THE STRUCTURE AND FUNCTION OF INTEGRINS

WENDY A. DOUGLASS

Wolfson College, Oxford

A thesis submitted for the degree of

Doctor of Philosophy

Trinity Term, 1997

MRC Immunochemistry Unit,

Department of Biochemistry,

University of Oxford.

RADCLIFFE SCIENCE LIBRARY OXFORD
DEPOSITED
19 JAN 1998
THESIS

ABSTRACT

THE STRUCTURE AND FUNCTION OF INTEGRINS

Wendy Ann Douglass
Wolfson College

Trinity Term 1997
Submitted for the degree of D. Phil

Integrins are a family of αβ heterodimeric cell surface glycoproteins formed by the non-covalent association of a specific integrin α and β subunit. At present 16 different integrin α subunits and 8 different integrin β subunits have been identified, which can associate in various combinations to produce over 20 different integrin αβ heterodimeric receptors. The leukocyte integrins LFA-1 (αLβ2, CD11a/CD18), Mac-1 (αMβ2, CD11b/CD18) and p150,95 (αXβ2, CD11c/CD18) are formed by the non-covalent association of the αL, αM or αX subunits with the β2 subunit. In order to determine the regions of the β2 subunit which are involved in its heterodimeric interaction with the αL, αM and αX subunits, eight variant β2 subunits were analysed for their ability to form LFA-1, Mac-1 and p150,95 heterodimeric complexes. Three chimeric β2/β1 subunits: β2V1, β2V12 and β2NS1, and three analogous chimeric β2/β7 subunits: β2V7, β2V72 and β2NS7, as well as a soluble and a truncated β2 subunit: β2sol and β2tr, were studied. All of the variant β2 subunits retained the ability to associate with the αL subunit, suggesting that the N-terminal 436 amino acids of the β2 subunit are sufficient to provide the specificity for LFA-1 heterodimer formation. In contrast, all the β2 variants associated inefficiently with the αM and αX subunits, suggesting that the heterodimeric interactions between the α and β subunits in Mac-1 and p150,95 are more extensive, and perhaps more complicated than those in LFA-1. The ability of the modified LFA-1 heterodimers formed with the variant β2 subunits to bind to the LFA-1 ligand ICAM-1 was also studied. All of the modified LFA-1 receptors retained the ability to bind to ICAM-1, suggesting that in LFA-1, the ICAM-1 binding site in the β2 subunit must be located within its N-terminal 436 amino acids. In addition, unlike the wildtype LFA-1 receptor, all of the modified LFA-1 receptors were constitutively active with respect to ICAM-1 binding. It therefore appears that specific interactions between different regions of the β2 subunit are required to constrain the LFA-1 receptor in its inactive, resting state, and that disruption of any one of these intramolecular interactions results in release of the receptor into its high affinity ligand binding conformation. This "constraint model" for the regulation of LFA-1 activity may also be applicable to other integrins. Analysis of a number of mutant β2 subunits carrying leukocyte adhesion deficiency (LAD) mutations, and their ability to form LFA-1, Mac-1 and p150,95 heterodimers, provided results consistent with those obtained with the variant β2 subunits.

ACKNOWLEDGEMENTS

I am very grateful to my supervisor, Dr. Alex Law, for his guidance throughout the course of my studies.

I would also like to thank Dr. G. Otulakowski for her contribution in constructing the αL cDNA, Miss J. Shaw for constructing the αM cDNA, Dr. M.K. Robinson for providing the αX cDNA and the KIM mAbs, Dr. M. Puklavec for providing the COS 7 cells, Professor A.J. McMichael for providing the MHM24 and MHM23 mAbs, Dr. K. Micklem for providing the LPM19C and KB23 mAbs, Dr. V. Horejse for providing the MEM83 mAb, and the Cellular Immunology Unit, Oxford, for providing the OX33 and OX34 mAbs.

I gratefully acknowledge the financial support of the Medical Research Council.

Thanks are also due to the staff and students of the MRC Immunochemistry Unit who were always ready to help when things went wrong. In particular I should like to thank Dr. A.H. Wright for helping me with the DNA techniques when I first arrived, and Miss B. Moffat for her invaluable help with the tissue culture, as well as members of F7, past and present, for being such fun to work with.

I would also like to thank my friends who have kept me going through the bad times and celebrated the good times with me. In particular, I would like to thank Mihaela Gadjeva, Amanda Jackson, Susan Kettle, Ashley Vaughan and Ann Wright, without whose encouragement this thesis would not have been completed.

Finally, I would like to thank my parents and sister for their endless support and encouragement throughout my time in higher education, and for always being there for me.

CONTENTS

ABSTRACT		i
ACKNOWLEDGEMENTS		ii
CONTENTS		iii
ABBREVIATIONS		xi
CHAPTER ONE: INTRODUCTION		
1.1	CELL ADHESION MOLECULES (CAMs)	1
1.1.1	CADHERINS	2
1.1.2	SELECTINS	2
1.1.3	THE IMMUNOGLOBULIN SUPERFAMILY (IgSF)	3
1.1.4	INTEGRINS	4
1.2	THE INTEGRIN SUPERFAMILY	5
1.2.1	INTEGRIN LIGANDS	7
1.2.2	THE STRUCTURE OF INTEGRINS AND THEIR DIVALENT CATION/LIGAND BINDING SITES	9
1.2.2.1	The Structure of Integrin α Subunits	9
1.2.2.2	The Structure of Integrin β Subunits	16
1.2.2.3	The Structure of Integrin αβ Heterodimers	21
1.2.3	REGULATION OF INTEGRIN MEDIATED CELL ADHESION	22
1.2.3.1	Affinity Modulation of Integrins ("Inside-Out" Signalling)	22
1.2.3.2	Avidity Modulation of Integrins	27
1.2.3.2.1	Upregulation of Integrin Receptors	27
1.2.3.2.2	Clustering	27
1.2.3.2.3	Cell Spreading	28
1.2.4	SIGNAL TRANSDUCTION BY INTEGRINS ("OUTSIDE-IN" SIGNALLING)	29
1.2.5	THE LEUKOCYTE INTEGRINS	30
1.2.5.1	Counter-Receptors and Functions of the Leukocyte Integrins	31
1.2.5.1.1	LFA-1	31
1.2.5.1.2	Mac-1	32
1.2.5.1.3	p150,95	33
1.2.5.1.4	αDβ2	34

1.2.5.2 Contribution of The Leukocyte Integrins to Transendothelial Migration 34
1.2.5.3 Leukocyte Adhesion Deficiency I (LAD-I) 36

1.3 PROJECT AIMS 38

CHAPTER TWO: MATERIALS AND METHODS

2.1 MATERIALS 40
2.1.1 GENERAL REAGENTS 40
2.1.2 RADIOCHEMICALS 40
2.1.3 ENZYMES 40
2.1.4 COMMERCIALLY AVAILABLE KITS 40
2.1.5 DNA VECTORS 41
2.1.6 MONOCLONAL ANTIBODIES 41
2.1.7 LABORATORY STOCKS 42
2.1.8 SOLUTIONS AND BUFFERS 42
2.1.9 MEDIA 44

2.2 METHODS 45
2.2.1 GENERAL METHODS FOR DNA MANIPULATION 45
2.2.1.1 Phenol/Chloroform Extraction 45
2.2.1.2 Ethanol Precipitation of DNA 45
2.2.1.3 Isopropanol Precipitation of DNA 45
2.2.1.4 Concentrating DNA by Butanol Extraction 46
2.2.1.5 Quantitation of DNA 46
2.2.1.6 Restriction Endonuclease Digestion of DNA 46
2.2.1.7 Synthesis and Purification of Oligonucleotides 46
2.2.1.8 Autoradiography 47

2.2.2 RADIOACTIVE LABELLING OF NUCLEIC ACIDS 48
2.2.2.1 Radiolabelling of Double-Stranded DNA Fragments 48
2.2.2.2 Preparation of Radiolabelled Oligonucleotide Probes 49

2.2.3 TRANSFER OF DNA TO FILTERS AND HYBRIDISATION 49
2.2.3.1 Transfer of DNA to Filters after Agarose Gel Electrophoresis (Southern Blot Hybridisation) 49
2.2.3.2 Transfer of Bacterial Colonies to Filters (Colony Hybridisation) 50
2.2.3.3 Transfer of Bacteriophage Plaques to Filters (Plaque Hybridisation) 51
2.2.3.4 Hybridisation Conditions 51
2.2.3.5 Removal of Unbound Probe from Filters 51
2.2.3.6 Removing Specifically Bound Probe from Filters 52

2.2.4	BACTERIOPHAGE LAMBDA VECTORS	52
2.2.4.1	Plating Bacteriophage Lambda	52
2.2.4.2	Purification of Bacteriophage Lambda DNA	53
2.2.5	DNA SEPARATION AND PURIFICATION BY GEL ELECTROPHORESIS	54
2.2.5.1	Agarose Gel Electrophoresis	54
2.2.5.2	Recovery of DNA Fragments From Agarose Gels	55
2.2.5.3	Polyacrylamide Gel Electrophoresis	56
2.2.5.4	Recovery of DNA From Polyacrylamide Gels	57
2.2.6	THE POLYMERASE CHAIN REACTION (PCR)	57
2.2.6.1	Standard Protocol	57
2.2.6.2	Combination of Two PCR Products Via PCR	58
2.2.6.3	Preparation of PCR Products for Cloning	58
2.2.6.4	Screening for Recombinant Plasmids Using PCR	59
2.2.7	CLONING DNA FRAGMENTS INTO PLASMID VECTORS	59
2.2.7.1	Preparation of Vector DNA	59
2.2.7.2	Preparation of Insert DNA	60
2.2.7.3	"End Filling" of DNA Fragments With Recessed 3' Ends	60
2.2.7.4	Ligations	60
2.2.7.5	Preparation of E. coli Competent Cells	61
2.2.7.6	Transformation of E. coli Competent Cells with Plasmid DNA	61
2.2.7.7	Identification of Colonies That Contain Recombinant Plasmids	61
2.2.7.8	Purification of Plasmid DNA	62
2.2.8	DNA SEQUENCING	63
2.2.8.1	Sequencing Reactions	63
2.2.8.2	Polyacrylamide Gel Electrophoresis of Sequencing Reactions	64
2.2.9	COS 7 CELL CULTURE PROCEDURES	64
2.2.9.1	Normal Culture of COS 7 Cells	64
2.2.9.2	Storage of COS 7 Cell Stocks In Liquid Nitrogen	65
2.2.9.3	Recovering COS 7 Cell Stocks From Liquid Nitrogen	65
2.2.10	TRANSFECTION OF COS 7 CELLS	65
2.2.11	ANALYSIS OF COS 7 TRANSFECTANTS	66
2.2.11.1	Harvesting Transfected COS 7 Cells	66
2.2.11.2	FACS Analysis of Transfected COS 7 Cells	67
2.2.11.3	Immunoprecipitation Analysis of Transfected COS 7 Cells	67
2.2.11.4	Adhesion Assays With Transfected COS 7 Cells	71

CHAPTER THREE: GENERATING CHIMERIC, SOLUBLE, TRUNCATED AND WILDTYPE INTEGRIN CONSTRUCTS

3.1	INTRODUCTION	73
3.2	RESULTS	75
3.2.1	GENERATING CHIMERIC β2/β1 AND β2/β7 CLONES	75
3.2.1.1	Overall Strategy For Constructing Chimeric cDNAs	75
3.2.1.2	Obtaining Wildtype β2, β1 and β7 cDNA Clones	76
3.2.1.2.1	Obtaining a Full length Wildtype β2 cDNA Clone	76
3.2.1.2.2	Obtaining a Partial β1 cDNA and a Full length β7 cDNA Clone	76
3.2.1.3	Constructing Chimeric β2V1 and β2V7 cDNA Clones	78
3.2.1.3.1	Cloning the Wildtype β2 cDNA into pBluescript, Creating pBS/β2C	78
3.2.1.3.2	Engineering an EcoRV Site into pBS/β2C, Creating pBS/β2V	78
3.2.1.3.3	Constructing the Chimeric β2V1 cDNA from pBS/β2V, Creating pBS/β2V1	79
3.2.1.3.4	Constructing the Chimeric β2V7 cDNA from pBS/β2V, Creating pBS/β2V7	79
3.2.1.3.5	Cloning the Chimeric β2V1 and β2V7 cDNAs into Expression Vectors	80
3.2.1.3.5.1	Constructing the pKG4/β2V1 Clone	80
3.2.1.3.5.2	Constructing the pKG4/β2V7 Clone	80
3.2.1.3.5.3	Constructing the pSVL/β2V1 Clone	80
3.2.1.3.5.4	Constructing the pSVL/β2V7 Clone	81
3.2.1.3.5.5	Constructing the pcDNA3/β2V1 Clone	81
3.2.1.3.5.6	Constructing the pcDNA3/β2V7 Clone	81
3.2.1.4	Constructing the Chimeric β2V12 and β2V72 cDNA Clones	83
3.2.1.4.1	Modifying the β2 cDNA Sequence of pBS/β2V, Creating pBS/β2M	83
3.2.1.4.2	Constructing the Chimeric β2V12 cDNA from pBS/β2M, Creating pBS/β2V12	83
3.2.1.4.3	Constructing the Chimeric β2V72 cDNA from pBS/β2M, Creating pBS/β2V72	84
3.2.1.4.4	Cloning the β2V12 and β2V72 cDNAs into Expression Vectors	85
3.2.1.4.4.1	Constructing the pSVL/β2V12 Clone	85
3.2.1.4.4.2	Constructing the pSVL/β2V72 Clone	85
3.2.1.4.4.3	Constructing the pcDNA3/β2V12 Clone	85
3.2.1.4.4.4	Constructing the pcDNA3/β2V72 Clone	85

3.2.1.5	Constructing the Chimeric β2NS1 and β2NS7 cDNA Clones	87
3.2.1.5.1	Modifying the J8 Clone, Creating J8.1N	87
3.2.1.5.2	Constructing the Chimeric β2NS1 cDNA from J8.1N, Creating pATX/β2NS1	87
3.2.1.5.3	Constructing the Chimeric β2NS7 cDNA from J8.1N, Creating pATX/β2NS7	87
3.2.1.5.4	Cloning the β2NS1 and β2NS7 cDNAs into Expression Vectors	88
3.2.1.5.4.1	Constructing the pSVL/β2NS1 Clone	88
3.2.1.5.4.2	Constructing the pSVL/β2NS7 Clone	88
3.2.1.5.4.3	Constructing the pcDNA3/β2NS1 Clone	89
3.2.1.5.4.4	Constructing the pcDNA3/β2NS7 Clone	89
3.2.2	GENERATING SOLUBLE AND TRUNCATED β2 CLONES	90
3.2.2.1	Cloning the β2sol and β2tr cDNAs into Expression Vectors	90
3.2.2.1.1	Constructing the pSVL/β2sol Clone	90
3.2.2.1.2	Constructing the pSVL/β2tr Clone	90
3.2.2.1.3	Constructing the pcDNA3/β2tr Clone	90
3.2.3	GENERATING WILDTYPE β2 CLONES	91
3.2.3.1	Cloning the Wildtype β2 cDNA into Expression Vectors	91
3.2.3.1.1	Constructing the pSVL/β2 Clone	91
3.2.3.1.2	Constructing the pcDNA3/β2 Clone	91
3.2.4	GENERATING WILDTYPE αL, αM and αX CLONES	92
3.2.4.1	Generating Wildtype αL Clones	92
3.2.4.1.1	Constructing a Full Length Wildtype αL cDNA	92
3.2.4.1.2	Cloning the Wildtype αL cDNA into Expression Vectors	93
3.2.4.1.2.1	Constructing the pSVL/αL Clone	93
3.2.4.1.2.2	Constructing pcDNA3/αL	93
3.2.4.2	Generating Wildtype αM Clones	94
3.2.4.2.1	Obtaining a Full Length Wildtype αM cDNA	94
3.2.4.2.2	Cloning the Wildtype αM cDNA into Expression Vectors	94
3.2.4.2.2.1	Constructing the pcDNA1/αM Clone	94
3.2.4.2.2.2	Constructing the pSVL/αM Clone	94
3.2.4.2.2.3	Constructing the pcDNA3/αM Clone	95
3.2.4.3	Generating Wildtype αX Clones	95
3.2.4.3.1	Obtaining a Full Length Wildtype αX cDNA	95
3.2.4.3.2	Cloning the Wildtype αX cDNA into Expression Vectors	95

3.2.4.3.2.1 Constructing the pSVL/αX Clone 95
3.2.4.3.2.2 Constructing the pcDNA3/αX Clone 96

3.3 SUMMARY 97

CHAPTER FOUR: THE EXPRESSION OF VARIANT β2 SUBUNITS IN COS 7 CELLS AND THE FORMATION OF MODIFIED LFA-1, MAC-1 AND p150,95 HETERODIMERS

4.1 INTRODUCTION 99

4.2 RESULTS 101

4.2.1 EXPRESSION OF WILDTYPE AND MODIFIED LFA-1, Mac-1 AND p150,95 IN COS 7 CELLS 101

4.2.1.1 Expression of Wildtype LFA-1, Mac-1 and p150,95 101
4.2.1.1.1 Expression of the Wildtype αL, αM and αX Subunits 101
4.2.1.1.2 Expression of the Wildtype β2 Subunit 102
4.2.1.1.3 Summary of the Expression of the Wildtype α and β Subunits 103

4.2.1.2 Expression of Modified LFA-1, Mac-1 and p150,95 104
4.2.1.2.1 Expression of the Chimeric β2 Subunits and their Heterodimer Formation with the Wildtype αL, αM and αX Subunits 105
4.2.1.2.1.1 Expression of the Chimeric β2V1 and β2V7 Subunits 105
4.2.1.2.1.2 Expression of the Chimeric β2V12 and β2V72 Subunits 106
4.2.1.2.1.3 Expression of the Chimeric β2NS1 and β2NS7 Subunits 108
4.2.1.2.2 Expression of the Soluble and Truncated β2 Subunits and their Heterodimer Formation with the Wildtype αL, αM and αX Subunits 110
4.2.1.2.2.1 Expression of the β2sol and β2tr Subunits 110
4.2.1.2.3 Summary of the Expression of the Chimeric, Soluble and Truncated β2 Subunits 111

4.2.2 THE BINDING OF WILDTYPE AND MODIFIED LFA-1 TO ICAM-1 112

4.2.3 EPITOPE MAPPING OF ANTI-β2 MONOCLONAL ANTIBODIES 114

4.3 SUMMARY 115

CHAPTER FIVE: LEUKOCYTE ADHESION DEFICIENCY-I (LAD-I): TRANSIENT EXPRESSION OF MUTANT LFA-1, MAC-1 AND p150,95 IN COS 7 CELLS

5.1	INTRODUCTION	119
5.2	RESULTS	120
5.2.1	CHARACTERISATION OF THREE NOVEL LAD MUTATIONS WITHIN THE CODING REGION OF THE β2 GENE	120
5.2.1.1	Identifying Mutations Within the Coding Region of the β2 Gene	120
5.2.1.2	Constructing Full Length Mutant β2 cDNAs	121
5.2.1.3	Subcloning the Full Length Mutant β2 cDNAs into the pSVL Expression Vector	121
5.2.1.3.1	Cloning the Mutant β2(A270V) cDNA into pSVL, Creating pSVL/β2(A270V)	122
5.2.1.3.2	Cloning the Mutant β2(G284S) cDNA into pSVL, Creating pSVL/β2(G284S)	122
5.2.1.3.3	Cloning the Mutant β2($T418_{fr*}$) cDNA into pSVL, Creating pSVL/β2($T418_{fr*}$)	122
5.2.1.4	Expressing the Mutant β2 Subunits on COS 7 Cells	123
5.2.1.4.1	Expression of the Mutant β2(A270V) Subunit	123
5.2.1.4.2	Expression of the Mutant β2(G284S) Subunit	124
5.2.1.4.3	Expression of the Mutant β2($T418_{fr*}$) Subunit	125
5.2.1.4.4	Summary of the Expression of the Mutant β2(A270V), Mutant β2(G284S) and Mutant β2($T418_{fr*}$) Subunits on COS 7 Cells	125
5.3	SUMMARY	127

CHAPTER SIX: DISCUSSION

6.1	THE EFFECT OF A SERIES OF CHIMERIC, SOLUBLE AND TRUNCATED β2 SUBUNITS ON αβ HETERODIMER FORMATION AND LIGAND BINDING	132
6.1.1	REGIONS OF THE β2 SUBUNIT INVOLVED IN LFA-1, Mac-1 AND p150,95 HETERODIMER FORMATION	132

6.1.2	REGIONS OF THE β2 SUBUNIT INVOLVED IN LFA-1 BINDING TO ICAM-1	133
6.1.3	THE ROLE OF THE β2 SUBUNIT IN THE REGULATION OF LFA-1 BINDING TO ICAM-1	134
6.2	THE EFFECT OF A SERIES OF LAD MUTATIONS ON αβ HETERODIMER FORMATION AND LIGAND BINDING	135
6.3	A "CONSTRAINT MODEL" FOR THE REGULATION OF INTEGRIN-LIGAND BINDING EVENTS	136
REFERENCES		139

ABBREVIATIONS

ATP	adenosine triphosphate
bp	base pair(s)
BSA	bovine serum albumin
CCM	chemical cleavage at mismatch
CD	cluster of differentiation
cDNA	complementary DNA
cpm	counts per minute
DMSO	dimethyl sulphoxide
DNAse	deoxyribonuclease
dNTP	deoxynucleotide triphosphate
dATP	deoxyadenosine triphosphate
dCTP	deoxycytidine triphosphate
dGTP	deoxyguanidine triphosphate
dTTP	deoxythymidine triphosphate
DTT	dithiothreitol
DNA	deoxyribonucleic acid
ECL	enhanced chemiluminescence
EDTA	ethylene-diamine-tetra acetic acid
ELISA	enzyme linked immunoabsorbent assay
FACS	fluorescent activated cell sorter
kbp	kilobase pairs
kDa	kilodaltons
h	hour(s)
Ig	immunoglobulin
IP	immunoprecipitation
µCi	microcurie
mAb	monoclonal antibody
min	minute(s)
mRNA	messenger ribonucleic acid
MW	molecular weight
O.D.	optical density
PAGE	polyacrylamide gel electrophoresis
PBS	phosphate buffered saline
PBS/O	phosphate buffered saline (without calcium and magnesium)
PMA	phorbol myristate acetate
PMSF	phenylmethylsulphonyl fluoride
RNA	ribonucleic acid
RNAse	ribonuclease

MTT	3-[4,5-Dimethylthiazol-2-yl]-2,5-diphenyltetrazolium bromide

rpm	revolutions per minute
r.t.	room temperature
SSC	standard saline citrate
SDS	sodium dodecyl sulphate
sec	second(s)
TEMED	N, N, N', N'-tetramethylethylenediamine
tRNA	transfer ribonucleic acid
Tris	Tris (hydroxymethyl)-aminoethane
UV	ultraviolet
v/v	volume per volume
w/v	weight per volume
w/w	weight per weight

The single-letter and triplet codes for amino acid residues are used. Restriction enzymes are referred to by their three-letter names derived from that of the source microorganism. Other abbreviations are defined in the text where first encountered.

CHAPTER ONE

INTRODUCTION

1.1 CELL ADHESION MOLECULES (CAMs)

Cell adhesion is vital for the development, maintenance and function of multicellular organisms. Each cell interacts with its neighbouring cells or with the surrounding extracellular matrix (ECM) via specific cell surface glycoproteins termed cell adhesion molecules (or CAMs). By regulating the activity or the expression pattern of its particular array of CAMs, a cell can alter its adhesive phenotype, enabling it to participate in complex adhesive events such as those governing morphogenesis and development, haemostasis, the immune response, and wound healing (Hynes and Lander, 1992; Gumbiner, 1996).

CAMs are typically transmembrane glycoproteins which adhere at their extracellular face to components of the ECM or to CAMs on other cells, and interact at their intracellular face with peripheral membrane and cytoplasmic plaque proteins which tether them to the actin cytoskeleton (Gumbiner, 1993). Apart from providing structural pegs which anchor a cell in place, CAMs can also transmit signals in a bidirectional fashion across the cell membrane, and can form highly organised multiprotein adhesive structures, such as focal adhesion complexes and synaptic and adherens junctions, which appear to act as signal transduction centres, capable of generating and receiving extracellular and intracellular signals (Yamada and Geiger, 1997). In addition, CAMs can operate in synergy with other cell surface receptors, and can network with other intracellular signalling systems, such as the mitogenic signalling pathways initiated by growth factors, to orchestrate a complex and finely regulated pattern of adhesion.

In the past two decades, many CAMs have been identified and characterised at the molecular level. The majority have been found to belong to one of four major superfamilies of structurally related proteins: the cadherins (Takeichi, 1988, 1990, 1991), the selectins (Bevilacqua *et al.*, 1991; Bevilacqua and Belson, 1993; Lasky, 1992; 1995), certain members of the immunoglobulin superfamily (Williams, 1987; Williams and Barclay, 1988), and the integrins (Hynes, 1987; 1992). The basic structural and functional features of these CAM superfamilies, which are discussed below, are illustrated in Figure 1.1.

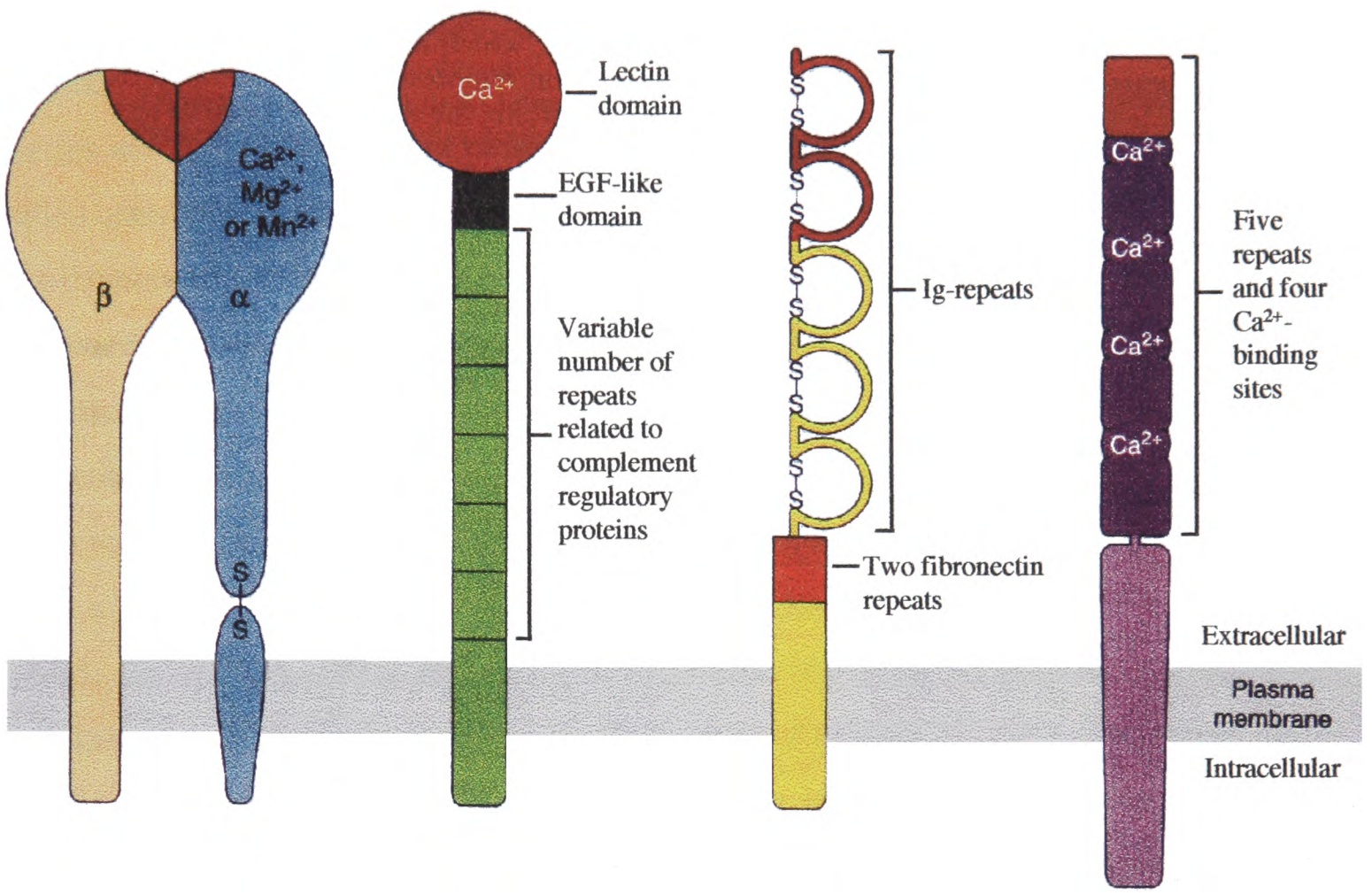


Figure 1.1: The Four Major Classes of Cell Adhesion Molecules (CAMs)

The basic structural features of the four major classes of cell surface adhesion molecules (CAMs) are shown, with regions thought to be involved in ligand binding shaded red. The selectins, the immunoglobulin superfamily (IgSF) members and the cadherins all mediate cell-cell adhesive interactions, whereas the more complex integrin family of $\alpha\beta$ heterodimers mediate both cell-cell, cell-extracellular matrix (ECM) and cell-soluble ligand binding. Adhesion mediated by these CAMs, with the exception of the IgSF members, is characteristically divalent cation dependent.

This figure was taken from: Horwitz and Hunter (1996).

1.1.1 CADHERINS

The cadherins are a family of calcium dependent cell-cell adhesion molecules which bind via homophilic, and less commonly heterophilic, interactions with cadherins on other cells (Takeichi, 1988; 1990; 1991). They play an important role in the segregation of cells during embryonic development (Ranscht, 1994; Huber *et al.*, 1996), and are fundamental in maintaining the tissue architecture of the mature organism. At least twelve different cadherins are known (Suzuki *et al.*, 1991; 1996), but the most extensively studied are the so called classic cadherins: E(epithelial)-, N(neuronal)- and P(placental)-cadherin. These have a cannonic structure, consisting of a long extracellular domain of five repeats (EC1-5), followed by a single transmembrane domain and a short, highly conserved cytoplasmic domain that associates indirectly with the actin cytoskeleton via the catenin (α, β, and γ) and α-actinin proteins (Ozawa *et al.*, 1989). The binding site on most cadherins has been mapped to EC1 (Nose *et al.*, 1990; Overduin *et al.*, 1995; Shapiro *et al.*, 1995), and recently a "zipper" model for homophilic cadherin binding has been proposed (Shapiro *et al.*, 1995; Weis, 1995), in which cadherin molecules associate to form dimers that interdigitate with other cadherin dimers on the surface of the opposing cell. Cadherins are the major components of adherens junctions, and the importance of E-cadherin in the formation of epithelial tissues has been demonstrated by lethal E-cadherin gene knockouts in mice (Laure *et al.*, 1994). E-cadherin is also thought to act as an important tumour suppressor, as deficiencies or mutations in E-cadherin correlate with the invasiveness and metastasis of certain human tumours (Birchmeier and Behrens, 1994; Takeichi, 1993)

1.1.2 SELECTINS

The selectins are a family of calcium-dependent carbohydrate binding proteins which mediate adhesive interactions between leukocytes and the endothelium/platelets (Rosen and Bertozzi, 1994; Lasky, 1992; 1995; Tedder *et al.*, 1995; Kansas *et al.*, 1996). There are three closely related members of the selectin family: E(endothelial)-, L(leukocyte)-, and P(platelet)-selectin. Each member typically consists of an N-terminal C-type lectin domain (carbohydrate recognition domain), followed by an epidermal growth factor (EGF)-like motif, varying numbers of short consensus repeats (SCRs) similar to those found in complement-regulatory proteins, a transmembrane domain, and a short cytoplasmic tail. Soluble forms of E- and L-selectin can also arise through proteolytic cleavage of these

receptors from the cell surface, and alternative RNA splicing can also create a soluble form of P-selectin lacking the transmembrane anchoring domain (Gearing *et al.*, 1992; Gearing and Newman, 1993; Kahn *et al.*, 1994). Selectins recognise fucosylated carbohydrate ligands, especially structures containing sialyl-Lewis^x, and both the lectin and the EGF domains appear to be involved in ligand binding (Kansas *et al.*, 1994). Selectins are involved in mediating the initial attachment of rolling leukocytes to the blood vessel wall during the inflammatory response. Their importance in this process is highlighted in the disorder leukocyte adhesion deficiency II (LAD II), where selectin ligands are absent, and neutrophils are unable to recruit to sites of inflammation (von Andrian *et al.*, 1993; Etzioni, 1994).

1.1.3 THE IMMUNOGLOBULIN SUPERFAMILY (IgSF)

The immunoglobulin superfamily (IgSF) are an abundant family of cell surface glycoproteins whose extracellular structure is characterised by variable numbers of repeating immunoglobulin-like domains (Ig domains). Although many IgSF members are receptors for soluble ligands (e.g. PDGF-receptor and the Fc-receptors), the majority are cell adhesion molecules, mediating divalent cation independent homophilic or heterophilic cell-cell interactions. The IgSF CAMs are expressed on a wide variety of cell types, including neuronal cells (e.g. NCAM, telencephalin), red blood cells (e.g. ICAM-4) and endothelial cells (e.g. VCAM, MAdCAM, ICAM-1, ICAM-2, CD31), but are particularly abundant on leukocytes, where they represent approximately 50% of the cell surface glycoproteins (e.g. ICAM-1, -2, and -3, LFA-2, LFA-3, CD31) (Cunningham *et al.*, 1987; Williams and Barclay, 1988; Springer, 1990). Some members of the family are transmembrane receptors, whilst others are attached to the membrane via glycosylphosphatidyl inositol tails, and several occur in both forms with varying cytoplasmic domains derived by alternative RNA splicing (Cunningham *et al.*, 1987; Santoni *et al.*, 1989). The non-lymphocyte members of the family often contain several membrane proximal fibronectin type III repeats (Hynes, 1990), which are similar in structure to the Ig domain repeats. In spite of the very conserved pattern of domain folding and organisation seen in members of the IgSF, there is considerable diversity in their modes of binding. The adhesive binding sites may be located on either the N-terminal membrane distal domains, the internal domains, or the membrane proximal domains, and

can be localised to either a single domain, or may be more extensive, encompassing several Ig domains (Holness and Simmons, 1994).

1.1.4 INTEGRINS

The integrins are the most complex and widespread family of CAMs discovered to date. They are expressed on almost every cell type (Albelda and Buck, 1990) and can mediate cell-cell, cell-ECM and cell-multivalent ligand adhesive events (Hynes, 1987; 1992; Hemler, 1990; Ruoslahti, 1991; Garratt and Humphries, 1995; Newham and Humphries, 1996). They are heterodimers, formed by the non-covalent association of a larger α subunit (120-180 kDa) with a smaller β subunit (90-110 kDa). Ligand binding requires the presence of both subunits, and is also divalent cation-dependent. Multiple integrin α and β subunits have been discovered, which combine selectively to form a variety of functional αβ heterodimeric complexes, each with distinct ligand binding properties. Integrin α and β subunits are type I transmembrane glycoproteins, consisting of large extracellular domains, followed by classic hydrophobic transmembrane segments and generally short cytoplasmic tails. The extracellular N-terminal regions of the α and β subunits associate to form the adhesive ligand binding site, whilst their C-terminal cytoplasmic tails interact with cytoskeletal and intracellular signalling proteins. A fundamental property of integrins is their ability to transmit signals in a bidirectional fashion across the cell membrane. Response to cytoplasmic signals can regulate the functional activity and surface expression levels of receptors (termed inside-out signalling), whilst binding to extracellular ligands can induce changes in cell shape, gene expression and the activation state of a cell (termed outside-in signalling) (Garratt and Humphries, 1995; Schwartz *et al.*, 1995). The ability to integrate information between the cytoskeleton and the ECM gave the name to the superfamily (Tamkun *et al.*, 1986), and enables precise coordination of adhesion with other cellular events. Integrins participate in numerous complex biological processes, including cell growth and differentiation, fertilisation, tissue organisation, cell migration, blood clotting, inflammation and target recognition by lymphocytes. Their importance is highlighted by several genetic disorders, including Leukocyte Adhesion Deficiency I (LAD-I) (Springer *et al.*, 1984) and Glanzmann's Thrombasthenia (Nurden and Caen, 1974), in which the expression or function of a particular integrin or integrin subset is severely compromised. Targetted gene knockout studies in mice have also demonstrated the

fundamental importance of the integrin superfamily in foetal development (Yang *et al.*, 1993; Hynes, 1996). As the work described in this thesis focuses on the integrins, this family of cell adhesion molecules are discussed in greater detail in the following sections.

1.2 THE INTEGRIN SUPERFAMILY

When integrins were first classified as a CAM superfamily, they were thought to comprise of three distinct subfamilies formed by the association of a specific β subunit (either the β1, β2 or β3 subunit) with an exclusive set of α subunits (Ginsberg *et al.*, 1987; Hynes, 1987). The β1 subfamily (formed by association with the α1, α2, α3, α4, α5, or α6 subunits) were the largest subfamily, expressed on a wide variety of cell types. They were also refered to as the VLA (Very Late after Activation) antigens, because α1β1 (VLA-1) and α2β1 (VLA-2) appear on lymphocytes several days after mitogen activation (Albelda and Buck, 1990). The β1 integrins consist mainly of receptors involved in cell-ECM interactions, like the fibronectin receptor (α5β1, VLA-5) and the laminin receptor (α6β1, VLA-6). The β2 (CD18) subfamily (formed by association with the αL(CD11a), αM(CD11b) or αX(CD11c) subunits) are exclusively expressed on leukocytes, and were therefore also refered to as the leukocyte integrins (Larson and Springer, 1990). They consisted of the LFA-1 (Leukocyte Function Associated molecule-1) receptor (αLβ2, CD11a/CD18), and the Mac-1 (αMβ2, CD11b/CD18) and p150,95 (αXβ2, CD11c/CD18) receptors, and mediate various adhesive interactions of the immune system. Finally, the β3 integrin subfamily (formed by association with the αIIb or αV subunits), consisted of the platelet gpIIbIIIa (αIIbβ3) and the vitronectin receptor (αVβ3), which are expressed primarily on platelets and endothelial cells respectively. As each integrin β subunit combined with several unique α subunits, but each α subunit only combined with one particular β subunit, it was thought that the α and β subunits of each integrin subfamily shared specific structural features which made them exclusively compatible.

Since this initial classification, it has become apparent that the integrin superfamily is far more extensive and complicated than originally proposed. Five additional β subunits (β4-β8) and five additional α subunits (α7-α9, αD and αE) have been identified, and there are now a total of 8 different integrin β subunits and 16 different integrin α subunits which can associate in various combinations to form over 20 different integrin αβ heterodimeric

complexes (see Figure 1.2). Subfamilies with shared β subunits can still be defined, and infact the β1 subfamily (which has been extended to include the α7β1, α8β1, α9β1 and αVβ1 integrins), the β2 subfamily (which has been extended to include the αDβ2 integrin), and the β3 subfamily are still the most extensively studied integrins. However, it has become apparent that the original classification of integrins into β subunit subfamilies was an innacurate description of the superfamily. Some of the α subunits are far more promiscuous than originally suggested. For instance, the α4 subunit can combine with both the β1 and β7 subunits, the α6 subunit with both the β1 and β4 subunits, and the αV subunit with the β1, β3, β5, β6 and β8 subunits.

One of the enigmas of the integrin superfamily is how the specificity of αβ heterodimer formation is achieved. The 16 different α subunits and 8 different β subunits could combine to form a total of 128 (16 x 8) different αβ heterodimeric pairs, and yet at present, only 22 different αβ heterodimers have been identified. Although it is possible that some additional αβ combinations may be permisable but remain undiscovered, perhaps because they are expressed at very low levels or because the α and β subunits in question are never expressed at the same time in the same cell, there are also some known forbidden combinations (see Figure 1.2). Patients suffering from the genetic disorder leukocyte adhesion deficiency I (LAD-I) have defects in the gene encoding the β2 subunit which often results in severely reduced expression levels of β2 on the surface of their leukocytes (Anderson and Springer, 1987; Arnaout, 1990). In such cases, the αL, αM, and αX subunits are also not expressed on the cell surface, even though alternative β subunits (β1, β3 and β7) can be detected at high expression levels on the same cells. This implies that the leukocyte integrin α subunits (αL, αM, and αX) are unable to associate with the β1, β3 and β7 subunits. Conversely, it appears that the α1-α6, αV and αE subunits are unable to associate with the β2 subunit, as these combinations have also never been detected. It is possible that other forbidden αβ combinations also exist, but await identification. Integrin αβ heterodimer formation is therefore a highly selective and complex event, with each integrin subunit associating with only a specific subset of partner subunits, and at present, it is unclear exactly how the specificity of these interactions is achieved.

Figure 1.2: Members of the Integrin Superfamily and Their Ligands

Members of the integrin superfamily of adhesion molecules are heterodimeric, each consisting of a non-covalently associated α and β subunit. To date, 16 different α subunits and 8 different β subunits have been characterised, which associate in the various combinations shown opposite to form 22 different integrin αβ heterodimeric complexes (grey shaded squares). Many αβ heterodimeric combinations have not been reported, and it is unclear whether these combinations are permissible or not (unshaded boxes), whereas some αβ combinations are definitely not permissible (black shaded boxes). Integrins can bind to proteins of the extracellular matrix (ECM), to members of the cadherin and immunoglobulin superfamily (IgSF) of CAMs expressed on opposing cells, to soluble multivalent ligands involved in the blood clotting and complement cascades, and to a variety of microbial surface components. The ligand(s) for each specific αβ heterodimer are indicated where known. The ligand(s) for the integrin αVβ8 have not yet been identified, as indicated by the "?" sign.

Key to Ligands:

Extracellular Matrix (ECM) Components: CO = Collagen; LM = Laminin; FN = Fibronectin; VN = Vitronectin; KN = Kalinin; EP = Epiligrin; OP = Osteopontin; TN = Tenascin; TS = Thrombospondin.

Members of the Immunoglobulin Superfamily (IgSF) of CAMs: VCAM-1 = Vascular Adhesion Molecule-1; ICAM-1, -2, -3 and -4 = Intercellular Adhesion Molecules-1,-2, -3, and -4; MadCAM-1 = Mucosal Adressin Adhesion Molecule-1; TLN = Telencephalin; CD31 = PECAM-1 = Platelet Endothelial Cell Adhesion Molecule.

Members of the Cadherin Family of CAMs: E-Cadherin = Endothelial Cadherin.

Proteins of the Blood Clotting and Complement Cascades: FB = Fibrinogen; FX = Coagulation Factor X; vWF = von Willebrand Factor; iC3b = Complement Component iC3b.

Microbial Surface Components: LPS = Lipopolysaccharide, LPG = Lipophosphoglycan.

	β1	β2	β3	β4	β5	β6	β7	β8
α1	CO, LM							
α2	CO, LM, FN							
α3	CO, LM, FN, EP, KN							
α4	FN, TS VCAM-1 MAdCAM-1						FN, VCAM-1 MAdCAM-1	
α5	FN							
α6	LM			LM, KN				
α7	LM							
α8	FN							
α9	TN							
αL		ICAM-1, -2, -3, -4, TLN						
αM		ICAM-1, -2, -4, FB iC3b, FX LPS, LPG						
αX		iC3b, FB LPS, LPG						
αD		ICAM-3						
αIIb			FB, FN, vWF, VN, CO, TS					
αV	VN, FN, FB, vWF CO		VN, FN, FB, vWF, LM,TS,CO OP, CD31		VN, FN, FB	FN		?
αE							E-Cadherin	

1.2.1 INTEGRIN LIGANDS

Integrins can bind to a wide variety of ligands (Humphries, 1990; Hynes, 1992; Haas and Plow, 1994; Garratt and Humphries, 1995; Newham and Humphries, 1996). They can mediate cell-substratum interactions by binding to ECM proteins (such as fibronectin, vitronectin, laminin and collagen), cell-cell interactions by binding to CAM counter-receptors expressed on other cells (like the ICAMs, VCAM-1, CD31 and E-cadherin), and cell aggregation by binding to soluble multivalent ligands (like fibrinogen and von Willibrand factor). They can also adhere to a variety of soluble plasma proteins (such as factor X and iC3b). Individual integrins can often bind multiple ligands, whilst individual ligands may be recognised by several different integrins (see Figure 1.2). Many viral, bacterial and parasitic proteins have also been identified which can interact with integrins: The tat protein of human immunodeficiency virus (HIV) type-1 can bind to $\alpha 5\beta 1$ and $\alpha V\beta 3$ (Barillari *et al.*, 1993), adenovirus to $\alpha V\beta 3$ and $\alpha V\beta 5$ (Wickham *et al.*, 1993), echovirus to $\alpha 2\beta 1$ (Bergelson *et al.*, 1993), the Lyme disease spirochete *Borrelia burgdorferi* to $\alpha IIb\beta 3$ (Coburn *et al.*, 1993) and the neutrophil inhibitory factor (NIF) protein of canine hookworm to $\alpha M\beta 2$ (Moyle *et al.*, 1994; Muchowski *et al.*, 1994). In addition, snake venom and cellular disintegrins can bind to certain integrin family members (Blobel and White, 1992; Weskamp and Blobel, 1994).

Many integrin ligands appear to use short linear peptides (of three or four amino acids in length) as recognition motifs for receptor binding. The Arg-Gly-Asp (RGD) sequence within the central cell-binding domain of fibronectin was the first of these motifs to be discovered (Pierschbacher and Ruoslhati, 1984; Ruoslahti and Pierschbacher, 1987). Fibronectin, vitronectin, von Willibrand factor and the foot and mouth disease virus (FMDV) all bind to integrins via their RGD motifs (Aota *et al.*, 1991; Beacham *et al.*, 1992). However, not all integrin ligands possess RGD sequences, whilst other ligands (like iC3b, fibrinogen and laminin) contain RGD sequences which are not involved in receptor binding (Taniguchi-Sidle and Isenman, 1992; Farrel and Thiagarajan, 1994). Another commonly used recognition motif, first identified in the IIICS region of fibronectin (Komoriya *et al.*, 1991) is the LDVP motif. Whilst RGD sites are invariant in sequence, LDVP sequences can vary within a defineable consensus (L/I-D/E-S/T/V/A-P/S). Many integrin-binding members of the IgSF have been shown to use LDVP-like sequences: in

VCAM-1 the active sequence is IDSP, in MAdCAM-1 it is LDTS, whilst in the ICAMs-1-3 it is either IETP or LETS (Staunton *et al.*, 1990; Li *et al.*, 1993; Clements *et al.*, 1994; Vonderheide *et al.*, 1994; Holness *et al.*, 1995). Other short sequences recognised by integrins include QAGDV in fibrinogen (Kloczewiak *et al.*, 1984), EILDV in fibronectin, and DGEA in collagen (Staatz *et al.*, 1991). All these motifs are characterised by the presence of an acidic residue (either an Asp or a Glu) which is essential for receptor binding. Ligand binding by integrins is divalent cation dependent, and it has been suggested that the acidic residues in ligands are required to directly coordinate with divalent cations in the integrin ligand binding pocket. The crystal structure of the RGD site in the tenth type III module of fibronectin (Dickinson *et al.*, 1994) and in the FMDV (Logan *et al.*, 1993) has been determined. In both cases, the RGD sequence was present in a flexible loop extending outwards from the protein core. The crystal structure of the two N-terminal Ig domains of VCAM-1 has also been determined (Jones *et al.*, 1995), and the IDSP site in domain 1 is also located in an exposed loop, favouring receptor recognition. As all Ig-CAMs are likely to adopt the same folding pattern, the LDVP motifs in the ICAMs-1-3 and MAdCAM are probably located in similar positions, and it has been suggested that all integrin ligand binding motifs may share the same broadly related topology (Newham and Humphries, 1996).

As integrins recognise and bind to such small and highly related peptide motifs in ligands, it is somewhat surprising that individual ligands can exhibit such discrete receptor binding specificities. It has been suggested that additional discontinuous sites within ligands may act in synergy with the peptide recogniton motifs, and that the combination of multiple integrin-ligand contacts provides a mechansim for selective receptor binding. There is in fact considerable evidence that the RGD site in fibronectin requires a second synergy sequence for optimal receptor binding activity (Aota *et al.*, 1991; Nagai *et al.*, 1991). This sequence has been mapped to the pentapeptide PHSRN in the centre of the ninth type III repeat, and mutation or deletion of this synergy site greatly diminishes integrin adhesion to fibronectin (Aota *et al.*, 1994; Bowditch *et al.*, 1994). In addition, mutational analysis of ICAM-1 and VCAM-1 has identified residues, either close to the LDVP site or more distant, which are also required for $\alpha L\beta 2$ and $\alpha 4\beta 1$ binding (Staunton *et al.*, 1990; Osborn *et al.*, 1994; Vonderheide *et al.*, 1994). It therefore appears that short peptide recognition motifs within ligands represent their main adhesive sites of contact with integrins, but that

the actual specificity of integrin-ligand interactions is determined by the more global structure of the ligand.

1.2.2 THE STRUCTURE OF INTEGRINS AND THEIR DIVALENT CATION/LIGAND BINDING SITES

Each integrin receptor is an αβ heterodimer, formed by the non-covalent association of a specific integrin α and β subunit. The primary structure of the 16 different integrin α subunits and 8 different integrin β subunits has been determined, and all the α subunits share extensive sequence homology with one another and have a similar overall structure, as do all the β subunits. Both are type I transmembrane glycoproteins, with large N-terminal extracellular domains, of about 1100 amino acids for the α subunits and 670 amino acids for the β subunits, followed by classic hydrophobic transmembrane segments, and short C-terminal cytoplasmic tails ranging from 15-77 amino acids in length. The exception is the β4 subunit, which has an extended cytoplasmic tail of about 1000 amino acids. Although information on the higher order structure of integrins is limited, several structural features have been identified which are characteristic of integrin α and β subunits (see Figure 1.3), and as all the α subunits are similar, as are all the β subunits, it has been suggested that all integrin αβ heterodimers share the same overall consensus structure, and that each receptor is simply a variant of this consensus.

1.2.2.1 The Structure of Integrin α Subunits

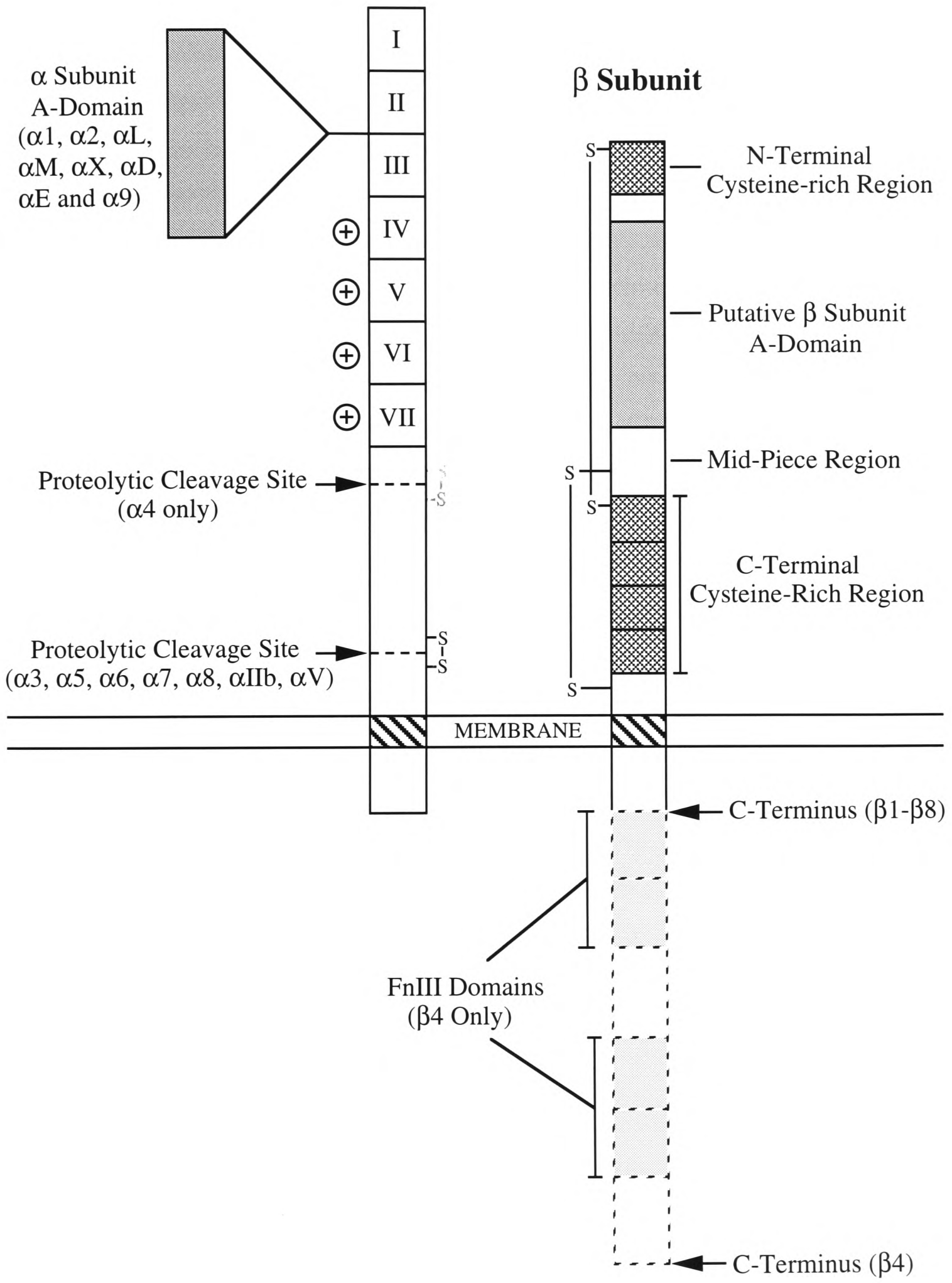
The 16 different integrin α subunits are 25-65% homologous, and vary in size between 100-200 kDa. Their extracellular domains are characterised by the presense of seven N-terminal tandem repeats of approximately 60 amino acids each (repeats I-VII), which share weak sequence homology with one another. Embedded in the last three repeats (V-VII) of all α subunits, and in the last four repeats (IV-VII) of some α subunits, are stretches of oxygen-rich residues which share sequence homology with the calcium binding EF-hand motifs present in calmodulin, troponin C and parvalbumin (Strynadka and James, 1989), and are therefore thought to represent divalent cation binding sites. In some α subunits (α1, α2, αL, αM, αX, αD, αE and α9) there is an additional region of around 200 amino acids between repeats II and III, which is known as the "inserted/interactive" or I-domain. This region is homologous to the family of von Willibrand Factor (vWF) A-type domains

Figure 1.3: A Schematic Representation of Integrin α and β Subunits

Integrin receptors are αβ heterodimers formed by the non-covalent association of a specific integrin α and β subunit. To date, sixteen different integrin α subunits, and eight different integrin β subunits have been identified, which can associate in various combinations to give rise to over 20 different receptors (see Figure 1.2). The basic structural features of integrin α and β subunits are shown opposite. Both are type I transmembrane glycoproteins, with large N-terminal extracellular domains, followed by single pass transmembrane spanning regions and small (with the exception of the β4 subunit) C-terminal intracellular domains.

The α subunits are characterised by the presence of seven N-terminal repeats (I-VII) which are weakly homologous with one another. The last three or four of these repeats contain divalent cation binding sites, and all seven repeats are thought to fold into a cylindrical β-propellor-like ligand binding domain, with the N-terminus of repeat I folded into close proximity with the C-terminus of repeat VII. Some α subunits also contain an additional domain inserted between repeats II and III, which has an A-domain-like structure, and is also capable of binding both ligands and divalent cations. Many of the α subunits are postranslationally cleaved into two chains which are then held together by disulphide bonds, and the approximate position of these proteolytic cleavage sites is shown.

The β subunits are characterised by their high cysteine content of around 7%. Some of these cysteines are located in a small N-terminal cysteine-rich region, but the majority are concentrated within a much larger C-terminal cysteine-rich region, where they represent one in every five residues. The extracellular region of integrin β subunits is thought to fold into two large loops held in position by two long-range disulphide bonds. Within the N-terminal loop is a region which appears to be involved in ligand and divalent cation binding, and may have an A-domain-like structure, similar to the A-domain found in some of the α subunits. The role of the C-terminal loop, containing the C-terminal cysteine-rich region, is unclear, but it has been suggested that it may play a role in regulating the ligand binding activities of the receptor.


α Subunit
α Subunit
A-Domain
(α1, α2, αL,
αM, αX, αD,
αE and α9)
I
II
III
IV
V
VI
VII
Proteolytic Cleavage Site
(α4 only)
Proteolytic Cleavage Site
(α3, α5, α6, α7, α8, αIIb, αV)
S
S
S
S
MEMBRANE
β Subunit
N-Terminal
Cysteine-rich Region
Putative β Subunit
A-Domain
Mid-Piece Region
C-Terminal
Cysteine-Rich Region
C-Terminus (β1-β8)
FnIII Domains
(β4 Only)
C-Terminus (β4)

(Colombatti and Bonaldo, 1991), and hence is also refered to as the α subunit A-domain. This region will be refered to as the A-domain throughout this thesis. Both the A-domains and the seven N-terminal repeats of integrin α subunits have been implicated in divalent cation and ligand binding events. Interestingly, the α subunits which contain an A-domain only have divalent cation binding motifs in repeats V-VII, whereas those lacking an A-domain have divalent cation binding motifs in repeats IV-VII, and also have a membrane proximal proteolytic cleavage site in their extracellular domains. The exception is the α4 subunit, which lacks an A-domain and yet only has divalent cation binding motifs in repeats V-VII, and also contains a unique proteolytic cleavage site which is C-terminal of repeat VII (see Figure 1.3). Subunits with proteolytic sites are posttranslationally cleaved into two chains which are held together by a single disulphide bond. There are between 18-22 cysteine residues in the extracellular portions of integrin α subunits. Most of these cysteines are conserved upon alignment, and unconserved residues tend to fall into one of two different alignment patterns, correlating with the presence/absence of A-domains (Takada and Hemler, 1989). The glycosylation sites in the extracellular region of integrin α subunits also vary, but are notably sparse in the A-domain, indicating that this region may be highly accessible for divalent cation/ligand binding, and may also be capable of conformational changes which could be important in the regulation of these binding events.

The A-domain has been the most extensively studied region of the integrin α subunit, and appears to play a crucial role in the functioning of the A-domain containing integrins. Ligand binding sites have been mapped to the A-domains of the VLA-1 (Kern *et al.*, 1994), VLA-2 (Kamata and Takada, 1994; Tuckwell *et al.*, 1995), LFA-1 (Landis *et al.*, 1994; Randi and Hogg, 1994; Huang and Springer, 1995), Mac-1 (Diamond *et al.*, 1993; Michishita *et al.*, 1993; Ueda *et al.*, 1994; Zhou *et al.*, 1994; Xie *et al.*, 1995; Zhang and Plow, 1996) and p150,95 receptors (Bilsland *et al.*, 1994), and the A-domain also appears to be a target for pathogens, with the echovirus adhering to the A-domain of VLA-2 (King *et al.*, 1995) and the neutrophil inhibitory factor (NIF) protein of canine hookworm to the A-domain of Mac-1 (Muchowski *et al.*, 1994; Rieu *et al.*, 1994). Ligand binding to A-domains is generally divalent cation dependent, and a divalent cation binding site, which was first identified in the A-domain of Mac-1 (Michishita *et al.*, 1993), is present in all integrin A-domains. Comparison of the intron/exon boundaries of integrin α subunits suggests that the A-domain has been inserted into the basic integrin structure as an

evolutionary conserved unit (Landis *et al.*, 1994), and A-domains do appear to be capable of independent functioning, as recombinant A-domains isolated from VLA-2 (Kamata and Takada, 1994; Tuckwell *et al.*, 1995), LFA-1 (Randi and Hogg, 1994) and Mac-1 (Michishita *et al.*, 1993; Rieu *et al.*, 1994; Ueda *et al.*, 1994; Zhou *et al.*, 1994; Xie *et al.*, 1995) have been shown to retain many of the structural and functional binding properties of their intact integrin receptors.

The crystal structures of the A-domains from LFA-1 and Mac-1 have been determined (Lee *et al.*, 1995a, 1995b; Qu and Leahy, 1995). Both domains comprise of alternating α-helices and β-strands which adopt a classic α/β open sheet (or "Rossmann", "dinucleotide-binding" or "doubly wound") fold structure which is also found in nucleotide-binding enzymes, small G proteins and heterotrimeric G-protein α subunits. In the integrin A-domains, five parallel and one short anti-parallel β-strand are arranged to form a central hydrophobic β-sheet which is surrounded on both faces by a total of by seven amphipathic α-helices. The divalent cation binding site is located on the surface of the A-domain, in a crevice at the "top" of the β-sheet. Specific oxygen-rich residues lining this crevice serve to coordinate the bound metal ion, and represent a divalent cation binding motif which is conserved in all integrin A-domains. This motif is composed of a "DxSxS" sequence (single letter amino acid code, where x represents any amino acid), with contributions from a "T" and a "D" residue from discontinuous regions of the sequence. Six coordination sites are required to bind divalent cations. In the crystal structure obtained for the Mac-1 A-domain with Mg^{2+} bound (Lee *et al.*, 1995a), the sixth coordination site was provided by a Glu residue in another A-domain molecule. As all known integrin ligands contain either an Asp or a Glu residue as a key feature of their integrin binding motifs (see Section 1.2.1), it was suggested that the second A-domain molecule was acting as a ligand mimetic, and that the A-domain divalent cation binding motif represents a metal ion dependent adhesion site (or MIDAS motif) for the binding of integrin ligands (Lee *et al.*, 1995a; Bergelson and Hemler, 1995). This is supported by the fact that various point mutations in the MIDAS motif have been shown to abrogate divalent cation and ligand binding (Michishita *et al.*, 1993; Kamata *et al.*, 1994, 1995; Lee *et al.*, 1995a; Tuckwell *et al.*, 1995). Interestingly, when the Mac-1 A-domain was crystallised in the presence of Mn^{2+} rather than Mg^{2+} (Lee *et al.*, 1995b), a slightly different structure for the A-domain was obtained, in which the

MIDAS was disrupted so that direct coordination with ligand was no longer favoured and the sixth metal coordination site was occupied by a water molecule instead of an acidic protein ligand. A similar crystal structure has also been obtained for the LFA-1 A-domain with Mn^{2+} bound at the MIDAS (Qu *et al.*, 1995). As Mn^{2+} is a well known activator of LFA-1 and Mac-1 ligand binding, it has been suggested that divalent cations may also be able to support ligand binding to A-domains indirectly, perhaps by causing a conformational change within the A-domain which activates the ligand binding site. In the Mn^{2+}-bound crystal structure of the LFA-1 A-domain (Qu *et al.*, 1995), a ridge of hydrophobic residues, which were predicted to be buried in the absence of Mn^{2+}, were exposed adjacent to the metal binding site, and it was suggested that these residues might represent a site for the hydrophobic binding of integrin ligands. As ligand bound at this site would be in close proximity to bound divalent cation, direct coordination between ligand and cation might also be possible under certain circumstances. Residues surrounding the MIDAS in LFA-1 have also been shown to determine the specificity of LFA-1 ligand binding (Huang and Springer, 1995), indicating that the MIDAS region in the A-domains of integrin α subunits may well represent the main ligand binding site in the A-domain containing integrins.

The structure of the putative divalent cation binding sites in repeats IV/V-VII of integrin α subunits is unknown. However, as they share sequence homology with EF-hand motifs, it has been suggested that they may adopt a similar structure. EF-hands have a characteristic "helix-loop-helix" structure, in which the oxygen-rich divalent cation binding residues are present in a peptide loop which is flanked on either side by helices (Tufty and Kretsinger, 1975). A modelling study of hybrid integrin-calmodulin EF-hands has demonstrated that the integrin sequences can closely resemble conventional EF-hands, and are also highly likely to bind calcium ions *in vivo* (Tuckwell *et al.*, 1992). Each repeat does appear to be able to bind a single divalent cation, as the αVβ3 receptor, which lacks an A-domain but has 4 divalent cation binding repeats, binds an average of 3-4 divalent cations (Smith and Cheresh, 1991), and a recombinant fragment of the αIIb subunit spanning its 4 divalent cation binding repeats IV-VII binds an average of 4 calcium ions (Gulino *et al.*, 1992). However, there are several significant differences between the divalent cation binding sequences found in integrin α subunits and those found in EF-hand-type proteins. One of

the cation-coordinating oxygen-rich residues in the "loop" region of the EF-hand motif is missing in the integrin divalent cation binding sequences. This has lead to the suggestion that integrin ligands may contribute the extra electron donor required for divalent cation binding (Corbi *et al.*, 1987; Edwards *et al.*, 1988; Tuckwell *et al.*, 1992). There is some evidence that integrin ligands can interact with the divalent cation binding repeats: An 11mer peptide from the fibrinogen γ chain can bind to repeat V of the αIIb subunit (D'Souza *et al.*, 1990, 1991), and conversely a peptide encoding the EF-hand-like motif from repeat V of the αIIb subunit can bind fibrinogen, and can also inhibit the binding of the αIIbβ3 receptor to fibrinogen in a calcium dependent manner (D'Souza *et al.*, 1991). RGD-containing peptides have also been chemically cross-linked to a region spanning repeats II-VI of the αV subunit (Smith and Cheresh, 1990), and a recombinant fragment of the αL subunit spanning repeats V-VI can inhibit LFA-1 binding to ICAM-1 (Stanley *et al.*, 1994). However, direct coordination between bound divalent cations and integrin ligands has never been demonstrated, and although mutations in the EF-hand-like sequences of the α4 subunit have been shown to reduce the ligand binding ability of the α4β1 receptor (Masumoto and Hemler, 1993), the VCAM-1 and fibronectin binding sites of α4β1 have subsequently been mapped to a region of the α4 subunit (residues 108-268) which is N-terminal of the divalent cation binding repeats (Kamata *et al.*, 1995), indicating that divalent cation binding at repeats IV/V-VII may influence ligand binding indirectly by causing a conformational change within the α subunit which alters the activity of a nearby ligand binding site. Another difference between the integrin and EF-hand divalent cation binding sequences is that regions in the integrin sequences which are predicted to be the "helix" parts of the "helix-loop-helix" EF-hand motifs contain residues, such as Pro , which are strong helix breakers. It therefore seems unlikely that these regions would fold into the helix secondary structures required for functional EF-hand sites. It has also been noted that the spacings between the divalent cation binding motifs in integrins (~60 residues) are significantly larger than those found in EF-hand-type proteins (~40 residues) (Weitzman and Law, 1993). Therefore, although it appears that the oxygen rich residues within repeats IV/V-VII of integrin α subunits do represent divalent cation binding sites, it is clear that they fold into a structure distinct from that of EF-hands. Also, although integrin ligands appear to interact with this region, the location of the ligand binding sites and the manner in which ligand interacts with these sites, remains to be determined.

Apart from the crystal structures which have been obtained for the LFA-1 and Mac-1 A-domains, and the EF-hand structures which have been proposed for the divalent cation binding motifs in repeats IV/V-VII, there is very little information available on the higher order structure of integrin α subunits. The complete disulphide bond pattern of the αIIb subunit has been determined (Calvete *et al.*, 1989), and each cysteine residue, starting from the N-terminus, was found to pair with the next available cysteine in the sequence. Although the disulphide bonds in the other integrin α subunits are not known, they can be tentatively predicted from homology to αIIb and from analysis of multiple alignment patterns. From this limited information, integrin α subunits have been envisaged folding into a linear structure containing a series of disulphide bonded loops.

A recent structure prediction for the seven N-terminal repeats of integrin α subunits has however provided significant insight into the structure of integrin α subunits and their divalent cation/ligand binding sites. These seven N-terminal repeats have previously been assumed to fold into seven independent domains which are arranged linearly along the α subunit like beads on a string. It has now been suggested that these repeats are actually folded into a single globular domain, and that this domain has an overall cylindrical structure which is known as a β-propellor (Springer, 1997). In this proposed structure, seven four stranded anti-parallel β-sheets are arranged radially and pseudosymmetrically around a central cylindrical axis. The first strand of each β-sheet lies closest to and parallel with this axis, so that each successive strand is positioned further from the axis and the fourth strand of each β-sheet forms the outer curved surface of the cylinder. As β-sheets have an inherent twist, the angle of the succesive strands in each β-sheet increases with respect to the central axis, giving rise to a propellor pattern in which each sheet represents a single propellor blade. There are no α helices in this structure, as the β-strands in each β-sheet are connected to one another by successive hairpin turns, and the last strand of each β-sheet is connected to the first strand of the next β-sheet by a polypeptide loop. The amino acid sequence threads through the β-propellor in a circular fashion, so that the N- and C-termini are adjacent in the structure. Homologous β-propellors have been identified in the enzymes galactose oxidase and methylamine dehydrogenase, but the most closely related β-propellor appears to be the heterotrimeric G protein β subunit. Integrin ligands and a single Mg^{2+} ion are predicted to bind in the central cavity on the upper face of the β-propellor. This face binds substrates in β-propellor enzymes and is also used by the G protein β

subunit to bind the G protein α subunit. Each of the seven α subunit repeats are thought to contribute to the ligand binding site, explaining the results of other studies, which have mapped ligand binding sites to regions within repeats I-II (Zhang *et al.*, 1997), repeat III (Irie *et al.*, 1995; Schiffer *et al.*, 1995; Kamata *et al.*, 1995, 1996; Zhang *et al.*, 1997), repeat V (D'Souza *et al.*, 1990, 1991), repeats I-V (Loftus *et al.*, 1996), repeats V-VI (Stanley *et al.*, 1994) and repeats II-VI (Smith and Cheresh, 1990) of integrin α subunits. The binding site for the Mg^{2+} ion is predicted to be similar to the MIDAS in integrin A-domains, with one of the coordination sites provided by an acidic residue in the integrin ligand. As one of the metal ion coordination sites in the A-domain MIDAS is missing in the proposed β-propellor MIDAS, it has been suggested that a polypeptide finger from the β subunit may protrude up the central cavity of the β-propellor to provide the missing coordination site required for Mg^{2+} binding. The A-domain, which is structurally homologous to the G protein α subunit, is predicted to be tethered to the top of the β-propellor by a hinge which may permit movement of the domains relative to one another. The putative divalent cation binding sites in repeats IV/V-VII are positioned near one another on the lower face of the β-propellor. In contrast to the EF-hand "helix-loop-helix" structures which have previously been predicted for these sites, the Ca^{2+} ions are predicted to be coordinated by residues from the β-strands in these repeats and their connecting polypeptide loops. As removal of calcium activates ligand binding in many integrins and destablises association with the β subunit in several integrins (Smyth *et al.*, 1993; Diamond and Springer, 1994; Loftus *et al.*, 1994), the lower face of the β-propellor is predicted to be involved in interactions with the β subunit and in conformational changes which may regulate the activity of the ligand binding site on the upper face of the β-propellor. Strong support for a β-propellor domain in integrin α subunits can be provided by secondary structure and threading predictions, as well as by the disulphide bond topology of integrin α subunits (Springer, 1997). It therefore seems highly likely that the seven N-terminal repeats of integrin α subunits do fold into a β-propellor domain, and as the β-propellor is a highly stereotyped protein fold, with all known β-propellors containing four β-strands per β-sheet and having an invariant pattern of threading the amino acid sequence through the structure (Murzin, 1992), the predicted disposition of amino acids within the proposed integrin β-propellor is likely to be highly accurate.

Unlike their extracellular domains, the cytoplasmic domains of integrin α subunits are not strongly related to one another at the sequence level, although each domain is highly conserved across species (Sastry and Horwitz, 1993). The only feature which is conserved in all α subunit cytoplasmic domains is the membrane proximal sequence KxGFFKR (single letter amino acid code, where x represents a non-conserved amino acid), indicating that this region may play a crucial role in the functioning of all integrin receptors (Hynes, 1992; Williams *et al.*, 1994). The "K" residue at the beginning of this conserved sequence is thought to be located at the interface between the transmembrane and cytoplasmic domains, and may act as a weak transmembrane "stop-transfer" sequence (Williams *et al.*, 1994), whereas the membrane-proximal GFFKR motif appears to be involved in maintaining integrin receptors in their default low affinity binding state (see Section 1.2.3.1), as mutations which eliminate this motif have been shown to constitutively activate integrin receptors (O'Toole *et al.*, 1991; 1994). The intracellular calcium binding protein calreticulin appears to bind to the α subunits of integrin receptors via the KxGFFKR motif (Rojiani *et al.*, 1991; Dedhar, 1994). Suppression of calreticulin biosynthesis can inhibit integrin-mediated cell adhesion (Leung-Hagesteijn *et al.*, 1994), and as calreticulin preferentially binds to the activated form of the α2β1 receptor (Coppolino *et al.*, 1995), it has been suggested that calreticulin binding to the GFFKR motif may stabilise integrins in their high affinity ligand binding state. In the α5 subunit, the membrane proximal cytoplasmic region has also been implicated in cytoskeletal organisation and cell motility (Bauer *et al.*, 1993), whereas in the αL subunit, it has been suggested that it might stabilise αLβ2 heterodimer formation (Pardi *et al.*, 1995). However, in contrast to the cytoplasmic tails of integrin β subunits, which are known to interact with several cytoskeletal and signalling proteins (see Section 1.2.2.2), the only intracellular protein which has been found to bind to the cytoplasmic tails of integrin α subunits is calreticulin, indicating that the main function of the α subunit cytoplasmic domains may be to modulate the ligand binding affinities of their integrin receptors.

1.2.2.2 The Structure of Integrin β Subunits

The 8 different integrin β subunits are 37-45% homologous and vary in size between 90-130 kDa. Like the integrin α subunits, they are type I transmembrane glycoproteins, with large N-terminal extracellular domains of about 670 amino acids, followed by single pass

hydrophobic transmembrane segments and short C-terminal cytoplasmic tails of between 40-60 amino acids in length. The exception is the β4 subunit, which has an extended cytoplasmic tail of approximately 1000 amino acids (Suzuki and Naitoh, 1990; Hogervorst *et al.*, 1990). Although the primary sequence of all eight β subunits is known, progress has been relatively slow in determining their higher order structure. Unlike the α subunits, the β subunits are not obviously homologous to any other known proteins at the primary structure level. They also have a very complex secondary disulphide-bonded structure (see below), which has made it difficult to assign functions to specific regions, and has hampered the expression of putative domains and subdomains for structural and functional analysis. However, several structural features have been identified which are characteristic of integrin β subunits, and these are illustrated in Figure1.3.

The most striking feature of the β subunits is their high cysteine content. The extracellular regions of the β1, β2, β3, β5, and β6 subunits all contain 56 cysteine residues, whereas the β4, β7 and β8 subunits contain 48, 54 and 50 cysteines respectively. Upon alignment, these cysteine residues appear to be highly conserved, not only in the 8 different human β subunits, but also in each subunit across species, indicating their importance to the structure and function of the β subunit. The majority of the cysteine residues are concentrated within two different regions of the β subunit: 7 cysteines are located within a small N-terminal cysteine-rich region of approximately 60 amino acids, but most of the cysteines, between 35-39 depending on the subunit, are located within a much larger and more complex C-terminal cysteine-rich region of approximately 200 amino acids (see Figure 1.3). Analysis of the primary amino acid sequences of β subunits suggests that the larger C-terminal cysteine-rich region contains four cysteine-rich repeats, with each of these repeats containing 8 cysteine residues, but the exact boundaries of these repeats, and hence their definition, is unclear (Weitzman and Law, 1993). A complete disulphide bond pattern has been proposed for the extracellular region of the β3 subunit (Calvete *et al.*, 1991). Due to its high cysteine content, many of the disulphide bonds within the C-terminal cysteine-rich region could not be determined by traditional protein chemistry methods, and were instead predicted from steric rather than physical considerations. However, the disulphide bond pairing of the remaining cysteines was unambiguously determined. The majority of these cysteines were found to pair either with the next available cysteine in the sequence or with a cysteine residue proximal in the sequence, but two long range disulphide bonds

were also discovered: Labelling the cysteine residues 1-56 along the mature β3 polypeptide, C1 was found to pair with C16, and C14 with C54. Hence the extracellular region of the β3 subunit is envisaged folding into a secondary structure consisting of two large disulphide bonded loops, with the C1-C16 bond connecting the N-terminus to the beginning of the C-terminal cysteine-rich region, and the C14-C54 bond connecting the regions immediately before and after the C-terminal cysteine-rich region. As the cysteine residues in integrin β subunits are highly conserved, and the C1, C14, C16 and C54 residues are completely conserved, it seems highly likely that all integrin β subunits adopt the same overall disulphide bonded structure, and that the long range C1-C16 and C14-C54 disulphide bonds are intrinsic to this structure. Although it has been suggested that the C-terminal cysteine-rich repeats may represent a regulatory domain (Shih *et al.*, 1993), the function of both the N- and C-terminal cysteine-rich regions is unknown.

Between the N- and C-terminal cysteine rich regions of integrin β subunits is a highly conserved region of approximately 200 amino acids which appears to be involved in both ligand and divalent cation binding. RGD-containing peptides have been chemically crosslinked to this region in the β3 subunit (D'Souza *et al.*, 1988; Smith and Cheresh, 1988), and a peptide from this region in β3 can inhibit the binding of fibrinogen to the αIIbβ3 receptor (Charo *et al.*, 1991). Various point mutations within this conserved region have also been shown to inhibit ligand binding to the β1 (Takada *et al.*, 1992), β2 (Bajt *et al.*, 1995; Zhang and Plow, 1996), β3 (Loftus *et al.*, 1990; Bajt *et al.*, 1992a; Bajt and Loftus, 1994; Tozer *et al.*, 1996) and β6 integrins (Huang *et al.*, 1994), and have demonstrated that a highly conserved DxSxS motif (single amino acid code, where x represents a non-conserved amino acid) within this region is crucial for ligand binding. The DxSxS motif also appears to be involved in binding divalent cations, as a peptide derived from the β3 subunit spanning its DxSxS motif can directly bind both RGD-containing peptides and the Ca^{2+} analogue Tb^{3+} (terbium), and mutation of the conserved "D" residue within the DxSxS motif dramatically reduces the formation of peptide-Tb^{3+} complexes (D'Souza *et al.*, 1994). The DxSxS motif occurs in a region of integrin β subunits which is rich in oxygenated residues. As the linear spacing of these residues approximates that of oxygenated residues in the calcium binding loop of EF-hand-type proteins (Kretsinger, 1980), it has been suggested that they may represent an EF-hand

divalent cation-binding motif (Loftus *et al.*, 1990). However, while mutations of the DxSxS sequence have been found to abolish ligand binding in several integrin β subunits (Loftus *et al.*, 1990; Takada *et al.*, 1992; Bajt and Loftus, 1994; Huang *et al.*, 1994; Bajt *et al.*, 1995; Zhang and Plow, 1996), mutations of aspartate residues immediately downstream, which would form part of the putative EF-hand, have no effect on ligand binding (Bajt and Loftus, 1994). A similar highly conserved DxSxS motif is also present in the A-domains of integrin α subunits, where it forms part of a MIDAS motif within an A-domain-like structure (see Section 1.2.2.1). Although the conserved 200 amino acid ligand binding region in integrin β subunits is not obviously homologous to the α subunit A-domain at the primary amino acid level, hydropathy plots comparing these two regions are strikingly similar, indicating that they could in fact share the same overall structure (Lee *et al.*, 1995). Two separate modelling studies have indeed predicted that the conserved ligand binding region in integrin β subunits does fold into an A-type domain (Tozer *et al.*, 1996; Tuckwell and Humphries, 1997), and as residues downstream of the DxSxS motif, which could form part of a non-contiguous MIDAS, have been shown to be essential for ligand binding (Tozer *et al.*, 1996), it appears that the A-domains in integrin α and β subunits may utilise a similar mechanism for the binding of divalent cations and ligands.

The cytoplasmic domains of the β subunits, unlike those of the α subunits, are homologous to one another at the primary amino acid level, suggesting that they may perform a similar function in all integrin receptors. The noteable exceptions are the β4 and β8 subunits, whose cytoplasmic regions bear little homology with those of the other subunits. The β4 cytoplasmic domain is in fact over 20 times the length of the other β cytoplasmic domains, and contains regions which are homologous to fibronectin type III repeats (Quaranta, 1990). The differences between the cytoplasmic domains of the β4 and β8 subunits and those of the other β subunits may reflect the fact that they have evolved to perform unique functions. For instance, the extended cytoplasmic tail of the β4 subunit may be essential for the formation of hemidesmosomes by the α6β4 receptor (Quaranta and Jones, 1991). The cytoplasmic domains of the other integrin β subunits are characterised by the presence of several sequence motifs which are conserved to varying degrees in each subunit. Immediately downstream of a highly conserved "K" residue, which is thought to reside at the boundary between the transmembrane and cytoplasmic domains, is the conserved "LLvxihDRrE" sequence motif (single letter amino acid code, where upper case

corresponds to invariant or near invariant residues, lower case to partially conserved residues, and x to a completely unconserved residue). This membrane proximal sequence appears to behave in a similar fashion to the membrane proximal "GFKKR" motif in the α cytoplasmic domains (see Section 1.2.2.1), as deletions in this region have been shown to constitutively activate integrin receptors (Crowe *et al.*, 1994; Hughes *et al.*, 1995). It has been suggested that the "D" residue within the β subunit "LLvxihDRrE" motif may form a salt bridge with the "R" residue in the α subunit "GFFKR" motif, and that this bridge may serve to constrain integrins in their default low affinity binding state (Hughes *et al.*, 1996). Intracellular proteins which bind to this membrane proximal "hinge" region may therefore be involved in regulating the ligand binding affinity of integrin receptors. Calreticulin can bind to the GFFKR motif in integrin α subunits (see Section 1.2.2.1), whereas the focal adhesion kinase $pp125^{FAK}$ and paxillin can bind to β1 peptides containing the LLvxihDRrE motif (Otey *et al.*, 1994; Schaller *et al.*, 1995) and filamin can also bind to this motif in the β2 subunit (Sharma *et al.*, 1995). Whether these proteins can actually regulate integrin affinity remains to be determined. Downstream of the conserved "LLvxihDRrE" motif are two conserved NPxY/F motifs (single letter amino acid code, where x is any amino acid). The NPxY/F motif is required for internalisation of the low density lipoprotein (LDL) receptor via clathrin coated pits (Chen *et al.*, 1990), and mutation of the first NPxF motif in the β2 cytoplasmic domain has been shown to dramatically reduce coated pit internalisation of the αMβ2 receptor (Rabb *et al.*, 1993). The NPxY/F motifs may also be involved in regulating integrin affinity, as mutations within the first NPxY motifs of the β1 and β3 cytoplasmic domains can alter the affinity status of chimeric integrin receptors (O'Toole *et al.*, 1995). Another motif which is reasonably conserved in the cytoplasmic domains of integrin β subunits is the "TTT" motif, which is located between the two NPxY/F motifs. This motif appears to be important for integrin/cytoskeletal interactions. Mutation of the "TST" motif in the β3 subunit impairs interaction of αIIbβ3 with the cytoskeleton (Chen *et al.*, 1994; Ylanne *et al.*, 1995), and the "TTT" motif in the β2 subunit appears to be required for LFA-1 mediated cell adhesion, spreading and focal contact formation (Hibbs *et al.*, 1991; Peter and O'Toole, 1995). In contrast to the cytoplasmic domains of the α subunits, which are only known to interact with calreticulin, the β subunit cytoplasmic domains have been found to interact with several intracellular cytoskeletal and signalling proteins. The β1 cytoplasmic domain can interact with talin (Horwitz *et al.*, 1986), α-actinin (Otey *et al.*, 1990), integrin-linked kinase (ILK) (Hannigann *et al.*, 1996),

pp125^{FAK} and paxillin (Otey *et al.*, 1994; Schaller *et al.*, 1995), whereas the β2 cytoplasmic domain can interact with filamin (Sharma *et al.*, 1995) and cytohesin-1 (Kolanus *et al.*, 1996), and the β3 cytoplasmic domain can interact with β3-endonexin (Shattil, S.J. *et al.*, 1995). Although integrin receptors usually only interact with the intracellular cytoskeletal/signalling network after they have bound ligand, isolated β cytoplasmic domains can readily associate with focal adhesions (LaFlamme *et al.*, 1992) and can also initiate phosphorylation of pp125^{FAK} (Lukashev *et al.*, 1994, Akiyama *et al.*, 1994). Deletion of the α cytoplasmic domains from intact integrins also appears to promote both these processes (Ylanne *et al.*, 1993; Briesewitz *et al.*, 1993). Therefore, although the α cytoplasmic domain may not interact directly with the cytoskeleton/signalling network, it appears to play an important role in negatively regulating the intracellular interactions of the β subunit.

1.2.2.3 The Structure of Integrin αβ Heterodimers

The higher order structure of two integrins, αIIbβ3 (Carrell *et al.*, 1985; Weisel *et al.*, 1992) and α5β1 (Nermut *et al.*, 1988), has been studied by electron microscopy. Both receptors were found to comprise of a large globular "head" of approximately 10 nm in diameter followed by two "tails" which were extended into the membrane in a "two pronged plug" fashion. Hence the extracellular regions of integrin α and the β subunits are envisaged associating at their N-termini to form a ligand binding globular head (Weisel *et al.*, 1992), and this region is thought to extend from the surface of the cell on two extracellular "stalks" whose C-termini are inserted separately into the plasma membrane (see Figure 1.1). In this proposed structure, the globular ligand binding region would presumably be formed from the β-propellor domain in the α subunit and the putative A-domain in the β subunit. The A-domain which is present in almost half of integrin α subunits, is thought to be attached to the surface of this globular "head" by a flexible hinge (Springer, 1997). Hence, all the regions in integrin α and β subunits which have been implicated in ligand and divalent cation binding (see Sections 1.2.2.1 and 1.2.2.2) would be concentrated within this N-terminal globular "head", and the "stalks" anchoring this region to the cell membrane would be formed from the C-terminal extracellular region of the α subunit and the C-terminal cysteine-rich region of the β subunit. The expression of soluble forms of the α1β1 (Briesewitz *et al.*, 1993), αMβ2 (Dana *et al.*, 1991; Berman *et*

al., 1993) and αIIbβ3 receptors (Bennett *et al.*, 1993; Gulino *et al.*, 1995) have demonstrated that the transmembrane and cytoplasmic domains of these α and β subunits are not required for the formation of these particular αβ heterodimeric complexes. Two truncated αIIbβ3 receptors have also been expressed, one comprising of the entire extracellular region of αIIb associated with only the N-terminal cysteine-rich region and A-domain of β3 (Wippler *et al.*, 1994), and another of only the first three N-terminal repeats of αIIb (repeats I-III) and the putative A-domain of β3 (McKay *et al.*, 1996). It therefore appears that only the very N-terminal regions of the αIIb and β3 subunits are required for αIIbβ3 heterodimer formation. Whether these regions form the heterodimeric interface in all integrin receptors is not known, but as all integrin α subunits have a very similar overall structure, as do all integrin β subunits, it has been generally assumed that all integrin αβ heterodimeric complexes must also share a very similar overall consensus structure.

1.2.3 REGULATION OF INTEGRIN MEDIATED CELL ADHESION

Cell adhesion mediated by integrins can be regulated by altering the affinity and/or the avidity of integrin receptors for their ligands (Stewart and Hogg, 1996). Changes in avidity can be achieved by altering the number of integrin receptors on the cell surface (up/down regulation), the distribution of receptors on the cell surface (clustering), or even the shape of the cell (cell spreading), whereas alterations in individual integrin receptors can lead to enhanced affinity for ligand (termed "inside to out signalling"). Cells often use a combination of these processes to alter their adhesive properties, but affinity modulation of integrins appears to be particularly important, as it enables cells to respond very rapidly to their surrounding environment.

1.2.3.1 Affinity Modulation of Integrins ("Inside-Out" Signalling)

Cells can convert between adhesive and non-adhesive states by modifying the ligand binding affinities of their integrin receptors (Hynes, 1992; Diamond and Springer, 1994; Faull and Ginsberg, 1995; Schwartz *et al.*, 1995; Stuiver and O'Toole, 1995). On resting cells, integrins are expressed on the cell surface in a low affinity state, and require activation from an intracellular source in order to bind ligand. The activation signal is transmitted from the cytoplasmic domains of the integrin receptors through to their extracellular ligand binding sites, and hence is often refered to as "inside-out" signalling.

Affinity modulation of integrins is indispensible to a variety of biological processes, including platelet aggregation and leukocyte extravasation (see Section 1.2.5.2), where a rapid switch between a non-adhesive and a fully adhesive state is required.

A variety of soluble agonists can stimulate cells to increase the ligand binding affinities of their integrin receptors. Thrombin and adenine nucleotides, for example, can activate αIIbβ3-mediated platelet aggregation (Smyth *et al.*, 1993), whereas chemoattractants and inflammatory mediators can activate αMβ2 on the surface of neutrophils (Law and Weitzman, 1993). The cross-linking of receptors on the surface of T Cells has also been demonstrated to activate the binding of αLβ2 to ICAM-1 (Dustin and Springer, 1989; van Kooyk *et al.*, 1989). Although the intracellular pathways which result in integrin activation are poorly understood, they appear to involve the engagement of "classic" signal transduction systems. The binding of agonists to their cell surface receptors often results in activation of G-proteins and tyrosine kinases, which in turn leads to the activation of phospholipase C, changes in cytosolic calcium, and activation of intracellular protein kinases, including protein kinase C (PKC) (Schwartz *et al.*, 1995). The cytoplasmic domains of several integrin subunits become phosphorylated upon PKC activation (Chatila *et al.*, 1989; Shaw *et al.*, 1990; Pardi *et al.*, 1992), but the functional significance of this is unclear. Agonist-induced integrin activation is not always accompanied by receptor phosphorylation (Merrill *et al.*, 1990; Buyon *et al.*, 1990), and mutation of the phosphorylation sites in integrin receptors does not seem to affect their inside-out signalling abilities (Hibbs *et al.*, 1991; Hogervorst *et al.*, 1993; Shaw and Mercurio, 1993).

The activity of integrin receptors appears to be a reflection on the cellular background in which they are expressed. The α2β1 receptor, for example, binds to both laminin and collagen when expressed on endothelial cells, but only binds to collagen when expressed on leukocytes (Kirchhofer *et al.*, 1990), indicating that cell-type specific factors can influence its ligand binding specificity. Integrin affinity also appears to be affected by the cellular background. For example, when expressed in K562 cells, the α5β1 receptor has a low affinity for fibronectin, but when expressed in CHO cells it becomes activated and binds fibronectin with high affinity. O'Toole *et al.* (1994) showed that the cell-type specific signals which modulate integrin affinity are transmitted through the α cytoplasmic domains of integrin receptors: Chimeras composed of the cytoplasmic domains of α5β1 fused to the

extracellular and transmembrane domains of αIIbβ3 exibited the same pattern of affinity modulation in K562 and CHO cells as the wildtype α5β1 receptor, even though they bound the αIIbβ3 ligand fibrinogen. In addition, coexpression of the chimeric αIIb/α5 subunit with the wildtype β3 subunit in CHO cells retained the high α5β1-like binding affinity for fibrinogen, whereas coexpression of the chimeric β3/β1 subunit with the wildtype αIIb subunit reverted the receptors back to their normal αIIbβ3-like low affinity. Interestingly, cotransfection of CHO cells with the chimeric αIIb/α5 subunit and a truncated β3 subunit lacking its entire intracellular domain abolished high affinity binding, indicating that although the cytoplamic tails of the α subunits appear to determine the cell-specific affinity state of an integrin, the cytoplasmic tails of the β subunits are also required for inside-out signalling. The high affinity chimeras were also dependent on cellular metabolism, indicating that inside-out signalling is an active process, requiring energy as well as the correct cell-specific intracellular machinery.

The putative transmembrane-cytoplasmic interface in integrin α and β subunits is at a conserved lysine residue. In both subunits, this lysine is immediately followed by a short (four to six residue) apolar segment and a charged region (Williams *et al.*, 1994). The corresponding conserved sequences for the α and β subunits are "xGFFKR" and "LLvxihDRrE" (single letter amino acid code, with partially conserved amino acids in the lower case, and unconserved amino acids represented by an "x"). Apart from this highly conserved membrane-proximal region, there are no other conserved motifs in the α cytoplasmic domains, although the middle and distal regions of the β cytoplasmic domains also contain two conserved "NPXY/F" motifs and a "TTT" motif (see Section 1.2.2.2). Partial truncations of β cytoplasmic domains which only remove their distal and mid-regions prevent integrin activation (Hibbs *et al.*, 1991b; Crowe *et al.*, 1994; O'Toole *et al.*, 1994; Hughes *et al.*, 1995), whereas complete truncation of the entire β cytoplasmic domain constitutively activates integrin receptors (Rabb *et al.*, 1993; Crowe *et al.*, 1994; Hughes *et al.*, 1995), as does complete truncation of the α cytoplasmic domain (O'Toole *et al.*, 1991; Rabb *et al.*, 1993). It has therefore been suggested that the distal region of the β cytoplasmic domain may play a positive regulatory role in inside-out signalling (Crowe *et al.*, 1994), whereas the membrane proximal regions in both the α and β cytoplasmic domains have a negative regulatory function, and are required to constrain integrin receptors in their default low affinity state (O'Toole *et al.*, 1994; Hughes *et al.*, 1995). The

cytoplasmic tails of the αIIbβ3 receptor appear to interact in synthetic neo-protein mimics of the integrin cytoplasmic face (Muir *et al.*, 1994), and studies involving mutation of the conserved "R" residue within the membrane proximal "GFFKR" motif of the αIIb subunit (R995D) and the conserved "D" residue within the "LLvxihDRrE" motif of the β3 subunit (D723R) suggest that R995 of αIIb and D723 of β3 may be connected by a salt bridge (Hughes *et al.*, 1996): The αIIb(R995D) and β3(D723R) mutants, when combined with their respective wildtype counter-subunits, formed αIIbβ3 variants which were constitutively active, but the double "charge-reversal" mutant αIIb(R995D)β3(D723R) was not. It was therefore suggested that a salt bridge between the membrane proximal cytoplasmic regions of αIIb and β3 is required to constrain the αIIbβ3 receptor in its inactive state, and that disruption of this salt bridge releases the receptor into its high affinity ligand binding state. As the membrane proximal cytoplasmic regions in integrin α and β subunits are highly conserved, a similar regulatory mechanism may operate in all integrin receptors. Several intracellular proteins, including calreticulin, focal adhesion kinase $pp125^{FAK}$, paxillin and filamin (Rojiani *et al.*, 1991; Dedhar, 1994; Otey *et al.*, 1994; Schaller *et al.*, 1995; Sharma *et al.*, 1995), can interact with the membrane proximal cytoplasmic "hinge" region in integrin receptors, and may therefore be involved in regulating the ligand binding affinity of integrins.

Exactly how the activating signal is transmitted from the cytoplasmic domains of integrin receptors through to their extracellular ligand binding sites is unknown, but is thought to involve some kind of a long range conformational change (Du *et al.*, 1993; Hughes *et al.*, 1996). Changes in the spatial relationship between the cytoplasmic tails of the α and β subunits is thought to initiate this conformational change, which then proceeds through the transmembrane helices to the N-terminal extracellular ligand binding site. Studies based primarily on the use of mAbs suggest that integrin receptors can alternate between different conformational states which reflect their functional activity. At least three different conformational states have been defined: an inactive state (which is unable to bind ligand), an active state (which is capable of binding ligand), and a ligand-occupied state (which has bound ligand). The active state can be induced physiologically by cell agonists, but can also be induced *in vitro* by manipulating the extracellular concentration of divalent cations (Altieri, 1991; Gailit and Ruoslhati, 1988; Dransfield *et al.*, 1992), or by using activating mAbs which bind to inactive receptors and switch them to their active form. The mAb

MEM83, which binds to the A-domain of the αL subunit and directly induces the binding of LFA-1 to ICAM-1 (Landis *et al.*, 1993), is an example of an activating mAb. Although it is unclear exactly how such mAbs activate integrin receptors, it has been suggested that they may bind preferentially to the active conformation and may therefore tip the equilibrium between the inactive-active conformations in favour of the activated state (Diamond and Springer, 1994). Evidence for a conformational change between inactive and active integrins is also provided by another class of mAbs which recognise epitopes that are only expressed on activated integrin receptors. As the binding of these mAbs can be used as an indicator of the activated state, they are often refered to as activation reporters. The PAC-1 mAb, which recognises a neo-epitope only expressed on the activated form of the αIIbβ3 receptor, is an example of an activation reporter (Shattil *et al.*, 1985). Numerous activating mAbs and activation reporters have been described, and the epitopes which they recognise have been mapped to diverse regions of integrin α and β subunits, indicating that a very widespread conformational change occurs upon integrin activation. A conformational change also appears to occur after ligand binding, as a third class of mAbs have been described which bind preferentially to the ligand-occupied form of integrin receptors. The epitopes which these mAbs recognise are known as ligand induced binding sites (or LIBS epitopes), and if they are also cation sensitive, as cation and ligand influenced binding sites (or CLIBS epitopes). Certain mAbs, by binding to a particular LIBS, can in turn increase the affinity of an integrin receptor for its ligand. The anti-LIBS1 and anti-LIBS2 mAbs can, for example, induce the binding of fibrinogen to platelets (Frelinger *et al.*, 1991; Du *et al.*, 1993). Studies using activating, activation reporter and anti-LIBS/CLIBS mAbs have therefore demonstrated that integrin receptors can cycle through multiple activation states on the cell surface, and that conversion between these different activation states is accompanied by widespread conformational changes in integrin receptors. Inside-out signalling appears to be mediated by the transmission of a long range conformational change from the cytoplasmic tails of an integrin receptor, through its transmembrane domains and C-terminal extracellular "stalk" regions, to its N-terminal globular "head" region, where it results in an increase in the affinity of an integrin receptor for its ligand. Conversely, the propogation of conformational changes in the opposite direction, from the extracellular ligand binding site through to the intracellular cytoplasmic tails, may be involved in mediating outside-in signalling by integrins (see Section 1.2.4).

1.2.3.2 Avidity Modulation of Integrins

In the absence of high affinity integrin receptors, efficient cell adhesion can still occur via the coordinated effort of a large number of low affinity receptors. The translocation of additional integrin receptors to the cell surface (up-regulation), or the redistribution of receptors already present on the surface (clustering), can increase the overall binding strength of a cell for a particular ligand. In addition, cells can undergo morphological changes (such as cell spreading) which can increase the avidity of their adhesive interactions.

1.2.3.2.1 Upregulation of Integrin Receptors

A number of integrins, including the α5β1, α6β1, αMβ2, αXβ2 and αIIbβ3 receptors, can be stored within the cell in intracellular pools which can be rapidly translocated to the cell surface in response to a variety of activating stimuli (Berger *et al.*, 1984; Wencel-Drake *et al.*, 1986; Miller *et al.*, 1987; Yoon *et al.*, 1987). By up-regulating the translocation of specific pools of integrin receptors to the cell surface, a cell can rapidly increase its avidity for a particular array of ligands. In addition, a specific receptor may be stored in different types of subcellular organelles which differ in their mode of mobilisation, and may be used in response to different stimuli. The up-regulation of Mac-1 on the surface of neutrophils is a typical example. In unstimulated neutrophils, only about 5% of the Mac-1 population is actually expressed on the cell surface, and the remaining population is stored intracellularly within granules (75%) and secretory vesicles (20%) (Sengelov *et al.*, 1993). Stimulation with inflammatory mediators, such as f-Met-Leu-Phe (fMLP), leads to selective mobilisation of secretory vesicles to the cell surface, whereas stimulation with PMA results in the translocation of both secretory vesicles and granules. It has therefore been suggested that for inflammatory processes, such as chemotaxis and diapedesis, where a very rapid response is required, Mac-1 is up-regulated from secretory vesicles, whereas for other functions, such as adherence to iC3b-opsonised particles, it is stored in granules which are mobilised during the process of phagocytosis (Sengelov *et al.*, 1993).

1.2.3.2.2 Clustering

An increase in avidity for ligand can also be achieved by organising the integrin receptors already present on the cell surface into clusters or focal adhesions. Even if low affinity

receptors are clustered, the multiple receptor-ligand interactions occuring at these sites can result in stable cell adhesion. Probably the best known example of integrin clustering is the formation of focal adhesion complexes by the β1 integrins (Burridge *et al.*, 1988). Increased cell adhesion through receptor clustering has also been reported for the β2 integrins. Stimulation with phorbol esters can cause cytoskeletal-dependent capping of LFA-1 on lymphocytes (Haverstick *et al.*, 1992) and aggregation of Mac-1 on neutrophils (Detmers *et al.*, 1987), both of which enhance their integrin-mediated adhesion. Calcium appears to be instrumental for the clustering of LFA-1 on T-cells (van Kooyk *et al.*, 1994), and it has been suggested that Ca^{2+} may regulate LFA-1 mediated adhesion through avidity changes, whereas Mg^{2+} plays an important role in the affinity modulation of this integrin.

1.2.3.2.3 Cell Spreading

Cells often spread over an apposing surface in an attempt to increase the avidity of their integrin-ligand interactions. One of the most extensively studied examples of cell spreading is the transmigration of leukocytes through the endothelium to sites of inflammation. Once leukocytes have attached to the vessel wall, they flatten against the endothelial cells, and hence streamline themselves from the shear stress imposed on them by the vascular flow (Springer, 1994; 1995). Cell spreading also forces a larger area of the cell into closer apposition with ligand, and may provide an opportunity for integrin receptors to bind to ligands via a zipper-like mechanism (Singer, 1992). The increase in cell adhesion mediated by cell spreading appears to be mainly due to changes in the avidity of integrins for their ligands. The spreading of T cells onto fibronectin through α5β1 (Faull *et al.*, 1994), and onto ICAM-1 through LFA-1 (Stewart *et al.*, 1996), occurs without an increase in the affinity of these receptors for their ligands, but is dependent on cytoskeletal alterations. Mutational analysis has indicated that specific motifs in the cytoplasmic domains of integrin β subunits are responsible for the cytoskeletal alterations which allow cell spreading to take place. The conserved "TTT" motif in the β cytoplasmic tail appears to be particularly important (see Section 1.2.2.2). Cell adhesion, spreading and focal contact formation have been found to be dependent on the "TTT" motif in the β2 subunit (Peter and O'Toole, 1995), and this motif also appears to play a role in cell spreading and cytoskeletal interactions mediated by the β3 subunit (Ylanne *et al.*, 1995).

1.2.4 SIGNAL TRANSDUCTION BY INTEGRINS ("OUTSIDE-IN" SIGNALLING)

Integrin receptors are also capable of transmitting signals from the exterior into the interior of cells. Such "outside-in" signalling informs cells of their surrounding environment, and enables them to mount appropriate responses, which can involve changes in morphology, migration, phagocytosis, proliferation and gene expression. Integrin-dependent signal transduction is a highly complex event, involving a wide variety of different signal transduction pathways, which can interact with one another, and can also crosstalk or synergise with the signalling pathways initiated by other cell surface receptors. To add to this complexity, different integrin receptors can induce different signalling pathways, and a given integrin receptor can induce different pathways in different cell types. At present, there is no comprehensive model for integrin mediated signal transduction, although several general themes have been identified (Juliano and Haskill, 1993; Sastry and Horwitz, 1993; Schwartz *et al.*, 1995; Lafrenie and Yamada, 1996): The short cytoplasmic tails of integrin receptors do not contain any obvious catalytic domains, such as kinase or phosphatase domains, indicating that integrins must mediate their signal transduction events indirectly, through associations with intracellular signalling molecules. Several cytoskeletal and signalling proteins become associated with the cytoplasmic tails of integrin receptors after ligand occupation and receptor clustering. These proteins form signalling complexes, which can transmit signals from the cytoplasmic tails of integrin receptors into the interior of the cell. The activation of an intracellular protein tyrosine kinase, termed focal adhesion kinase, or $pp125^{FAK}$, often plays a central role in the formation of these signalling complexes (Schaller and Parsons, 1993; Richardson and Parsons, 1995; Llic *et al.*, 1997). FAK can associate with the membrane proximal cytoplasmic region of integrin β subunits (Otey *et al.*, 1994; Schaller *et al.*, 1995) and can phosphorylate both itself and another intracellular protein, paxillin. These tyrosine phosphorylated proteins may serve as a scaffold to recruit other signalling molecules, such as the Src-family of kinases, via SH2/SH3 domain interactions. Both tyrosine kinases and G-protein signalling molecules become associated with integrin-signalling complexes, resulting in the activation of other protein kinases, such as PKC and MAP kinases, as well as changes in phospholipid metabolism, and changes in the intracellular Ca^{2+} levels and pH. Together with the various

cytoskeletal proteins, which interact either directly or indirectly with the cytoplasmic tails of integrin receptors, these intracellular signals appear to be able to regulate diverse cell functions, such as cell growth and differentiation, and can also control gene expression, presumably by activating transcription factors which then promote the transcription of specific genes.

1.2.5 THE LEUKOCYTE INTEGRINS

The β2 subfamily of integrin receptors are exclusively expressed on white blood cells, and are therefore also refered to as the leukocyte integrins. They comprise of the LFA-1 (αLβ2, CD11a/CD18), Mac-1 (αMβ2, CD11b/CD18) and p150,95 (αXβ2, CD11c/CD18) receptors (Hogg, 1989; Kishimoto *et al.*, 1989; Arnaout, 1990a; Larson and Springer, 1990) and the more recently identified αDβ2 (CD11d/CD18) receptor (Danilenko *et al.*, 1995; Van der Vieren, 1995). Each of these receptors consists of a unique integrin α subunit, either the αL (CD11a), αM (CD11b), αX (CD11c) or αD (CD11d) subunit, non-covalently associated with the common β2 subunit (CD18) (see Table 1.1). The four leukocyte integrin α subunits (CD11) are only known to associate with the β2 subunit, and conversely, the β2 subunit only appears to associate with these four α subunits. The β2 gene has been localised to chromosome 21 (at 21q22.3), whereas the α subunit genes (with the possible exception of the αD gene, whose location has not yet been determined) have all been localised to a cluster on chromosome 16 (at 16p11.1-p13), and may therefore have arisen by gene duplication (Marlin *et al.*, 1986; Corbi *et al.*, 1988; Solomon *et al.*, 1988). The four leukocyte integrin α subunits are all closely related, but the αM, αX and αD subunits are more homologous to each other (αM-αX, 61%; αM-αD, 60%; αX-αD, 66%) than they are to the αL subunit (αL-αM, 35.7%; αL-αX, 37.4%; αL-αD, 36%), indicating that gene duplication initally gave rise to the αL gene and an αM/αX/αD primordal gene, and that this primordal gene was then further duplicated to produce the αM, αX and αD genes. The LFA-1 receptor is expressed on virtually all mature leukocytes, whereas the Mac-1 and p150,95 receptors are primarily expressed on cells of the myelo-monocytic lineage, and expression of the αDβ2 receptor appears to be mainly restricted to tissue macrophages (see Table 1.1). The leukocyte integrins play a prominent role in mediating the adhesion-dependent leukocyte functions of the immune system (Springer, 1990), and their importance is highlighted by the genetic disorder leukocyte adhesion deficiency I

Table 1.1: The Leukocyte Integrins

Integrin	Other Names	Molecular Mass (kDa)	Ligands	Tissue Distribution	Functions
αLβ2	CD11a/CD18 LFA-1	175/95	ICAM-1 ICAM-2 ICAM-3 ICAM-4 TLN	All mature leukocytes	Interactions between T cells and B cells, T cells and targets, leukocyte-endothelial interaction and leukocyte migration
αMβ2	CD11b/CD18 Mac-1 CR3	165/95	ICAM-1 ICAM-2 ICAM-4 iC3b, FB FX, LPS LPG, and others	Monocytes, macrophages neutrophils, NK cells, $CD8^+$ T cells, and some cytotoxic T cells	Promotion of phagocytic activity via iC3b, neutrophil and monocyte aggregation, leukocyte-endothelial interaction, leukocyte migration and chemotaxis
αXβ2	CD11c/CD18 p150,95 CR4	150/95	ICAM-1 (?) iC3b, FB, LPS, LPG and others	Monocytes, macrophages, neutrophils, eosinophils, NK cells, activated B cells, and some cytotoxic T cells	Leukocyte-endothelial interaction, iC3b affinity and adhesive function
αDβ2	CD11d/CD18	155/95	ICAM-3	Macrophages, $CD8^+$ T cells	?

(LAD-I) (see Section 1.2.5.3), where defects in the gene encoding the common β2 subunit result in impaired leukocyte adhesion, and recurrent, often lethal, bacterial infections (Anderson and Springer, 1987; Arnaout, 1990b).

1.2.5.1 Counter-Receptors and Functions of the Leukocyte Integrins

1.2.5.1.1 LFA-1

LFA-1 is expressed on virtually all leukocytes, and mediates a wide range of adhesion-dependent immune functions (see Table 1.1). The receptor was first identified by screening for mAbs which block cytotoxic T cell (CTL)-mediated killing (Davignon *et al.*, 1981), and mAbs directed against LFA-1 have subsequently been shown to inhibit virtually every immune function involving T cell-mediated adhesion, including CTL-mediated killing, antigen-specific T-cell proliferation and T cell dependent antibody responses. Several other immune functions that involve cell-cell adhesion are also inhibited by anti-LFA-1 mAbs, including the extravasation of leukocytes to sites of inflammation, leukocyte trafficking, natural killer (NK) cell activity, and monocyte and B-cell homotypic adhesion (Larson and Springer, 1990). Apart from these functions, which have been studied extensively, LFA-1 may also be involved in mediating cellular interactions between the immune system and the central nervous system (CNS), and in regulating the turnover of red blood cells (see below).

All the known ligands of LFA-1 are members of the immunoglobulin superfamily (IgSF) of adhesion molecules (see Section 1.1.3), and are single chain transmembrane glycoproteins, whose extracellular N-terminal regions contain variable numbers of tandom, repeating immunoglobulin like domains (Ig domains). Five different LFA-1 ligands have been identified: The intercellular adhesion molecules ICAM-1 (Marlin and Springer, 1987), ICAM-2 (Staunton *et al.*, 1989), ICAM-3 (de Fougerolles and Springer, 1992; Fawcett *et al.*, 1992; de Fougerolles *et al.*, 1993) and ICAM-4 (Bailly *et al.*, 1995), and the recently identified IgSF member telencephalin (TLN) (Tian *et al.*, 1997). ICAM-1 (CD54) contains five Ig domains, and is found in relatively low amounts on resting leukocytes and on endothelial cells, but is rapidly up-regulated in response to inflammatory mediators such as IL-1, interferon (IFN)-γ and tumour necrosis factor (TNF)-α (Pober *et al.*, 1986; Springer, 1990). In contrast, ICAM-2 (CD102) has only two Ig domains, and is constitutively expressed on leukocytes and endothelial cells (Staunton *et al.*, 1989; de Fougerolles *et al.*,

1991; Nortamo *et al.*, 1991). ICAM-1 appears to be the major ligand for LFA-1 during inflammatory and immune responses, whereas ICAM-2 may play a role in the trafficking of resting leukocytes through tissue endothelium. ICAM-3 (CD50) has five Ig domains and is absent on endothelial cells, but is present on resting lymphocytes, monocytes and neutrophils, and can be up-regulated upon activation, although not to the same extent as ICAM-1 (de Fougerolles and Springer, 1992). ICAM-3 appears to be involved in facilitating the interaction of T cells with antigen presenting B cells, and there is also some evidence that it may regulate the LFA-1/ICAM-1 adhesion pathway (Campanero *et al.*, 1993). The fourth LFA-1 ligand ICAM-4 has only two Ig domains, and is expressed on red blood cells. The function of ICAM-4 is unknown, but it has been suggested that it may be involved in the turnover of red blood cells, with spleen macrophages expressing β2 integrins binding to senescent red blood cells via ICAM-4 (Bailly *et al.*, 1995). Telencephalin (TLN) is the most recently identified LFA-1 ligand. It has nine Ig domains, and is only expressed on neuronal cells, in the telencephalic regions of the brain. It has been suggested that TLN may be involved in interactions between the immune system and the CNS, facilitating direct interaction of activated microglia (the resident macrophages of the CNS) with injured neurones, or the infiltration of monocytes to sites of neuronal inflammation (Tian *et al.*, 1997). The LFA-1 binding site has been mapped to the NH_2-terminal Ig domain (domain 1) in ICAM-1 (Staunton *et al.*, 1990), ICAM-2 (Li *et al.*, 1993), and ICAM-3 (Fawcett *et al.*, 1992; de Fougerolles *et al.*, 1994; Holness *et al.*, 1995), and to within the five N-terminal Ig domains (domains 1-5) of TLN (Tian *et al.*, 1997). Although domain 1 appears to be dominant with respect to ligand binding, domain 2 may play a less critical role, as mutations within domain 2 of ICAM-3 result in reduced LFA-1 binding, whereas mutations in domain 1 completely inhibit LFA-1 binding (Holness and Simmons, 1994; Holness *et al.*, 1995).

1.2.5.1.2 Mac-1

Although Mac-1 can be expressed on certain lymphocyte populations (see Table 1.1), it is mainly expressed on cells of the myeloid lineage, such as monocytes, macrophages and neutrophils. Mac-1 was first identified as an iC3b receptor, equivalent to the complement receptor type 3 (CR3) (Beller *et al.*, 1982), but has subsequently been found to bind to a wide variety of both soluble and cellular ligands, many of which appear to be involved the migration of phagocytes from the bloodstream to sites of inflammation, and in the

subsequent phagocytosis of infectious agents. The binding of Mac-1 to the third Ig domain (domain 3) of ICAM-1 (Diamond *et al.*, 1990; 1991) and to ICAM-2 (Xie *et al.*, 1995) appears to be involved in the transmigration of leukocytes from the bloodstream into extravascular tissues, and the ability of Mac-1 to bind to extracellular matix molecules, such as fibronectin, laminin and collagen (Bohnsack *et al.*, 1990) and to denatured proteins (Davis, 1992), may contribute to the subsequent migration of leukocytes through tissues to inflammatory sites. Mac-1 can also bind to microorganisms, either by direct interaction with natural microbial surface components, such as β-glucan (Ross *et al.*, 1987), lipopolysaccharide (LPS) (Wright and Jong, 1986; van Strijp *et al.*, 1993) and lipophosphoglycan (LPG) (Talamas-Rohana *et al.*, 1990), or by interacting with iC3b deposited on the surface of pathogens after activation of the complement pathways (Beller *et al.*, 1982; Wright *et al.*, 1983). Such interactions play a vital role in mediating the elimination of microorganisms by phagocytic ingestion. In addition, Mac-1 can also bind to proteins of the blood clotting system, such as fibrinogen (Altieri *et al.*, 1988; Wright *et al.*, 1988) and factor X (Altieri and Edgington, 1988), and may therefore be involved in regulating the clotting process, and by binding to the erythrocyte ligand ICAM-4 (Bailly *et al.*, 1995), Mac-1 may also be involved in regulating the turnover of red blood cells.

1.2.5.1.3 p150,95

The role of p150,95 is less well defined, mainly because its cellular distribution is very similar to that of Mac-1 (see Table 1.1), while its level of expression is much lower, making its study problematic. Many of the functions of p150,95 appear to overlap those of Mac-1. mAbs against p150,95 can inhibit the adhesion of peripheral blood monocytes and neutrophils to the endothelium, as well as chemotaxis and phagocytosis (Larson and Springer, 1990). p150,95 was initially defined as a receptor for iC3b (Micklem and Sim, 1985; Myones *et al.*, 1988; Bisland *et al.*, 1994), and hence is also refered to as complement receptor type 4 (CR4). However, like Mac-1, p150,95 can bind to a variety of ligands, including fibrinogen (Loike *et al.*, 1991; Postigo *et al.*, 1991), lipopolysaccharide (LPS) (Wright and Jong, 1986), lipophosphoglycan (LPG) (Talamas-Rohana *et al.*, 1990) and denatured proteins (Davis, 1992). In addition, the p150,95 receptor appears to bind to at least one counter-receptor on endothelium (Stacker and Springer, 1991), and there is evidence to suggest that the cellular ligand for p150,95 may be ICAM-1 (Blackford *et al.*, 1996).

1.2.5.1.4 αDβ2

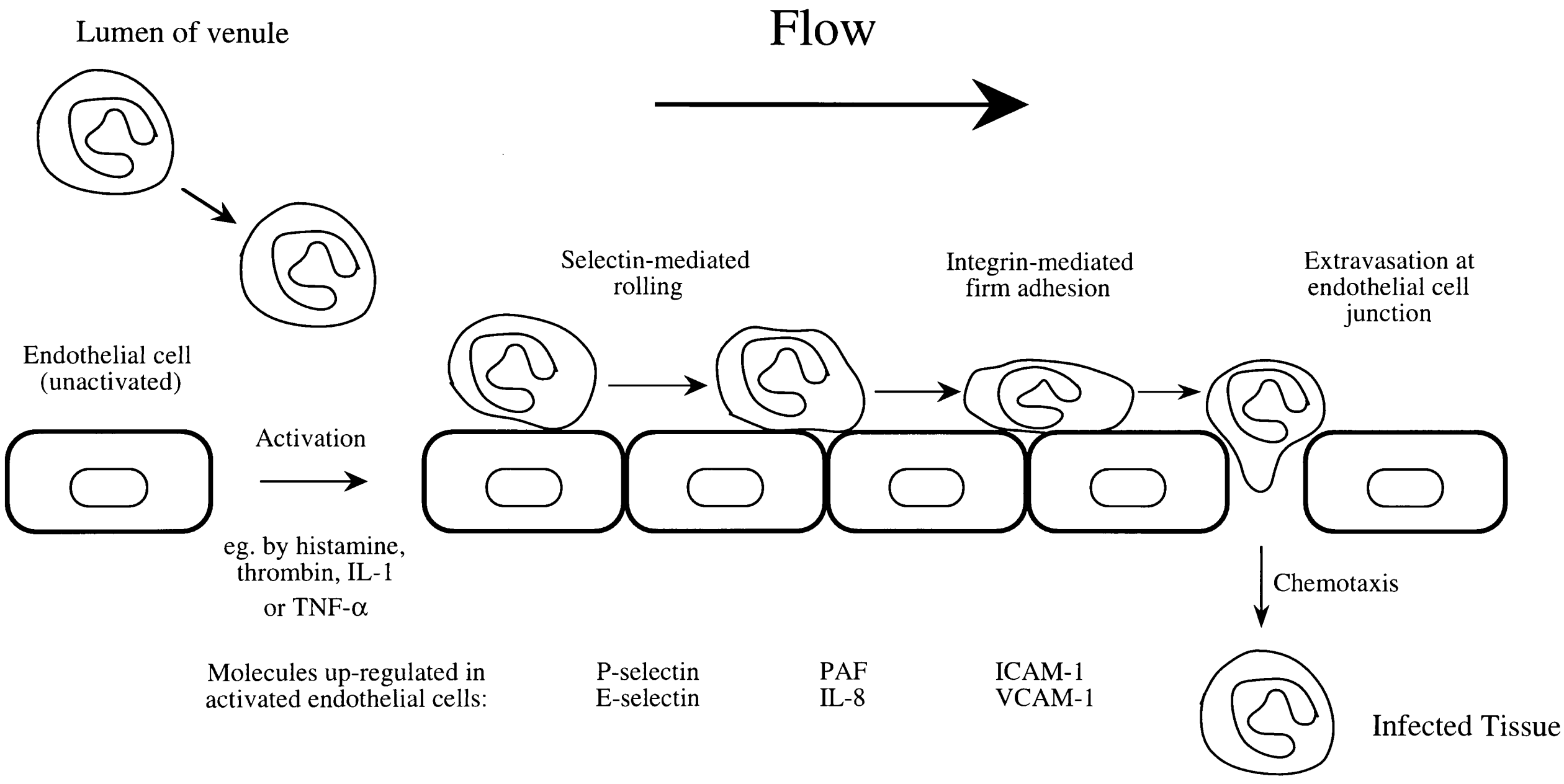
As the αDβ2 (CD11d/CD18) receptor has only recently been identified (Danilenko *et al.*, 1995; Van der Vieren, 1995), information on its ligand binding profile and functions is limited. Initial investigations have demonstrated that αDβ2 is primarily expressed on tissue compartmentalised cells, such as splenic red pulp macrophages and the foam cell macrophages present in athlerosclerotic streaks. It has therefore been suggested that αDβ2 may be involved in the phagocytosis of effete erythrocytes or modified lipoproteins (Van der Vieren *et al.*, 1995). In contrast to the other leukocyte integrins, αDβ2 is only expressed at low levels on myelo-monocytic cells, and does not appear to bind to ICAM-1. At present, the only ligand which has been demonstrated to bind to αDβ2 is ICAM-3 (Van der Vieren *et al.*, 1995), but the functional significance of this interaction remains to be determined.

1.2.5.2 Contribution of The Leukocyte Integrins to Transendothelial Migration

The adhesion of leukocytes to the vascular endothelium is the first step in the traffic of leukocytes from the bloodstream into the surrounding tissues, and is therefore of paramount importance to the inflammatory response. The involvement of the leukocyte integrins in this process was initially demonstrated by the study of patients suffering from the genetic disorder leukocyte adhesion deficiency I (LAD-I), in whom expression of functional β2 integrin receptors is severely reduced (see Section 1.2.5.3). LAD patients suffer from recurrent life-threatening bacterial infections, and tissue biopsies of infected areas from these patients revealed that their neutrophils were abundant within venules, but were literally absent in the surrounding extravascular tissue (reviewed by: Anderson and Springer, 1987; Arnaout, 1990b). Subsequent studies have provided substantial insights into the sequence of steps involved in the migration of leukocytes into inflammed tissues, and have also identified the indispensable contribution of the leukocyte integrins to this process (reviewed by: McEver, 1992; Shimizu *et al.*, 1992; Zimmerman *et al.*, 1992; Bevilacqua, 1993; Godin *et al.*, 1993; Springer, 1994; 1995). An adhesion cascade model, involving members of the selectin, integrin, and immunoglobulin superfamilies of adhesion molecules, has been proposed (see Figure 1.4). The initial contact between flowing leukocytes and the endothelium is thought to be mediated by selectin receptors expressed

Figure 1.4: The Transendothelial Migration of Leukocytes From The Bloodstream to Sites of Tissue Inflammation

Infected and damaged cells release a variety of inflammatory mediators into their surroundings which activate their localised endothelium, initiating a response which culminates in the extravasation and migration of leukocytes from the bloodstream into the infected extravascular site. This transendothelial migration of leukocytes begins with the activation of resting endothelial cells with inflammatory mediators, such as histamine, thrombin, IL-1 or TNF-α. Once activated, endothelial cells up-regulate expression of adhesive and signalling molecules, including P-selectin, E-selectin, ICAM-1, VCAM-1, PAF and IL-8, which facilitate interactions with leukocytes flowing past in the vasculature. The initial contact between leukocytes and endothelial cells is mediated by selectins, and is weak and reversible, resulting in the "rolling" of leukocytes along the vessel wall. With respect to the leukocyte, this primary adhesion is activation-independent. However, the subsequent interaction of chemoattractants, such as PAF and IL-8, with receptors on the surface of rolling leukocytes stimulates them to rapidly activate their integrin receptors, and they become arrested and firmly attached to the vessel wall via much stronger, integrin-mediated interactions with the endothelial adhesion molecules ICAM-1, ICAM-2 and VCAM-1. This step is essential for leukocyte transmigration, and in the absence of functional β2 integrin receptors, phagocytic cells such as neutrophils are unable to adhere tightly enough to the activated endothelial site, and eventually roll off the vessel wall and back into the bloodstream, resulting in many of the clinical symptoms exhibited by LAD-I patients. After firm adhesion to the vessel wall, leukocytes extravasate through the endothelium at cell junctions, and using strong-integrin mediated adhesion for traction, migrate through the extravascular tissue to the inflammed site following directional cues from chemoattractants.


Lumen of venule
Flow
Endothelial cell
(unactivated)
Selectin-mediated
rolling
Integrin-mediated
firm adhesion
Extravasation at
endothelial cell
junction
Activation
eg. by histamine,
thrombin, IL-1
or TNF-α
Chemotaxis
Molecules up-regulated in
activated endothelial cells:
P-selectin
E-selectin
PAF
IL-8
ICAM-1
VCAM-1
Infected Tissue

on both leukocytes and endothelial cells. E- and P-selectin are rapidly up-regulated on the surface of endothelial cells in response to inflammatory mediators, such as thrombin, histamine, interleukin-1 (IL-1) and tumour necrosis factor (TNF-α), and bind to specific carbohydrate mucin-like ligands expressed on the surface of leukocytes. Inflammatory mediators also result in the endothelial up-regulation of a ligand for L-selectin, a receptor which is constitutively expressed on leukocytes. These localised inflammatory responses result in a "sticky" vessel wall to which flowing leukocytes become attached. As the adhesive bonds between selectins and their ligands are relatively weak, they are insufficient to completely immobilise leukocytes under conditions of blood flow. Therefore, once leukocytes have become attached, they begin to roll along the vessel wall via transient selectin-mediated adhesive interactions. This rolling process brings leukocytes into close proximity with inflammatory chemoattractants, such as platelet activating factor (PAF) and interleukin-8 (IL-8), which are either displayed on or released from the activated endothelium. Chemoattractants stimulate rolling leukocytes to activate their surface integrin receptors, and once activated, integrins bind to ligands expressed on the surface of the endothelium, rapidly increasing adhesiveness and resulting in the arrest of rolling leukocytes and their firm adhesion to the vessel wall. The leukocyte integrins LFA-1, Mac-1 and possibly also p150,95, as well as another integrin, VLA-4, are all involved at this stage. The leukocyte integrins bind to the endothelial ligands ICAM-1 and ICAM-2, whereas VLA-4 binds to VCAM-1. Although ICAM-2 is constitutively expressed on endothelial cells, expression of both ICAM-1 and VCAM-1 is substantially up-regulated in response to inflammatory mediators, increasing the avidity of integrin-ligand interactions. As expression of the VLA-4 receptor is restricted on immune cells to monocytes, and B and T lymphocytes, the firm adhesion of phagocytic cells to blood vessel walls, and in particular the firm adhesion of neutrophils, is completely dependent on the leukocyte integrins at this stage, explaining the inability of LAD neutrophils to migrate to sites of tissue infection. After firm attachment, leukocytes extravasate through the blood vessel wall into the extravascular tissue. Although this extravasation process is poorly understood, it appears to involve CD31-CD31 interactions, and may also require adhesion between LFA-1/Mac-1 and ICAM-1. Mac-1, and possibly also p150,95, have also been implicated in the subsequent migration of extravasated leukocytes through tissues to inflammed sites, and are also known to play a crucial role in the phagocytosis of infectious agents at these sites. Therefore, not only are the leukocyte integrins indispensible for the

recruitment of leukocytes, and in particular the recruitment of neutrophils, to sites of tissue infection, but they also play a vital role in the destruction of infectious agents at these sites, as well as being involved in a variety of T and B cell mediated immune responses.

1.2.5.3 Leukocyte Adhesion Deficiency I (LAD-I)

Leukocyte adhesion deficiency I (LAD-I) is an inherited autosomal reccessive disorder caused by mutations in the gene encoding the integrin β2 subunit (CD18) on chromosome 21q22.3 (reviewed by: Anderson and Springer, 1987; Arnaout, 1990b). These mutations result in impaired expression and/or functioning of β2 integrin receptors on the surface of leukocytes, and consequently, to dysfunctions in immune processes requiring participation of the leukocyte integrins. Affected individuals characteristically suffer from chronic and recurrent bacterial infections, particularly of the soft tissues, with superficial infections on body surfaces rapidly invading locally as well as systemically. Infected areas are characterised by their lack of pus formation, even though patients often have much higher than normal levels of neutrophils in the bloodstream. Two LAD phenotypes, designated "severe" and "moderate", have been described. Patients with the severe phenotype generally have no detectable CD18 on their leukocytes, and usually succumb to infections in early infancy, whereas patients with the moderate phenotype have up to 10% of the normal levels of CD18 expression, and can survive into their 20's or 30's. Although cells from LAD patients have been shown *in vitro* to be deficient in various T cell-mediated functions, including antigen-induced proliferation, T cell mediated killing, and heterotypic adhesion of T and B cells, the major clinical problems seen in LAD patients appear to be the result of impaired phagocyte function, and in particular, the deficient transendothelial migration of neutrophils to sites of tissue infection. Although LAD was initially characterised in humans, examples of bovine and canine LAD have also been described (reviewed by: Shuster *et al.*, 1992; Trowald-Wigh *et al.*, 1992).

LAD was first recognised as an immune disorder in the mid-1980's: Several independent reports had identified a group of patients with high white blood cell counts, of about 5-15 times that of normal, that suffered from severe and recurrent bacterial infections (Reviewed by: Anderson and Springer, 1987). *In vitro*, granulocytes from these patients showed severely reduced capacity for phagocytosis, adhesion and chemotaxis, and Crowley *et al.*,

(1980) proposed that the underlying cause of the disease was defective neutrophil adhesion due to the absence of a cell surface protein now known to be the αM subunit of Mac-1. Subsequent studies (Dana *et al.*, 1983; Anderson *et al.*, 1984; Beatty *et al.*, 1984; Springer *et al.*, 1984; Arnaout *et al.*, 1984) showed that both the α and β subunits of Mac-1 were deficient on patient leukocytes, and that expression of LFA-1 and p150,95 was also severely reduced. It was therefore suggested that a primary defect in the common β2 subunit of LFA-1, Mac-1 and p150,95 could account for the disease. Somatic cell complementation studies further indicated a pathologic role for the β2 subunit in LAD (Marlin *et al.*, 1986): In hybrids of human and mouse lymphocytes, human LFA-1 α and β subunits from healthy individuals associated with mouse LFA-1 α and β subunits to form interspecies LFA-1 hybrids. However, when human lymphocytes from LAD patients were used, αL(human)β2(murine) hybrids, but not αL(murine)β2(human) hybrids, were detected. Firm evidence that the presence of a defective β2 subunit correlated with LAD came from the study of a large family described by Kishimoto *et al.* (1987). In this family, the incidence of an aberrantly small β subunit precurser invariably coincided, in homozygous individuals, with LAD. Members of the family who were heterozygous, with both normal sized and small precursor, had approximately 50% of normal levels of the leukocyte integrins, whilst those who had only normal precursors showed normal levels of expression. Finally, transfection of LAD cells with wildtype CD18 cDNA was shown to restore LFA-1 expression and function (Hibbs *et al.*, 1990), providing conclusive proof that LAD is caused by defective CD18.

The defects which result in LAD have been found to be very heterogeneous. In a study of 14 LAD patients by Kishimoto *et al.* (1987), five distinct phenotypes of CD18 expression and structure were identified: (i) The CD18 mRNA and protein precursor were undetectable; (ii) the levels of CD18 mRNA and protein precursor were diminished; (iii) the levels of CD18 mRNA were normal, but the protein precursor was aberrantly large; (iv) the levels of the CD18 mRNA were again normal, but protein precursor was aberrantly small; and (v) no gross abnormalities in the CD18 mRNA or protein precursor were detected. Subsequent analysis of numerous patients at the nucleic acid level has identified over 25 different mutations, dispersed throughout the entire β2 gene, which can result in LAD. A complete summary of these mutations is provided in Chapter Five (see Figure 5.7). The diminished mRNA levels characterised by LAD phenotypes (i) and (ii) appear to be mainly

caused by frameshifts resulting from deletions within exonic regions of the CD18 gene. Such mutations seem to lead to decreased mRNA stability, presumably because translation is inevitably terminated prematurely and dissociation of the ribosomal complex leaves the mutant mRNA molecule exposed to excessive degradation. The gross abnormalities characterised by phenotypes (iii) and (iv) appear to be caused by point mutations at mRNA splice sites, which result in abberant splicing events such as deletions of entire exons, or inframe additions of intronic material. Phenotype (v) appears to be the result of subtle point mutations within the coding regions of the β2 gene. Over 15 different point mutations have been identified, which are mainly concentrated within the putative A-domain and C-terminal cysteine-rich regions of the β2 subunit. These mutations can affect αβ heterodimer formation, ligand binding or the activation state of receptors, and their study has therefore been beneficial to the mapping of functional regions within the β2 subunit (see Chapter Five).

It is therefore clear that LAD is a highly complex disorder resulting from an array of different mutations in the β2 gene. These mutations can lead to a variety of different LAD phenotypes, ranging from severe LAD through to the more moderate forms of the disease. As LAD is a recessive disorder, two defective alleles are required to manifest clinical symptoms. Although patients can be homozygous for a particular mutant allele, they are more often compound heterozygotes, deriving two different LAD mutations from their maternal and paternal alleles, which adds even greater phenotypic diversity to the disease. At present, the main treatment for LAD centres around aggressive antibiotic therapy during infectious episodes. Bone marrow transplantation has also been employed to treat some severe LAD patients (Fischer *et al.*, 1983), and preliminary efforts towards developing gene therapy for the treatment of LAD have also been reported (Krauss *et al.*, 1991; Yorifuji *et al.*, 1992).

1.3 PROJECT AIMS

Although the integrin family of cell adhesion molecules have been extensively studied over the past two decades, many important questions concerning their structure and function remain unanswered. It is unclear for instance, exactly how the specificity of αβ heterodimer formation is achieved, and exactly how the ligand binding regions in integrin α

and β subunits cooperate to form highly specific ligand binding sites. The precise conformational changes which occur upon integrin activation, and exactly how these conformational changes are controlled from within the cell, also remain to be determined. In an attempt to answer some of these questions, a series of chimeric and truncated integrin β2 variants were constructed, and the effect that these changes have on the formation and ligand binding activities of the leukocyte integrins LFA-1, Mac-1 and p150,95 was examined. In addition, the effect of three different LAD mutations on the expression of the β2 subunit, and on its ability to form functional LFA-1, Mac-1 and p150,95 heterodimeric complexes, was also assessed.

CHAPTER TWO

MATERIALS AND METHODS

2.1 MATERIALS

2.1.1 GENERAL REAGENTS

General reagents and solvents were AnalaR grade, and were obtained from BDH Chemicals Ltd., Rose Chemicals Ltd., Fisons, May and Baker Ltd., Hayman Ltd., Boehringer Mannheim Ltd., Sigma Chemical Company Ltd., Aldrich Chemical Company Ltd., Oxoid Ltd., Difco Laboratories, FMC BioProducts, Gibco-BRL Ltd., Pharmacia Fine Chemicals, Becton Dickinson or FSA Laboratory Supplies, unless otherwise stated. Solutions were sterilised where required, by autoclaving at 15 pounds per square inch for 20 min, or by passing through a 0.22µm filter (Millipore, Costar or Sartorius).

2.1.2 RADIOCHEMICALS

Radioisotopes were obtained from Amersham International plc.

		Specific Activity
[α-^{32}P]-dATP	10 mCi/ml	3000 Ci/mmol
[α-^{32}P]-dCTP	10 mCi/ml	3000 Ci/mmol
[γ-^{32}P]-dATP	10 mCi/ml	3000 Ci/mmol
[α-^{35}S]-dATP	10 mCi/ml	600 Ci/mmol
[α-^{35}S]dCTP	10 mCi/ml	600 Ci/mmol

2.1.3 ENZYMES

Restriction endonucleases and other enzymes were purchased from Promega Corporation, New England Biolabs Inc., Amersham International plc., Bethesda Research Laboratories (BRL), Boehringer Mannheim Ltd. or Pharmacia Inc. unless otherwise stated, and were used according to the supplier's recommendations.

2.1.4 COMMERCIALLY AVAILABLE KITS

Magic™ Minipreps DNA Purification System	Promega Corporation.
QIAprep Spin Miniprep Kit	QIAGEN Inc.
Plasmid Midi Kit	QIAGEN Inc.
Plasmid Maxi Kit	QIAGEN Inc.

QIAquick Gel Extraction Kit	QIAGEN Inc.
T7 Sequencing™ Kit	Pharmacia LKB Biotechnology.
Multiprime™ Labelling Kit (1601Z)	Amersham International plc.
ECL Detection Reagents	Amersham International plc.

2.1.5 DNA VECTORS

λGT10	Clonetech Ltd. (Murray *et al.*, 1977)
pAT-X	Gift from Dr. G. Brownlee, (Knott *et al.*, 1988)
pBluescript KS (-)	Stratagene Cloning Systems, (Short *et al.*, 1988).
pEE6.HCMV.GS	Celltech Ltd. (Bebbington *et al.*, 1987; Cockett *et al.*, 1990)
pSVL	Pharmacia LKB Biotechnology, (Sprague *et al.*, 1983).
pcDNA3	Invitrogen Corp. (Boshart *et al.*, 1985; Riviere *et al.*, 1991)

2.1.6 MONOCLONAL ANTIBODIES

MHM24	Mouse Anti-Human αL	IgG1	(Hildreth and August, 1985)
MEM83	Mouse Anti-Human αL	IgG1	(Landis *et al.*, 1993)
LPM19C	Mouse Anti-Human αM	IgG2a	(Uciechowski and Schmidt, 1989)
KB23	Mouse Anti-Human αX		
KB90	Mouse Anti-Human αX		
H52	Mouse Anti-Human β2	IgG1	(Hildreth and August, 1985)
MHM23	Mouse Anti-Human β2	IgG1	(Hildreth and August, 1985)
IB4	Mouse Anti-Human β2	IgG2a	(Wright *et al.*, 1983)
KIM89	Mouse Anti-Human β2	IgG2a	(Stephens *et al.*, 1995)
KIM127	Mouse Anti-Human β2	IgG1	(Robinson *et al.*, 1992)
KIM170	Mouse Anti-Human β2	IgG1	(Stephens *et al.*, 1995)
KIM182	Mouse Anti-Human β2	IgG1	(Stephens *et al.*, 1995)
KIM185	Mouse Anti-Human β2	IgG1	(Andrew *et al.*, 1993)
KIM202	Mouse Anti-Human β2	IgG1	(Stephens *et al.*, 1995)
KIM215	Mouse Anti-Human β2	IgG1	(Stephens *et al.*, 1995)
OX33	Mouse Anti-Rat CD2	IgG1	
OX34	Mouse Anti-Rat CD2	IgG2a	

MHM24 and MHM23 were gifts from Professor A.J. McMichael (John Radcliffe Hospital, Oxford); MEM83 was a gift from Dr. V. Horejse (Prague, Czech Rebublic); LPM19c and KB23 were gifts from the LRF Diagnostic Unit (John Radcliffe Hosptal, Oxford); KIM89, KIM127, KIM170, KIM182, KIM185, KIM202 and KIM215 were gifts from Dr. M.K. Robinson (Celltech Therapeutics Ltd., Slough); OX33 and OX34 were gifts from the MRC Cellular Immunology Unit (CIU), Oxford.

2.1.7 LABORATORY STOCKS

1 M Tris-HCl, pH 8.0	Stored at room temperature
1 M $MgCl_2$	Stored at room temperature
3 M NaCl	Stored at room temperature
5 M NaCl	Stored at room temperature
3 M NaAc, pH 6.0	Stored at room temperature
3 M NaAc, pH 4.8	Stored at room temperature
10% (w/v) SDS	Stored at room temperature
0.5 M EDTA, pH 7.5	Stored at room temperature
0.1 M DTT	Stored at -20°C
1 M DTT	Stored at -20°C
10 mg/ml BSA	Stored at -20°C
100 mM Spermidine	Stored at -20°C
0.1% Ethidium Bromide	Stored at 4°C
1 M Hepes, pH 7.4	Stored at 4°C

2.1.8 SOLUTIONS AND BUFFERS

TE Buffer	10 mM Tris, 0.1 mM EDTA pH 8.0.
Phenol	Solid phenol was melted and was extracted several times with 1 M Tris-HCl pH 8.0, followed by 20 mM Tris-HCl pH 8.0 until the pH of the aqueous phase was > 7.6. The phenol was then aliquoted and stored at -20°C, or at 4°C under 20 mM Tris-HCL pH 8.0.
Phenol:Chloroform	Equal volumes of chloroform and phenol (prepared as above) were mixed and stored at 4°C
10 x TBE	0.89 M Tris, 0.89 M Boric Acid, 25 mM EDTA.
Formamide Loading Dye	80% (v/v) deionised formamide, 10mM EDTA pH 7.5, 0.1% (w/v) xylene cyanol FF, 0.1% (w/v) bromophenol blue. Stored at 4°C.
Glycerol Loading Dye	30% (w/v) glycerol, 5 mM EDTA pH 7.5, 0.1% (w/v) xylene cyanol FF, and 0.1% (w/v) bromophenol blue. Stored at 4°C.

50 x Denhardt's Solution	1% (w/v) BSA, 1% (w/v) Ficoll 400, 1% (w/v) polyvinylpyrrolidine.
12 x NET	1.8 M NaCl, 0.18 M Tris-HCl pH 7.4, 12 mM EDTA.
Hybridisation Buffers	
For cDNA Probes:	50% (v/v) deionised formamide, 50 mM Tris-HCl pH 7.4, 1M NaCl, 10% (w/v) Dextran sulphate, 10 x Denhardt's solution, 0.1% (w/v) SDS, 0.1% (w/v) sodium pyrophosphate, 0.1 mg/ml sonicated salmon sperm DNA (Sigma Type III). Stored at 4°C.
For Oligonucleotide Probes:	5 x Denhardt's solution, 6 x NET, 0.5% (w/v) Dextran sulphate, 0.5% (w/v) SDS, 0.1% (w/v) sodium pyrophosphate, 0.1 mg/ml sonicated salmon sperm DNA (Sigma Type III), 0.1 mg/ml tRNA. Stored at 4°C.
20 x SSC	3 M NaCl, 0.3 M tri-sodium citrate, pH 7.0.
20 x SSPE	3 M NaCl, 0.2 M sodium phosphate, 20 mM EDTA, pH 7.4.
TfB-I	100 mM KCl, 50 mM $MnCl_2$, 30 mM KOAc, 10 mM $CaCl_2$, 15% (v/v) glycerol. Stored at 4°C
TfB-II	75 mM $CaCl_2$, 10 mM KCl, 10 mM MOPS pH 7.0, 15% (v/v) glycerol. Stored at 4°C.
Hogness Buffer	4% (v/v) glycerol, 3.6 mM Na_2HPO_4, 1.3 mM NaH_2PO_4, 2 mM tri-sodium citrate, 1 mM $MgSO_4$, pH 7.5.
SM Buffer	50 mM Tris-HCL pH 7.5, 100 mM NaCl, 10 mM $MgSO_4$, 0.01% (w/v) Gelatin, pH 7.5.
IP Buffer	10 mM Tris.HCL pH 8.0, 150 mM NaCl, 2.5 mM EDTA pH 7.5, 1% (v/v) NP40, 0.1% (w/v) BSA, 0.2% (w/v) sodium azide, pH 8.0. Stored at 4°C.
SDS-PAGE:	
2 x Sample Loading Buffer	8 M Urea, 0.2 M Tris.HCL pH 8.0, 2% (w/v) SDS, 0.08% (w/v) Bromophenol Blue, pH 8.0. To reduce samples prior to electrophoresis, DTT was included in the sample buffer at 40 mM.
4 x Upper Gel Buffer	0.5 M Tris, 0.4% (w/v) SDS, pH 6.8.
4 x Lower Gel Buffer	1.5 M Tris, 0.4% (w/v) SDS, pH 8.8.

10 x Running Buffer	0.25 M Tris, 1.9 M Glycine, 1.0% (w/v) SDS, pH 8.8.

2.1.9 MEDIA

All media were sterilised by autoclaving for 20 minutes at 15 lb/sq. in. on liquid cycle.

LB Medium	1% (w/v) bacto-tryptone, 0.5% (w/v) yeast extract, 1% (w/v) NaCl, pH 7.4.
LB Agar	LB medium plus 1.5% (w/v) bacto-agar.
LA Plates	LB agar plates containing 100 μg/ml ampicillin
2 x TY Medium	1.5% (w/v) bacto-tryptone, 1% (w/v) yeast extract, 0.5% (w/v) NaCl, pH 7.4.
TYM Broth	2% (w/v) bacto-tryptone, 0.5% (w/v) yeast extract, 0.1 M NaCl, 10 mM $MgSO_4$, pH 7.5.
T Broth	1.0% (w/v) bacto-tryptone, 0.5% (w/v) NaCl
T-Mg Broth	1.0% (w/v) bacto-tryptone, 0.5% (w/v) NaCl, 10 mM $MgSO_4$, pH 7.4.
T Broth Agar	T-Mg Broth plus 1.2% (w/v) bacto-agar.
T Broth Agarose	T-Mg Broth plus 0.7% (w/v) agarose.

Ampicillin was prepared at 20 mg/ml in water and was sterilised by filtration through a 0.22 μm filter. When appropriate, it was included in liquid cultures and in agar plates at an end concentration of 100 μg/ml. As ampicillin is heat sensitive, autoclaved media and molten agar were cooled to below 55°C before addition of sterile ampicilin.

2.2 METHODS

2.2.1 GENERAL METHODS FOR DNA MANIPULATION

Many of the methods used are modifications of those described by Sambrook *et al.* (1989).

2.2.1.1 Phenol/Chloroform Extraction

Contaminating proteins were removed from DNA solutions by extraction with phenol/chloroform. Phenol/chloroform (1:1 v/v) was added in equal volume to the aqueous solution of DNA and proteins. The mixture was vortexed for 30 sec to ensure thorough mixing of the phases, and then centrifuged (12 000 g, 1 min, r.t.) to separate the phases. The top (aqueous) phase was transferred to a new tube, avoiding protein at the interface, and the procedure was repeated until no protein was visable at the interface. Traces of phenol were removed by another extraction with an equal volume of chloroform alone.

2.2.1.2 Ethanol Precipitation of DNA

DNA was precipitated, to increase its concentration or to change the buffer, using ethanol. Sodium acetate at pH 6.0 was added to a final concentration of 0.3 M, followed by 2.5 to 3 volumes of absolute ethanol. After incubation at -70°C for at least 30 min, or in a dry ice/ethanol bath for 15 min, the DNA was pelleted by centrifugation (12 000 g, 30 min, r.t.). The pellet was washed with chilled 70% ethanol to remove salt contamination, and was then dried briefly on the bench and resuspended in the appropriate volume of TE buffer pH 8.0.

2.2.1.3 Isopropanol Precipitation of DNA

DNA was precipitated by the addition of 7/10 volume of isopropanol pre-equilibrated to room temperature. Following centrifugation at 12 000 g for 30 min at 4°C, the DNA pellet was washed with chilled 70% ethanol to remove salt contamination, and was then dried briefly on the bench and resuspended in the appropriate volume of TE buffer pH 8.0.

2.2.1.4 Concentrating DNA by Butanol Extraction

Butanol was added to DNA solutions, mixed thoroughly by vortexing for 1 min, and centrifuged briefly at room temperature, then the upper organic phase discarded. This procedure was repeated until the desired volume of DNA was achieved. Subsequently a chloroform extraction was performed to remove traces of butanol.

2.2.1.5 Quantitation of DNA

Concentration of DNA was determined by its absorbance at a wavelength of 260 nm (OD_{260}; Cecil CE292 digital ultraviolet spectrophotometer) based on the following calculation: A solution of 50 µg/ml double-stranded DNA or 33 µg/ml single-stranded DNA gives an OD_{260} unit of 1. The OD_{280} was also read and the ratio of OD_{260}/OD_{280} calculated to estimate the purity of DNA solutions. An OD_{260}/OD_{280} ratio between 1.6-2.0 was satisfactory. In most cases, the amount of double-stranded DNA was also estimated by its fluorescence intensity in an ethidium bromide-stained mini-agarose gel. A DNA size standard (1 kb ladder, BRL) was usually included for comparison.

2.2.1.6 Restriction Endonuclease Digestion of DNA

Restriction endonuclease digestions were usually carried out in a 20-100 µl volume reaction, where 2-5 units of enzymes were used for up to 500 ng of DNA, for 4 to 18 hours at an appropriate temperature. The reaction buffers were 10 mM Tris pH 8, 10 mM $MgCl_2$, 1 mM DTT, 100 µg/ml BSA, with the appropriate concentration of NaCl (either 0 mM, 50 mM, 100 mM or 150 mM). 5 mM spermidine was usually included in the final reaction except when the reaction buffer contained no NaCl. Commercially available 10 x buffers were also used according to the manufacturer's instructions. Digestions with more than one enzyme were carried out simultaneously in a suitable common buffer whenever possible. When the buffer requirements were incompatible, digestions were performed sequentially with phenol:chloroform extraction and ethanol precipitation between digests.

2.2.1.7 Synthesis and Purification of Oligonucleotides

Oligonucleotides were synthesised in an Applied Biosystems Model 381A DNA Synthesiser. The design of the oligonucleotides varied according to their intended use. For example, those intended for use as PCR primers were matched for melting/annealing

temperature (Tm), the temperature at which half of the molecules will be dissociated from a complementary DNA strand. Tm is calculated according to the formula:

$$Tm = 4(G+C) + 2(A+T) \qquad \text{(Wallace and Miyada, 1987)}$$

For PCR, the oligonucleotides were commonly about 20 bases long, with a Tm around 60°C. During synthesis, the oligonucleotides were attached to a solid support in a column, and β-cyanoethyl phosphoramidite nucleoside derivatives were added to the 5' end of the molecules. To remove the protecting groups and cleave the oligonucleotides from their solid support, concentrated ammonia solution (2 ml, ~30%) was passed through the column in 0.5 ml aliquots at 15 min intervals: the oligonucleotides in ammonia solution were then incubated at 55°C for 14-16 h. The ammonia was subsequently removed by two ethanol precipitations, and the oligonucleotides resuspended in 500 µl TE pH 8.0 prior to determination of the concentration. Concentrations of around 200 µM were generally achieved. This concentrated stock was stored at -20°C and diluted with TE pH 8.0 as necessary.

2.2.1.8 Autoradiography

Radioactive gels and filters were exposed to Kodak X-OMAT S film in a radiographic cassette at 4°C or -70°C. Sequencing gels containing [^{35}S]-nucleotides were dried and exposed directly to the film at room temperature for the appropriate time (~24 hrs). To autoradiograph [^{32}P]-labelled DNA acrylamide gels or nitrocellulose filters, films were hypersensitised by pre-exposure to a flash of light, placed flash-side down onto the labelled gel or filter, and exposed with a calcium tungstate X-ray intensifying screen (Du Pont Lightning Plus) at -70°C. Fluorescent markers (Stratagene) were used when necessary to allow accurate orientation of films. Films were developed using a Kodak X-OMAT ME-1 processor.

2.2.2 RADIOACTIVE LABELLING OF NUCLEIC ACIDS

2.2.2.1 Radiolabelling of Double-Stranded DNA Fragments

a) "Multiprime" Labelling

Double-stranded DNA fragments were labelled using the Multiprime DNA Labelling System (Amersham International plc). Random hexanucleotide primers are hybridised with the DNA and extended using the Klenow fragment of *E. coli* polymerase I (Feinberg and Vogelstein, 1983) and [α^{32}P]-dCTP. 25-100 ng of DNA, made up to a volume of 30 µl with water, was denatured by heating to 100°C for 5 min, then cooled on ice and centrifuged briefly to spin the contents to the bottom of the tube. 10 µl of solution 1, containing dATP, dGTP and dTTP, and 5 µl solution 2 containing random hexanucleotides and BSA were added, followed by 3 µl [α^{32}P]-dCTP (30 µCi) and 2 U Klenow fragment. The reaction was incubated at room temperature for 3-5 h, and then passed down a PD10 column (Pharmacia) containing Sephadex G-25 buffered in 10 mM Tris-HCl pH 7.5, 1 M NaCl and 1 mM EDTA, to separate the labelled DNA from unincorporated radiolabel. The eluate was collected in 8 fractions of 750 µl, and the separation was assessed by measuring the radioactivity in a 2 µl aliquot from each fraction using a scintillation counter (LKB-Wallac 1211 Minibeta). The probe was usually contained in fractions 4-5, which were then pooled.

b) "End-Filling"

Restriction fragments with recessed 3' ends were radiolabelled via an end-filling reaction with the Klenow fragment and suitable radionucleotides. Depending on the sequence of the 5' overhang, either [α^{32}P]-dCTP and/or [α^{32}P]-dATP were used as the label. Digested DNA was incubated with 4 U Klenow fragment in 10 mM Tris-HCl pH 8.0, 5 mM $MgCl_2$, 0.1 mM DTT, 0.05 mg/ml BSA, 50 µM dNTP (excluding the nucleotide(s) used as the label) and 0.5 µl (5 µCi) radionucleotide. After incubation for 15 min at r.t., the reaction was "chased" by the addition of non-radioactive nucleotide of the type used as the label, to a final concentration of 50 µM, and the reaction was incubated at r.t. for a further 15 min. The enzyme was inactivated by heating to 65°C for 10 min and the DNA was purified from proteins by phenol/chloroform extraction and was recovered by ethanol precipitation.

2.2.2.2 Preparation of Radiolabelled Oligonucleotide Probes

Oligonucleotides were radiolabelled by transferring a radioactive phosphate group to the 5' end using T4 polynucleotide kinase. 75 ng oligonucleotide DNA was incubated with 10 U polynucleotide kinase in a 20 µl reaction containing 50 mM Tris-HCl pH 8.0, 10 mM DTT, 10 mM $MgCl_2$ and 10-30 µCi [γ^{32}P]-ATP. After incubation at 37°C for 30-45 min, the reaction mixture was passed down a PD10 column (as in Section 2.2.2.1a) to separate the oligonucleotide from unincorporated label. The eluate was collected in 8 x 750 µl fractions and the separation and labelling was assessed by measuring the radioactivity in a 2 µl sample from each fraction using a scintillation counter.

2.2.3 TRANSFER OF DNA TO FILTERS AND HYBRIDISATION

DNA was transferred to nitrocellulose or nylon filters and cross-linked on to them in order to probe for specific DNA sequences using radiolabelled cDNA or oligonucleotide probes.

2.2.3.1 Transfer of DNA to Filters after Agarose Gel Electrophoresis (Southern Blot Hybridisation)

DNA fragments were transferred to filters by the method of capillary blotting first described by Southern (1975). After electrophoresis, agarose "minigels" were treated with alkali to denature the DNA. Firstly, the gels were rinsed with distilled water (5 min), then treated with denaturing buffer (0.5 M NaOH, 1.5 M NaCl) for 30-40 min with shaking, and then equilibrated for 10-15 min in alkali transfer buffer (0.25 M NaOH, 1.5 M NaCl). A capillary blot was then set up as follows: The gel was placed on top of two sponges and two layers of Whatman 3 MM filter paper, all pre-soaked with alkali transfer buffer, and with the bottom sponge sitting immersed in a tray of alkali transfer buffer. A nylon filter (Hybond-N, Amersham International plc) was cut to the same size as the gel and pre-wetted with water followed by alkali transfer buffer. This was then placed on top of the gel and on top of this were added two further pieces of Whatman 3 MM filter paper and a stack of paper towels 4 cm high. A glass plate and weight were placed on top. Blotting was carried out for a minimum of 15 min up to 16 h. If several blots were required from the same gel, the length of time for blotting was increased for each filter. After blotting, the membrane was washed with 2 x SSC for 10 min and dried briefly at 80°C for 5 min. The

filter was wrapped in Clingo-Rap® film and the DNA cross-linked to the filter by exposure to UV light at 254 nm for 2 min.

2.2.3.2 Transfer of Bacterial Colonies to Filters (Colony Hybridisation)

The method of colony hybridisation to select clones with specific inserts using [^{32}P]-labelled probes was first described by Grunstein and Hogness (1975). DNA from bacterial colonies is transferred to nitrocellulose and probed with radiolabelled cDNA or oligonucleotides to screen for the desired insert. Ampicillin-resistant transformants (cDNA libraries or subcloned DNA recombinants) were spread over the nitrocellulose filters (Hybond C, Amersham International plc.) on LA plates, and were incubated at 37°C until the colonies were about 1 mm in diameter. Usually, two replicas of each master filter were made, using fresh filters which were pre-wetted on fresh agar plates. The master filter was removed from the agar plate and placed on a layer of filter paper and a clean nitrocellulose filter was placed on top. The 2 filters were pressed together between glass plates, applying pressure evenly over the plates, to allow the transfer of some of the bacterial cells from the master plate to the replica. The filters were marked with asymmetric ink spots using a needle, to allow precise orientation of the filters at a later stage. The filters were then peeled apart and replaced colony side up on the agar plates. Alternatively, individual colonies were transferred onto gridded nitrocellulose membranes on LA plates in triplicate using sterile tips. All the plates were incubated at 37°C until the colonies had grown to a suitable size. The master plates were then stored at 4°C, whilst the replica filters were removed from their agar plates, and the bacterial cells were lysed and the DNA from them was fixed onto the nitrocellulose. The filters were placed sequentially, colony side up, on to Whatman 3 MM filter paper soaked in the following solutions: (i) 10% (w/v) SDS, (ii) 0.5 M NaOH, 1.5 M NaCl, (iii) 0.5 M Tris-HCl pH 7.5, 1.5 M NaCl. The filters were left for 5 min on each, then washed for 10 min in 0.5 M Tris-HCL pH 7.5, 1.5 M NaCl. The filters were then placed, DNA side up, on a clean dry tray and the cell debris was removed by wiping the filters with a tissue soaked in 2 x SSC, 0.1% SDS. Finally, the filters were washed in 2 x SSC for 10 min and air-dried for 10 min before baking at 80°C for 2 h to fix the DNA to the filter prior to hybridisation.

2.2.3.3 Transfer of Bacteriophage Plaques to Filters (Plaque Hybridisation)

Recombinant phage containing the desired insert were selected by screening with radioactively labelled probes using a plaque hybridisation protocol. Replica filters were prepared by placing a moist nitrocellulose filter (Hybond C, Amersham International plc.) onto chilled (4°C) top agarose containing plated phage particles (lambda libraries or putative positives). The filters were left for 1 min and orientation marks made by stabbing filters and agar with an ink-coated needle. Filters were carefully removed and a second copy made by placing on another filter. Phage was lysed by placing filters (plaque-side up) onto the surface of lysis buffer (0.5 M NaOH, 1.5 M NaCl) for 7 min, then neutralising buffer (0.5 M Tris-HCL pH 7.5, 1.5 M NaCl) for 3 min, and were then immersed in neutralising buffer (0.5 M Tris-HCL pH 7.5, 1.5 M NaCl) for another 3 min, before being briefly washed in 2 x SSC solution. Filters were dried briefly on Whatman 3MM paper and the DNA was fixed to the filters by baking at 80°C for 2-3 h.

2.2.3.4 Hybridisation Conditions

Before hybridisation, nitrocellulose filters were pre-wetted in 10 mM Tris-HCL pH 7.5, 1 mM EDTA, 1 M NaCl for 30 min at r.t. Filters were prehybridised at 42°C for 3 h in hybridisation buffer in sealed plastic bags or crystallising dishes. Radioactive hybridisation solution was prepared by adding to a fresh aliquot of hybridisation buffer sonicated salmon sperm DNA to a final concentration of 0.1 μg/ml and radiolabelled DNA probe to a concentration of 2 x 10^5-1 x 10^6 cpm/ml. This mixture was boiled for 5 min, cooled on ice and then added to the pre-wetted filters in a hybridisation bag or in a crystallising dish, ensuring that there was a layer of buffer between the filters. The filters were then hybridised overnight (14-18 h) at 42°C with constant agitation.

2.2.3.5 Removal of Unbound Probe from Filters

After hybridisation, filters were washed to remove excess, non-specifically bound probe. Where a cDNA probe had been used, filters were washed with 2 x SSC for 10 min at r.t. with constant agitation. This was followed by 2 x 15 min washes at 65°C, the first with 0.2 x SSC, 0.1% SDS and the second with 0.2 x SSC. Filters hybridised with

oligonucleotide probes were washed with constant agitation in 6 x SSC at r.t. (10 min), and then at 5°C below the Tm of the oligonucleotide (see Section 2.2.1.7) firstly in 6 x SSC, 0.1% SDS and then in 6 x SSC (2 x 15 min washes). Washed filters were dried briefly (10 min) on Whatman 3MM paper, wrapped in Clingo-Rap® film and autoradiographed at -70°C for 4-48 h.

2.2.3.6 Removing Specifically Bound Probe from Filters

If the filters were to be re-screened with a different probe, a solution of 0.1 x SSPE, 0.1% SDS was boiled and poured on to the filters, and allowed to cool to r.t. The removal of the probe could be checked by autoradiography, and the filters were then hybridised with a new probe.

2.2.4 BACTERIOPHAGE LAMBDA VECTORS

2.2.4.1 Plating Bacteriophage Lambda

A human peripheral blood monocyte cDNA library cloned into the lambda vector λGT10 (Clonetech Ltd.) was plated and screened for desired cDNA inserts as follows: A single isolated bacterial colony, strain C600 *hfl*, was used to innocluate 10 ml T-Mg broth supplemented with 0.4% (w/v) maltose, and the culture was incubated overnight at 37°C with shaking. A total of ~$1x10^6$ pfu were plated onto 4 x large square (22 x 22 cm) culture plates and were screened for the desired insert. For each culture plate, a sample of the phage library diluted in 0.1 ml SM buffer was prepared, so that it would yield a maximum of ~$2.5x10^5$ pfu/plate. To each sample of diluted phage, 0.9 ml SM buffer and 1.8 ml host cell culture were added, and the mixtures were incubated at 37°C for 20 min without agitation. After this incubation period, 30 ml molten (45°C) top agarose was added per sample, and after mixing, each sample was poured onto a warm T-Broth agar plate (22 x 22 cm). The plates were swirled quickly to allow even spreading of the agarose over the surface. After plates had set, they were inverted and incubated at 37°C until the plaques had reached a diameter of no greater than 0.25 mm, or were just beginning to make contact with one another (3-8 h). Confluent lysis was avoided. The plates were then chilled at 4°C to allow the top agarose to harden, and were then screened for positive recombinants using the plaque hybridisation protocol (see Section 2.2.3.3). Putative positive recombinants

identified by hybridisation were picked by extracting a plug of agar using cut-off sterile pipette tips, and phage particles were eluted in 1.5 ml SM buffer (with 10 µl chloroform) and were stored at 4°C. Eluted phage samples were then diluted and replated at a lower density of ~500 pfu/round (150 mm) plate. For these plates, 250 µl diluted phage, 500 µl host cells and 9 ml top agarose were used. After rescreening, agar plugs containing putative positive recombinants were repicked as before, and the eluted phage were again diluted and replated at ~50 pfu/round (90 mm) plate. For these plates, 100 µl diluted phage, 200 µl host cells and 3.5 ml top agarose were used. This procedure was repeated, replating at successively lower densities, until single plaques were obtained.

2.2.4.2 Purification of Bacteriophage Lambda DNA

Small-scale preparations of bacteriophage lambda DNA were performed using the liquid lysate method (Leder *et al.*, 1977). A single isolated bacterial colony (strain C600 *hfl*) was used to innocluate 10 ml T-Mg broth supplemented with 0.4% (w/v) maltose, and the culture was incubated overnight at 37°C with shaking. Single isolated plaques of lambda recombinants were picked from culture plates using cut-off automatic piptette tips, and the phage eluted in 1.5 ml SM buffer overnight at 4°C. The bacteriophage eluate (200 µl plus 250 µl SM Buffer) was added to the fresh overnight bacterial C600 *hfl* culture (250 µl), and incubated at 37°C for 15 min to allow bacteriophage particles to absorb. T-Mg medium containing 5 mM $CaCl_2$ (5 ml) was added and incubated for a further 5 h at 37°C with vigorous shaking until the solution became clear. After lysis occured, chloroform (100 µl) was added and incubated for 7 min at 37°C before centrifugation (2 500 rpm, 10 min, 4°C, MSE 6L) to pellet the bacterial cells and debris. The bacteriophage particles were purified by the addition of polyethylene glycol (PEG MW 8000) solution (5 ml 20% PEG in 2M NaCl) and incubatioin on ice for at least 60 min. The bacteriophage were recovered by centrifugation (2 500 rpm, 20 min, 4°C, MSE 6L) and the PEG supernatant removed fully. The pellet was resuspended in 0.6 ml T-Mg medium pH 7.0-7.3, and 0.6 ml DE52 in T-Mg pH 7.0 was added. After inversion several times, the mixture was centrifuged (12 000 g, 5 min, MSE Micro Centaur) twice to remove all DE52 and the supernatant removed. Proteinase K (1 µl of freshly prepared 2 mg/ml solution) and 20% SDS (14 µl) were added. Following incubation at room temperature for 15 min, 3 M KOAc (110 µl) was added and a precipitate allowed to form (15 min at r.t). The tubes were heated to 88°C for

20 min and then incubated on ice for 10 min. The mixture was centrifuged (12 000 g, 10 min), the supernanant removed and re-centrifuged. The bacteriophage DNA was then precipitated by addition of an equal volume (700 µl) of isopropanol. After incubation at -70°C for 30 min, the DNA precipitate was pelleted (12 000 g, 10 min, 4°C), washed with 70% ethanol and resupended in 50 µl TE pH 8.0.

2.2.5 DNA SEPARATION AND PURIFICATION BY GEL ELECTROPHORESIS

2.2.5.1 Agarose Gel Electrophoresis

Agarose gel electrophoresis was carried out to separate DNA fragments of between 70 bp-12 kbp for analytical and preparative purposes. For fragments of over 200 bp, 0.6-1.5% (w/v) agarose gels were prepared by melting 0.3-0.75 g agarose (SeaKem GTG, FMC BioProducts) in 50 mls 1 x TBE (using a microwave), followed by cooling to 55°C before adding ethidium bromide (1 µg/ml) and casting in a horizontal "minigel" apparatus (105 x 105 x 45 mm). For fragments of DNA between around 70 bp and 200 bp, the same procedure was carried out, except that a mixture of 1% (w/v) SeaKem GTG agarose and 3% (w/v) NuSieve GTG agarose (FMC BioProducts) in 1 x TBE was used. Gels were allowed to set for at least 20 min at room temperature before use. Electrophoresis was carried out in a horizontal "minigel" apparatus with the gel submerged in 1 x TBE containing 0.5 µg/ml ethidium bromide. DNA samples were prepared for loading by adding one-fifth volume of glycerol loading dye. A standard with DNA fragments of known length (BRL 1 kb ladder, 20 ng/µl, loading 100 ng/lane) was also run to allow estimation of the sizes of the sample DNA fragments. Gels were run at a current of up to 150 mA at room temperature until the indicator dyes (xylene cyanol and bromophenol blue) in the glycerol loading buffer had migrated to appropriate positions (after about 45 min). The DNA fragments within gels were then visualised using UV light (302 nm, UV transilluminator TM-20, UVP), under which DNA/ethidium bromide complexes fluoresce (Sharp *et al.*, 1973), and the image was recorded using a Mitsubishi video copy processor.

2.2.5.2 Recovery of DNA Fragments From Agarose Gels

When a particular fragment of DNA in a mixture of fragments was required, e.g. in ligations or as a PCR template, it was routinely separated from other fragments by agarose gel electrophoresis. Gel slices containing the desired DNA fragments were cut from agarose mini-gels using a razor blade, carefully avoiding their exposure to U.V light. Three different methods were employed to recover DNA fragments from agarose gel slices:

(i) Electroelution

For this method, 0.8% (w/v) SeaKem agarose minigels were used. Dialysis tubing was prepared by boiling in 10 mM EDTA and was stored in this solution at 4°C. Just before use, the tubing was rinsed with 1 x TBE. The gel slice containing the DNA fragment of interest was placed in a dialysis bag with enough 1 x TBE to immerse the slice (1-2 ml). The bag was sealed and placed in the gel tank, at right angles to the direction of the current, and submerged in 1 x TBE. An electric current was passed through the bag, such that the voltage was 4-5 V/cm, for 2-4 hours at room temperature. The current was then reversed for 1 min to detach DNA from the inner wall of the bag. The eluted DNA solution was then collected, concentrated by butanol extraction if necessary, phenol/chloroform extracted and then ethanol precipitated and resuspended in an appropriate volume of TE buffer pH 8.0.

(ii) Spinning The DNA Through Glass Wool

For this method, 0.6% (w/v) SeaKem agarose minigels were used. The gel slice was put into a 0.5-ml Eppendorf tube which had been punctured at the base and packed with glass wool (2-3 mm at the bottom). This tube was then placed in a 1.5-ml Eppendorf tube and both tubes were centrifuged in a microfuge (MSE Micro Centaur) at low speed (6 000 rpm) for 10 min, and then at full speed (13 000 rpm) for another 5-10 min. The eluate which collects in the bottom tube was examined under UV light to verify the recovery of the DNA by fluorescence. The solution was phenol/chloroform extracted and the DNA precipitated with ethanol, washed with 80% ethanol and resuspended in TE pH 8.0. This method proved suitable for purifying DNA fragments of between 300 bp and 5 kbp (Heery *et al.*, 1990).

(iii) Using The QIAquick Gel Extraction Kit (Qiagen Ltd)

The QIAquick Gel Extraction Kit (Qiagen Ltd) was used according to the manufacturer's instructions.

2.2.5.3 Polyacrylamide Gel Electrophoresis

a) Non-Denaturing Gels

Non denaturing polyacrylamide gels were used to separate DNA fragments of less than 1.5 kbp. The DNA was radiolabelled so that it could be visualised by autoradiography. Polyacrylamide gels were prepared in volumes of 40 ml using appropriate amounts of 40% acrylamide:bisacrylamide (19:1; Accugel 40™, National Diagnostics) in 1 x TBE. The percentage of acrylamide in the gel varied between 3.75 and 5%, depending on the size of the DNA fragments. Gels were polymerised by the addition of 400 µl 10% ammonium persulphate and 40 µl TEMED, and cast between glass plates (20 x 39 cm) separated by 0.5 mm spacers. One plate was siliconised with dimethyldichlorosilane (BDH). Before the gel had set, wells of an appropriate size were made with a well-former. Gels were allowed to set for at least 2 h before use. Radiolabelled standard (1 kb ladder, BRL) was prepared by end-filling with both [α-^{32}P]dATP and [α-^{32}P]dCTP and was used as a size marker. The samples were prepared by adding a 1/5 volume of glycerol loading dye. The gels were run in a vertical electrophoresis apparatus using 1 x TBE as electrophoresis buffer, at 25 mA for about 2-4 h, until the indicator dyes had migrated to appropriate positions. The siliconised plate was removed and the gel, still attached to the other glass plate, was wrapped in Clingo-rap® film and exposed to X-ray film. The DNA was visualised by autoradiography.

b) Denaturing Gels

Single-stranded DNA was separated on denaturing gels containing 6% acrylamide (from stock Accugel 40™ as before) and 8 M urea in 1 x TBE. Gels were cast between glass plates (20 x 39 cm) with 0.2 mm spacers and well-formers. One plate was siliconised: the other was treated with bind-silane (silane A-174, LKB). Ammonium persulphate (300 µl, from a 10% (w/v) stock solution) and TEMED (30 µl) were added to 40 ml gel mix to polymerise the acrylamide. Samples were prepared by adding a 1/5 volume of formamide

loading dye, and heating to 85-90°C for 2 min before loading. The electrophoresis buffer was 1 x TBE. A current of 25 mA was applied across the gel for the appropriate time: if this was longer than 2 h the buffer was changed every 2-3 h. After electrophoresis was complete, the siliconised plate was removed and the gel was fixed in 10% methanol (v/v) 10% acetic acid (v/v) for 15 min, rinsed with water (15 min) and baked at 110°C until it was dry (~30 min). X-ray film was placed directly on to the dry gel and exposed at -70°C for 12-70 h.

2.2.5.4 Recovery of DNA From Polyacrylamide Gels

Double-stranded DNA fragments were purified from 3.75 to 4% non-denaturing gels. After electrophoresis, the gel was autoradiographed with fluorescent markers to allow accurate orientation of the gel with the film. After the film was developed, it was aligned with the gel and the desired band was excised with a razor blade. The gel slice was then placed in a screw-top tube (2 ml, Sarstedt) and crushed with a disposable pipette tip, and the DNA was then eluted from the gel fragments in 800 µl 2 M ammonium acetate by shaking overnight at 37-55°C. The acrylamide gel fragments were pelleted by centrifugation (12 000 g) for 3 min and the supernatant collected, phenol/chloroform extracted, and the DNA ethanol precipitated and resuspended in a suitable volume of TE buffer pH 8.0.

2.2.6 THE POLYMERASE CHAIN REACTION (PCR)

The polymerase chain reaction was used to amplify specific fragments between two oligonucleotide primers via a succession of "cycles" where the DNA template is denatured, allowed to anneal with the primers and a new strand synthesised using a thermostable DNA polymerase (Saiki *et al.*, 1988).

2.2.6.1 Standard Protocol

Typically, preparative PCR reactions were performed in a volume of 100 µl containing 100 µM each dNTP, 1 µM each oligonucleotide primer and < 1 µg template DNA. Either 2.5 U *Taq* DNA polymerase (from *Thermus aquaticus,* Perkin Elmer Cetus) or 5 U *Pfu* DNA polymerase (from *Pyrococcus furiosus,* Stratagene) which possesses a 3'-5' proofreading activity resulting in a 12-fold increase in fidelity of DNA synthesis over *Taq* DNA

polymerase, were included in the reactions. PCR reactions using *Taq* DNA polymerase were performed in 10 mM Tris-HCl pH 8.3, 50 mM KCl, 0.01% (w/v) gelatin, and 1.5 mM $MgCl_2$. *Pfu* DNA polymerase was supplied with a buffer which contained 20 mM Tris-HCl pH 8.75, 10 mM KCl, 10 mM $(NH_4)_2SO_4$, 2 mM $MgCl_2$, 0.1% Triton X-100, and 0.1 mg/ml BSA. The reaction mixtures were overlayed with paraffin oil to prevent evaporation and were subjected to a varying number of cycles of amplification in a DNA Thermal Cycler automated machine (Perkin Elmer Cetus). Generally, each cycle encompassed three stages: the DNA was denatured at 94°C (1 min): the annealing step was 1 min between 45 and 65°C (depending on the primers) and for the final extension stage the temperature was set at 72°C for 1-2 min per kbp of desired product. After amplification, the PCR products were analysed by agarose gel electrophoresis (see Section 2.2.5.1).

2.2.6.2 Combination of Two PCR Products Via PCR

When the products of two separate PCR reactions had an overlapping sequence of at least 15 bp at the end, they could be combined using PCR. The two PCR products were separated from their original templates and oligonucleotide primers, either by agarose gel or non-denaturing polyacrylamide gel electrophoresis, and were then used as templates in the combination PCR reaction: The denaturation step was followed by an annealing step in which some of the positive DNA strands from one PCR product annealed to some of the negative DNA stands from the other PCR product, via the overlapping > 15 bp sequence at their 3' ends. The annealed 3' ends were then extended via PCR to obtain a combined PCR product, which was then amplified by PCR, using the original outside oligonucleotides as primers.

2.2.6.3 Preparation of PCR Products for Cloning

PCR products were cloned either by making use of restriction sites that lay within the product or by designing oligonucleotides containing mismatches or tails at their 5' ends which artificially created suitable restriction enzyme sites at the 5' ends of the product. After amplification, the products were phenol/chloroform extracted and the DNA precipitated with ethanol. After digestion with suitable restriction enzymes, the insert was usually gel purified (see Sections 2.2.5.2 and 2.2.5.4) before ligation with the desired vector (see Section 2.2.7.4).

2.2.6.4 Screening for Recombinant Plasmids Using PCR

In some cases, PCR was employed after ligation and transformation to identify colonies which contained the desired recombinant plasmid (Section 2.2.7.7), either using two primers which annealed to the desired vector or one which annealed to the vector and one annealing within the desired insert. In this way, colonies containing the desired vector with an insert of the desired size could be selected: where one primer annealed within the insert, orientation of the insert could also be checked. Single colonies growing on LA plates were picked using sterile pipette tips and used to inoculate 15 µl LB medium. 1 µl of this was used as the template in a 20 µl PCR reaction containing 10 x PCR buffer, 100 µM dNTP, 1 µM each oligonucleotide primer and 0.5 U *Taq* DNA polymerase. Samples were usually subjected to 30 cycles of amplification, the first two being long cycles with 5 and 3 min denaturation at 94°C respectively. A 1 min denaturation step was employed in the other 28 cycles, with 30 sec annealing at an appropriate temperature, depending on the oligonucleotides used, and 2 min extension for all cycles. After the PCR reaction was complete, the products (5 µl each) were analysed on 0.8% agarose gels.

2.2.7 CLONING DNA FRAGMENTS INTO PLASMID VECTORS

2.2.7.1 Preparation of Vector DNA

Vectors for cloning were prepared by digestion of plasmid vectors with appropriate restriction endonucleases within the polylinker, in order to produce termini which were compatible with the ends of the insert which was to be used. A large scale digest was set up, with ~5 µg DNA and ~50 U enzyme plus 1 U calf intestinal phosphatase (Boehringer Mannheim) which was included in the digest in order to reduce re-circularisation during subsequent ligations. A small amount (50 ng) was electrophoresed on 0.8% agarose to check that digestion was complete: the linearised vector was then purified from a preparative agarose gel (Section 2.2.5.2). After phenol/chloroform extraction and ethanol precipitation, the purified vector was resuspended in TE pH 7.5 at a concentration of 10 ng/µl and stored at -20°C.

2.2.7.2 Preparation of Insert DNA

Insert DNA was digested with restriction endonucleases, in such a way as to produce ends which were compatible with those formed by digestion of the vector, by using the same enzymes, different enzymes which produced compatible ends, or by end-filling digested insert to produce blunt ends (see Section 2.2.7.3). Where the insert was to be subcloned from another vector, this vector was usually further cleaved with a restriction endonuclease with no sites in the insert, in order to reduce the incidence of re-formation of the original clone. After digestion and end-filling (where used), the extent of the digestion was checked by electrophoresis (~50 ng on 0.8% agarose) and the insert was then purified from a preparative agarose or acrylamide gel (Sections 2.2.5.2 and 2.2.5.4). After phenol/chloroform extraction and ethanol precipitation, the purified insert was resuspended in TE pH 8.0 at a concentration of 5-20 ng/µl.

2.2.7.3 "End Filling" of DNA Fragments With Recessed 3' Ends

DNA with 5' overhangs resulting from restriction endonuclease digestion were end-filled using the Klenow fragment of *E. coli* DNA polymerase to produce blunt ends. The reaction was performed immediately after the digest, in Klenow buffer (10 mM Tris-HCl pH 8.0, 5 mM $MgCl_2$, 0.1 mM DTT, 0.05 mg/ml BSA) with 0.05 mM dNTP and Klenow fragment (1 U/µg DNA), at r.t. for 30 min. The enzyme was inactivated by heating at 65°C for 10 min, and was then removed by phenol/chloroform extraction. The DNA was precipitated with ethanol and resuspended in TE pH 8.0 to a concentration of 5-20 ng/µl.

2.2.7.4 Ligations

Ligations were performed in a reaction volume of 10 µl with 10 ng vector DNA and a range of concentrations of insert (5-20 ng) in ligation buffer (1 mM ATP, 50 mM Tris-HCl pH 8.0, 20 mM DTT, 10 mM $MgCl_2$, 0.05 mg/ml BSA) with 2.5 U of T4 DNA ligase. The following controls were included: a ligation with 1 ng uncut vector (to test the efficiency of the transformation); a ligation with 10 ng cut vector with no insert (to assess the extent of vector recircularisation) and, in cases where the insert had been cleaved from another vector, a ligation with insert only (~10 ng) to give an indication of the background due to re-formation of the original clone or recircularisation of this vector. Ligations were incubated at r.t. for 3 h, or at 16°C overnight.

2.2.7.5 Preparation of *E. coli* Competent Cells

The NM554 *E. coli* strain was used for all transformations. Competent cells were prepared in advance and stored at -70°C. The strain was streaked on to a 2 x Ty agar plate and incubated at 37°C overnight (14-18 h). A single culture from the plate was inoculated into 20 ml TYM broth and the culture was incubated at 37°C with shaking, until midlog phase was reached ($O.D._{600}$ ~ 0.2-0.8). The culture was then transferred to a fresh flask containing 100 ml TYM and grown until the $O.D_{600}$ reached 0.5-0.9. A further 380 ml warmed TYM broth was then added to the flask and the culture was grown until a final $O.D_{600}$ of 0.6 was attained. The culture flask was placed in a tray of ice/water and agitated to ensure rapid cooling. The culture was then centrifuged (10 x 50 ml tubes) at 2 000 g (4°C, Beckman GPR benchtop centrifuge) for 15 min, and the resulting supernatant was discarded before each pellet was resuspended in 10 ml cold TfB-I by gentle pipetting and shaking on ice. The suspension was centrifuged at 2 000 g for 8 min (4°C, Beckman GPR benchtop centrifuge) and each pellet resuspended in 3 ml cold TfB-II. 0.6 ml aliquots of this cell suspension were placed in screw-top tubes, snap frozen in liquid nitrogen and were then stored at -70°C.

2.2.7.6 Transformation of *E. coli* Competent Cells with Plasmid DNA

Competent cells were thawed for 20 min on ice. 100 µl cells were added to an aliquot (2.5-10 µl) of each ligation mix and the mixture incubated on ice for 30 min. The tubes were then transferred to a water bath at 37°C and given a 5 min heat shock before the addition of 2 x Ty broth (300 µl, pre-warmed to 37°C). After a 45 min incubation at 37°C, to allow the transformed cells to start expressing their ampicillin resistance gene, an aliquot (100-300 µl) of the mixture was spread on to LA plates (90 mm) or on to nitrocellulose filters (Hybond C: Amersham International) on LA plates. The plates were allowed to dry and were then inverted and incubated overnight (14-18 h) at 37°C. The remaining transformation mix was stored at 4°C and was re-plated if necessary.

2.2.7.7 Identification of Colonies That Contain Recombinant Plasmids

If the number of colonies growing on the vector only and insert only control plates (i.e. background) was low in comparison with the number growing on the experimental plates, then screening was not usually performed, and colonies were picked at random, using

sterile pipettes, and used to inoculate media. Plasmid DNA was then prepared using the mini-prep protocol (Section 2.2.7.8) and the plasmids analysed by restriction enzyme digestion and agarose gel electrophoresis. If the background was high, colonies containing the desired plasmid were identified by screening, either with radioactive cDNA or oligonucleotide probes, or by PCR. Colony hybridisation was performed as described in Section 2.2.3.2, and PCR screening as described in Section 2.2.6.4. Plasmid DNA was then prepared from colonies which hybridised with the insert-specific radiolabelled probe or which contained inserts of the desired size.

2.2.7.8 Purification of Plasmid DNA

a) Small-Scale Preparation

Plasmid DNA was prepared on a small scale from 2-10 ml bacterial cultures, grown overnight (14-18 h) in LB medium containing ampicillin (100 μg/ml) at 37°C with shaking, either by a modification of the rapid alkaline lysis method procedure (Birnboim and Doly, 1979; Ish-Horowicz and Burke, 1981) or by using the Magic Minipreps™ kit (Promega Inc.) or the QIAprep Spin Miniprep Kit (Qiagen Inc.) according to the manufacturer's instructions. These small scale plasmid preparations typically yielded ~ 5 μg DNA.

The rapid alkaline lysis procedure was as follows: The bacterial cells (1.5 ml) were transfered to Eppendorf tubes and were pelleted by centrifugation (12 000 g, 1 min, r.t.). The pellets were then resuspended in 100 μl chilled lysis buffer (50 mM glucose, 25 mM Tris-HCl pH 8.0, 10 mM EDTA pH 7.5) by vortexing, and were incubated on ice for 5 min. Then, 200 μl of freshly prepared NaOH/SDS solution (0.2 M NaOH, 1% SDS) was added to each tube, mixed by inversion, and incubated on ice for 5 min, followed by 150 μl chilled sodium acetate (3 M, pH 4.8), the tubes inverted and the mixture incubated on ice for a further 5 min. The tubes were centrifuged (12 000 g, 5 min, 4°C, MSE Micro Centaur) to pellet the bacterial DNA precipitate: the supernatant was transferred to fresh tubes and re-spun (12 000 g, 5 min, 4°C). The supernatant was extracted once with phenol/chloroform, then once with chloroform, and the DNA then precipitated with twice the volume of ice cold ethanol. After 30 min on ice, the DNA was pelleted (12 000 g, 10 min, 4°C), washed with ice-cold 70% ethanol and resuspended in TE (50 μl, pH 8.0) containing RNase A (Sigma Type II-A from bovine pancreas) at 0.2 μg/μl.

b) Large-Scale Preparation

For large scale preparation of plasmid DNA, the Plasmid Midi, Maxi or Mega Kits (QIAGEN Inc.) were used according to the manufacturer's recommendations. These kits routinely yielded between 75-100 µg DNA (Plasmid Midi Kit), 100-500 µg DNA (Plasmid Maxi Kit) or 500-2500 µg DNA (Plasmid Mega Kit) from 25-100 ml (Plasmid Midi Kit), 100-500 ml (Plasmid Maxi Kit) or 500-2500 ml (Plasmid Mega Kit) of overnight bacterial cultures, depending on the copy number of the plasmid vector. This DNA was of transfection quality, and was used in COS-7 cell transfections (See Section 2.2.10).

2.2.8 DNA SEQUENCING

DNA sequencing was performed by the dideoxy chain termination method devised by Sanger *et al.* (1977) with double-stranded templates in the vector pBluescript, using the T7™ Sequencing kit (Pharmacia). This method depends on base-specific termination of enzyme-catalysed primer extension. Four separate reactions are performed, all containing a specific primer annealed to the template to be sequenced, all four dNTPs and one dideoxynucleic acid. The extension of the primer yields a nested set of fragments which are electrophoresed side by side in order to ascertain the order in which successively larger fragments occur in the four lanes.

2.2.8.1 Sequencing Reactions

Plasmid DNA (1-1.5 µg) was denatured for 10 min at r.t. using NaOH (0.4 M) and then precipitated with ethanol and pelleted by centrifugation (12 000 g, 4°C, 10 min). The DNA was washed with cold 80% ethanol and resuspended in water (10 µl). 2 µl sequencing primer (0.75-1.5 µM) was annealed to the template in a 14 µl reaction containing 2 µl annealing buffer (1 M Tris-HCl pH 7.6, 100 mM $MgCl_2$, 160 mM DTT) during a 20 min incubation at 37°C. The reactions were left at r.t. for at least 10 min before the labelling reaction. The labelling reaction was performed at r.t. (5 min) in labelling buffer (0.2 µM dNTP, 50 mM NaCl) containing 10 µCi [α^{35}S]-dATP and 3 U T7 polymerase, in a reaction volume of 20 µl. The termination reactions were carried out at 37°C, by the addition of 4.5 µl of labelled template to the four sequencing mixes, each containing one dideoxy nucleic acid (ddATP at 14 µM, ddCTP at 17 µM, ddGTP at 14 µM or ddTTP at 14 µM) with the corresponding dNTP at 93.5 µM and the other dNTPs at 840 µM. After 5

min the reactions were terminated by the addition of 5 µl stop solution (formamide loading dye).

2.2.8.2 Polyacrylamide Gel Electrophoresis of Sequencing Reactions

Sequencing reactions were electrophoresed on denaturing polyacrylamide gels, which were prepared as described in Section 2.2.5.3b. The wells used were approximately 4 mm wide and held about 3 µl solution. Samples were heated to 85-90°C for 5 min before loading (2 µl per lane) and electrophoresis was carried out at a constant current of 25 mA. "Short" gels (~ 1.5 h run) allowed the sequence close to the primer to be read (from about 40 bases from the primer). Longer electrophoresis times were employed if sequences further from the primer were required. After electrophoresis, the gel was treated as described in Section 2.2.5.3b.

2.2.9 COS 7 CELL CULTURE PROCEDURES

COS 7 cells are an SV40 transformed cell line originally derived from African green monkey kidney fibroblasts. The COS 7 cells used in this study were obtained from Dr. M. Puklavec, MRC Cellular Immunology Unit (CIU), Oxford.

2.2.9.1 Normal culture of COS 7 Cells

COS 7 cells were grown in cell culture flasks (Nunc, Life Tech.) in RPMI 1640 + L-Gln medium (Gibco/BRL) supplemented with 10% fetal calf serum (FCS, heat inactivated, Gibco/BRL) and kanamycin (100 µg/ml; Gibco/BRL) in a humidified tissue culture incubator (Heraeus Inc.) at 37°C, 5% CO_2. Cells were split 1/6-1/10 when they were still subconfluent (when ~80% confluency was reached) to maintain them in the fast growing logarithmic state. They were washed twice in PBS/O (GIBCO/BRL), and were then treated with trypsin (0.25% (w/v) trypsin in Gibco Solution A, ~ 0.5-1.0 ml/80 cm^2 tissue culture flask) at r.t for 5 min. Cells were then detached from the surface of the culture flasks by gentle tapping, and the trypsin inactivated by addition of full media. Cells were then either directly seeded into fresh culture flasks at the desired dilutions, or were pelleted by centrifugation (1 000 g, 10 min, r.t), resuspended in full culture medium, and then seeded into fresh culture flasks. Cells were then gassed with 5% CO_2 before being replaced into the incubator (37°C, 5% CO_2). Cells were propagated indefinitely without

any effect on transfection efficiency.

2.2.9.2 Storage of COS 7 Cell Stocks In Liquid Nitrogen

Subconfluent fast growing cells in 80 cm^2 tissue culture flasks were trypsinised as described above and sedimented by centrifugation (1 000 g, 10 min, r.t., Denley BS400 centrifuge). Each cell pellet was then resuspended in 1 ml freezing medium (heat inactivated FCS (GIBCO/BRL) + 10% DMSO (Sigma)) and was transferred into a cell freezing vial (Cryo Vials, Greiner Lab.). Vials were then frozen in a Freezing Container (Nalgene Company) at -70°C for 24 h to achieve a slow rate of cooling (1°C/min) before transfer into liquid nitrogen for long term storage.

2.2.9.3 Recovering COS 7 Cell Stocks From Liquid Nitrogen

To recover cells from liquid nitrogen, frozen vials were removed and defrosted quickly in a 37°C water bath (~ 3 min). Cells were then diluted with full culture medium (9 ml), and were sedimented (1 000 g, 10 min, r.t.) to remove DMSO in the freezing medium. Each cell pellet was then resuspended in complete medium and cultured in an 80 cm^2 flask as described above.

2.2.10 TRANSFECTION OF COS 7 CELLS

COS 7 cells were transfected by the DEAE-dextran method (Seed and Aruffo, 1987; Simmons, 1993). Constructs were cloned into either the pSVL (Pharmacia) or pcDNA3 (Invitrogen) expression vectors designed for high level transient expression in COS cell lines. COS 7 cells were seeded at ~4 x 10^6 cells/80 cm^2 flask, gassed (5% CO_2) and left at 37°C (5% CO_2). Transfections were performed 16-24 h later when cells were ~80% confluent. The medium in each flask was discarded and the cells were washed twice with 25 ml RPMI 1640 + L-Gln medium (without FCS/kanamycin). Then, 5 ml transfection mix containing 5 µg each DNA construct (prepared using the QIAGEN maxiprep Kit, in TE Buffer pH 8.0), 20 µl DEAE dextran (100 mg/ml in PBS/O, pH 7.0, stored at 4°C; Sigma) and 50 µl chloroquine (10 mM in PBS/O, made fresh, Sigma) in RPMI 1640 + L-Gln medium (without FCS/kanamycin) was added directly to the cells, and the flasks were gassed with 5% CO_2 and returned to the incubator (37°C, 5% CO_2). Cells were incubated

with the transfection mixes for 2.5-3 h. To increase transfection efficiency, flasks were removed from the incubator at roughly half-way through the incubation period and were gently swirled for ~15 sec before being returned to the incubator. After 2.5-3 h, endocytosed vesicles could be seen in the cells. The transfection mixes were then discarded and each flask washed with 25 ml PBS prior to a DMSO shock (10% DMSO in PBS, 2 min, r.t), and were then washed twice with 25 ml PBS before the addition of 30 ml complete medium. The cells were then gassed with 5% CO_2 and left at 37°C overnight (~20 h, 5% CO_2). On the following day, the cells were reseeded into fresh flasks by trypsinisation, and were then gassed with 5% CO_2 and left at 37°C, 5% CO_2 for a minimum of 24 h (24-36 h) before harvesting. When transectants were to be analysed by FACS only, transfections were performed in 80 cm^2 flasks, but when analysis by both FACS and immunoprecipitation or cell adhesion assays was required, transfections were scaled-up and performed in 175 cm^2 flasks.

2.2.11 ANALYSIS OF COS 7 TRANSFECTANTS

The expression of integrin subunits on the surface of transfected COS 7 cells was assessed using a panel of leukocyte integrin specific mouse mAbs (see Section 2.1.6). Fluorescent labelling of transfectants with specific mAbs followed by FACS analysis using a Becton Dickinson FACScan flow cytometer gave information on the level of cell surface expression, and was routinely used to monitor the efficiency of a particular set of transfections. Immunoprecipitation of integrin subunits from the surface of COS 7 transfectants using specific mAbs provided additional information on cell surface expression, whereas the ability of surface integrins to bind to ligands was assessed by analysing the performance of COS 7 transfectants in cell adhesion assays.

2.2.11.1 Harvesting Transfected COS 7 Cells

Transfected COS 7 cells were harvested 48-72 h after transfection. Each flask (80 cm^2) was washed with 10 ml detach buffer (0.5 mM EDTA in PBS/O) and the cells were then incubated for 15 min, r.t. in 5 ml detach buffer with constant agitation. Flasks were then tapped and the detached cells (5 ml) were mixed with RPMI 1640 + L-Gln medium (without FCS/kanamycin) (5 ml) and were transfered to sterilin tubes on ice.

2.2.11.2 FACS Analysis of Transfected COS 7 Cells

Harvested cells were sedimented by centrifugation (1 000 g, 10 min, r.t.) and were resuspended in PBS/O at approximately 1 x 10^7cells/ml. This cell suspension was then aliquoted into round bottom microtitre plates (Nunc/Gibco): 50 µl (~5 x 10^5 cells) were aliquoted into each well. Microtitre plates were then centrifuged (1000 g, 5 min, 4˚C) and the cell pellets resuspended in 50 µl of the desired mouse mAb (either tissue culture supernatant or purified mAb diluted in wash buffer (PBS/O, 0.1% BSA) to 20 µg/ml) and were incubated at 4˚C for 45 min. Cells were then re-pelleted by centrifugation (1000 g, 5 min, 4˚C), and were washed twice in 200 µl wash buffer (PBS/O, 0.1% BSA), before resuspension in 50 µl of the FITC-conjugated second antibody (rabbit $F(ab')_2$ anti-mouse IgG-FITC conjugate, Serotec, diluted 1/400 in wash buffer). Cells were incubated in second antibody for 30 min at 4˚C, and then the contents of each well were transfered into a FACS tube (Becton Dickinson) containing 0.5 ml fixative solution (PBS/O, 1% formaldehyde). Samples were then either stored overnight at 4˚C, or were analysed immediately on a FACScan flow cytometer (Becton Dickinson).

2.2.11.3 Immunoprecipitation Analysis of Transfected COS 7 Cells

Whole cell lysates of surface biotinylated COS 7 transfectants were immunoprecipitated using mAbs specific for the leukocyte integrin CD11 and CD18 subunits (see Section 2.1.6). Immunoprecipitated proteins were run on SDS-PAGE gels and were western blotted onto PVDF membranes. The presence of biotinylated proteins on membranes was then revealed by labelling with a streptavidin-HRP conjugate followed by enhanced chemiluminescence (ECL).

(i) Surface Biotinylation of Cells and the Preparation of Whole Cell Lysates

Harvested cells were pelleted by centrifugation (1000 g, 5 min, 4˚C) and washed twice in ice cold PBS. Cells were then resupended in ice cold PBS at ~2.5 x 10^6 cells/ml, and 200 µl cells were mixed with 200 µl sulpho-NHS-biotin (Pierce; 1 mg/ml freshly prepared in PBS) and were incubated on ice for 30 min. Labelling was quenched by addition of 5 ml ice-cold PBS-G8 (PBS containing 20 mM glycine, pH 8.0), and cells were then washed twice in 5 ml PBS-G8 to remove any unbound biotin, and were resupended in 200 µl PBS-

G8 and transfered to 1.5 ml Eppendorf tubes. Cells were lysed by addition of 1 ml freshly prepared ice cold IP-PIA buffer (Immunoprecipitation Buffer: 10 mM Tris-HCL pH 8.0, 150 mM NaCl, 2.5 mM EDTA, 1% NP40, 1 mg/ml BSA, 0.2% (w/v) sodium azide, pH 8.0, stored at 4°C, with the addition of 2.5 mM iodoacetamide, 1 mM PMSF and 75 µg/ml aprotinin) and incubation on ice, 30 min. Cell nuclei and debris were then removed by centrifugation at 13 000 g, 4°C, 15 min, and the cell lysates were transfered to fresh Eppendorf tubes and were stored at 4°C, or at -70°C for prolonged storage.

(ii) Preparation of Protein A Sepharose Conjugated to Rabbit Anti-Mouse IgG (PAS-RAM)

1 g Protein A Sepharose (PAS; Sigma) was placed in a 50 ml Falcon tube with 40 ml PBS and incubated at 4°C overnight with constant rotation. The swollen PAS (occupying a bed volume of 4 ml) was sedimented by centrifugation (3000 g, 5 min, 4°C), washed twice in 40 ml PBS, and was resupended in 16 ml PBS. 2 ml rabbit anti-mouse IgG (RAM; Sigma) was added to the PAS, and the mixture was rotated for 1 h at 4°C. The PAS-RAM conjugate was then washed once in 40 ml PBS, once in 40 ml IP Buffer (10 mM Tris-HCL pH 8.0, 150 mM NaCl, 2.5 mM EDTA, 1% NP40, 1 mg/ml BSA, 0.2% (w/v) sodium azide, pH 8.0) and was then resuspended at 25% (v/v) in a total of 16 ml IP Buffer and was stored at 4°C.

(iii) Immunoprecipitation of Biotinylated Cell Lysates

For each immunoprecipitation (IP), 100 µl cell lysate (from ~1 x 10^5 cells) was transfered to a pre-chilled 1.5 ml Eppendorf and kept on ice. Cell lysates were precleared using a mixture of two irrelevant mAbs: OX33 (IgG1) and OX34 (IgG2a), both tissue culture supernatants. 50 µl (~1 µg) OX33/OX34 was added to each cell lysate and the mixture was incubated on ice for 30 min. 25 µl PAS-RAM (25% (v/v) suspension) was then added, and the mixture rotated at 4°C for 30 min. The PAS-RAM was sedimented by centrifugation (13 000 g, 2 min, 4°C) and the lysates transfered to fresh, pre-chilled Eppendorf tubes. A further 25 µl PAS-RAM (25% (v/v) suspension) was added and the process repeated. The precleared lysates were centrifuged (13 000 g, 5 min, 4°C) to ensure thorough removal of PAS-RAM, and were transfered to fresh pre-chilled Eppendorf tubes containing 50 µl (~1 µg) of primary mAb (either tissue culture supernatant or purified mAb diluted to 20 µg/ml in PBS/O, 0.1% BSA) and were incubated on ice, 1 h. 50 µl PAS-

RAM (25% (v/v) suspension) was added and the mixtures rotated at 4°C for 1 h. The PAS-RAM was then sedimented by centrifugation (13 000 g, 2 min, 4°C) and washed once in 0.5 ml freshly prepared ice cold IP-PI 500 (IP Buffer: 10 mM Tris-HCL pH 8.0, 150 mM NaCl, 2.5 mM EDTA, 1% NP40, 1 mg/ml BSA, 0.2% (w/v) sodium azide, pH 8.0, with the NaCl concentration adjusted to 500 mM, and with the addition of 1 mM PMSF and 2.5 mM iodoacetamide), and once in 0.5 ml freshly prepared ice cold IP-PI (IP Buffer with addition of 1 mM PMSF and 2.5 mM iodoacetamide). The PAS-RAM was then resupended in 0.5 ml IP-PI and was layered over 0.5 ml sucrose cushion (IP Buffer containing 30% (w/v) sucrose), and again the PAS-RAM was sedimented by centrifugation (13 000 g, 2 min, 4°C). The supernatant was carefully removed, making sure not to disturb material at the IP-PI/sucrose cushion interface, and the PAS-RAM pellet was washed once in 0.5 ml ice cold 10 mM Tris-HCL pH 8.0, 0.05% SDS, and was then resuspended in 100 µl SDS-PAGE sample loading buffer and was vortexed gently, heated at 85°C for 3 min, vortexed again, and re-sedimented by centrifugation (13 000 g, 2 min, r.t). The resulting IP supernatants were removed and were either run directly on SDS-PAGE gels, or were stored at -20°C until use.

(iv) Polyacrylamide Gel Electrophoresis in Sodium Dodecyl Sulphate (SDS-PAGE)

Immunoprecipitation (IP) samples were run in SDS-polyacrylamide gels using a Bio-Rad vertical electrophoresis apparatus (SE 500, 12 x 14 cm) according to the method of Laemmli (1970). Lower resolving gels (containing 8.2% polyacrylamide) were made by mixing together 6.5 ml Protogel (30% acrylamide, 0.8% bisacrylamide; Ultrapure), 6 ml Lower Gel Buffer (1.5 M Tris-HCL, 0.4% SDS, pH 8.8), 11.5 ml MilliQ water, 125 µl 10% ammonium persulphate, and 12.5 µl TEMED, and were left to set overnight, before overlaying with upper stacking gels (containing 3% polyacrylamide), made by mixing together 2.5 ml Protogel (30% acrylamide, 0.8% bisacrylamide; Ultrapure), 4 ml Upper Gel Mix (0.5 M Tris-HCL, 0.4% SDS, pH 6.8), 10 ml MilliQ water, 160 µl 10% ammonium persulphate and 16 µl TEMED. Upper stacking gels were left to set for a minimum of 2 hr before use. 30 µl each IP sample was reduced in ~30-40 mM DTT by addition of 1 µl 1 M DTT followed by heating at 65°C for 5 min, as were 30 µl Prestained High Range Molecular Weight Protein Markers (Sigma) and/or 30 µl Biotinylated High Range Molecular Weight Protein Markers (Bio-Rad) (both diluted according to the manufacturer's instructions in SDS-PAGE sample loading buffer). The protein samples

were electrophoresed (at a constant voltage of 200 V for ~3 h, or at a constant current of 7 mA for ~ 18 h) until the dye marker had run off the bottom of the gel.

(v) Western Blotting

Proteins separated by SDS-PAGE were transfered to a PVDF membrane (Immobilon-P; Millipore) by western blotting. The PVDF membrane was equilibrated by washing in ethanol for 5-10 sec, then MilliQ water for 10 min, and then in Blotting Buffer (12 mM Tris-HCL, 95 mM Glycine, 10% (v/v) ethanol) for 10 min. The SDS-polyacrylamide gel was equilibrated in Blotting Buffer for 15 min. Two western blot sponges, a piece of Whatmann 3MM filter paper cut to the size of the gel (9 x 14 cm), and another piece of Whatman 3MM filter paper cut to a size slightly larger than the gel, were also pre-soaked in western blot buffer. A gel sandwich consisting of: one sponge, followed by the larger piece of Whatman 3MM filter paper, the protein gel, the PVDF membrane, the smaller piece of Whatman 3MM filter paper, and finally the second sponge, was assembled and placed in a Bio-Rad "wet blot" Western Blot Apparatus, completely immersed in western blot buffer (12 mM Tris-HCL, 95 mM Glycine, 10% (v/v) ethanol), and was western blotted at 100 V for 3 h, with the apparatus packed in ice and the buffer constantly mixed by a magnetic stirrer. After protein transfer, the PVDF membrane was transfered to blocking buffer (10 mM Tris-HCL pH 8.0, 150 mM NaCl, 0.05 % (v/v) Tween-20, 1 % (w/v) Sainsburys dried skimmed milk) and was agitated at r.t for 4-18 h.

(vi) Detection of Biotinylated Proteins on Western Blots

Biotinylated proteins which had been transfered onto PVDF membranes by western blotting were labelled with a streptavidin-HRP (Horse Radish Peroxidase) conjugate and were then detected by enhanced chemiluminescence (ECL). Membranes were removed from blocking buffer and were washed three times in PBS-T (PBS, 0.1% Tween-20) at r.t, 10 min per wash. Membranes were then incubated with the streptavidin-HRP conjugate (Amersham Int.; diluted 1:1000 in PBS-T) at r.t for 30 min with gentle agitation, and were then washed again three times in PBS-T (PBS, 0.1% Tween-20) at r.t, 10 min per wash. The membranes were then developed using an ECL Detection Kit (Amersham Int.) according to the manufacturer's recommendations, resulting in fluoresence at HRP labelled sites. Membranes were then exposed to Kodak X-Omat S film and were developed using a

Kodak X-OMAT ME-1 processor. The initial exposure time was very short (~ 1 min), and on the basis of its appearance, the exposure times for subsequent films varied (5 min-2 h).

2.2.11.4 Adhesion Assays With Transfected COS 7 Cells

An ICAM-1 fusion protein, consisting of all five IgSF domains of ICAM-1 fused to a human IgG1 Fc fragment (ICAM-1/Fc) was obtained from Dr. D.L. Simmons, Institute of Molecular Medicine, John Radcliffe Hospital, Oxford. Goat anti-human IgG (Fc specific) (SIGMA) was diluted to 10 µg/ml in 50 mM $NaHCO_3$, pH 9.0, and 100 µl was added to each well of a microtitre plate (Polysorb, Nunc Immuno-Plate). The microtitre plates were left at room temperature for 3-4 h, and were then transfered to 4 °C (cold room) overnight. The solution was then discarded and the wells washed twice with 150 µl PBS/O per well. A solution of 0.5 % BSA in PBS/O was added to each well (150 µl per well) and the plates were incubated at 37 °C for 30-45 min, and were then washed twice with PBS containing 0.1 % BSA (150 µl per well) before the addition of 50 µl per well of ICAM-1/Fc (5 µg/ml in PBS containing 0.1 % BSA). After 2-3 h at rt. the plates were washed once in PBS containing 0.1 % BSA, and then once in RPMI/HEPES/FCS (RPMI 1640 + L-Gln medium (Gibco), supplemented with 10 mM HEPES, pH 7.4 and 5% heat inactivated FCS) before use. The anti-LFA-1 mAbs (MHM23 and 1B4) were coated directly onto microtitre plates at 10 µg/ml in $NaHCO_3$, pH 9. Harvested cells were sedimented by centrifugation (1000 g, 10 min, r.t.) and were resuspended at ~4-6 x 10^5/ml in RPMI/HEPES/FCS. 50 µl cell suspension (~2-3 x 10^4 cells) was added to each ligand-coated and each anti-LFA-1 mAb-coated well. Activating and/or inhibiting mAb, when used, were mixed with cells at a final concentration of 10 µg/ml before delivery of cells into wells. The plates were incubated at 37°C for 30 min, and were then washed 3-4 times with RPMI/HEPES/FCS at r.t and were left in 100 µl RPMI/HEPES/FCS. 20 µl of freshly prepared MTT (Sigma; at 5 mg/ml in PBS, filtered through a 0.22 µm filter) was then added to each well, and the plates were incubated at 37°C for 3-4 h, during which time the MTT was taken up by cells and cleaved intracellularly to produce an insoluble formazan product (Mosmann, 1983). The plates were then centrifuged (1000 g, 5 min), the supernatants removed from wells, and 200 µl DMSO was added per well to solubilise the formazan crystals. The amount of MTT uptake by cells, which was proportional to the number of cells bound to each well, was quantitated by measuring the OD at 562 nm, using

an ELISA plate reader (Titertek Multiscan PLUS, Labsystems, Finland). To determine the amount of MTT uptake that would have been achieved by the total number cells initially aliquoted into each well, 50 µl of the initial cell suspension (~2-3 x 10^4 cells) was aliquoted into the uncoated microtitre wells of a tissue culture plate (Microwell, Nunc), and the volume was adjusted to 100 µl before the addition of 20 µl of freshly prepared MTT (Sigma; at 5 mg/ml in PBS, filtered through a 0.22 µm filter). The number of cells bound per well was then quantitated similarly. All measurements in the adhesion assay were done in triplicate.

CHAPTER THREE

GENERATING CHIMERIC, SOLUBLE TRUNCATED AND WILDTYPE INTEGRIN CONSTRUCTS

3.1 INTRODUCTION

The main aim of this project was to evaluate the role of the β subunit C-terminal cysteine-rich region in integrin structure and function. For this purpose, a series of chimeric, soluble and truncated β2 subunits were constructed, in which various segments of the C-terminal cysteine-rich, membrane proximal, transmembrane and cytoplasmic domains of β2 were either removed or were replaced with the corresponding regions from other integrin β subunits. In order to maximise the probability of retaining the overall β subunit structure, the chimeric variants were constructed from β subunits exhibiting the highest homology to β2. The β7 subunit is the most homologous to β2 at the primary amino acid level (46.5 % homologous). However, mature β7 only has 54 extracellular cysteine residues, whereas mature β2 has 56. As all 56 cysteine residues are highly conserved in the β2 subunit across species, there was concern that chimeric β2/β7 subunits might fold incorrrectly due to aberrant disulphide bond pairing. The β2 subunit is also closely related to β1 (45.7 % homologous), and all 56 extracellular cysteine residues are conserved in the mature β1 subunit. Two sets of chimeras were therefore constructed: a set of β2/β7 chimeras, and a corresponding set of β2/β1 chimeras (see Figure 3.1). The largest chimeric interchange was made in the β2V1 and β2V7 constructs. In these chimeras, the entire C-terminal cysteine-rich, membrane proximal, transmembrane and cytoplasmic domains of β2 were substituted with the corresponding regions from β1 and β7 respectively. Smaller chimeric interchanges were then made within this region. In the β2V12 and β2V72 constructs, only the C-terminal cysteine-rich and membrane proximal domains were substituted, and in the β2NS1 and β2NS7 constructs, only a small section of the C-terminal cysteine-rich region was substituted. A soluble β2 subunit, β2sol, lacking the cytoplasmic and transmembrane domains, and a truncated β2 subunit, β2tr, lacking the cytoplasmic, transmembrane, and membrane proximal regions, as well as almost the entire C-terminal cysteine-rich region, were also constructed (see Figure 3.1).

This chapter describes the construction of the chimeric, soluble, truncated and wildtype β2 cDNAs, and their cloning into expression vectors for subsequent expression studies in COS 7 cells. As COS 7 cells do not express any of the leukocyte integrin subunits, cotransfection of a wildtype αL, αM or αX construct with a β2 construct was required to produce LFA-1, Mac-1 or p150,95 heterodimers. Therefore, the construction of wildtype

Figure 3.1: The Chimeric, Soluble and Truncated β2 Subunits

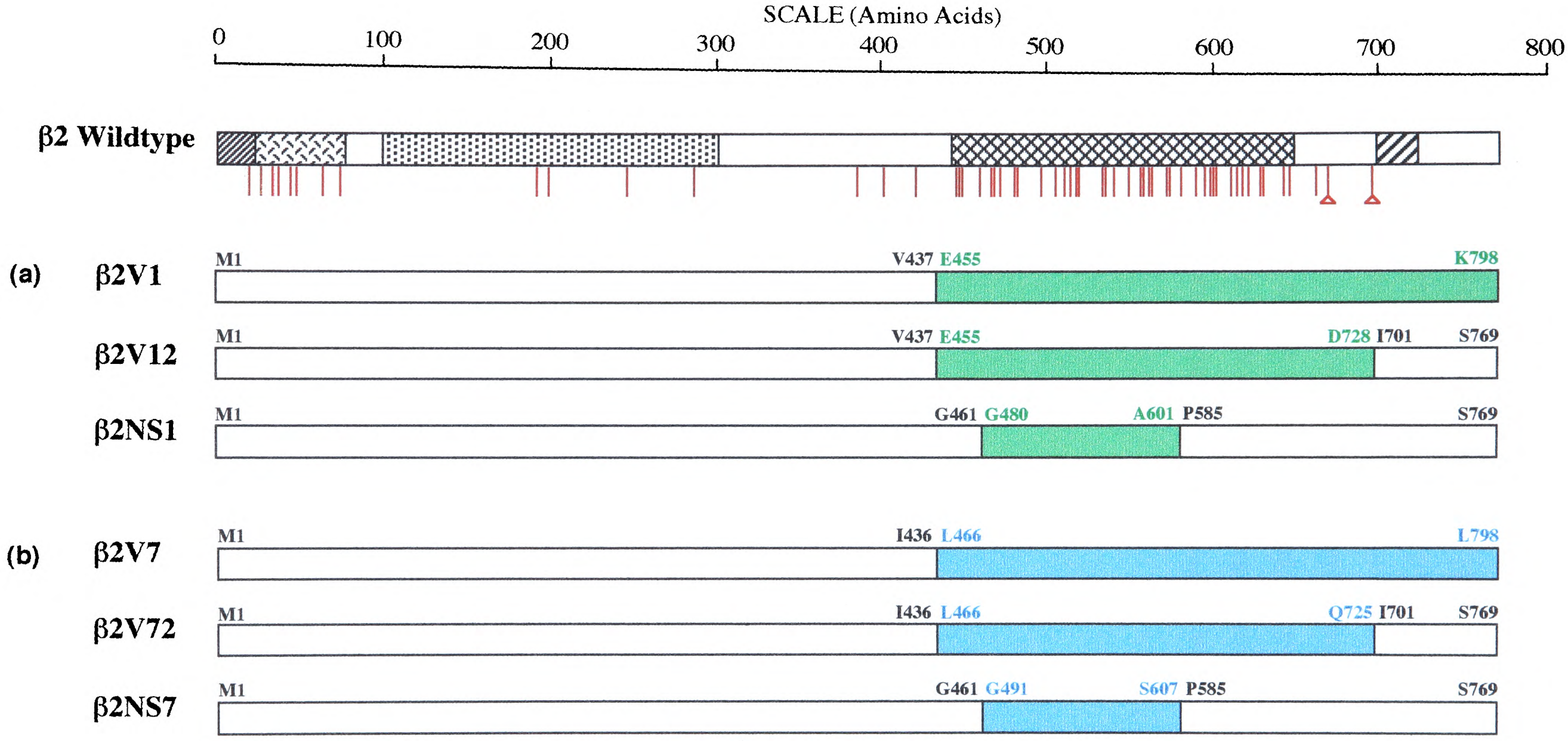
The chimeric, soluble and truncated β2 subunits discussed in this thesis are illustrated in the figure below. The wildtype β2 subunit is shown, with the narrow diagonal lines (▨) representing the leader sequence, the dashed lines (▩) the N-terminal cysteine-rich region, the dots (□) the putative A-domain, the crosshatches (▩) the C-terminal cysteine-rich region, and the larger diagonal lines (▨) the transmembrane region. The position of the single cysteine residue in the leader sequence, and the positions of the 56 extracellular cysteine residues present in the mature β2 subunit, are indicated by the vertical red lines below the β2 subunit, with each red line representing a single cysteine residue, and with the two cysteine residues missing in the β7 subunit indicated by the red triangles. Eight β2 variant subunits were constructed:

(a) three β2/β1 chimeras: β2V1, β2V12 and β2NS1,

(b) three β2/β7 chimeras: β2V7, β2V72 and β2NS7,

(c) and one soluble and one truncated β2 subunit: β2sol and β2tr.

The unshaded areas within the variant β2 subunits represent the wildtype β2 regions, the green shaded areas the wildtype β1 regions, and the blue shaded areas the wildtype β7 regions. The N- and C-terminal amino acid residues in each variant subunit are also shown, along with the residues at the beginning and the ends of each chimeric interchange (using the single letter amino acid code): the β2 residues are in black, the β1 residues are in green, and the β7 residues are in blue.


SCALE (Amino Acids)
0
100
200
300
400
500
600
700
800
β2 Wildtype
(a)
β2V1
M1
V437 E455
K798
β2V12
M1
V437 E455
D728 I701
S769
β2NS1
M1
G461 G480
A601 P585
S769
(b)
β2V7
M1
I436 L466
L798
β2V72
M1
I436 L466
Q725 I701
S769
β2NS7
M1
G461 G491
S607 P585
S769
(c)
β2sol
M1
G698
β2tr
M1
N480

αL, αM and αX cDNAs, and their cloning into expression vectors, is also described. Initially, COS 7 cells were transfected with constructs cloned into the pSVL expression vector (Pharmacia). However, subsequent transfections showed that the pcDNA1 expression vector (Invitrogen), and then its updated counterpart pcDNA3 (Invitrogen), gave much higher expression levels. The majority of the cDNAs were therefore also cloned into the pcDNA3 vector to obtain maximum expression levels on the surface of COS 7 transfectants. Since the main purpose of this chapter is to describe how the various cDNA clones were constructed, all the figures refering to each cDNA are collated and presented after the section of text which describes their construction.

3.2 RESULTS

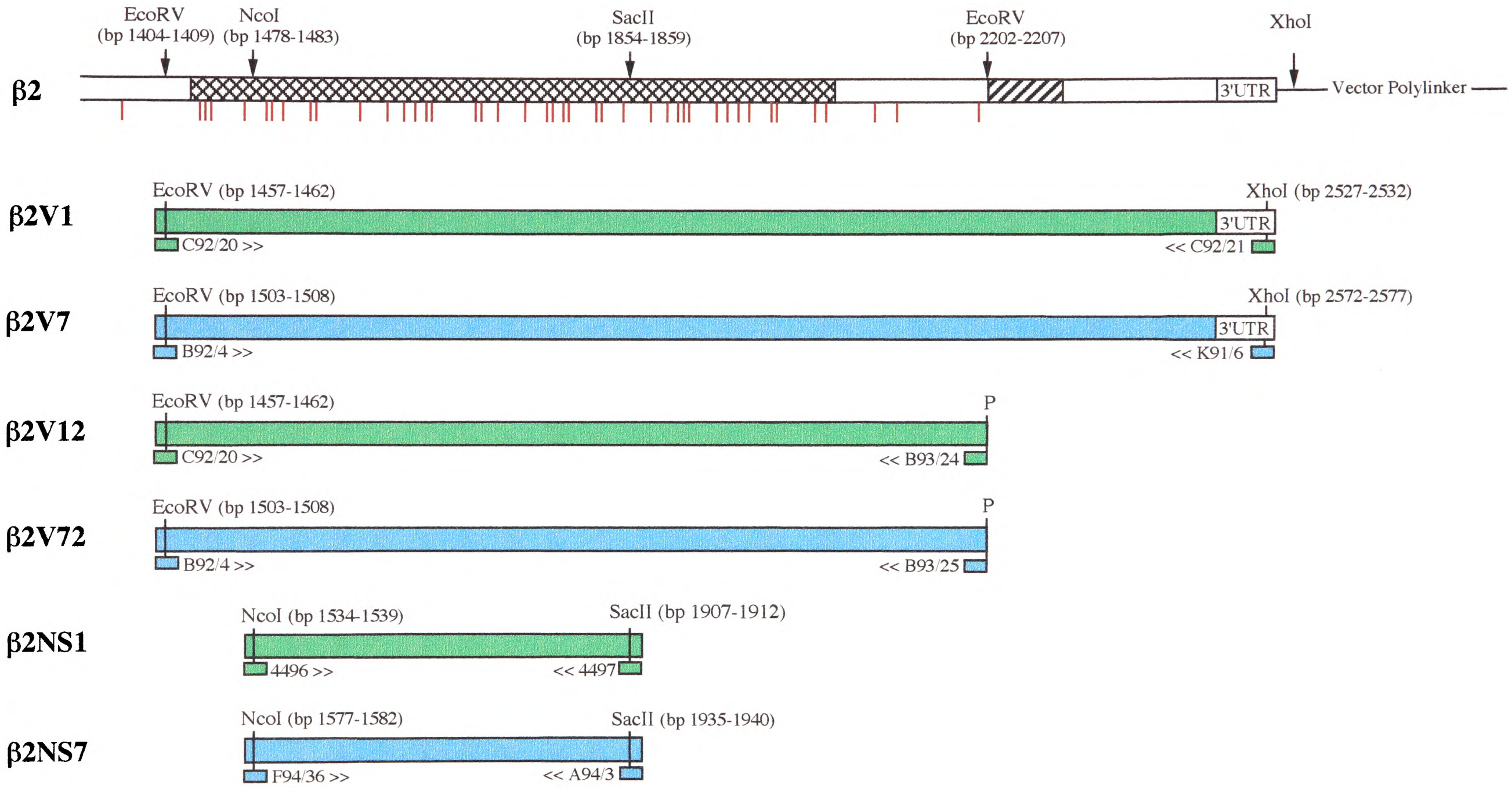
3.2.1 GENERATING CHIMERIC β2/β1 AND β2/β7 CLONES

3.2.1.1 Overall Strategy For Constructing Chimeric cDNAs

Three chimeric β2/β1 cDNAs: β2V1, β2V12, and β2NS1, and three chimeric β2/β7 cDNAs: β2V7, β2V72 and β2NS7, were constructed from a full length β2 cDNA clone as summarised in Figure 3.2. Exchanges between the β2 and the β1 and β7 cDNAs were facilitated using pairs of unique restriction enzyme sites in the β2 cDNA sequence. These sites were either present in the wildtype sequence, or were engineered into the sequence at convenient locations by oligonucleotide-directed mutagenesis. The β1 and β7 cDNA fragments spanning exchanged regions were synthesised by PCR, engineering compatible restriction enzyme sites into homologous regions with oligonucleotide primers. Chimeric β2/β1 and β2/β7 cDNAs were then constructed by digesting the β1 and β7 PCR products with the appropriate restriction enzymes, and ligating them into β2 cDNA clones cut with compatible enzymes. The resulting chimeric cDNAs were then nucleotide sequenced to confirm the correct formation of the chimeric junctions, and to confirm the absence of PCR errors in β1 and β7 cDNA sections derived from PCR amplified fragments.

Figure 3.2: Overall Strategy for Constructing Chimeric β2/β1 and β2/β7 cDNAs

Three chimeric β2/β1 cDNAs: β2V1, β2V12 and β2NS1, and three chimeric β2/β7 cDNAs: β2V7, β2V72 and β2NS7, were constructed from a full length wildtype β2 cDNA clone as summarised below. The 3' end of the wildtype β2 cDNA clone is shown, with the region encoding the C-terminal cysteine-rich region crosshatched, and the region encoding the transmembrane domain indicated by diagonal lines. Regions of the β2 cDNA encoding cysteine residues are also shown, with each vertical red line below the β2 cDNA representing a single cysteine codon. Exchanges between the wildtype β2 cDNA and the β1 and β7 cDNAs were facilitated using the unique restriction enzyme sites shown above the β2 cDNA. The NcoI site (bp 1478-1483) and the SacII site (bp 1854-1859) are present in the wildtype β2 sequence, whereas the EcoRV site (bp 1404-1409) and another EcoRV site (bp 2202-2207) were engineered into β2 cDNA clones by oligonucleotide-directed mutagenesis, and the XhoI site was located within the polylinker of the vector containing the β2 cDNA insert. β1 cDNA fragments (coloured green) and β7 cDNA fragments (coloured blue) were PCR amplified from wildtype cDNA clones using the pairs of oligonucleotide primers shown below each PCR amplified fragment. In most cases, these oligonucleotides were designed to engineer a unique restriction enzyme site into the 5' and 3' end of each PCR derived fragment, which corresponded to the site shown above in the wildtype β2 cDNA clone. Chimeric cDNAs were then constructed by exchanging the β2 cDNA fragment between two unique restriction enzyme sites with the homologous β1 or β7 PCR derived cDNA fragment which had the same two restriction enzyme sites engineered into its 5' and 3' ends. The construction of the β2V12 and β2V72 chimeric cDNAs was slightly different: an EcoRV site was introduced at the 5'end of the β1 and β7 PCR amplified fragments, but no restriction enzyme site was introduced into their 3'ends. The β1 and β7 PCR products were phosphorylated (as indicated in the figure below by a "P") and were digested with EcoRV (which cuts DNA to create a blunt end), and the β2 cDNA fragment between the two EcoRV sites was exchanged for the β1 and β7 blunt-ended PCR products. In all cases, the chimeric β2/β1 and β2/β7 junctions were created without changing the wildtype β2 and β1 or β7 amino acid sequences, and all the chimeric cDNAs clones were nucleotide sequenced to confirm the correct formation of these chimeric junctions, and to confirm the absence of PCR errors in the β1 or β7 cDNA sections derived by PCR.


β2
EcoRV
(bp 1404-1409)
NcoI
(bp 1478-1483)
SacII
(bp 1854-1859)
EcoRV
(bp 2202-2207)
XhoI
3'UTR
Vector Polylinker
β2V1
EcoRV (bp 1457-1462)
XhoI (bp 2527-2532)
3'UTR
C92/20 >>
<< C92/21
β2V7
EcoRV (bp 1503-1508)
XhoI (bp 2572-2577)
3'UTR
B92/4 >>
<< K91/6
β2V12
EcoRV (bp 1457-1462)
P
C92/20 >>
<< B93/24
β2V72
EcoRV (bp 1503-1508)
P
B92/4 >>
<< B93/25
β2NS1
NcoI (bp 1534-1539)
SacII (bp 1907-1912)
4496 >>
<< 4497
β2NS7
NcoI (bp 1577-1582)
SacII (bp 1935-1940)
F94/36 >>
<< A94/3

3.2.1.2 Obtaining Wildtype β2, β1 and β7 cDNA Clones

A full length wildtype β2 cDNA, and 3' sections of the β1 and β7 cDNAs (encoding the C-terminal region of the "mid-piece", followed by the C-terminal cysteine-rich, membrane proximal, transmembrane and cytoplasmic regions of the β1 and β7 subunits), were required to construct the chimeric β2/β1 and β2/β7 cDNA clones.

3.2.1.2.1 Obtaining a Full length Wildtype β2 cDNA Clone

A PMA-stimulated U937 cDNA library, cloned into the vector pATX, had previously been screened in Dr. Law's laboratory for β2 cDNA clones (Law *et al.*, 1987). One clone isolated from this cDNA library, named J8, contained a full length β2 cDNA insert with 101 bp of the 5' UTR and a complete 3' UTR and poly (A) tail. The J8 clone was used throughout this study as a source of wildtype β2 cDNA.

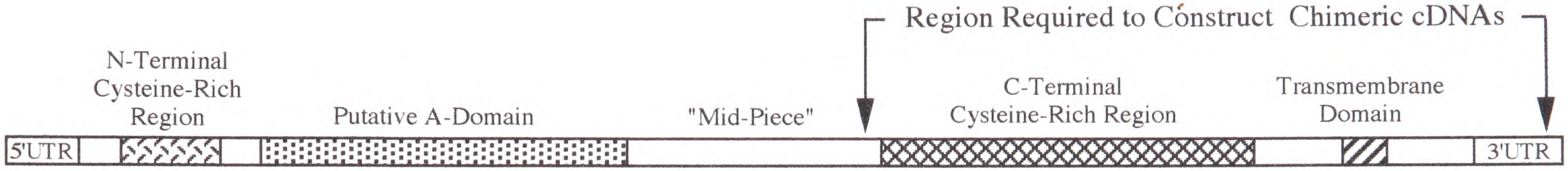
3.2.1.2.2 Obtaining a Partial β1 cDNA and a Full length β7 cDNA Clone

A human peripheral blood monocyte cDNA library, cloned into the EcoRI site of the bacteriophage lambda vector λGT10 (Clontech), was screened for β1 and β7 cDNA clones as illustrated in Figure 3.3. The 3' end of the β1 cDNA (bp, 1454-2537) and the 3' end of the β7 cDNA (bp 1500-2581) were amplified by PCR, using the cDNA library as template and the oligonucleotides C92/20 and C92/21 as primers for PCR amplification of the β1 cDNA fragment, and the oligonucleotides B92/4 and K91/6 as primers for PCR amplification of the β7 fragment (see Figure 3.3). Radiolabelled probes were then prepared from these PCR products using the cDNA Multiprime Labelling Kit (Amersham Int.), and these probes were used to screen the λGT10 cDNA library. Several recombinant bacteriophage clones positive for β1 or β7 cDNA inserts were isolated. Clones containing cDNA inserts spanning the 3' end of the β1 cDNA (bp, 1454-2537) and the 3' end of the β7 cDNA (bp 1500-2581) were then selected by PCR screening, using the oligonucleotides C92/20 and C92/21 to screen for β1 positives, and the oligonucleotides B92/4 and K91/6 to screen for β7 positives. One clone positive for the 3' end of the β1 cDNA, and one clone positive for the 3' end of the β7 cDNA, were detected. Recombinant lambda DNA was prepared from these clones and was digested with EcoRI to excise the β1 and β7 cDNA inserts. These inserts were then subcloned into EcoRI cut pBluescript, creating the clones

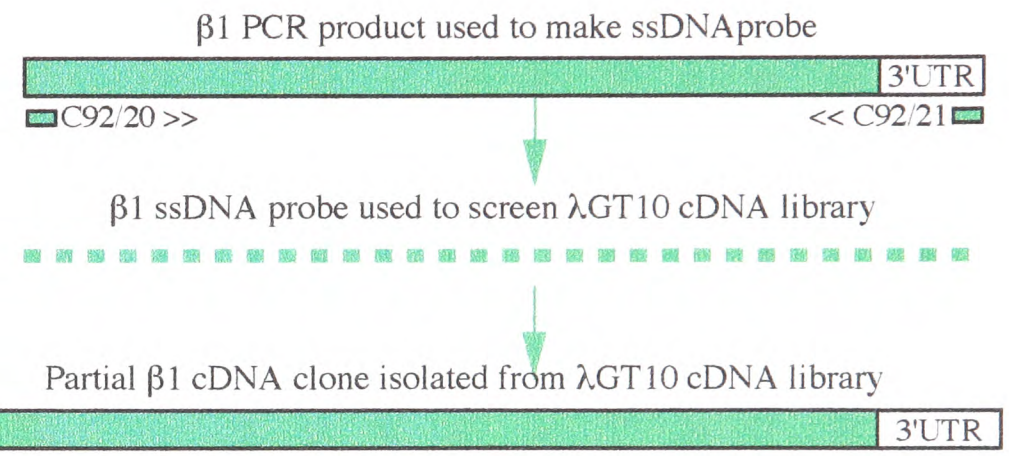
pBS/β1 and pBS/β7, which were then nucleotide sequenced to determine the exact boundaries of the β1 and β7 cDNAs. The β1 cDNA was a partial clone (bp 1369-2648), whereas the β7 cDNA was a full length clone (bp 1-2740) containing a 5' UTR and a complete 3' UTR and Poly (A) tail. Two sequences have been published for the human β7 subunit (Yuan *et al.*, 1990; Erle *et al.*, 1991) which differ by 9 amino acid residues. The full length β7 cDNA clone isolated from the lambda library was identical to the β7 sequence published by Erle *et al.* (1991). The pBS/β1 and pBS/β7 clones were used as a source of wildtype β1 and β7 cDNAs.

Figure 3.3: Screening a cDNA Library for β1 and β7 cDNA Clones

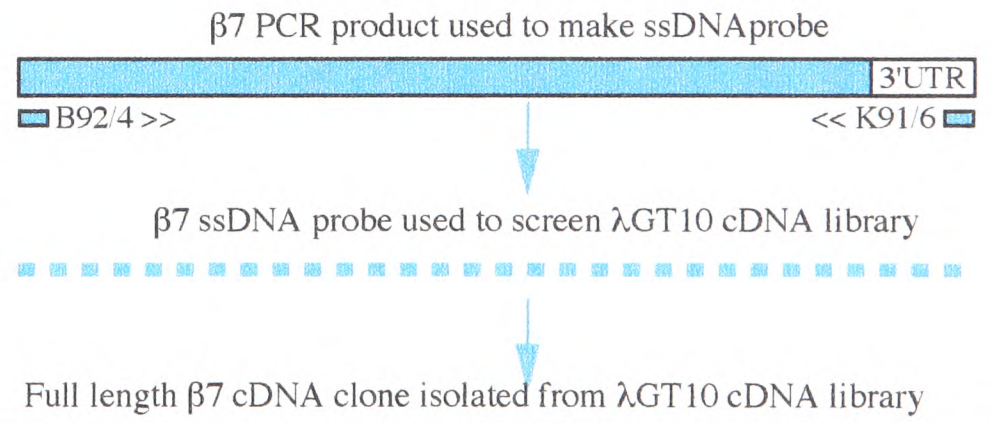
A human peripheral blood monocyte cDNA library, cloned into the bacteriophage vector λGT10 (Clonetech), was screened for β1 and β7 cDNAs as shown below. The cDNA library was used as a template to amplify the 3' end of the β1 cDNA (bp 1454-2537) with oligonucleotides C92/20 and C92/21, and the 3' end of the β7 cDNA (bp 1500-2581) with oligonucleotides B92/4 and K91/6, using the taq DNA polymerase enzyme (Stratagene). Radiolabelled DNA probes were then prepared from these PCR products using the cDNA Multiprime Labelling Kit (Amersham Int.), and the cDNA library was screened with these probes for β1 and β7 cDNAs. A partial β1 cDNA clone (bp 1369-2684) and a full length β7 cDNA clone (bp 1-2740) were obtained, and these clones were used as a source of wildtype β1 and β7 cDNAs in the subsequent construction of β2/β1 and β2/β7 chimeras.



(i) Screening for β1 cDNA clones:



(ii) Screening for β7 cDNA clones:



3.2.1.3 Constructing the Chimeric β2V1 and β2V7 cDNA Clones

3.2.1.3.1 Cloning the Wildtype β2 cDNA into pBluescript, Creating pBS/β2C

To simplify the construction of the β2V1 and β2V7 cDNAs, the wildtype β2 cDNA was subcloned into a modified pBluescript vector, pBSH. The pBSH vector was constructed as illustrated in Figure 3.4. pBluescript KS(-) was digested with SacI and EcoRV, and the SacI site 3' overhang was removed using T4 DNA polymerase. The modified pBluescript vector was then religated, creating pBSH. In this manoeuvre, a section of the pBluescript polylinker, containing the EcoRI, SacII and EcoRV sites, was removed. The full length β2 cDNA was then cloned into pBSH as illustrated in Figure 3.5. The J8 clone was digested with ClaI/XhoI, and the ClaI-XhoI β2 cDNA fragment was then cloned into ClaI/XhoI cut pBSH. This created pBS/β2C, a full length β2 cDNA clone (bp 1-2843) in pBluescript, which had restriction enzyme polylinker sites convenient for the subsequent construction of the β2V1 and β2V7 chimeric cDNAs.

3.2.1.3.2 Engineering an EcoRV Site into pBS/β2C, Creating pBS/β2V

In order to construct the chimeric β2V1 and β2V7 cDNAs, a unique EcoRV site (β2, bp 1404-1409) was engineered into pBS/β2C, creating a clone named pBS/β2V. The construction of pBS/β2V is summarised in Figure 3.6a. A β2 PCR product (bp 962-1910), incorporating the EcoRV site mutation (bp 1404-1409), was synthesised using the site-directed mutagenesis procedure described in Figure 3.6b. Four oligonucleotides: K89/17, J91/26, J91/27 and E89/02, were designed for this purpose. The sequences of these oligonucleotides and their positions in the β2 cDNA sequence are shown in Figure 3.6c. The mutant PCR product (bp 962-1910) was cloned into pBS/β2C using the unique EcoRI (β2, bp 993-998) and SacII (β2, bp 1854-1859) sites. pBS/β2C was digested with EcoRI/SacII, and the normal EcoRI-SacII fragment replaced with the mutant EcoRI-SacII fragment. This created pBS/β2V, a full length β2 cDNA clone (β2V, bp 1-2843) in pBluescript, containing a convenient EcoRV site (β2V, bp 1404-1409). The pBS/β2V clone was then nucleotide sequenced to confirm the presence of the EcoRV site, and to confirm the absence of PCR errors in the EcoRI-SacII PCR derived section. Two DNA point mutations, C to T^{1406} and A to C^{1409}, were introduced into the wildtype β2 cDNA

sequence to create pBS/β2V. However, both these mutations were silent, and did not alter the resulting β2 coding sequence. pBS/β2V was used to construct the chimeric β2V1 and β2V7 cDNAs.

3.2.1.3.3 Constructing the Chimeric β2V1 cDNA from pBS/β2V, Creating pBS/β2V1

The chimeric β2V1 cDNA was constructed from pBS/β2V as illustrated in Figure 3.7a, creating a clone named pBS/β2V1. Exchanges between the β2 and the β1 subunit were facilitated using the pBS/β2V unique EcoRV site (β2V, bp 1404-1409) and unique XhoI site (pBS/β2V, 3' polylinker). pBS/β2V was digested with EcoRV and XhoI, which excised the β2 cDNA fragment encoding the C-terminal cysteine-rich, membrane proximal, transmembrane and cytoplasmic domains. The β1 cDNA encoding these domains was then synthesised by PCR, using the pBS/β1 clone as template and the oligonucleotides C92/20 and C92/21. The C92/20 oligonucleotide was designed to engineer an EcoRV site into the 5' end of the PCR product (β1, bp 1457-1462) and the C92/21 oligonucleotide to engineer an XhoI site into the 3' end (β1, bp 2527-2532). The sequences of these oligonucleotides and their positions in the β1 cDNA sequence are shown in Figure 3.7b. The β1 PCR product was digested with EcoRV and XhoI, and the chimeric β2V1 cDNA was then constructed by replacing the pBS/β2V EcoRV-XhoI fragment with the β1 EcoRV-XhoI fragment. The resulting pBS/β2V1 clone was then nucleotide sequenced to confirm the correct formation of the chimeric β2/β1 junction at the EcoRV site, and to confirm the absence of PCR errors in the PCR derived β1 section. The construction of the β2V1 EcoRV site chimeric junction is shown in detail in Figure 3.7c. The β2V1 chimera was created without introducing any amino acid mutations into the β2 and β1 sections.

3.2.1.3.4 Constructing the Chimeric β2V7 cDNA from pBS/β2V, Creating pBS/β2V7

The chimeric β2V7 cDNA was constructed from pBS/β2V in a similar way, creating a clone named pBS/β2V7. The construction of pBS/β2V7 is illustrated in Figure 3.8a. The β7 cDNA spanning the exchanged region was synthesised by PCR, using pBS/β7 as template and the oligonucleotides B92/4 and K91/6. The B92/4 oligonucleotide was designed to engineer an EcoRV site into the 5' end of the PCR product (β7, bp 1503-1508), and the

oligonucleotide K91/6 to engineer an XhoI site into the 3' end (β7, bp 2572-2577). The sequences of these oligonucleotides and their positions in the β7 cDNA sequence are shown in Figure 3.8b. This β7 PCR product was digested with EcoRV and XhoI, and the chimeric β2V7 cDNA was then constructed by replacing the pBS/β2V EcoRV-XhoI fragment with the β7 EcoRV-XhoI fragment. The resulting pBS/β2V7 clone was then nucleotide sequenced to confirm the correct formation of the chimeric β2/β7 junction at the EcoRV site, and to confirm the absence of PCR errors in the PCR derived β7 section. The construction of the β2V7 EcoRV site chimeric junction is shown in detail in Figure 3.8c. The β2V7 chimera was also created without introducing any amino acid mutations into the β2 and β7 sections.

3.2.1.3.5 Cloning the Chimeric β2V1 and β2V7 cDNAs into Expression Vectors

The full length β2V1 and β2V7 cDNAs were initially subcloned from pBluescript into the vector pKG4 (from Dr G.K. Gould) for stable expression in B cell lines. They were then subcloned from the pKG4 vector into the pSVL vector (Pharmacia), and subsequently into the pcDNA3 vector (Invitrogen), for transient expression in COS 7 cells.

3.2.1.3.5.1 Constructing the pKG4/β2V1 Clone

The β2V1 cDNA was subcloned from pBluescript into the pKG4 expression vector as illustrated in Figure 3.9a. The entire coding region of the β2V1 cDNA was excised from pBS/β2V1 by digestion with HindIII (pBS/β2V1, 5' polylinker) and XhoI (β2V1 cDNA, 3' UTR), and was cloned into HindIII/XhoI cut pKG4, creating a clone named pKG4/β2V1.

3.2.1.3.5.2 Constructing the pKG4/β2V7 Clone

The β2V7 cDNA was subcloned from pBluescript into the pKG4 expression vector as illustrated in Figure 3.9b. The entire coding region of the β2V7 cDNA was excised from pBS/β2V7 by digestion with HindIII (pBS/β2V7, 5' polylinker) and XhoI (β2V7 cDNA, 3' UTR), and was cloned into HindIII/XhoI cut pKG4, creating a clone named pKG4/β2V7.

3.2.1.3.5.3 Constructing the pSVL/β2V1 Clone

The β2V1 cDNA was subcloned from pKG4 into the pSVL expression vector as illustrated in Figure 3.9c. pKG4/β2V1 was digested with XhoI (β2V1 cDNA, 3' UTR) and the

resultant 5' overhang was blunted using the end-filling reaction. The entire coding region of the β2V1 cDNA was then excised by digestion with XbaI (β2V1, 5' UTR) and was purified by agarose gel electrophoresis. The pSVL/αL clone (which was a gift of Dr. G. Otulakuski, Toronto) was used as a source of pSVL vector. pSVL/αL was digested with XbaI (pSVL, 5' polylinker) and SmaI (pSVL, 3' polylnker), and the pSVL vector purified by agarose gel electrophoresis. pSVL/β2V1 was then constructed by ligating the XbaI/XhoI-endfilled β2V1 cDNA insert into the XbaI/SmaI cut pSVL vector.

3.2.1.3.5.4 Constructing the pSVL/β2V7 Clone

The β2V7 cDNA was subcloned from pKG4 into the pSVL expression vector as illustrated in Figure 3.9d. pKG4/β2V7 was digested with XhoI (β2V7 cDNA, 3' UTR) and the resultant 5' overhang was blunted using the end-filling reaction. The entire coding region of the β2V7 cDNA was then excised by digestion with XbaI (β2V7, 5' UTR). The β2V7 cDNA insert was then purified by agarose gel electrophoresis. The pSVL/αL clone (which was a gift of Dr. G. Otolakuski, Toronto) was used as a source of pSVL vector. pSVL/αL was digested with XbaI (pSVL, 5' polylinker) and SmaI (pSVL, 3' polylinker), and the pSVL vector was purified by agarose gel electrophoresis. pSVL/β2V7 was then constructed by ligating the XbaI/XhoI-endfilled β2V7 cDNA insert into the XbaI/SmaI cut pSVL vector.

3.2.1.3.5.5 Constructing the pcDNA3/β2V1 Clone

The β2V1 cDNA was subcloned from pSVL into the pcDNA3 expression vector as illustrated in Figure 3.9e. The entire coding region of the β2V1 cDNA was excised from pSVL/β2V1 by digestion with XhoI (pSVL/β2V1, 5' polylinker; β2V1 cDNA, 3' UTR) and was ligated into XhoI cut pcDNA3, creating a clone named pcDNA3/β2V1. The orientation of the β2V1 cDNA in the expression vector was determined by EcoRV digestion. Clones producing a 1.45 kbp restriction fragment were in the correct orientation.

3.2.1.3.5.6 Constructing the pcDNA3/β2V7 Clone

The β2V7 cDNA was subcloned from pSVL into the pcDNA3 expression vector as illustrated in Figure 3.9f. The entire coding region of the β2V7 cDNA was excised from pSVL/β2V7 by digestion with XhoI (pSVL/β2V7, 5' polylinker; β2V7 cDNA, 3' UTR),

and was ligated into XhoI cut pcDNA3. The orientation of the β2V7 cDNA in the expression vector was then determined by EcoRV digestion. Clones producing a 1.45 kbp restriction fragment were in the correct orientation.

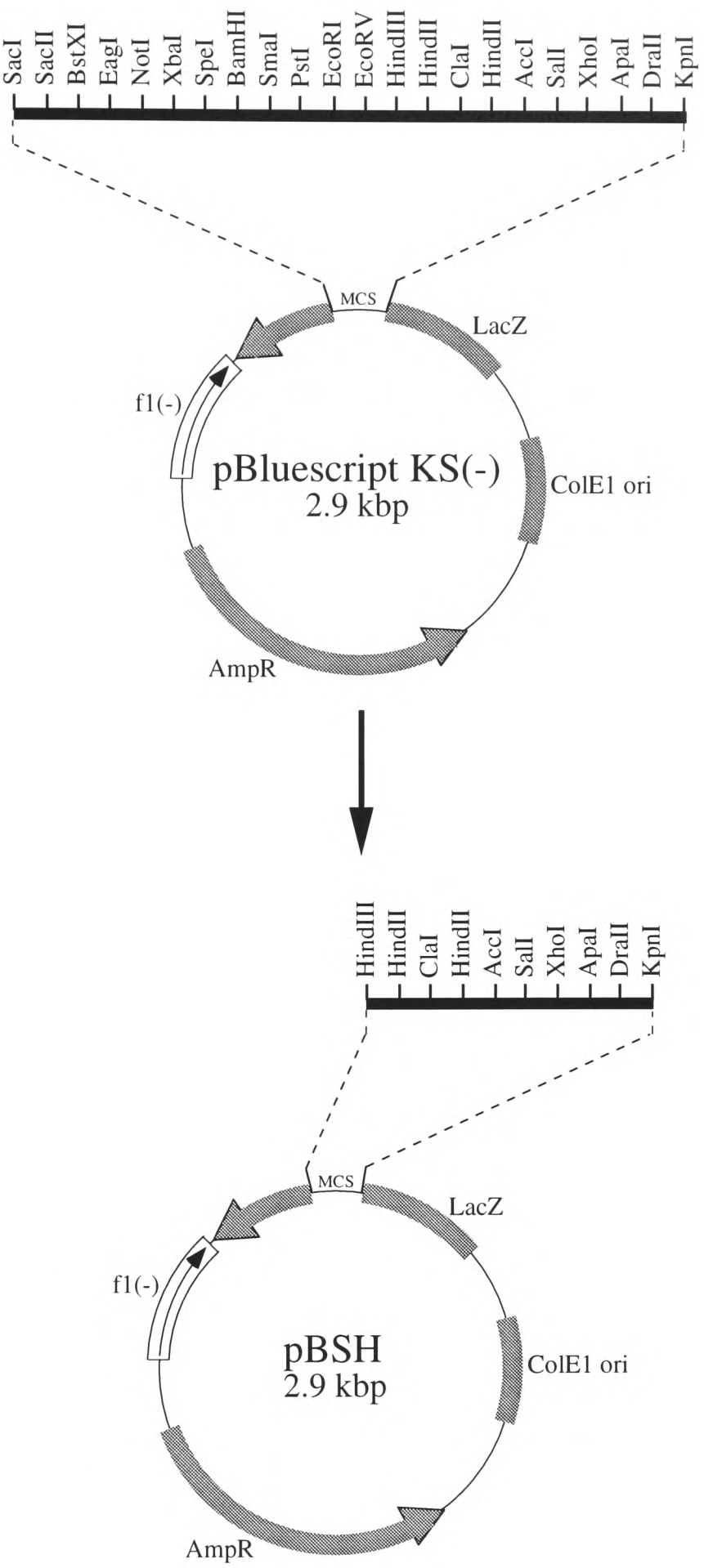


Figure 3.4: Constructing pBSH

pBluescript KS(-) (Stratagene) was modified to remove the EcoRI, SacII and EcoRV restriction enzyme polylinker sites, creating a clone named pBSH. The pBluescript vector was digested with SacI and EcoRV, and the SacI site 3' overhang blunted using T4 DNA polymerase. The 2.9 kbp vector band was then purified by agarose gel electrophoresis and was religated, creating pBSH. The modified sequence of the pBSH polylinker was confirmed by nucleotide sequencing.

Figure 3.5: Constructing pBS/β2C

The full length β2 cDNA (bp 1-2843) was cloned into the modified pBluescript vector pBSH, creating pBS/β2C, as follows:

(1) J8 was digested with ClaI and XhoI to excise the 2.8 kbp β2 cDNA insert, which was then purified from the pATX vector by agarose gel electrophoresis.

(2) pBSH was digested with ClaI and XhoI, and the 2.9 kbp pBSH vector was also purified by agarose gel electrophoresis.

(3) The pBSH vector and β2 cDNA insert were then ligated, creating a full length β2 cDNA clone in pBluescript, named pBS/β2C.

In the figure opposite, the region in the β2 cDNA encoding the N-terminal cysteine rich region is represented by the dashed lines, the region encoding the putative A-domain by the dots, the region encoding the C-terminal cysteine-rich region by the crosshatches, and the region encoding the transmembrane domain by the diagonal lines. The 5' and 3' untranslated regions (UTRs) of the β2 cDNA are also shown.

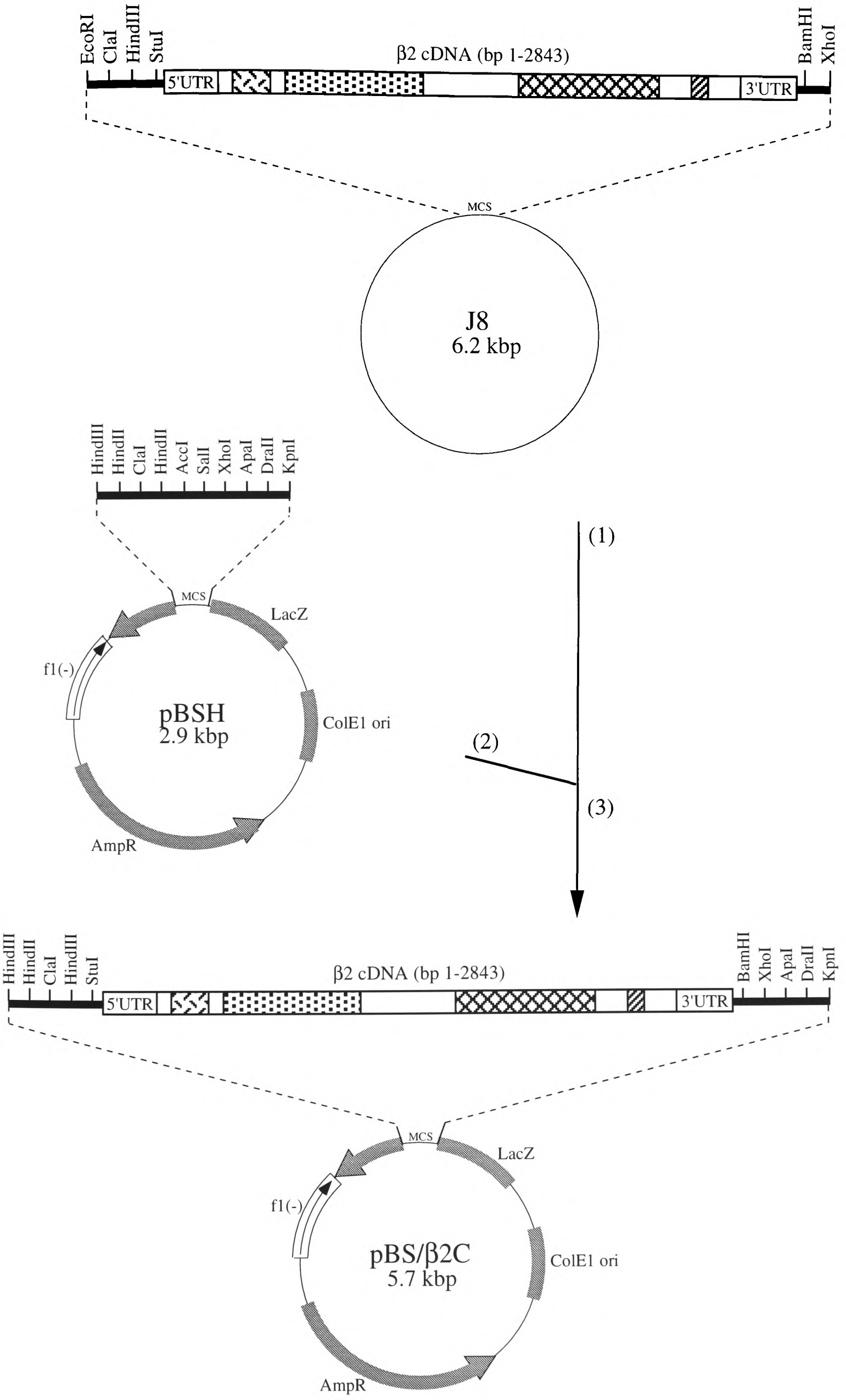

EcoRI
ClaI
HindIII
StuI
β2 cDNA (bp 1-2843)
BamHI
XhoI
5'UTR
3'UTR
MCS
J8
6.2 kbp
HindIII
HindII
ClaI
HindII
AccI
SalI
XhoI
ApaI
DraII
KpnI
MCS
LacZ
f1(-)
pBSH
2.9 kbp
ColE1 ori
AmpR
(1)
(2)
(3)
HindIII
HindII
ClaI
HindIII
StuI
β2 cDNA (bp 1-2843)
BamHI
XhoI
ApaI
DraII
KpnI
5'UTR
3'UTR
MCS
LacZ
f1(-)
pBS/β2C
5.7 kbp
ColE1 ori
AmpR

Figure 3.6a: Constructing pBS/β2V

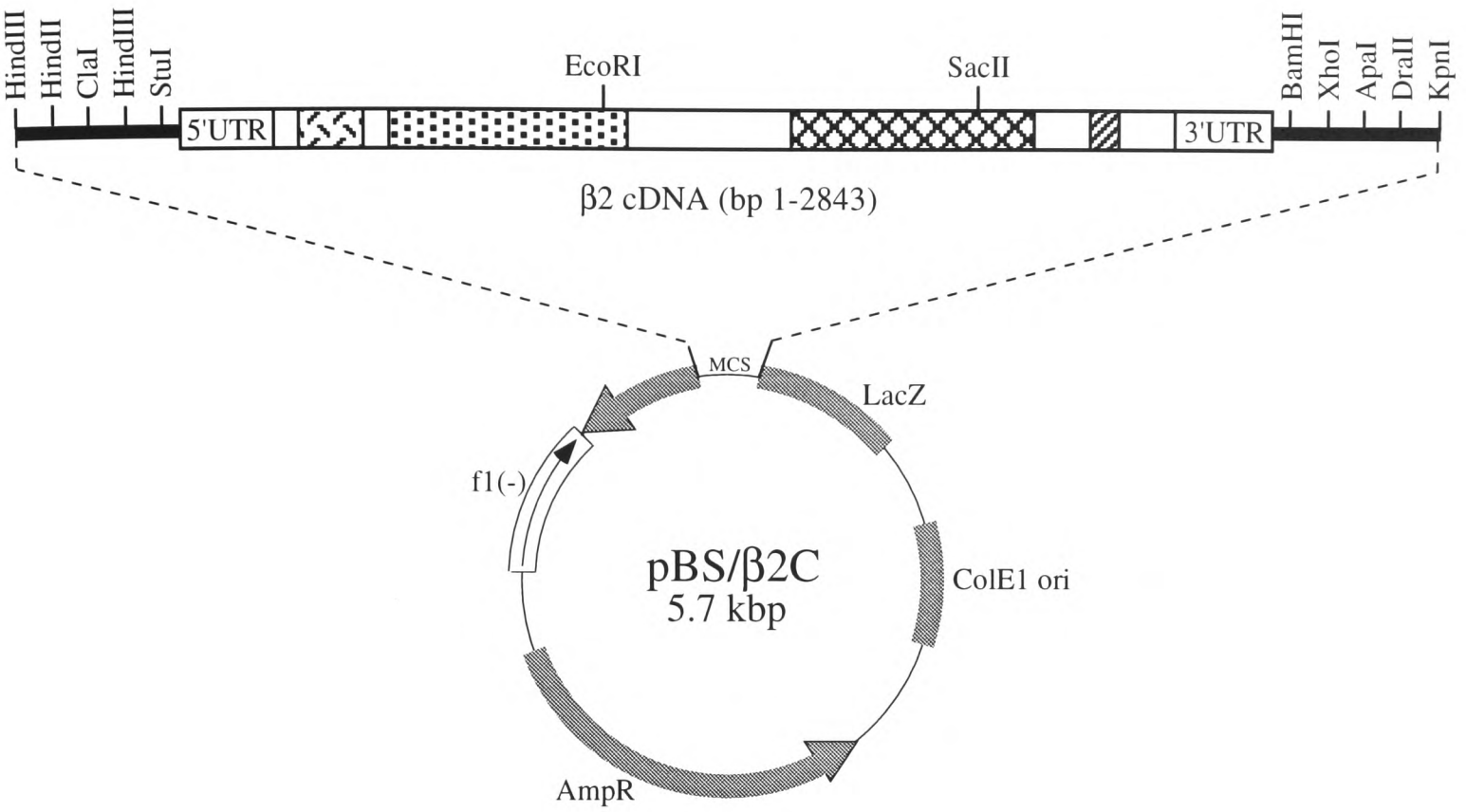
A unique EcoRV site was engineered into the wildtype β2 cDNA (bp 1404-1409) of the pBS/β2C clone, creating a clone named pBS/β2V, as follows:

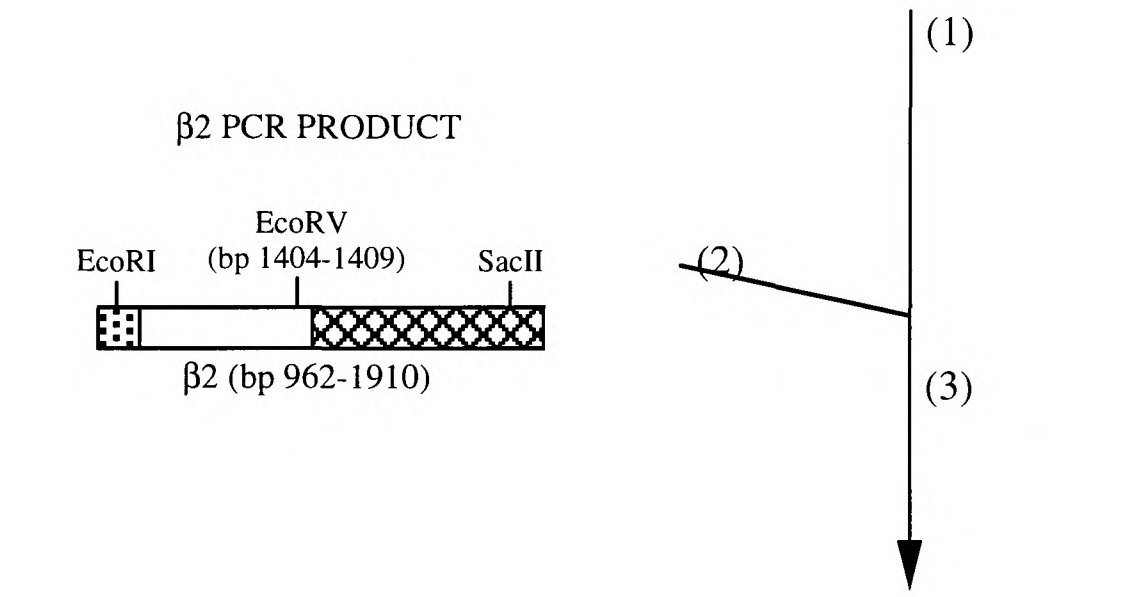
(1) pBS/β2C was digested with EcoRI (β2 cDNA, bp 993-998) and SacII (β2 cDNA, bp 1854-1859), and the larger 4.75 kbp pBS/β2C fragment was purified by agarose gel electrophoresis.

(2) A β2 PCR product (bp 962-1910), incorporating the EcoRV site mutation (bp 1404-1409), was synthesised using the site-directed mutagenesis procedure described in Figures 3.6b and 3.6c. This PCR product was digested with EcoRI and SacII, and the 950 bp EcoRI-SacII PCR fragment was also purified by agarose gel electrophoresis.

(3) The 950 bp PCR fragment and the 4.75 kbp pBS/β2C fragment were then ligated, creating pBS/β2V, a full length β2 cDNA (bp 1-2843), containing a unique EcoRV site (bp 1404-1409), in pBluescript. The pBS/β2V clone was nucleotide sequenced to confirm the presence of the EcoRV site, and to confirm the absence of PCR errors in the EcoRI-SacII section derived by PCR. The EcoRV site was introduced into the β2 cDNA without altering the amino acid sequence of the resulting β2 subunit.

In the figure opposite, the region in the β2 cDNA encoding the N-terminal cysteine rich region is represented by the dashed lines, the region encoding the putative A-domain by the dots, the region encoding the C-terminal cysteine-rich region by the crosshatches, and the region encoding the transmembrane domain by the diagonal lines. The 5' and 3' untranslated regions (UTRs) of the β2 cDNA are also shown.


HindIII
HindII
ClaI
HindIII
StuI
EcoRI
SacII
BamHI
XhoI
ApaI
DraII
KpnI
5'UTR
3'UTR
β2 cDNA (bp 1-2843)
MCS
LacZ
f1(-)
pBS/β2C
5.7 kbp
ColE1 ori
AmpR


β2 PCR PRODUCT
EcoRV
EcoRI
(bp 1404-1409)
SacII
β2 (bp 962-1910)
(1)
(2)
(3)

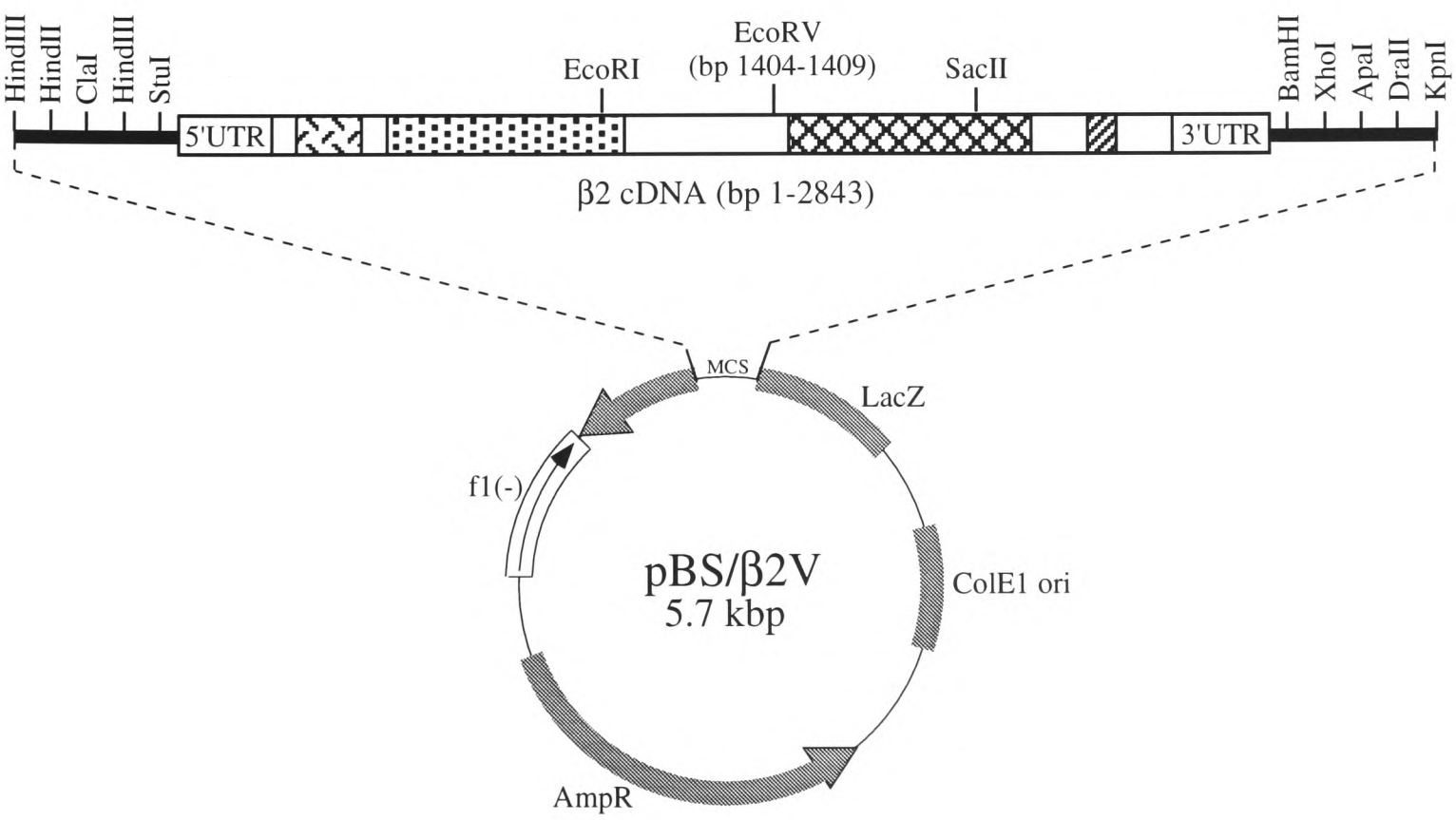

HindIII
HindII
ClaI
HindIII
StuI
EcoRI
EcoRV
(bp 1404-1409)
SacII
BamHI
XhoI
ApaI
DraII
KpnI
5'UTR
3'UTR
β2 cDNA (bp 1-2843)
MCS
LacZ
f1(-)
pBS/β2V
5.7 kbp
ColE1 ori
AmpR

Figure 3.6b: Engineering an EcoRV Site into the Wildtype β2 cDNA Clone by PCR Generated Site-Directed Mutagenesis

Four oligonucleotide primers; K89/17, J91/26, J91/27 and E89/02 were designed to create the EcoRV site. The position of these oligonucleotides in the β2 cDNA sequence is indicated by the arrows, with the raised region representing the EcoRV site mutation. J91/26 and J91/27 were designed to anneal to exactly the same section of the β2 cDNA but to opposite strands, and contained the EcoRV site mutation (see Figure 3.6c). PCR 1 and PCR 2 were performed separately, using pBS/β2C as template and taq DNA polymerase. The resulting PCR products were then separated from template and excess primers by agarose gel electrophoresis, and were then mixed, denatured and allowed to reanneal. Some of the molecules recombined as shown through the overlap made by the J91/26 and J91/27 primers. These recombinants were then DNA chain extended, producing a molecule which could be used as a template for PCR 3. The resulting PCR 3 product, containing the EcoRV site mutation, was then cloned into the wildtype β2 cDNA using the unique EcoRI and SacII restriction enzyme sites (see Figure 3.6a). pBS/β2C was cut with EcoRI and SacII, and the normal EcoRI-SacII fragment replaced with the PCR 3 mutant EcoRI-SacII fragment. The resulting clone, pBS/β2V, was then nucleotide sequenced to confirm the presence of the EcoRV site mutation and to confirm the absence of taq DNA polymerase errors in the PCR derived EcoRI-SacII section.

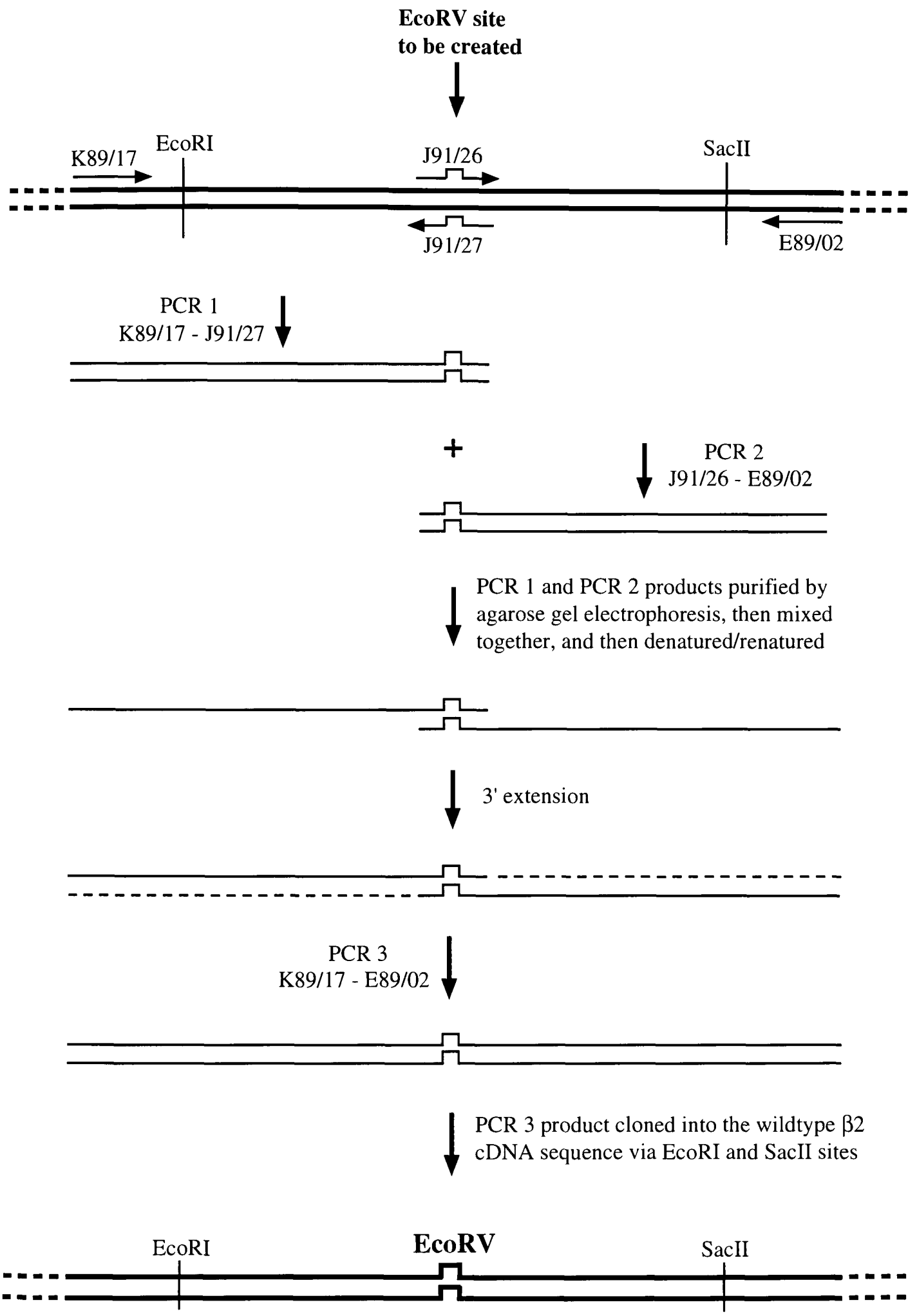

EcoRV site
to be created
K89/17
EcoRI
J91/26
SacII
J91/27
E89/02
PCR 1
K89/17 - J91/27
+
PCR 2
J91/26 - E89/02
PCR 1 and PCR 2 products purified by
agarose gel electrophoresis, then mixed
together, and then denatured/renatured
3' extension
PCR 3
K89/17 - E89/02
PCR 3 product cloned into the wildtype β2
cDNA sequence via EcoRI and SacII sites
EcoRI
EcoRV
SacII

Figure 3.6c: The Sequence and Position of the Oligonucleotides K89/17, J91/26, J91/27 and E89/02

The oligonucleotides K89/17, J91/26, J91/27 and E89/02 were designed to engineer an EcoRV site into the wildtype β2 cDNA sequence (at position: bp 1404-1409). Relevant sections of the wildtype β2 cDNA sequence are shown in the figure opposite, with the amino acid residues encoded by these sections shown above the cDNA sequence (using the single letter amino acid code), and nucleotide residues representing relevant restriction enzyme sites coloured pink. The cysteine residues, which are numbered in accordance with the first cysteine residue in the extracellular region of the mature β2 polypeptide being designated C1 and the last being designated C56, are coloured red. The sequence of the K89/17, J91/26, J91/27 and E89/02 oligonucleotides and their annealing positions in the β2 cDNA sequence is shown, with residues matching the wildtype sequence marked by vertical lines and any mismatched residues by dots. The J91/26 and J91/27 oligonucleotides were designed to anneal to exactly the same section of the β2 cDNA but to opposite strands, and contained the EcoRV site mutation, whilst the K89/17 and E89/02 oligonucleotides matched the wildtype sequence. K89/17 and J91/27 were used to synthesise PCR product 1, and J91/26 and E89/02 PCR product 2 (see Figure 3.6b). These two PCR products were then mixed together and were used to make PCR product 3, using the outside primers K89/17 and E89/02 (see Figure 3.6b). This PCR product was then digested with EcoRI and SacII, and the EcoRI-SacII wildtype fragment from pBS/β2C was substituted with the mutant EcoRI-SacII PCR derived fragment, creating a full length β2 cDNA clone in pBluescript with a unique EcoRV site at position: bp 1404-1409, clone pBS/β2V (see Figure 3.6a).

```
D  G  R C11 H  L  E  D  N  L  Y  K  R  S  N  E  F  D
      K89/17» CCTGGAGGACAACTTGTAC »K89/17
              ||||||||||||||||||||
GACGGCCGCTGTCACCTGGAGGACAACTTGTACAAGAGGAGCAACGAATTCGAC - - -
950       960       970       980       990  EcoRI
CTGCCGGCGACAGTGGACCTCCTGTTGAACATGTTCTCCTCGTTGCTTAAGCTG - - -
```

EcoRV Site to be Created

```
F  V  I  R  A  L  G  F  T  D  I  V  T  V  Q  V  L  P  Q C15 E
          J91/26>> GCTTCACGGATATCGTGACCGTGC >>J91/26
                   ||||||||||·||·||||||||||
- - - TTTGTCATCCGGGCGCTGGGCTTCACGGACATAGTGACCGTGCAGGTCCTTCCCCAGTGTGAG - -
      1380      1390      1400      1410      1420      1430
- - - AAACAGTAGGCCCGCGACCCGAAGTGCCTGTATCACTGGCACGTCCAGGAAGGGGTCACACTC - -
                   ||||||||||·||·||||||||||
                J91/27<< CGAAGTGCCTATAGCACTGGCACG <<J91/27
```

```
   N  P  R  R  V  E C41 S  G  R  G  R C42 R C43 N  V C44 E C45 H  S  G  Y
- - AACCCGCGGCGTGTTGAGTGTAGTGGTCGTGGCCGGTGCCGCTGCAACGTATGCGAGTGCCATTCAGGCT
     SacII        1870      1880      1890      1900      1910      1920
- - TTGGGCGCCGCACAACTCACATCACCAGCACCGGCCACGGCGACGTTGCATACGCTCACGGTAAGTCCGA
                                                ||||||||||||||||||
                                          E89/02« GACGTTGCATACGCTCACG «E89/02
```

Figure 3.7a: Constructing the Chimeric β2V1 cDNA in pBluescript, Creating pBS/β2V1

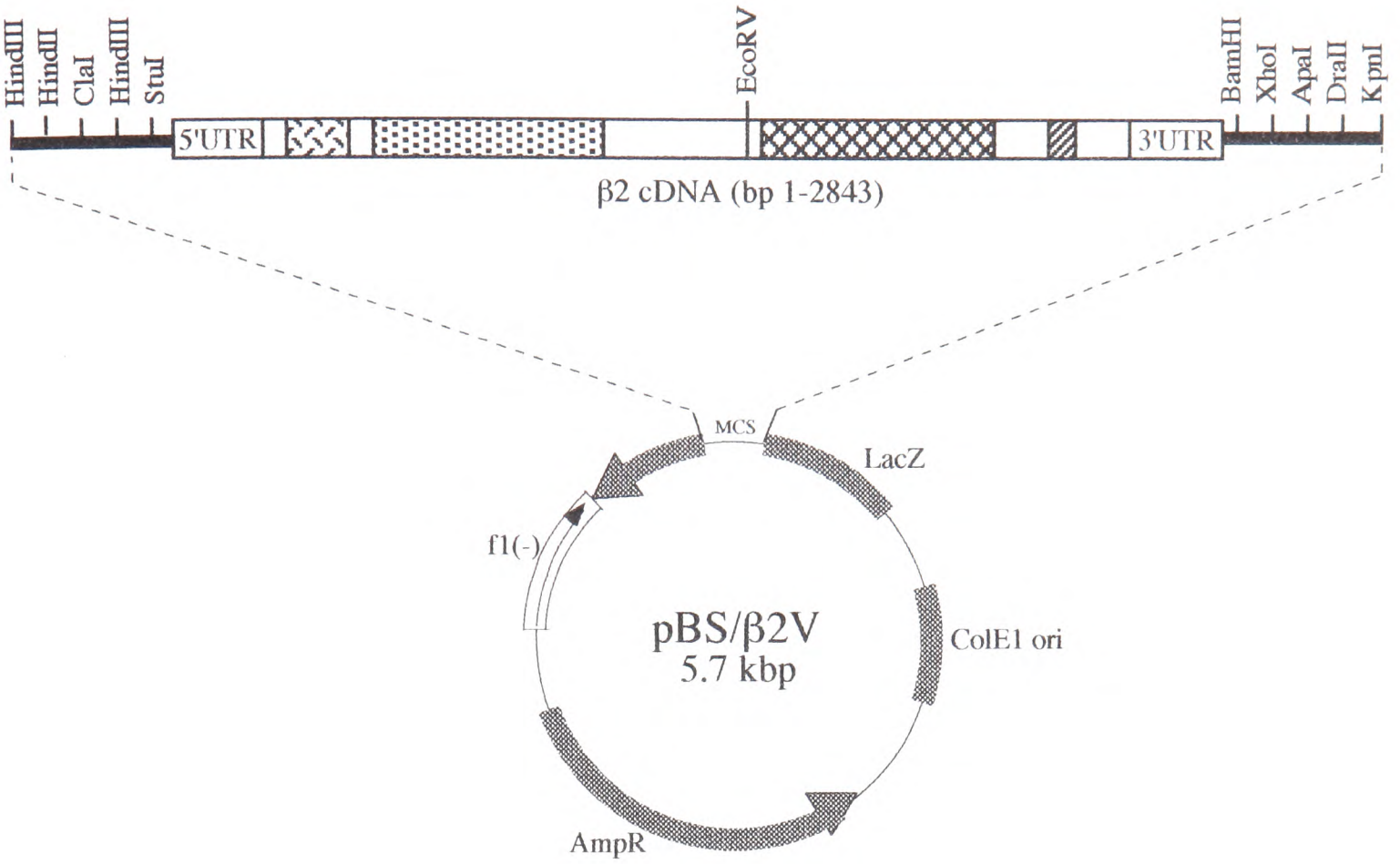
The chimeric β2V1 cDNA in pBluescript, pBS/β2V1, was constructed from the pBS/β2V clone as follows:

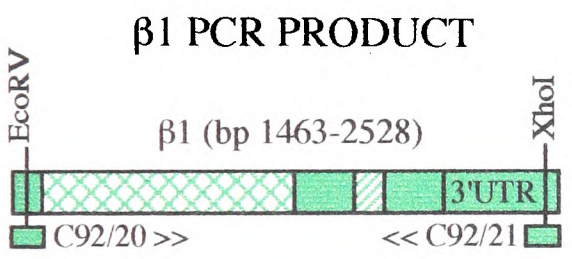
(1) pBS/β2V was digested with EcoRV (β2V, bp 1404-1409) and XhoI (pBS/β2V, 3' polylinker), and the larger 4.3 kbp pBS/β2V fragment was purified by agarose gel electrophoresis.

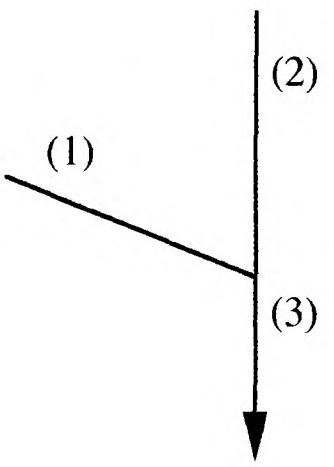
(2) A β1 PCR product (bp 1463-2528) was synthesised using the wildtype pBS/β1 clone as template, the oligonucleotides C92/20 and C92/21 as primers, and the taq DNA polymerase enzyme. The C92/20 oligonucleotide was designed to engineer an EcoRV site into the 5' end of the PCR product, whereas the C92/21 oligonucleotide was designed to engineer an XhoI site into the 3' end (see Figure 3.7b). The β1 PCR product was digested with EcoRV and XhoI, and the 1 kbp EcoRV-XhoI β1 PCR fragment was purified by agarose gel electrophoresis.

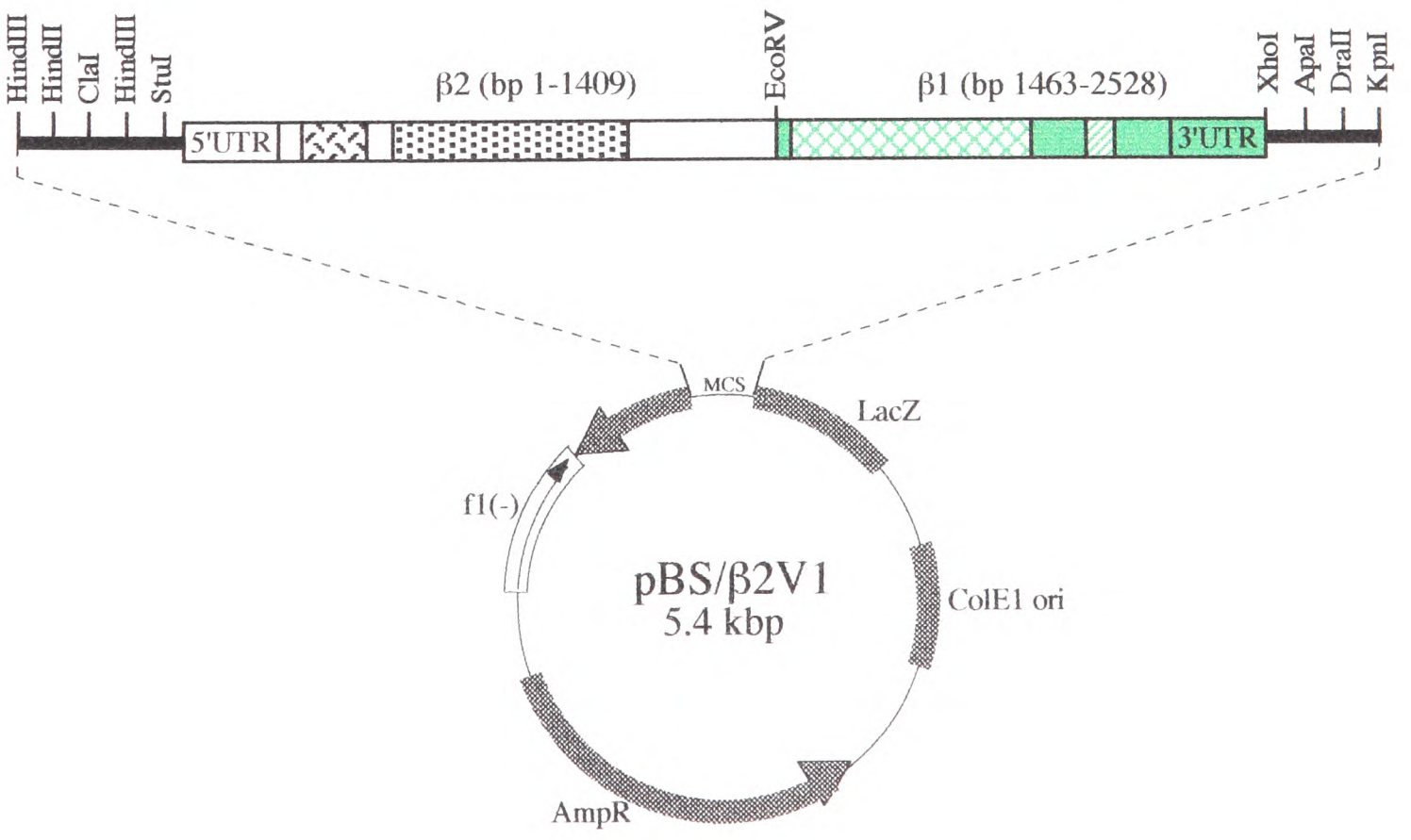
(3) The 1 kbp β1 PCR fragment and the 4.3 kbp pBS/β2V fragment were then ligated, creating a full length chimeric β2V1 cDNA in pBluescript, clone pBS/β2V1. The pBS/β2V1 clone was nucleotide sequenced to confirm the correct formation of the β2/β1 chimeric junction, and to confirm the absence of PCR errors in the EcoRV-XhoI β1 section derived by PCR. No amino acid mutations were introduced into the β2 or β1 subunits at the β2V1 chimeric junction (see Figure 3.7c).

In the figure opposite, the β2 cDNA regions are unshaded, whereas the β1 cDNA regions are shaded green. The regions encoding the N-terminal cysteine rich region are represented by dashed lines, the regions encoding the putative A-domain by dots, the regions encoding the C-terminal cysteine-rich region by crosshatches, and the regions encoding the transmembrane domain by diagonal lines. The 5' and 3' untranslated regions (UTRs) of the β cDNAs are also shown.


HindIII
HindII
ClaI
HindIII
StuI
EcoRV
BamHI
XhoI
ApaI
DraII
KpnI
5'UTR
3'UTR
β2 cDNA (bp 1-2843)
MCS
LacZ
f1(-)
pBS/β2V
5.7 kbp
ColE1 ori
AmpR


β1 PCR PRODUCT
EcoRV
β1 (bp 1463-2528)
XhoI
3'UTR
C92/20 >>
<< C92/21


(2)
(1)
(3)


HindIII
HindII
ClaI
HindIII
StuI
β2 (bp 1-1409)
EcoRV
β1 (bp 1463-2528)
XhoI
ApaI
DraII
KpnI
5'UTR
3'UTR
MCS
LacZ
f1(-)
pBS/β2V1
5.4 kbp
ColE1 ori
AmpR

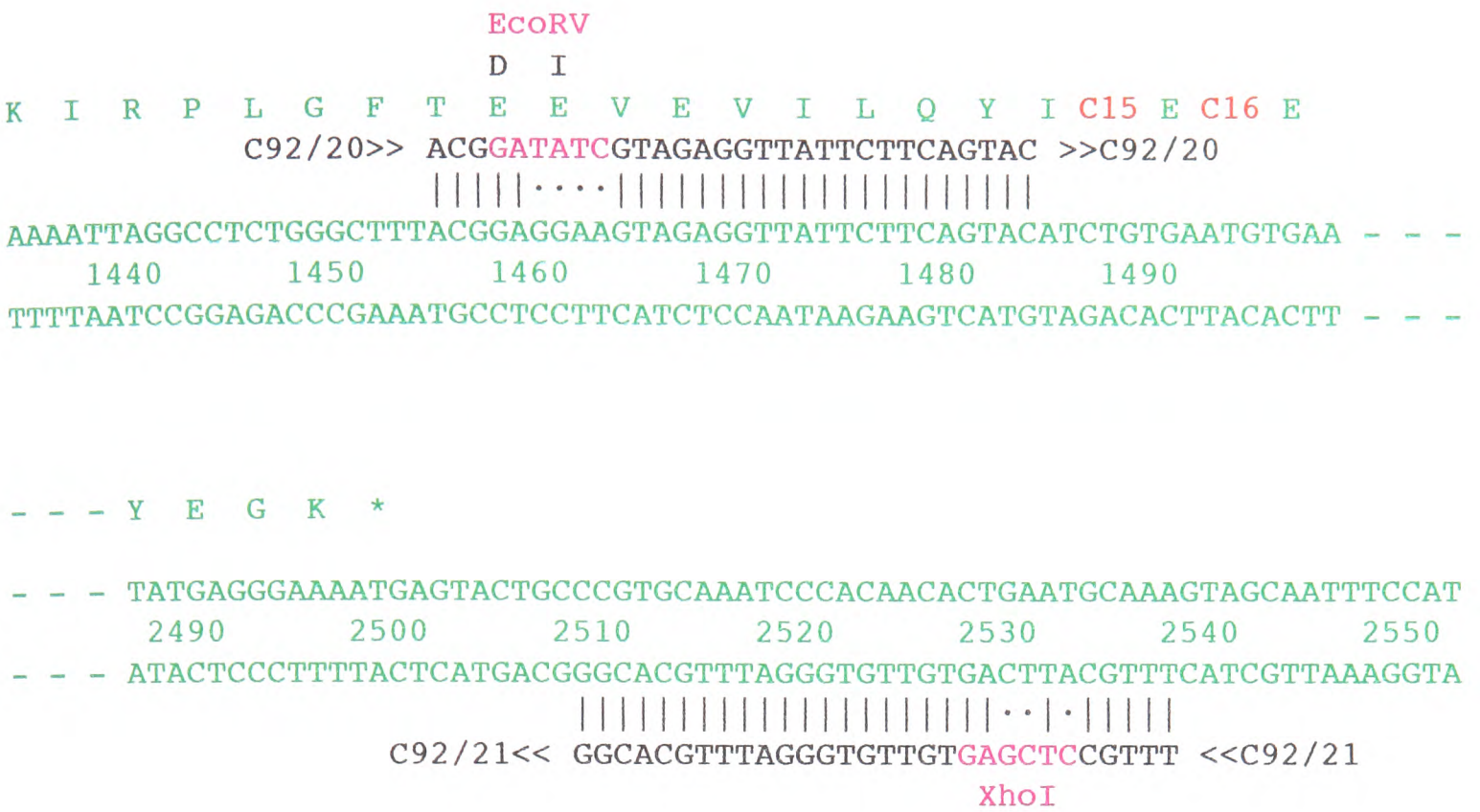


Figure 3.7b: The C92/20 and C92/21 Oligonucleotides used to Synthesise the β1 cDNA Section of the Chimeric β2V1 cDNA

The β1 cDNA section of the chimeric β2V1 cDNA was synthesised by PCR, using the wildtype pBS/β1 clone as template and the C92/20 and C92/21 oligonucleotides as primers. The oligonucleotide C90/20 was designed to engineer an EcoRV site into the 5' end of the PCR product (β1 cDNA: bp 1457-1462), whilst the C92/21 oligonucleotide was designed to engineer an XhoI site into the 3' end of the PCR product (β1 cDNA: bp 2527-2532). The sequences of these two oligonucleotides, and their annealing positions in the wildtype β1 cDNA template are shown above. The relevant sections of the wildtype β1 cDNA are shown in green, and the amino acids that these sections encode are shown above the cDNA sequence (using the single letter amino acid code), also in green. The annealing position of the C92/20 and C92/21 oligonucleotides is shown next to the β1 cDNA sequence, with residues that match the wildtye sequence indicated by vertical lines and mismatched residues by dots, and with the residues representing the EcoRV and XhoI sites shown in pink. The DNA mutations engineered into the 5' end of the β1 PCR product to create the EcoRV site resulted in two amino acid substitutions, E452D and E453I, shown above the wildtype β1 sequence. However, as these residues correspond to the wildtype β2 residues at these positions, no amino acid changes were introduced into the β1 section of the resulting β2V1 chimera (see Figure 3.7c).

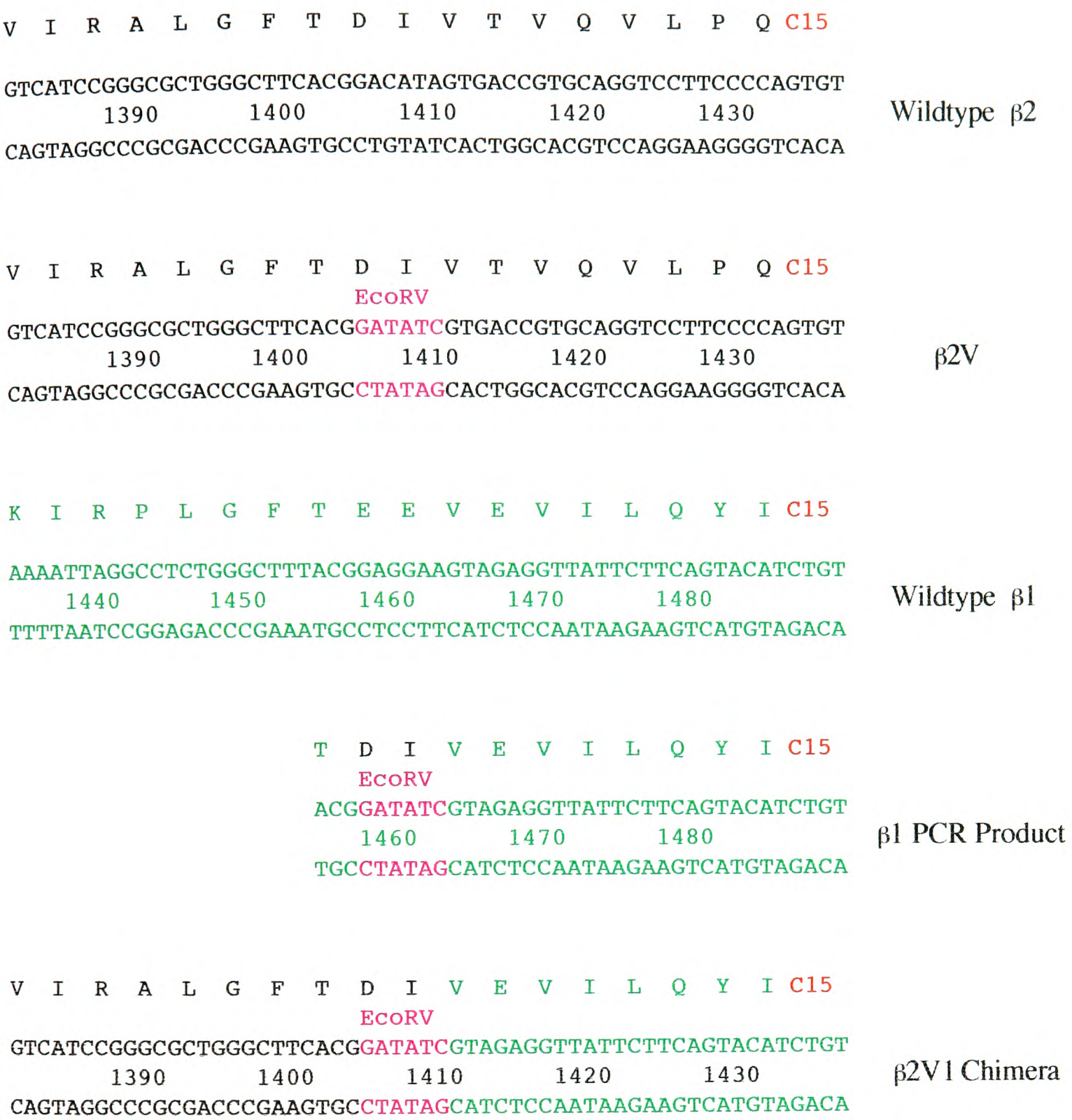


Figure 3.7c: Formation of the β2V1 Chimeric Junction

The figure above shows the formation of the β2/β1 chimeric junction in the β2V1 chimera. The wildtype β2 cDNA and amino acid sequences are shown in black, whereas the wildtype β1 cDNA and amino acid sequences are shown in green, and the nucleotide residues which represent the EcoRV site are shown in pink. Cysteine residues are shown in red, and are numbered such that the first cysteine residue in the mature β polypeptide would be numbered C1 and the last would be numbered C56. It should be noted that the β2V1 chimeric junction was created without introducing any amino acid mutations into the β2 or the β1 sections.

Figure 3.8a: Constructing the Chimeric β2V7 cDNA in pBluescript, Creating pBS/β2V7

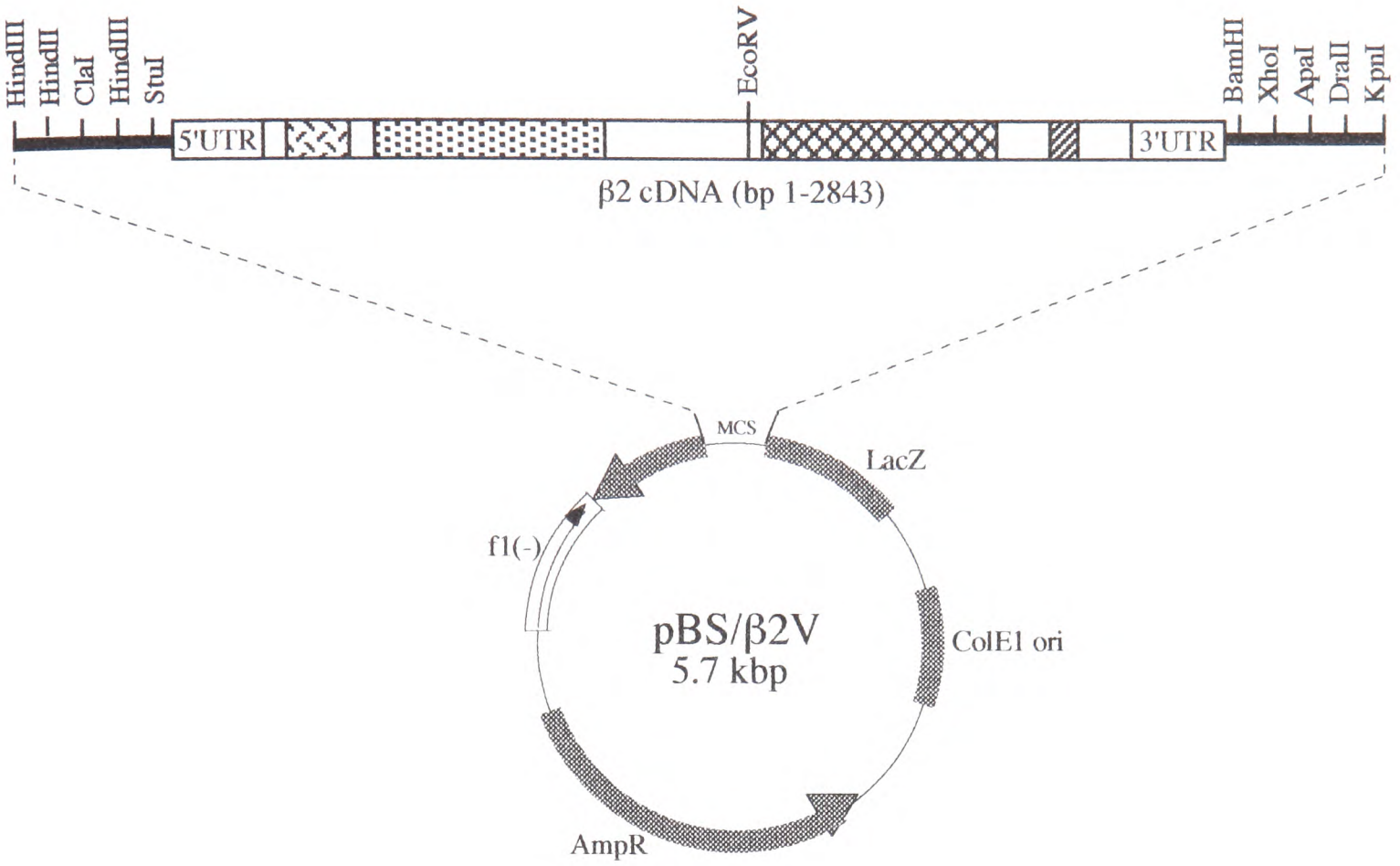
The chimeric β2V7 cDNA in pBluescript, pBS/β2V7, was constructed from the pBS/β2V clone as follows:

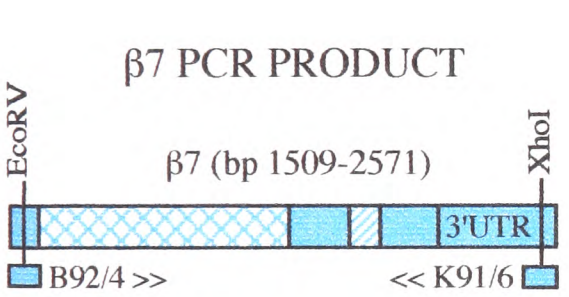
(1) pBS/β2V was digested with EcoRV (β2V, bp 1404-1409) and XhoI (pBS/β2V, 3' polylinker), and the larger 4.3 kbp pBS/β2V fragment was purified by agarose gel electrophoresis.

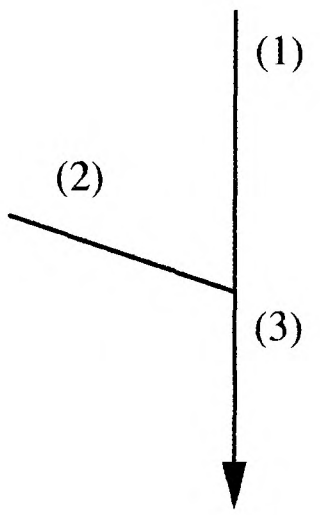
(2) A β7 PCR product (bp 1509-2571) was synthesised using the wildtype pBS/β7 clone as template, the oligonucleotides B92/4 and K91/6 as primers, and the taq DNA polymerase enzyme. The B92/4 oligonucleotide was designed to engineer an EcoRV site into the 5' end of the PCR product, whereas the K91/6 oligonucleotide was designed to engineer an XhoI site into the 3' end (see Figure 3.8b). The β7 PCR product was digested with EcoRV and XhoI, and the 1 kbp EcoRV-XhoI β7 PCR fragment was purified by agarose gel electrophoresis.

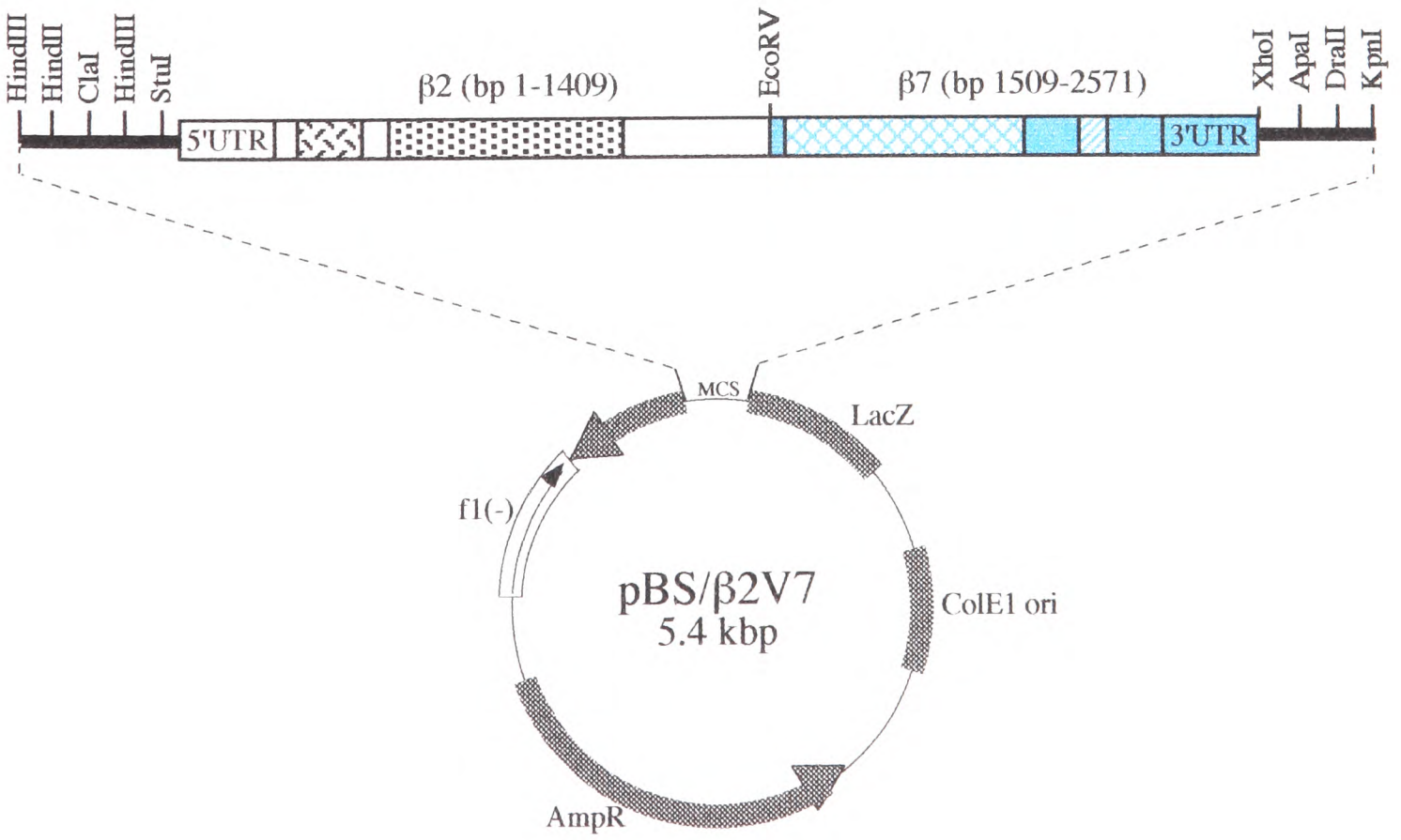
(3) The 1 kbp β7 PCR fragment and the 4.3 kbp pBS/β2V fragment were then ligated, creating a full length chimeric β2V7 cDNA in pBluescript, clone pBS/β2V7. The pBS/β2V7 clone was nucleotide sequenced to confirm the correct formation of the β2/β7 chimeric junction, and to confirm the absence of PCR errors in the EcoRV-XhoI β7 section derived by PCR. No amino acid mutations were introduced into the β2 or β7 subunits at the β2V7 chimeric junction (see Figure 3.8c).

In the figure opposite, the β2 cDNA regions are unshaded, whereas the β7 cDNA regions are shaded blue. The regions encoding the N-terminal cysteine rich region are represented by dashed lines, the regions encoding the putative A-domain by dots, the regions encoding the C-terminal cysteine-rich region by crosshatches, and the regions encoding the transmembrane domain by diagonal lines. The 5' and 3' untranslated regions (UTRs) of the β cDNAs are also shown.


HindIII
HindII
ClaI
HindIII
StuI
EcoRV
BamHI
XhoI
ApaI
DraII
KpnI
5'UTR
3'UTR
β2 cDNA (bp 1-2843)
MCS
LacZ
f1(-)
pBS/β2V
5.7 kbp
ColE1 ori
AmpR


β7 PCR PRODUCT
EcoRV
β7 (bp 1509-2571)
XhoI
3'UTR
B92/4 >>
<< K91/6


(1)
(2)
(3)


HindIII
HindII
ClaI
HindIII
StuI
β2 (bp 1-1409)
EcoRV
β7 (bp 1509-2571)
XhoI
ApaI
DraII
KpnI
5'UTR
3'UTR
MCS
LacZ
f1(-)
pBS/β2V7
5.4 kbp
ColE1 ori
AmpR

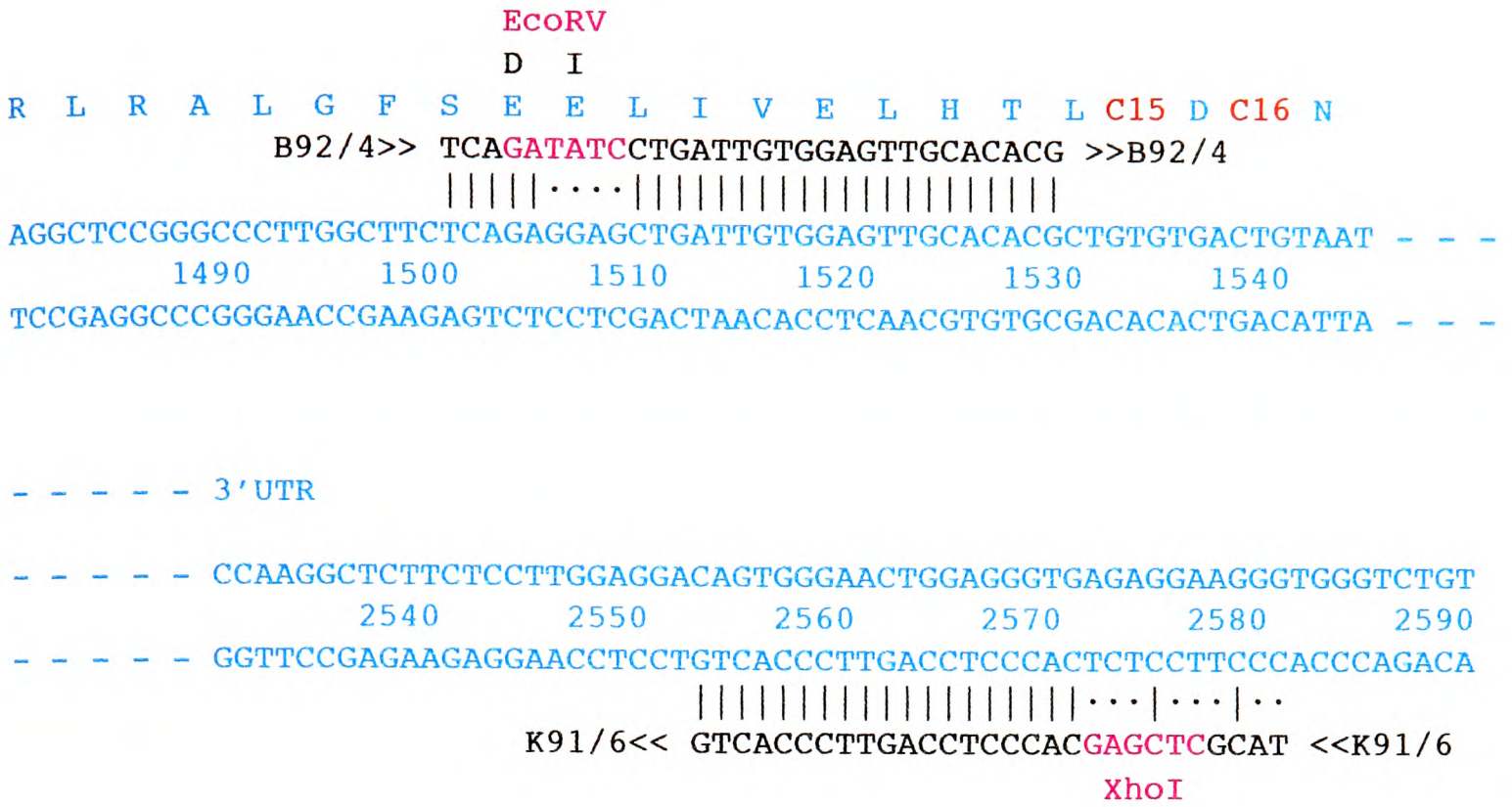


Figure 3.8b: The B92/4 and K91/6 Oligonucleotides used to Synthesise the β7 cDNA Section of the Chimeric β2V7 cDNA

The β7 cDNA section of the chimeric β2V7 cDNA was synthesised by PCR, using the wildtype pBS/β7 clone as template and the B92/4 and K91/6 oligonucleotides as primers. The oligonucleotide B92/4 was designed to engineer an EcoRV site into the 5' end of the PCR product (β7 cDNA: bp 1503-1508), whilst the K91/6 oligonucleotide was designed to engineer an XhoI site into the 3' end of the PCR product (β7 cDNA: bp 2572-2577). The sequences of these two oligonucleotides, and their annealing positions in the wildtype β7 cDNA template are shown above. The relevant sections of the wildtype β7 cDNA are shown in blue, and the amino acids that these sections encode are shown above the cDNA sequence (using the single letter amino acid code), also in blue. The annealing position of the B92/4 and K91/6 oligonucleotides is shown next to the β7 cDNA sequence, with residues that match the wildtye sequence indicated by vertical lines and mismatched residues by dots, and with the residues representing the EcoRV and XhoI sites shown in pink. The DNA mutations engineered into the 5' end of the β7 PCR product to create the EcoRV site resulted in two amino acid substitutions, E464D and E465I, shown above the wildtype β7 sequence. However, as these residues correspond to the wildtype β2 residues at these positions, no amino acid changes were introduced into the β7 section of the resulting β2V7 chimera (see Figure 3.8c).

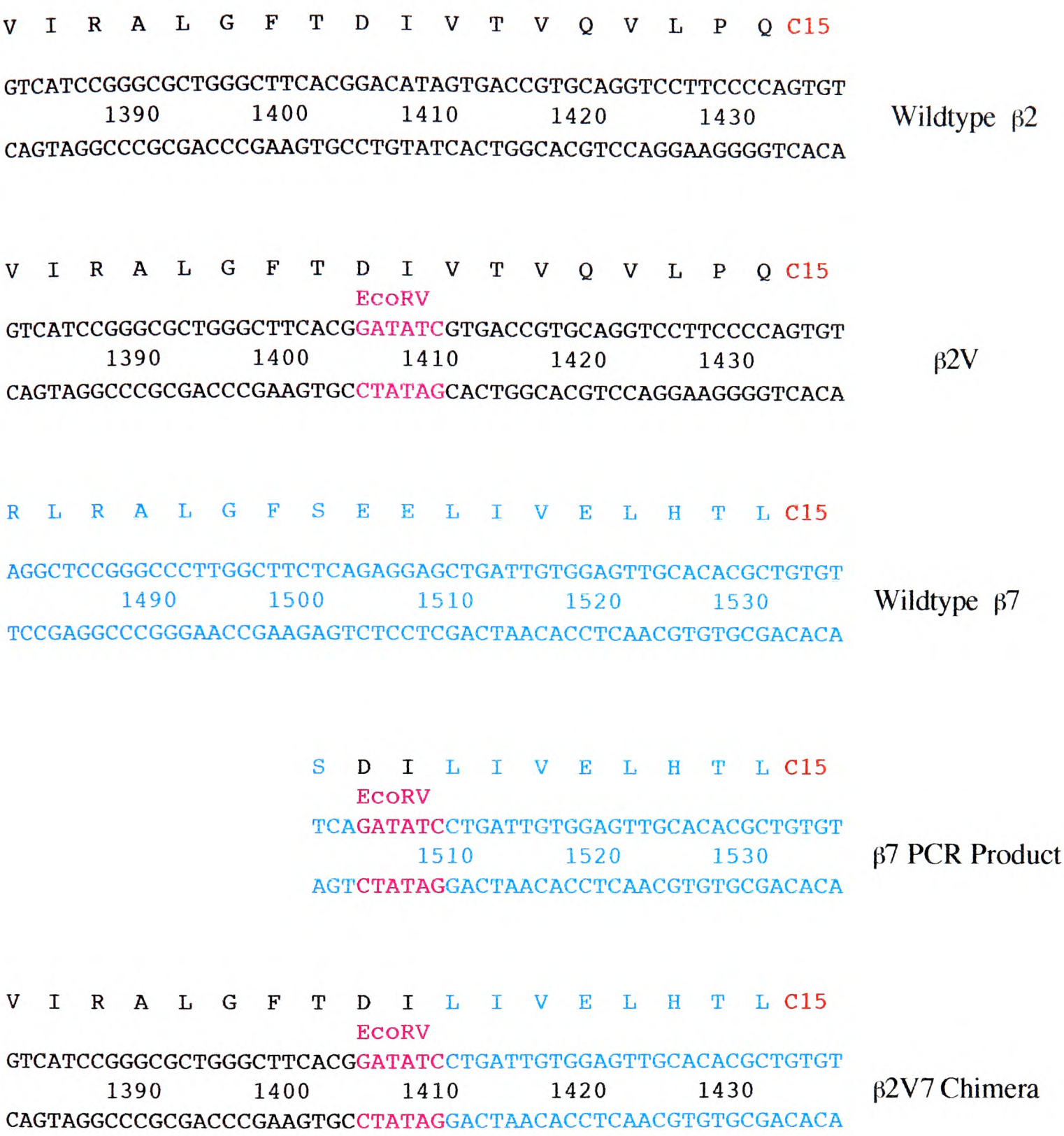


Figure 3.8c: Formation of the β2V7 Chimeric Junction

The figure above shows the formation of the β2/β7 chimeric junction in the β2V7 chimera. The wildtype β2 cDNA and amino acid sequences are shown in black, whereas the wildtype β7 cDNA and amino acid sequences are shown in blue, and the nucleotide residues which represent the EcoRV site are shown in pink. Cysteine residues are shown in red, and are numbered such that the first cysteine residue in the mature β polypeptide would be numbered C1 and the last would be numbered C56. It should be noted that the β2V7 chimeric junction was created without introducing any amino acid mutations into the β2 or the β7 sections.

Figure 3.9a: Constructing pKG4/β2V1

The entire coding region of the β2V1 cDNA was subcloned from pBluescript into the pKG4 vector as follows:

(1) pBS/β2V1 was digested with HindIII (pBS/β2V1, 5' polylinker) and XhoI (β2V1 cDNA, 3' UTR), and the 2.5 kbp β2V1 cDNA insert was purified by agarose gel electrophoresis.

(2) pKG4 was digested with HindIII and XhoI, and the 5.8 kbp pKG4 vector was also purified by agarose gel electrophoresis.

(3) The pKG4 vector and the β2V1 cDNA insert were then ligated, creating a clone named pKG4/β2V1.

In the figure opposite, the β2 cDNA regions are unshaded, whereas the β1 cDNA regions are shaded green. The cDNA regions encoding the N-terminal cysteine rich region are represented by dashed lines, the regions encoding the putative A-domain by dots, the regions encoding the C-terminal cysteine-rich region by crosshatches, and the regions encoding the transmembrane domain by diagonal lines. The 5' and 3' untranslated regions (UTRs) of the cDNAs are also shown.

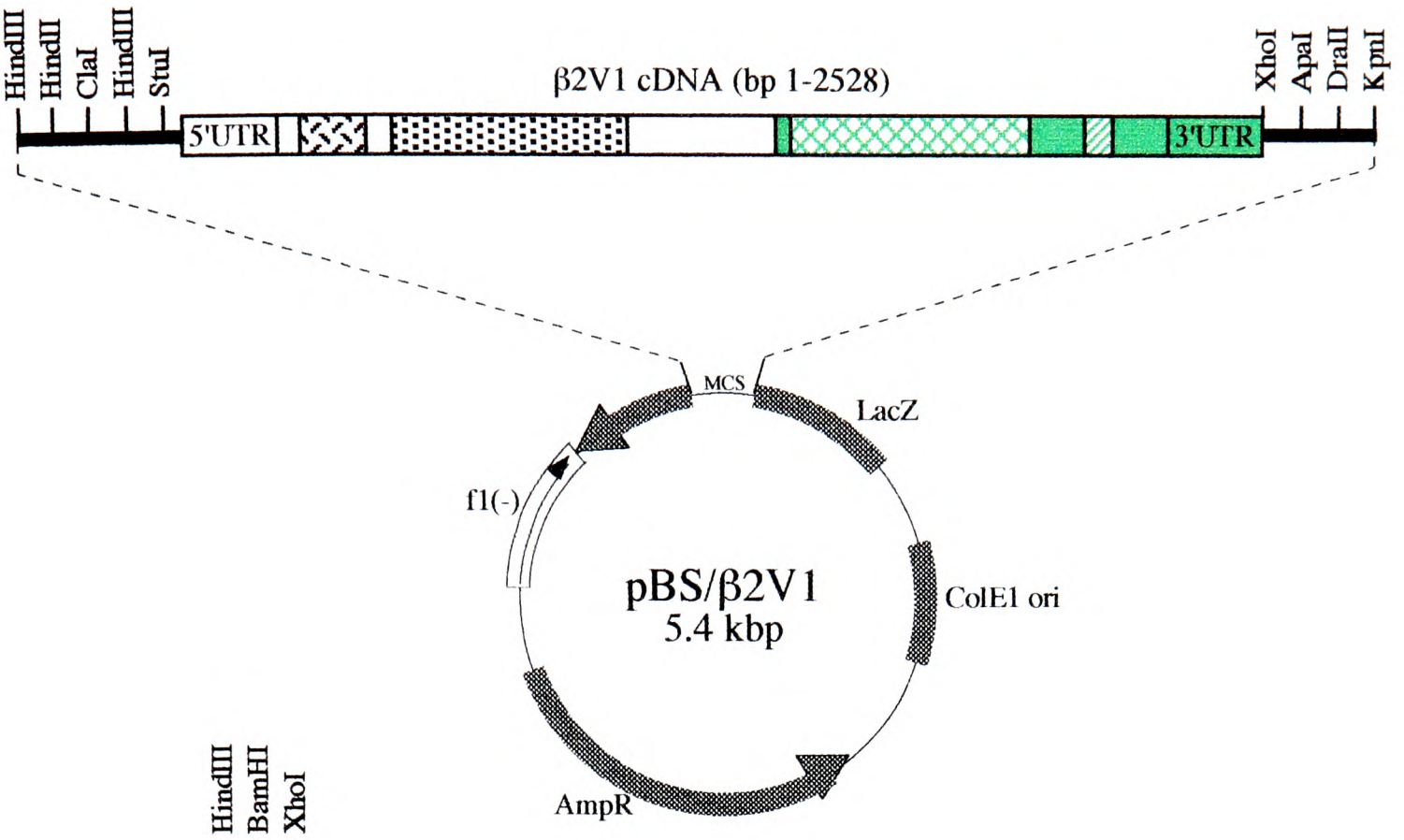

HindIII
HindII
ClaI
HindIII
StuI
β2V1 cDNA (bp 1-2528)
XhoI
ApaI
DraII
KpnI
5'UTR
3'UTR
MCS
LacZ
f1(-)
pBS/β2V1
5.4 kbp
ColE1 ori
AmpR
HindIII
BamHI
XhoI
MCS
SV40 Early Promoter
SV40 pA
pBR322
ori
pKG4
5.8 kbp
NeoR
AmpR
(1)
(2)
(3)
HindIII
StuI
β2V1 cDNA (bp 1-2528)
XhoI
5'UTR
3'UTR
MCS
SV40 Early Promoter
SV40 pA
pBR322
ori
pKG4/β2V1
8.3 kbp
NeoR
AmpR

Figure 3.9b: Constructing pKG4/β2V7

The entire coding region of the β2V7 cDNA was subcloned from pBluescript into the pKG4 vector as follows:

(1) pBS/β2V7 was digested with HindIII (pBS/β2V7, 5' polylinker) and XhoI (β2V7 cDNA, 3' UTR), and the 2.5 kbp β2V7 cDNA insert was purified by agarose gel electrophoresis.

(2) pKG4 was digested with HindIII and XhoI, and the 5.8 kbp pKG4 vector was also purified by agarose gel electrophoresis.

(3) The pKG4 vector and the β2V7 cDNA insert were then ligated, creating a clone named pKG4/β2V7.

In the figure opposite, the β2 cDNA regions are unshaded, whereas the β7 cDNA regions are shaded blue. The cDNA regions encoding the N-terminal cysteine rich region are represented by dashed lines, the regions encoding the putative A-domain by dots, the regions encoding the C-terminal cysteine-rich region by crosshatches, and the regions encoding the transmembrane domain by diagonal lines. The 5' and 3' untranslated regions (UTRs) of the cDNAs are also shown.

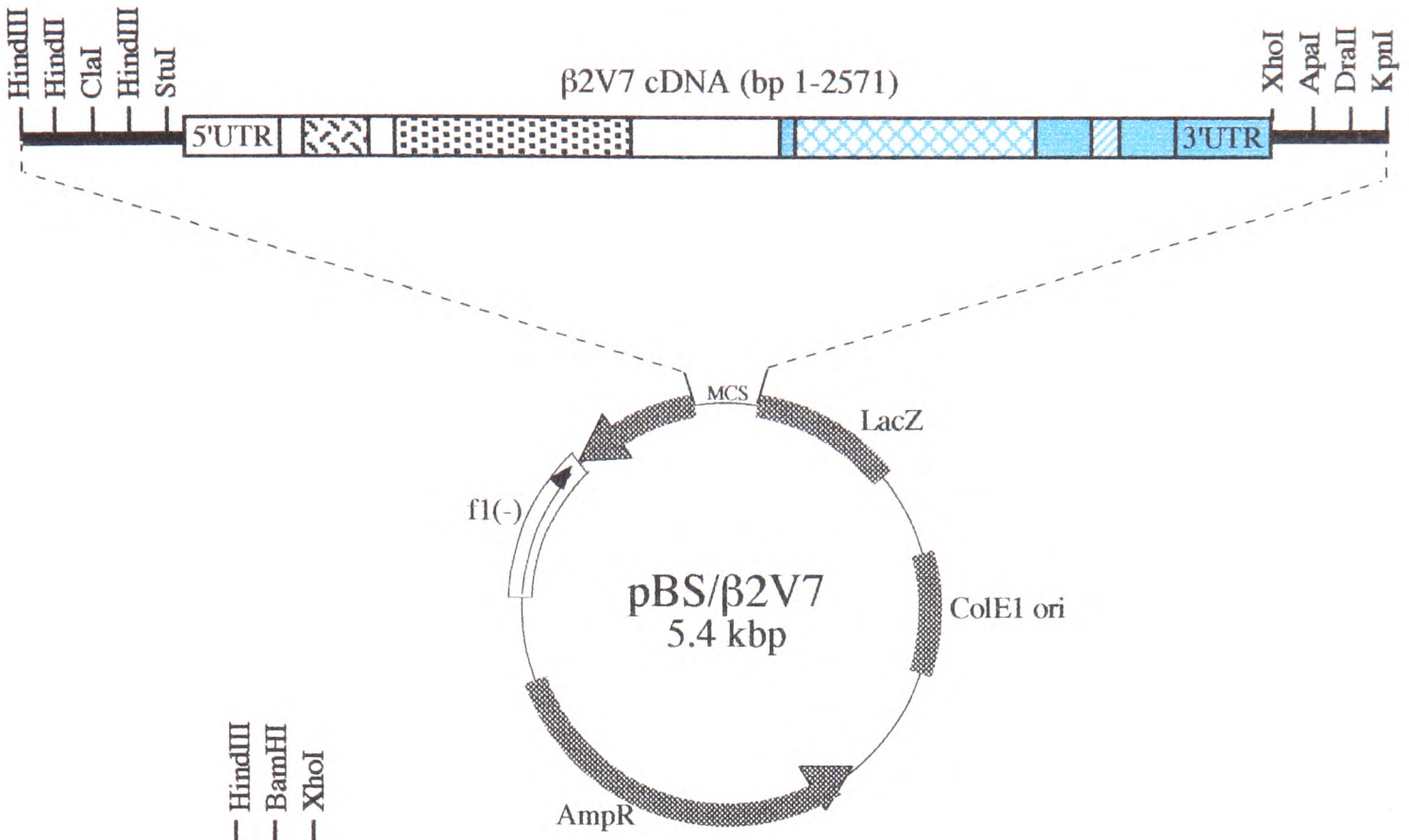

HindIII
HindII
ClaI
HindIII
StuI
β2V7 cDNA (bp 1-2571)
XhoI
ApaI
DraII
KpnI
5'UTR
3'UTR
MCS
LacZ
f1(-)
pBS/β2V7
5.4 kbp
ColE1 ori
AmpR
HindIII
BamHI
XhoI
MCS
SV40 Early Promoter
SV40 pA
pBR322
ori
pKG4
5.8 kbp
NeoR
AmpR
(1)
(2)
(3)
HindIII
StuI
β2V7 cDNA (bp 1-2571)
XhoI
5'UTR
3'UTR
MCS
SV40 Early Promoter
SV40 pA
pBR322
ori
pKG4/β2V7
8.3 kbp
NeoR
AmpR

Figure 3.9c: Constructing pSVL/β2V1

The entire coding region of the β2V1 cDNA was subcloned from pKG4 into the pSVL vector as follows:

(1) pKG4/β2V1 was digested with XhoI (β2V1 cDNA, 3' UTR) and the resultant 5' overhang was blunted using the end-filling reaction. The 2.5 kbp β2V1 cDNA insert was then excised from pKG4 by digestion with XbaI (β2V1 cDNA, 5' UTR), and was purified by agarose gel electrophoresis.

(2) pSVL/αL was digested with XbaI (pSVL, 5' polylinker) and SmaI (pSVL, 3' polylinker), and the 4.8 kbp pSVL vector was also purified by agarose gel electrophoresis.

(3) The pSVL vector and the β2V1 cDNA insert were then ligated, creating a clone named pSVL/β2V1.

In the figure opposite, the β2 cDNA regions are unshaded, whereas the β1 cDNA regions are shaded green. The cDNA regions encoding the N-terminal cysteine rich region are represented by dashed lines, the regions encoding the putative A-domain by dots, the regions encoding the C-terminal cysteine-rich region by crosshatches, and the regions encoding the transmembrane domain by diagonal lines. The 5' and 3' untranslated regions (UTRs) of the cDNAs are also shown.

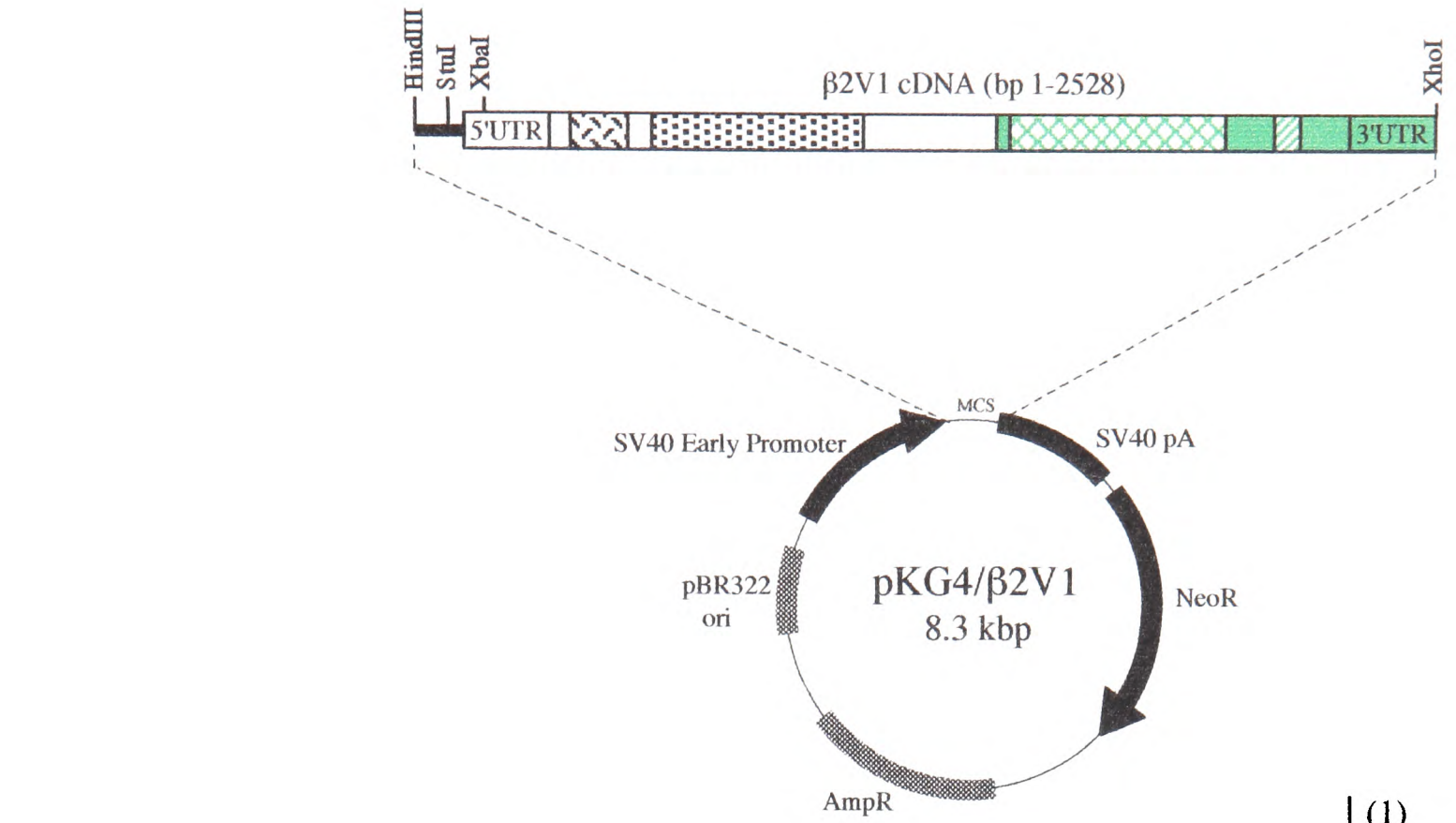

HindIII
SmaI
XbaI
β2V1 cDNA (bp 1-2528)
XhoI
5'UTR
3'UTR
MCS
SV40 Early Promoter
SV40 pA
pBR322
ori
pKG4/β2V1
8.3 kbp
NeoR
AmpR
(1)
XhoI
XbaI
αL (bp 27-3640)
EcoRI
PstI
SmaI
EcoRI
SacI
BamHI
5'UTR
3'UTR
MCS
SV40 Late Promoter
/ VP1 Intron
SV40 Late
Polyadenylation
pSVL/αL
8.4 kbp
SV40
ori
pBR322
ori
AmpR
(2)
(3)
XhoI
XbaI
β2V1 cDNA (bp 17-2528)
XhoI
EcoRI
SacI
BamHI
5'UTR
3'UTR
MCS
SV40 Late Promoter
/ VP1 Intron
SV40 Late
Polyadenylation
pSVL/β2V1
7.3 kbp
SV40
ori
pBR322
ori
AmpR

Figure 3.9d: Constructing pSVL/β2V7

The entire coding region of the β2V7 cDNA was subcloned from pKG4 into the pSVL vector as follows:

(1) pKG4/β2V7 was digested with XhoI (β2V7 cDNA, 3' UTR) and the resultant 5' overhang was blunted using the end-filling reaction. The 2.5 kbp β2V7 cDNA insert was then excised from pKG4 by digestion with XbaI (β2V7 cDNA, 5' UTR), and was purified by agarose gel electrophoresis.

(2) pSVL/αL was digested with XbaI (pSVL, 5' polylinker) and SmaI (pSVL, 3' polylinker), and the 4.8 kbp pSVL vector was also purified by agarose gel electrophoresis.

(3) The pSVL vector and the β2V7 cDNA insert were then ligated, creating a clone named pSVL/β2V7.

In the figure opposite, the β2 cDNA regions are unshaded, whereas the β7 cDNA regions are shaded blue. The cDNA regions encoding the N-terminal cysteine rich region are represented by dashed lines, the regions encoding the putative A-domain by dots, the regions encoding the C-terminal cysteine-rich region by crosshatches, and the regions encoding the transmembrane domain by diagonal lines. The 5' and 3' untranslated regions (UTRs) of the cDNAs are also shown.

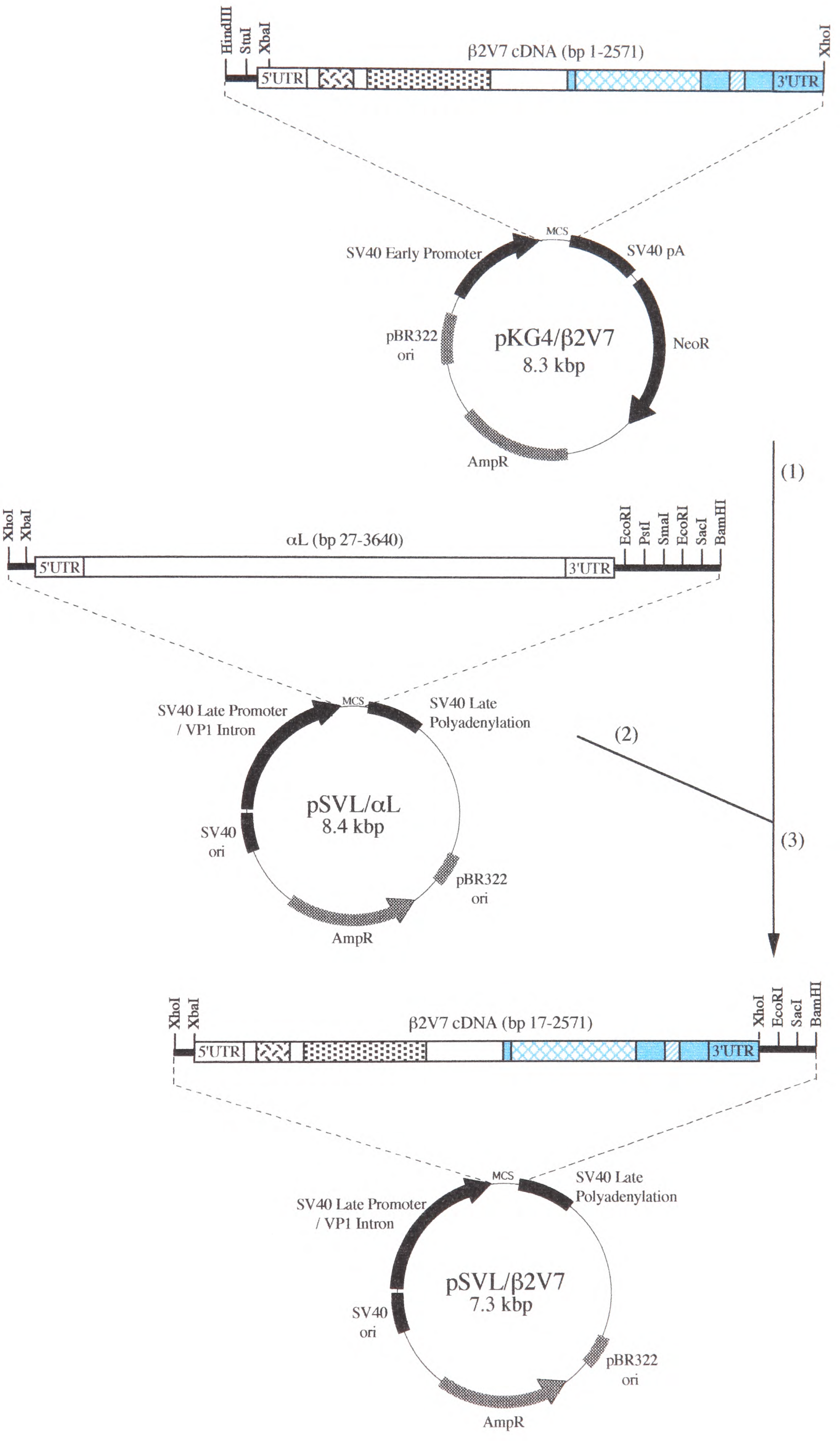

HindIII
StuI
XbaI
β2V7 cDNA (bp 1-2571)
XhoI
5'UTR
3'UTR
MCS
SV40 Early Promoter
SV40 pA
pBR322
ori
pKG4/β2V7
8.3 kbp
NeoR
AmpR
(1)
XhoI
XbaI
αL (bp 27-3640)
EcoRI
PstI
SmaI
EcoRI
SacI
BamHI
5'UTR
3'UTR
MCS
SV40 Late Promoter
/ VP1 Intron
SV40 Late
Polyadenylation
pSVL/αL
8.4 kbp
SV40
ori
pBR322
ori
AmpR
(2)
(3)
XhoI
XbaI
β2V7 cDNA (bp 17-2571)
XhoI
EcoRI
SacI
BamHI
5'UTR
3'UTR
MCS
SV40 Late Promoter
/ VP1 Intron
SV40 Late
Polyadenylation
pSVL/β2V7
7.3 kbp
SV40
ori
pBR322
ori
AmpR

Figure 3.9e: Constructing pcDNA3/β2V1

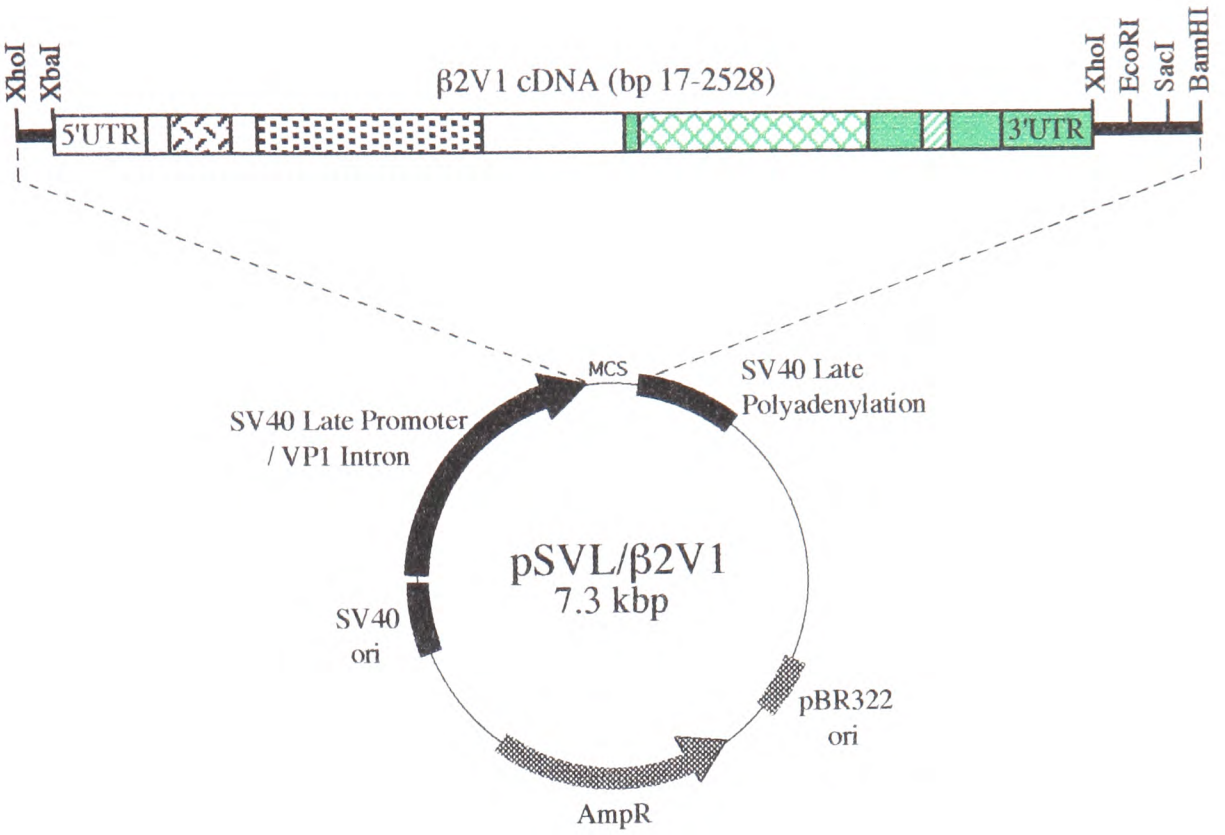
The entire coding region of the β2V1 cDNA was subcloned from pSVL into the pcDNA3 vector as follows:

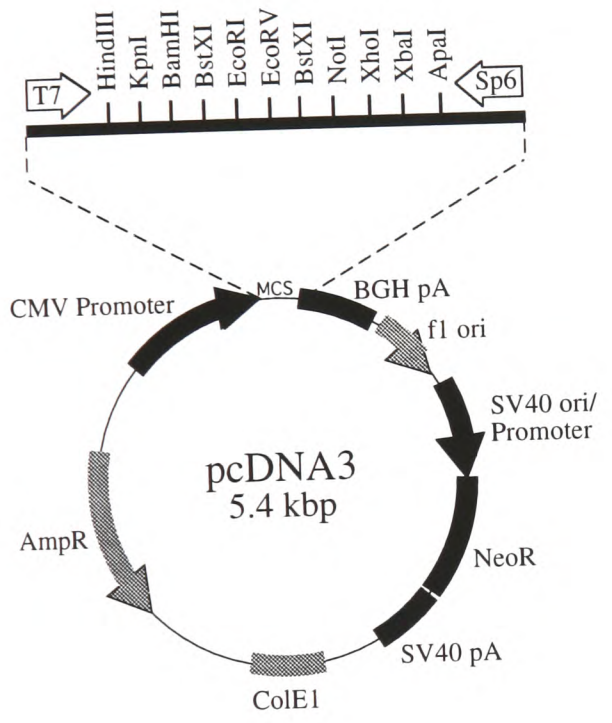
(1) pSVL/β2V1 was digested with XhoI (pSVL/β2V1, 5' polylinker; β2V1 cDNA, 3' UTR) and the 2.5 kbp β2V1 cDNA insert was purified by agarose gel electrophoresis.

(2) pcDNA3 was also digested with XhoI, and the 5.4 kbp pcDNA3 vector was purified by agarose gel electrophoresis.

(3) The pcDNA3 vector and the β2V1 cDNA insert were then ligated, creating a clone named pcDNA3/β2V1. The orientation of the β2V1 cDNA in the pcDNA3 vector was determined by EcoRV digestion. Clones producing a 1.45 kbp restriction fragment were in the correct orientation.

In the figure opposite, the β2 cDNA regions are unshaded, whereas the β1 cDNA regions are shaded green. The cDNA regions encoding the N-terminal cysteine rich region are represented by dashed lines, the regions encoding the putative A-domain by dots, the regions encoding the C-terminal cysteine-rich region by crosshatches, and the regions encoding the transmembrane domain by diagonal lines. The 5' and 3' untranslated regions (UTRs) of the cDNAs are also shown.


XhoI
XbaI
β2V1 cDNA (bp 17-2528)
XhoI
EcoRI
SacI
BamHI
5'UTR
3'UTR
MCS
SV40 Late
Polyadenylation
SV40 Late Promoter
/ VP1 Intron
pSVL/β2V1
7.3 kbp
SV40
ori
pBR322
ori
AmpR


HindIII
KpnI
BamHI
BstXI
EcoRI
EcoRV
BstXI
NotI
XhoI
XbaI
ApaI
T7
Sp6
MCS
CMV Promoter
BGH pA
f1 ori
SV40 ori/
Promoter
pcDNA3
5.4 kbp
AmpR
NeoR
SV40 pA
ColE1

(1)

(2)

(3)

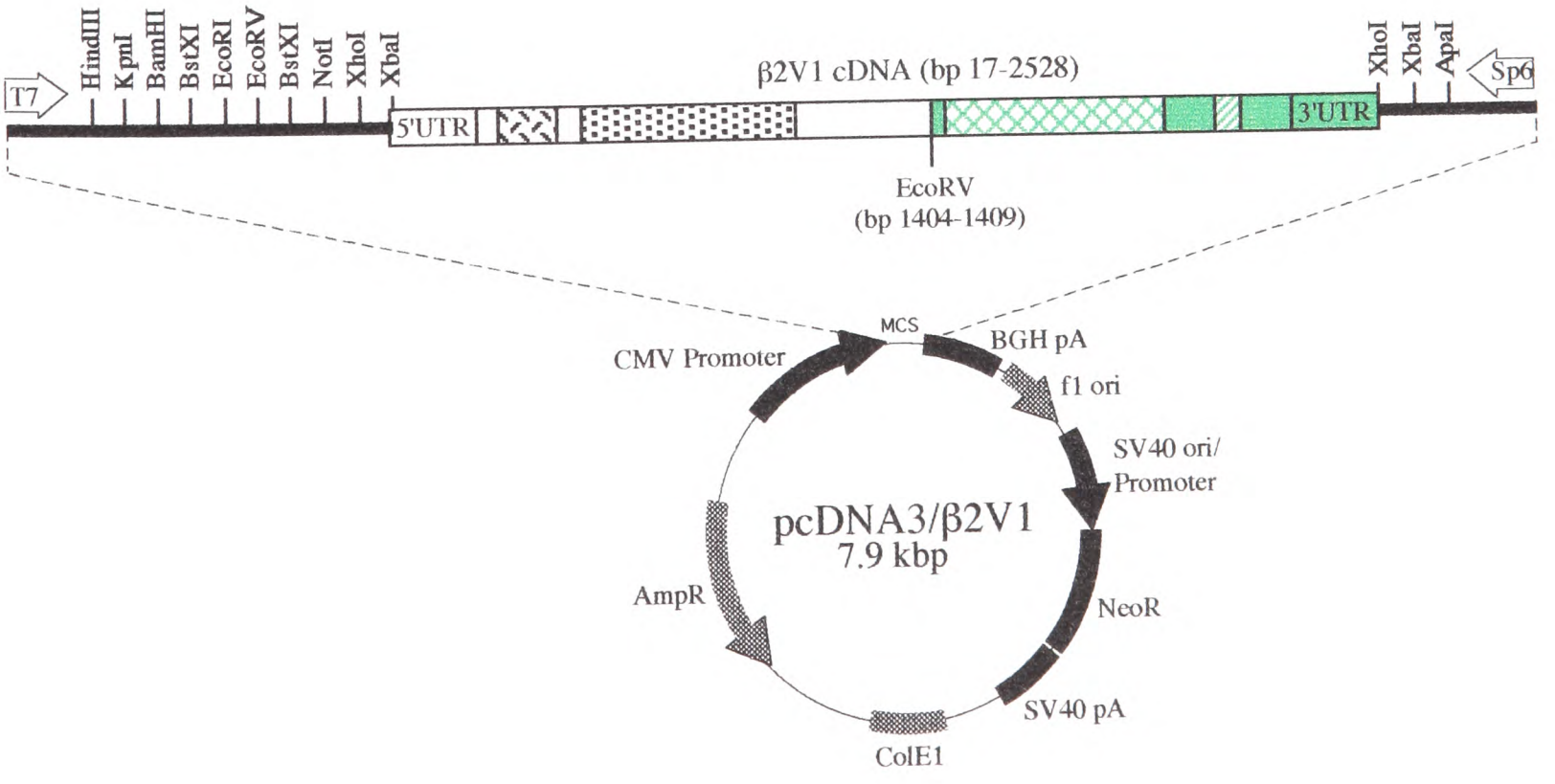

HindIII
KpnI
BamHI
BstXI
EcoRI
EcoRV
BstXI
NotI
XhoI
XbaI
T7
β2V1 cDNA (bp 17-2528)
XhoI
XbaI
ApaI
Sp6
5'UTR
3'UTR
EcoRV
(bp 1404-1409)
MCS
CMV Promoter
BGH pA
f1 ori
SV40 ori/
Promoter
pcDNA3/β2V1
7.9 kbp
AmpR
NeoR
SV40 pA
ColE1

Figure 3.9f: Constructing pcDNA3/β2V7

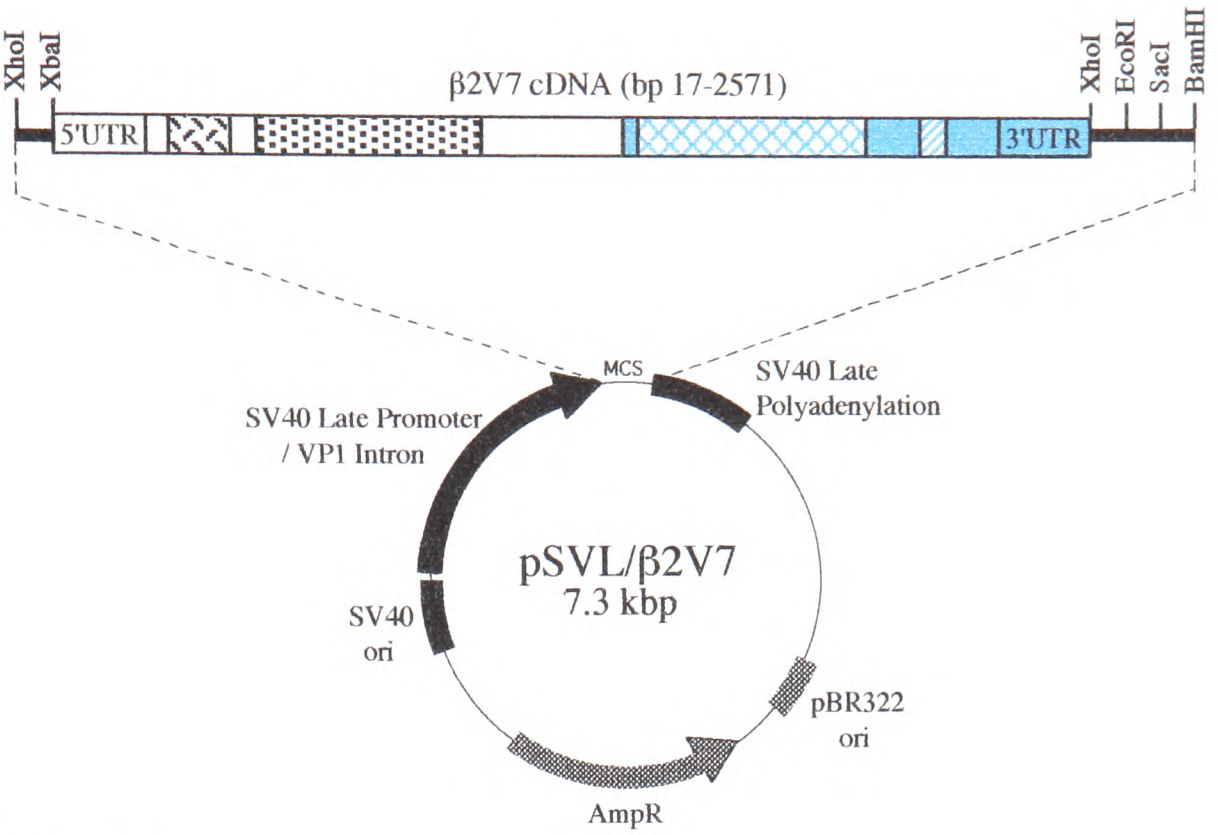
The entire coding region of the β2V7 cDNA was subcloned from pSVL into the pcDNA3 vector as follows:

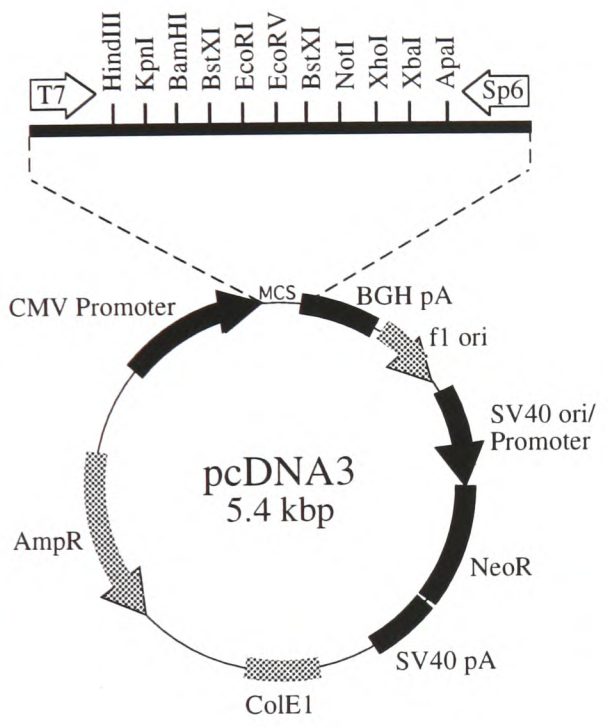
(1) pSVL/β2V7 was digested with XhoI (pSVL/β2V7, 5' polylinker; β2V7 cDNA, 3' UTR) and the 2.5 kbp β2V7 cDNA insert was purified by agarose gel electrophoresis.

(2) pcDNA3 was also digested with XhoI, and the 5.4 kbp pcDNA3 vector was purified by agarose gel electrophoresis.

(3) The pcDNA3 vector and the β2V7 cDNA insert were then ligated, creating a clone named pcDNA3/β2V7. The orientation of the β2V7 cDNA in the pcDNA3 vector was determined by EcoRV digestion. Clones producing a 1.45 kbp restriction fragment were in the correct orientation.

In the figure opposite, the β2 cDNA regions are unshaded, whereas the β7 cDNA regions are shaded blue. The cDNA regions encoding the N-terminal cysteine rich region are represented by dashed lines, the regions encoding the putative A-domain by dots, the regions encoding the C-terminal cysteine-rich region by crosshatches, and the regions encoding the transmembrane domain by diagonal lines. The 5' and 3' untranslated regions (UTRs) of the cDNAs are also shown.

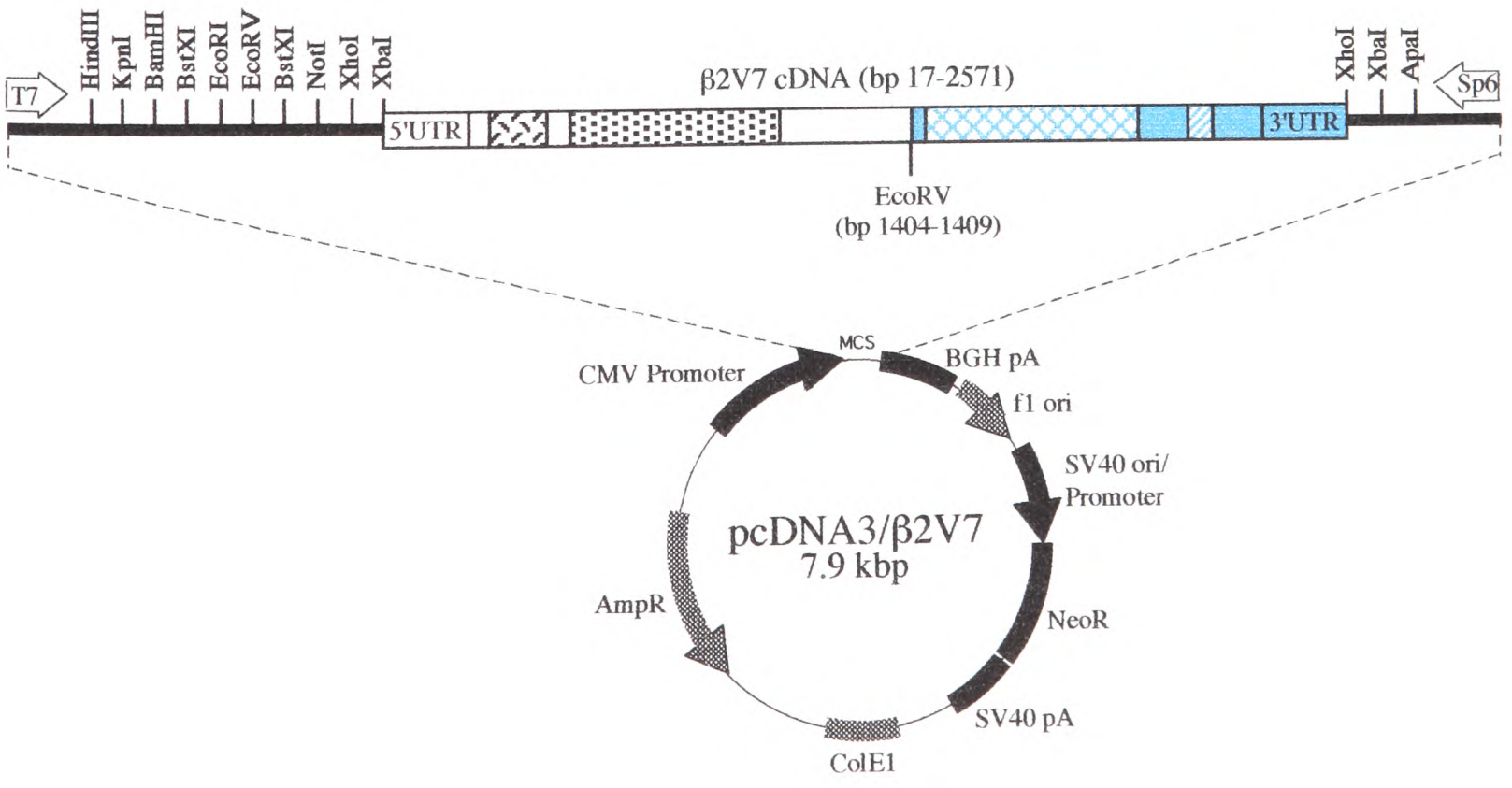

XhoI
XbaI
β2V7 cDNA (bp 17-2571)
XhoI
EcoRI
SacI
BamHI
5'UTR
3'UTR
MCS
SV40 Late Promoter / VP1 Intron
SV40 Late Polyadenylation
pSVL/β2V7
7.3 kbp
SV40 ori
pBR322 ori
AmpR


T7
HindIII
KpnI
BamHI
BstXI
EcoRI
EcoRV
BstXI
NotI
XhoI
XbaI
ApaI
Sp6
MCS
CMV Promoter
BGH pA
f1 ori
SV40 ori/ Promoter
pcDNA3
5.4 kbp
AmpR
NeoR
SV40 pA
ColE1

(1)

(2)

(3)


T7
HindIII
KpnI
BamHI
BstXI
EcoRI
EcoRV
BstXI
NotI
XhoI
XbaI
β2V7 cDNA (bp 17-2571)
XhoI
XbaI
ApaI
Sp6
5'UTR
3'UTR
EcoRV
(bp 1404-1409)
MCS
CMV Promoter
BGH pA
f1 ori
SV40 ori/ Promoter
pcDNA3/β2V7
7.9 kbp
AmpR
NeoR
SV40 pA
ColE1

3.2.1.4 Constructing the Chimeric β2V12 and β2V72 cDNA Clones

3.2.1.4.1 Modifying the β2 cDNA Sequence of pBS/β2V, Creating pBS/β2M

In order to construct the chimeric β2V12 and β2V72 cDNAs, a modified β2 cDNA clone in pBluescript, pBS/β2M, was constructed from pBS/β2V as illustrated in Figure 3.10a. pBS/β2V was digested with EcoRV (β2V cDNA, bp 1404-1409) and XhoI (pBS/β2V, 3' polylinker) to excise the β2 cDNA fragment encoding the C-terminal cysteine-rich, membrane proximal, transmembrane and cytoplasmic domains. A β2 cDNA fragment encoding only the transmembrane and cytoplasmic domains was then synthesised by PCR, using the oligonucleotide primers B93/23 and B93/22. Figure 3.10b shows the sequences of these oligonucleotides and their positions in the β2 cDNA sequence. B93/23 was designed to engineer an EcoRV site into the β2 cDNA sequence between the extracellular and transmembrane domains (bp 2199-2204), whereas B93/22 was designed to engineer an XhoI site into the 3' UTR (bp 2435-2440). By replacing the pBS/β2V EcoRV-XhoI fragment (spanning the C-terminal cysteine-rich, membrane proximal, transmembrane and cytoplasmic domains) with the PCR synthesised EcoRV-XhoI fragment (spanning only the transmembrane and cytoplasmic domains), a modified β2 cDNA clone, β2M, was created, in which the C-terminal cysteine-rich and membrane proximal domains had been deleted. The nucleotide and amino acid sequences at the resulting junction between the extracellular and transmembrane domains in β2M are shown in Figure 3.10c. The EcoRV site was reformed at this junction (β2M cDNA, bp 1404/2204). No amino acid mutations were introduced into the β2 coding sequence to create pBS/β2M.

3.2.1.4.2 Constructing the Chimeric β2V12 cDNA from pBS/β2M, Creating pBS/β2V12

The chimeric β2V12 cDNA was constructed from pBS/β2M as illustrated in Figure 3.11a, creating a clone named pBS/β2V12. Exchanges between the β2 and the β1 subunit were facilitated using the pBS/β2M unique EcoRV site (β2M cDNA, bp 1404/2204). A β1 cDNA fragment encoding the C-terminal cysteine-rich and membrane proximal domains was synthesised by PCR, using the pBS/β2V1 clone as template and the oligonucleotides C92/20 and B93/24. The C92/20 oligonucleotide was designed to engineer an EcoRV site into the 5' end of the PCR product (β1 cDNA, bp 1457-1462), whereas the B93/24

oligonucleotide was complementary to the wildtype β1 cDNA sequence at the 3' end of the PCR product. The sequences of these oligonucleotides and their positions in the β1 cDNA sequence are shown in Figure 3.11b. The chimeric β2V12 cDNA was constructed by phosphorylating the β1 PCR product using T4 polynucleotide kinase, digesting it with EcoRV, and then cloning the resulting β1 cDNA fragment (encoding the β1 C-terminal cysteine-rich and membrane proximal domains) into EcoRV cut pBS/β2M. The resulting pBS/β2V12 clone was nucleotide sequenced to confirm the correct formation of the β2/β1 chimeric junctions, and to confirm the absence of PCR errors in the β1 PCR derived section. The construction of the β2V12 chimeric junctions is shown in detail in Figure 3.11c. The EcoRV site chimeric junction in the β2V12 cDNA is exactly the same as the EcoRV site chimeric junction in the β2V1 cDNA. No amino acid mutations were introduced into the β2 or the β1 subunit at the β2V12 chimeric junctions.

3.2.1.4.3 Constructing the Chimeric β2V72 cDNA from pBS/β2M, Creating pBS/β2V72

The chimeric β2V72 cDNA was constructed from pBS/β2M in a similar way, creating a clone named pBS/β2V72. The construction of pBS/β2V72 is illustrated in Figure 3.12a. The β7 cDNA spanning the exchanged region was synthesised by PCR, using pBS/β2V7 as template and the oligonucleotides B92/4 and B93/25. The B92/4 oligonucleotide was designed to engineer an EcoRV site into the 5' end PCR product (β7 cDNA, bp 1503-1508), whereas the B93/25 oligonucleotide was complementary to the wildtype β7 cDNA sequence at the 3' end PCR product. The sequences of these oligonucleotides and their positions in the β7 cDNA sequence are shown in Figure 3.12b. The chimeric β2V72 cDNA was constructed by phosphorylating the β7 PCR product using T4 polynucleotide kinase, digesting it with EcoRV, and then cloning the resulting β7 cDNA fragment (encoding the β7 C-terminal cysteine-rich and membrane proximal domains) into EcoRV cut pBS/β2M. The resulting pBS/β2V72 clone was nucleotide sequenced to confirm the correct formation of the β2/β7 chimeric junctions, and to confirm the absence of PCR errors in the β7 PCR derived section. The construction of the β2V72 chimeric junctions is shown in detail in Figure 3.12c. The EcoRV site chimeric junction in the β2V72 cDNA is exactly the same as the EcoRV site chimeric junction in the β2V7 cDNA. No amino acid mutations were introduced into the β2 or the β7 subunit at the β2V72 chimeric junctions.

3.2.1.4.4 Cloning the β2V12 and β2V72 cDNAs into Expression Vectors

The entire coding regions of the β2V12 and β2V72 cDNAs were subcloned from pBluescript into the vectors pSVL (Pharmacia) and pcDNA3 (Invitrogen) for transient expression in COS 7 cells.

3.2.1.4.4.1 Constructing the pSVL/β2V12 Clone

The β2V12 cDNA was subcloned from pBluescript into the pSVL vector as illustrated in Figure 3.13a. pBS/β2V12 was digested with XhoI (β2V12 cDNA, 3' UTR) and the resultant 5' overhang was blunted using the end-filling reaction. The β2V12 cDNA insert was then excised by digestion with XbaI (β2V12 cDNA, 5' UTR), and was cloned into XbaI/SmaI cut pSVL, creating a clone named pSVL/β2V12.

3.2.1.4.4.2 Constructing the pSVL/β2V72 Clone

The β2V72 cDNA was subcloned from pBluescript into the pSVL vector as illustrated in Figure 3.13b. pBS/β2V72 was digested with XhoI (β2V72 cDNA, 3' UTR) and the resultant 5' overhang was blunted using the end-filling reaction. The β2V72 cDNA insert was then excised by digestion with XbaI (β2V72 cDNA, 5' UTR), and was cloned into XbaI/SmaI cut pSVL, creating a clone named pSVL/β2V72.

3.2.1.4.4.3 Constructing the pcDNA3/β2V12 Clone

The β2V12 cDNA was subcloned from pSVL into the pcDNA3 vector as illustrated in Figure 3.13c. The β2V12 cDNA insert was excised from pSVL/β2V12 by digestion with XhoI (pSVL/β2V12, 5' polylinker; 2V12 cDNA, 3' UTR) and was cloned into XhoI cut pcDNA3, creating pcDNA3/β2V12. The orientation of the β2V12 cDNA in the expression vector was determined by EcoRI digestion. Clones producing a 1 kbp restriction fragment were in the correct orientation.

3.2.1.4.4.4 Constructing the pcDNA3/β2V72 Clone

The β2V72 cDNA was subcloned from pSVL into the pcDNA3 vector as illustrated in Figure 3.13d. The β2V72 cDNA insert was excised from pSVL/β2V72 by digestion with XhoI (pSVL/β2V72, 5' polylinker; 2V72 cDNA, 3' UTR) and was cloned into XhoI cut pcDNA3, creating pcDNA3/β2V72. The orientation of the β2V72 cDNA in the expression

vector was determined by EcoRI digestion. Clones producing a 1 kbp restriction fragment were in the correct orientation.

Figure 3.10a: Constructing the Clone pBS/β2M from pBS/β2V

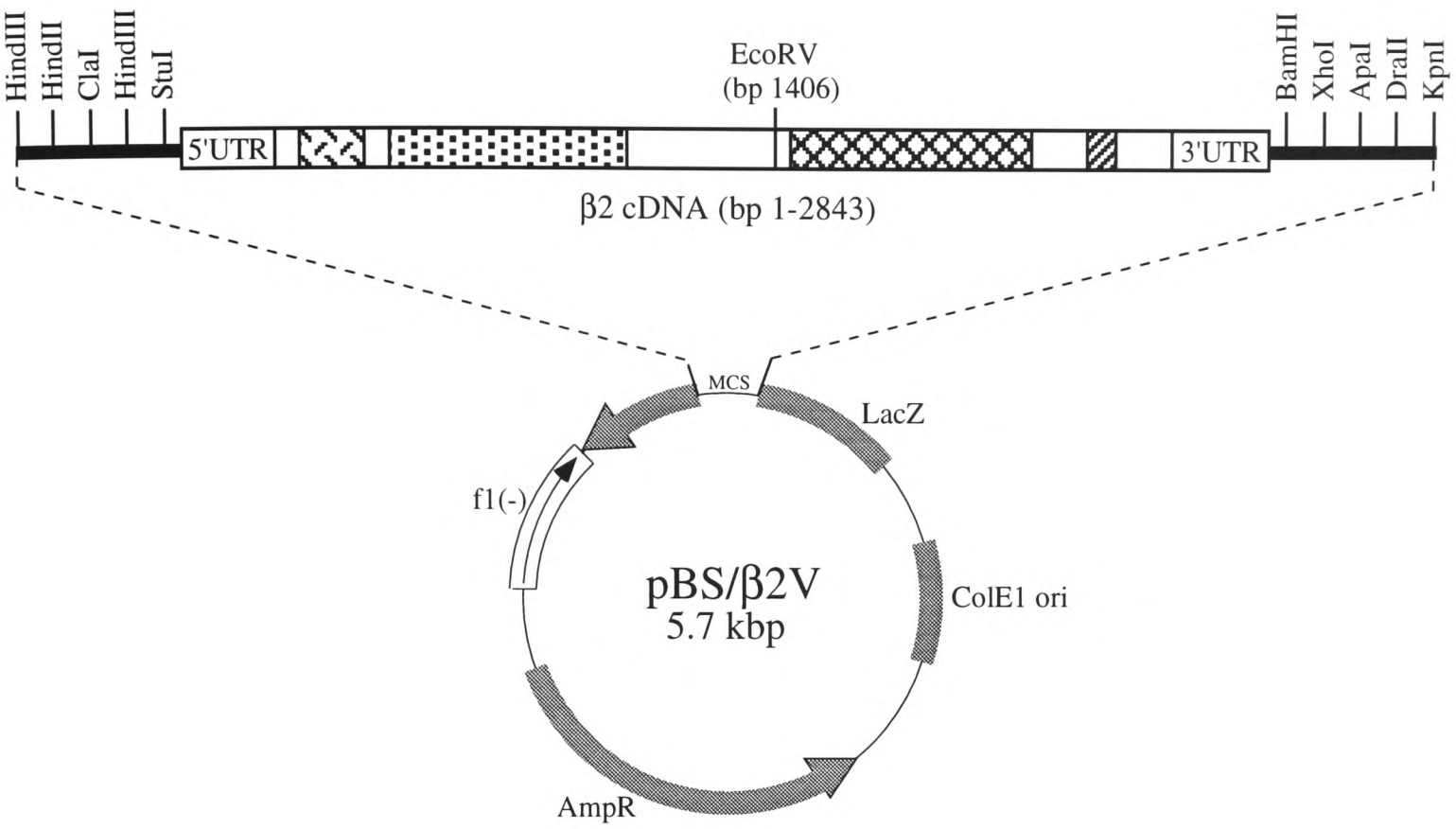
A modified β2 cDNA, β2M, in which the cDNA regions encoding the C-terminal cysteine-rich region, and the membrane proximal, transmembrane and cytoplasmic domains were deleted, was constructed in pBluescript from the pBS/β2V clone as follows:

(1) pBS/β2V was digested with EcoRV (β2V, bp 1404-1409) and XhoI (pBS/β2V, 3' polylinker), and the larger 4.3 kbp pBS/β2V fragment was purified by agarose gel electrophoresis.

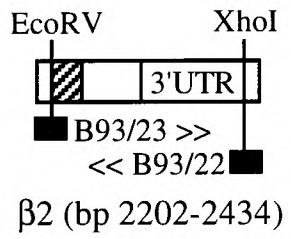
(2) A β2 PCR product (bp 2202-2434) was synthesised using the wildtype J8 clone as template, the oligonucleotides B93/23 and B93/22 as primers, and the Pfu DNA polymerase enzyme. The B93/23 oligonucleotide was designed to engineer an EcoRV site into the 5' end of the PCR product, whereas the B93/22 oligonucleotide was designed to engineer an XhoI site into the 3' end (see Figure 3.10b). The β2 PCR product was digested with EcoRV and XhoI, and the 232 bp EcoRV-XhoI β2 PCR fragment was purified by agarose gel electrophoresis.

(3) The 232 bp β2 PCR fragment and the 4.3 kbp pBS/β2V fragment were then ligated, creating a modified β2 cDNA in pBluescript, clone pBS/β2M, in which the β2 cDNA regions encoding the C-terminal cysteine-rich region, and the membrane proximal, transmembrane and cytoplasmic domains, were deleted. The pBS/β2M clone was nucleotide sequenced to confirm the correct formation of the EcoRV site at the junction between the cDNA regions encoding the "mid-piece" and transmembrane domains, and to confirm the absence of PCR errors in the EcoRV-XhoI section derived by PCR. No amino acid mutations were introduced into the β2 coding sequence to create the β2M cDNA (see Figure 3.10c).

In the figure opposite, the region encoding the N-terminal cysteine rich region is represented by dashed lines, the region encoding the putative A-domain by dots, the region encoding the C-terminal cysteine-rich region by crosshatches, and the region encoding the transmembrane domain by diagonal lines. The 5' and 3' untranslated regions (UTRs) of the β2 cDNA are also shown.



PCR PRODUCT



β2 (bp 2202-2434)

(1)

(2)

(3)

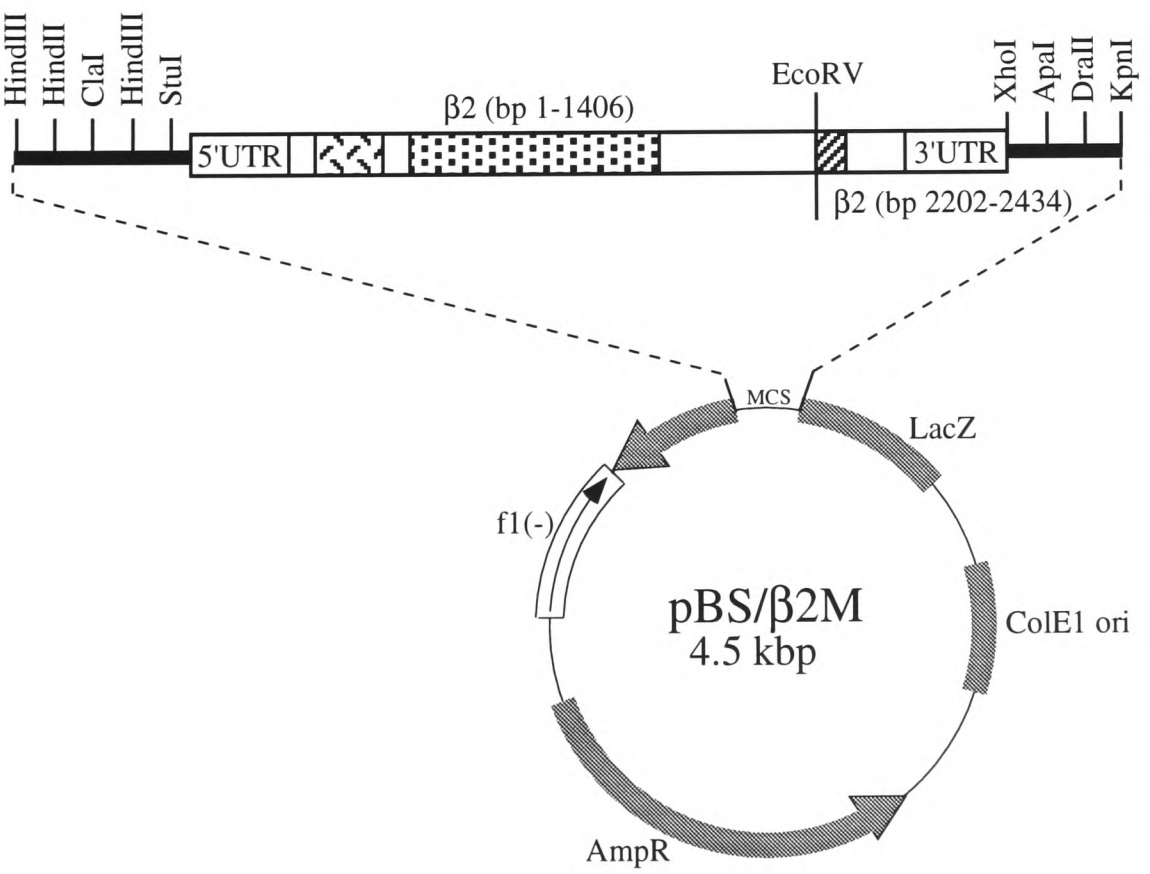


Figure 3.10b: The Sequences and Annealing Positions of the B93/23 and B93/22 Oligonucleotides

A section of the β2 cDNA encoding the transmembrane and cytoplasmic domains was synthesised by PCR, using the wildtype β2 cDNA clone J8 as template and the oligonucleotides B93/23 and B93/22 as primers. The B93/23 oligonucleotide was designed to engineer an EcoRV site into the 5' end of the PCR product (β2 cDNA, bp 2199-2204), whereas the B93/22 oligonucleotide was designed to engineer an XhoI site into the 3' end of the PCR product (β2 cDNA, bp 2435-2440). The relevant section of the wildtype β2 cDNA is shown in the figure opposite, with the amino acids it encodes shown above the cDNA sequence (using the single letter amino acid code), and with the residues representing the transmembrane domain underlined. The sequences of the B93/23 and B93/22 oligonucleotides, and their annealing positions in the wildtype β2 cDNA template are also shown, with residues that match the wildtype sequence indicated by vertical lines and mismatched residues by dots, and with the residues representing the EcoRV and XhoI sites shown in pink. The DNA mutations engineered into the 5' end of the β2 PCR product to create the EcoRV site resulted in a single amino acid substitution, N700D, shown above the wildtype β2 sequence. However, as the PCR product was subsequently digested with EcoRV and XhoI, and only the EcoRV-XhoI fragment was used to create the modified β2M cDNA construct, this mutation was not introduced into the pBS/β2M clone (see Figure 3.10c).

EcoRV
D
R E C56 V A G P N I A A I V G G T V A G I V L I
B93/23>> CCCGATATCGCCGCCATCGTCGG >>B93/23
CCGAGAGTGTGTGGCAGGCCCCAACATCGCCGCCATCGTCGGGGGCACCGTGGCAGGCATCGTGCTGATC
2180 2190 2200 2210 2220 2230 2240
GGCTCTCACACACCGTCCGGGGTTGTAGCGGCGGTAGCAGCCCCCGTGGCACCGTCCGTAGCACGACTAG

G I L L L V I W K A L I H L S D L R E Y R R F E

GGCATTCTCCTGCTGGTCATCTGGAAGGCTCTGATCCACCTGAGCGACCTCCGGGAGTACAGGCGCTTTG
2250 2260 2270 2280 2290 2300 2310
CCGTAAGAGGACGACCAGTAGACCTTCCGAGACTAGGTGGACTCGCTGGAGGCCCTCATGTCCGCGAAAC

K E K L K S Q W N N D N P L F K S A T T T V M

AGAAGGAGAAGCTCAAGTCCCAGTGGAACAATGATAATCCCCTTTTCAAGAGCGCCACCACGACGGTCAT
2320 2330 2340 2350 2360 2370 2380
TCTTCCTCTTCGAGTTCAGGGTCACCTTGTTACTATTAGGGGAAAAGTTCTCGCGGTGGTGCTGCCAGTA

N P K F A E S * 3'UTR

GAACCCCAAGTTTGCTGAGAGTTAGGAGCACTTGGTGAAGACAAGGCCGTCAGGACCCACCATGTCTGCC
2390 2400 2410 2420 2430 2440 2450
CTTGGGGTTCAAACGACTCTCAATCCTCGTGAACCACTTCTGTTCCGGCAGTCCTGGGTGGTACAGACGG
B93/22<< TGAACCACTTCTGTTCCGGGAGCTCTG <<B93/22
XhoI

Figure 3.10c: The Nucleotide and Amino Acid Sequences at the Junction Between the "Mid-Piece" and Transmembrane Domains in the Modified β2 cDNA, β2M

A modified β2 cDNA, β2M, lacking the β2 cDNA section encoding the C-terminal cysteine-rich and membrane proximal regions, was constructed from the β2V cDNA and a β2 PCR product as summarised in Figure 3.10a. The figure below shows the formation of the junction between the "mid-piece" and the transmembrane domain in β2M. The relevant sections of the wildtype β2 cDNA are shown for reference, along with the relevent sections of the β2V cDNA and the β2 PCR product. The amino acid residues these sections encode are shown above the cDNA sequence (using the single letter amino acid code), with residues representing the transmembrane domain underlined. The junction between the "mid-piece" and the transmembrane domain in β2M was constructed using the EcoRV sites in the β2V cDNA and the β2 PCR product. The nucleotide residues representing these EcoRV sites are shown in the figure below in pink. The β2V cDNA and the β2 PCR product were both digested with EcoRV, and their resultant blunt ends were ligated together (as indicated in the figure below by the arrows), reforming the EcoRV site and creating the β2M "mid-piece"/transmembrane junction. As can be seen in the figure below, no amino acid mutations were introduced into the β2 coding sequence to create this junction.

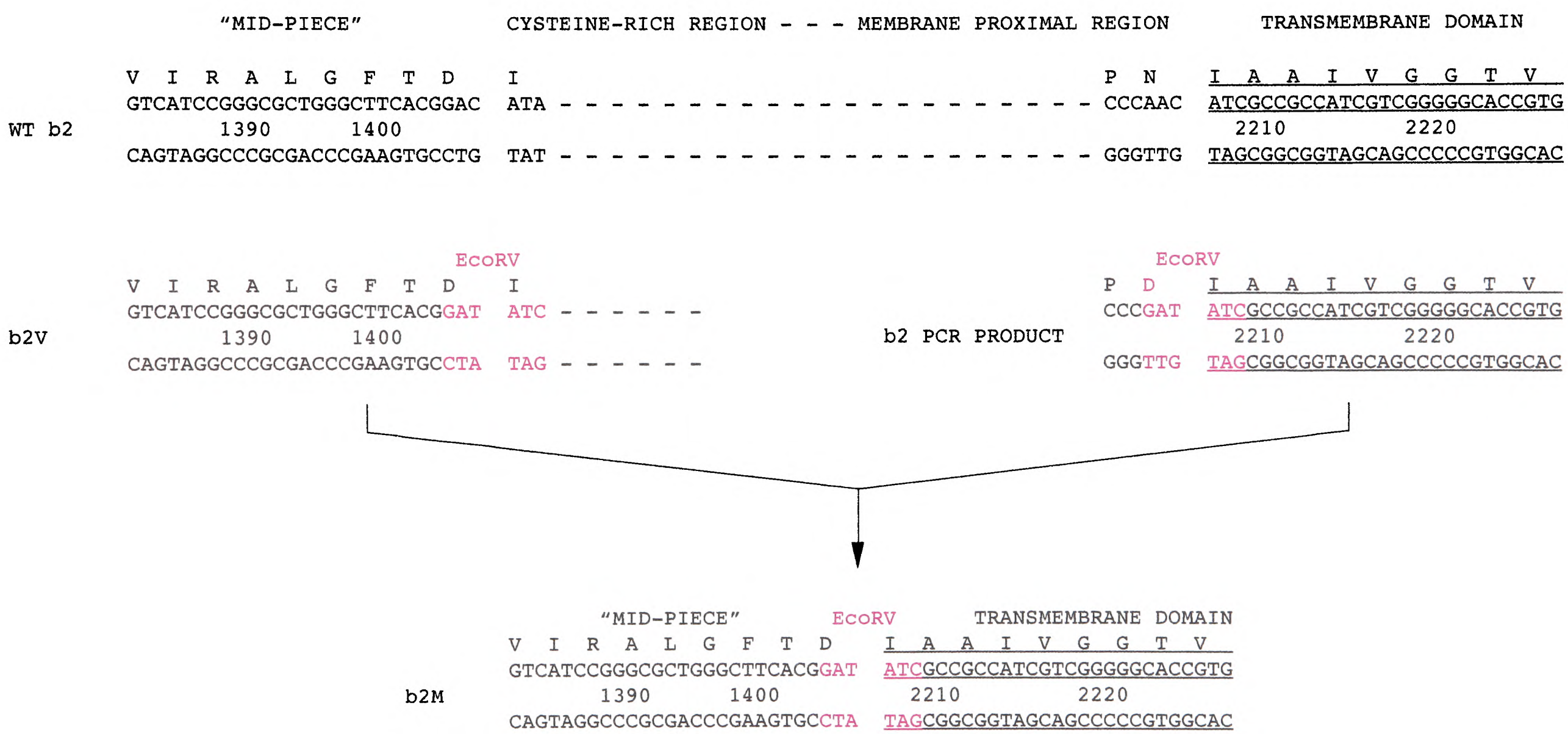

"MID-PIECE"
CYSTEINE-RICH REGION - - - MEMBRANE PROXIMAL REGION
TRANSMEMBRANE DOMAIN
V I R A L G F T D
I
P N
I A A I V G G T V
GTCATCCGGGCGCTGGGCTTCACGGAC
ATA - - -

Figure 3.11a: Constructing the Chimeric β2V12 cDNA in pBluescript, Creating pBS/β2V12

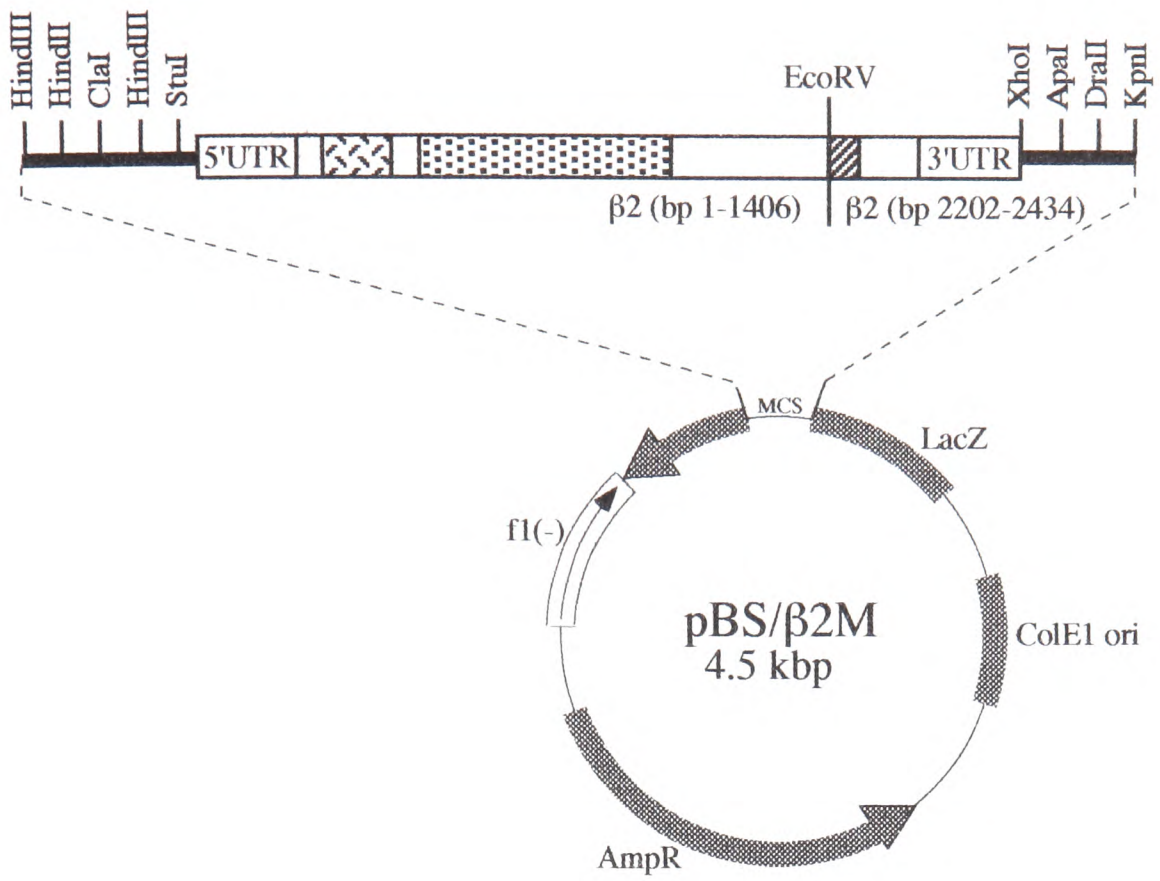
The chimeric β2V12 cDNA in pBluescript, pBS/β2V12, was constructed from the pBS/β2M clone as follows:

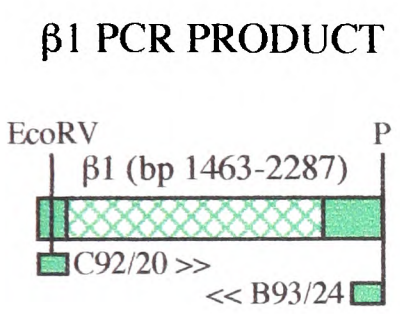
(1) pBS/β2M was digested with EcoRV (β2M cDNA, bp 1404/2204), and the 4.5 kbp pBS/β2M fragment was purified by agarose gel electrophoresis.

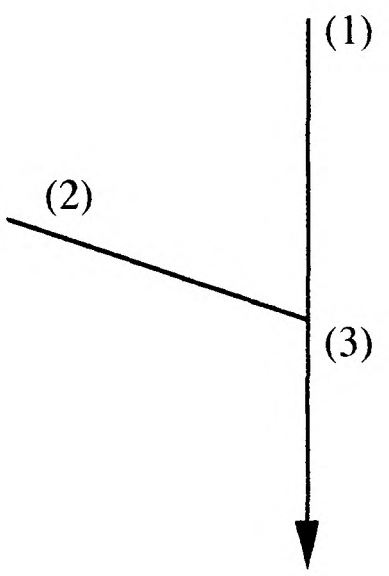
(2) A β1 PCR product (bp 1463-2287) was synthesised using the pBS/β2V1 clone as template, the oligonucleotides C92/20 and B93/24 as primers, and the Pfu DNA polymerase enzyme. The C92/20 oligonucleotide was designed to engineer an EcoRV site into the 5' end of the PCR product, whereas the B93/24 oligonucleotide was complementary to the wildtype β1 cDNA sequence at the 3' end of the PCR product (see Figure 3.11b). The β1 PCR product was phosphorylated using T4 polynucleotide kinase and was then digested with EcoRV, and the 824 bp PCR fragment was purified by agarose gel electrophoresis.

(3) The 824 kbp β1 PCR fragment and the 4.5 kbp pBS/β2M fragment were then ligated, creating a full length chimeric β2V12 cDNA in pBluescript, clone pBS/β2V12. The pBS/β2V12 clone was nucleotide sequenced to confirm the correct formation of the β2/β1 chimeric junctions, and to confirm the absence of PCR errors in the β1 cDNA section derived by PCR. No amino acid mutations were introduced into the β2 or β1 subunits at both β2V12 chimeric junctions (see Figure 3.11c).

In the figure opposite, the β2 cDNA regions are unshaded, whereas the β1 cDNA regions are shaded green. The regions encoding the N-terminal cysteine rich region are represented by dashed lines, the regions encoding the putative A-domain by dots, the regions encoding the C-terminal cysteine-rich region by crosshatches, and the regions encoding the transmembrane domain by diagonal lines. The 5' and 3' untranslated regions (UTRs) of the β cDNAs are also shown.


HindIII
HindII
ClaI
HindIII
StuI
EcoRV
XhoI
ApaI
DraII
KpnI
5'UTR
3'UTR
β2 (bp 1-1406)
β2 (bp 2202-2434)
MCS
LacZ
f1(-)
pBS/β2M
4.5 kbp
ColE1 ori
AmpR


β1 PCR PRODUCT
EcoRV
P
β1 (bp 1463-2287)
C92/20 >>
<< B93/24


(1)
(2)
(3)

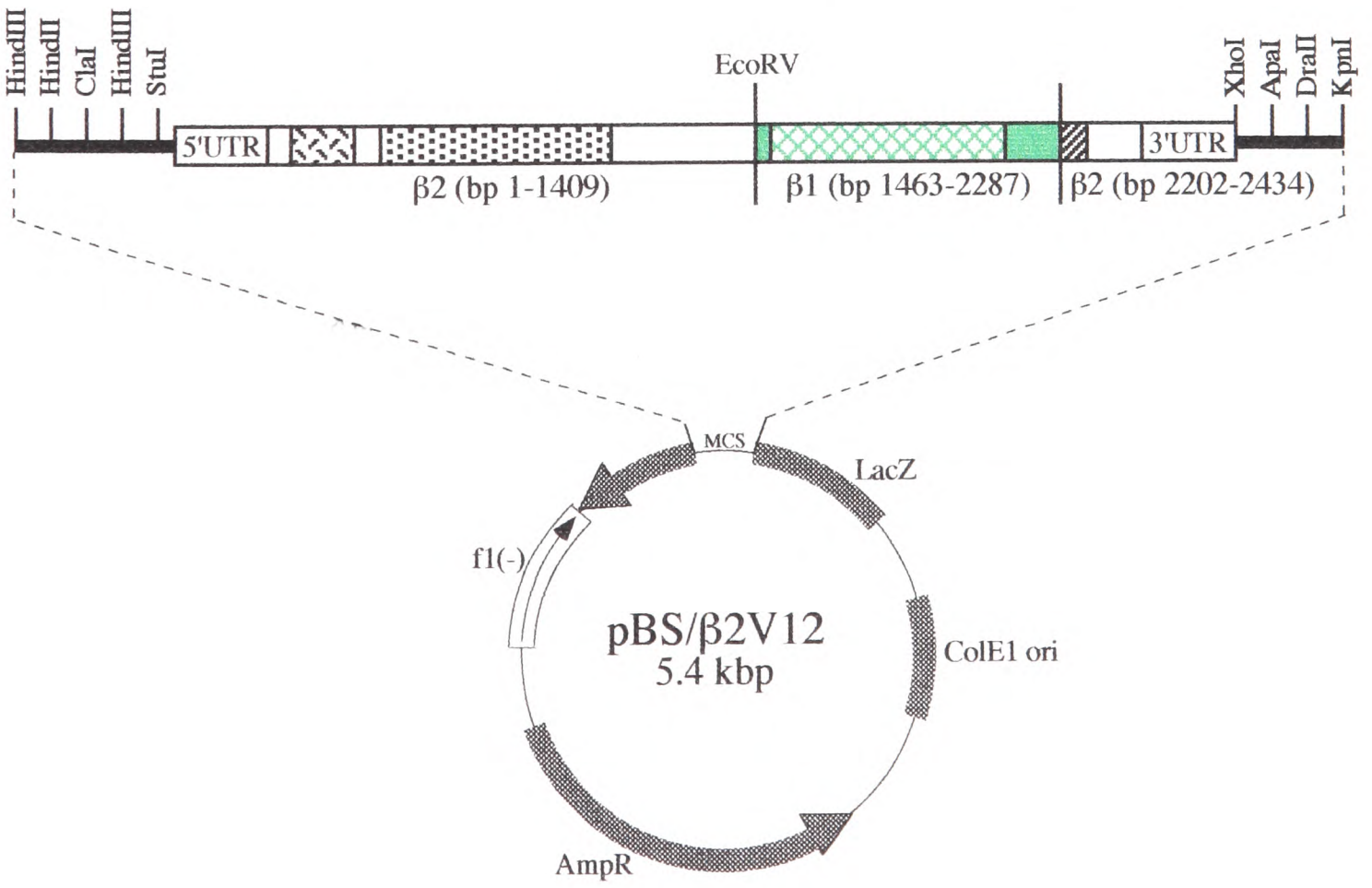

HindIII
HindII
ClaI
HindIII
StuI
EcoRV
XhoI
ApaI
DraII
KpnI
5'UTR
3'UTR
β2 (bp 1-1409)
β1 (bp 1463-2287)
β2 (bp 2202-2434)
MCS
LacZ
f1(-)
pBS/β2V12
5.4 kbp
ColE1 ori
AmpR



Figure 3.11b: The C92/20 and B93/24 Oligonucleotides used to Synthesise the β1 cDNA Section of the Chimeric β2V12 cDNA

The β1 cDNA section of the chimeric β2V12 cDNA was synthesised by PCR, using the pBS/β2V1 clone as template and the C92/20 and B93/24 oligonucleotides as primers. The oligonucleotide C90/20 was designed to engineer an EcoRV site into the 5' end of the PCR product (β1 cDNA: bp 1457-1462), whilst the B93/24 oligonucleotide was complimentary to the wildtype β1 cDNA sequence at the 3' end of the PCR product. The relevant sections of the wildtype β1 cDNA are shown in the figure above in green, and the amino acids that these sections encode are shown above the cDNA sequence (using the single letter amino acid code), also in green, with the residues representing the transmembrane domain underlined. The sequences and annealing positions of the C92/20 and the B93/24 oligonucleotides are also shown, with residues that match the wildtype sequence indicated by vertical lines and mismatched residues by dots, and with the residues representing the EcoRV site shown in pink. The DNA mutations engineered into the 5' end of the β1 PCR product to create the EcoRV site resulted in two amino acid substitutions, E452D and E453I, shown above the wildtype β1 sequence. However, as these residues correspond to the wildtype β2 residues at these positions, no amino acid changes were introduced into the β1 section of the resulting β2V12 chimera (see Figure 3.11c).

Figure 3.11c: Formation of the β2V12 Chimeric Junctions

The figure below shows the formation of the β2/β1 chimeric junctions in the β2V12 chimera. The wildtype β2 cDNA and amino acid sequences are shown in black, whereas the wildtype β1 cDNA and amino acid sequences are shown in green, and the nucleotide residues which represent the EcoRV site are shown in pink. Cysteine residues are shown in red, and are numbered such that the first cysteine residue in the mature β polypeptide would be numbered C1 and the last would be numbered C56. The residues which represent the β subunit transmembrane domain are underlined. It should be noted that both of the β2V12 chimeric junctions were created without introducing any amino acid mutations into the β2 or the β1 sections.

"MID-PIECE" CYSTEINE-RICH REGION MEMBRANE PROXIMAL REGION TRANSMEMBRANE DOMAIN

WT b2

```
R A L G F T D   I V T V Q V L                   E C56 V A G P N   I A A I V G G
CGGGCGCTGGGCTTCACGGAC ATAGTGACCGTGCAGGTCCTT - - - - - - - - - - GAGTGTGTGGCAGGCCCCAAC ATCGCCGCCATCGTCGGGGGC
 1390      1400       1410      1420                              2190      2200      2210      2220
GCCCGCGACCCGAAGTGCCTG TATCACTGGCACGTCCAGGAA - - - - - - - - - - CTCACACACCGTCCGGGGTTG TAGCGGCGGTAGCAGCCCCCG
```

b2M

```
                  EcoRV                                                                EcoRV
R A L G F T D                                                                          I A A I V G G
CGGGCGCTGGGCTTCACGGAT                                                                  ATCGCCGCCATCGTCGGGGGC
 1390      1400                                                                            2210      2220
GCCCGCGACCCGAAGTGCCTA                                                                  TAGCGGCGGTAGCAGCCCCCG
```

WT b1

```
R P L G F T E   E V E V I L Q                   E C56 P T G P D   I I P I V A G
AGGCCTCTGGGCTTTACGGAG GAAGTAGAGGTTATTCTTCAG - - - - - - - - - - GAGTGTCCCACTGGTCCAGAC ATCATTCCAATTGTAGCTGGT
      1450                1470      1480                        2270      2280            2300      2310
TCCGGAGACCCGAAATGCCTC CTTCATCTCCAATAAGAAGTC - - - - - - - - - - CTCACAGGGTGACCAGGTCTG TAGTAAGGTTAACATCGACCA
```

b1 PCR PRODUCT

```
      EcoRV
T D   I V E V I L Q                             E C56 P T G P D
ACGGAT ATCGTAGAGGTTATTCTTCAG - - - - - - - - - - GAGTGTCCCACTGGTCCAGAC
                  1470      1480                  2270      2280
TGCCTA TAGCATCTCCAATAAGAAGTC - - - - - - - - - - CTCACAGGGTGACCAGGTCTG
```

b2V12

```
                  EcoRV                                                                ~~EcoRV~~
R A L G F T D   I V E V I L Q                   E C56 P T G P D   I A A I V G G
CGGGCGCTGGGCTTCACGGAT ATCGTAGAGGTTATTCTTCAG - - - - - - - - - - GAGTGTCCCACTGGTCCAGAC ATCGCCGCCATCGTCGGGGGC
 1390      1400       1410      1420                              2220      2230      2240      2250
GCCCGCGACCCGAAGTGCCTA TAGCATCTCCAATAAGAAGTC - - - - - - - - - - CTCACAGGGTGACCAGGTCTG TAGCGGCGGTAGCAGCCCCCG
```

Figure 3.12a: Constructing the Chimeric β2V72 cDNA in pBluescript, Creating pBS/β2V72

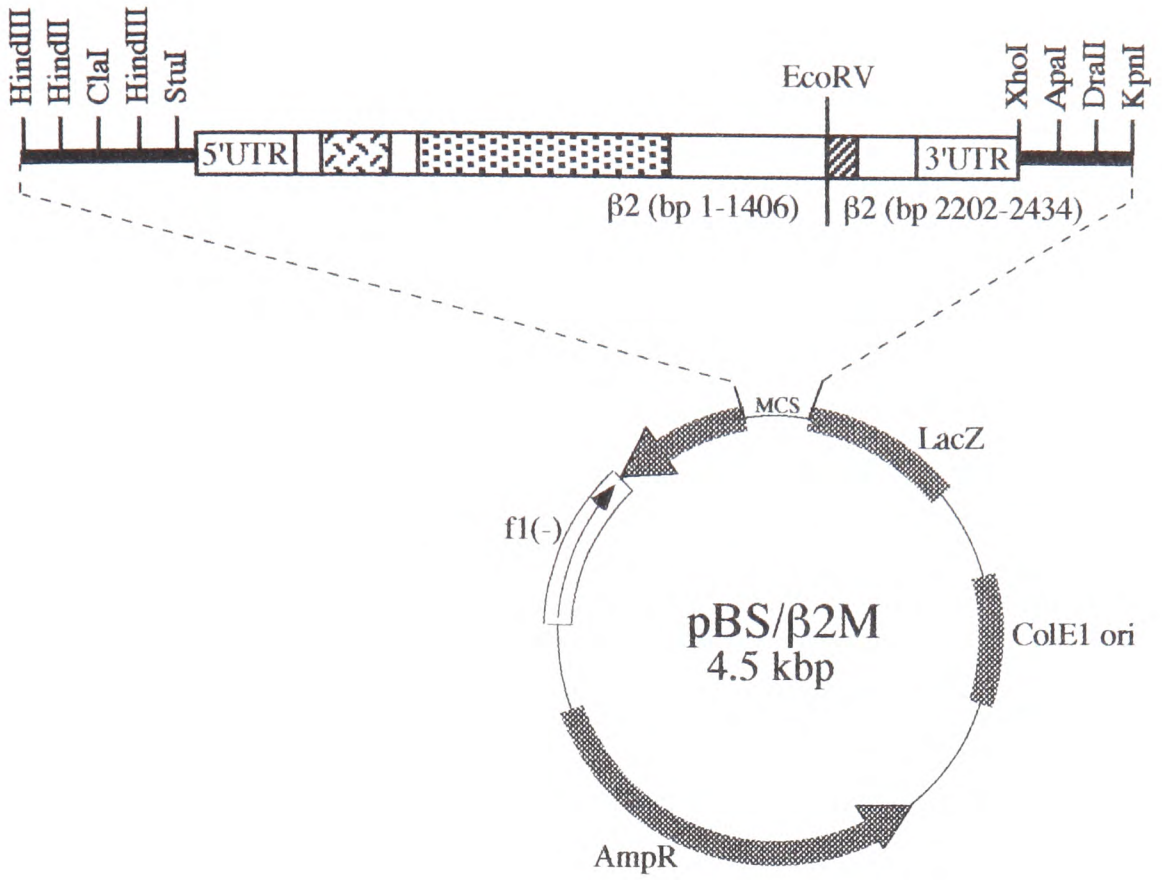
The chimeric β2V72 cDNA in pBluescript, pBS/β2V72, was constructed from the pBS/β2M clone as follows:

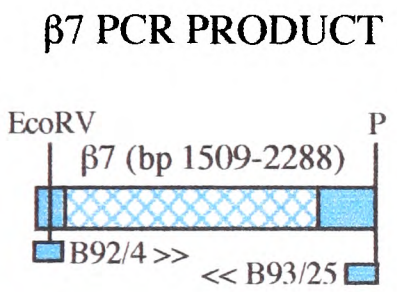
(1) pBS/β2M was digested with EcoRV (β2M cDNA, bp 1404/2204), and the 4.5 kbp pBS/β2M fragment was purified by agarose gel electrophoresis.

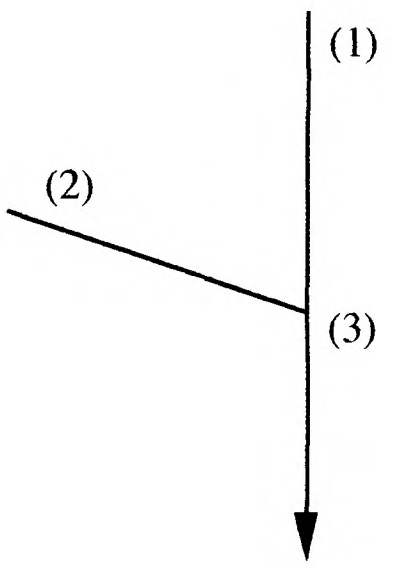
(2) A β7 PCR product (bp 1509-2288) was synthesised using the pBS/β2V7 clone as template, the oligonucleotides B92/4 and B93/25 as primers, and the Pfu DNA polymerase enzyme. The B92/4 oligonucleotide was designed to engineer an EcoRV site into the 5' end of the PCR product, whereas the B93/25 oligonucleotide was complementary to the wildtype β7 cDNA sequence at the 3' end of the PCR product (see Figure 3.12b). The β7 PCR product was phosphorylated using T4 polynucleotide kinase and was then digested with EcoRV, and the 779 kbp PCR fragment was purified by agarose gel electrophoresis.

(3) The 779 kbp β7 PCR fragment and the 4.5 kbp pBS/β2M fragment were then ligated, creating a full length chimeric β2V72 cDNA in pBluescript, clone pBS/β2V72. The pBS/β2V72 clone was nucleotide sequenced to confirm the correct formation of the β2/β7 chimeric junctions, and to confirm the absence of PCR errors in the β7 cDNA section derived by PCR. No amino acid mutations were introduced into the β2 or β7 subunits at both β2V72 chimeric junctions (see Figure 3.12c).

In the figure opposite, the β2 cDNA regions are unshaded, whereas the β7 cDNA regions are shaded blue. The regions encoding the N-terminal cysteine rich region are represented by dashed lines, the regions encoding the putative A-domain by dots, the regions encoding the C-terminal cysteine-rich region by crosshatches, and the regions encoding the transmembrane domain by diagonal lines. The 5' and 3' untranslated regions (UTRs) of the β cDNAs are also shown.


HindIII
HindII
ClaI
HindIII
StuI
EcoRV
XhoI
ApaI
DraII
KpnI
5'UTR
3'UTR
β2 (bp 1-1406)
β2 (bp 2202-2434)
MCS
LacZ
f1(-)
pBS/β2M
4.5 kbp
ColE1 ori
AmpR


β7 PCR PRODUCT
EcoRV
P
β7 (bp 1509-2288)
B92/4 >>
<< B93/25


(1)
(2)
(3)

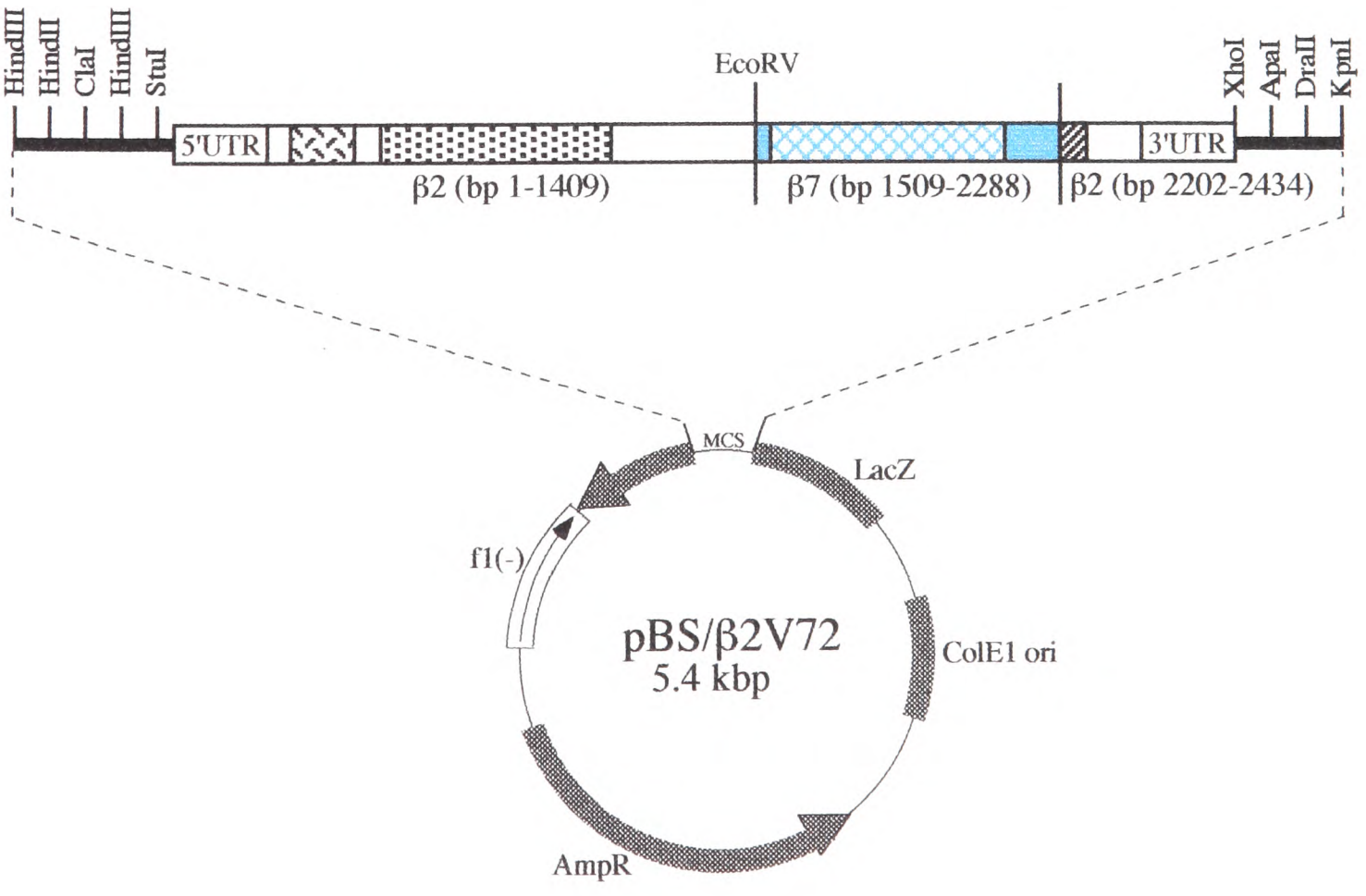

HindIII
HindII
ClaI
HindIII
StuI
EcoRV
XhoI
ApaI
DraII
KpnI
5'UTR
3'UTR
β2 (bp 1-1409)
β7 (bp 1509-2288)
β2 (bp 2202-2434)
MCS
LacZ
f1(-)
pBS/β2V72
5.4 kbp
ColE1 ori
AmpR



Figure 3.12b: The B92/4 and B93/25 Oligonucleotides used to Synthesise the β7 cDNA Section of the Chimeric β2V72 cDNA

The β7 cDNA section of the chimeric β2V72 cDNA was synthesised by PCR, using the pBS/β2V7 clone as template and the B92/4 and B93/25 oligonucleotides as primers. The oligonucleotide B92/4 was designed to engineer an EcoRV site into the 5' end of the PCR product (β7 cDNA: bp 1503-1508), whilst the B93/25 oligonucleotide was complimentary to the wildtype β7 cDNA sequence at the 3' end of the PCR product. The relevant sections of the wildtype β7 cDNA are shown in the figure above in blue, and the amino acids that these sections encode are shown above the cDNA sequence (using the single letter amino acid code), also in blue, with the residues representing the transmembrane domain underlined. The sequences and annealing positions of the B92/4 and the B93/25 oligonucleotides are also shown, with residues that match the wildtype sequence indicated by vertical lines and mismatched residues by dots, and with the residues representing the EcoRV site shown in pink. The DNA mutations engineered into the 5' end of the β7 PCR product to create the EcoRV site resulted in two amino acid substitutions, E464D and E465I, shown above the wildtype β7 sequence. However, as these residues correspond to the wildtype β2 residues at these positions, no amino acid changes were introduced into the β7 section of the resulting β2V72 chimera (see Figure 3.12c).

Figure 3.12c: Formation of the β2V72 Chimeric Junctions

The figure below shows the formation of the β2/β7 chimeric junctions in the β2V72 chimera. The wildtype β2 cDNA and amino acid sequences are shown in black, whereas the wildtype β7 cDNA and amino acid sequences are shown in blue, and the nucleotide residues which represent the EcoRV site are shown in pink. Cysteine residues are shown in red, and are numbered such that the first cysteine residue in the mature β polypeptide would be numbered C1 and the last would be numbered C56. The residues which represent the β subunit transmembrane domain are underlined. It should be noted that both of the β2V72 chimeric junctions were created without introducing any amino acid mutations into the β2 or the β7 sections.

"MID-PIECE" CYSTEINE-RICH REGION MEMBRANE PROXIMAL REGION TRANSMEMBRANE DOMAIN

WT b2

```
R A L G F T D   I V T V Q V L                   E C56 V A G P N   I A A I V G G
CGGGCGCTGGGCTTCACGGAC ATAGTGACCGTGCAGGTCCTT - - - - - - - - - - GAGTGTGTGGCAGGCCCCAAC ATCGCCGCCATCGTCGGGGGC
 1390      1400       1410      1420                              2190      2200      2210      2220
GCCCGCGACCCGAAGTGCCTG TATCACTGGCACGTCCAGGAA - - - - - - - - - - CTCACACACCGTCCGGGGTTG TAGCGGCGGTAGCAGCCCCCG
```

b2M

```
                  EcoRV                                                              EcoRV
R A L G F T D                                                                        I A A I V G G
CGGGCGCTGGGCTTCACGGAT                                                              ATCGCCGCCATCGTCGGGGGC
 1390      1400                                                                        2210      2220
GCCCGCGACCCGAAGTGCCTA                                                              TAGCGGCGGTAGCAGCCCCCG
```

WT b7

```
R A L G F S E   E L I V E L H                   K G A D H T Q   A I V L G C V
CGGGCCCTTGGCTTCTCAGAG GAGCTGATTGTGGAGTTGCAC - - - - - - - - - - AAGGGAGCAGACCACACGCAG GCCATTGTGCTGGGCTGCGTA
 1490      1500       1510      1520                              2280      2300
GCCCGGGAACCGAAGAGTCTC CTCGACTAACACCTCAACGTG - - - - - - - - - - TTCCCTCGTCTGGTGTGCGTC CGGTAACACGACCCGACGCAT
```

b7 PCR

```
          EcoRV
S D   I L I V E L H                             K G A D H T Q
TCAGAT ATCCTGATTGTGGAGTTGCAC - - - - - - - - - - AAGGGAGCAGACCACACGCAG
       1510      1520                                2280
AGTCTA TAGGACTAACACCTCAACGTG - - - - - - - - - - TTCCCTCGTCTGGTGTGCGTC
```

b2V72

```
                  EcoRV                                                              ~~EcoRV~~
R A L G F T D   I L I V E L H                   K G A D H T Q                       I A A I V G G
CGGGCGCTGGGCTTCACGGAT ATCCTGATTGTGGAGTTGCAC - - - - - - - - - - AAGGGAGCAGACCACACGCAG ATCGCCGCCATCGTCGGGGGC
 1390      1400       1410      1420                              2180                2200      2210
GCCCGCGACCCGAAGTGCCTA TAGGACTAACACCTCAACGTG - - - - - - - - - - TTCCCTCGTCTGGTGTGCGTC TAGCGGCGGTAGCAGCCCCCG
```

Figure 3.13a: Constructing pSVL/β2V12

The entire coding region of the β2V12 cDNA was subcloned from pBluescript into the pSVL vector as follows:

(1) pBS/β2V12 was digested with XhoI (β2V12 cDNA, 3' UTR) and the resultant 5' overhang was blunted using the end-filling reaction. The β2V12 cDNA insert was then excised by digestion with XbaI (β2V12 cDNA, 5' UTR), and the 2.4 kbp β2V12 cDNA insert was purified by agarose gel electrophoresis.

(2) pSVL was digested with XbaI and SmaI, and the 4.8 kbp pSVL vector was also purified by agarose gel electrophoresis.

(3) The pSVL vector and the β2V12 cDNA insert were then ligated, creating a clone named pSVL/β2V12.

In the figure opposite, the β2 cDNA regions are unshaded, whereas the β1 cDNA regions are shaded green. The cDNA regions encoding the N-terminal cysteine rich region are represented by dashed lines, the regions encoding the putative A-domain by dots, the regions encoding the C-terminal cysteine-rich region by crosshatches, and the regions encoding the transmembrane domain by diagonal lines. The 5' and 3' untranslated regions (UTRs) of the cDNAs are also shown.

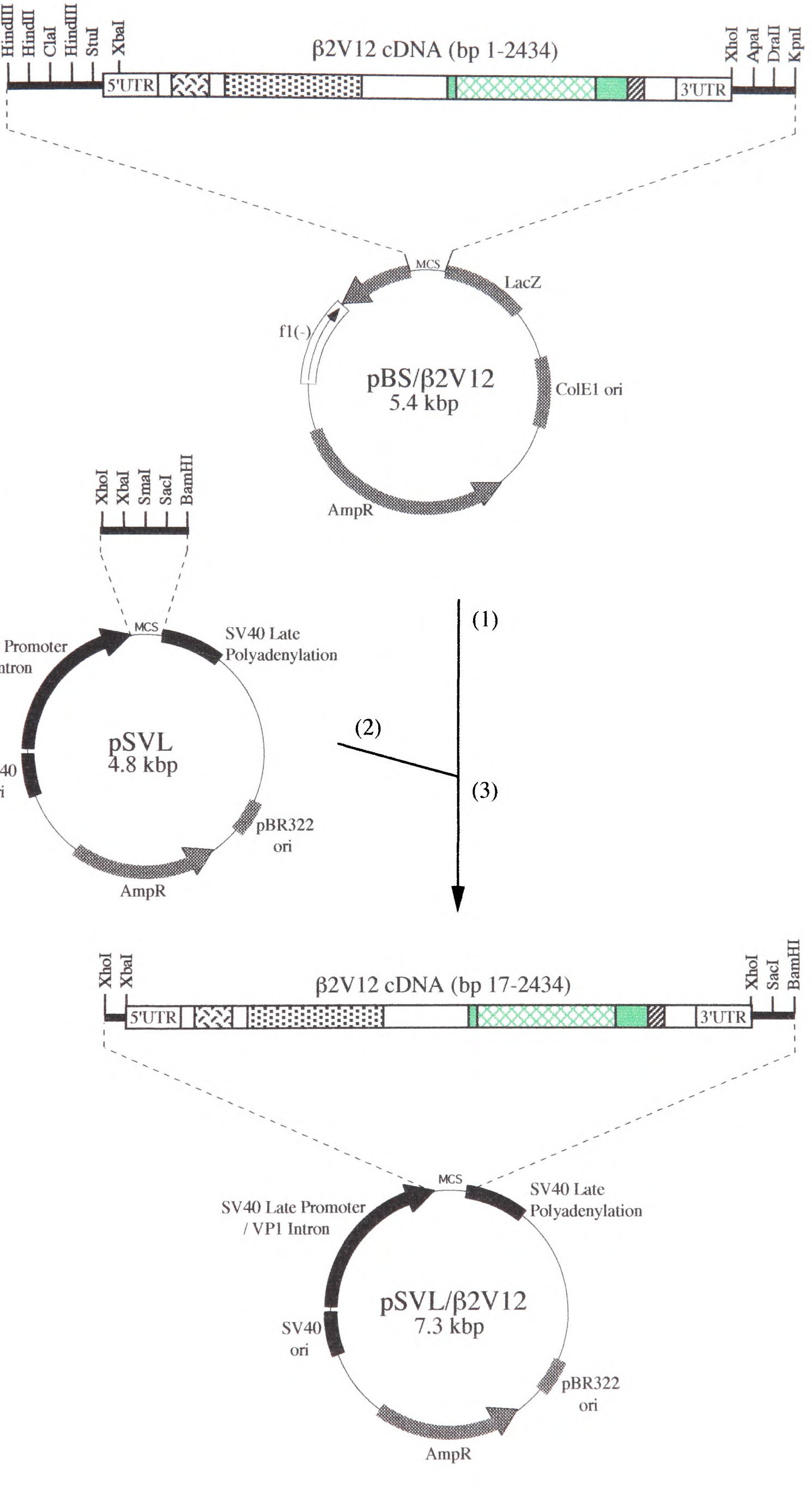

HindIII
HindII
ClaI
HindIII
StuI
XbaI
β2V12 cDNA (bp 1-2434)
XhoI
ApaI
DraII
KpnI
5'UTR
3'UTR
MCS
LacZ
f1(-)
pBS/β2V12
5.4 kbp
ColE1 ori
AmpR
XhoI
XbaI
SmaI
SacI
BamHI
MCS
SV40 Late Promoter
/ VP1 Intron
SV40 Late
Polyadenylation
pSVL
4.8 kbp
SV40
ori
pBR322
ori
AmpR
(1)
(2)
(3)
XhoI
XbaI
β2V12 cDNA (bp 17-2434)
XhoI
SacI
BamHI
5'UTR
3'UTR
MCS
SV40 Late Promoter
/ VP1 Intron
SV40 Late
Polyadenylation
pSVL/β2V12
7.3 kbp
SV40
ori
pBR322
ori
AmpR

Figure 3.13b: Constructing pSVL/β2V72

The entire coding region of the β2V72 cDNA was subcloned from pBluescript into the pSVL vector as follows:

(1) pBS/β2V72 was digested with XhoI (β2V72 cDNA, 3' UTR) and the resultant 5' overhang was blunted using the end-filling reaction. The β2V72 cDNA insert was then excised by digestion with XbaI (β2V72 cDNA, 5' UTR), and the 2.4 kbp β2V72 cDNA insert was purified by agarose gel electrophoresis.

(2) pSVL was digested with XbaI and SmaI, and the 4.8 kbp pSVL vector was also purified by agarose gel electrophoresis.

(3) The pSVL vector and the β2V72 cDNA insert were then ligated, creating a clone named pSVL/β2V72.

In the figure opposite, the β2 cDNA regions are unshaded, whereas the β7 cDNA regions are shaded blue. The cDNA regions encoding the N-terminal cysteine rich region are represented by dashed lines, the regions encoding the putative A-domain by dots, the regions encoding the C-terminal cysteine-rich region by crosshatches, and the regions encoding the transmembrane domain by diagonal lines. The 5' and 3' untranslated regions (UTRs) of the cDNAs are also shown.

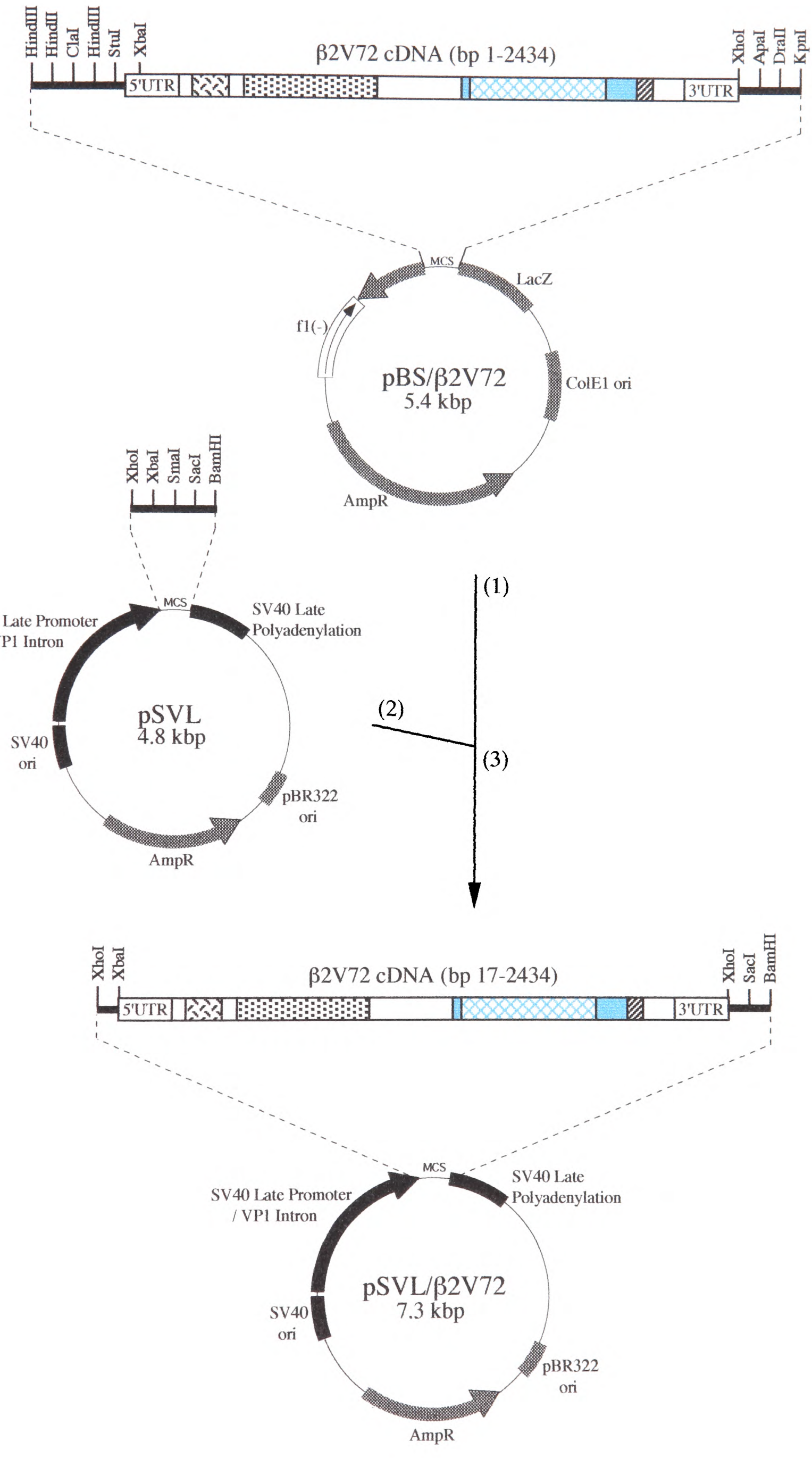

HindIII
HindII
ClaI
HindIII
StuI
XbaI
β2V72 cDNA (bp 1-2434)
XhoI
ApaI
DraII
KpnI
5'UTR
3'UTR
MCS
LacZ
f1(-)
pBS/β2V72
5.4 kbp
ColE1 ori
AmpR
XhoI
XbaI
SmaI
SacI
BamHI
MCS
SV40 Late Promoter
/ VP1 Intron
SV40 Late
Polyadenylation
pSVL
4.8 kbp
SV40
ori
pBR322
ori
AmpR
(1)
(2)
(3)
XhoI
XbaI
β2V72 cDNA (bp 17-2434)
XhoI
SacI
BamHI
5'UTR
3'UTR
MCS
SV40 Late Promoter
/ VP1 Intron
SV40 Late
Polyadenylation
pSVL/β2V72
7.3 kbp
SV40
ori
pBR322
ori
AmpR

Figure 3.13c: Constructing pcDNA3/β2V12

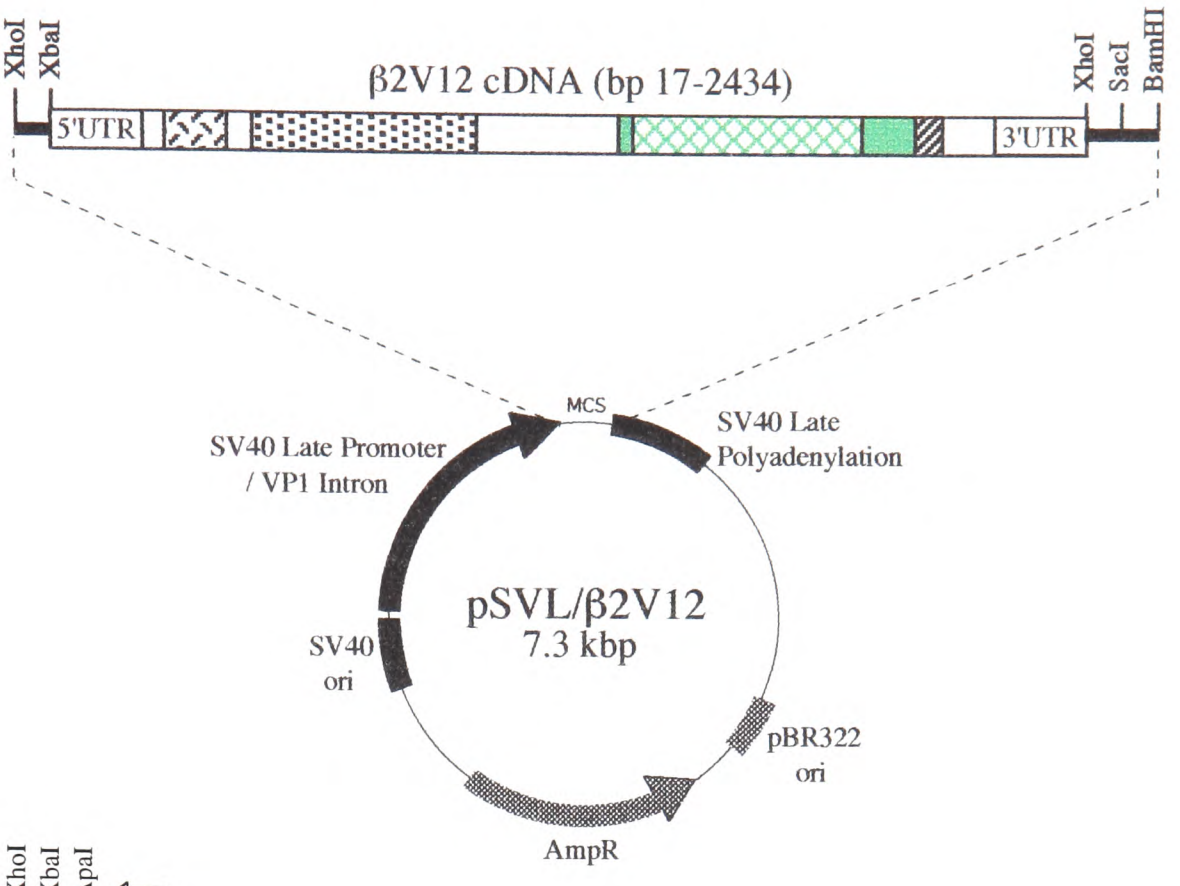
The entire coding region of the β2V12 cDNA was subcloned from pSVL into the pcDNA3 vector as follows:

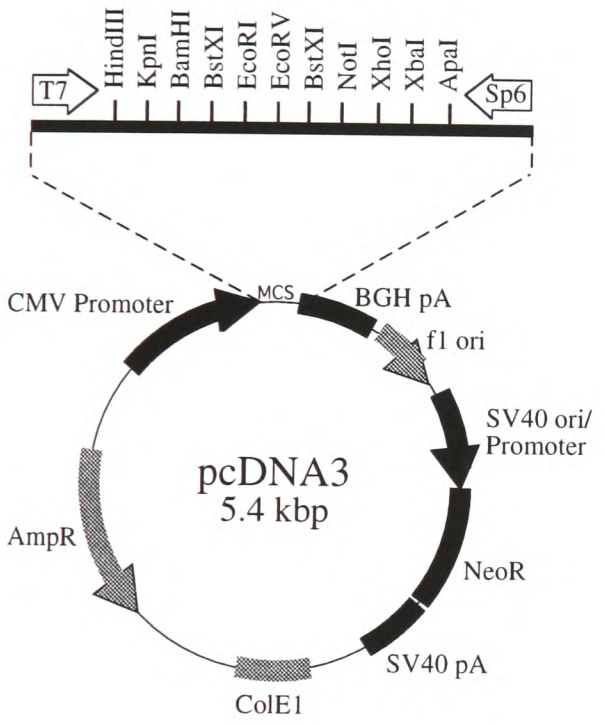
(1) pSVL/β2V12 was digested with XhoI (pSVL/β2V12, 5' polylinker; β2V12 cDNA, 3' UTR) and the 2.4 kbp β2V12 cDNA insert was purified by agarose gel electrophoresis.

(2) pcDNA3 was also digested with XhoI, and the 5.4 kbp pcDNA3 vector was purified by agarose gel electrophoresis.

(3) The pcDNA3 vector and the β2V12 cDNA insert were then ligated, creating a clone named pcDNA3/β2V12. The orientation of the β2V12 cDNA in the pcDNA3 vector was determined by EcoRI digestion. Clones producing a 1 kbp restriction fragment were in the correct orientation.

In the figure opposite, the β2 cDNA regions are unshaded, whereas the β1 cDNA regions are shaded green. The cDNA regions encoding the N-terminal cysteine rich region are represented by dashed lines, the regions encoding the putative A-domain by dots, the regions encoding the C-terminal cysteine-rich region by crosshatches, and the regions encoding the transmembrane domain by diagonal lines. The 5' and 3' untranslated regions (UTRs) of the cDNAs are also shown.


XhoI
XbaI
β2V12 cDNA (bp 17-2434)
XhoI
SacI
BamHI
5'UTR
3'UTR
MCS
SV40 Late Promoter / VP1 Intron
SV40 Late Polyadenylation
pSVL/β2V12
7.3 kbp
SV40 ori
pBR322 ori
AmpR


T7
HindIII
KpnI
BamHI
BstXI
EcoRI
EcoRV
BstXI
NotI
XhoI
XbaI
ApaI
Sp6
CMV Promoter
MCS
BGH pA
f1 ori
SV40 ori/ Promoter
pcDNA3
5.4 kbp
AmpR
NeoR
SV40 pA
ColE1

(1)

(2)

(3)

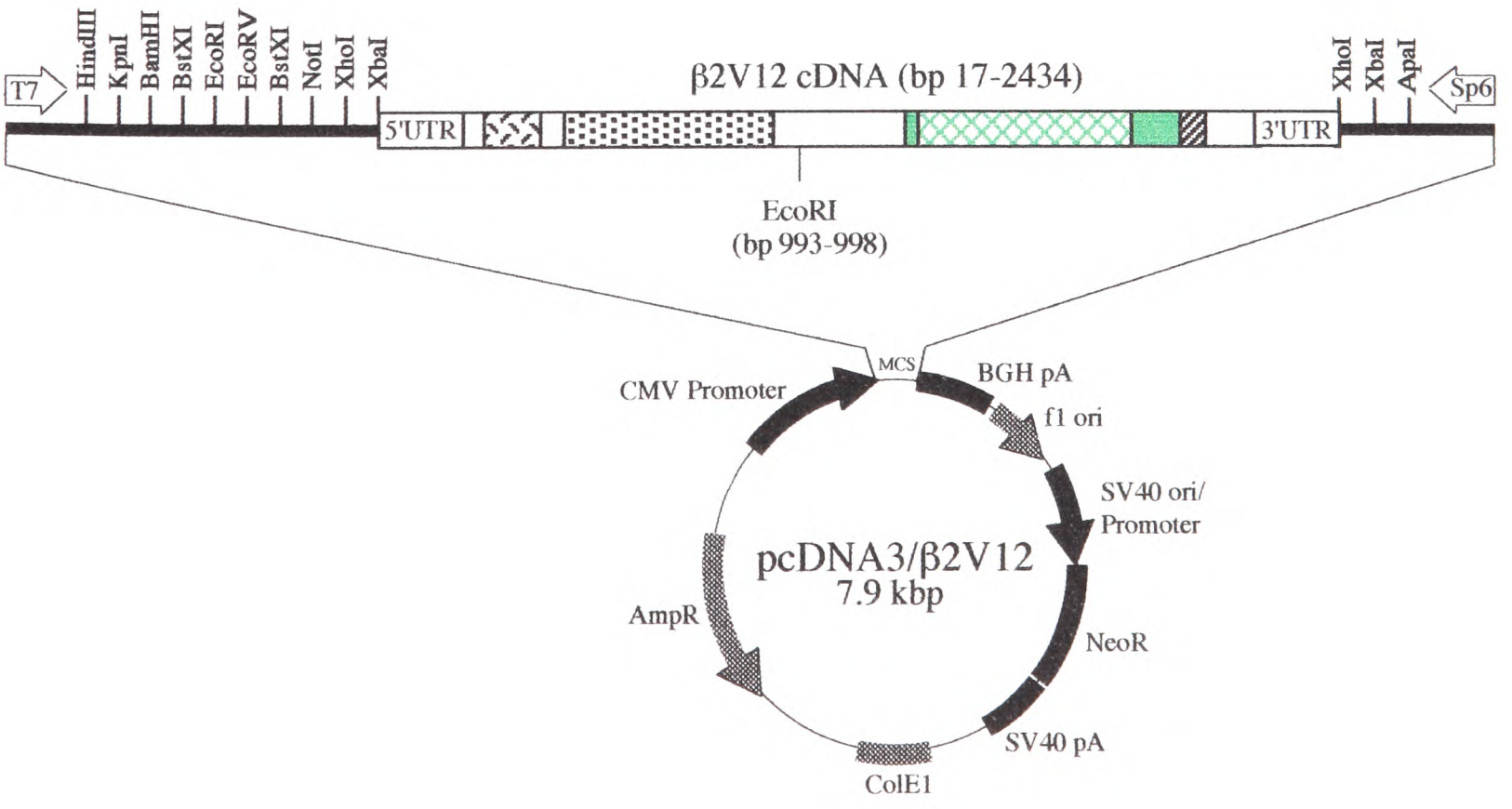

T7
HindIII
KpnI
BamHI
BstXI
EcoRI
EcoRV
BstXI
NotI
XhoI
XbaI
β2V12 cDNA (bp 17-2434)
XhoI
XbaI
ApaI
Sp6
5'UTR
3'UTR
EcoRI
(bp 993-998)
MCS
CMV Promoter
BGH pA
f1 ori
SV40 ori/ Promoter
pcDNA3/β2V12
7.9 kbp
AmpR
NeoR
SV40 pA
ColE1

Figure 3.13d: Constructing pcDNA3/β2V72

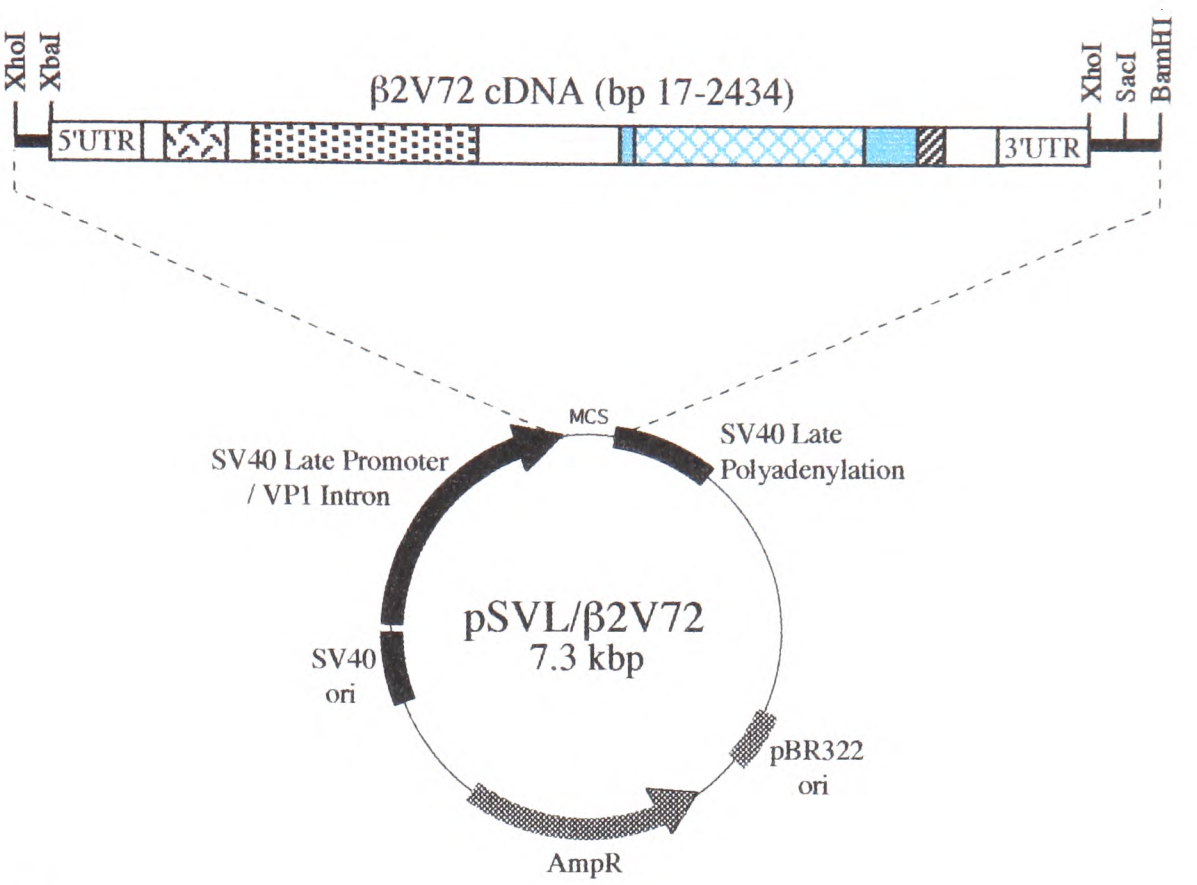
The entire coding region of the β2V72 cDNA was subcloned from pSVL into the pcDNA3 vector as follows:

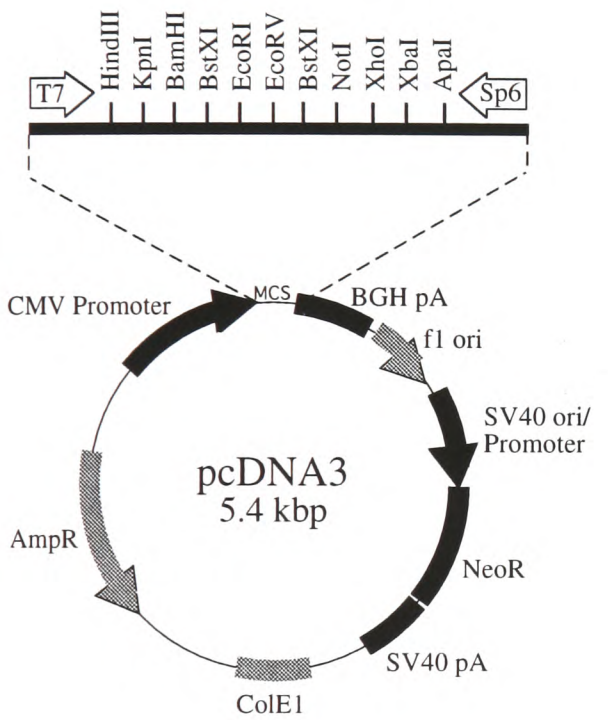
(1) pSVL/β2V72 was digested with XhoI (pSVL/β2V72, 5' polylinker; β2V72 cDNA, 3' UTR) and the 2.4 kbp β2V72 cDNA insert was purified by agarose gel electrophoresis.

(2) pcDNA3 was also digested with XhoI, and the 5.4 kbp pcDNA3 vector was purified by agarose gel electrophoresis.

(3) The pcDNA3 vector and the β2V72 cDNA insert were then ligated, creating a clone named pcDNA3/β2V72. The orientation of the β2V72 cDNA in the pcDNA3 vector was determined by EcoRI digestion. Clones producing a 1 kbp restriction fragment were in the correct orientation.

In the figure opposite, the β2 cDNA regions are unshaded, whereas the β7 cDNA regions are shaded blue. The cDNA regions encoding the N-terminal cysteine rich region are represented by dashed lines, the regions encoding the putative A-domain by dots, the regions encoding the C-terminal cysteine-rich region by crosshatches, and the regions encoding the transmembrane domain by diagonal lines. The 5' and 3' untranslated regions (UTRs) of the cDNAs are also shown.

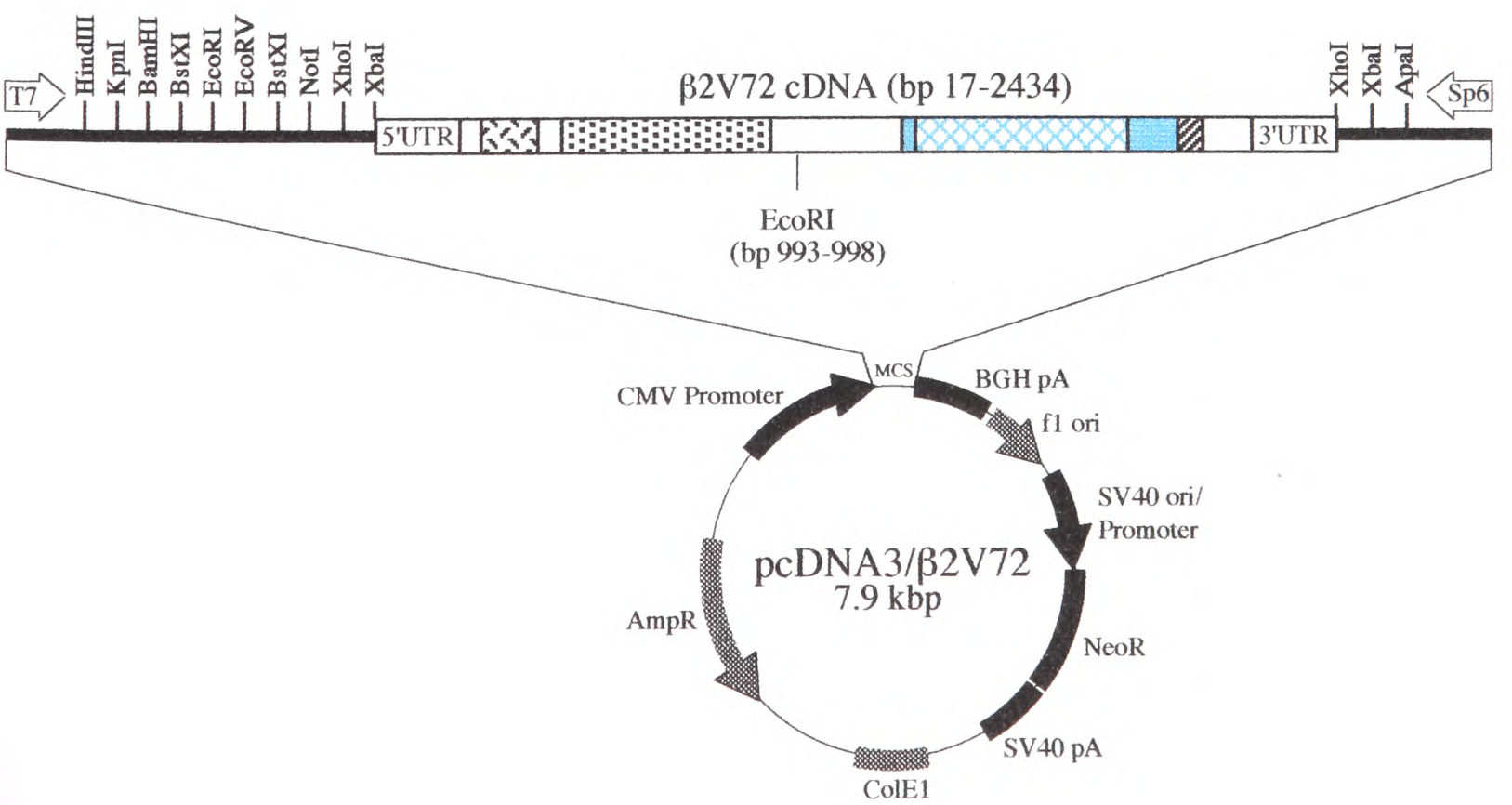

XhoI
XbaI
β2V72 cDNA (bp 17-2434)
XhoI
SacI
BamHI
5'UTR
3'UTR
MCS
SV40 Late Promoter / VP1 Intron
SV40 Late Polyadenylation
pSVL/β2V72
7.3 kbp
SV40 ori
pBR322 ori
AmpR


T7
HindIII
KpnI
BamHI
BstXI
EcoRI
EcoRV
BstXI
NotI
XhoI
XbaI
ApaI
Sp6
CMV Promoter
MCS
BGH pA
f1 ori
SV40 ori/ Promoter
pcDNA3
5.4 kbp
AmpR
NeoR
SV40 pA
ColE1

(1)

(2)

(3)


T7
HindIII
KpnI
BamHI
BstXI
EcoRI
EcoRV
BstXI
NotI
XhoI
XbaI
β2V72 cDNA (bp 17-2434)
XhoI
XbaI
ApaI
Sp6
5'UTR
3'UTR
EcoRI
(bp 993-998)
MCS
CMV Promoter
BGH pA
f1 ori
SV40 ori/ Promoter
pcDNA3/β2V72
7.9 kbp
AmpR
NeoR
SV40 pA
ColE1

3.2.1.5 Constructing the Chimeric β2NS1 and β2NS7 cDNA Clones

3.2.1.5.1 Modifying the J8 Clone, Creating J8.1N

A J8 derivative, J8.1N, had previously been constructed in Dr. Law's laboratory (by Miss S. Nolan). A section of the J8 wildtype β2 cDNA (β2 3' UTR, bp 2554-2843), which contained two NcoI sites (β2, bp 2549-2554; β2, bp 2818-2823), had been removed. This made the remaining NcoI site (β2, bp 1478-1483) a unique restriction enzyme site. The J8.1N clone was used to construct the chimeric β2NS1 and β2NS7 cDNAs.

3.2.1.5.2 Constructing the Chimeric β2NS1 cDNA from J8.1N, Creating pATX/β2NS1

The chimeric β2NS1 cDNA was constructed from J8.1N as illustrated in Figure 3.14a, creating a clone named pATX/β2NS1. Exchanges between the β2 and β1 subunit were facilitated using the J8.1N unique NcoI site (β2, bp 1478-1483) and unique SacII site (β2, bp 1854-1859), which are naturally present in the wildtype β2 cDNA sequence. J8.1N was digested with NcoI and SacII to excise a β2 cDNA fragment encoding part of the C-terminal cysteine-rich region. The β1 cDNA encoding this region was then synthesised by PCR, using the pBS/β2V1 clone as template and the oligonucleotides 4496 and 4497 as primers. The 4496 oligonucleotide was designed to engineer an NcoI site into the 5' end PCR product (β1, bp 1534-1539) and the 4497 oligonucleotide to engineer a SacII site into the 3' end (β1, bp 1907-1912). The sequences of these oligonucleotides and their positions in the β1 cDNA sequence are shown in Figure 3.14b. The β1 PCR product was digested with NcoI and SacII, and the chimeric β2NS1 cDNA was constructed by replacing the J8.1N NcoI-SacII fragment with the β1 NcoI-SacII fragment. The resulting pATX/β2NS1 clone was then nucleotide sequenced to confirm the correct formation of the β2/β1 chimeric junctions, and to confirm the absence of PCR errors in the β1 PCR derived section. The construction of the β2NS1 chimeric junctions is shown in detail in Figure 3.14c. No amino acid mutations were introduced into the β2 or the β1 subunit at these junctions.

3.2.1.5.3 Constructing the Chimeric β2NS7 cDNA from J8.1N, Creating pATX/β2NS7

The chimeric β2NS7 cDNA was constructed from J8.1N in a similar way, creating a clone named pATX/β2NS7. The construction of pATX/β2NS7 is illustrated in Figure 3.15a.

The β7 cDNA spanning the exchanged region was synthesised by PCR, using the pBS/β2V7 clone as template and the oligonucleotides F94/36 and A94/3. The F94/36 oligonucleotide was designed to engineer an NcoI site into the 5' end of the PCR product (β7, bp 1577-1582) and the A94/3 oligonucleotide to engineer a SacII site into the 3' end (β7, bp 1935-1940). The sequences of these oligonucleotides and their positions in the β7 cDNA sequence are shown in Figure 3.15b. The β7 PCR product was digested with NcoI and SacII, and the chimeric β2NS7 cDNA was constructed by replacing the J8.1N NcoI-SacII fragment with the β7 NcoI-SacII fragment. The resulting pATX/β2NS7 clone was then nucleotide sequenced to confirm the correct formation of the β2/β7 chimeric junctions, and to confirm the absence of PCR errors in the β7 PCR derived section. The construction of the β2NS7 chimeric junctions is shown in detail in Figure 3.15c. No amino acid changes were introduced into the β2 or the β7 subunits at these junctions.

3.2.1.5.4 Cloning the β2NS1 and β2NS7 cDNAs into Expression Vectors

The entire coding regions of the β2NS1 and β2NS7 cDNAs were then subcloned from pATX into the vectors pSVL (Pharmacia) and pcDNA3 (Invitrogen) for transient expression in COS 7 cells.

3.2.1.5.4.1 Constructing the pSVL/β2NS1 Clone

The β2NS1 cDNA was subcloned from pATX into the pSVL vector as illustrated in Figure 3.16a. The β2NS1 cDNA was excised from pATX/β2NS1 by digestion with XbaI (β2NS1 cDNA, 5'UTR; pATX/β2NS1, 3' polylinker), and the resultant 5' overhangs were blunted using the end-filling reaction. The blunted β2NS1 cDNA insert was then cloned into SmaI cut pSVL, creating a clone named pSVL/β2NS1. The orientation of the cDNA in the expression vector was determined by BamHI digestion. Clones producing a 2.3 kbp restriction fragment were in the correct orientation.

3.2.1.5.4.2 Constructing the pSVL/β2NS7 Clone

The β2NS7 cDNA was subcloned from pATX into the pSVL vector as illustrated in Figure 3.16b. The β2NS7 cDNA was excised from pATX/β2NS7 by digestion with XbaI (β2NS7 cDNA, 5'UTR; pATX/β2NS7, 3' polylinker), and the resultant 5' overhangs were blunted using the end-filling reaction. The blunted β2NS7 cDNA insert was then cloned into SmaI cut pSVL, creating a clone named pSVL/β2NS7. The orientation of the cDNA in the

expression vector was determined by BamHI digestion. Clones producing a 2.3 kbp restriction fragment were in the correct orientation.

3.2.1.5.4.3 Constructing the pcDNA3/β2NS1 Clone

The β2NS1 cDNA was subcloned from pATX into the pcDNA3 vector as illustrated in Figure 3.16c. The β2NS1 cDNA was excised from pATX/β2NS1 by digestion with XbaI (β2NS1 cDNA, 5'UTR; pATX/β2NS1, 3'polylinker) and was cloned into XbaI cut pcDNA3. The orientation of the cDNA in the expression vector was determined by BamHI digestion. Clones producing a 300 bp restriction fragment were in the correct orientation.

3.2.1.5.4.4 Constructing the pcDNA3/β2NS7 Clone

The β2NS7 cDNA was subcloned from pATX into the pcDNA3 vector as illustrated in Figure 3.16d. The β2NS7 cDNA was excised from pATX/β2NS7 by digestion with XbaI (β2NS7 cDNA, 5'UTR; pATX/β2NS7, 3' polylinker) and was cloned into XbaI cut pcDNA3. The orientation of the cDNA in the expression vector was determined by BamHI digestion. Clones producing a 300 bp restriction fragment were in the correct orientation.

Figure 3.14a: Constructing the Chimeric β2NS1 cDNA in pATX, Creating pATX/β2NS1

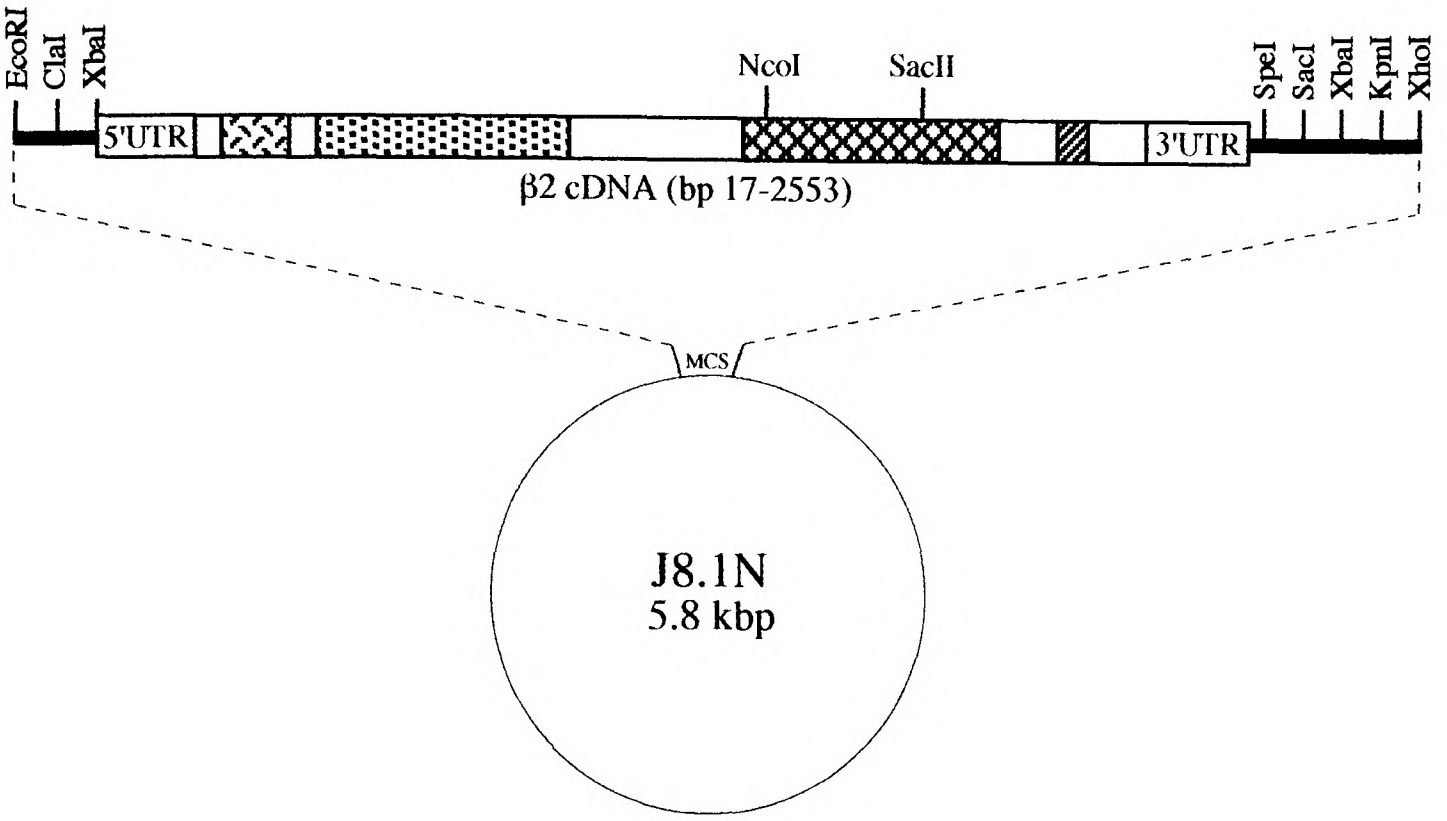
The chimeric β2NS1 cDNA in pATX, pATX/β2NS1, was constructed from the J8.1N clone as follows:

(1) J8.1N was digested with NcoI (β2 cDNA, bp 1478-1483) and SacII (β2 cDNA, bp 1854-1859), and the 5.4 kbp J8.1N fragment was purified by agarose gel electrophoresis.

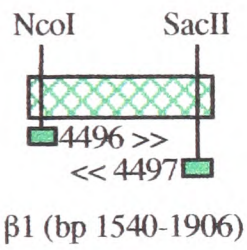
(2) A β1 PCR product (bp 1540-1906) was synthesised using the pBS/β2V1 clone as template, the oligonucleotides 4496 and 4497 as primers, and the Pfu DNA polymerase enzyme. The 4496 oligonucleotide was designed to engineer an NcoI site into the 5' end of the PCR product, whereas the 4497 oligonucleotide was designed to engineer a SacII site into the 3' end (see Figure 3.14b). The β1 PCR product was digested with NcoI and SacII, and the 366 bp PCR fragment was purified by agarose gel electrophoresis.

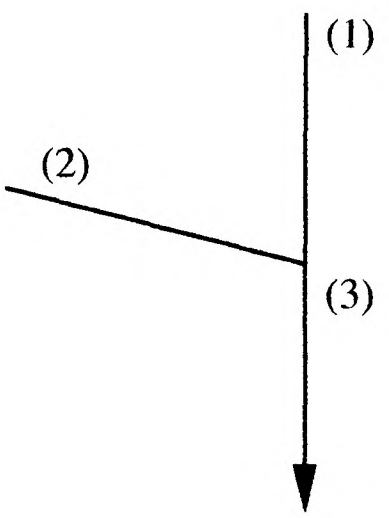
(3) The 366 bp β1 PCR fragment and the 5.4 kbp J8.1N fragment were then ligated, creating a full length chimeric β2NS1 cDNA in pATX, clone pATX/β2NS1. The pATX/β2NS1 clone was nucleotide sequenced to confirm the correct formation of the β2/β1 chimeric junctions, and to confirm the absence of PCR errors in the β1 cDNA section derived by PCR. No amino acid mutations were introduced into the β2 or β1 subunits at the β2NS1 chimeric junctions (see Figure 3.14c).

In the figure opposite, the β2 cDNA regions are unshaded, whereas the β1 cDNA regions are shaded green. The regions encoding the N-terminal cysteine rich region are represented by dashed lines, the regions encoding the putative A-domain by dots, the regions encoding the C-terminal cysteine-rich region by crosshatches, and the regions encoding the transmembrane domain by diagonal lines. The 5' and 3' untranslated regions (UTRs) of the β cDNAs are also shown.



β1 PCR PRODUCT





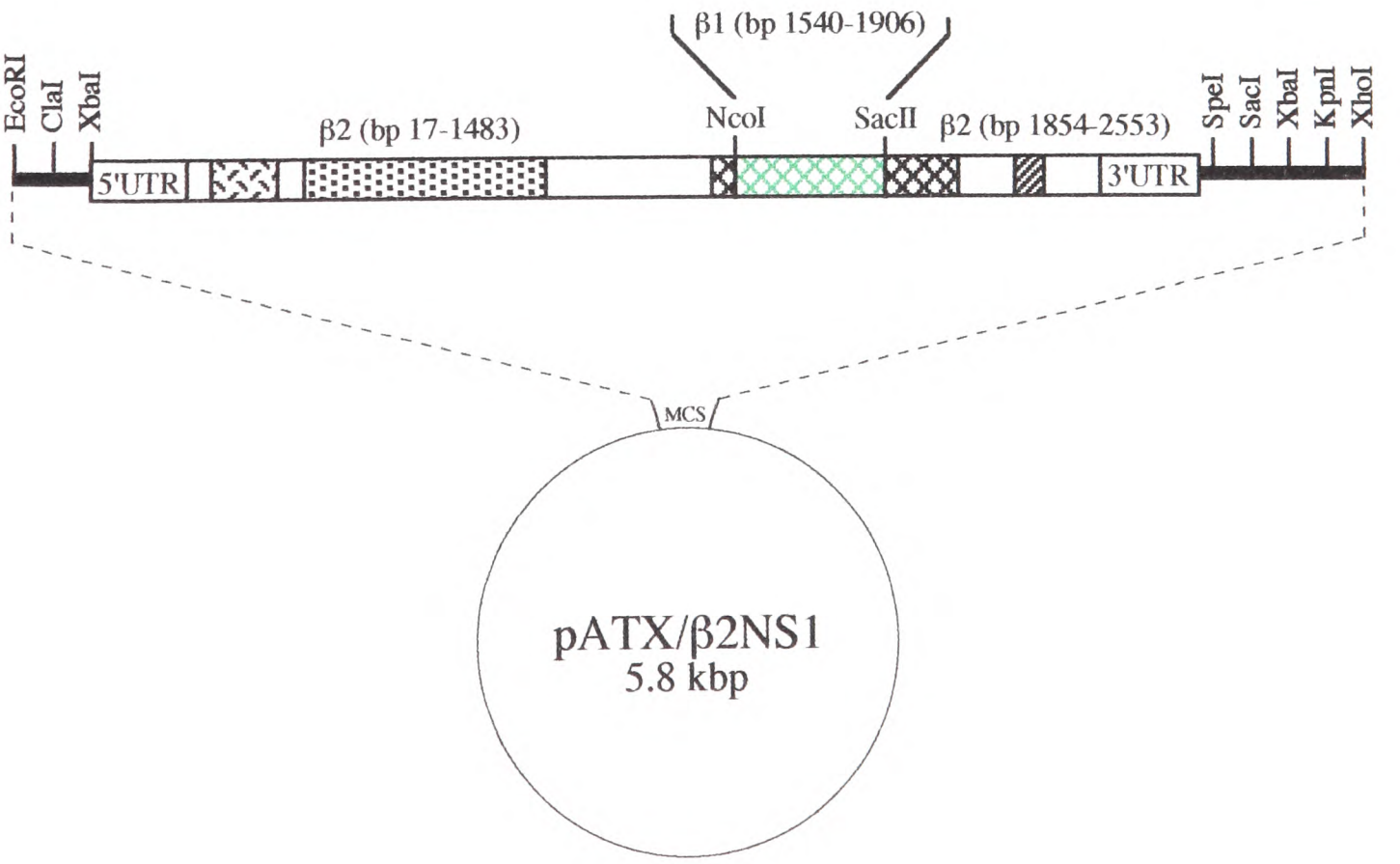




Figure 3.14b: The 4496 and 4497 Oligonucleotides used to Synthesise the β1 cDNA Section of the Chimeric β2NS1 cDNA

The β1 cDNA section of the chimeric β2NS1 cDNA was synthesised by PCR, using the pBS/β2V1 clone as template and the 4496 and 4497 oligonucleotides as primers. The oligonucleotide 4496 was designed to engineer an NcoI site into the 5' end of the PCR product (β1 cDNA: bp 1534-1539), whilst the 4497 oligonucleotide was designed to engineer a SacII site into the 3' end of the PCR product (β1 cDNA: bp 1907-1912). The relevant sections of the wildtype β1 cDNA are shown in the figure above in green, and the amino acids that these sections encode are shown above the cDNA sequence (using the single letter amino acid code), also in green. The sequences and annealing positions of the 4496 and the 4497 oligonucleotides are also shown, with residues that match the wildtype sequence indicated by vertical lines and mismatched residues by dots, and with the residues representing the NcoI and SacII sites shown in pink. The DNA mutations engineered into the 5' end of the β1 PCR product to create the NcoI site resulted in a single amino acid substitution, E479G, and the DNA mutations engineered into the 3' end of the PCR product to create the SacII site resulted in two amino acid substitutions, S602P and N603R. These amino acid mutations are shown above the wildtype β1 sequence. However, as these amino acids correspond to the wildtype β2 residues at these positions, no amino acid changes were introduced into the β1 section of the resulting β2NS1 chimera (see Figure 3.14c).

Figure 3.14c: Formation of the β2NS1 Chimeric Junctions

The figure below shows the formation of the β2/β1 chimeric junctions in the β2NS1 chimera. The wildtype β2 cDNA and amino acid sequences are shown in black, whereas the wildtype β1 cDNA and amino acid sequences are shown in green, and the nucleotide residues which represent the NcoI and SacII sites are shown in pink. Cysteine residues are shown in red, and are numbered such that the first cysteine residue in the mature β polypeptide would be numbered C1 and the last would be numbered C56. It should be noted that the β2NS1 chimeric junctions were created without introducing any amino acid mutations into the β2 or the β1 sections.

WT b2

```
                    NcoI                                                                                                SacII
                D   R   S   L C18 H   G     K   G   F   L   E C19 G                                   T   T   E   G C40 L   N     P   R   R   V   E C41 S
                GACCGCAGCCTCTGCCATGG CAAGGGCTTCTTGGAGTGCGGC - - - - - - - - - - ACCACTGAGGGCTGCCTGAAC CCGCGGCGTGTTGAGTGTAGT
                   1470       1480       1490       1500                                              1840       1850       1860       1870
                CTGGCGTCGGAGACGGTACC GTTCCCGAAGAACCTCACGCCG - - - - - - - - - - TGGTGACTCCCGACGGACTTG GGCGCCGCACAACTCACATCA
```

WT b1

```
                E   S   P   K C18 H   E     G   N   G   T   F   E C19                                   D   T   S   T C40 E   A     S   N   G   Q   I C41 N
                GAAAGTCCCAAGTGTCATGA AGGAAATGGGACATTTGAGTGT - - - - - - - - - - GATACTAGTACTTGTGAAGCC AGCAACGGACAGATCTGCAAT
                      1530      1539         1550       1560                                             1890       1900         1910       1920
                CTTTCAGGGTTCACAGTACT TCCTTTACCCTGTAAACTCACA - - - - - - - - - - CTATGATCATGAACACTTCGG TCGTTGCCTGTCTAGACGTTA
```

b1 PCR PRODUCT

```
                    NcoI                                                                                                SacII
                C18 H   G     G   N   G   T   F   E C19                                   D   T   S   T C40 E   A     P   R   G
                 TGCCATGG AGGAAATGGGACATTTGAGTGT - - - - - - - - - - GATACTAGTACTTGTGAAGCC CCGCGGGG
                     1539         1550       1560                                             1890       1900         1910
                 ACGGTACC TCCTTTACCCTGTAAACTCACA - - - - - - - - - - CTATGATCATGAACACTTCGG GGCGCCCC
```

b2NS1

```
                    NcoI                                                                                                SacII
                D   R   S   L C18 H   G     G   N   G   T   F   E C19                                   D   T   S   T C40 E   A     P   R   R   V   E C41 S
                GACCGCAGCCTCTGCCATGG AGGAAATGGGACATTTGAGTGT - - - - - - - - - - GATACTAGTACTTGTGAAGCC CCGCGGCGTGTTGAGTGTAGT
                   1470       1480           1550       1560                                             1890       1900           1860       1870
                CTGGCGTCGGAGACGGTACC TCCTTTACCCTGTAAACTCACA - - - - - - - - - - CTATGATCATGAACACTTCGG GGCGCCGCACAACTCACATCA
```

Figure 3.15a: Constructing the Chimeric β2NS7 cDNA in pATX, Creating pATX/β2NS7

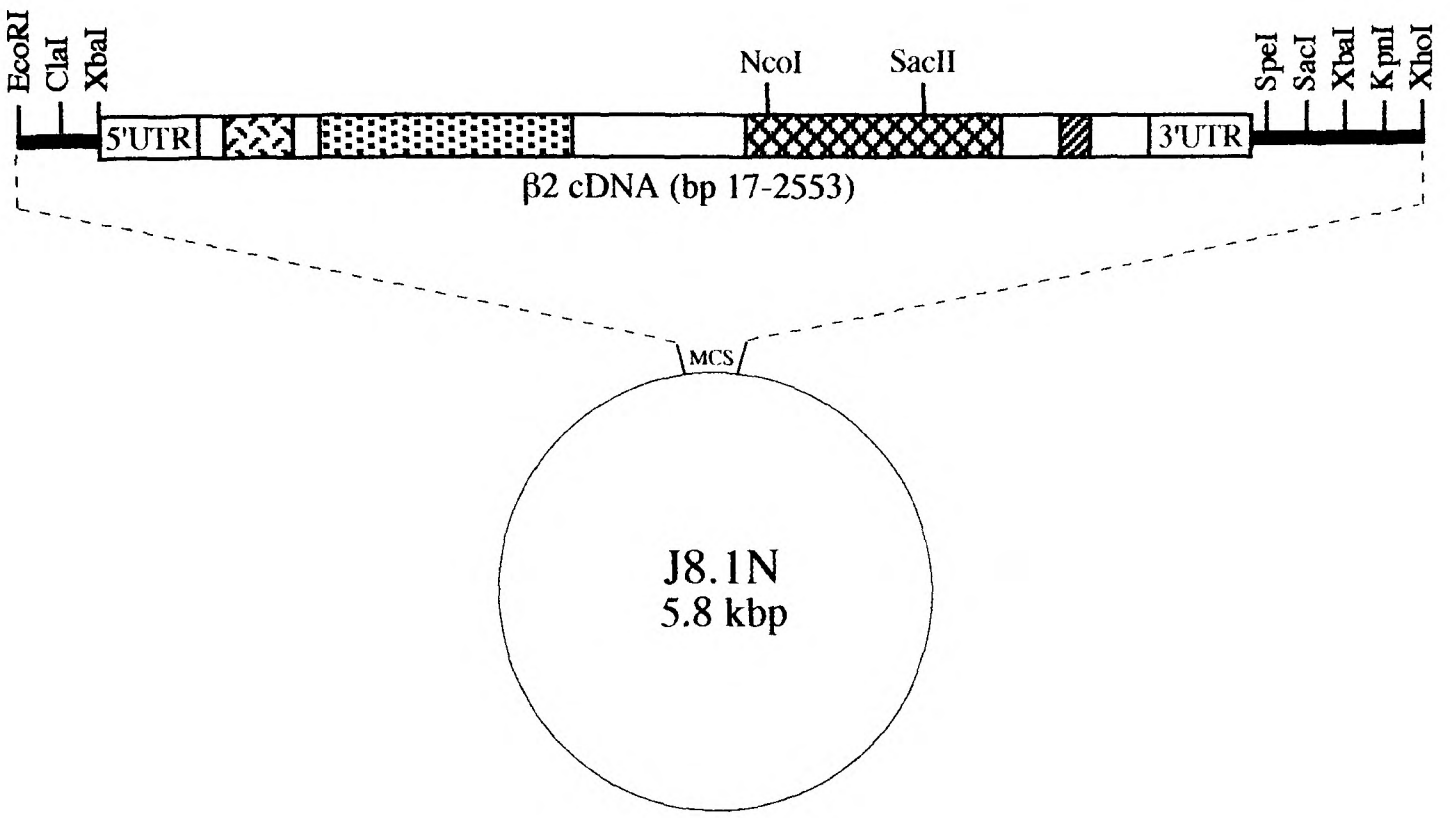
The chimeric β2NS7 cDNA in pATX, pATX/β2NS7, was constructed from the J8.1N clone as follows:

(1) J8.1N was digested with NcoI (β2 cDNA, bp 1478-1483) and SacII (β2 cDNA, bp 1854-1859), and the 5.4 kbp J8.1N fragment was purified by agarose gel electrophoresis.

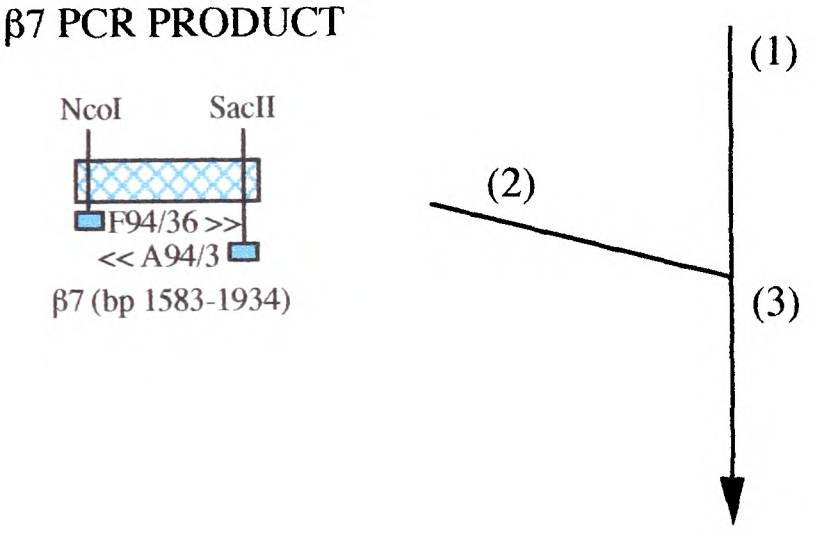
(2) A β7 PCR product (bp 1583-1934) was synthesised using the pBS/β2V7 clone as template, the oligonucleotides F94/36 and A94/3 as primers, and the Pfu DNA polymerase enzyme. The F94/36 oligonucleotide was designed to engineer an NcoI site into the 5' end of the PCR product, whereas the A94/3 oligonucleotide was designed to engineer a SacII site into the 3' end (see Figure 3.15b). The β7 PCR product was digested with NcoI and SacII, and the 351 bp PCR fragment was purified by agarose gel electrophoresis.

(3) The 351 bp β7 PCR fragment and the 5.4 kbp J8.1N fragment were then ligated, creating a full length chimeric β2NS7 cDNA in pATX, clone pATX/β2NS7. The pATX/β2NS7 clone was nucleotide sequenced to confirm the correct formation of the β2/β7 chimeric junctions, and to confirm the absence of PCR errors in the β7 cDNA section derived by PCR. No amino acid mutations were introduced into the β2 or β7 subunits at the β2NS7 chimeric junctions (see Figure 3.15c).

In the figure opposite, the β2 cDNA regions are unshaded, whereas the β7 cDNA regions are shaded blue. The regions encoding the N-terminal cysteine rich region are represented by dashed lines, the regions encoding the putative A-domain by dots, the regions encoding the C-terminal cysteine-rich region by crosshatches, and the regions encoding the transmembrane domain by diagonal lines. The 5' and 3' untranslated regions (UTRs) of the β cDNAs are also shown.



β7 PCR PRODUCT



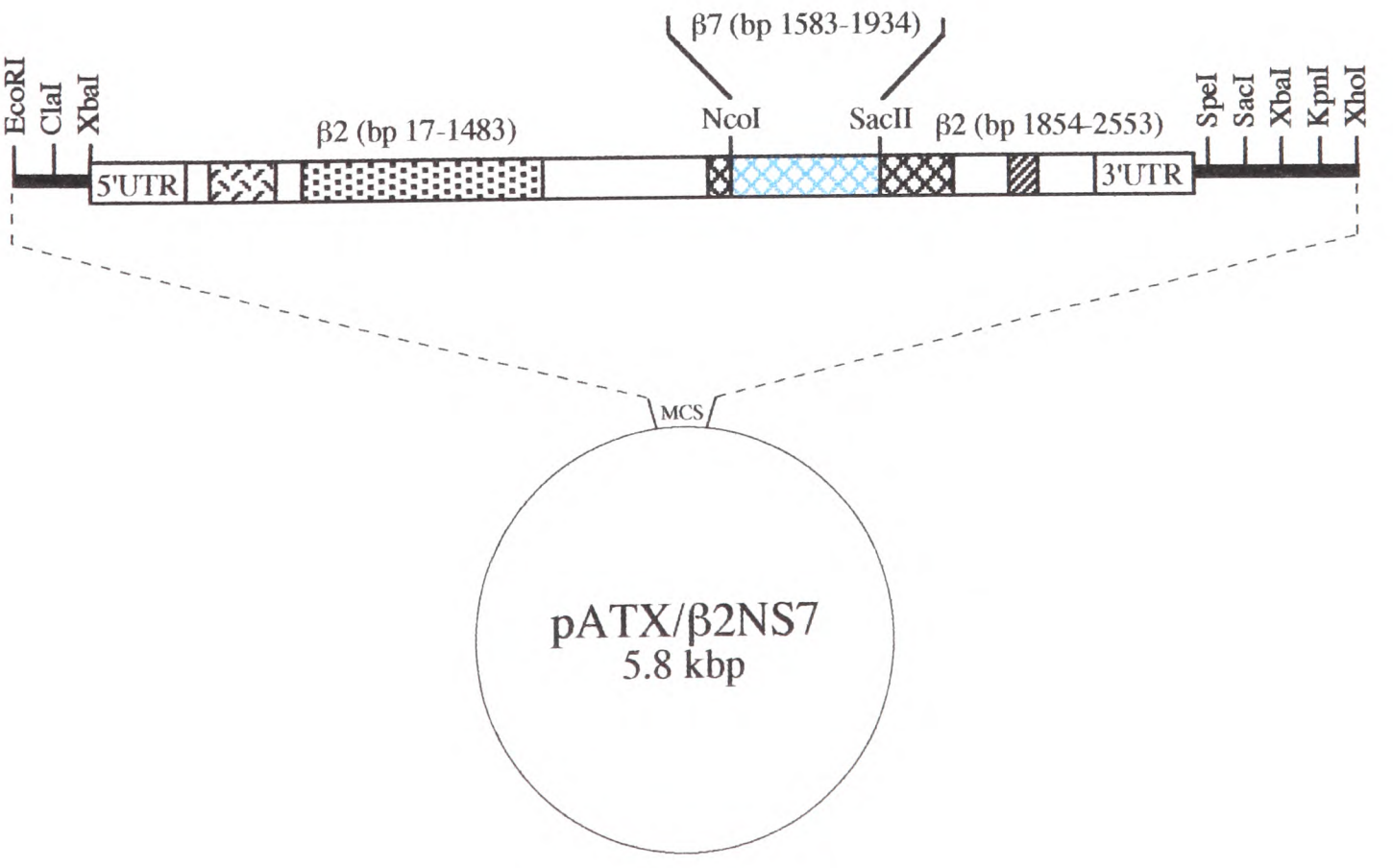




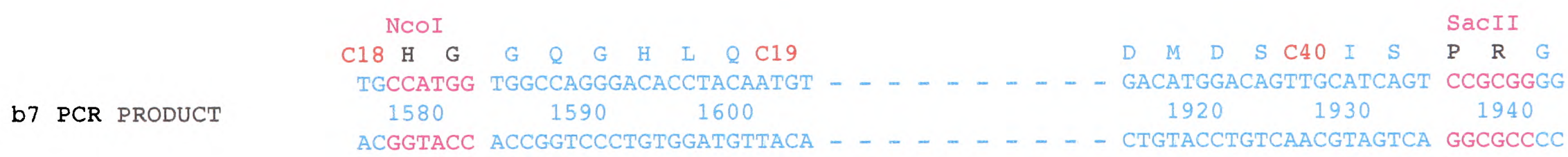
Figure 3.15b: The F94/36 and A94/3 Oligonucleotides used to Synthesise the β7 cDNA Section of the Chimeric β2NS7 cDNA

The β7 cDNA section of the chimeric β2NS7 cDNA was synthesised by PCR, using the pBS/β2V7 clone as template and the F94/36 and A94/3 oligonucleotides as primers. The oligonucleotide F94/36 was designed to engineer an NcoI site into the 5' end of the PCR product (β7 cDNA: bp 1577-1582), whilst the A94/3 oligonucleotide was designed to engineer a SacII site into the 3' end of the PCR product (β7 cDNA: bp 1935-1940). The relevant sections of the wildtype β7 cDNA are shown in the figure above in blue, and the amino acids that these sections encode are shown above the cDNA sequence (using the single letter amino acid code), also in blue. The sequences and annealing positions of the F94/36 and the A94/3 oligonucleotides are also shown, with residues that match the wildtype sequence indicated by vertical lines and mismatched residues by dots, and with the residues representing the NcoI and SacII sites shown in pink. The DNA mutations engineered into the 5' end of the β7 PCR product to create the NcoI site resulted in two amino acid substitutions, S489H and D490G, and the DNA mutations engineered into the 3' end of the PCR product to create the SacII site resulted in a single amino acid substitution, E609R. These amino acid mutations are shown above the wildtype β7 sequence. However, as these amino acids correspond to the wildtype β2 residues at these positions, no amino acid changes were introduced into the β7 section of the resulting β2NS7 chimera (see Figure 3.15c).

Figure 3.15c: Formation of the β2NS7 Chimeric Junctions

The figure below shows the formation of the β2/β7 chimeric junctions in the β2NS7 chimera. The wildtype β2 cDNA and amino acid sequences are shown in black, whereas the wildtype β7 cDNA and amino acid sequences are shown in blue, and the nucleotide residues which represent the NcoI and SacII sites are shown in pink. Cysteine residues are shown in red, and are numbered such that the first cysteine residue in the mature β polypeptide would be numbered C1 and the last would be numbered C56. It should be noted that the β2NS7 chimeric junctions were created without introducing any amino acid mutations into the β2 or the β7 sections.


NcoI
SacII
D R S L C18 H G K G F L E C19 G T T E G C40 L N P R R V E C41 S
GACCGCAGCCTCTGCCATGG CAAGGGCTTCTTGGAGTGCGGC - - - - - - - - - - ACCACTGAGGGCTGCCTGAAC CCGCGGCGTGTTGAGTGTAGT
1470 1480 1490 1500 1840 1850 1860 1870
WT b2
CTGGCGTCGGAGACGGTACC GTTCCCGAAGAACCTCACGCCG - - - - - - - - - - TGGTGACTCCCGACGGACTTG GGCGCCGCACAACTCACATCA
Q A P H C18 S D G Q G H L Q C19 D M D S C40 I S P E G G L C41 S
CAGGCTCCCCACTGCAGTGA TGGCCAGGGACACCTACAATGT - - - - - - - - - - GACATGGACAGTTGCATCAGT CCCGAGGGAGGGCTCTGCAGT
1570 1580 1590 1600 1920 1930 1940 1950
WT b7
GTCCGAGGGGTGACGTCACT ACCGGTCCCTGTGGATGTTACA - - - - - - - - - - CTGTACCTGTCAACGTAGTCA GGGCTCCCTCCCGAGACGTCA


NcoI
SacII
C18 H G G Q G H L Q C19 D M D S C40 I S P R G
TGCCATGG TGGCCAGGGACACCTACAATGT - - - - - - - - - - GACATGGACAGTTGCATCAGT CCGCGGGG
1580 1590 1600 1920 1930 1940
b7 PCR PRODUCT
ACGGTACC ACCGGTCCCTGTGGATGTTACA - - - - - - - - - - CTGTACCTGTCAACGTAGTCA GGCGCCCC


NcoI
SacII
D R S L C18 H G G Q G H L Q C19 D M D S C40 I S P R R V E C41 S
GACCGCAGCCTCTGCCATGG TGGCCAGGGACACCTACAATGT - - - - - - - - - - GACATGGACAGTTGCATCAGT CCGCGGCGTGTTGAGTGTAGT
1470 1480 1590 1600 1920 1930 1860 1870
b2NS7
CTGGCGTCGGAGACGGTACC ACCGGTCCCTGTGGATGTTACA - - - - - - - - - - CTGTACCTGTCAACGTAGTCA GGCGCCGCACAACTCACATCA

Figure 3.16a: Constructing pSVL/β2NS1

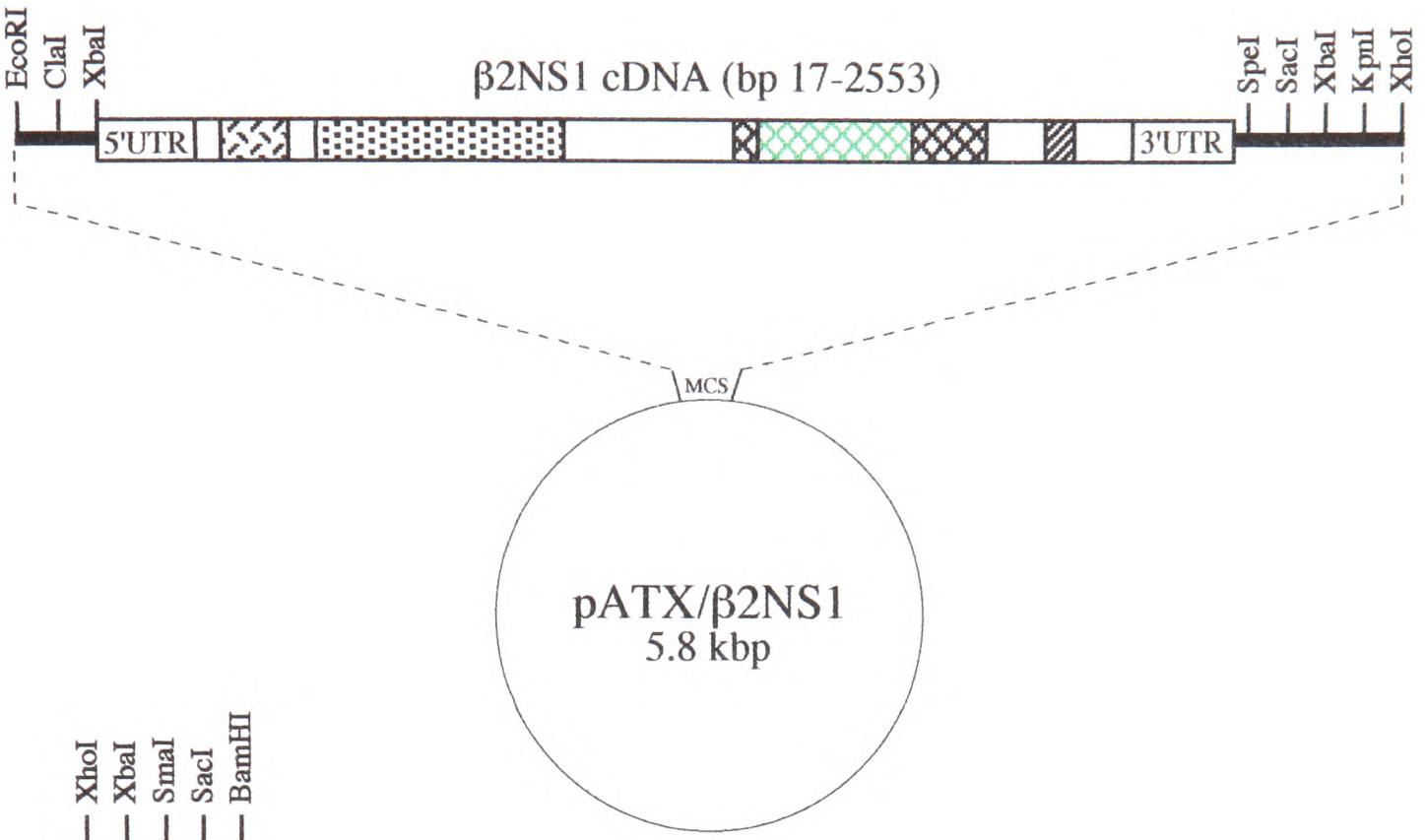
The entire coding region of the β2NS1 cDNA was subcloned from pATX into the pSVL vector as follows:

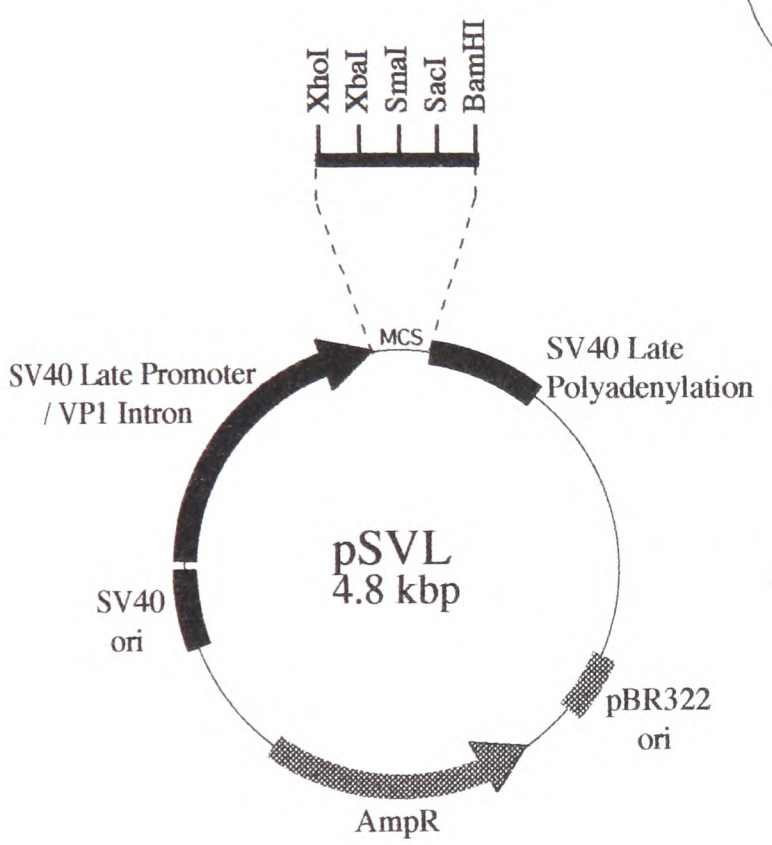
(1) pATX/β2NS1 was digested with XbaI (β2NS1 cDNA, 5' UTR; pATX/β2NS1, 3' polylinker) and the resultant 5' overhangs were blunted using the end-filling reaction before the 2.5 kbp β2NS1 cDNA insert was purified by agarose gel electrophoresis.

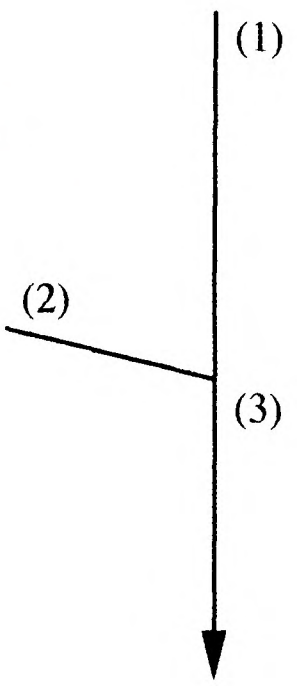
(2) pSVL was digested with SmaI, and the 4.8 kbp pSVL vector was also purified by agarose gel electrophoresis.

(3) The pSVL vector and the β2NS1 cDNA insert were then ligated, creating a clone named pSVL/β2NS1. The orientation of the β2NS1 cDNA insert in the pSVL vector was determined by BamHI digestion. Clones producing a 2.3 kbp restriction fragment were in the correct orientation.

In the figure opposite, the β2 cDNA regions are unshaded, whereas the β1 cDNA regions are shaded green. The cDNA regions encoding the N-terminal cysteine rich region are represented by dashed lines, the regions encoding the putative A-domain by dots, the regions encoding the C-terminal cysteine-rich region by crosshatches, and the regions encoding the transmembrane domain by diagonal lines. The 5' and 3' untranslated regions (UTRs) of the cDNAs are also shown.


EcoRI
ClaI
XbaI
β2NS1 cDNA (bp 17-2553)
SpeI
SacI
XbaI
KpnI
XhoI
5'UTR
3'UTR
MCS
pATX/β2NS1
5.8 kbp


XhoI
XbaI
SmaI
SacI
BamHI
MCS
SV40 Late Promoter
/ VP1 Intron
SV40 Late
Polyadenylation
pSVL
4.8 kbp
SV40
ori
pBR322
ori
AmpR


(1)
(2)
(3)

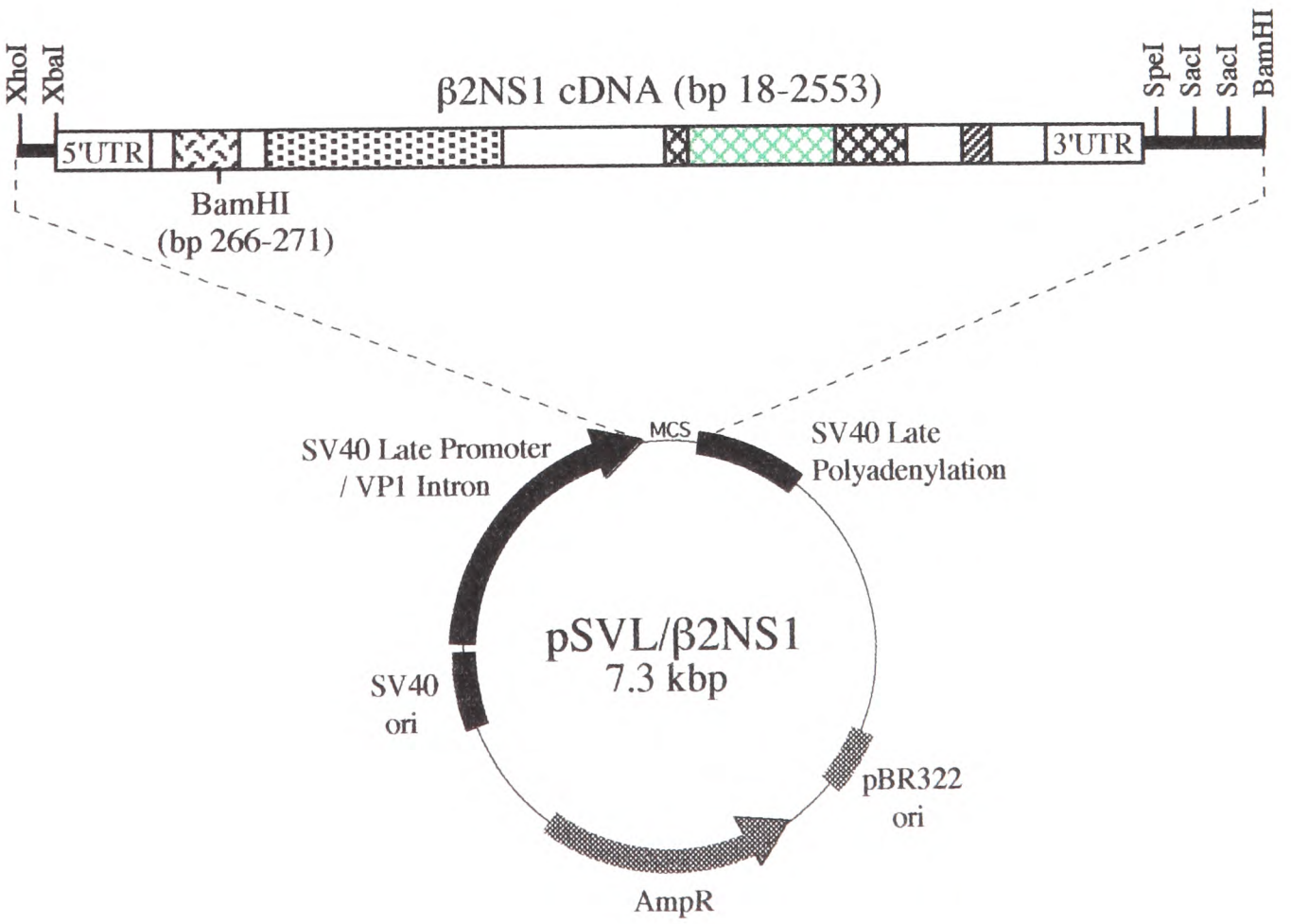

XhoI
XbaI
β2NS1 cDNA (bp 18-2553)
SpeI
SacI
SacI
BamHI
5'UTR
3'UTR
BamHI
(bp 266-271)
SV40 Late Promoter
/ VP1 Intron
MCS
SV40 Late
Polyadenylation
pSVL/β2NS1
7.3 kbp
SV40
ori
pBR322
ori
AmpR

Figure 3.16b: Constructing pSVL/β2NS7

The entire coding region of the β2NS7 cDNA was subcloned from pATX into the pSVL vector as follows:

(1) pATX/β2NS7 was digested with XbaI (β2NS7 cDNA, 5' UTR; pATX/β2NS7, 3' polylinker) and the resultant 5' overhangs were blunted using the end-filling reaction before the 2.5 kbp β2NS7 cDNA insert was purified by agarose gel electrophoresis.

(2) pSVL was digested with SmaI, and the 4.8 kbp pSVL vector was also purified by agarose gel electrophoresis.

(3) The pSVL vector and the β2NS7 cDNA insert were then ligated, creating a clone named pSVL/β2NS7. The orientation of the β2NS7 cDNA insert in the pSVL vector was determined by BamHI digestion. Clones producing a 2.3 kbp restriction fragment were in the correct orientation.

In the figure opposite, the β2 cDNA regions are unshaded, whereas the β7 cDNA regions are shaded blue. The cDNA regions encoding the N-terminal cysteine rich region are represented by dashed lines, the regions encoding the putative A-domain by dots, the regions encoding the C-terminal cysteine-rich region by crosshatches, and the regions encoding the transmembrane domain by diagonal lines. The 5' and 3' untranslated regions (UTRs) of the cDNAs are also shown.

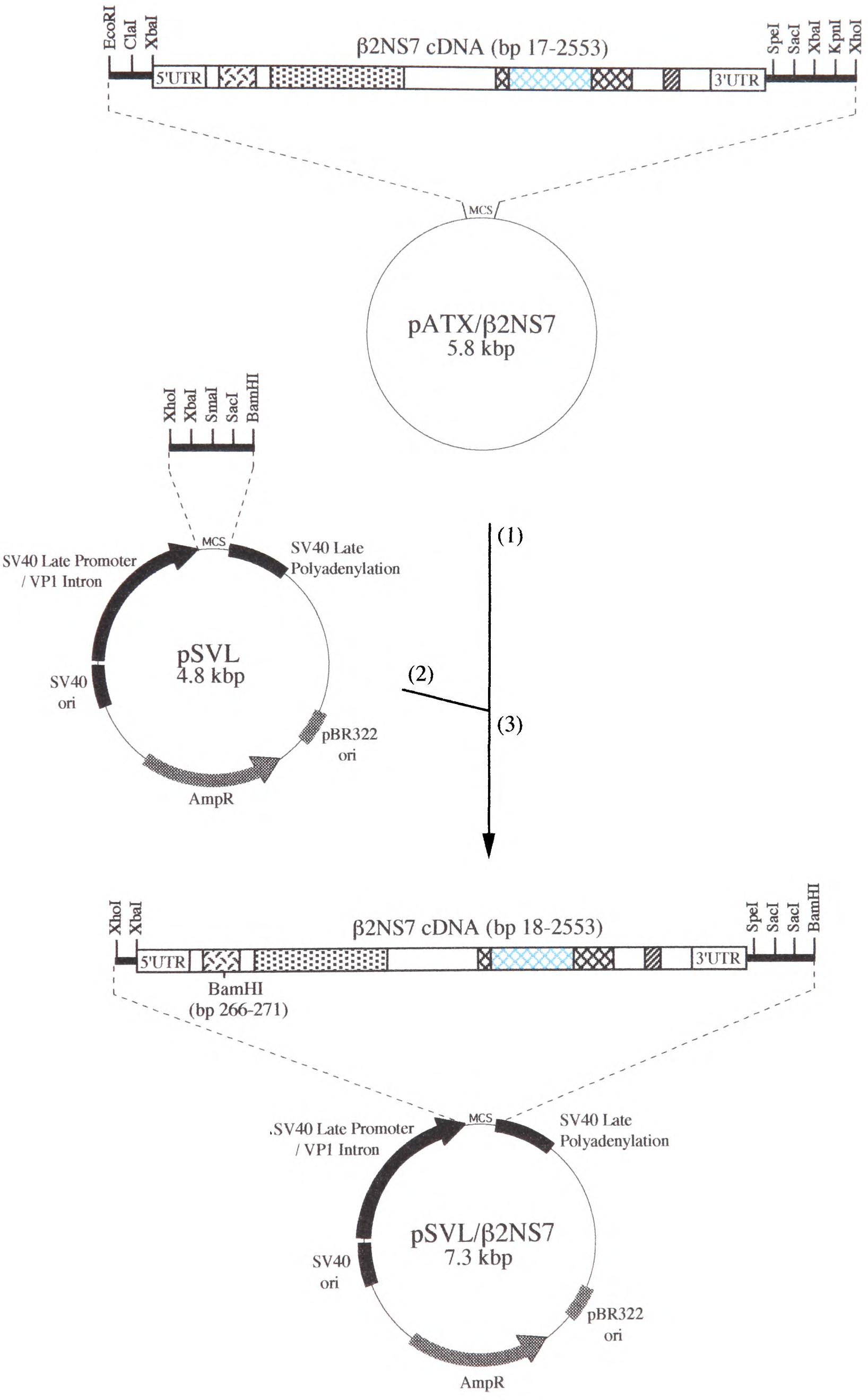

EcoRI
ClaI
XbaI
β2NS7 cDNA (bp 17-2553)
5'UTR
3'UTR
SpeI
SacI
XbaI
KpnI
XhoI
MCS
pATX/β2NS7
5.8 kbp
XhoI
XbaI
SmaI
SacI
BamHI
MCS
SV40 Late Promoter
/ VP1 Intron
SV40 Late
Polyadenylation
pSVL
4.8 kbp
SV40
ori
pBR322
ori
AmpR
(1)
(2)
(3)
XhoI
XbaI
β2NS7 cDNA (bp 18-2553)
SpeI
SacI
SacI
BamHI
5'UTR
3'UTR
BamHI
(bp 266-271)
SV40 Late Promoter
/ VP1 Intron
MCS
SV40 Late
Polyadenylation
pSVL/β2NS7
7.3 kbp
SV40
ori
pBR322
ori
AmpR

Figure 3.16c: Constructing pcDNA3/β2NS1

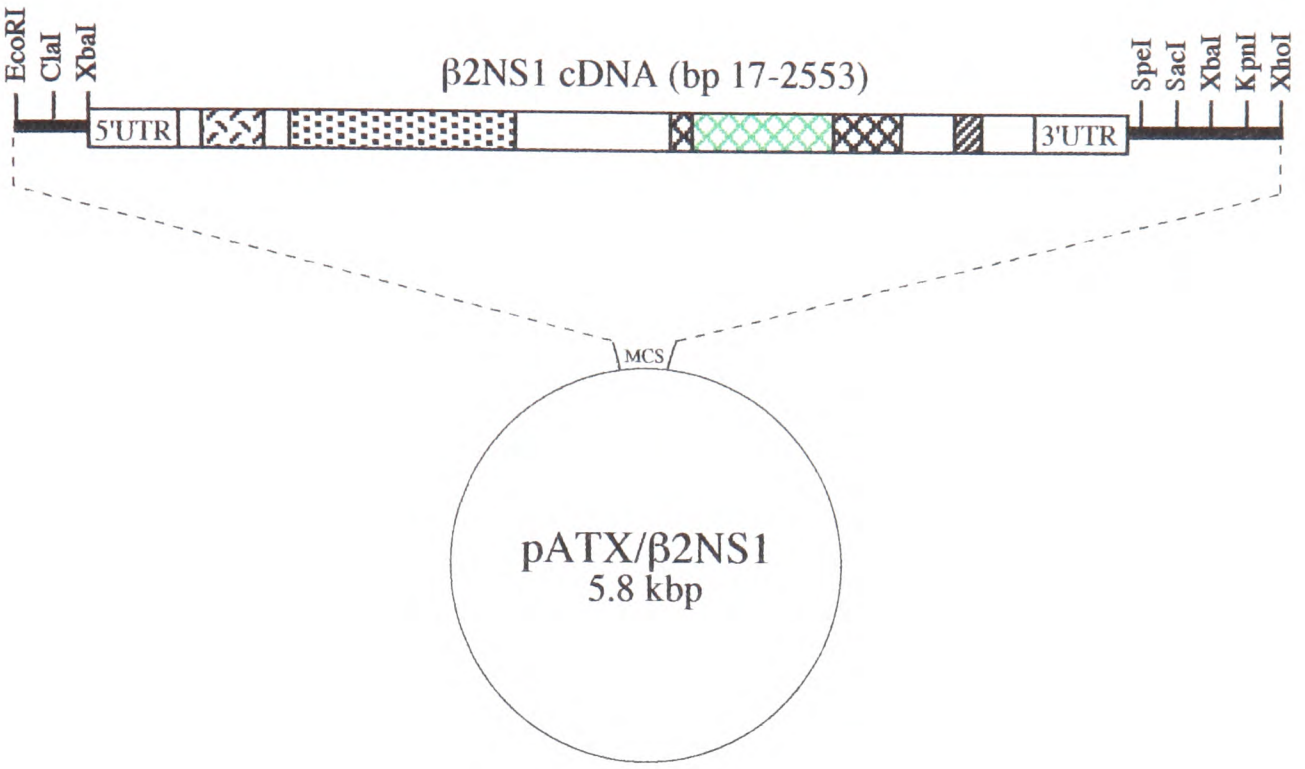
The entire coding region of the β2NS1 cDNA was subcloned from pATX into the pcDNA3 vector as follows:

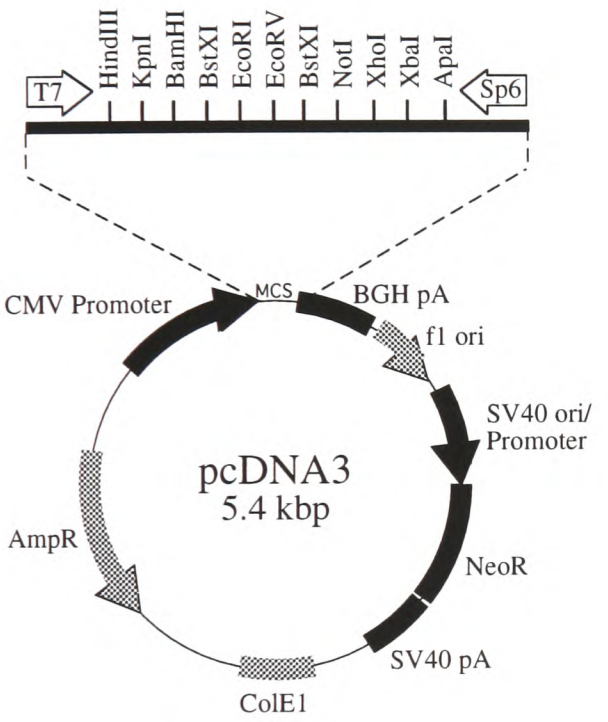
(1) pATX/β2NS1 was digested with XbaI (β2NS1 cDNA, 5' UTR; pATX/β2NS1, 3' polylinker) and the 2.5 kbp β2NS1 cDNA insert was purified by agarose gel electrophoresis.

(2) pcDNA3 was also digested with XbaI, and the 5.4 kbp pcDNA3 vector was purified by agarose gel electrophoresis.

(3) The pcDNA3 vector and the β2NS1 cDNA insert were then ligated, creating a clone named pcDNA3/β2NS1. The orientation of the β2NS1 cDNA in the pcDNA3 vector was determined by BamHI digestion. Clones producing a 300 bp restriction fragment were in the correct orientation.

In the figure opposite, the β2 cDNA regions are unshaded, whereas the β1 cDNA regions are shaded green. The cDNA regions encoding the N-terminal cysteine rich region are represented by dashed lines, the regions encoding the putative A-domain by dots, the regions encoding the C-terminal cysteine-rich region by crosshatches, and the regions encoding the transmembrane domain by diagonal lines. The 5' and 3' untranslated regions (UTRs) of the cDNAs are also shown.


EcoRI
ClaI
XbaI
β2NS1 cDNA (bp 17-2553)
SpeI
SacI
XbaI
KpnI
XhoI
5'UTR
3'UTR
MCS
pATX/β2NS1
5.8 kbp


T7
HindIII
KpnI
BamHI
BstXI
EcoRI
EcoRV
BstXI
NotI
XhoI
XbaI
ApaI
Sp6
MCS
CMV Promoter
BGH pA
f1 ori
SV40 ori/
Promoter
pcDNA3
5.4 kbp
AmpR
NeoR
SV40 pA
ColE1

(1)

(2)

(3)

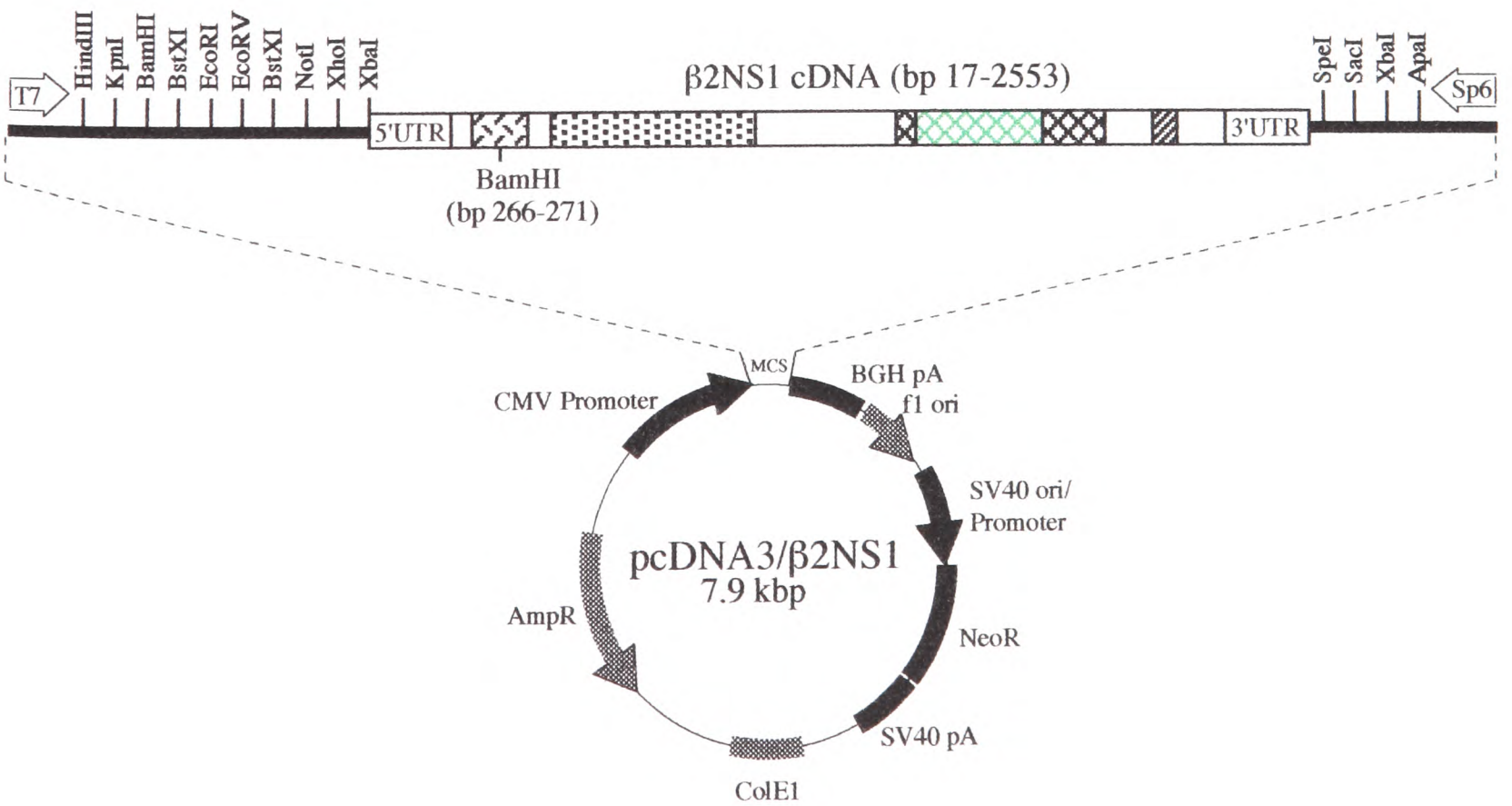

T7
HindIII
KpnI
BamHI
BstXI
EcoRI
EcoRV
BstXI
NotI
XhoI
XbaI
β2NS1 cDNA (bp 17-2553)
SpeI
SacI
XbaI
ApaI
Sp6
5'UTR
3'UTR
BamHI
(bp 266-271)
MCS
CMV Promoter
BGH pA
f1 ori
SV40 ori/
Promoter
pcDNA3/β2NS1
7.9 kbp
AmpR
NeoR
SV40 pA
ColE1

Figure 3.16d: Constructing pcDNA3/β2NS7

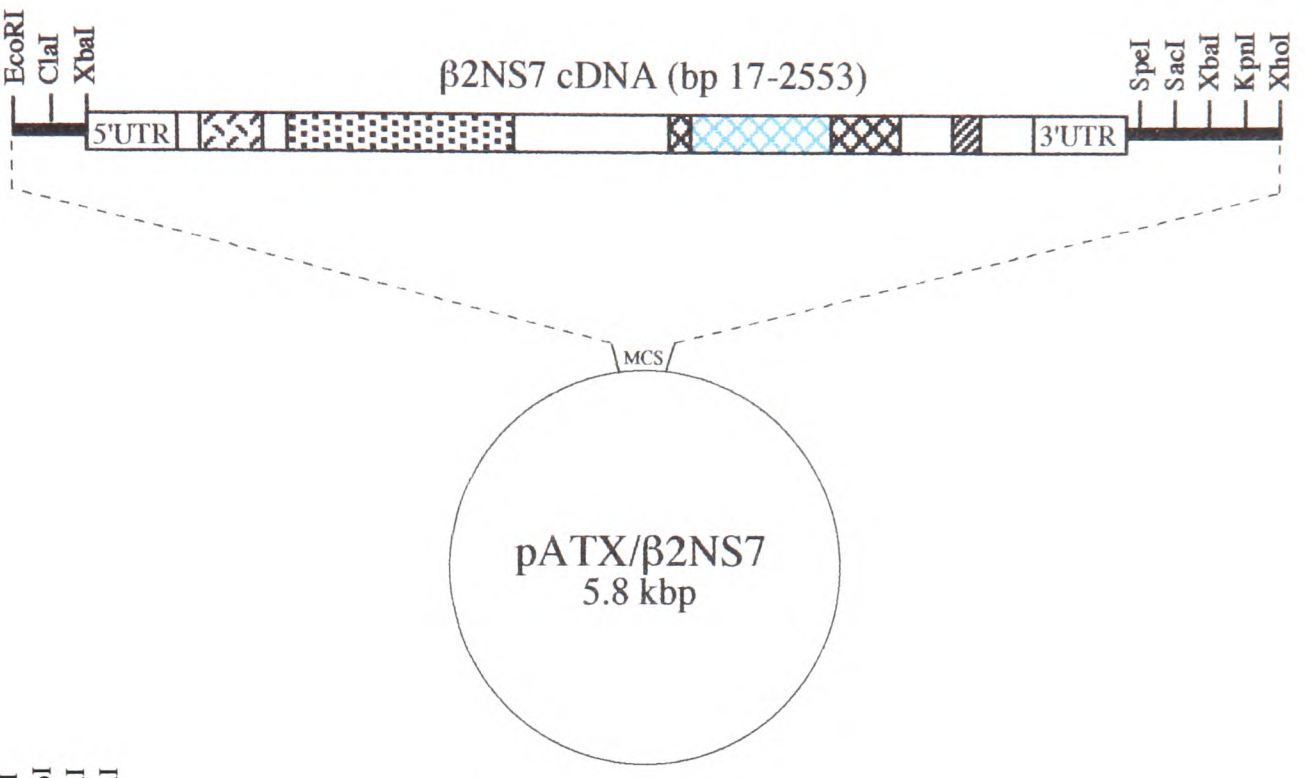
The entire coding region of the β2NS7 cDNA was subcloned from pATX into the pcDNA3 vector as follows:

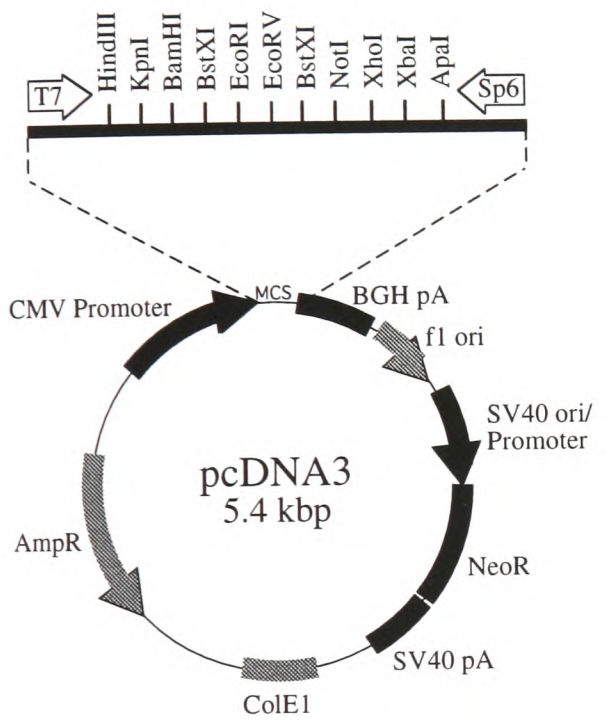
(1) pATX/β2NS7 was digested with XbaI (β2NS7 cDNA, 5' UTR; pATX/β2NS7, 3' polylinker) and the 2.5 kbp β2NS7 cDNA insert was purified by agarose gel electrophoresis.

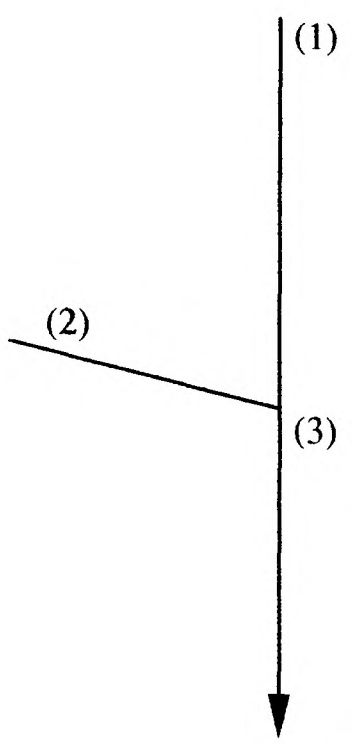
(2) pcDNA3 was also digested with XbaI, and the 5.4 kbp pcDNA3 vector was purified by agarose gel electrophoresis.

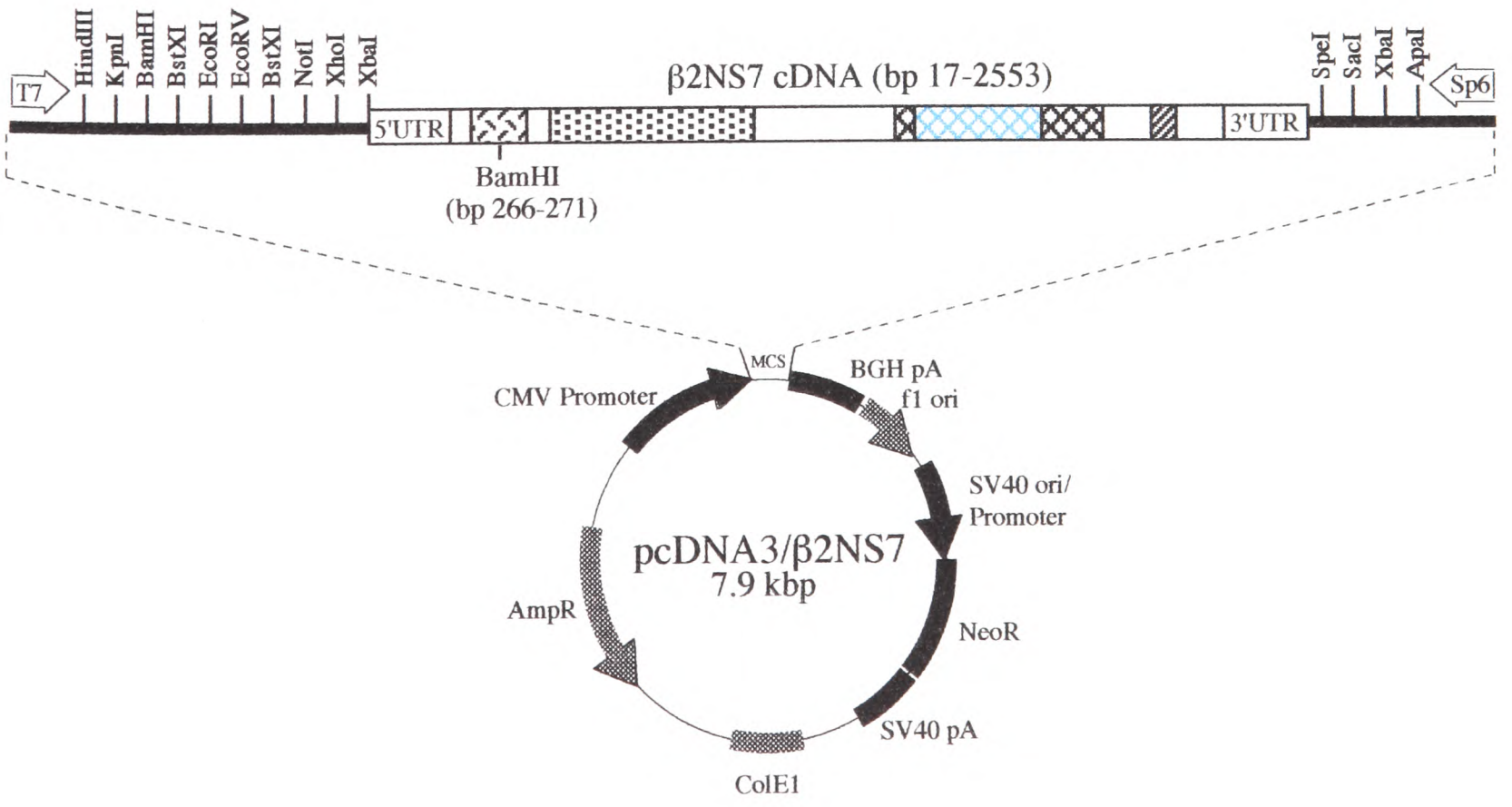
(3) The pcDNA3 vector and the β2NS7 cDNA insert were then ligated, creating a clone named pcDNA3/β2NS7. The orientation of the β2NS7 cDNA in the pcDNA3 vector was determined by BamHI digestion. Clones producing a 300 bp restriction fragment were in the correct orientation.

In the figure opposite, the β2 cDNA regions are unshaded, whereas the β7 cDNA regions are shaded blue. The cDNA regions encoding the N-terminal cysteine rich region are represented by dashed lines, the regions encoding the putative A-domain by dots, the regions encoding the C-terminal cysteine-rich region by crosshatches, and the regions encoding the transmembrane domain by diagonal lines. The 5' and 3' untranslated regions (UTRs) of the cDNAs are also shown.


EcoRI
ClaI
XbaI
β2NS7 cDNA (bp 17-2553)
SpeI
SacI
XbaI
KpnI
XhoI
5'UTR
3'UTR
MCS
pATX/β2NS7
5.8 kbp


HindIII
KpnI
BamHI
BstXI
EcoRI
EcoRV
BstXI
NotI
XhoI
XbaI
ApaI
T7
Sp6
MCS
CMV Promoter
BGH pA
f1 ori
SV40 ori/
Promoter
pcDNA3
5.4 kbp
AmpR
NeoR
SV40 pA
ColE1


(1)
(2)
(3)


HindIII
KpnI
BamHI
BstXI
EcoRI
EcoRV
BstXI
NotI
XhoI
XbaI
SpeI
SacI
XbaI
ApaI
T7
Sp6
β2NS7 cDNA (bp 17-2553)
5'UTR
3'UTR
BamHI
(bp 266-271)
MCS
CMV Promoter
BGH pA
f1 ori
SV40 ori/
Promoter
pcDNA3/β2NS7
7.9 kbp
AmpR
NeoR
SV40 pA
ColE1

3.2.2 GENERATING SOLUBLE AND TRUNCATED β2 CLONES

A soluble β2 cDNA, β2sol, encoding the entire extracellular region of the β2 subunit (amino acids 1-698), and a truncated β2 cDNA, β2tr, encoding amino acids 1-480 of the β2 subunit, had previously been constructed by Dr. A. Law. The nucleotide sequences at the 3' termini of the β2sol and β2tr cDNAs, and the amino acids that these residues encode, are shown in Figure 3.17.

3.2.2.1 Cloning the β2sol and β2tr cDNAs into Expression Vectors

The β2sol and β2tr cDNAs had been constructed in pBluescript, creating clones named pBS/β2sol and pBS/β2tr respectively. The β2sol and β2tr cDNA inserts were subcloned from pBluescript into the expression vectors pSVL (Pharmacia) and pcDNA3 (Invitrogen) for transient expression in COS 7 cells.

3.2.2.1.1 Constructing the pSVL/β2sol Clone

The β2sol cDNA was subcloned from pBluescript into the pSVL expression vector as illustrated in Figure 3.18a. The β2sol cDNA insert was excised from pBS/β2sol by digestion with XhoI (pBS/β2sol, 5' polylinker) and SacI (pBS/β2sol, 3' polylinker) and was cloned into XhoI/SacI cut pSVL, creating a clone named pSVL/β2sol.

3.2.2.1.2 Constructing the pSVL/β2tr Clone

The β2tr cDNA was subcloned from pBluescript into the pSVL expression vector as illustrated in Figure 3.18b. The β2tr cDNA insert was excised from pBS/β2tr by digestion with XhoI (pBS/β2tr, 5' polylinker) and SacI (β2tr cDNA, 3' terminus) and was cloned into XhoI/SacI cut pSVL, creating a clone named pSVL/β2tr.

3.2.2.1.3 Constructing the pcDNA3/β2tr Clone

The β2tr cDNA was subcloned from pBluescript into the pcDNA3 expression vector as illustrated in Figure 3.18c. The β2tr cDNA insert was excised from pBS/β2tr by digestion with KpnI (pBS/β2tr, 5' polylinker) and Ecl136II (β2tr, 3' terminus), and was cloned into KpnI/EcoRV cut pcDNA3, creating a clone named pcDNA3/β2tr.

Figure 3.17: The Nucleotide and Resulting Amino Acid Sequences at the 3' Termini of the β2sol and β2tr cDNAs

The 3' termini of the β2sol and β2tr cDNAs are shown in the figure above, along with the relevant sections of the wildtype β2 cDNA. The amino acids that these cDNA regions encode are shown above the cDNA sequences (using the single letter amino acid code), and with the cysteine residues coloured red, and numbered such that the first cysteine residue in the extracellular portion of the mature β2 polypeptide would be numbered C1 and the last C56. Residues representing the transmembrane domain are underlined. The β2sol and β2tr cDNAs were constructed by engineering a stop codon into the desired position in the wildtype β2 cDNA sequence. For cloning purposes, a convenient restriction enzyme site was also engineered into the modified cDNAs. The mutated nucleotide and amino acid residues are shown, coloured in pink. The β2tr cDNA encodes the wildtype 1-480 β2 amino acids, whereas the β2sol cDNA encodes the wildtype 1-698 β2 amino acids followed by a single amino acid point mutation, P699L.

(i) The 3' terminus of the β2sol cDNA clone:

```
D  E  S  R  E C56 V  A  G  P  N  I  A  A  I  V  G  G  T
GATGAGAGCCGAGAGTGTGTGGCAGGCCCCAACATCGCCGCCATCGTCGGGGGCACC
        2180       2190       2200       2210       2220          WT β2
CTACTCTCGGCTCTCACACACCGTCCGGGGTTGTAGCGGCGGTAGCAGCCCCCGTGG

D  E  S  R  E C56 V  A  G  L  *
GATGAGAGCCGAGAGTGTGTGGCAGGCCTCTAGA
        2180       2190      XbaI                                  β2sol
CTACTCTCGGCTCTCACACACCGTCCGGAGATCT
```

(ii) The 3' terminus of the β2tr cDNA clone:

```
C19G  I C20 R C21 D  T  G  Y  I  G  K  N C22 E C23 Q  T  Q  G
TGCGGCATCTGCAGGTGTGACACTGGCTACATTGGGAAAAACTGTGAGTGCCAGACACAGGGC
       1510       1520       1530       1540       1550       1560    WT β2
ACGCCGTAGACGTCCACACTGTGACCGATGTAACCCTTTTTGACACTCACGGTCTGTGTCCCG

C19G  I C20 R C21 D  T  G  Y  I  G  K  N  *
TGCGGCATCTGCAGGTGTGACACTGGCTACATTGGGAAAAACTGAGCTC
       1510       1520       1530       1540  SacI                  β2tr
ACGCCGTAGACGTCCACACTGTGACCGATGTAACCCTTTTTGACTCGAG
```

Figure 3.18a: Constructing pSVL/β2sol

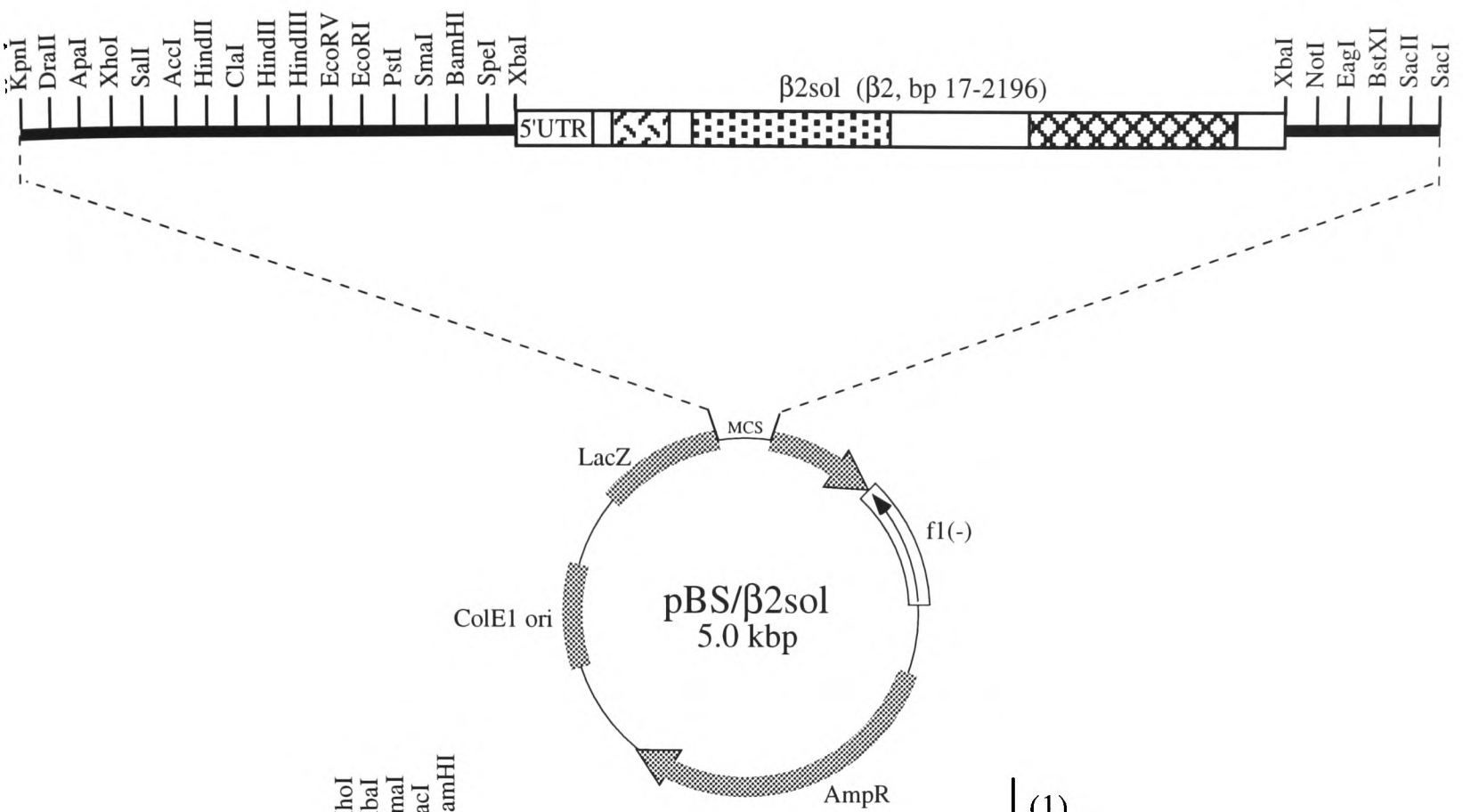
The β2sol cDNA was subcloned from pBluescript into the pSVL vector as follows:

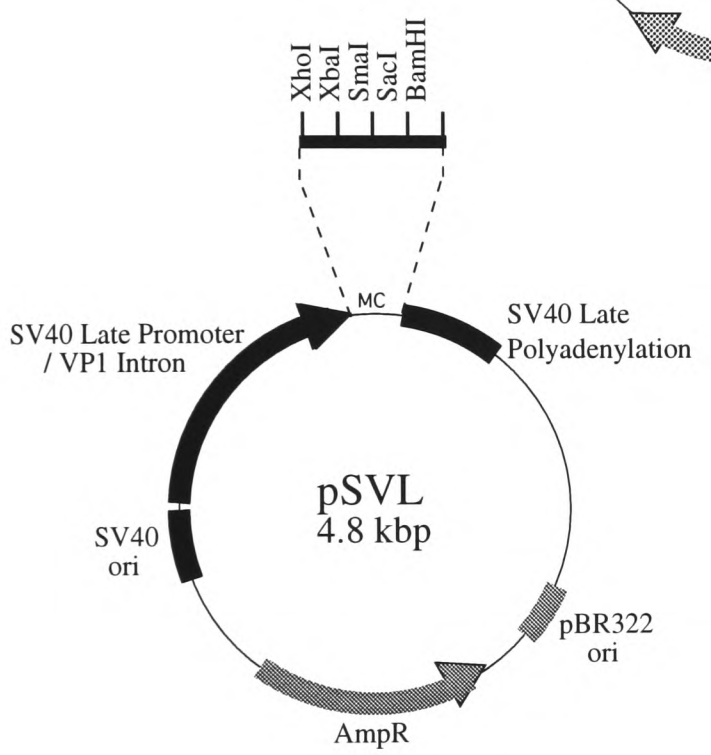
(1) pBS/β2sol was digested with XhoI (pBS/β2sol, 5' polylinker) and SacI (pBS/β2sol, 3' polylinker) and the 2.2 kbp β2sol cDNA insert was purified by agarose gel electrophoresis.

(2) pSVL was digested with XhoI and SacI, and the 4.8 kbp pSVL vector was also purified by agarose gel electrophoresis.

(3) The pSVL vector and the β2sol cDNA insert were then ligated, creating a clone named pSVL/β2sol.

In the figure opposite, the β2 cDNA region encoding the N-terminal cysteine rich region is represented by dashed lines, the region encoding the putative A-domain by dots, and the region encoding the C-terminal cysteine-rich region by crosshatches. The 5' untranslated region (5' UTR) of the β2 cDNA is also shown.


KpnI
DraII
ApaI
XhoI
SalI
AccI
HindII
ClaI
HindII
HindIII
EcoRV
EcoRI
PstI
SmaI
BamHI
SpeI
XbaI
β2sol (β2, bp 17-2196)
5'UTR
XbaI
NotI
EagI
BstXI
SacII
SacI
MCS
LacZ
f1(-)
ColE1 ori
pBS/β2sol
5.0 kbp
AmpR


XhoI
XbaI
SmaI
SacI
BamHI
MC
SV40 Late Promoter
/ VP1 Intron
SV40 Late
Polyadenylation
pSVL
4.8 kbp
SV40
ori
pBR322
ori
AmpR

(1)

(2)

(3)

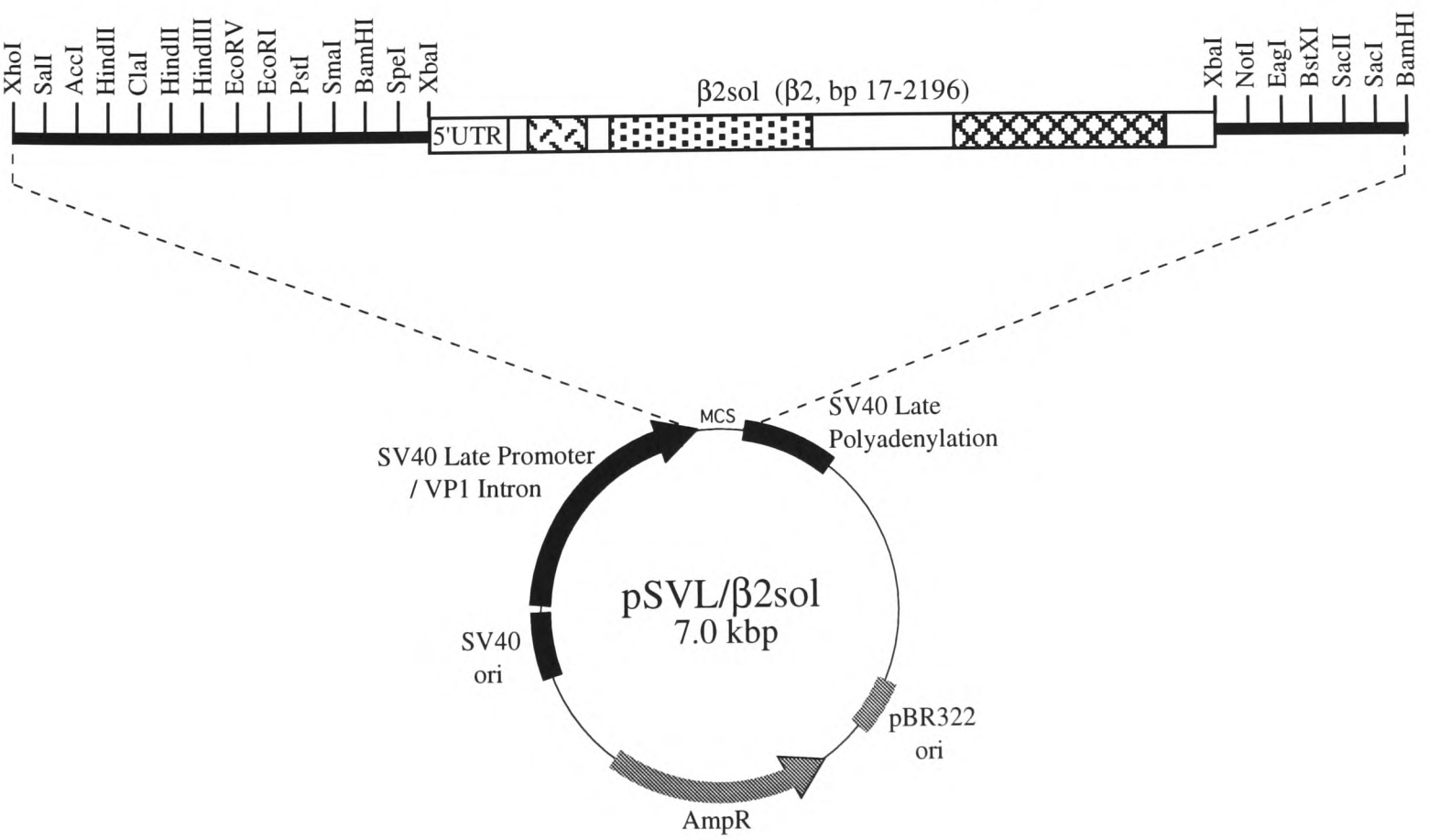

XhoI
SalI
AccI
HindII
ClaI
HindII
HindIII
EcoRV
EcoRI
PstI
SmaI
BamHI
SpeI
XbaI
β2sol (β2, bp 17-2196)
5'UTR
XbaI
NotI
EagI
BstXI
SacII
SacI
BamHI
MCS
SV40 Late
Polyadenylation
SV40 Late Promoter
/ VP1 Intron
pSVL/β2sol
7.0 kbp
SV40
ori
pBR322
ori
AmpR

Figure 3.18b: Constructing pSVL/β2tr

The β2tr cDNA was subcloned from pBluescript into the pSVL vector as follows:

(1) pBS/β2tr was digested with XhoI (pBS/β2tr, 5' polylinker) and SacI (β2tr cDNA, 3' terminus) and the 1.5 kbp β2tr cDNA insert was purified by agarose gel electrophoresis.

(2) pSVL was digested with XhoI and SacI, and the 4.8 kbp pSVL vector was also purified by agarose gel electrophoresis.

(3) The pSVL vector and the β2tr cDNA insert were then ligated, creating a clone named pSVL/β2tr.

In the figure opposite, the β2 cDNA region encoding the N-terminal cysteine rich region is represented by dashed lines, the region encoding the putative A-domain by dots, and the region encoding the C-terminal cysteine-rich region by crosshatches. The 5' untranslated region (5' UTR) of the β2 cDNA is also shown.

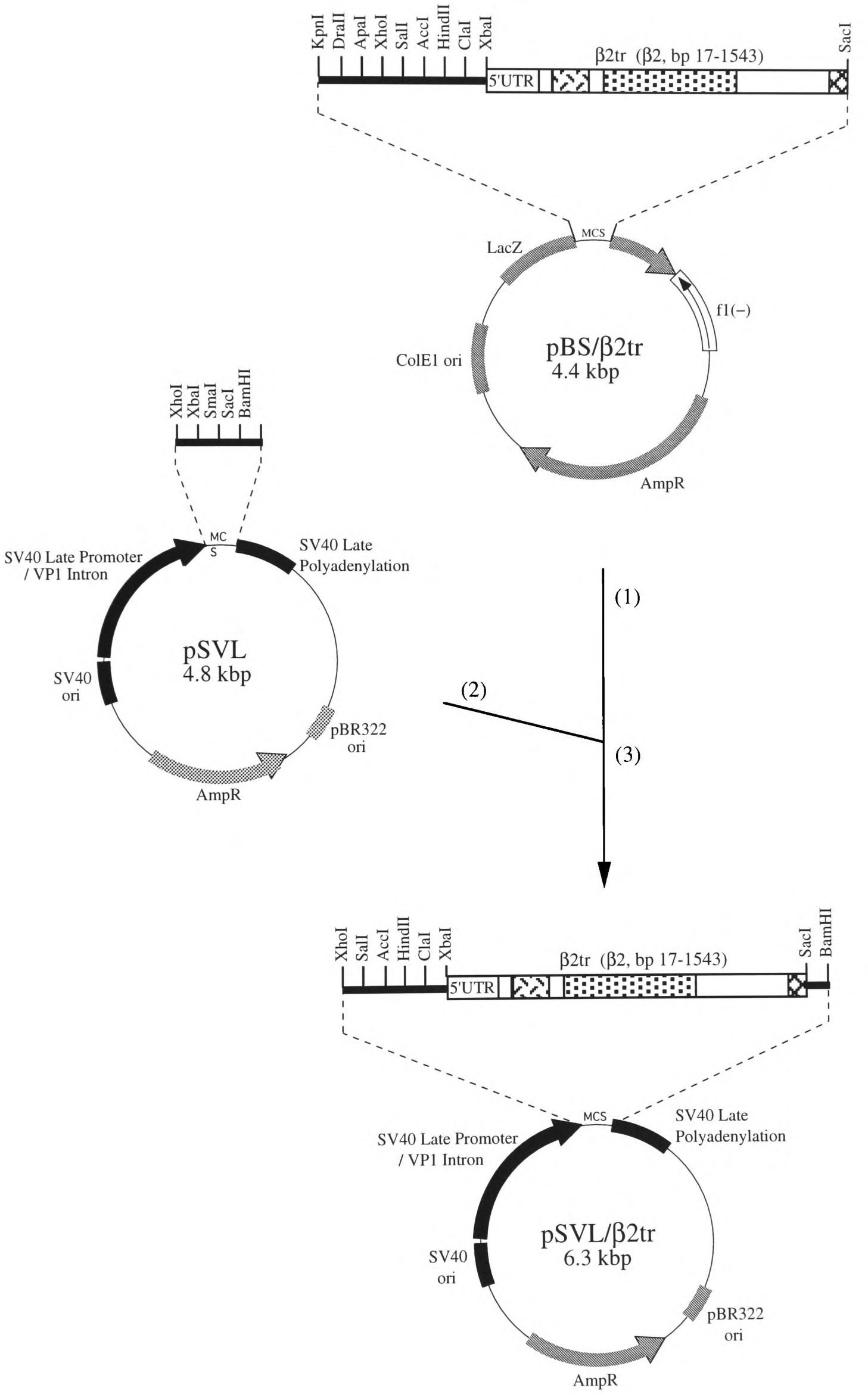

KpnI
DraII
ApaI
XhoI
SalI
AccI
HindII
ClaI
XbaI
β2tr (β2, bp 17-1543)
SacI
5'UTR
MCS
LacZ
f1(−)
ColE1 ori
pBS/β2tr
4.4 kbp
AmpR
XhoI
XbaI
SmaI
SacI
BamHI
MC
S
SV40 Late Promoter
/ VP1 Intron
SV40 Late
Polyadenylation
pSVL
4.8 kbp
SV40
ori
pBR322
ori
AmpR
(1)
(2)
(3)
XhoI
SalI
AccI
HindII
ClaI
XbaI
β2tr (β2, bp 17-1543)
SacI
BamHI
5'UTR
MCS
SV40 Late Promoter
/ VP1 Intron
SV40 Late
Polyadenylation
pSVL/β2tr
6.3 kbp
SV40
ori
pBR322
ori
AmpR

Figure 3.18c: Constructing pcDNA3/β2tr

The β2tr cDNA was subcloned from pBluescript into the pcDNA3 vector as follows:

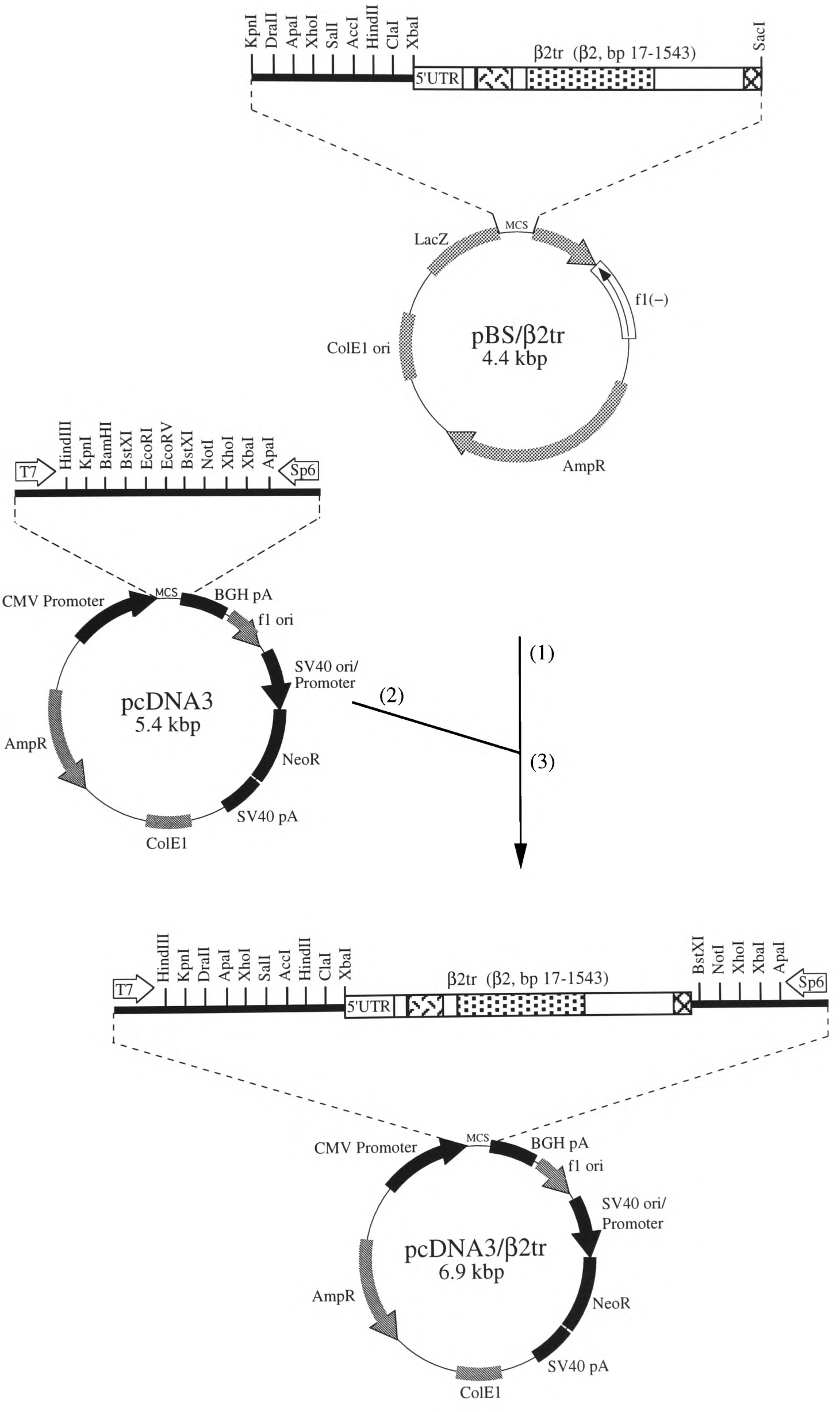
(1) pBS/β2tr was digested with KpnI (pBS/β2tr, 5' polylinker) and Ecl136II [1] (β2tr cDNA, 3' terminus) and the 1.5 kbp β2tr cDNA insert was purified by agarose gel electrophoresis.

(2) pcDNA3 was digested with KpnI and EcoRV, and the 5.4 kbp pcDNA3 vector was also purified by agarose gel electrophoresis.

(3) The pcDNA3 vector and the β2tr cDNA insert were then ligated, creating a clone named pcDNA3/β2tr.

In the figure opposite, the β2 cDNA region encoding the N-terminal cysteine rich region is represented by dashed lines, the region encoding the putative A-domain by dots, and the region encoding the C-terminal cysteine-rich region by crosshatches. The 5' untranslated region (5' UTR) of the β2 cDNA is also shown.

1 Ecl136II is an isoschizomer of SacI


KpnI
DraII
ApaI
XhoI
SalI
AccI
HindII
ClaI
XbaI
β2tr (β2, bp 17-1543)
SacI
5'UTR
MCS
LacZ
f1(−)
ColE1 ori
pBS/β2tr
4.4 kbp
AmpR
T7
HindIII
KpnI
BamHI
BstXI
EcoRI
EcoRV
BstXI
NotI
XhoI
XbaI
ApaI
Sp6
MCS
CMV Promoter
BGH pA
f1 ori
SV40 ori/
Promoter
pcDNA3
5.4 kbp
AmpR
NeoR
SV40 pA
ColE1
(1)
(2)
(3)
HindIII
KpnI
DraII
ApaI
XhoI
SalI
AccI
HindII
ClaI
XbaI
β2tr (β2, bp 17-1543)
BstXI
NotI
XhoI
XbaI
ApaI
T7
5'UTR
Sp6
MCS
CMV Promoter
BGH pA
f1 ori
SV40 ori/
Promoter
pcDNA3/β2tr
6.9 kbp
AmpR
NeoR
SV40 pA
ColE1

3.2.3 GENERATING WILDTYPE β2 CLONES

3.2.3.1 Cloning the Wildtype β2 cDNA into Expression Vectors

The entire coding region of the wildtype β2 cDNA was cloned into the vectors pSVL (Pharmacia) and pcDNA3 (Invitrogen) for transient expression in COS 7 cells.

3.2.3.1.1 Constructing the pSVL/β2 Clone

The wildtype β2 cDNA was subcloned from J8 into the pSVL vector as illustrated in Figure 3.19a. The β2 cDNA insert was excised from J8 by digestion with XbaI (β2 cDNA, 5' UTR) and NaeI (β2 cDNA, 3' UTR), and was ligated into XbaI/SmaI cut pSVL, creating a clone named pSVL/β2. Both the NaeI and SmaI sites were destroyed in this cloning procedure.

3.2.3.1.2 Constructing the pcDNA3/β2 Clone

The wildtype β2 cDNA was subcloned from J8.1N into the pcDNA3 vector as illustrated in Figure 3.19b. The β2 cDNA insert was excised from J8.1N by digestion with XbaI (β2 cDNA, 5' UTR; J8.1N, 3' polylinker), and was ligated into XbaI cut pcDNA3, creating a clone named pcDNA3/β2. The orientation of the β2 cDNA in the expression vector was determined by BamHI digestion. Clones producing a 350 bp restriction fragment were in the correct orientation.

Figure 3.19a: Constructing pSVL/β2

The wildtype β2 cDNA was subcloned from J8 into the pSVL vector as follows:

(1) J8 was digested with XbaI (β2 cDNA, 5' UTR) and NaeI (β2 cDNA, 3' UTR) and the 2.8 kbp β2 cDNA insert was purified by agarose gel electrophoresis.

(2) pSVL was digested with XbaI and SmaI, and the 4.8 kbp pSVL vector was also purified by agarose gel electrophoresis.

(3) The pSVL vector and the β2 cDNA insert were then ligated, creating a clone named pSVL/β2.

In the figure opposite, the β2 cDNA region encoding the N-terminal cysteine rich region is represented by dashed lines, the region encoding the putative A-domain by dots, and the region encoding the C-terminal cysteine-rich region by crosshatches, and the region encoding the transmembrane domain by diagonal lines. The 5' and 3' untranslated regions (UTRs) of the β2 cDNA are also shown.

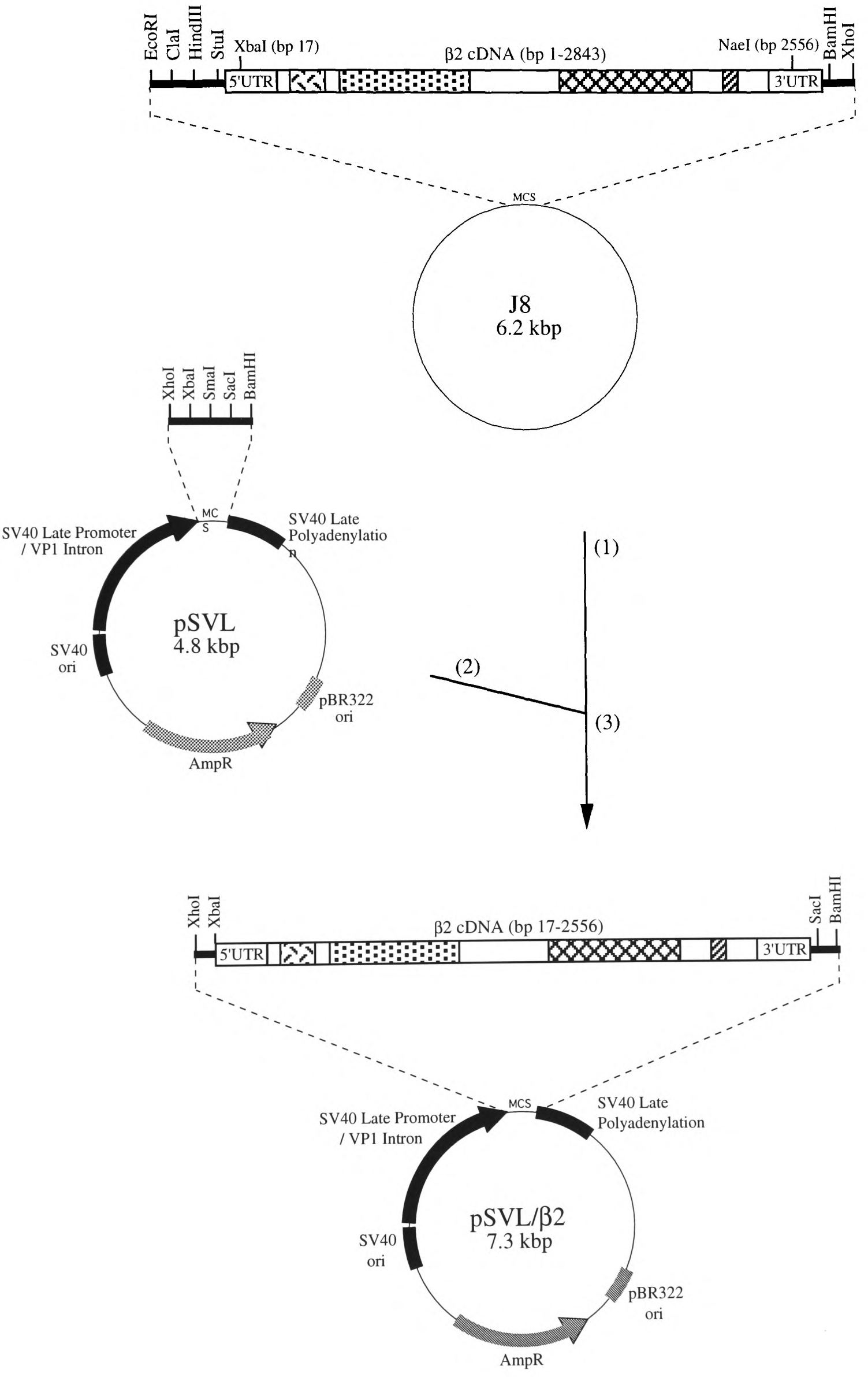

EcoRI
ClaI
HindIII
StuI
XbaI (bp 17)
β2 cDNA (bp 1-2843)
NaeI (bp 2556)
BamHI
XhoI
5'UTR
3'UTR
MCS
J8
6.2 kbp
XhoI
XbaI
SmaI
SacI
BamHI
MC
S
SV40 Late Promoter
/ VP1 Intron
SV40 Late
Polyadenylatio
n
pSVL
4.8 kbp
SV40
ori
pBR322
ori
AmpR
(1)
(2)
(3)
XhoI
XbaI
β2 cDNA (bp 17-2556)
SacI
BamHI
5'UTR
3'UTR
MCS
SV40 Late Promoter
/ VP1 Intron
SV40 Late
Polyadenylation
pSVL/β2
7.3 kbp
SV40
ori
pBR322
ori
AmpR

Figure 3.19b: Constructing pcDNA3/β2

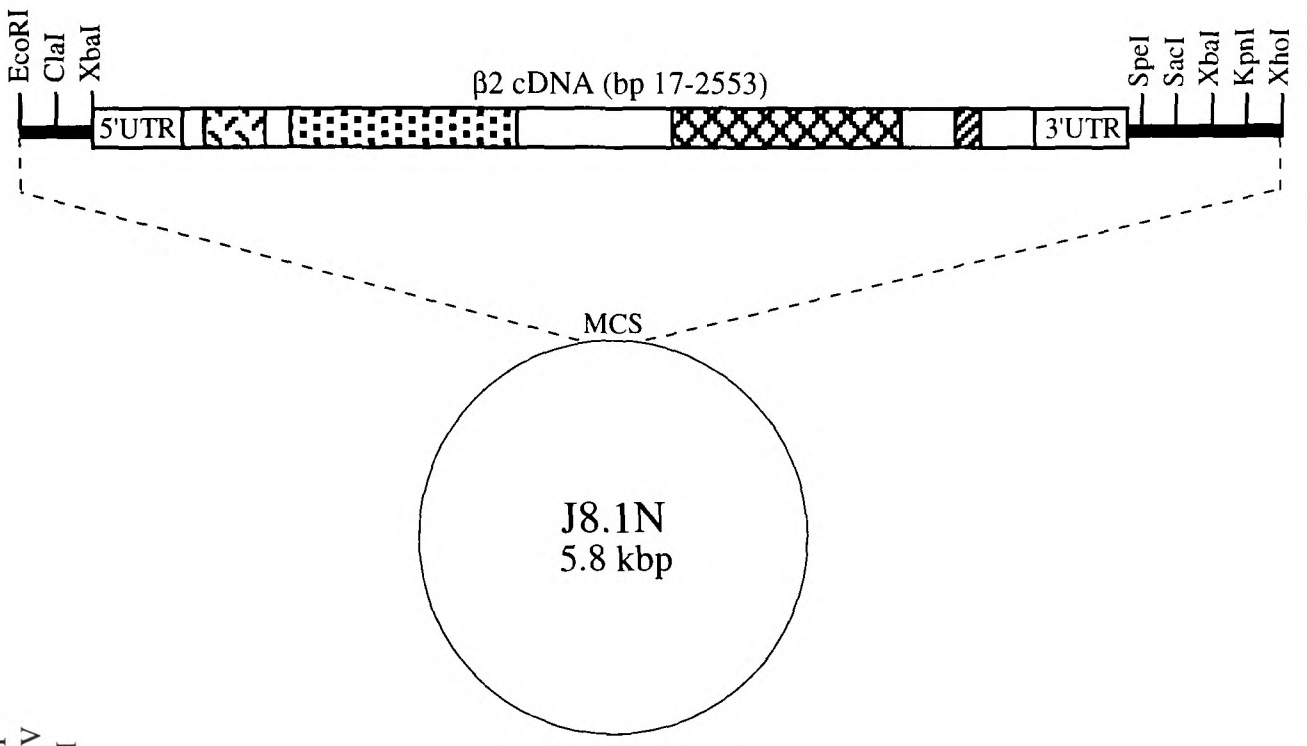
The wildtype β2 cDNA was subcloned from J8.1N into the pcDNA3 vector as follows:

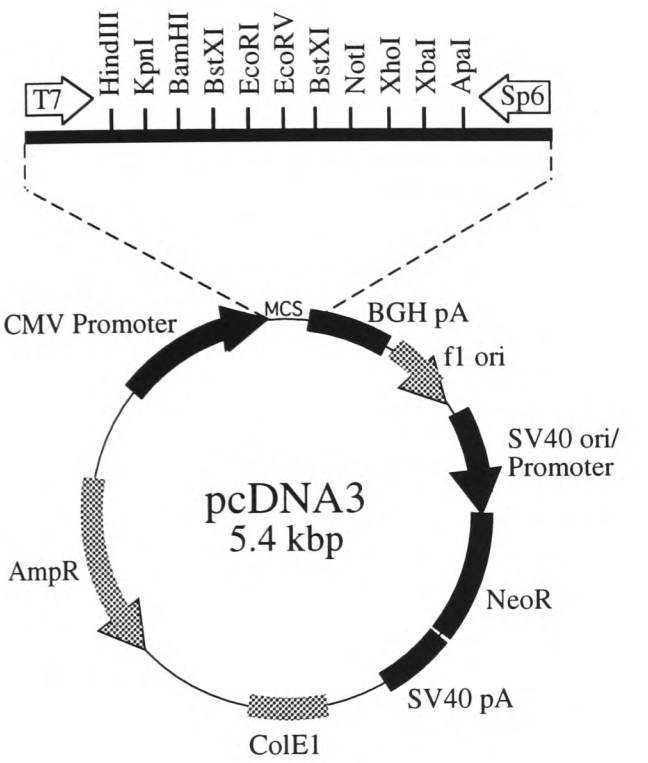
(1) J8.1N was digested with XbaI (β2 cDNA, 5' UTR; J8.1N, 3' polylinker) and the 2.5 kbp β2 cDNA insert was purified by agarose gel electrophoresis.

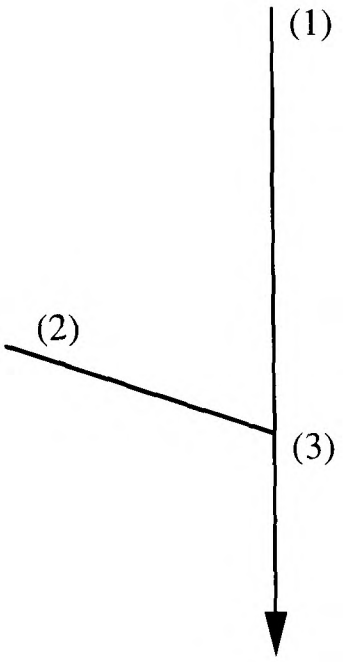
(2) pcDNA3 was digested with XbaI, and the 5.4 kbp pcDNA3 vector was also purified by agarose gel electrophoresis.

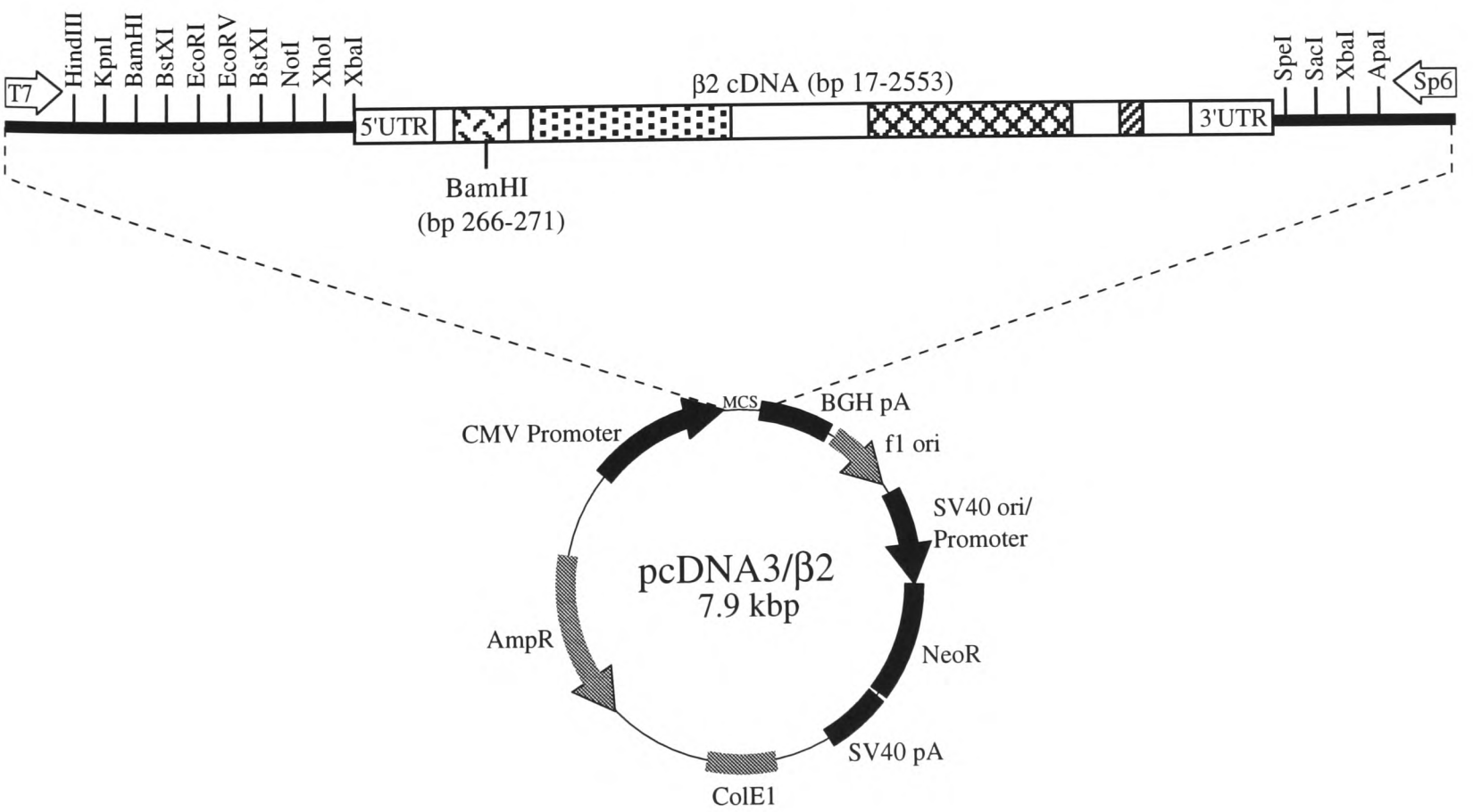
(3) The pcDNA3 vector and the β2 cDNA insert were then ligated, creating a clone named pcDNA3/β2. The orientation of the β2 cDNA in the pcDNA3 vector was determined by BamHI digestion. Clones producing a 350 bp restriction fragment were in the correct orientation.

In the figure opposite, the β2 cDNA region encoding the N-terminal cysteine rich region is represented by dashed lines, the region encoding the putative A-domain by dots, and the region encoding the C-terminal cysteine-rich region by crosshatches, and the region encoding the transmembrane domain by diagonal lines. The 5' and 3' untranslated regions (UTRs) of the β2 cDNA are also shown.


EcoRI
ClaI
XbaI
β2 cDNA (bp 17-2553)
SpeI
SacI
XbaI
KpnI
XhoI
5'UTR
3'UTR
MCS
J8.1N
5.8 kbp


T7
HindIII
KpnI
BamHI
BstXI
EcoRI
EcoRV
BstXI
NotI
XhoI
XbaI
ApaI
Sp6
MCS
CMV Promoter
BGH pA
f1 ori
SV40 ori/
Promoter
pcDNA3
5.4 kbp
AmpR
NeoR
SV40 pA
ColE1


(1)
(2)
(3)


T7
HindIII
KpnI
BamHI
BstXI
EcoRI
EcoRV
BstXI
NotI
XhoI
XbaI
β2 cDNA (bp 17-2553)
SpeI
SacI
XbaI
ApaI
Sp6
5'UTR
3'UTR
BamHI
(bp 266-271)
MCS
CMV Promoter
BGH pA
f1 ori
SV40 ori/
Promoter
pcDNA3/β2
7.9 kbp
AmpR
NeoR
SV40 pA
ColE1

3.2.4 GENERATING WILDTYPE αL, αM and αX CLONES

The chimeric, soluble, truncated, and wildtype β2 constructs were to be transiently expressed in COS 7 cells. Because these cells do not express any of the leukocyte integrin subunits, cotransfection of the α subunits αL, αM and αX with the β2 constructs was required to produce LFA-1, Mac-1 and p150,95 heterodimers.

3.2.4.1 Generating Wildtype αL Clones

3.2.4.1.1 Constructing a Full Length Wildtype αL cDNA

A full length wildtype αL cDNA (bp 27-3640) was constructed as summarised in Figure 3.20.

A U937 cDNA library, cloned via XbaI into the vector pCDM8 (Stratagene), was screened for clones containing αL cDNA inserts. The 5' end of the αL cDNA (bp 93-933) was amplified by PCR, using the cDNA library as template and the oligonucleotides OL2 and OL3 as primers. A radiolabelled DNA probe was then prepared from this PCR product using the cDNA Multiprime Labelling Kit (Amersham), and this probe was used to screen the U937 cDNA library. No full length αL cDNA clones were obtained. However, several cDNA clones spanning the 5' end of the αL cDNA were isolated. The largest of these clones, αL5' (αL cDNA, bp 27-2187), was subcloned from the library vector pCDM8 into pBluescript KS(-) via XbaI, creating a clone named pBS/αL5'.

Construction of a full length αL cDNA from pBS/αL5' was carried out in collaboration with Dr. G. Otulakowski (R.W. Johnson PRI, Canada). The remaining 3' end of the αL cDNA was synthesised by PCR (bp 1899-3649), using a Jurkat cDNA library as template and oligonucleotides L1 (bp 1899-1920) and L2 (bp 3621-3649). For subsequent cloning purposes, oligo L2 was designed to engineer an EcoRI site (bp 3641-3646, CAGGAT to GAATTC) into the 3' UTR of the αL cDNA. The full length coding sequence was then constructed making use of a unique BstEII site in αL (bp 1942-1948) and the unique engineered EcoRI site (bp 3641-3646). pBS/αL5' was digested with BstEII and EcoRI, and ligated with the PCR product also digested with BstEII and EcoRI, creating a full length αL cDNA in pBluescript KS(-), pBS/αL.

The entire coding region of the αL cDNA in pBS/αL was then nucleotide sequenced. Three sequence discrepancies were discovered between the pBS/αL clone and the published αL cDNA sequence (Larson *et al..*, 1989) derived from an HL-60 cDNA library: (i) bp 2066-2067, TA to AT (Y689I); (ii) bp 2323-2325, GCA deleted (Q775 deleted); (iii) bp 2460, G to C (R820T). To determine whether these discrepancies represented true variations in the αL sequence or simply PCR errors, PCR products were resynthesised from the Jurkat and U937 cDNA libraries, as well as from an HL-60 cDNA library, using the L1 and L2 oligonucleotides, and were cloned into pBluescript KS(-) and nucleotide sequenced. The first two sequence discrepancies were found in all PCR products amplified from the Jurkat, U937 and HL-60 cDNA libraries. It was therefore assumed that these differences were due to errors in the published αL sequence. The third sequence discrepancy was found in all PCR products amplified from the Jurkat and U937 cDNA libraries, but in no PCR products amplified from the HL-60 cDNA library. This sequence variation was therefore assumed to represent a polymorphic difference in Jurkat/U937 cells versas HL-60 cells.

3.2.4.1.2 Cloning the Wildtype αL cDNA into Expression Vectors

The entire coding region of the wildtype αL cDNA was subcloned into the vectors pSVL (Pharmacia) and pcDNA3 (Invitrogen) for transient expression in COS 7 cells.

3.2.4.1.2.1 Constructing the pSVL/αL Clone

The αL cDNA was subcloned from pBluescript into the pSVL vector as summarised in Figure 3.21a. The αL cDNA insert was excised from pBS/αL by digestion with XbaI (pBS/αL, 5' polylinker) and EcoRV (pBS/αL, 3' polylinker), and was cloned into XbaI/SmaI cut pSVL, creating a clone named pSVL/αL.

3.2.4.1.2.2 Constructing the pcDNA3/αL Clone

The αL cDNA was subcloned from pBluescript into the pcDNA3 vector as summarised in Figure 3.21b. pBS/αL was digested with NotI (pBS/αL, 5' polylinker) and the resultant 5' overhang was blunted using the end-filling reaction. The αL cDNA insert was then excised from pBS/αL by digestion with EcoRV (pBS/αL, 3' polylinker), and was ligated into EcoRV cut pcDNA3, creating a clone named pcDNA3/αL. The orientation of the αL

cDNA in the expression vector was determined by BamHI digestion. Clones producing a 3.5 kbp restriction fragment were in the correct orientation.

3.2.4.2 Generating Wildtype αM Clones

3.2.4.2.1 Obtaining a Full Length Wildtype αM cDNA

A full length wildtype αM cDNA was constructed in Dr. Law's laboratory (by Mrs. J. M. Shaw) by overlapping PCR using the Taq DNA polymerase enzyme. The complete αM cDNA was cloned into pBluescript KS (-), creating a clone named pBS/αM, and the entire coding region was nucleotide sequenced to check for PCR errors. The sequence of the pBS/αM clone is identical to the varient reported by Fleming *et al* (1993), in which the last 3 nucleotide base pairs in intron 13 are deleted (bp 1580) resulting in the deletion of Q500.

3.2.4.2.2 Cloning the Wildtype αM cDNA into Expression Vectors

The entire coding region of the wildtype αM cDNA was subcloned into the vectors pcDNA1 (Invitrogen), pSVL (Pharmacia) and pcDNA3 (Invitrogen) for transient expression in COS 7 cells.

3.2.4.2.2.1 Constructing the pcDNA1/αM Clone

The αM cDNA was subcloned from pBluescript into the pcDNA1 vector as summarised in Figure 3.22a. pBS/αM was digested with XbaI (pBS/αM, 5' polylinker) and HindIII (pBS/αM, 3' polylinker), and the resultant 5' overhangs were blunted using the end-filling reaction. The αM cDNA insert was then cloned into EcoRV cut pcDNA1, creating a clone named pcDNA1/αM. The orientation of the cDNA in the expression vector was determined by BamHI digestion. Clones producing a 7.2 kbp restriction fragment were in the correct orientation.

3.2.4.2.2.2 Constructing the pSVL/αM Clone

The αM cDNA was subcloned from pcDNA1 into the pSVL vector as summarised in Figure 3.22b. pcDNA1/αM was digested with HindIII (pcDNA1/αM, 5' polylinker) and the resultant 5' overhang was blunted using the end-filling reaction. The αM cDNA insert was then excised from the pcDNA1 vector by digestion with XbaI (pcDNA1/αM, 3' polylinker), and was purified by agarose gel electrophoresis. The pSVL vector was

digested with XhoI, the resultant 5' overhang blunted using the end-filling reaction, and was then digested with XbaI. The αM HindIII(blunted)-XbaI cDNA insert was then cloned into the XhoI(blunted)-XbaI pSVL vector, creating a clone named pSVL/αM.

3.2.4.2.2.3 Constructing the pcDNA3/αM Clone

The αM cDNA was subcloned from pBluescript into the pcDNA3 vector as summarised in Figure 3.22c. pBS/αM was digested with XbaI (pBS/αM, 5' polylinker) and HindIII (pBS/αM, 3' polylinker), and the resultant 5' overhangs were blunted using the end-filling reaction. The blunted αM cDNA insert was then ligated into EcoRV cut pcDNA3, creating a clone named pcDNA3/αM. The orientation of the cDNA in the expression vector was determined by BamHI digestion. Clones producing an 8.5 kbp restriction fragment were in the correct orientation.

3.2.4.3 Generating Wildtype αX Clones

3.2.4.3.1 Obtaining a Full Length Wildtype αX cDNA

A full length wildtype αX cDNA (approximately: bp 60-3560), cloned into the vector pEE6.hCMV.BglII.Neo (Celltech) was a generous gift of Dr. M.K.Robinson (Celltech).

3.2.4.3.2 Cloning the Wildtype αX cDNA into Expression Vectors

The entire coding region of the wildtype αX cDNA was subcloned from the pEE6.hCMV.BglII.Neo vector into the pSVL (Pharmacia) and pcDNA3 (Invitrogen) expression vectors for transient expression in COS 7 cells.

3.2.4.3.2.1 Constructing the pSVL/αX Clone

The αX cDNA was subcloned from pEE6.hCMV.BglII.Neo into the pSVL expression vector as summarised in Figure 3.23a. pEE6.hCMV.BglII.Neo/αX was digested with HindIII, and the resultant 5' overhangs were partially end-filled using only the dATP and dGTP nucleotides. The 3.6 kbp αX cDNA insert was then purified by agarose gel electrophoresis. The pSVL vector was digested with XbaI, and the resultant 5' overhangs were also partially end-filled, using only the dCTP and dTTP nucleotides. The resulting two base pair 5' overhangs in the αX cDNA insert and the resulting 2 base pair 5'

overhangs in the pSVL vector were compatible, and the insert and vector were ligated, creating a clone named pSVL/αX. The orientation of the cDNA in the expression vector was determined by EcoRI digestion. Clones producing a 2.6 kbp restriction fragment were in the correct orientation.

3.2.4.3.2.2 Constructing the pcDNA3/αX Clone

The αX cDNA was subcloned from pEE6.hCMV.BglII.Neo into the pcDNA3 expression vector as summarised in Figure 3.23b. The αX cDNA was excised from pEE6.hCMV.BglIINeo/αX by digestion with HindIII, and was ligated into HindIII cut pcDNA3, creating a clone named pcDNA3/αX. The orientation of the cDNA in the expression vector was determined by EcoRI digestion. Clones producing a 2.9 kbp restriction fragment were in the correct orientation.

Figure 3.20: Construction of a Full Length Wildtype αL cDNA

A full length wildtype αL cDNA was constructed as summarised in the figure below. A U937 cDNA library, cloned via XbaI into the vector pCDM8 (Stratagene), was screened for clones containing αL cDNA inserts. The 5' end of the αL cDNA (bp 93-933) was amplified by PCR, using the cDNA library as template and the oligonucleotides OL2 and OL3 as primers. A radiolabelled DNA probe was then prepared from this PCR product using the cDNA Multiprime Labelling Kit (Amersham Int.), and this probe was used to screen the U937 cDNA library. A partial αL cDNA clone, αL5', spanning the 5' end of the wildtype αL cDNA (bp 27-2187) was obtained, and was subcloned from the library vector pCDM8 into pBluescript KS(-) via XbaI, creating a clone named pBS/αL5'. The remaining 3' end of the αL cDNA was synthesised by PCR (bp 1899-3649), using a Jurkat cDNA library as template and oligonucleotides L1 (bp 1899-1920) and L2 (bp 3621-3649). For subsequent cloning purposes, oligonucleotide L2 was designed to engineer an EcoRI site (bp 3641-3646, CAGGAT to GAATTC) into the 3' UTR of the αL cDNA. Oligonucleotide L1 was complementary to the wildtype αL cDNA sequence. A full length wildtype αL cDNA was then constructed from the partial αL cDNA clone isolated from the U937 cDNA library and the partial αL cDNA fragment synthesised by PCR, making use of a unique BstEII site in the αL cDNA (bp 1942-1948) and the unique EcoRI site engineered into the 3' end of the αL PCR product (3' UTR, bp 3641-3646): pBS/αL5' was digested with BstEII and EcoRI, and was ligated with the PCR product also digested with BstEII and EcoRI, creating a full length αL cDNA in pBluescript, pBS/αL.

In the figure below, the αL cDNA is represented by the boxed regions, with shaded areas representing the open reading frame (ORF), diagonal lines the DNA adapter derived from the cDNA library, and dashed lines the pBluescript polylinker. Relevant restriction enzyme sites are shown above the αL cDNA, and relevant oligonucleotides are shown below the αL cDNA. The positions of the three sequence discrepancies between the constructed αL cDNA and the published αL cDNA sequence (see main text): (i) bp 2066-2067, TA to AT, (Y689I); (ii) bp 2323-2325, GCA deleted, (Q775 deleted); (iii) bp 2460, G to C, (R820T), are indicated by arrows.

PCR Product used
to make DNA probe

DNA probe used for screening
the U937 cDNA library

Partial αL cDNA clone, αL5',
isolated from U937 cDNA library
and subcloned into pBluescript

Partial αL cDNA amplified by
PCR from a Jurkat cDNA library

Full length αL cDNA clone in
pBluescript, constructed from
αL5' and the PCR product
amplified from Jurkat cDNA
library

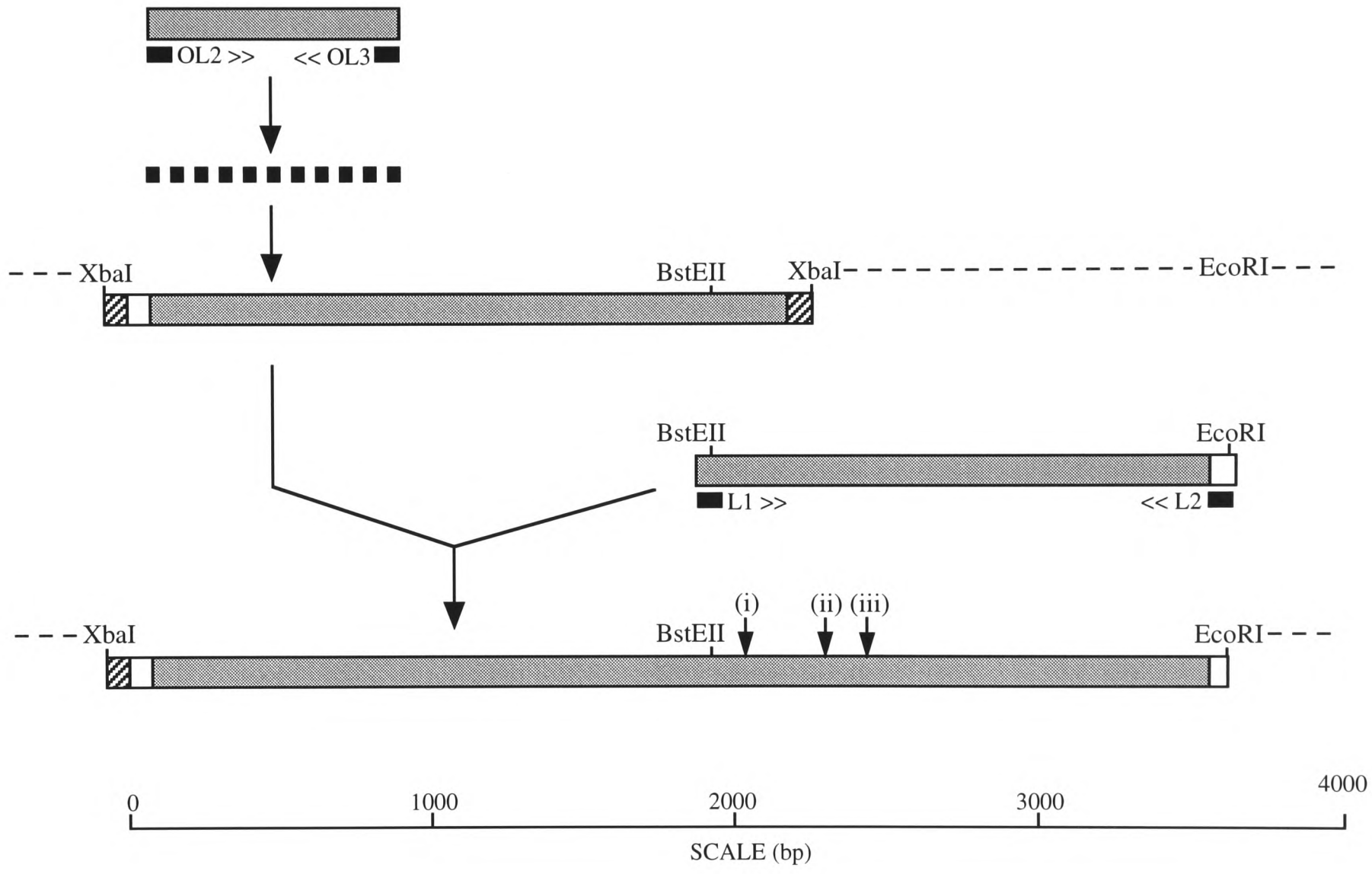


Figure 3.21a: Constructing pSVL/αL

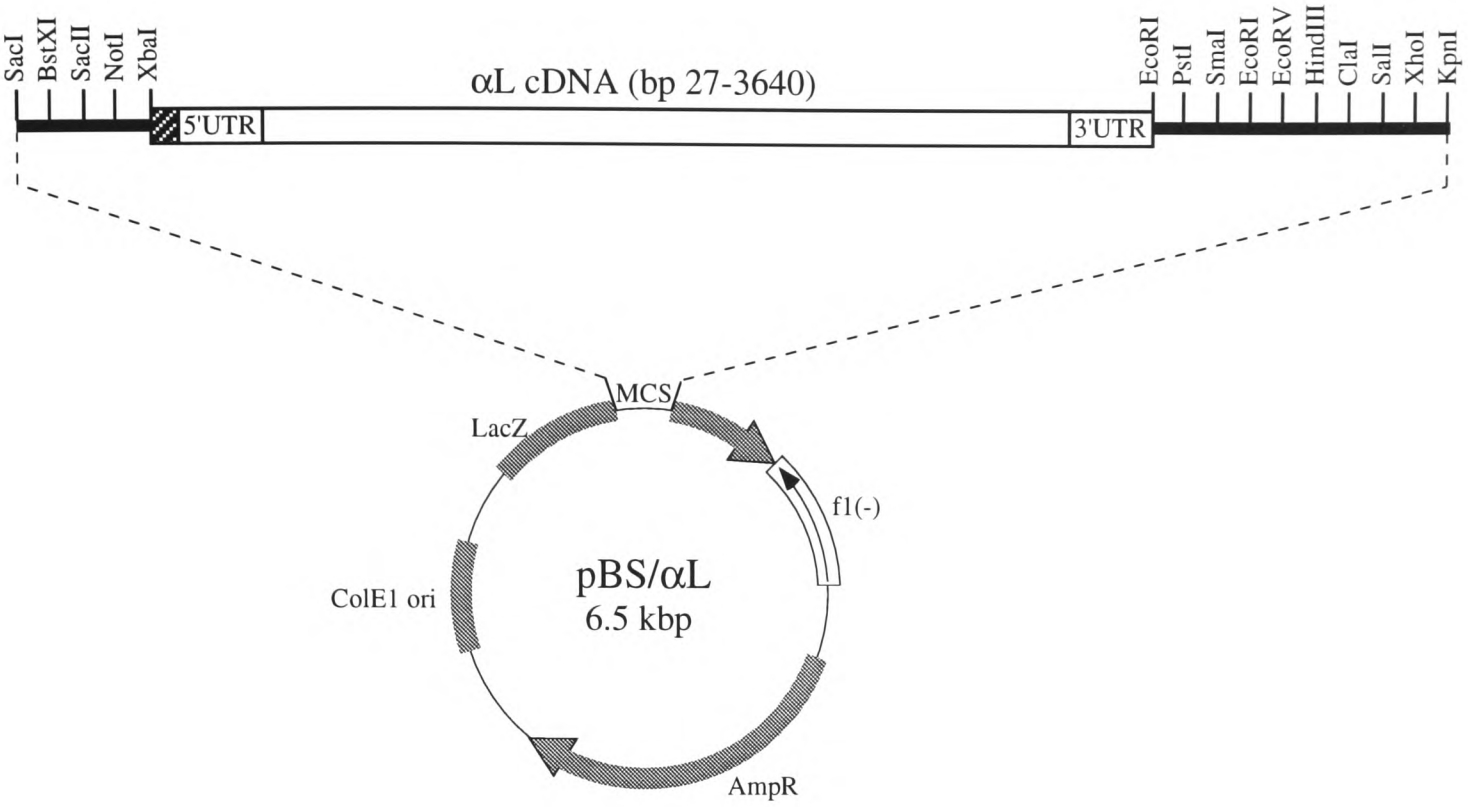
The wildtype αL cDNA was subcloned from pBluescript into the pSVL vector as follows:

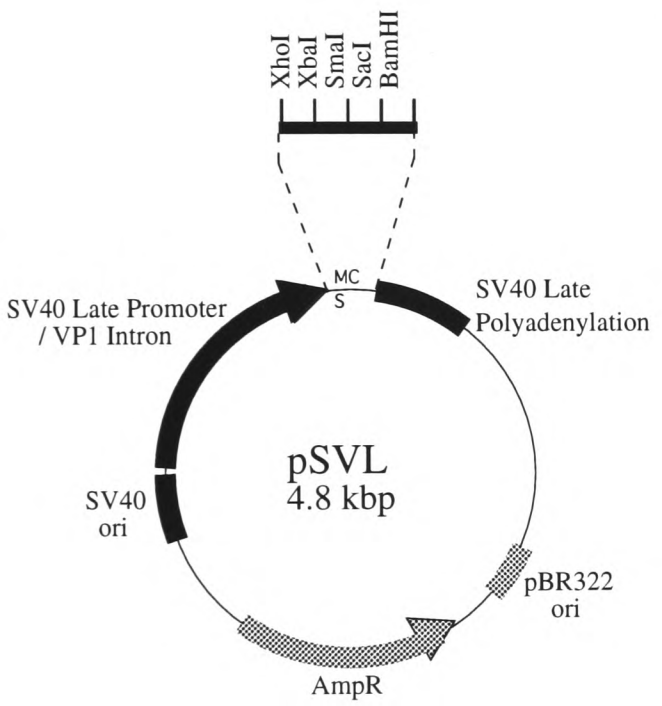
(1) pBS/αL was digested with XbaI (pBS/αL, 5' polylinker) and EcoRV (pBS/αL, 3' polylinker) and the 3.6 kbp αL cDNA insert was purified by agarose gel electrophoresis.

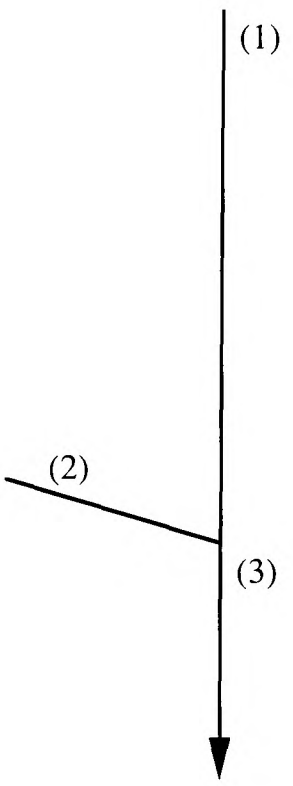
(2) pSVL was digested with XbaI and SmaI, and the 4.8 kbp pSVL vector was also purified by agarose gel electrophoresis.

(3) The pSVL vector and the αL cDNA insert were then ligated, creating a clone named pSVL/αL.

In the figure opposite, the boxed region represents the αL cDNA insert, and the diagonal lines within it represent the DNA adapter derived along with the 5' end of the αL cDNA clone from the U937 cDNA library. The 5' and 3' untranslated regions (UTRs) of the αL cDNA are also shown.


SacI
BstXI
SacII
NotI
XbaI
αL cDNA (bp 27-3640)
5'UTR
3'UTR
EcoRI
PstI
SmaI
EcoRI
EcoRV
HindIII
ClaI
SalI
XhoI
KpnI
MCS
LacZ
f1(-)
pBS/αL
6.5 kbp
ColE1 ori
AmpR


XhoI
XbaI
SmaI
SacI
BamHI
MC
S
SV40 Late Promoter
/ VP1 Intron
SV40 Late
Polyadenylation
pSVL
4.8 kbp
SV40
ori
pBR322
ori
AmpR


(1)
(2)
(3)

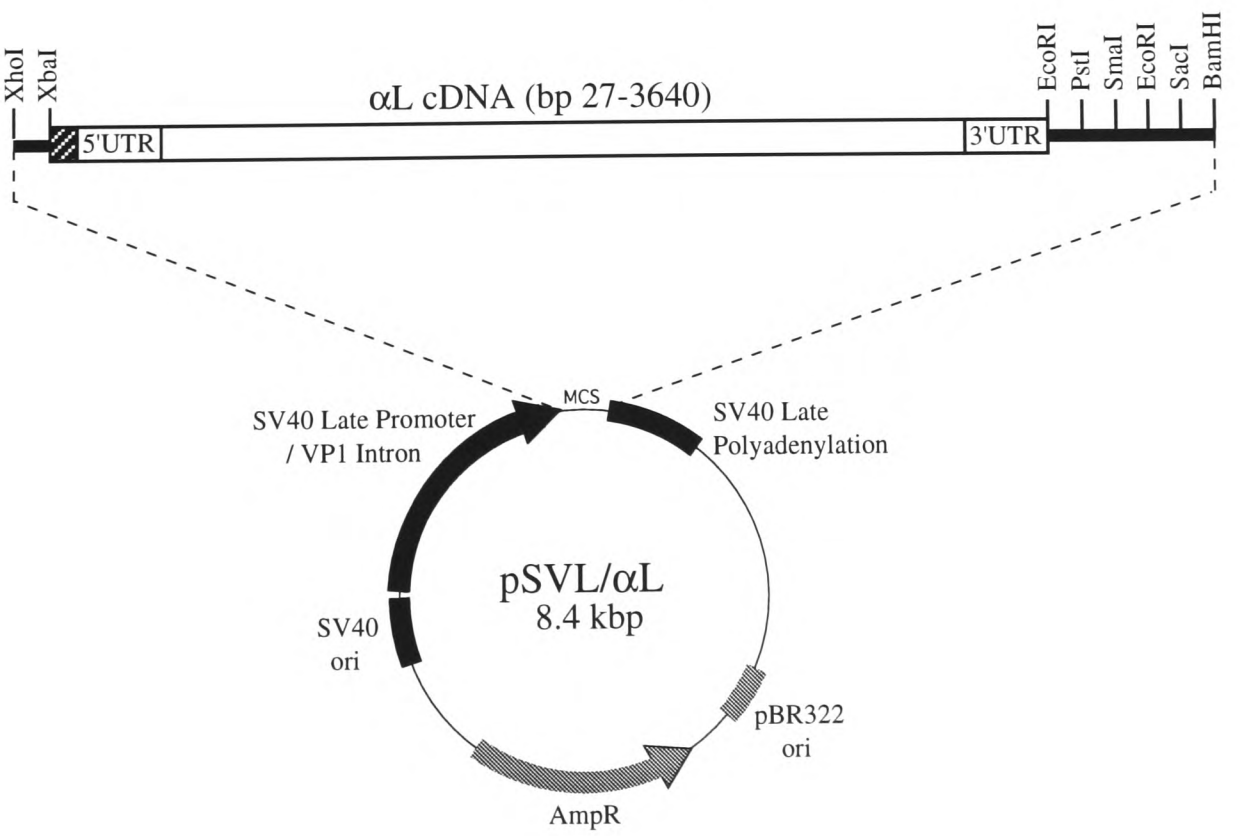

XhoI
XbaI
αL cDNA (bp 27-3640)
5'UTR
3'UTR
EcoRI
PstI
SmaI
EcoRI
SacI
BamHI
MCS
SV40 Late Promoter
/ VP1 Intron
SV40 Late
Polyadenylation
pSVL/αL
8.4 kbp
SV40
ori
pBR322
ori
AmpR

Figure 3.21b: Constructing pcDNA3/αL

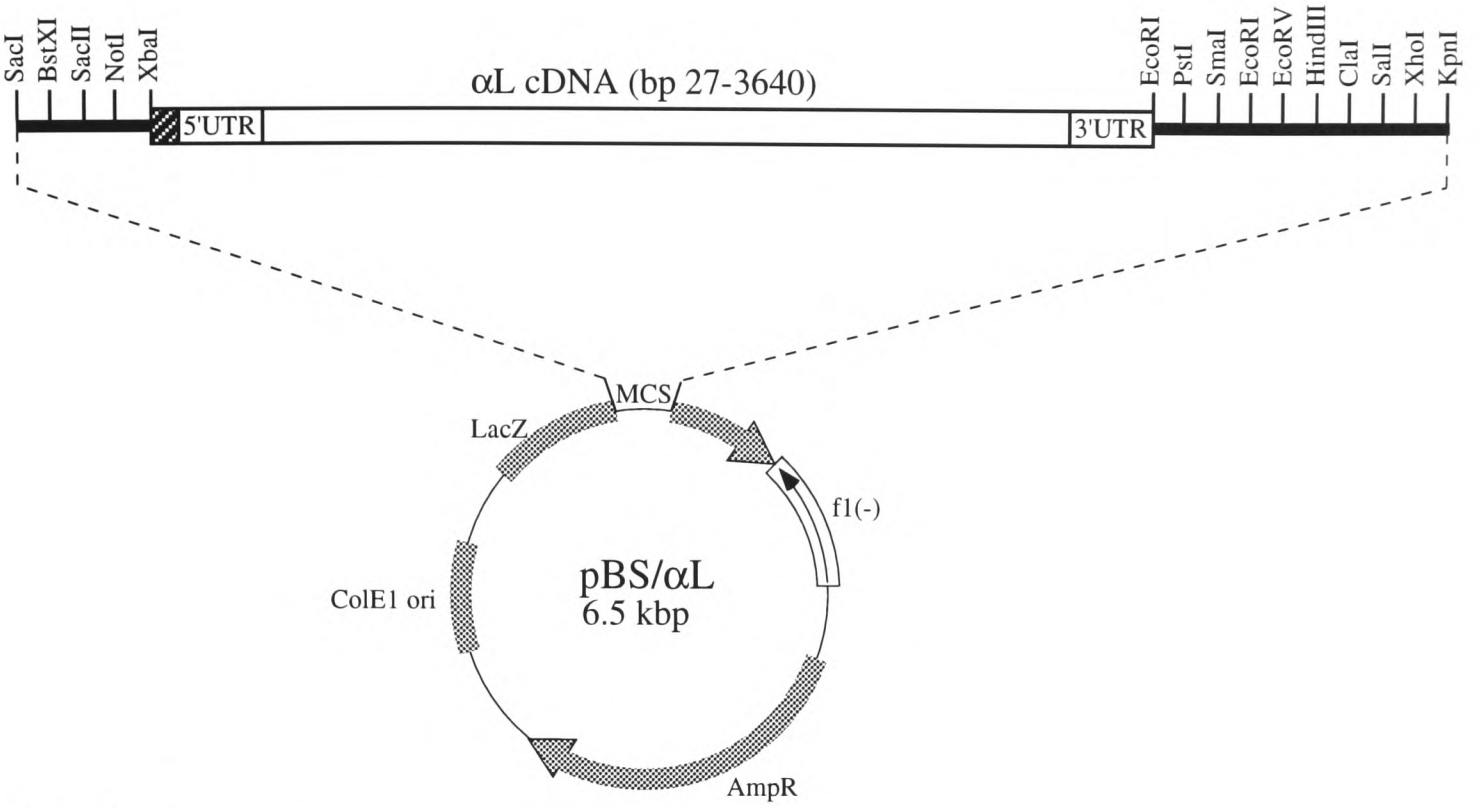
The wildtype αL cDNA was subcloned from pBluescript into the pcDNA3 vector as follows:

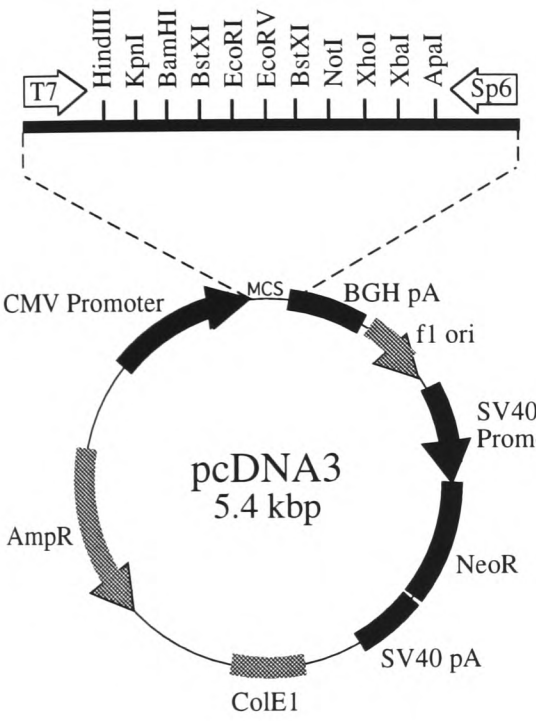
(1) pBS/αL was digested with NotI (pBS/αL, 5' polylinker) and the resultant 5' overhang was blunted using the end-filling reaction. The αL cDNA insert was then excised from pBS/αL by digestion with EcoRV (pBS/αL, 3' polylinker), and the 3.6 kbp αL cDNA insert was purified by agarose gel electrophoresis.

(2) pcDNA3 was digested with EcoRV, and the 5.4 kbp pcDNA3 vector was also purified by agarose gel electrophoresis.

(3) The pcDNA3 vector and the αL cDNA insert were then ligated, creating a clone named pcDNA3/αL. The orientation of the αL cDNA insert in the pcDNA3 vector was determined by BamHI digestion. Clones producing a 3.5 kbp restriction fragment were in the correct orientation.

In the figure opposite, the boxed region represents the αL cDNA insert, and the diagonal lines within it represent the DNA adapter derived along with the 5' end of the αL cDNA clone from the U937 cDNA library. The 5' and 3' untranslated regions (UTRs) of the αL cDNA are also shown.


SacI
BstXI
SacII
NotI
XbaI
αL cDNA (bp 27-3640)
EcoRI
PstI
SmaI
EcoRI
EcoRV
HindIII
ClaI
SalI
XhoI
KpnI
5'UTR
3'UTR
MCS
LacZ
f1(-)
pBS/αL
6.5 kbp
ColE1 ori
AmpR


HindIII
KpnI
BamHI
BstXI
EcoRI
EcoRV
BstXI
NotI
XhoI
XbaI
ApaI
T7
Sp6
MCS
CMV Promoter
BGH pA
f1 ori
SV40 ori/
Promoter
pcDNA3
5.4 kbp
AmpR
NeoR
SV40 pA
ColE1

(1)

(2)

(3)

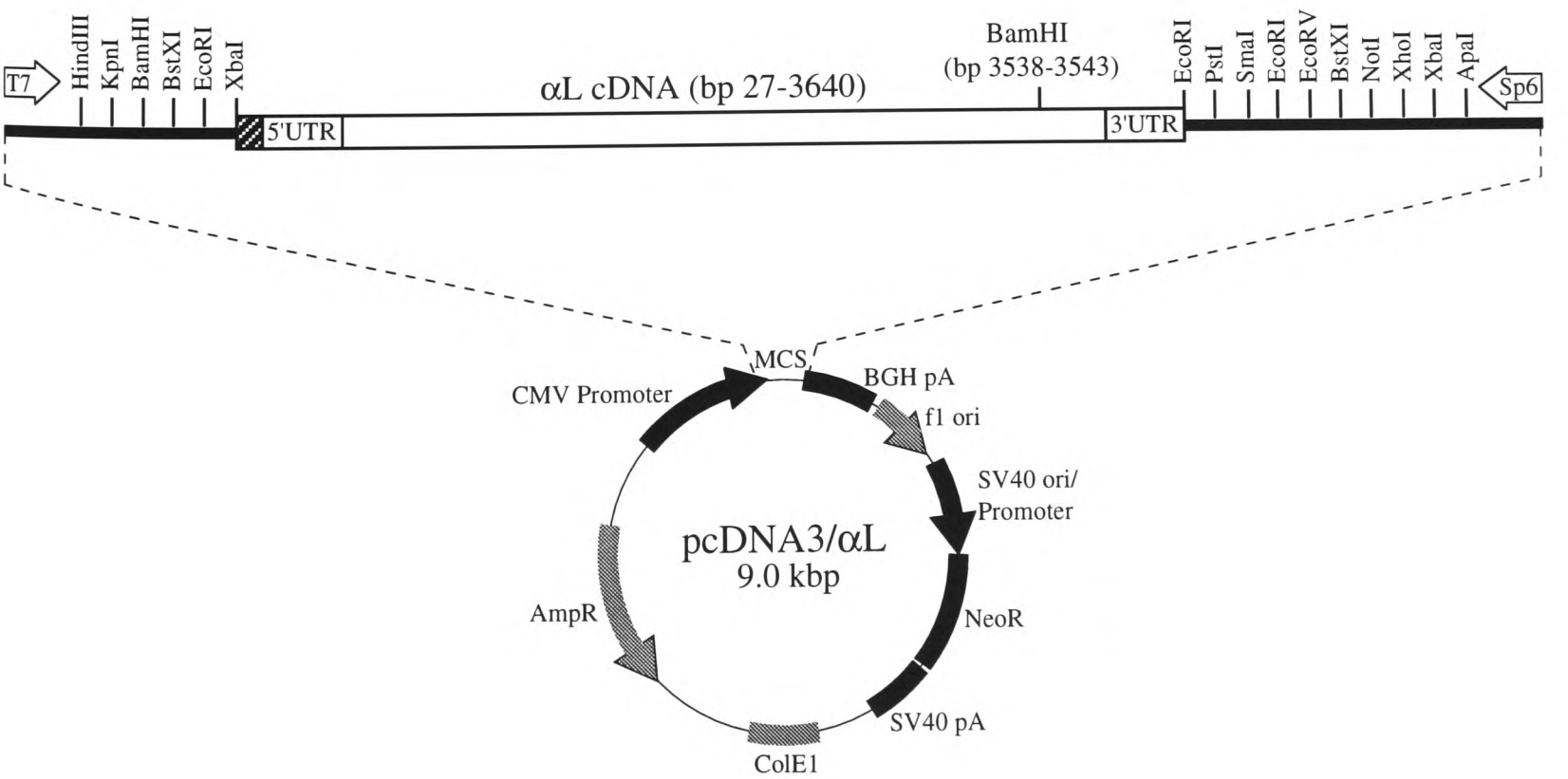

T7
HindIII
KpnI
BamHI
BstXI
EcoRI
XbaI
αL cDNA (bp 27-3640)
BamHI
(bp 3538-3543)
EcoRI
PstI
SmaI
EcoRI
EcoRV
BstXI
NotI
XhoI
XbaI
ApaI
Sp6
5'UTR
3'UTR
MCS
CMV Promoter
BGH pA
f1 ori
SV40 ori/
Promoter
pcDNA3/αL
9.0 kbp
AmpR
NeoR
SV40 pA
ColE1

Figure 3.22a: Constructing pcDNA1/αM

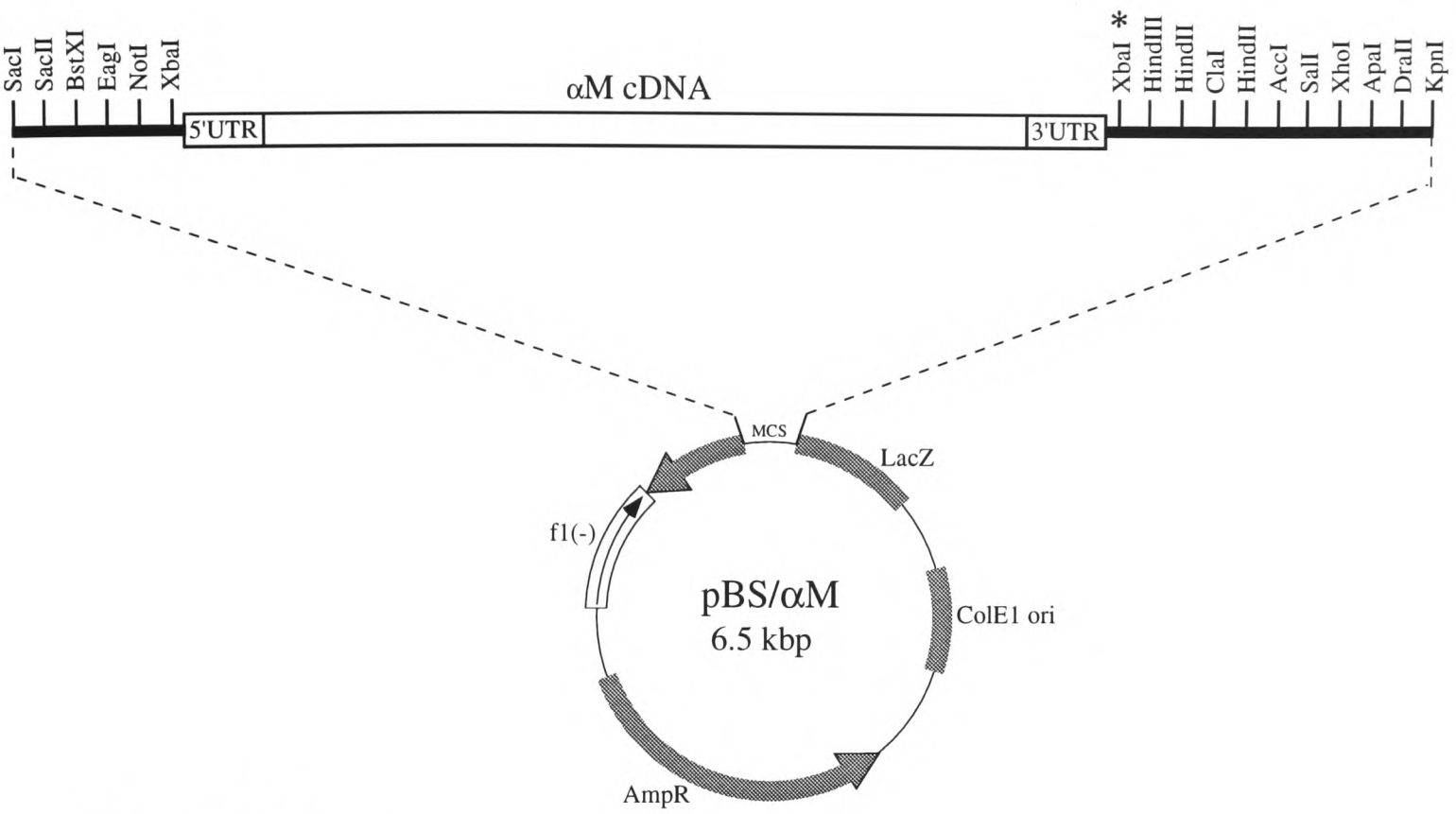
The wildtype αM cDNA was subcloned from pBluescript into the pcDNA1 vector as follows:

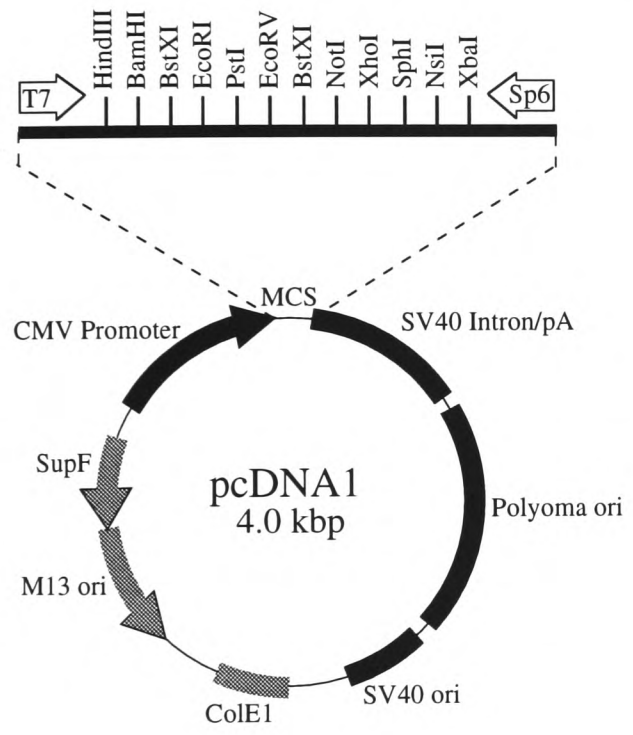
(1) pBS/αM was digested with XbaI (pBS/αM, 5' polylinker) and HindIII (pBS/αM, 3' polylinker) and the resultant 5' overhangs were blunted using the end-filling reaction. The 3.6 kbp αM cDNA insert was then purified by agarose gel electrophoresis.

(2) pcDNA1 was digested with EcoRV, and the 4.0 kbp pcDNA1 vector was also purified by agarose gel electrophoresis.

(3) The pcDNA1 vector and the αM cDNA insert were then ligated, creating a clone named pcDNA1/αM. The orientation of the αM cDNA in the expression vector was determined by BamHI digestion. Clones producing a 7.2 kbp restriction fragment were in the correct orientation.

* Blocked by overlapping Dam methylation


SacI
SacII
BstXI
EagI
NotI
XbaI
αM cDNA
5'UTR
3'UTR
XbaI *
HindIII
HindII
ClaI
HindII
AccI
SalI
XhoI
ApaI
DraII
KpnI
MCS
LacZ
f1(-)
pBS/αM
6.5 kbp
ColE1 ori
AmpR


T7
HindIII
BamHI
BstXI
EcoRI
PstI
EcoRV
BstXI
NotI
XhoI
SphI
NsiI
XbaI
Sp6
MCS
CMV Promoter
SV40 Intron/pA
SupF
pcDNA1
4.0 kbp
Polyoma ori
M13 ori
ColE1
SV40 ori

(1)

(2)

(3)

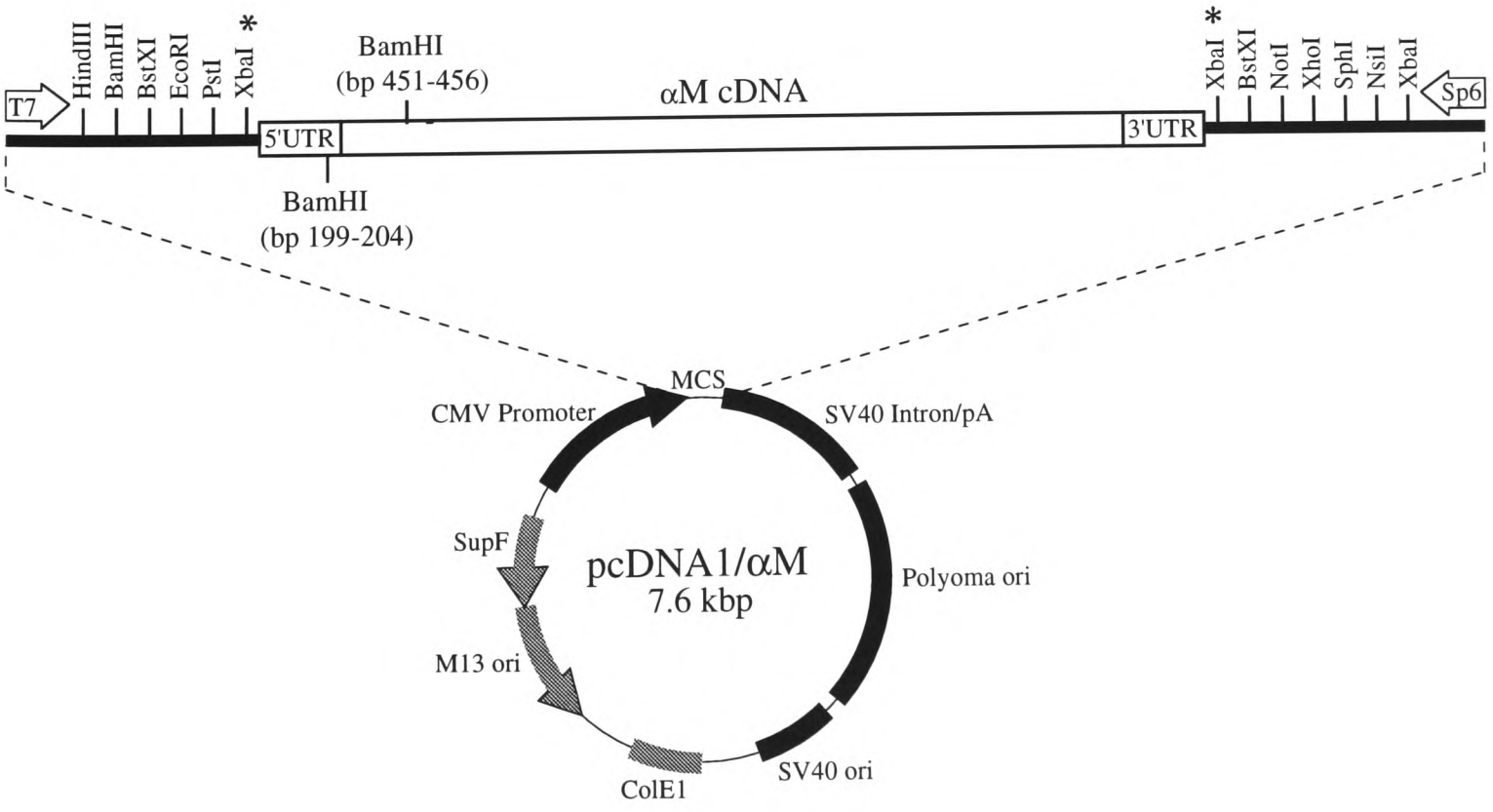

T7
HindIII
BamHI
BstXI
EcoRI
PstI
XbaI *
BamHI
(bp 451-456)
αM cDNA
5'UTR
3'UTR
BamHI
(bp 199-204)
XbaI *
BstXI
NotI
XhoI
SphI
NsiI
XbaI
Sp6
MCS
CMV Promoter
SV40 Intron/pA
SupF
pcDNA1/αM
7.6 kbp
Polyoma ori
M13 ori
ColE1
SV40 ori

Figure 3.22b: Constructing pSVL/αM

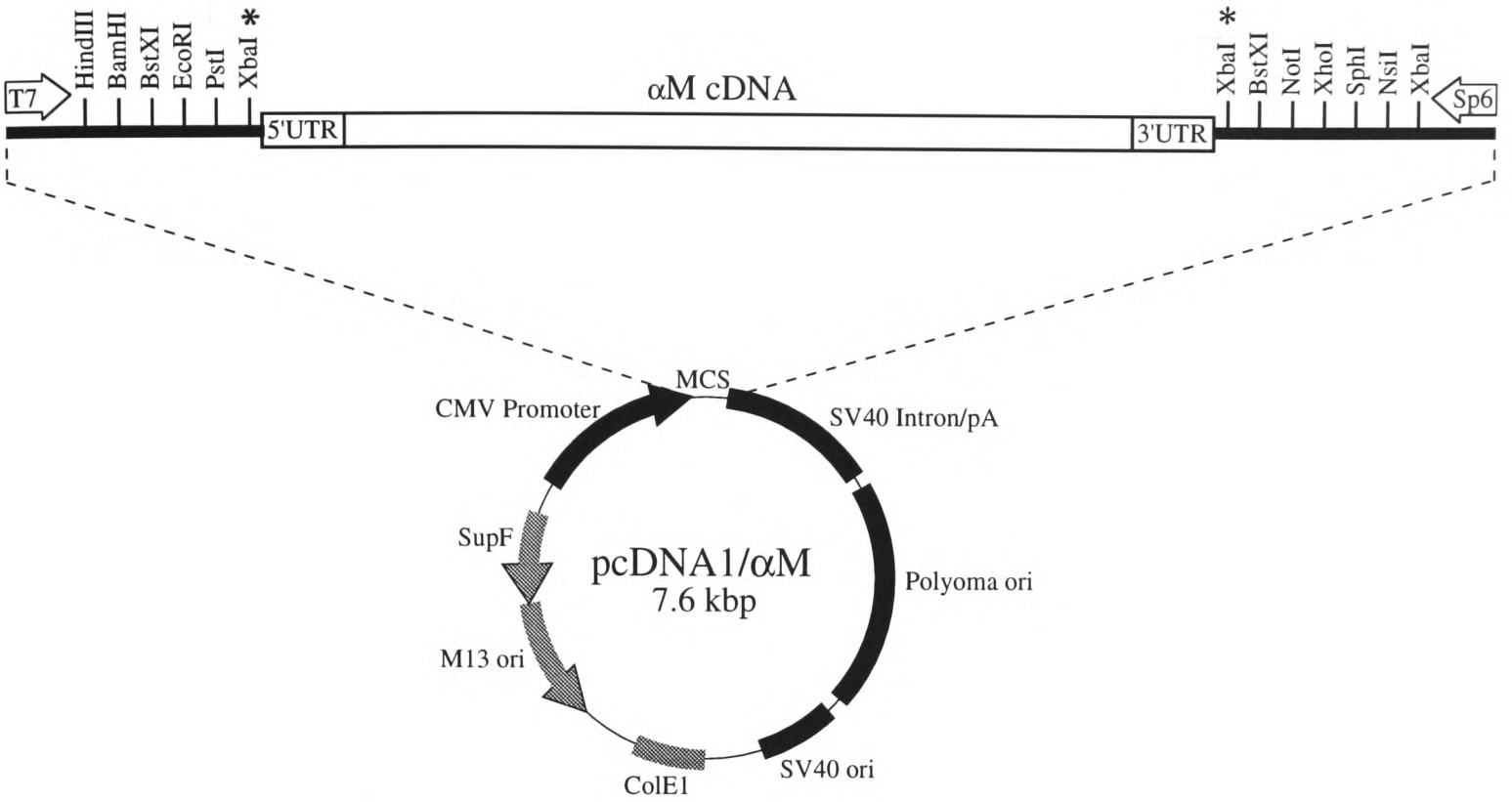
The wildtype αM cDNA was subcloned from pcDNA1 into the pSVL vector as follows:

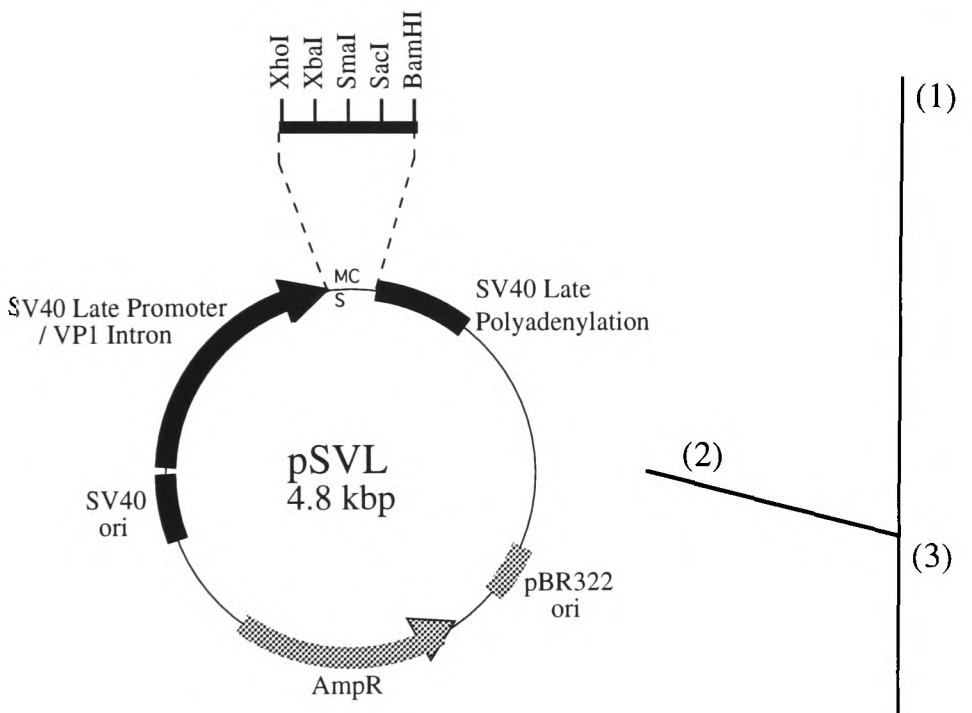
(1) pcDNA1/αM was digested with HindIII (pcDNA1/αM, 5' polylinker) and the resultant 5' overhang was blunted using the end-filling reaction. The αM cDNA insert was then excised from the pcDNA1 vector by digestion with XbaI (pcDNA1/αM, 3' polylinker), and was purified by agarose gel electrophoresis.

(2) The pSVL vector was digested with XhoI and the resultant 5' overhang was blunted, using the end-filling reaction, before digestion with XbaI. The pSVL vector was also purified by agarose gel electrophoresis.

(3) The pSVL vector and the αM cDNA insert were then ligated, creating a clone named pSVL/αM.

* Blocked by overlapping Dam methylation


T7
HindIII
BamHI
BstXI
EcoRI
PstI
XbaI *
αM cDNA
5'UTR
3'UTR
XbaI *
BstXI
NotI
XhoI
SphI
NsiI
XbaI
Sp6
MCS
CMV Promoter
SV40 Intron/pA
SupF
pcDNA1/αM
7.6 kbp
Polyoma ori
M13 ori
ColE1
SV40 ori


XhoI
XbaI
SmaI
SacI
BamHI
MC
S
SV40 Late Promoter
/ VP1 Intron
SV40 Late
Polyadenylation
pSVL
4.8 kbp
SV40
ori
pBR322
ori
AmpR

(1)

(2)

(3)

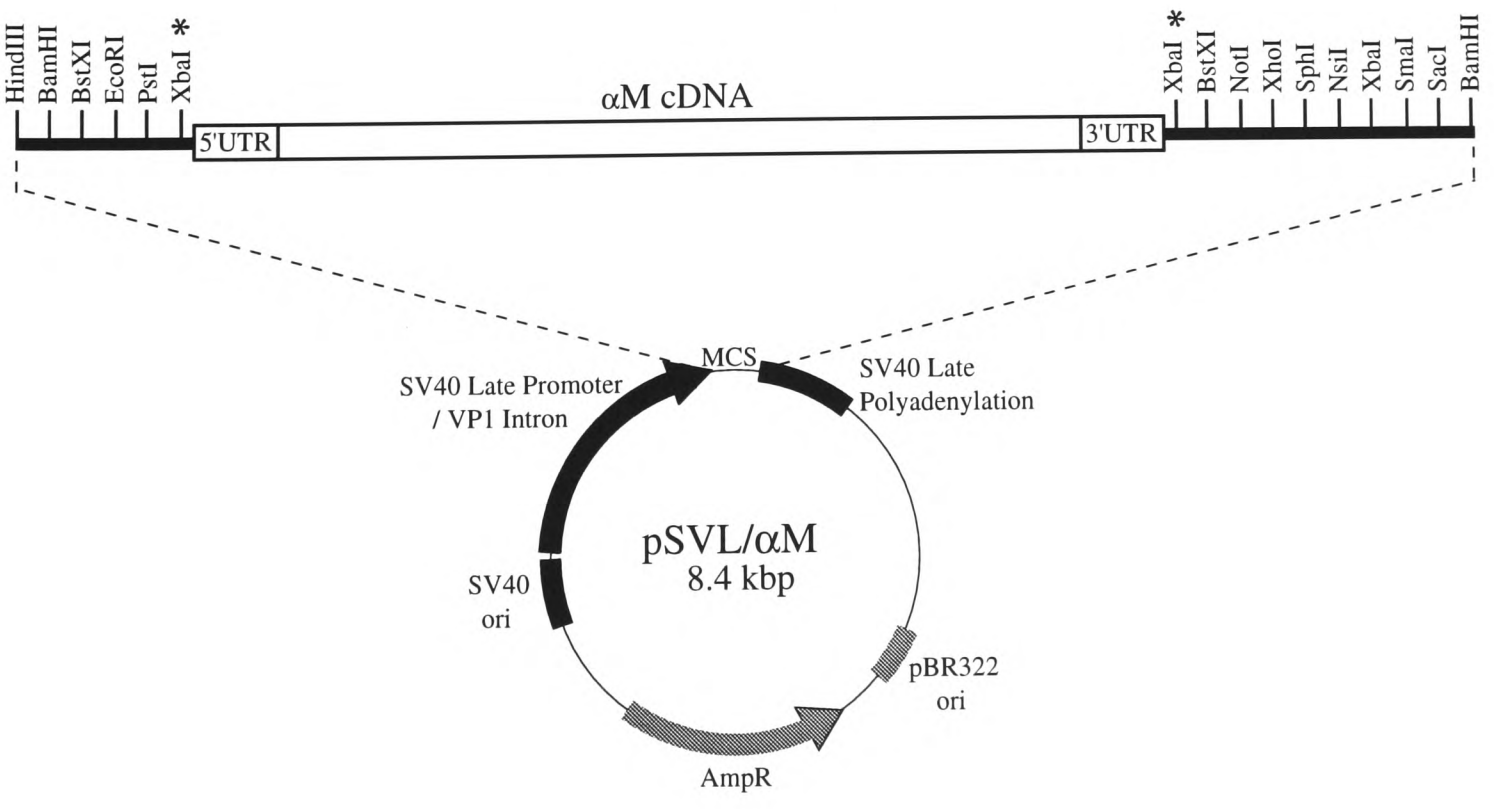

HindIII
BamHI
BstXI
EcoRI
PstI
XbaI *
αM cDNA
5'UTR
3'UTR
XbaI *
BstXI
NotI
XhoI
SphI
NsiI
XbaI
SmaI
SacI
BamHI
MCS
SV40 Late Promoter
/ VP1 Intron
SV40 Late
Polyadenylation
pSVL/αM
8.4 kbp
SV40
ori
pBR322
ori
AmpR

Figure 3.22c: Constructing pcDNA3/αM

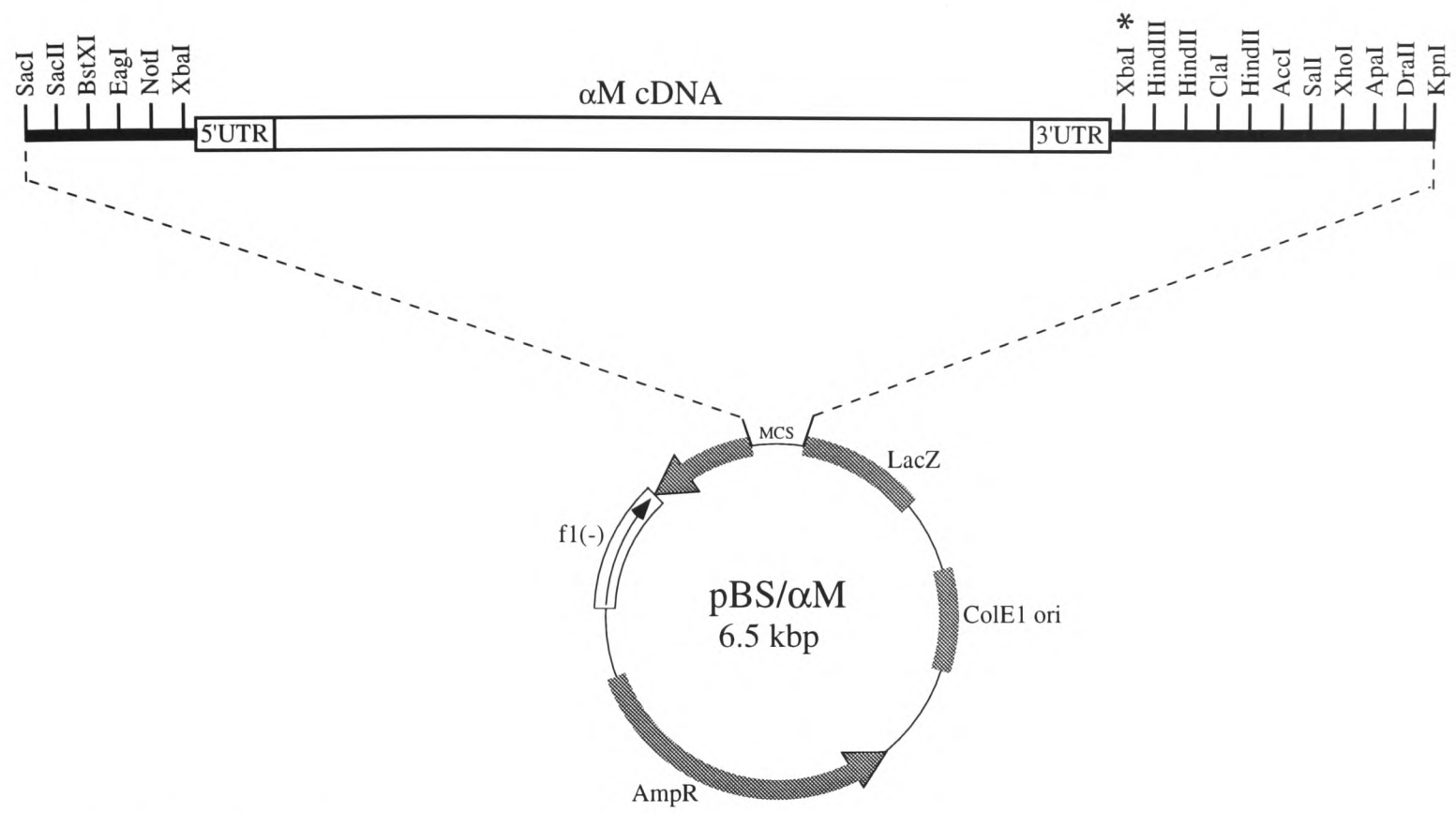
The wildtype αM cDNA was subcloned from pBluescript into the pcDNA3 vector as follows:

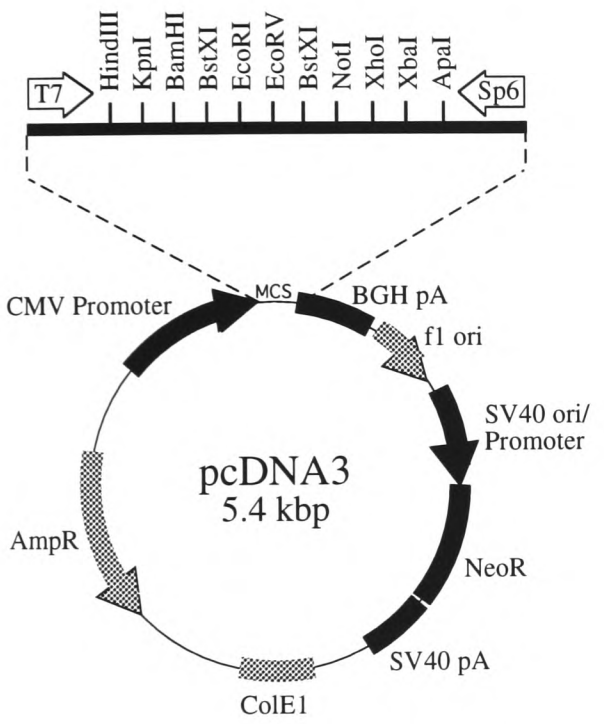
(1) pBS/αM was digested with XbaI (pBS/αM, 5' polylinker) and HindIII (pBS/αM, 3' polylinker), and the resultant 5' overhangs were blunted using the end-filling reaction. The 3.6 kbp αM cDNA insert was then purified by agarose gel electrophoresis.

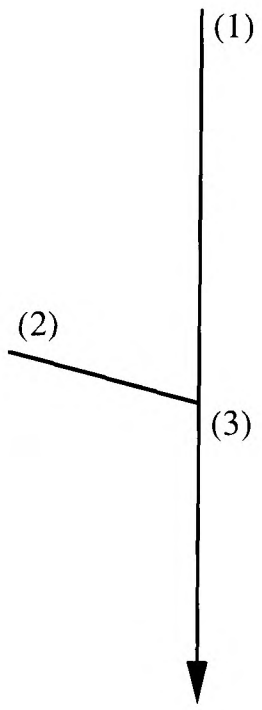
(2) pcDNA3 was digested with EcoRV, and the 5.4 kbp pcDNA3 vector was also purified by agarose gel electrophoresis.

(3) The pcDNA3 vector and the αM cDNA insert were then ligated, creating a clone named pcDNA3/αM. The orientation of the αM cDNA in the expression vector was determined by BamHI digestion. Clones producing an 8.5 kbp restriction fragment were in the correct orientation.

* Blocked by overlapping Dam methylation


SacI
SacII
BstXI
EagI
NotI
XbaI
αM cDNA
5'UTR
3'UTR
XbaI *
HindIII
HindII
ClaI
HindII
AccI
SalI
XhoI
ApaI
DraII
KpnI
MCS
LacZ
f1(-)
pBS/αM
6.5 kbp
ColE1 ori
AmpR


T7
HindIII
KpnI
BamHI
BstXI
EcoRI
EcoRV
BstXI
NotI
XhoI
XbaI
ApaI
Sp6
MCS
CMV Promoter
BGH pA
f1 ori
SV40 ori/
Promoter
pcDNA3
5.4 kbp
AmpR
NeoR
SV40 pA
ColE1


(1)
(2)
(3)

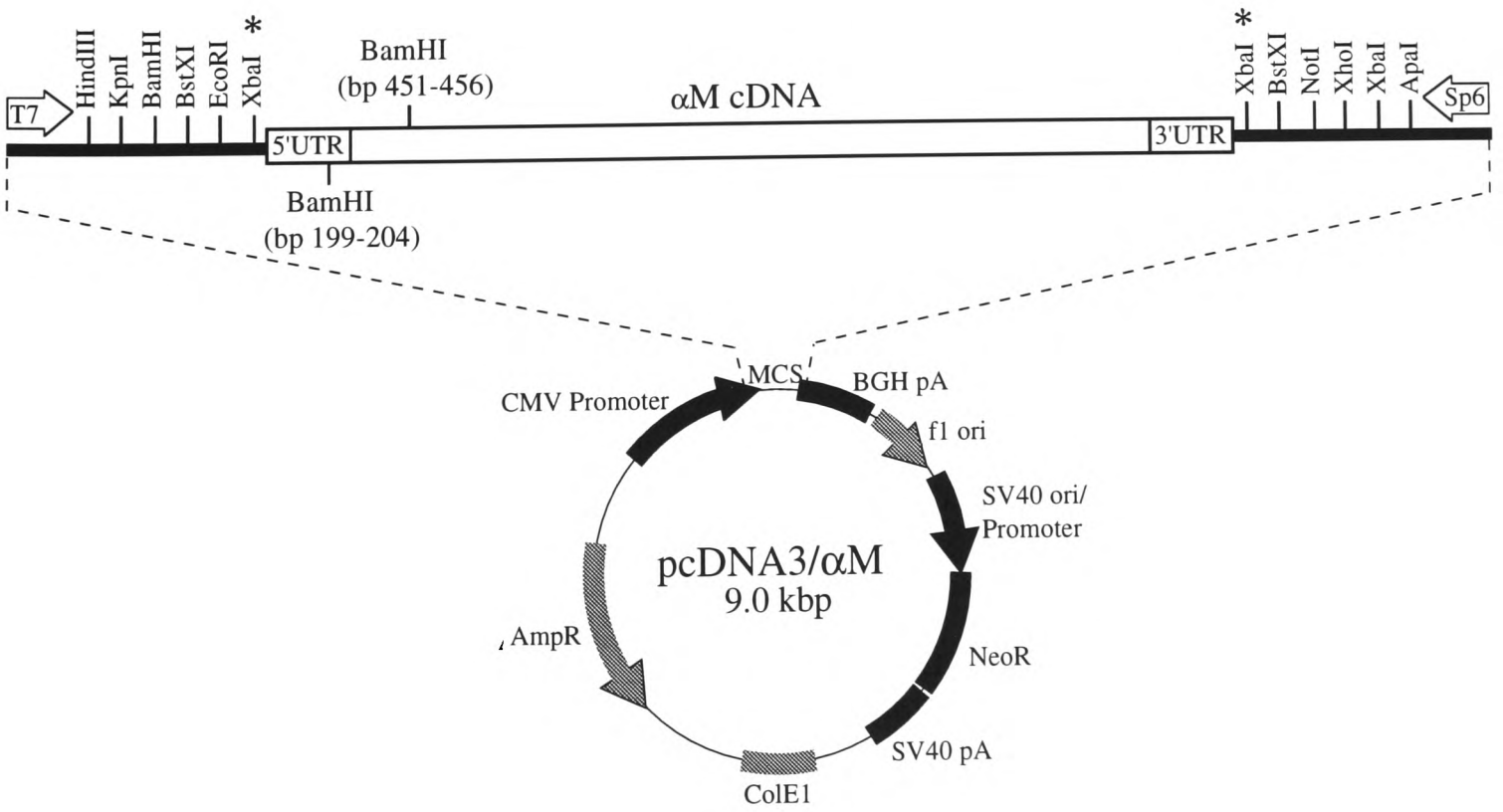

T7
HindIII
KpnI
BamHI
BstXI
EcoRI
XbaI *
BamHI
(bp 451-456)
BamHI
(bp 199-204)
αM cDNA
5'UTR
3'UTR
XbaI *
BstXI
NotI
XhoI
XbaI
ApaI
Sp6
MCS
CMV Promoter
BGH pA
f1 ori
SV40 ori/
Promoter
pcDNA3/αM
9.0 kbp
AmpR
NeoR
SV40 pA
ColE1

Figure 3.23a: Constructing pSVL/αX

The wildtype αX cDNA was subcloned from pEE6.hCMV.BglII.Neo into the pSVL expression vector as follows:

(1) pEE6.hCMV.BglII.Neo/αX was digested with HindIII, and the resultant 5' overhangs were partially end-filled using only the dATP and dGTP nucleotides. The 3.6 kbp αX cDNA insert was then purified by agarose gel electrophoresis.

(2) The pSVL vector was digested with XbaI, and the resultant 5' overhangs were also partially end-filled, using only the dCTP and dTTP nucleotides, so that the resulting two base pair 5' overhangs in the αX cDNA insert and the resulting 2 base pair 5' overhangs in the pSVL vector were compatible. The pSVL vector was also purified by agarose gel electrophoresis.

(3) The pSVL vector and the αX cDNA insert were then ligated, creating a clone named pSVL/αX. The orientation of the cDNA in the expression vector was determined by EcoRI digestion. Clones producing a 2.6 kbp restriction fragment were in the correct orientation.

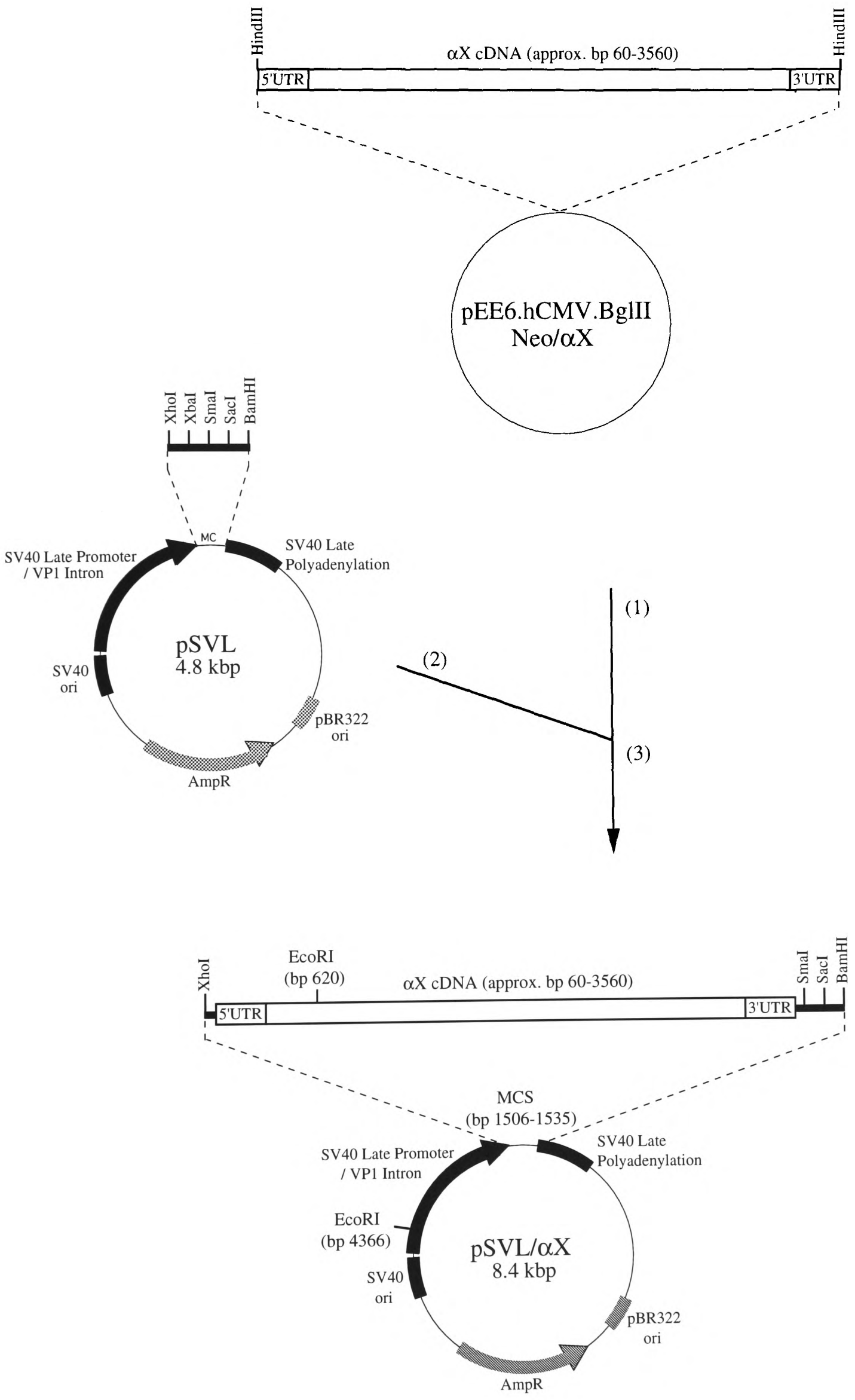

HindIII
αX cDNA (approx. bp 60-3560)
HindIII
5'UTR
3'UTR
pEE6.hCMV.BglII
Neo/αX
XhoI
XbaI
SmaI
SacI
BamHI
MC
SV40 Late Promoter
/ VP1 Intron
SV40 Late
Polyadenylation
pSVL
4.8 kbp
SV40
ori
pBR322
ori
AmpR
(1)
(2)
(3)
XhoI
EcoRI
(bp 620)
αX cDNA (approx. bp 60-3560)
SmaI
SacI
BamHI
5'UTR
3'UTR
MCS
(bp 1506-1535)
SV40 Late Promoter
/ VP1 Intron
SV40 Late
Polyadenylation
EcoRI
(bp 4366)
pSVL/αX
8.4 kbp
SV40
ori
pBR322
ori
AmpR

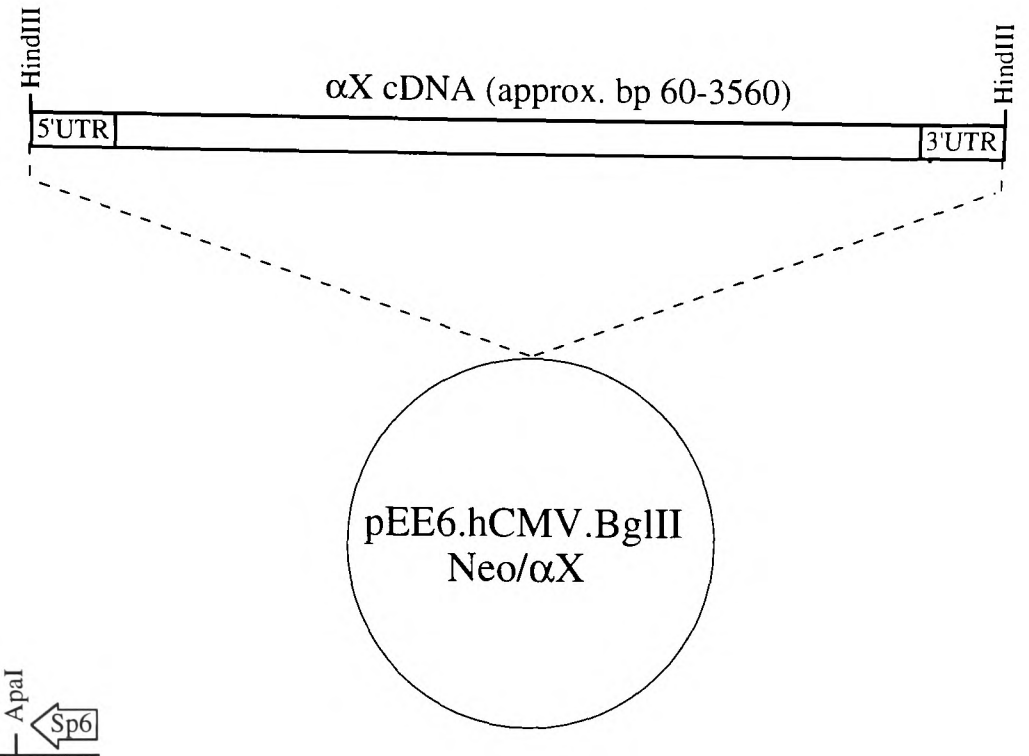
Figure 3.23b: Constructing pcDNA3/αX

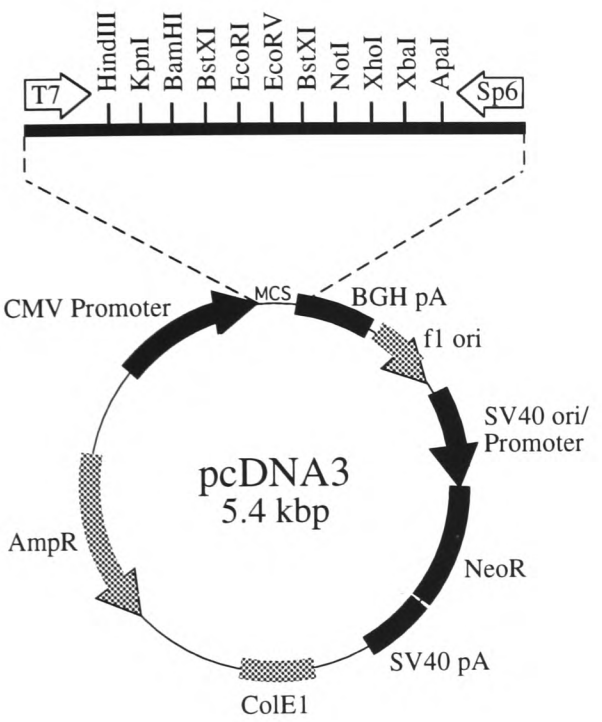
The wildtype αX cDNA was subcloned from pEE6.hCMV.BglII.Neo into the pcDNA3 expression vector as follows:

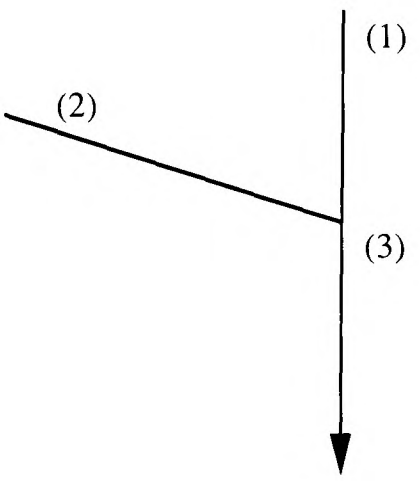
(1) pEE6.hCMV.BglII.Neo/αX was digested with HindIII, and the 3.6 kbp αX cDNA insert was purified by agarose gel electrophoresis.

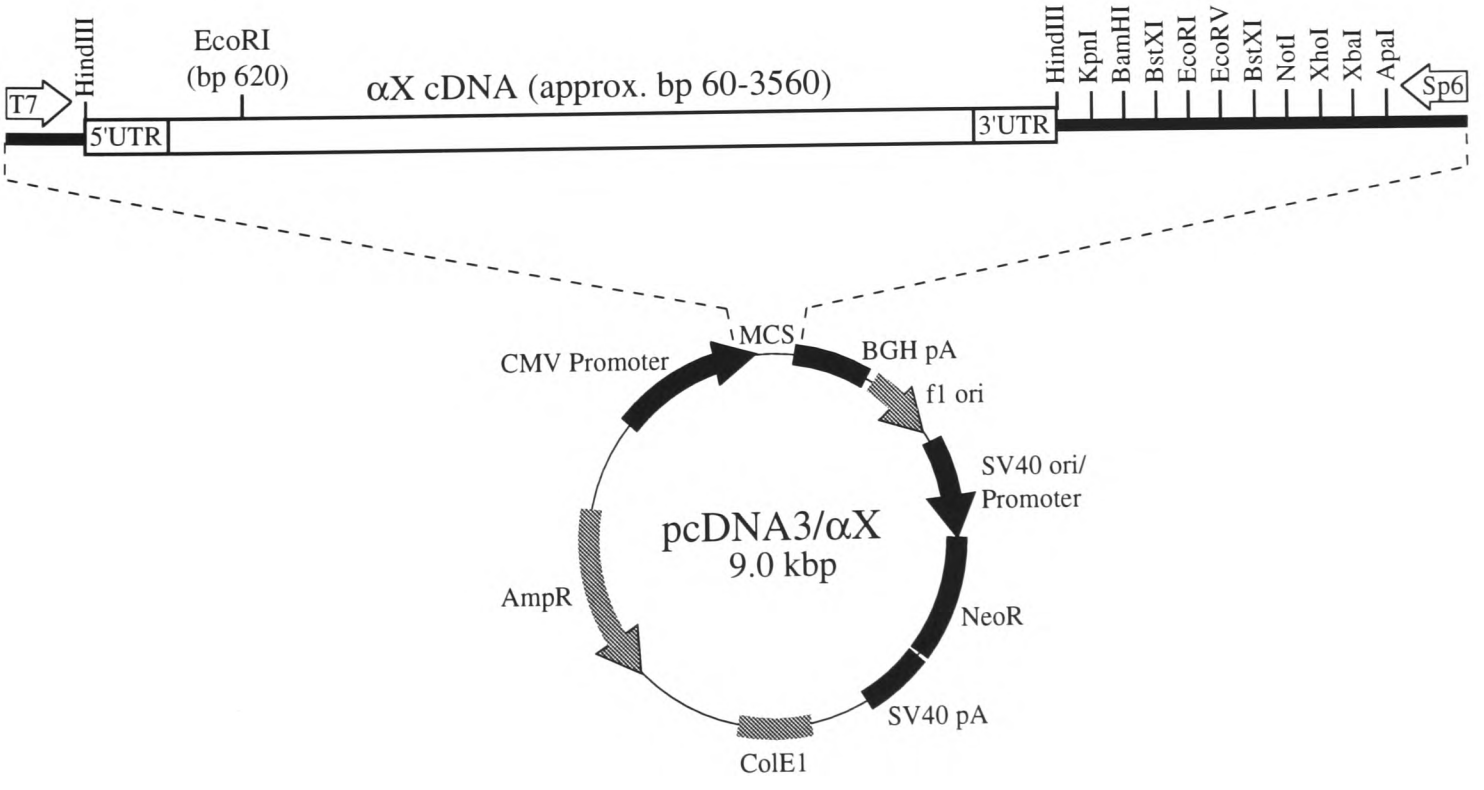
(2) The pcDNA3 vector was also digested with HindIII, and the 5.4 kbp pcDNA3 vector was purified by agarose gel electrophoresis.

(3) The pcDNA3 vector and the αX cDNA insert were then ligated, creating a clone named pcDNA3/αX. The orientation of the cDNA in the expression vector was determined by EcoRI digestion. Clones producing a 2.9 kbp restriction fragment were in the correct orientation.


HindIII
αX cDNA (approx. bp 60-3560)
HindIII
5'UTR
3'UTR
pEE6.hCMV.BglII
Neo/αX


T7
HindIII
KpnI
BamHI
BstXI
EcoRI
EcoRV
BstXI
NotI
XhoI
XbaI
ApaI
Sp6
MCS
CMV Promoter
BGH pA
f1 ori
SV40 ori/
Promoter
pcDNA3
5.4 kbp
AmpR
NeoR
SV40 pA
ColE1


(1)
(2)
(3)


T7
HindIII
EcoRI
(bp 620)
αX cDNA (approx. bp 60-3560)
HindIII
KpnI
BamHI
BstXI
EcoRI
EcoRV
BstXI
NotI
XhoI
XbaI
ApaI
Sp6
5'UTR
3'UTR
MCS
CMV Promoter
BGH pA
f1 ori
SV40 ori/
Promoter
pcDNA3/αX
9.0 kbp
AmpR
NeoR
SV40 pA
ColE1

3.3 SUMMARY

This chapter described the construction of a series of chimeric, soluble and truncated β2 cDNA variants and their cloning into suitable expression vectors for subsequent transient expression studies in COS 7 cells. Three β2/β1 chimeric cDNAs: β2V1, β2V12 and β2NS1, and three β2/β7 chimeric cDNAs: β2V7, β2V72 and β2NS7, as well as a soluble: β2sol, and a truncated: β2tr, cDNA were constructed, which encode the variant β2 subunits shown in Figure 3.1. A full length wildtype β2 cDNA was also obtained and was cloned into the same expression vectors. The construction of the various cDNA clones was rather convoluted. The initial plan was to clone the β cDNAs into the pKG4 vector (Gould, G.K. personal communication) for transfection by electroporation into EBV transformed cell lines derived from LAD patients, which express the αL subunit. However, the LAD cell lines were difficult to maintain in cell culture, and the transfections were unsuccessful. It was therefore decided to express constructs in COS 7 cells rather than the EBV-transformed B cells from LAD patients. As COS 7 cells do not express any of the leukocyte integrin subunits, cotransfection of a wildtype αL, αM, or αX construct with a β2 construct was required to produce LFA-1, Mac-1 and p150,95 heterodimers. Therefore, the construction of full length wildtype α cDNAs, and their cloning into suitable expression vectors, was also described in this chapter. The α and β cDNAs were initially cloned into the pSVL vector (Pharmacia), designed for transient expression in COS cell lines, because the full length αL cDNA from Dr. G. Otulakowski (R.W. Johnson PRI, Canada), which was the first α cDNA obtained, was cloned into this particular vector. However, it was later found that the cell surface expression levels achieved with this vector were very low, and a large amount of cell death also occured during the transfection process. The pSVL vector is a low copy number plasmid, and hence very large volumes of bacterial cultures were required to prepare sufficient DNA for transfections. As plasmid DNA prepared in this way is frequently contaminated with bacterial endotoxin, it is possible that high endotoxin levels within the DNA preps were toxic to the COS cells. Subsequent transfection experiments showed that much higher expression levels were obtained by cloning the α and β cDNAs into the pcDNA1 vector (Invitrogen), and later into its updated counter-part pcDNA3 (Invitrogen), and that cell death was also reduced using these vectors. As both pcDNA1 and pcDNA3 are high copy number plasmids, it is possible that the contaminating bacterial endotoxin levels in these DNA preps was within the tolerance limit of COS cells.

The majority of the cDNAs were therefore subcloned into the pcDNA3 vector, and the transfections were repeated using this vector to obtain clearer and more reproducible results. The results obtained with these transfectants are described in Chapter 4.

CHAPTER FOUR

THE EXPRESSION OF VARIANT β2 SUBUNITS IN COS 7 CELLS AND THE FORMATION OF MODIFIED LFA-1, MAC-1 AND p150,95 HETERODIMERS

4.1 INTRODUCTION

This chapter describes the analysis of eight variant β2 subunits and their ability to form modified LFA-1 (αLβ2), Mac-1 (αMβ2) and p150,95 (αXβ2) heterodimers with the wildtype αL, αM and αX subunits. Three β2/β1 chimeras: β2V1, β2V12 and β2NS1, three β2/β7 chimeras: β2V7, β2V72 and β2NS7, and a soluble and a truncated β2 subunit: β2sol and β2tr, were studied. In the β2V1 and β2V7 chimeras, the C-terminal cysteine-rich, membrane proximal, transmembrane and cytoplasmic domains of β2 are replaced with the homologous regions from β1 and β7 respectively, whereas in the β2V12 and β2V72 chimeras, only the C-terminal cysteine-rich and membrane proximal regions are substituted, and in the β2NS1 and β2NS7 chimeras only part of the C-terminal cysteine-rich region is substituted with the homologous regions from β1 and β7. The β2sol subunit (amino acids 1-698) consists of the entire extracellular region of β2, whereas the β2tr subunit (amino acids 1-480) is a β2 subunit truncated just after the beginning of the C-terminal cysteine-rich region. The chimeric, soluble and truncated β2 variants are illustrated in Chapter 3, Figure 3.1.

The ability of these variant β2 subunits to form functional LFA-1, Mac-1 and p150,95 heterodimeric complexes was analysed in a COS cell based transient expression system (Edwards and Aruffo, 1993). COS cells are SV40 transformed monkey fibroblastic cell lines which constitutively express the SV40 large T antigen. When COS cells are transfected with plasmids containing an SV40 origin of replication (SV40 *ori*), the SV40 large T antigen binds to the SV40 *ori* and initiates replication of the plasmid using COS cell DNA polymerases. Various expression vectors have been designed for transient expression in COS cells. In addition to an SV40 ori, these vectors contain prokaryotic origins of DNA replication and prokaryotic selectable markers for plasmid amplification in bacteria, and enhancer, promoter and polyadenylation sequences for efficient eukaryotic gene expression. Maximal replication of these plasmids in COS cells (~1000 fold) is generally achieved 48 h after transfection, with maximal protein synthesis occuring between 48-72 h post-transfection. COS expression systems can routinely produce > 10^5 copies per cell of a cell surface or intracellular protein, and up to 1 μg/ml of a secreted protein. The use of a COS based system for the expression of integrin receptors was first reported by Springer *et al* (1990): cotransfection of COS cells with wildtype LFA-1 α and

β constructs, or wildtype Mac-1 α and β constructs, resulted in the efficient expression of heterodimeric LFA-1 and Mac-1 on the COS cell surface, and the LFA-1 heterodimers were functional as they retained to ability to bind to ICAM-1. COS cell expression is now routinely used by many laboratories to analyse the effect of various mutations on the expression and function of different integrin receptors, and is often used as a method of quickly evaluating the effect of such mutations prior to the incorporation of constructs into stable cell lines. The COS expression system is particularly suitable for analysing the expression of the β2 integrins as untransfected COS cells do not express the αL, αM, αX, αD or β2 subunits.

In the previous chapter, the construction of cDNAs encoding the chimeric, soluble and truncated β2 variants, as well as the construction of cDNAs encoding the wildtype αL, αM, αX and β2 subunits, and the cloning of these cDNAs into the expression vectors pSVL (Pharmacia) and/or pcDNA3 (Invitrogen), was described. Both of these vectors are designed for high level expression in COS cell lines. The pSVL vector uses the SV40 late promoter and SV40 late polyadenylation signal for the transcription of cDNA inserts and the processing of the resultant mRNAs, whereas the pcDNA3 vector uses the human cytomegalovirus (CMV) promotor and the bovine growth hormone (BGH) polyadenylation signal. This chapter describes the results obtained when COS cells were transfected with either the pSVL or the pcDNA3 expression constructs. The effect of the various β2 subunit modifications on the formation of cell surface expressable LFA-1, Mac-1 and p150,95, as well as their effect on the ability of the LFA-1 receptor to bind to its ligand ICAM-1, are examined. The mapping of a number of anti-β2 monoclonal antibody epitopes using the chimeric β2/β7 subunits is also described.

4.2 RESULTS

4.2.1 EXPRESSION OF WILDTYPE AND MODIFIED LFA-1, Mac-1 AND p150,95 IN COS 7 CELLS

The cDNAs of the wildtype and modified leukocyte integrin α and β subunits were cloned into either the pSVL or pcDNA3 expression vectors (see Chapter 3) and were transfected into COS 7 cells using the DEAE-dextran method (see Chapter 2, Section 2.2.10). Cells were transfected with either an α or a β subunit alone, or were cotransfected with equal amounts of an α and a β subunit. The cells were harvested 48-72 h after transfection and the expression of the transfected subunits on the cell surface was analysed by flow cytometry (see Section 2.2.11.2) and immunoprecipitation (see Section 2.2.11.3) using the mAbs listed in Table 4.1.

4.2.1.1 Expression of Wildtype LFA-1, Mac-1 and p150,95

4.2.1.1.1 Expression of the Wildtype αL, αM and αX Subunits

The expression of the wildtype αL, αM and αX subunits was characterised using the mAbs MHM24, LPM19C and KB23. COS 7 cells were transfected with each wildtype α subunit alone, or were cotransfected with the αL and β2, αM and β2, or αX and β2 subunits, and the resulting cell surface expression was analysed by flow cytometry and immunoprecipitation. Mock transfected cells, and cells transfected with β2 alone, were also included as controls. The flow cytometry results obtained are shown in Figure 4.1a. Mock transfected cells and cells transfected with β2 alone did not express the MHM24, LPM19C or KB23 epitopes. The MHM24 epitope was however expressed at low levels on cells transfected with αL alone, and when cells were cotransfected with αL and β2, high expression levels of the MHM24 epitope were detected. In contrast, the LPM19C epitope was detected at equally high levels on cells transfected with αM alone and on cells cotransfected with αM and β2, whereas the KB23 epitope was not expressed at all on cells transfected with αX alone, but was detected at high expression levels on cells cotransfected with αX and β2. The results obtained by immunoprecipitation are shown in Figure 4.1b. MHM24 immunoprecipitated the αL subunit from the surface of the αL transfectants, and the αL and β2 subunits from the surface of the αLβ2 cotransfectants, and LPM19C immunoprecipitated the αM subunit from the surface of the αM transfectants, and the αM

Table.4.1: The Monoclonal Antibodies used for Flow Cytometric and Immunoprecipitation Analysis of Transfected COS 7 Cells

mAb	Isotype	Epitope Recognised	Reference
MHM24	IgG1	Human αL	Hildreth and August, 1985
LPM19C	IgG2a	Human αM	Uciechowski and Schmidt, 1989
KB23	not typed	Human αX	Dr. K. Micklem, personal communication
H52	IgG1	Human β2	Hildreth and August, 1985
MHM23	IgG1	Human β2	Hildreth and August, 1985
1B4	IgG2a	Human β2	Wright *et al.*, 1983
OX33	IgG1	Rat CD2	Cellular Immunology Unit, Oxford
OX34	IgG2a	Rat CD2	Cellular Immunology Unit, Oxford

This table lists the panel of anti-leukocyte integrin mAbs: MHM24, LPM19C, KB23, H52, MHM23 and 1B4, which were used for flow cytometric and immunoprecipitation analysis of transfected COS 7 cells. The mAbs OX33 and OX34, which recognise epitopes on rat CD2, were used as negative controls: in flow cytometry they were used to indicate the amount of fluorescence due to non-specific binding of mAbs, and in immunoprecipitations they were used in the pre-clearance step to remove proteins from cell lysates which bound non-specifically to mAbs.

Figure 4.1a: Analysis of the Expression of Wildtype Leukocyte Integrin Subunits on the Surface of COS 7 Transfectants By Flow Cytometry using the mAbs MHM24, LPM19c and KB23

COS 7 cells were either mock transfected, transfected with wildtype αL, αM, αX or β2 alone, or were cotransfected with wildtype αL and β2, wildtype αM and β2, or wildtype αX and β2, and the expression of the wildtype subunits on the COS 7 cell surface was analysed by flow cytometry. Transfectants were labelled with an irrelevant mAb (OX34; anti-rat CD2) to indicate the amount of fluorescence due to non-specific binding of mAbs to COS 7 cells (black profiles), or were labelled with the anti-human leukocyte integrin mAbs: MHM24 (anti-αL; green overlays), LPM19c (anti-αM; red overlays), or KB23 (anti-αX; mauve overlays). Samples were then stained with a fluorescently labelled rabbit anti-mouse second antibody, and the level of fluorescence on the surface of each cell was measured using a Becton Dickinson FACScan flow cytometer. In the profiles shown below, fluorescent intensity (in arbitary units) is plotted along the horizontal axis, and cell number is plotted along the vertical axis.

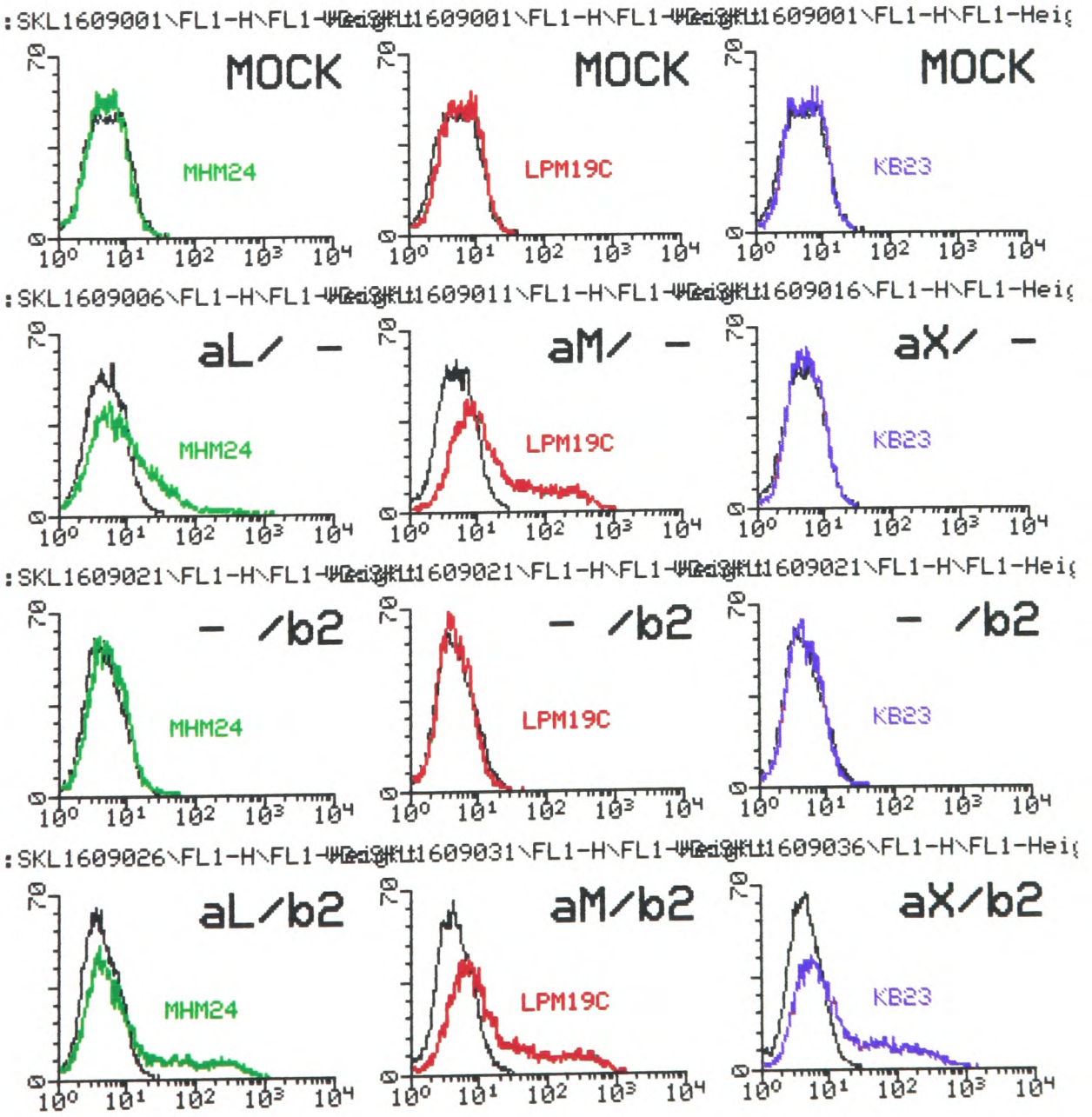
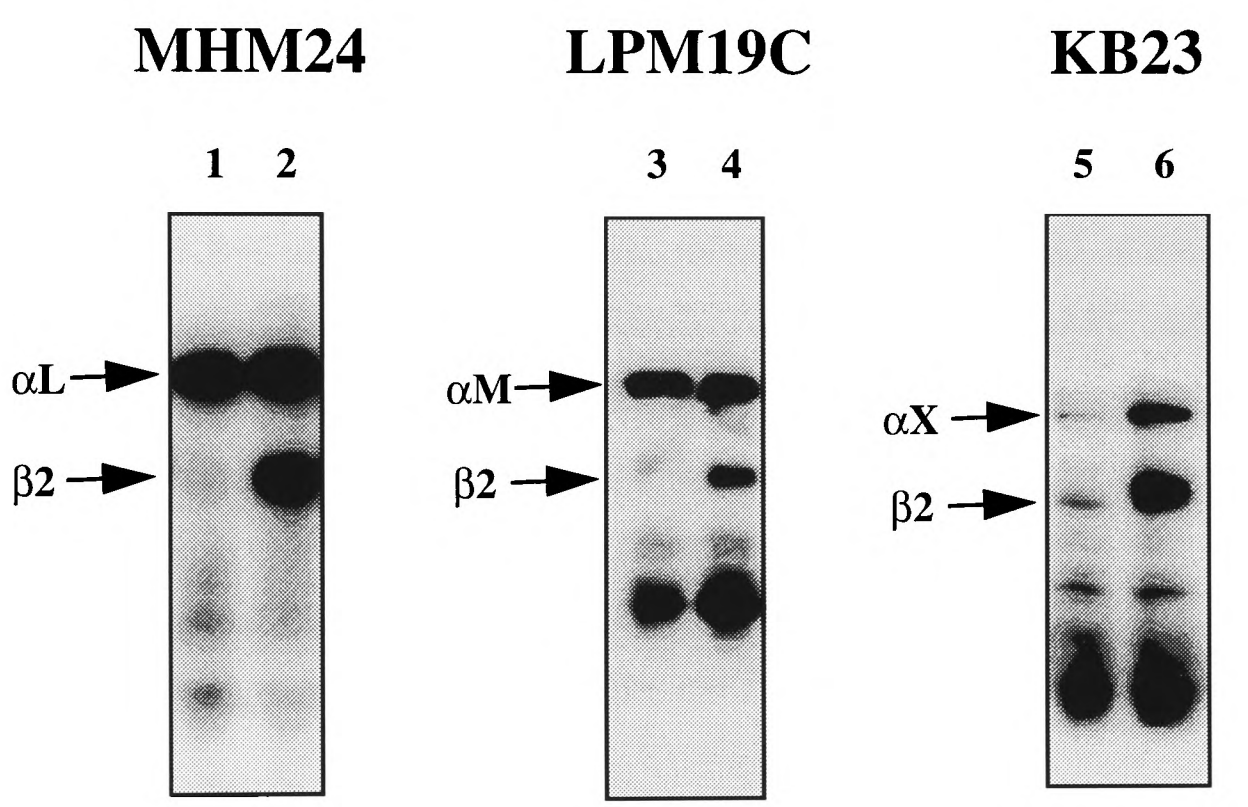


Figure 4.1b: Immunoprecipitation of Wildtype Leukocyte Integrin Subunits From the Surface of COS 7 Transfectants Using the mAbs MHM24, LPM19c and KB23

COS 7 cells were either transfected with wildtype αL, αM, or αX alone, or were cotransfected with wildtype αL and β2, wildtype αM and β2, or wildtype αX and β2, and the expression of the wildtype subunits on the COS 7 cell surface was analysed by immunoprecipitation. Transfectants were surface biotinylated and whole cell lysates were prepared from each sample. Wildtype subunits were then immunoprecipitated from lysates using the anti-α mAbs MHM24, LPM19C and KB23, and were run on SDS-PAGE gels and Western blotted onto PVDF membranes. The presence of biotinylated proteins on membranes was revealed by labelling with a streptavidin-HRP conjugate followed by enhanced chemiluminescence (ECL). The immunoprecipitation results obtained are shown opposite. The proteins in lanes 1-6 were immunoprecipitated from the following transfectants:

lane 1 = αL transfectants
lane 2 = αLβ2 transfectants
lane 3 = αM transfectants
lane 4 = αMβ2 transfectants
lane 5 = αX transfectants
lane 6 = αXβ2 transfectants


MHM24
LPM19C
KB23
1 2
3 4
5 6
αL
β2
αM
β2
αX
β2

and β2 subunits from the surface of the αMβ2 cotransfectants. In contrast, KB23 failed to immunoprecipitate the αX subunit from the surface of the αX transfectants, but did immunoprecipitate the αX and β2 subunits from the surface of the αXβ2 cotransfectants. It should be noted that when the αL subunit was immunoprecipitated from the αL transfectants by MHM24, and when the αM subunit was immunoprecipitated from the αM transfectants by LPM19c, no endogenous COS 7 cell counter-subunits were coprecipitated along with the transfected α subunits. Taken together, these results indicate that the leukocyte integrin αL and αM subunits can be expressed on the COS 7 cell surface either as α monomers or as αβ2 heterodimers. In contrast, the αX subunit was only detected on the cell surface in an αXβ2 heterodimeric form. Although it is possible that monomeric αX can be expressed on the cell surface but remained undetected in these experiments because it lacks expression of the KB23 epitope, similar results have also been obtained using two other anti-αX mAbs: KB90 and mAb 3.9. The αL monomers are expressed on the COS 7 cell surface at a low level, whereas the αM monomers and the αLβ2, αMβ2 and αXβ2 heterodimers are all expressed on the cell surface at very high levels. The MHM24 and LPM19C epitopes are expressed on both the monomeric and heterodimeric forms of the αL and αM subunits respectively, and the KB23 mAb epitope is expressed on the heterodimeric form of the αX subunit. Whether the KB23 epitope is also expressed on the monomeric form of αX can not be determined from these results.

4.2.1.1.2 Expression of the Wildtype β2 Subunit

Expression of the wildtype β2 subunit was characterised in a similar way, using the H52, MHM23 and 1B4 mAbs. COS 7 cells were transfected with the wildtype β2 subunit alone, or were cotransfected with αL and β2, αM and β2, or αX and β2, and the resulting cell surface expression was analysed by flow cytometry and immunoprecipitation. Mock transfected cells, and cells transfected with each wildtype α subunit alone, were also included as controls. The results obtained by flow cytometry are shown in Figure 4.2a. As expected, H52 did not label mock transfected cells, and the H52 epitope was not expressed on the surface of cells transfected with either αL alone, αM alone or αX alone. However, cells transfected with β2 alone, and cells cotransfected with αL and β2, αM and β2, and αX and β2, all expressed high levels of the H52 epitope. In contrast, the MHM23 and 1B4 mAbs did weakly label the mock transfected cells, as well as cells transfected with αM alone, αX alone, and β2 alone. Both MHM23 and 1B4 also labelled cells transfected

with αL alone slightly more than they labelled the mock transfectants, and cells cotransfected with αL and β2, αM and β2, and αX and β2, all expressed high levels of the MHM23 and 1B4 epitopes. The results obtained by immunoprecipitation are shown in Figure 4.2b. As expected, H52 failed to immunoprecipitate any integrin subunits from the surface of the αL, αM or αX transfectants, but did immunoprecipitate the β2 subunit from the surface of the β2 transfectants. It should be noted that no endogenous COS 7 cell counter-subunits were coprecipitated along with the β2 subunit. H52 also immunoprecipitated both the αL and β2 subunits from the surface of the αLβ2 cotransfectants, and the αM and β2 subunits from the surface of the αMβ2 cotransfectants, although the coprecipitation of the αM subunit was far less efficient than the coprecipitation of the αL subunit. In contrast, H52 only immunoprecipitated the β2 subunit from the surface of the αXβ2 cotransfectants. The 1B4 mAb failed to immunoprecipitate any integrin subunits from the surface of the αM transfectants, αX transfectants or β2 transfectants, but did weakly immunoprecipitate the αL subunit from the surface of the αL transfectants. 1B4 also immunoprecipitated the αL and β2 subunits from the surface of the αLβ2 cotransfectants, the αM and β2 subunits from the surface of the αMβ2 cotransfectants, and the αX and β2 subunits from the surface of the αXβ2 cotransfectants. Similar results were obtained with the MHM23 mAb (not shown). Taken together these results suggest that the β2 subunit can be efficiently expressed on the COS 7 cell surface either as a β2 monomer or as an αLβ2, αMβ2 or αXβ2 heterodimer. The H52 epitope is expressed efficiently on β2 monomers and on αLβ2 heterodimers, but is only weakly expressed on αMβ2 heterodimers, and is not expressed at all on αXβ2 heterodimers. In contrast, the MHM23 and 1B4 epitopes are expressed efficiently on αLβ2, αMβ2 and αXβ2 heterodimers, but are not expressed at all on β2 monomers. It should be noted that the MHM23 and 1B4 epitopes are also weakly expressed on αL monomers, and that both these mAbs also weakly label COS 7 cells in a non-specific manner.

4.2.1.1.3 Summary of the Expression of the Wildtype α and β Subunits

The conclusions derived from the results discussed in Sections 4.2.1.1.1 and 4.2.1.1.2 are summarised in Tables 4.2a and 4.2b. Flow cytometry and immunoprecipitation analysis established that the wildtype α and β subunits could be expressed on the COS 7 cell surface either as individual monomers or as αβ heterodimeric complexes (See Table 4.2a). The αL monomers are only weakly expressed on the COS 7 cell surface, whereas the αM

Figure 4.2a: Analysis of the Expression of Wildtype Leukocyte Integrin Subunits on the Surface of COS 7 Transfectants By Flow Cytometry using the mAbs H52, MHM23 and 1B4

COS 7 cells were either mock transfected, transfected with wildtype αL, αM, αX or β2 alone, or were cotransfected with wildtype αL and β2, wildtype αM and β2, or wildtype αX and β2, and the expression of the wildtype subunits on the COS 7 cell surface was analysed by flow cytometry. Transfectants were labelled with an irrelevant mAb (OX34; anti-rat CD2) to indicate the amount of fluorescence due to non-specific binding of mAbs to COS 7 cells (black profiles), or were labelled with the anti-human leukocyte integrin mAbs: H52 (anti-β2; light blue overlays), MHM23 (anti-β2; pink overlays) or 1B4 (anti-β2; dark blue overlays). Samples were then stained with a fluorescently labelled rabbit anti-mouse second antibody, and the level of fluorescence on the surface of each cell was measured using a Becton Dickinson FACScan flow cytometer. In the profiles shown opposite, fluorescent intensity (in arbitary units) is plotted along the horizontal axis, and cell number is plotted along the vertical axis.

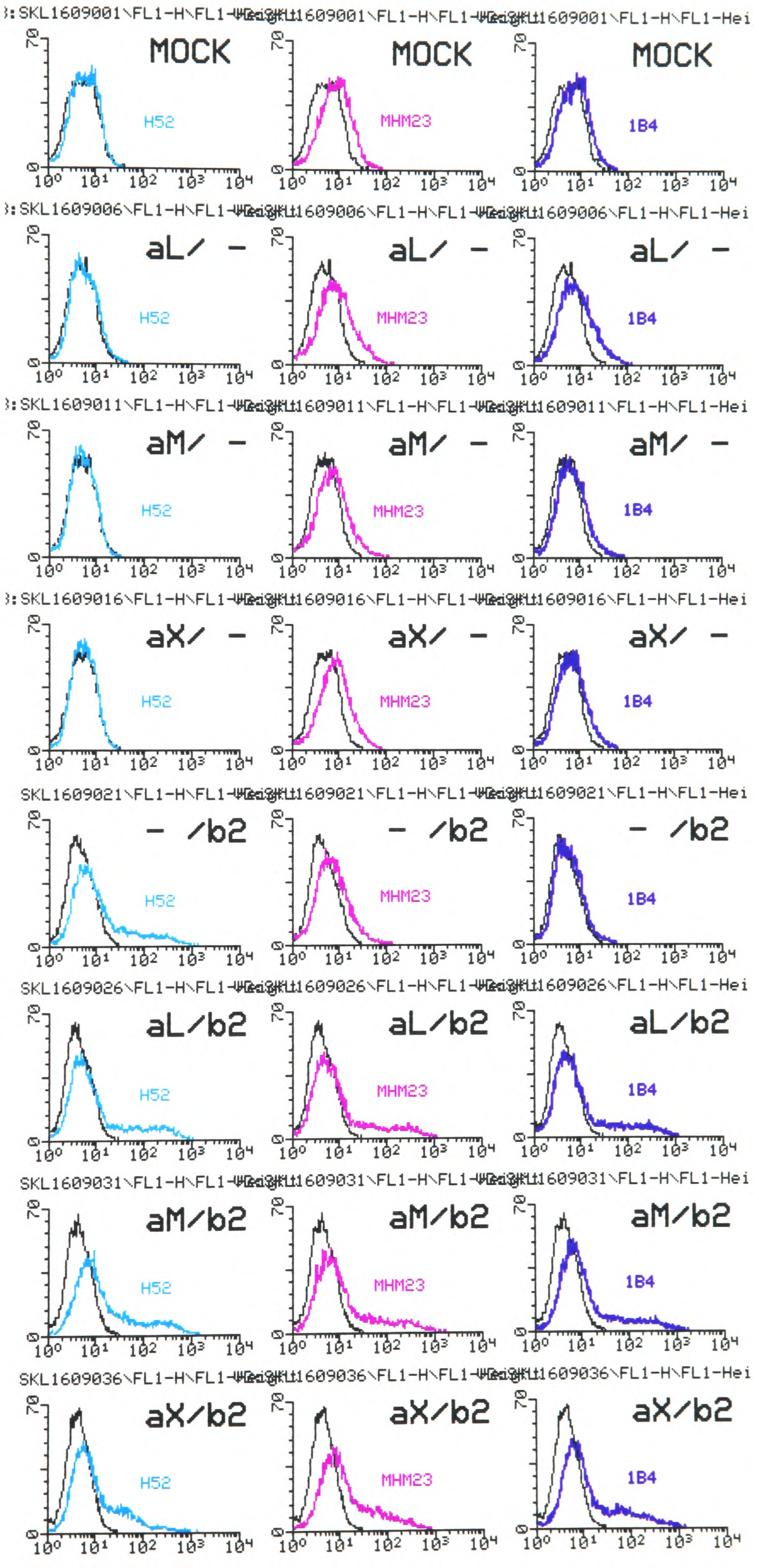
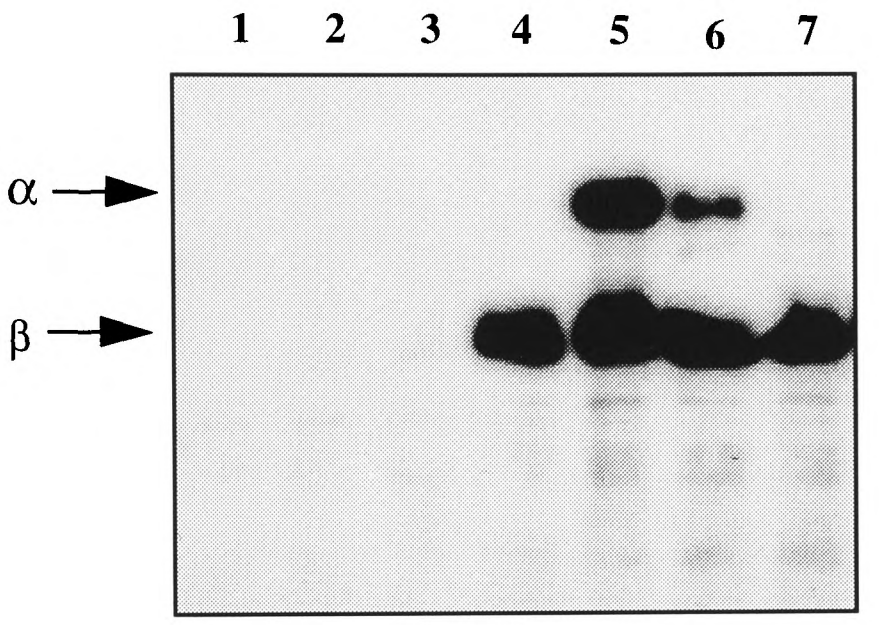

MOCK
H52
MHM23
1B4
aL/ -
aM/ -
aX/ -
- /b2
aL/b2
aM/b2
aX/b2

Figure 4.2b: Immunoprecipitation of Wildtype Leukocyte Integrin Subunits From the Surface of COS 7 Transfectants Using the mAbs H52 and 1B4

COS 7 cells were either transfected with wildtype αL, αM, αX or β2 alone, or were cotransfected with wildtype αL and β2, wildtype αM and β2, or wildtype αX and β2, and the expression of the wildtype subunits on the COS 7 cell surface was analysed by immunoprecipitation. Transfectants were surface biotinylated and whole cell lysates were prepared from each sample. Wildtype subunits were then immunoprecipitated from each lysate using the anti-β2 mAbs H52 and 1B4, and were run on SDS-PAGE gels and Western blotted onto PVDF membranes. The presence of biotinylated proteins on membranes was then revealed by labelling with a streptavidin-HRP conjugate followed by enhanced chemiluminescence (ECL). The immunoprecipitation results obtained are shown opposite. The proteins in lanes 1-7 were immunoprecipitated from the following transfectants:

lane 1 = αL transfectants
lane 2 = αM transfectants
lane 3 = αX transfectants
lane 4 = β2 transfectants
lane 5 = αLβ2 transfectants
lane 6 = αMβ2 transfectants
lane 7 = αXβ2 transfectants

H52



1B4

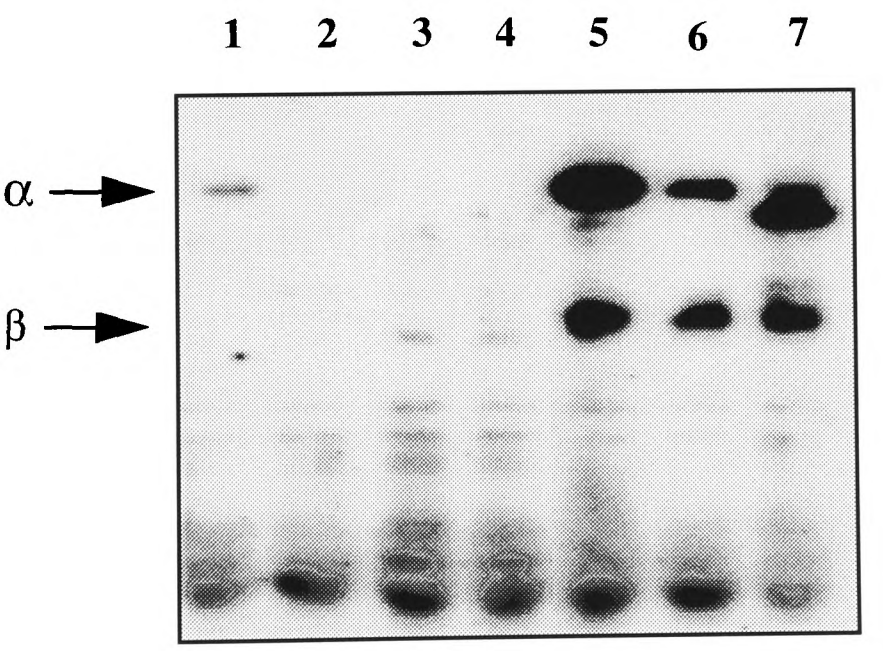


Table 4.2a: The Expression of Wildtype Monomers and Heterodimers on the Surface of COS 7 Transfectants

The table below summarises the cell surface expression of wildtype monomers and heterodimers resulting from the transfection of COS 7 cells with wildtype constructs. It is unclear whether the αX subunit can be expressed on the COS 7 cell surface in a monomeric form, as indicated in the table by the "?" signs. From the experimental results shown, it is also not possible to unequivocally determine if monomeric α and β subunits are expressed on the surface of αβ cotransfectants in addition to αβ heterodimers, as indicated in the table by the brackets.

Transfection	Resulting Cell Surface Expression		
	α Monomers	β Monomers	αβ Heterodimers
αL alone	αL		
αM alone	αM		
αX alone	?		
β2 alone		β2	
αL and β2	(αL)	(β2)	αLβ2
αM and β2	(αM)	(β2)	αMβ2
αX and β2	?	(β2)	αXβ2

Table 4.2b: Summary of the Expression of mAb Epitopes on the Wildtype Leukocyte Integrin Monomers and Heterodimers

The table below summarises the expression of the MHM24, LPM19C, KB23, H52, MHM23 and 1B4 mAb epitopes on the wildtype leukocyte integrin monomers and heterodimers. A "+" sign indicates expression of an epitope, a "(+)" sign weak expression of an epitope, a "-" sign no epitope expression, and a "?" sign that expression of the epitope could not be determined from the results presented in this thesis.

Subunit		MHM24	LPM19C	KB23	H52	MHM23	1B4
αL	Monomer	+			-	(+)	(+)
αM	Monomer		+		-	-	-
αX	Monomer			?	?	?	?
β2	Monomer	-	-	-	+	-	-
αLβ2	Heterodimer	+			+	+	+
αMβ2	Heterodimer		+		(+)	+	+
αXβ2	Heterodimer			+	-	+	+

monomers, β2 monomers, and αLβ2, αMβ2 and αXβ2 heterodimers are all very efficiently expressed on COS 7 cells. From these results, it is unclear whether the αX subunit can be expressed on the cell surface in a monomeric form. The flow cytometry and immunoprecipitation results also determined the expression of the MHM24, LPM19C, KB23, H52, MHM23 and 1B4 mAb epitopes on the wildtype monomers and heterodimers (See Table 4.2b). Although the MHM23 and 1B4 mAb epitopes are weakly expressed on αL monomers, they are strongly expressed on the β2 subunit when it was associated with either the αL, αM, or αX subunits in an αβ2 heterodimeric complex. Therefore, the expression of the MHM23 and 1B4 epitopes could be used to evaluate the formation of LFA-1, Mac-1, and p150,95 heterodimers: detection of these epitopes on the surface of αβ2 cotransfectants, at levels higher than those detected on either α transfectants or β2 transfectants, would indicate the expression of αβ2 heterodimeric complexes.

4.2.1.2 Expression of Modified LFA-1, Mac-1 and p150,95

The COS 7 cell expression system was then used to analyse the expression of the chimeric, soluble and truncated β2 subunits. COS 7 cells were transfected with each modified β2 subunit alone, or were cotransfected with a wildtype α subunit and a modified β2 subunit, and the resulting cell surface expression was then analysed by flow cytometry. The level of expression of the H52 epitope on the surface of cells transfected with a modified β2 subunit alone was used to evaluate the ability of the modified β2 subunits to express on the cell surface without associating with the wildtype αL, αM or αX counter-subunits, whereas the expression of the MHM23 and 1B4 epitopes on cells cotransfected with a wildtype α subunit and a modified β2 subunit (at levels higher than the background detected on cells transfected with either the wildtype α subunit or the modified β2 subunit alone) was used to evaluate the ability of the variant β2 subunits to form modified LFA-1, Mac-1 and p150,95 heterodimers with the wildtype αL, αM and αX subunits. In most cases, cell surface expression of variant β2 subunits detected by flow cytometry was subsequently confirmed by immunoprecipitation using the anti-β2 mAb H52.

4.2.1.2.1 Expression of the Chimeric β2 Subunits and Their Heterodimer Formation with the Wildtype αL, αM and αX Subunits

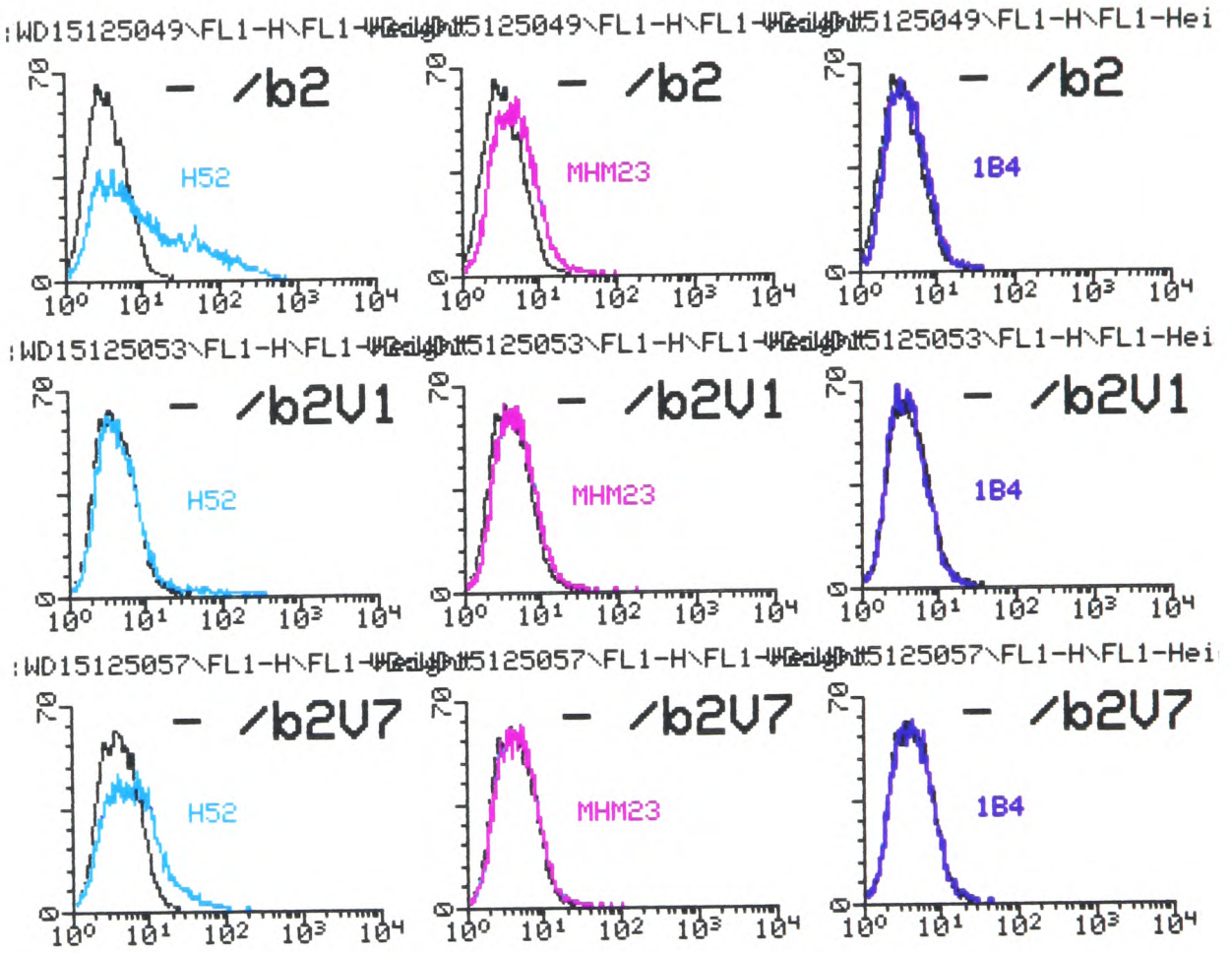
4.2.1.2.1.1 Expression of the Chimeric β2V1 and β2V7 Subunits

In the chimeric β2V1 and β2V7 subunits, the C-terminal cysteine-rich, membrane proximal, transmembrane and cytoplasmic domains of β2 are replaced with the homologous regions from the β1 and β7 subunits respectively (see Chapter 3, Figure 3.1). The flow cytometry results obtained with the β2V1 and β2V7 chimeras are shown in Figure 4.3a. When COS 7 cells were transfected with β2V1 alone, very low expression levels of the H52 epitope were detected on the cell surface, and the MHM23 and 1B4 epitopes were not detected. When cells were cotransfected with αL and β2V1, the H52 epitope was detected at slightly higher levels, and the 1B4, but not the MHM23 epitope, was detected at levels slightly higher than the background level detected on αL transfectants. However, when cells were cotransfected with αM and β2V1, or αX and β2V1, the expression of the H52 epitope was not enhanced, and the MHM23 and 1B4 epitopes were not expressed above the background levels observed with the αM and αX transfectants respectively. When cells were transfected with the β2V7 chimera alone, the H52 epitope was again expressed at low levels, and the MHM23 and 1B4 epitopes were not expressed. It should be noted that the H52 epitope was expressed on the β2V7 transfectants at slightly higher levels than on the β2V1 transfectants. When cells were cotransfected with αL and β2V7, the expression of the H52 epitope was significantly enhanced, and the MHM23 and 1B4 epitopes were detected at levels much higher than the background level detected on αL transfectants. When cells were cotransfected with αM and β2V7 the expression of the H52 epitope was slightly enhanced, and the MHM23 and 1B4 epitopes were detected at levels only slightly higher than the background level detected on the αM transfectants, and when cells were cotransfected with αX and β2V7 the expression of the H52 epitope was not enhanced, although the MHM23, and possibly also the 1B4 epitope, were detected at levels just above the background observed on αX transfectants. It should also be noted that the αXβ2V7 cotransfectants also very weakly expressed the KB23 epitope.

The expression of the chimeric β2V7 subunit and its heterodimer formation with the wildtype αL, αM and αX subunits was also analysed by immunoprecipitation with the H52 mAb (See Figure 4.3b). H52 immunoprecipitated the β2V7 subunit from the surface of the

Figure 4.3a: Analysis of the Expression of the Chimeric β2V1 and β2V7 Subunits and Their Ability to Form Heterodimers with the Wildtype αL, αM and αX Subunits by Flow Cytometry

COS 7 cells were transfected with wildtype αL, wildtype αM, wildtype αX, wildtype β2, chimeric β2V1 or chimeric β2V7 alone, or were cotransfected with wildtype αL, αM or αX and wildtype β2, chimeric β2V1 or chimeric β2V7, and the expression of the wildtype and chimeric subunits on the COS cell surface was analysed by flow cytometry. Transfectants were labelled with an irrelevant mAb (OX34; anti-rat CD2) to indicate the amount of fluorescence due to non-specific binding of mAbs to COS 7 cells (black profiles), or were labelled with the anti-human leukocyte integrin mAbs: MHM24 (anti-αL; green overlays), LPM19c (anti-αM; red overlays), KB23 (anti-αX; mauve overlays), H52 (anti-β2; light blue overlays), MHM23 (anti-β2 heterodimer; pink overlays) or 1B4 (anti-β2 heterodimer; dark blue overlays). Samples were then stained with a fluorescently labelled rabbit anti-mouse second antibody, and the level of fluorescence on the surface of each cell was measured using a Becton Dickinson FACScan flow cytometer. The flow cytometry profiles obtained are shown overleaf. In each profile, fluorescent intensity (in arbitary units) is plotted along the horizontal axis, and cell number is plotted along the vertical axis. Cell surface expression of wildtype and chimeric β2 subunits is indicated by detection of the H52 mAb epitope, whereas the expression of wildtype and modified LFA-1, Mac-1 or p150,95 heterodimers on the COS cell surface is indicated by the expression of the MHM23 and 1B4 mAb epitopes.


WD15125049\FL1-H\FL1-Height
5125049\FL1-H\FL1-Height
5125049\FL1-H\FL1-Hei
- /b2
H52
MHM23
1B4
WD15125053\FL1-H\FL1-Height
5125053\FL1-H\FL1-Height
5125053\FL1-H\FL1-Hei
- /b2V1
H52
MHM23
1B4
WD15125057\FL1-H\FL1-Height
5125057\FL1-H\FL1-Height
5125057\FL1-H\FL1-Hei
- /b2V7
H52
MHM23
1B4
WD15125049\FL1-H\FL1-Height
5125049\FL1-H\FL1-Height
5125049\FL1-H\FL1-Height
5125049\FL1-H\FL1-Hei
aL/ -
MHM24
H52
MHM23
1B4
WD15125049\FL1-H\FL1-Height
5125049\FL1-H\FL1-Height
5125049\FL1-H\FL1-Height
5125049\FL1-H\FL1-Hei
aL/b2
MHM24
H52
MHM23
1B4
WD15125053\FL1-H\FL1-Height
5125053\FL1-H\FL1-Height
5125053\FL1-H\FL1-Height
5125053\FL1-H\FL1-Hei
aL/b2V1
MHM24
H52
MHM23
1B4
WD15125057\FL1-H\FL1-Height
5125057\FL1-H\FL1-Height
5125057\FL1-H\FL1-Height
5125057\FL1-H\FL1-Hei
aL/b2V7
MHM24
H52
MHM23
1B4

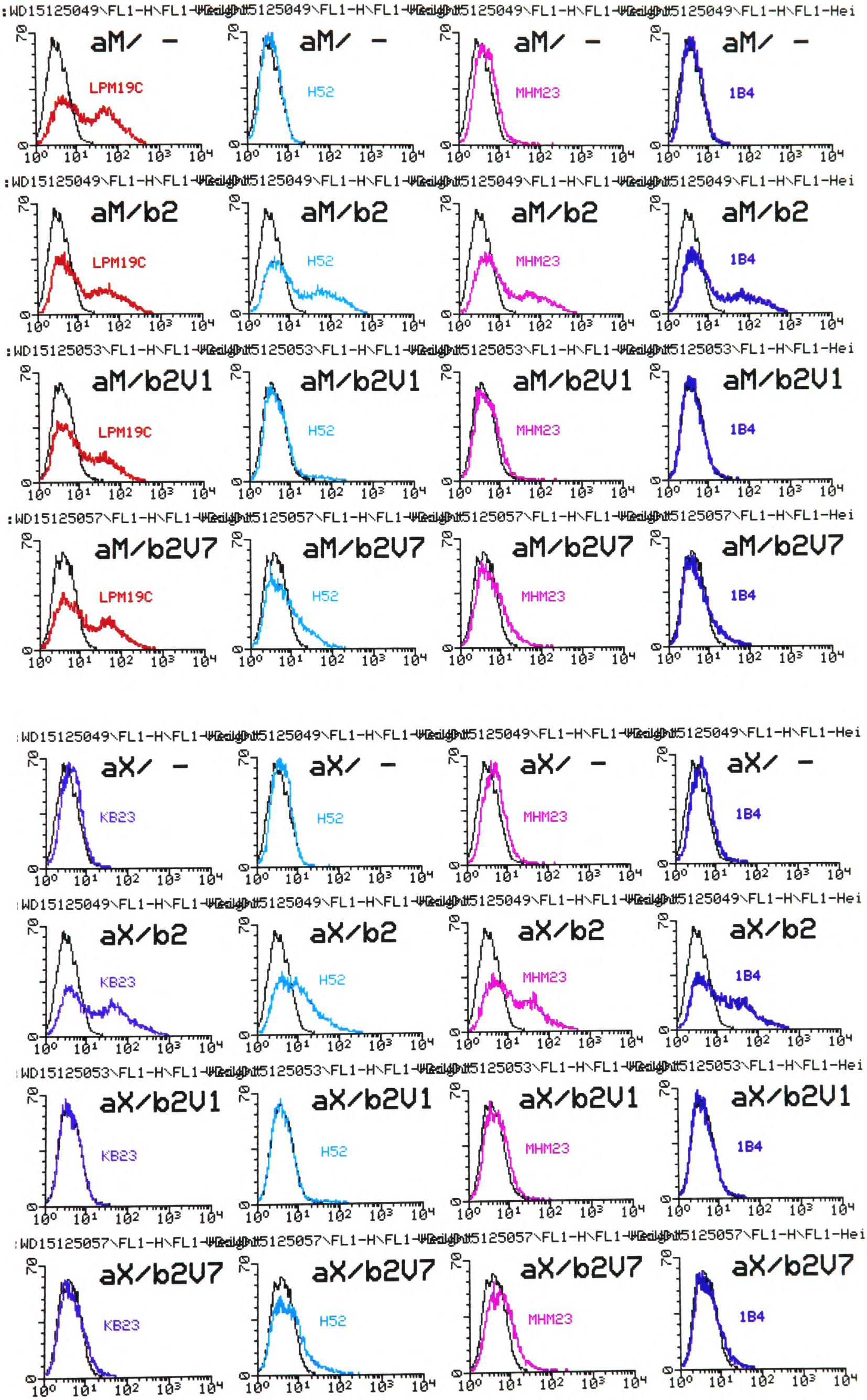
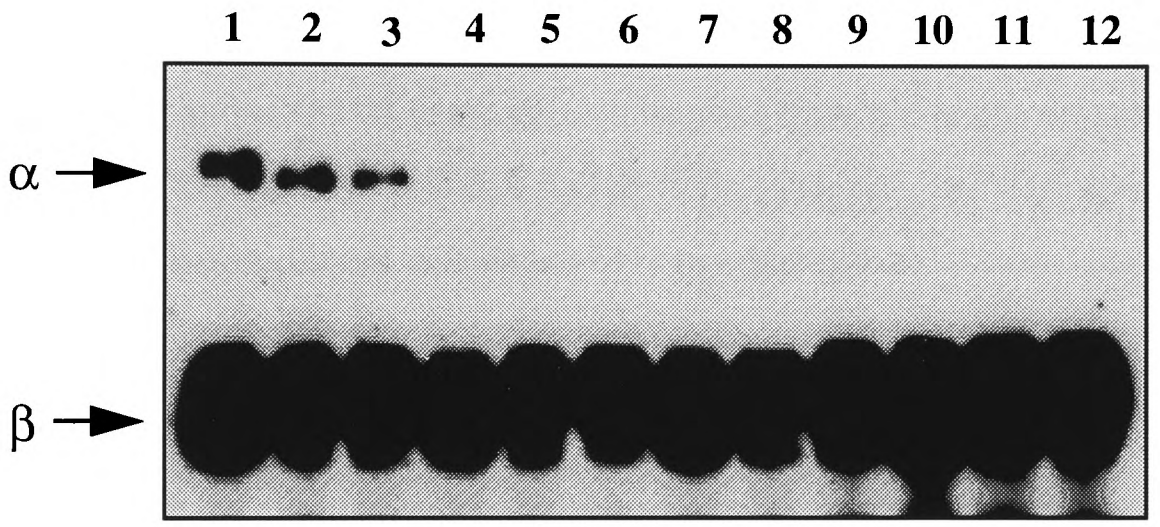

aM/ -
LPM19C
H52
MHM23
1B4
aM/b2
aM/b2V1
aM/b2V7
aX/ -
KB23
aX/b2
aX/b2V1
aX/b2V7

Figure 4.3b: Analysis of the Expression of the Chimeric β2V7 and β2V72 Subunits and Their Ability to Form Heterodimers with the Wildtype αL, αM and αX Subunits by Immunoprecipitation

COS 7 cells were transfected with wildtype β2, chimeric β2V7 or chimeric β2V72 alone, or were cotransfected with wildtype αL, αM or αX and wildtype β2, chimeric β2V7 or chimeric β2V72, and the expression of the wildtype and chimeric subunits on the COS cell surface was analysed by immunoprecipitation. Transfectants were surface biotinylated and whole cell lysates were prepared from each sample. Wildtype and chimeric subunits were then immunoprecipitated from each lysate using the anti-β2 mAb H52, and were run on an SDS-PAGE gel and Western blotted onto a PVDF membrane. The presence of biotinylated proteins on membranes was revealed by labelling with a streptavidin-HRP conjugate followed by enhanced chemiluminescence (ECL). The immunoprecipitation results obtained are shown opposite. Immunoprecipitation of a β subunit, without coprecipitation of an endogenous COS 7 cell α subunit, from a β transfectant indicates the expression of cell surface β monomers, whereas the coprecipitation of an α subunit along with a β subunit from an αβ cotransfectant indicates the expression of cell surface αβ heterodimers. The proteins in lanes 1-12 were immunoprecipitated from the following transfectants:

lane 1 = αLβ2 transfectants
lane 2 = αLβ2V7 transfectants
lane 3 = αLβ2V72 transfectants
lane 4 = αMβ2 transfectants
lane 5 = αMβ2V7 transfectants
lane 6 = αMβ2V72 transfectants
lane 7 = αXβ2 transfectants
lane 8 = αXβ2V7 transfectants
lane 9 = αXβ2V72 transfectants
lane 10 = β2 transfectants
lane 11 = β2V7 transfectants
lane 12 = β2V72 transfectants

H52



β2V7 transfectants without coprecipitating any endogenous COS 7 cell counter-subunits (Lane 11), and immunoprecipitated the αL and β2V7 subunits from the surface of the αLβ2V7 transfectants (Lane 2). In this set of immunoprecipitations, the coprecipitation of α subunits with the β2 subunit was very inefficient, and H52 failed to immunoprecipitate Mac-1 heterodimers from the surface of both the wildtype αMβ2 cotransfectants (Lane 4) and the αMβ2V7 cotransfectants (Lane 5). As p150,95 heterodimers do not express the H52 epitope, only β2 and β2V7 monomers were immunoprecipitated from the surface of the αXβ2 and αXβ2V7 cotransfectants (Lanes 7 & 8) respectively.

Taken together, these results indicate that the chimeric β2V1 and β2V7 subunits can be expressed on the COS 7 cell surface at very low levels on their own. The chimeric β2V1 subunit is able to support αLβ2V1 heterodimer formation, though at very low levels, and the expression of αMβ2V1 and αXβ2V1 heterodimers was not detected at all. In contrast, the expression of αLβ2V7 heterodimers was detected at moderate levels, and the expression of αMβ2V7 and αXβ2V7 heterodimers was detected above background levels, and their presence was confirmed by immunoprecipitation experiments.

4.2.1.2.1.2 Expression of the Chimeric β2V12 and β2V72 Subunits

In the chimeric β2V12 and β2V72 subunits, the C-terminal cysteine-rich and membrane proximal regions of β2 are replaced with the homologous regions from the β1 and β7 subunits respectively (see Chapter 3, Figure 3.1). The flow cytometry results obtained with the β2V12 and β2V72 chimeras, which are shown in Figure 4.4a, are very similar to the flow cytometry results obtained with the β2V1 and β2V7 chimeras (see Figure 4.3a). When COS 7 cells were transfected with β2V12 alone, very low expression levels of the H52 epitope were detected on the cell surface, and the MHM23 and 1B4 epitopes were not detected. When cells were cotransfected with αL and β2V12, the H52 epitope was detected at slightly higher levels and the MHM23 and 1B4 epitopes were both detected at levels slightly higher than the background level detected on αL transfectants. However, when cells were cotransfected with αM and β2V12, or αX and β2V12, the expression of the H52 epitope was not enhanced, and the MHM23 and 1B4 epitopes were not expressed above the background levels detected on the αM and αX transfectants respectively. When cells were transfected with β2V72 alone, the H52 epitope was again expressed at very low levels, and the MHM23 and 1B4 epitopes were not expressed. It should be noted that the

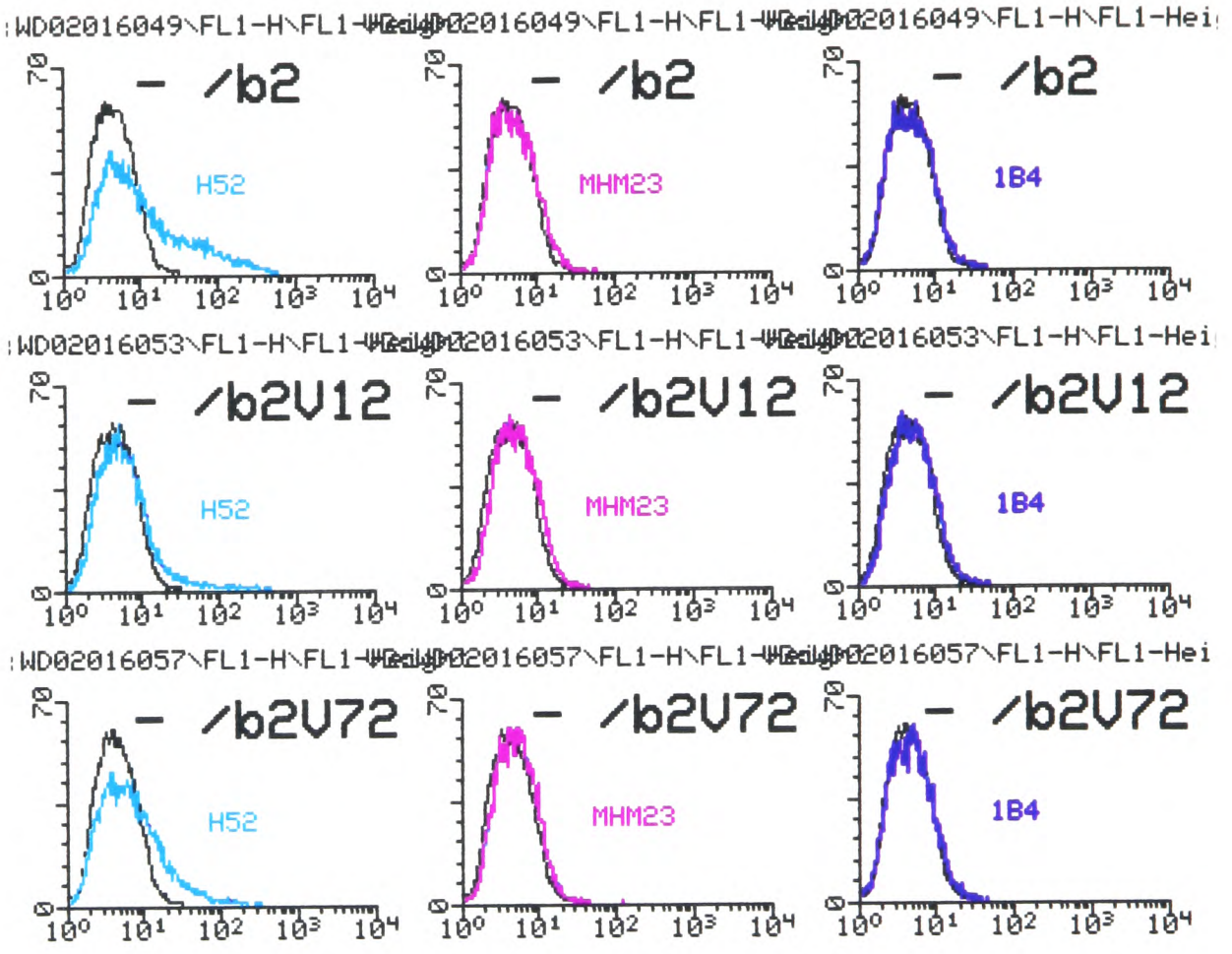
H52 epitope was expressed on the β2V72 transfectants at slightly higher levels than on the β2V12 transfectants. When cells were cotransfected with αL and β2V72, the expression of the H52 epitope was significantly enhanced, and the MHM23 and 1B4 epitopes were detected at levels much higher than the background level detected on αL transfectants. When cells were cotransfected with αM and β2V72, the expression of the H52 epitope was enhanced slightly, and the MHM23 and 1B4 epitopes were detected at levels slightly higher than the background detected on αM transfectants, but when cells were cotransfected with αX and β2V72, the expression of the H52 epitope was not enhanced and the MHM23 and 1B4 epitopes were not expressed above the background level detected on the αX transfectants.

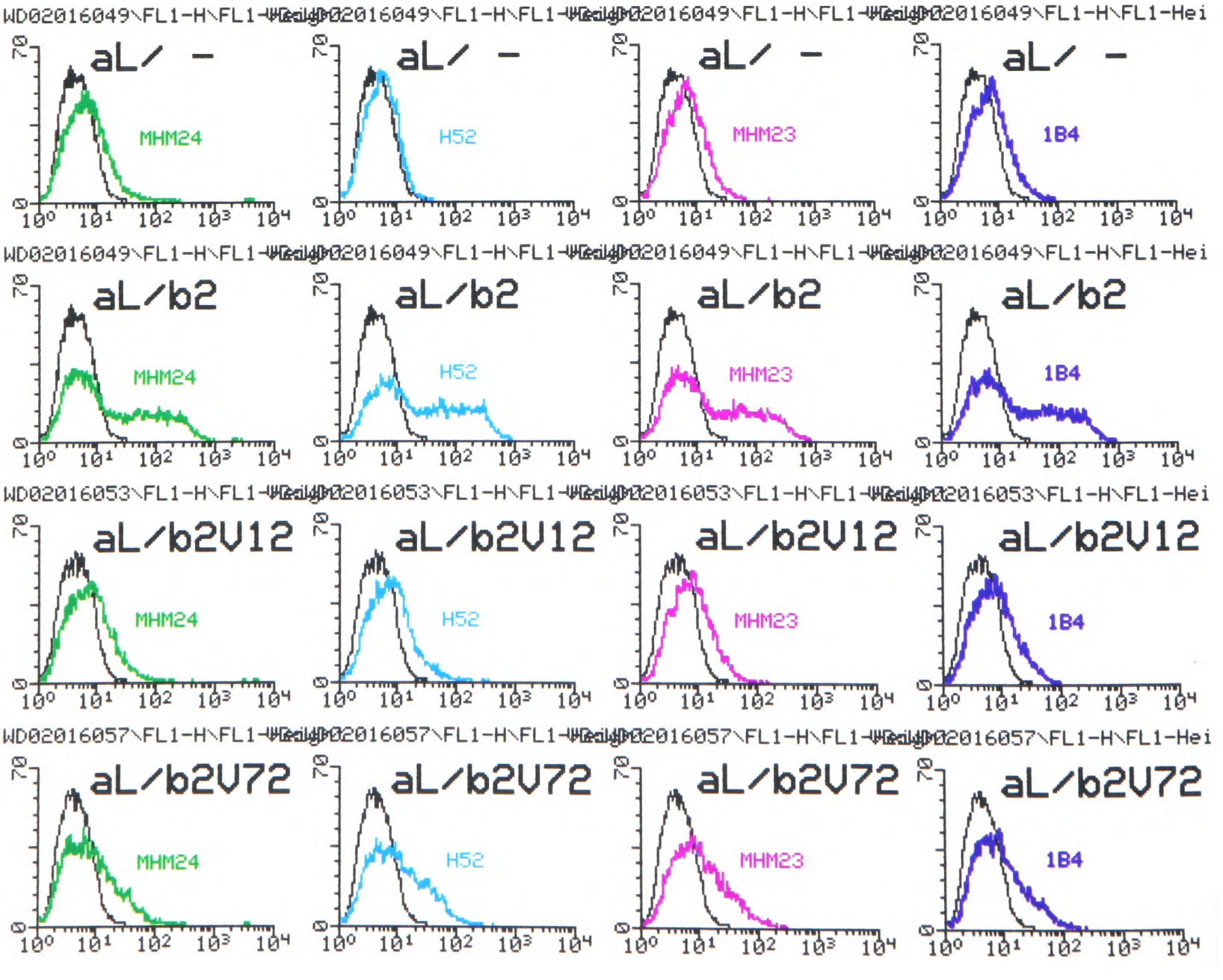
The expression of the chimeric β2V12 and β2V72 subunits, and their heterodimer formation with the wildtype αL, αM and αX subunits, was also analysed by immunoprecipitation with the H52 mAb (See Figure 4.4b). H52 immunoprecipitated the β2V12 subunit from the surface of the β2V12 transfectants, and the β2V72 subunit from the surface of the β2V72 transfectants (Lanes 3 & 4). No endogenous COS 7 cell counter-subunits were coprecipitated along with the β2V12 and β2V72 subunits. H52 also immunoprecipitated the αL and β2V12 subunits from the surface of the αLβ2V12 transfectants (Lane 7), and the αL and β2V72 subunits from the surface of the αLβ2V72 transfectants (Lane 8). It should be noted that although H52 did weakly immunoprecipitate the αL subunit from the surface of the αL transfectants (Lane 5), significantly higher levels of αL were immunoprecipitated from the surface of the αLβ2, αLβ2V12 and αLβ2V72 cotransfectants (Lanes 6, 7 & 8). Although αMβ2V72 heterodimers, but not αMβ2V12 heterodimers, had been detected at low expression levels by flow cytometry, H52 immunoprecipitated both αMβ2V12 and αMβ2V72 heterodimers from the surface of the αMβ2V12 and αMβ2V72 transfectants respectively (lanes 11 & 12). As the H52 epitope is not expressed on p150,95 heterodimers, only β2, β2V12 and β2V72 monomers were immunoprecipitated from the surface of the αXβ2, αXβ2V12 and αXβ2V72 transfectants respectively (lanes 14, 15 & 16). It should be noted that the immunoprecipitation of αLβ2V72 heterodimers was comparable to the immunoprecipitation of αLβ2V7 heterodimers (See Figure 4.3b).

Therefore, the expression of the β2V12 and β2V72 chimeras was very similar to the expression of the β2V1 and β2V7 chimeras. Both subunits were able to express weakly on

Figure 4.4a: Analysis of the Expression of the Chimeric β2V12 and β2V72 Subunits and Their Ability to Form Heterodimers with the Wildtype αL, αM and αX Subunits by Flow Cytometry

COS 7 cells were either transfected with wildtype αL, wildtype αM, wildtype αX, wildtype β2, chimeric β2V12 or chimeric β2V72 alone, or were cotransfected with wildtype αL, αM or αX and wildtype β2, chimeric β2V12 or chimeric β2V72, and the expression of the wildtype and chimeric subunits on the COS cell surface was analysed by flow cytometry. Transfectants were labelled with an irrelevant mAb (OX34; anti-rat CD2) to indicate the amount of fluorescence due to non-specific binding of mAbs to COS 7 cells (black profiles), or were labelled with the anti-human leukocyte integrin mAbs: MHM24 (anti-αL; green overlays), LPM19c (anti-αM; red overlays), KB23 (anti-αX; mauve overlays), H52 (anti-β2; light blue overlays), MHM23 (anti-β2 heterodimer; pink overlays) or 1B4 (anti-β2 heterodimer; dark blue overlays). Samples were then stained with a fluorescently labelled rabbit anti-mouse second antibody, and the level of fluorescence on the surface of each cell was measured using a Becton Dickinson FACScan flow cytometer. The flow cytometry profiles obtained are shown overleaf. In each profile, fluorescent intensity (in arbitary units) is plotted along the horizontal axis, and cell number is plotted along the vertical axis. Cell surface expression of wildtype and chimeric β2 subunits is indicated by detection of the H52 mAb epitope, whereas the expression of wildtype and modified LFA-1, Mac-1 or p150,95 heterodimers on the COS cell surface is indicated by the expression of the MHM23 and 1B4 mAb epitopes.


WD02016049\FL1-H\FL1-Hei
- /b2
H52
MHM23
1B4
WD02016053\FL1-H\FL1-Hei
- /b2V12
H52
MHM23
1B4
WD02016057\FL1-H\FL1-Hei
- /b2V72
H52
MHM23
1B4


WD02016049\FL1-H\FL1-Hei
aL/ -
MHM24
H52
MHM23
1B4
WD02016049\FL1-H\FL1-Hei
aL/b2
MHM24
H52
MHM23
1B4
WD02016053\FL1-H\FL1-Hei
aL/b2V12
MHM24
H52
MHM23
1B4
WD02016057\FL1-H\FL1-Hei
aL/b2V72
MHM24
H52
MHM23
1B4

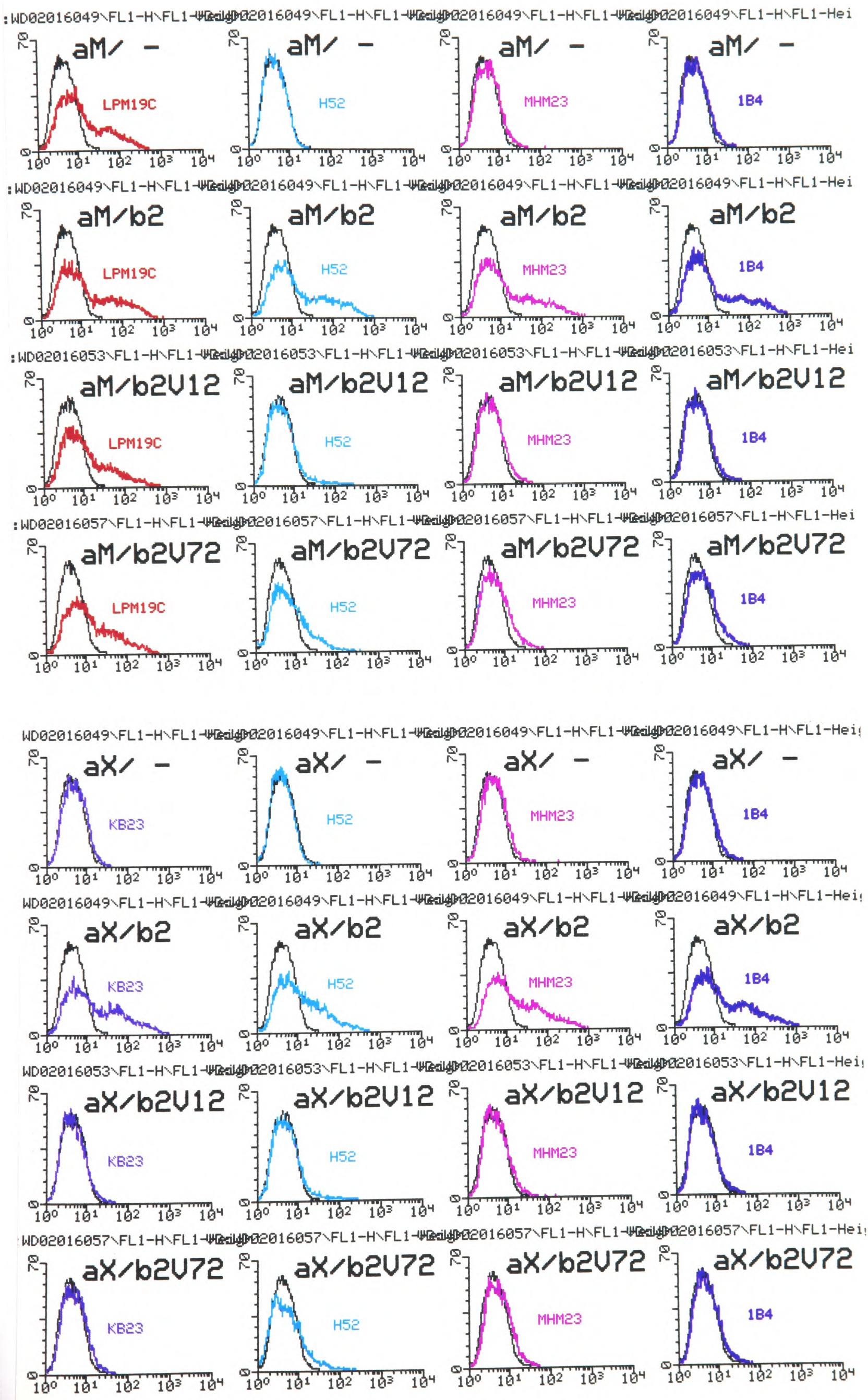
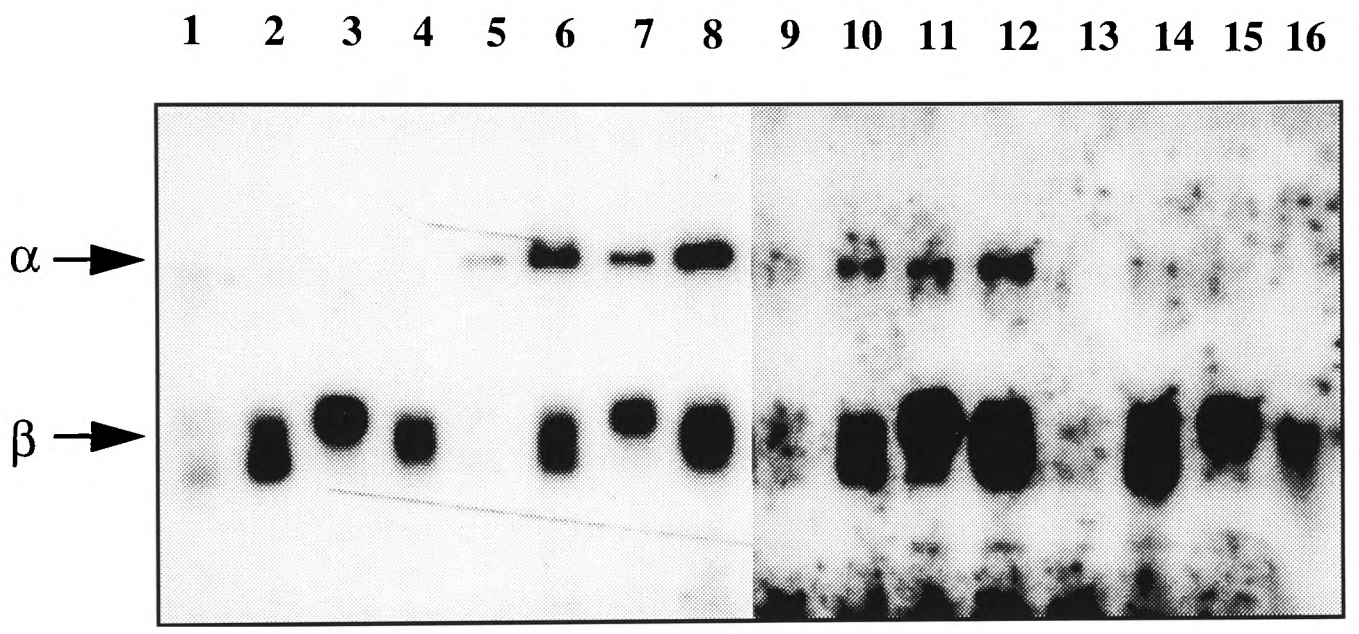

aM/ -
LPM19C
H52
MHM23
1B4
aM/b2
aM/b2V12
aM/b2V72
aX/ -
KB23
aX/b2
aX/b2V12
aX/b2V72

Figure 4.4b: Analysis of the Expression of the Chimeric β2V12 and β2V72 Subunits and Their Ability to Form Heterodimers with the Wildtype αL, αM and αX Subunits by Immunoprecipitation

COS 7 cells were either mock transfected, or were transfected with wildtype αL, wildtype αM, wildtype αX, wildtype β2, chimeric β2V12 or chimeric β2V72 alone, or were cotransfected with wildtype αL, αM or αX and wildtype β2, chimeric β2V12 or chimeric β2V72, and the expression of the wildtype and chimeric subunits on the COS cell surface was analysed by immunoprecipitation. Transfectants were surface biotinylated and whole cell lysates were prepared from each sample. Wildtype and chimeric subunits were then immunoprecipitated from each lysate using the anti-β2 mAb H52, and were run on an SDS-PAGE gel and Western blotted onto a PVDF membrane. The presence of biotinylated proteins on membranes was revealed by labelling with a streptavidin-HRP conjugate followed by enhanced chemiluminescence (ECL). The immunoprecipitation results obtained are shown opposite. Immunoprecipitation of a β subunit, without coprecipitation of an endogenous COS 7 cell α subunit, from a β transfectant indicates the expression of cell surface β monomers, whereas the coprecipitation of an α subunit along with a β subunit from an αβ cotransfectant indicates the expression of cell surface αβ heterodimers. The proteins in lanes 1-16 were immunoprecipitated from the following transfectants:

lane 1 = mock transfectants
lane 2 = β2 transfectants
lane 3 = β2V12 transfectants
lane 4 = β2V72 transfectants
lane 5 = αL transfectants
lane 6 = αLβ2 transfectants
lane 7 = αLβ2V12 transfectants
lane 8 = αLβ2V72 transfectants
lane 9 = αM transfectants
lane 10 = αMβ2 transfectants
lane 11 = αMβ2V12 transfectants
lane 12 = αMβ2V72 transfectants
lane 13 = αX transfectants
lane 14 = αXβ2 transfectants
lane 15 = αXβ2V12 transfectants
lane 16 = αXβ2V72 transfectants

H52



the cell surface as monomers, and both subunits also retained the ability to associate with the wildtype αL subunit to form variant LFA-1 heterodimers. The β2V12 monomers and αLβ2V12 heterodimers were expressed at very low levels, whereas the β2V72 monomers were expressed at slightly higher levels, and the αLβ2V72 heterodimers were very efficiently expressed. The β2V72 subunit was also able to weakly support αMβ2V72 heterodimer formation, and although αMβ2V12 heterodimers were not detected by flow cytometry, they were detected by immunoprecipitation, indicating that they were also expressed, but at extremely low levels. The expression of αXβ2V12 and αXβ2V72 heterodimers was not detected. However, it is possible that modified p150,95 heterodimers were expressed, but at levels too low to be detected by flow cytometric analysis alone. It should be noted that, like the wildtype β2 subunit, the β2V12 and β2V72 subunits were expressed more efficiently if they were able to associate with a wildtype α subunit to form variant αβ heterodimeric complexes.

4.2.1.2.1.3 Expression of the Chimeric β2NS1 and β2NS7 Subunits

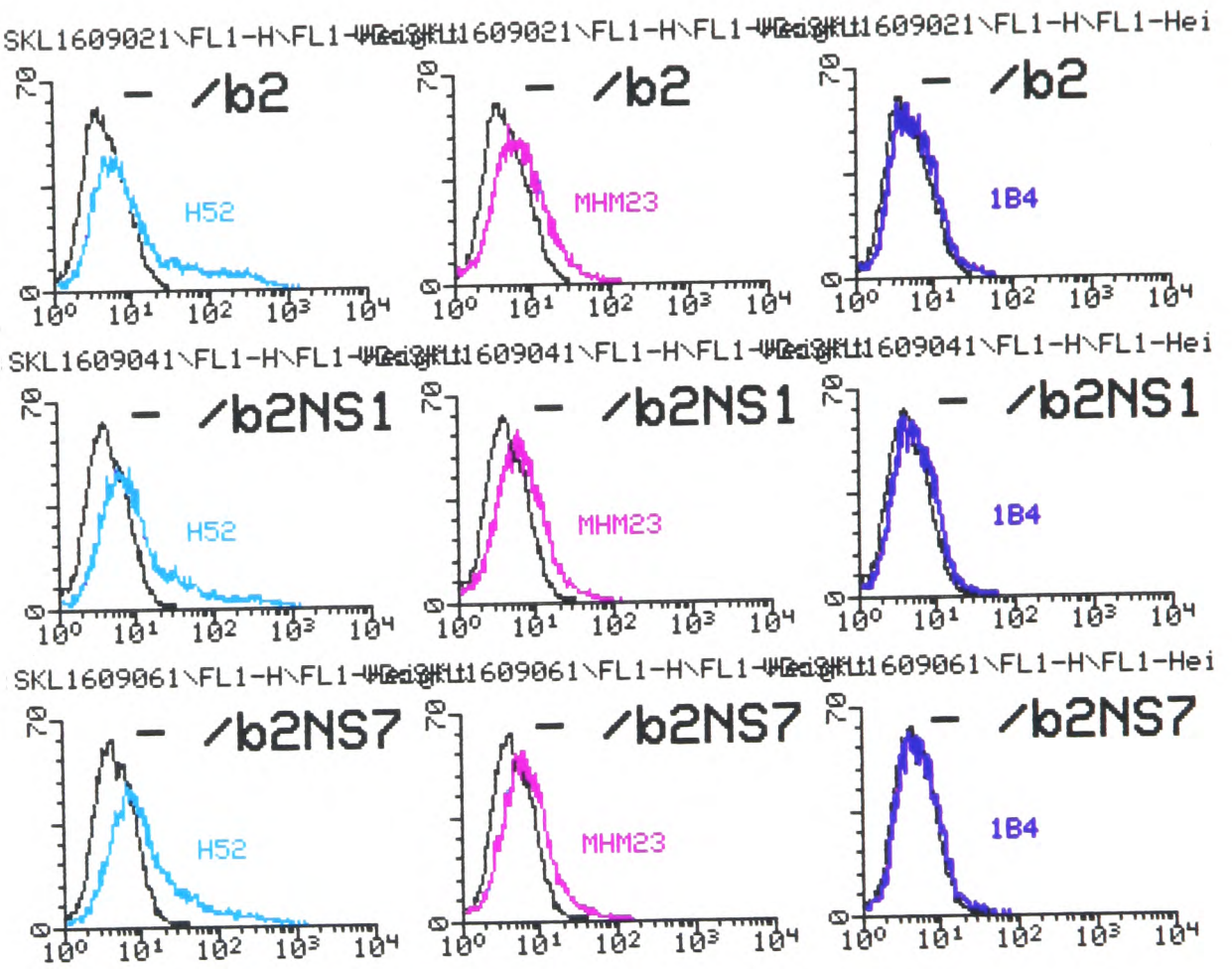
In the chimeric β2NS1 and β2NS7 subunits, a section of the C-terminal cysteine-rich region of β2 is replaced with the homologous region from the β1 and β7 subunits respectively (see Chapter 3, Figure 3.1). The flow cytometry results obtained for the β2NS1 and β2NS7 chimeras are shown in Figure 4.5a. When cells were transfected with β2NS1 alone, or β2NS7 alone, the H52 epitope was detected at very high levels, whereas the MHM23 and 1B4 epitopes were only detected at background levels. When cells were cotransfected with αL and β2NS1, or αL and β2NS7, the expression of the H52 epitope was slightly enhanced, and the MHM23 and 1B4 epitopes were expressed at levels much higher than the background level detected on the αL transfectants. However, when cells were cotransfected with αM and β2NS1, or αM and β2NS7, although the expression of the H52 epitope was again enhanced, the MHM23 and 1B4 epitopes were only expressed at levels slightly above the background detected on the αM transfectants, and when cells were cotransfected with αX and β2NS1, or αX and β2NS7, the expression of the H52 epitope was not enhanced, and the MHM23 and 1B4 epitopes were only expressed at levels just above the background detected on the αX transfectants. It should be noted that the KB23 epitope was also detected on the αXβ2NS1 and αXβ2NS7 transfectants, but only at levels slightly higher than the background level detected on the αX transfectants.

The expression of the chimeric β2NS1 and β2NS7 subunits, and their heterodimer formation with the wildtype αL, αM and αX subunits, was also analysed by immunoprecipitation with the H52 mAb (See Figure 4.5b). H52 immunoprecipitated the β2NS1 and β2NS7 subunits from the surface of the β2NS1 and β2NS7 transfectants (Lanes 8 and 12). No endogenous COS 7 cell counter-subunits were coprecipitated along with the β2NS1 and β2NS7 subunits. H52 also immunoprecipitated αLβ2NS1 and αLβ2NS7 heterodimers from the surface of the αLβ2NS1 and αLβ2NS7 cotransfectants (Lanes 9 and 13), and αMβ2NS1 and αMβ2NS7 heterodimers from the surface of the αMβ2NS1 and αMβ2NS7 cotransfectants (Lanes 10 and 14). Although flow cytometry had established that the αMβ2NS1 and αMβ2NS7 heterodimers were expressed on the cell surface at very low levels, it should be noted that these variant Mac-1 heterodimers were immunoprecipitated more efficiently than the wildtype Mac-1 heterodimers. It should also be noted that although H52 failed to immunoprecipitate wildtype p150,95 heterodimers from the surface of the wildtype αXβ2 cotransfectants (Lane 7), αXβ2NS1 and αXβ2NS7 heterodimers were weakly immunoprecipitated from the surface of the αXβ2NS1 and αXβ2NS7 cotransfectants (Lanes 11 and 15).

Taken together, these results indicate that the chimeric β2NS1 and β2NS7 subunits can be efficiently expressed on the cell surface as monomers, and that they also retain the ability to associate with the wildtype αL, αM and αX subunits to form variant LFA-1, Mac-1 and p150,95 heterodimers. Although the variant LFA-1 heterodimers were expressed on the cell surface almost as efficiently as the wildtype LFA-1 heterodimers, the variant Mac-1 heterodimers were expressed at lower levels, and the variant p150,95 heterodimers were very inefficiently expressed. It should be noted that the H52 epitope, which is expressed weakly on wildtype Mac-1 heterodimers and is not expressed at all on wildtype p150,95 heterodimers, was expressed very efficiently on the variant Mac-1 and variant p150,95 heterodimers. It should also be noted that the β2NS1 and β2NS7 subunits, like the wildtype β2 subunit, were expressed more efficiently on the cell surface when they were able to associate with a wildtype α subunit to form variant αβ heterodimeric complexes.

Figure 4.5a: Analysis of the Expression of the Chimeric β2NS1 and β2NS7 Subunits and Their Ability to Form Heterodimers with the Wildtype αL, αM and αX Subunits by Flow Cytometry

COS 7 cells were either transfected with wildtype αL, wildtype αM, wildtype αX, wildtype β2, chimeric β2NS1 or chimeric β2NS7 alone, or were cotransfected with wildtype αL, αM or αX and wildtype β2, chimeric β2NS1 or chimeric β2NS7, and the expression of the wildtype and chimeric subunits on the COS cell surface was analysed by flow cytometry. Transfectants were labelled with an irrelevant mAb (OX34; anti-rat CD2) to indicate the amount of fluorescence due to non-specific binding of mAbs to COS 7 cells (black profiles), or were labelled with the anti-human leukocyte integrin mAbs: MHM24 (anti-αL; green overlays), LPM19c (anti-αM; red overlays), KB23 (anti-αX; mauve overlays), H52 (anti-β2; light blue overlays), MHM23 (anti-β2 heterodimer; pink overlays) or 1B4 (anti-β2 heterodimer; dark blue overlays). Samples were then stained with a fluorescently labelled rabbit anti-mouse second antibody, and the level of fluorescence on the surface of each cell was measured using a Becton Dickinson FACScan flow cytometer. The flow cytometry profiles obtained are shown overleaf. In each profile, fluorescent intensity (in arbitary units) is plotted along the horizontal axis, and cell number is plotted along the vertical axis. Cell surface expression of wildtype and chimeric β2 subunits is indicated by detection of the H52 mAb epitope, whereas the expression of wildtype and modified LFA-1, Mac-1 or p150,95 heterodimers on the COS cell surface is indicated by the expression of the MHM23 and 1B4 mAb epitopes.


SKL1609021\FL1-H\FL1-Hei
- /b2
H52
MHM23
1B4
SKL1609041\FL1-H\FL1-Hei
- /b2NS1
H52
MHM23
1B4
SKL1609061\FL1-H\FL1-Hei
- /b2NS7
H52
MHM23
1B4
SKL1609006\FL1-H\FL1-Hei
aL/ -
MHM24
H52
MHM23
1B4
SKL1609026\FL1-H\FL1-Hei
aL/b2
MHM24
H52
MHM23
1B4
SKL1609046\FL1-H\FL1-Hei
aL/b2NS1
MHM24
H52
MHM23
1B4
SKL1609066\FL1-H\FL1-Hei
aL/b2NS7
MHM24
H52
MHM23
1B4

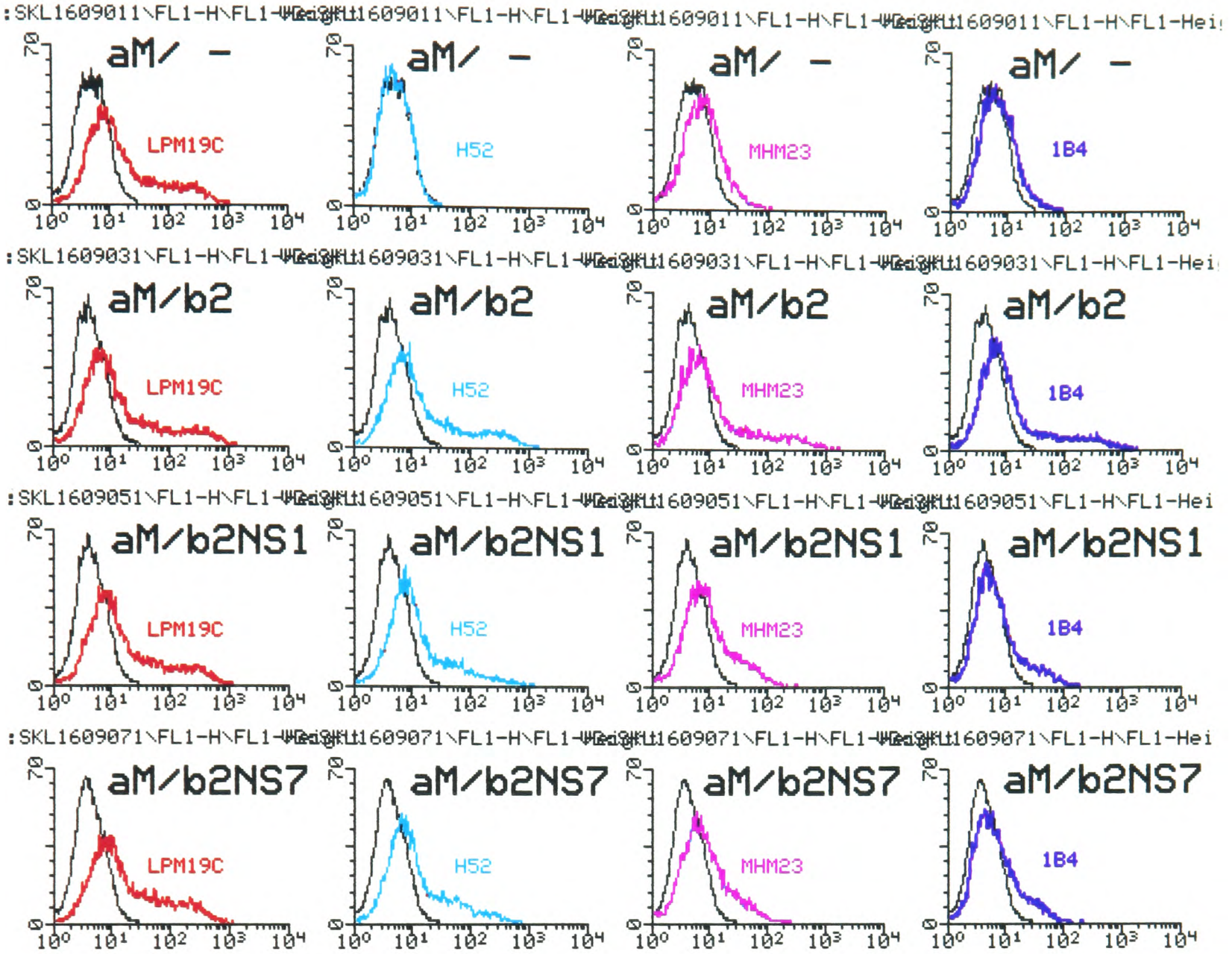
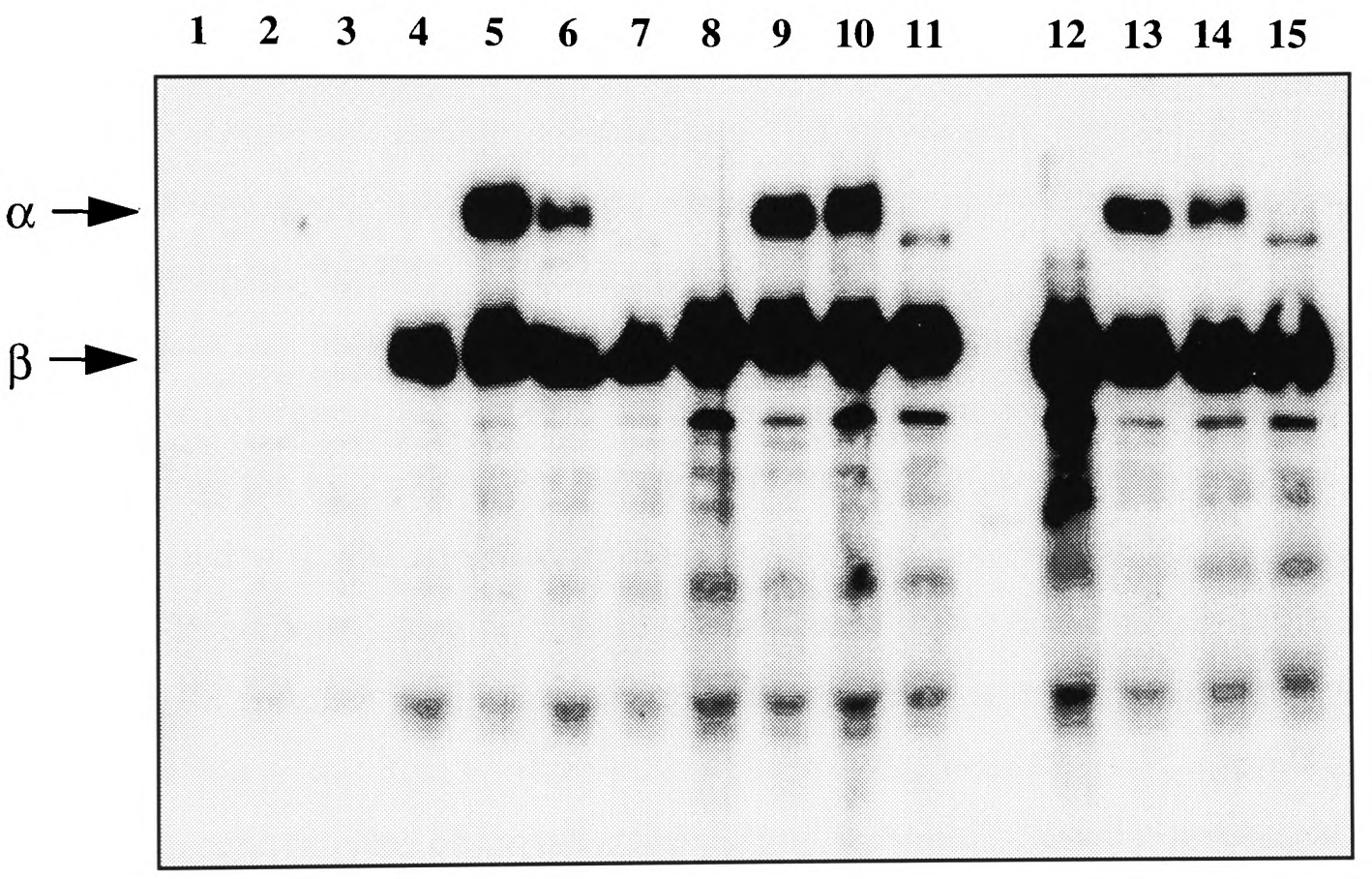

aM/ -
LPM19C
H52
MHM23
1B4
aM/b2
aM/b2NS1
aM/b2NS7
aX/ -
KB23
aX/b2
aX/b2NS1
aX/b2NS7

Figure 4.5b: Analysis of the Expression of the Chimeric β2NS1 and β2NS7 Subunits and Their Ability to Form Heterodimers with the Wildtype αL, αM and αX Subunits by Immunoprecipitation

COS 7 cells were either transfected with wildtype αL, wildtype αM, wildtype αX, wildtype β2, chimeric β2NS1 or chimeric β2NS7 alone, or were cotransfected with wildtype αL, αM or αX and wildtype β2, chimeric β2NS1 or chimeric β2NS7, and the expression of the wildtype and chimeric subunits on the COS cell surface was analysed by immunoprecipitation. Transfectants were surface biotinylated and whole cell lysates were prepared from each sample. Wildtype and chimeric subunits were then immunoprecipitated from each lysate using the anti-β2 mAb H52, and were run on an SDS-PAGE gel and Western blotted onto a PVDF membrane. The presence of biotinylated proteins on membranes was revealed by labelling with a streptavidin-HRP conjugate followed by enhanced chemiluminescence (ECL). The immunoprecipitation results obtained are shown opposite. Immunoprecipitation of a β subunit, without coprecipitation of an endogenous COS 7 cell α subunit, from a β transfectant indicates the expression of cell surface β monomers, whereas the coprecipitation of an α subunit along with a β subunit from an αβ cotransfectant indicates the expression of cell surface αβ heterodimers. The proteins in lanes 1-15 were immunoprecipitated from the following transfectants:

lane 1 = αL transfectants
lane 2 = αM transfectants
lane 3 = αX transfectants
lane 4 = β2 transfectants
lane 5 = αLβ2 transfectants
lane 6 = αMβ2 transfectants
lane 7 = αXβ2 transfectants
lane 8 = β2NS1 transfectants
lane 9 = αLβ2NS1 transfectants
lane 10 = αMβ2NS1 transfectants
lane 11 = αXβ2NS1 transfectants
lane 12 = β2NS7 transfectants
lane 13 = αLβ2NS7 transfectants
lane 14 = αMβ2NS7 transfectants
lane 15 = αXβ2NS7 transfectants

H52



4.2.1.2.2 Expression of the Soluble and Truncated β2 Subunits and their Heterodimer Formation with the Wildtype αL, αM and αX Subunits

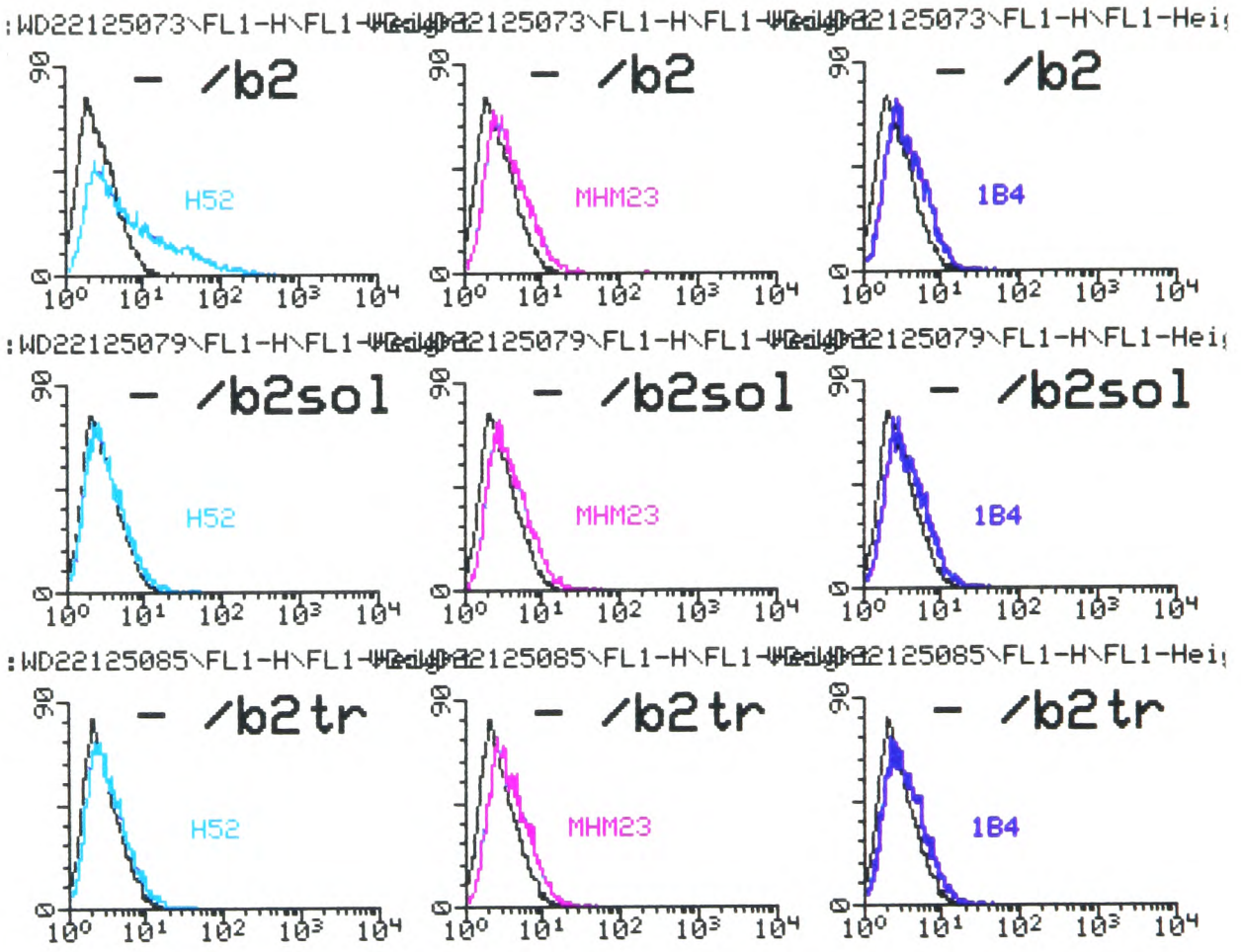
4.2.1.2.2.1 Expression of the β2sol and β2tr Subunits

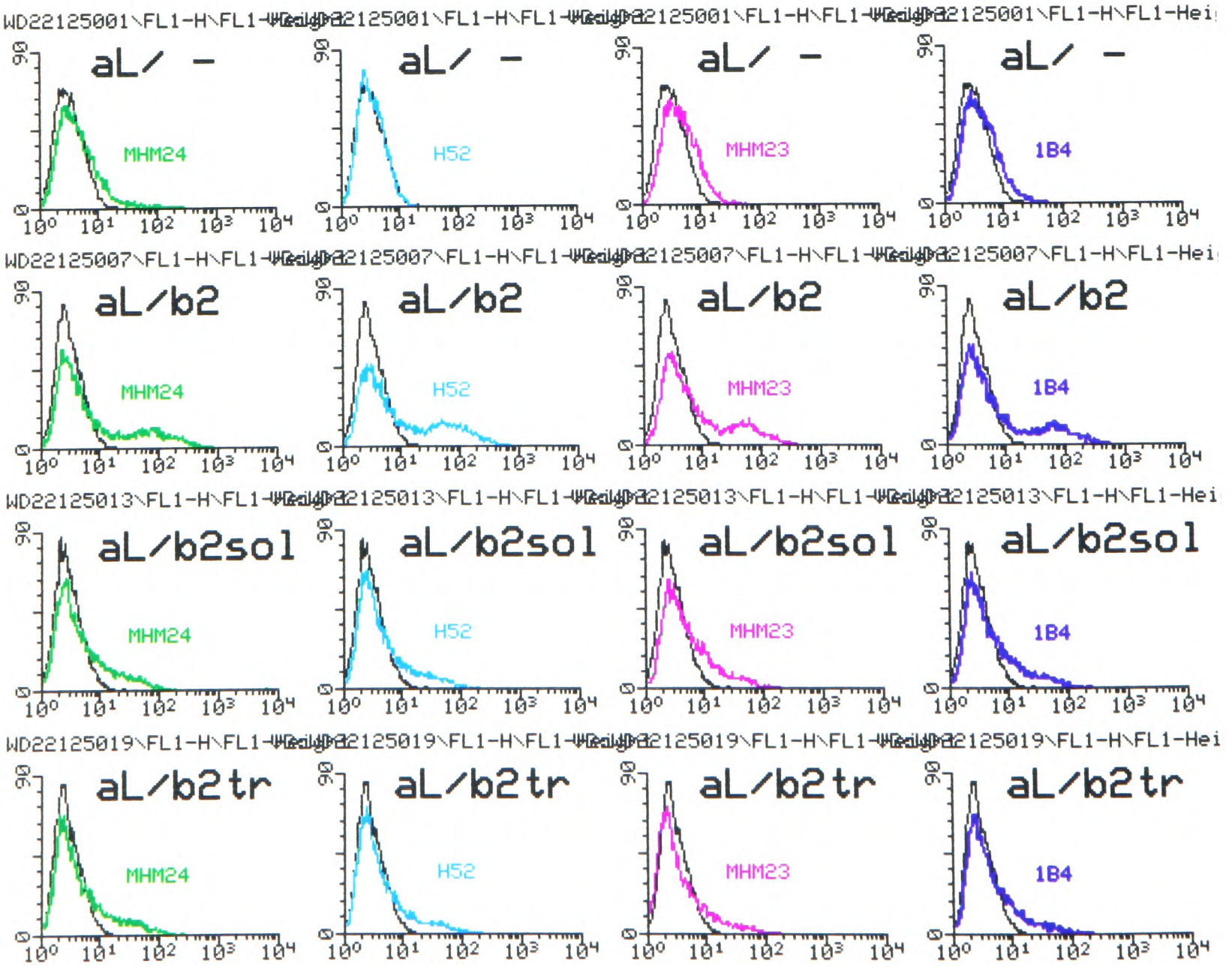
The β2sol subunit is a soluble β2 (amino acids 1-698) lacking the transmembrane and cytoplasmic domains of the β2 subunit, whereas the β2tr subunit is a truncated β2 (amino acids 1-480) lacking almost the entire C-terminal cysteine-rich region, as well as the membrane proximal, transmembrane and cytoplasmic domains of β2 (see Chapter 3, Figure 3.1). The flow cytometry results obtained with the β2sol and β2tr subunits are shown in Figure 4.6. When cells were transfected with β2sol alone, or with β2tr alone, the H52 epitope was not expressed, and the MHM23 and 1B4 mAbs only weakly labelled the transfected cells non-specifically. However, when cells were cotransfected with αL and β2sol, or αL and β2tr, the H52, MHM23 and 1B4 mAb epitopes were all expressed at levels higher than any background detected on the αL transfectants. When cells were cotransfected with αM and β2sol, the H52, MHM23 and 1B4 epitopes were only expressed at levels just above the background detected on the αM transfectants, whereas when cells were cotransfected with αM and β2tr, all three mAb epitopes were detected at slightly higher levels. In contrast, when cells were cotransfected with αX and β2sol, the H52, MHM23, and 1B4 epitopes were expressed at moderate levels, whereas when cells were cotransfected with αX and β2tr, all three mAb epitopes were only detected at levels just above the background detected on the αX transfectants. It should be noted that the level of expression of the MHM24 epitope on the surface of the αLβ2sol and αLβ2tr cotransfectants was similar to the level of expression of the H52, MHM23 and 1B4 epitopes, and that the level of expression of the KB23 epitope on the surface of the αXβ2sol and αXβ2tr cotransfectants was also similar to the level of expression of the H52, MHM23 and 1B4 epitopes. Immunoprecipitation analysis of the β2sol and β2tr transfectants was not performed.

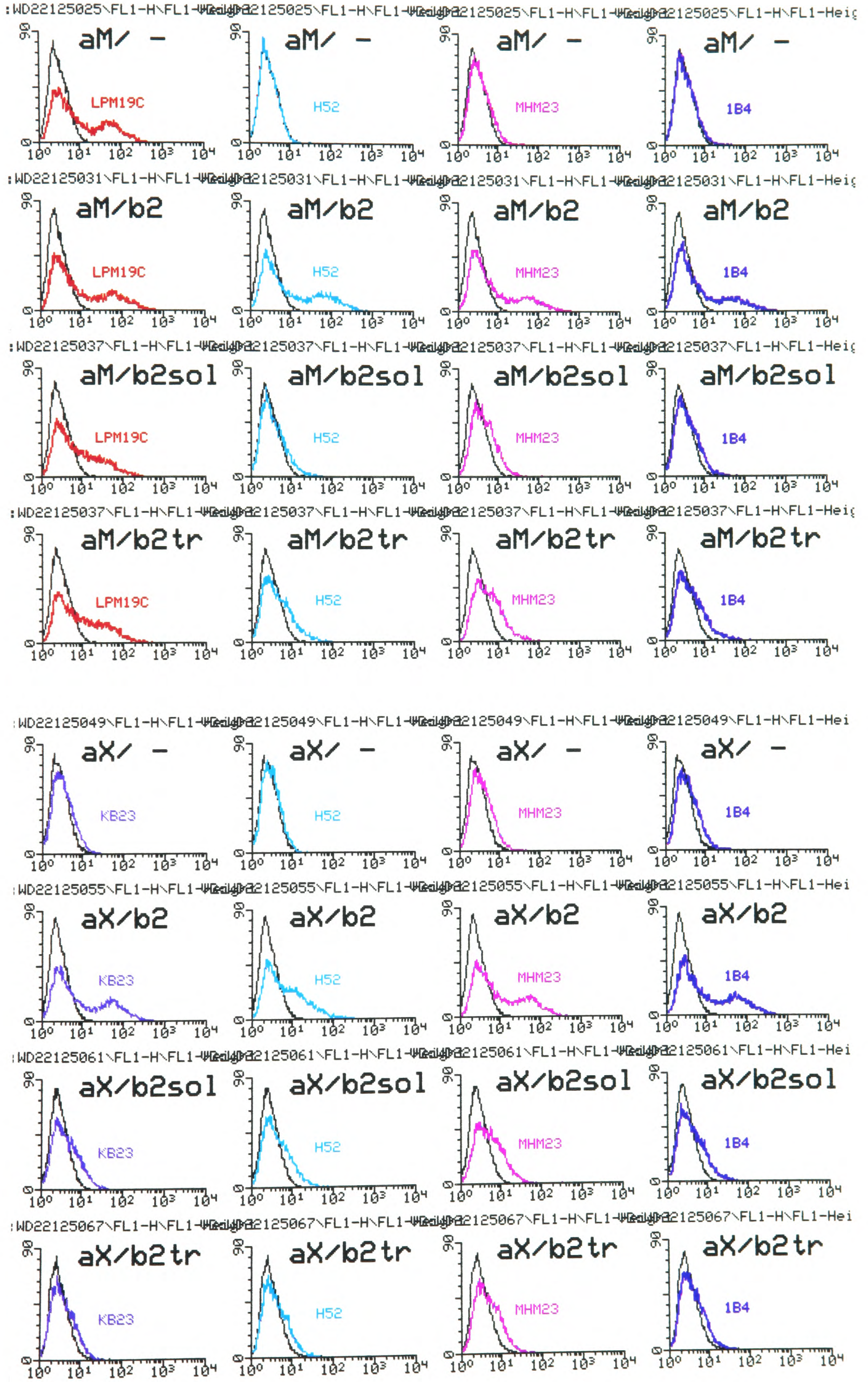
It was therefore concluded that when COS 7 cells are transfected with either β2sol or β2tr alone, the resulting β2sol and β2tr subunits are not expressed on the cell surface by association with an endogenous COS 7 cell counter-subunit, but are either retained and degraded within the cells or are secreted into the tissue culture media. However, when

Figure 4.6: Analysis of the Expression of the β2sol and β2tr Subunits and Their Ability to Form Heterodimers with the Wildtype αL, αM and αX Subunits by Flow Cytometry

COS 7 cells were either transfected with wildtype αL, wildtype αM, wildtype αX, wildtype β2, β2sol or β2tr alone, or were cotransfected with wildtype αL, αM or αX and wildtype β2, β2sol or β2tr, and the expression of the wildtype, soluble and truncated subunits on the COS cell surface was analysed by flow cytometry. Transfectants were labelled with an irrelevant mAb (OX34; anti-rat CD2) to indicate the amount of fluorescence due to non-specific binding of mAbs to COS 7 cells (black profiles), or were labelled with the anti-human leukocyte integrin mAbs: MHM24 (anti-αL; green overlays), LPM19c (anti-αM; red overlays), KB23 (anti-αX; mauve overlays), H52 (anti-β2; light blue overlays), MHM23 (anti-β2 heterodimer; pink overlays) or 1B4 (anti-β2 heterodimer; dark blue overlays). Samples were then stained with a fluorescently labelled rabbit anti-mouse second antibody, and the level of fluorescence on the surface of each cell was measured using a Becton Dickinson FACScan flow cytometer. The flow cytometry profiles obtained are shown overleaf. In each profile, fluorescent intensity (in arbitary units) is plotted along the horizontal axis, and cell number is plotted along the vertical axis. Cell surface expression of the wildtype, soluble and truncated β2 subunits is indicated by detection of the H52 mAb epitope, whereas the expression of wildtype and modified LFA-1, Mac-1 or p150,95 heterodimers on the COS cell surface is indicated by the expression of the MHM23 and 1B4 mAb epitopes.


:WD22125073\FL1-H\FL1-H
- /b2
H52
MHM23
1B4
:WD22125079\FL1-H\FL1-H
- /b2sol
H52
MHM23
1B4
:WD22125085\FL1-H\FL1-H
- /b2tr
H52
MHM23
1B4


WD22125001\FL1-H\FL1-H
aL/ -
MHM24
H52
MHM23
1B4
WD22125007\FL1-H\FL1-H
aL/b2
MHM24
H52
MHM23
1B4
WD22125013\FL1-H\FL1-H
aL/b2sol
MHM24
H52
MHM23
1B4
WD22125019\FL1-H\FL1-H
aL/b2tr
MHM24
H52
MHM23
1B4


aM/ -
LPM19C
H52
MHM23
1B4
aM/b2
aM/b2sol
aM/b2tr
aX/ -
KB23
aX/b2
aX/b2sol
aX/b2tr

COS 7 cells are cotransfected with either αL, αM or αX and β2sol or β2tr, the modified β2 subunits are able to associate with the wildtype α subunits and are expressed on the cell surface in modified αβ heterodimeric complexes. The modified LFA-1 heterodimers are efficiently expressed on the COS 7 cell surface, whereas the modified Mac-1 and p150,95 heterodimers are expressed at lower levels. Interestingly, although both modified subunits supported LFA-1 heterodimer formation equally well, the β2tr subunit appeared to support Mac-1 heterodimer formation more efficiently than the β2sol subunit, whereas the β2sol subunit appeared to support p150,95 heterodimer formation more efficiently than the β2tr subunit.

4.2.1.2.3 Summary of the Expression of the Chimeric, Soluble and Truncated β2 Subunits

The flow cytometry and immunoprecipitation results obtained with the chimeric, soluble and truncated β2 subunits are summarised in Tables 4.3a and 4.3b. All the β2/β1 and β2/β7 chimeras could be expressed on the cell surface as monomers. The β2NS1 and β2NS7 monomers were expressed at levels almost as high as the wildtype β2 monomers, whereas the β2V7 and β2V72 monomers were expressed less efficiently, and the β2V1 and β2V12 monomers were expressed at very low levels. All the chimeric subunits, as well as the β2sol and β2tr subunits, retained the ability to associate with the wildtype αL subunit to form variant LFA-1 heterodimers. The αLβ2sol and αLβ2tr heterodimers were expressed on the COS 7 cell surface at moderately high levels, and the chimeric LFA-1 heterodimers were expressed at levels equal to, or slightly higher than, the chimeric monomers. It was therefore concluded that all the modified β2 subunits could support LFA-1 heterodimer formation with similar efficiency, but that the level of expression of the variant LFA-1 heterodimers was limited by the level of expression of the modified β2 subunits. Interestingly, the chimeric, soluble, and truncated β2 subunits all supported LFA-1 heterodimer formation far more efficiently than Mac-1 or p150,95 heterodimer formation. Only the chimeric subunits which were most efficiently expressed on COS 7 cells, β2V7, β2V72, β2NS1 and β2NS7, formed variant Mac-1 or p150,95 heterodimers which could be detected on the cell surface by flow cytometry, and these chimeric subunits appeared to support Mac-1 heterodimer formation more efficiently than p150,95 heterodimer formation. However, it should be noted that αMβ2V12 heterodimers, which were not detected by flow cytometry, were detected by the more sensitive method of immunoprecipitation. It is

Table 4.3a: Summary of the Results Obtained by Flow cytometry

The table below summarises the expression results obtained by flow cytometry. The ability of the various chimeric, soluble and truncated β2 subunits to express on the COS 7 cell surface as monomers and as variant LFA-1, Mac-1 and p150,95 heterodimers is indicated by positive and negative signs, with "+++++" indicating very high expression levels, "++++" high expression levels, "+++" medium expression levels, "++" low expression levels, "+" very low expression levels, and "-" no expression detected by flow cytometry.

	Monomers	LFA-1	Mac-1	p150,95
WT β2	++++	+++++	+++++	+++++
β2V1	+	+	-	-
β2V7	++	+++	+	+
β2V12	+	+	-	-
β2V72	++	+++	+	-
β2NS1	+++	++++	++	+
β2NS7	+++	++++	++	+
β2sol		+++	+	++
β2tr		+++	++	+

Table 4.3b: Summary of the Results Obtained by Immunoprecipitation

The table below summarises the expression results obtained by immunoprecipitation, using the anti-β2 mAb H52. The ability of the various chimeric, soluble and truncated β2 subunits to express on the COS 7 cell surface as monomers and as variant LFA-1, Mac-1 and p150,95 heterodimers is indicated as follows: "+" indicates that expression of a particular monomer or heterodimer was detected by immunoprecipitation with H52, and "ND" that expression of a particular monomer or heterodimer was not determined by immunoprecipitation.

	Monomers	LFA-1	Mac-1	p150,95
WT β2	+	+	+	+
β2V1	ND	ND	ND	ND
β2V7	+	+	ND	ND
β2V12	+	+	+	ND
β2V72	+	+	+	ND
β2NS1	+	+	+	+
β2NS7	+	+	+	+
β2sol		ND	ND	ND
β2tr		ND	ND	ND

therefore possible that all the chimeric subunits can weakly support Mac-1 and p150,95 formation, but that the resulting heterodimers are often expressed at levels too low to be detected by flow cytometric analysis alone. Although the β2tr subunit, like the chimeric β2/β1 and β2/β7 subunits, also appeared to associate with the wildtype αM subunit more efficiently than with the wildtype αX subunit, it should be noted that the expression of the β2sol subunit was slightly different, as it appeared to associate with the wildtype αX subunit more efficiently than with the wildtype αM subunit.

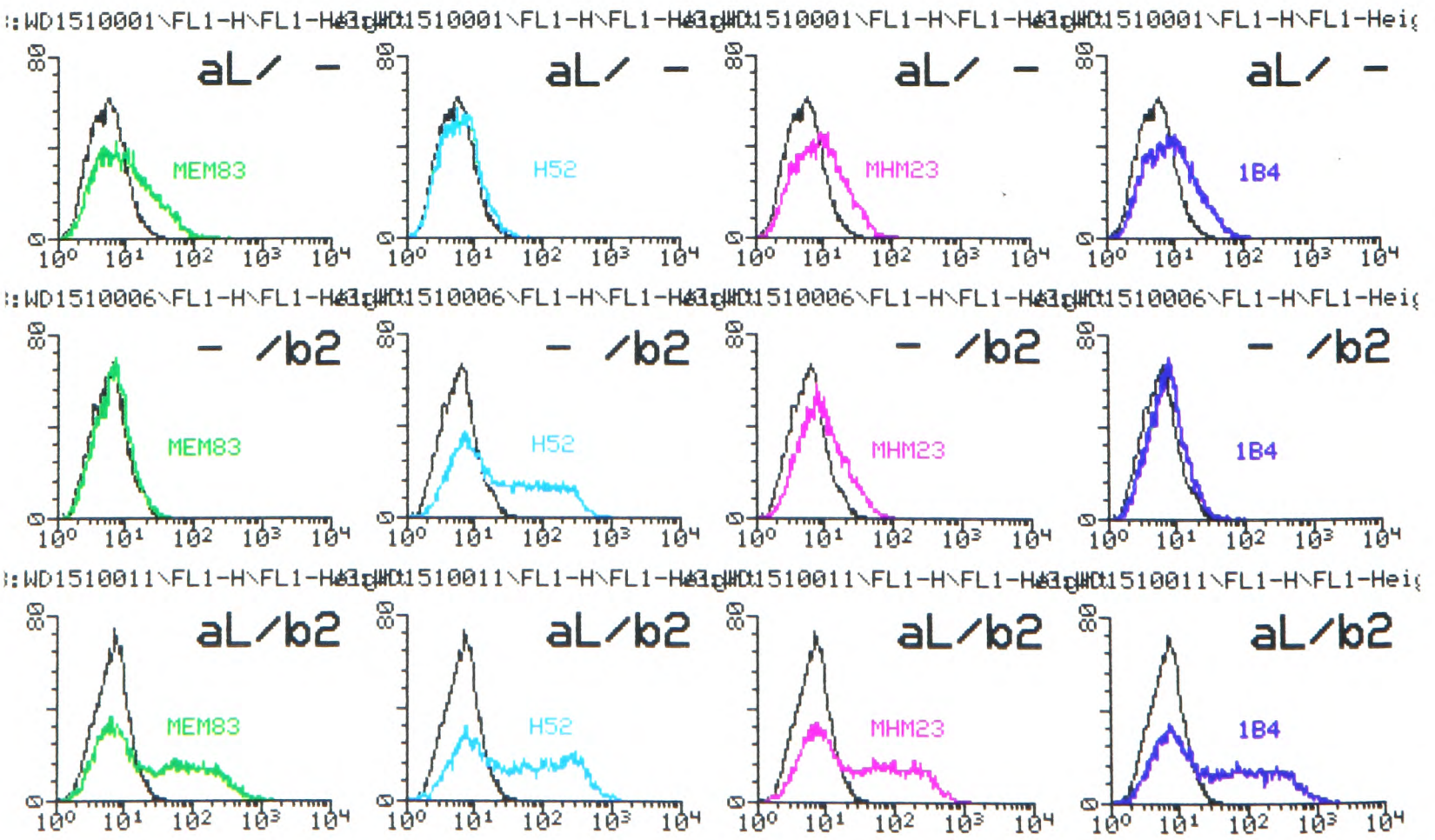
4.2.2 THE BINDING OF WILDTYPE AND MODIFIED LFA-1 TO ICAM-1

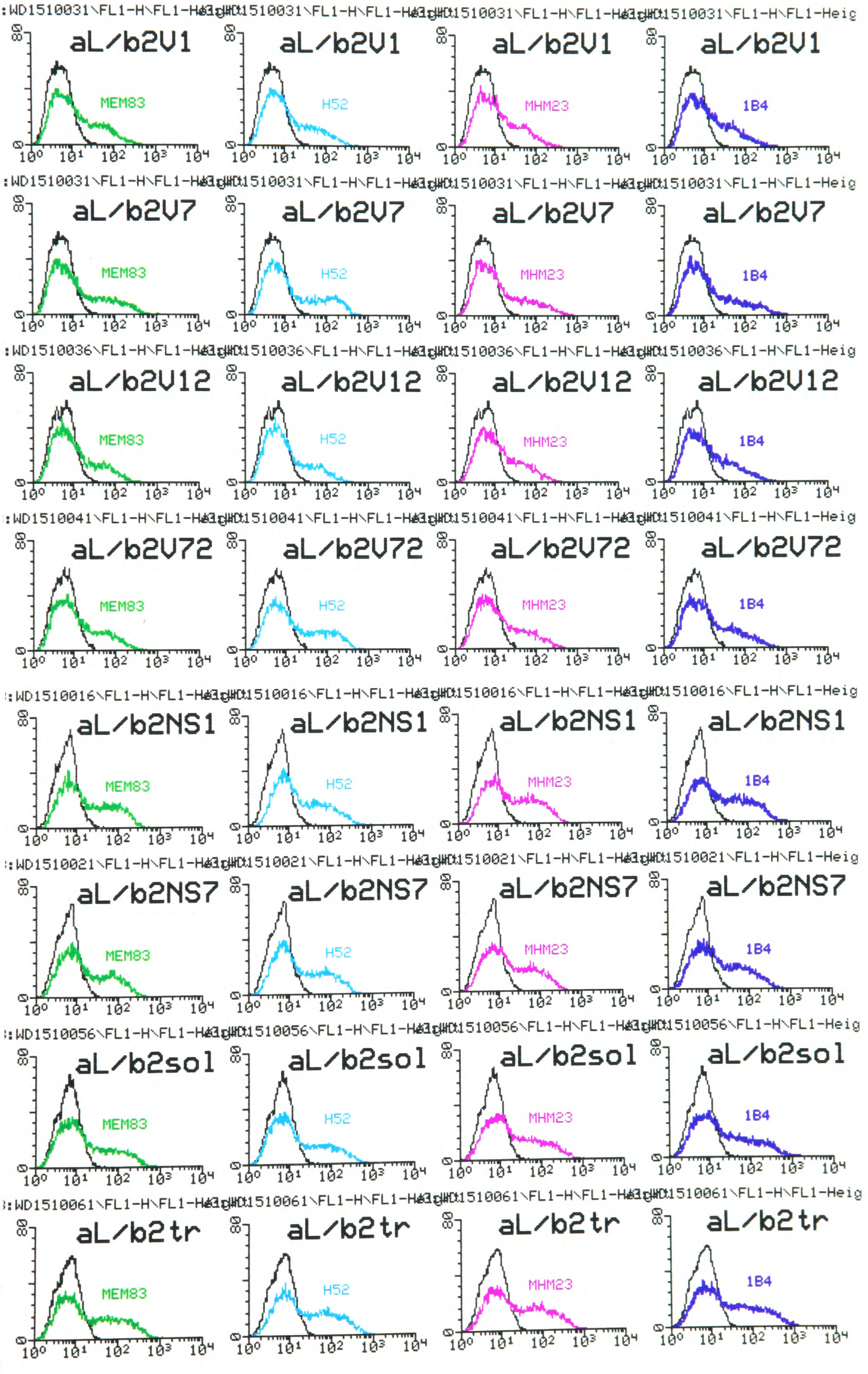
The COS 7 cell expression system was then used to analyse the effect that the variant β2 subunits have on the ligand binding properties of intact αβ integrin complexes. As the chimeric, soluble and truncated β2 subunits all supported LFA-1 heterodimer formation far more efficiently and uniformly than Mac-1 or p150,95 heterodimer formation, studies were focused on the ligand binding abilities of the modified LFA-1 heterodimers.

COS 7 cells were transfected with the wildtype αL or β2 subunits alone, or were cotransfected with the wildtype αL and β2 subunits, or the wildtype αL subunit and a variant β2 subunit, and the resulting transfectants were analysed by flow cytometry (See Figure 4.7). In this set of transfections, all the modifed β2 subunits were very efficiently expressed on the cell surface in LFA-1 heterodimeric complexes. The αLβ2sol, αLβ2tr, αLβ2NS1 and αLβ2NS7 heterodimers were all expressed at levels as high as wildtype αLβ2, whereas the αLβ2V1, αLβ2V7, αLβ2V12 and αLβ2V72 heterodimers were expressed at slightly lower levels. It should be noted that the activating mAb MEM83, which recognises the I-domain of the αL subunit (Landis *et al.*, 1993), was used for flow cytometric analysis instead of the MHM24 mAb. Like the MHM24 epitope, the MEM83 epitope was not detected on the surface of the β2 transfectants, but was expressed at low levels on the surface of the αL transfectants, and at very high levels on the surface of the αLβ2 cotransfectants, indicating that the MEM83 epitope is expressed on both the monomeric and heterodimeric forms of the αL subunit. As expression of the MEM83 epitope paralleled expression of the MHM23 and 1B4 epitopes on the wildtype and on the eight different variant αβ cotransfectants, it was also concluded that the MEM83 epitope is expressed on the wildtype and modified LFA-1 heterodimers with equal efficiency.

Figure 4.7: Flow Cytometric Analysis of the COS 7 Transfectants used in the Adhesion Assay to ICAM-1

COS 7 cells were either transfected with wildtype αL or wildtype β2 alone, or were cotransfected with wildtype αL and wildtype β2, β2V1, β2V7, β2V12, β2V72, β2NS1, β2NS7, β2sol or β2tr, and the expression of the wildtype and variant subunits on the COS cell surface was analysed by flow cytometry. Transfectants were labelled with an irrelevant mAb (OX34; anti-rat CD2) to indicate the amount of fluorescence due to non-specific binding of mAbs to COS 7 cells (black profiles), or were labelled with the anti-human leukocyte integrin mAbs: MEM83 (anti-αL; green overlays), LPM19c (anti-αM; red overlays), KB23 (anti-αX; mauve overlays), H52 (anti-β2; light blue overlays), MHM23 (anti-β2 heterodimer; pink overlays) or 1B4 (anti-β2 heterodimer; dark blue overlays). Samples were then stained with a fluorescently labelled rabbit anti-mouse second antibody, and the level of fluorescence on the surface of each cell was measured using a Becton Dickinson FACScan flow cytometer. In the flow cytometric profiles shown, fluorescent intensity (in arbitary units) is plotted along the horizontal axis, and cell number is plotted along the vertical axis. Cell surface expression of the wildtype and variant β2 subunits is indicated by detection of the H52 mAb epitope, whereas the expression of wildtype and modified LFA-1, Mac-1 or p150,95 heterodimers on the COS 7 cell surface is indicated by the expression of the MHM23 and 1B4 mAb epitopes.




aL/b2V1
MEM83
H52
MHM23
1B4
aL/b2V7
aL/b2V12
aL/b2V72
aL/b2NS1
aL/b2NS7
aL/b2sol
aL/b2tr

These COS 7 cell transfectants were tested for their ability to bind to the LFA-1 ligand ICAM-1 (See Figure 4.8). Microtitre wells were coated with a goat anti-human Fc (GAH) polyclonal antibody followed by an ICAM-1/Fc fusion protein, and the adhesion of the transfected cells to the resulting ICAM-1/Fc/GAH coated plates was studied (Figure 4.8a). To provide an estimate of the percentage of transfected cells expressing LFA-1 heterodimers at levels high enough to attach cells to plates, the binding of transfectants to microtitre wells coated with either the MHM23 or 1B4 mAbs was analysed (the last two columns on the right of each panel). It should be noted that the percentage of transfected cells binding to the MHM23 or 1B4 coated plates was comparable to the expression levels of the MHM23 and 1B4 epitopes detected by flow cytometry (See Figure 4.7). The ICAM-1 binding ability of unactivated transfectants (shown as open columns in each panel) and also of MEM83 activated transfectants (shown as grey shaded columns in each panel) was analysed. The αL transfectants and the β2 transfectants did not adhere to the ICAM-1 coated plates, even when activated with the MEM83 mAb, and the αLβ2 cotransfectants only adhered when activated with MEM83. However, the αLβ2sol, αLβ2tr, αLβ2V1, αLβ2V7, αLβ2V12, αLβ2V72, αLβ2NS1 and αLβ2NS7 cotransfectants all adhered readily to the ICAM-1 coated plates in the absence of the activating mAb, and the level of binding was actually higher than that observed with the activated wildtype αLβ2 cotransfectants. With the exception of the αLβ2V72 cotransfectants, the binding of the modified LFA-1 cotransfectants was enhanced to even higher levels upon activation with MEM83. It should be noted that the adhesion of transfected cells to the ICAM-1 coated plates was LFA-1 specific, as binding was blocked by the anti-LFA-1 mAb MHM23 (shown as overlapping columns in the foreground), and that adhesion was also ICAM-1 specific, as no binding was observed on plates coated with only the goat anti-human Fc (GAH) capture antibody (Figure 4.8b).

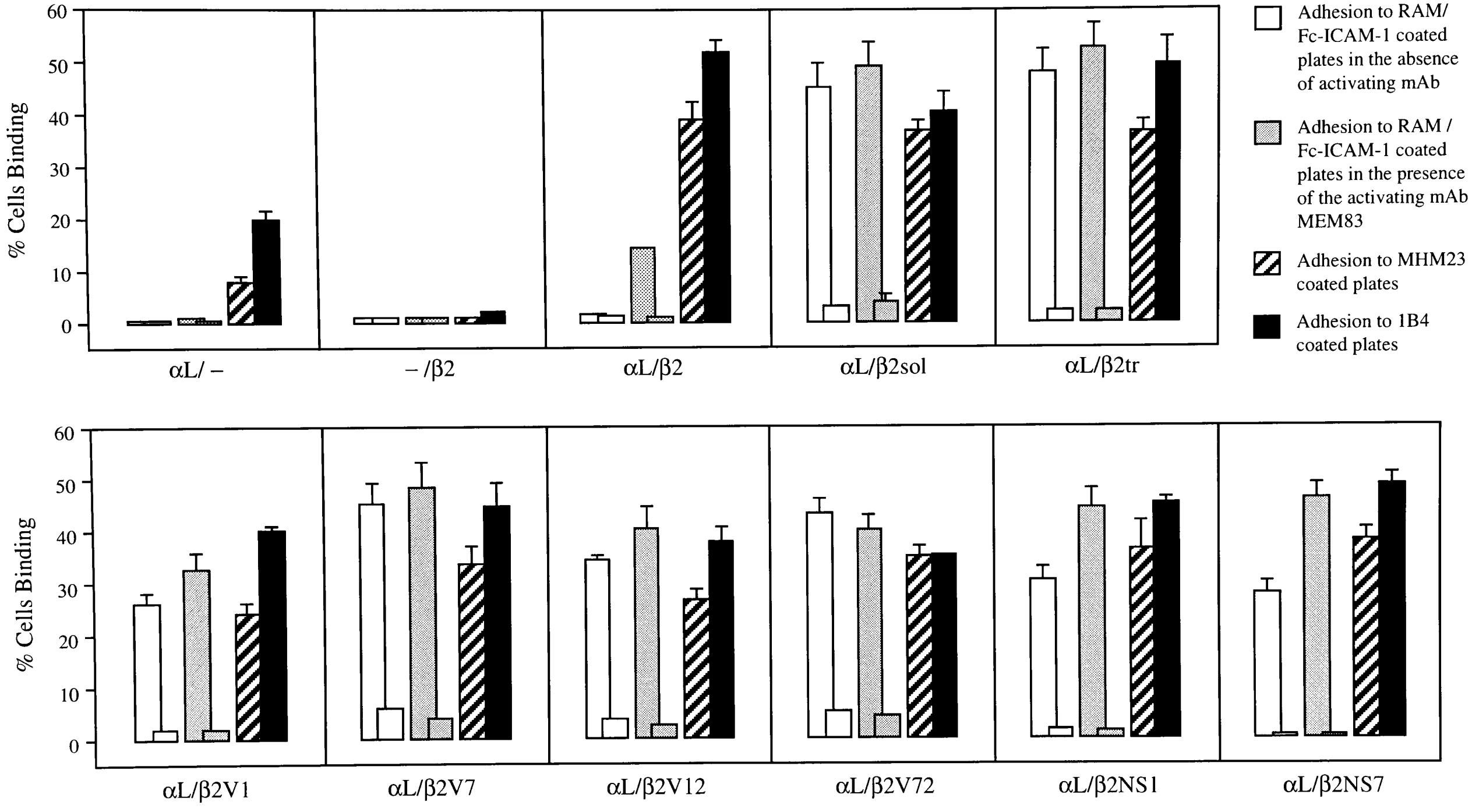
These results therefore suggest that the chimeric, soluble and truncated β2 subunits can all combine with the wildtype αL subunit to form modified LFA-1 heterodimeric complexes which retain the ICAM-1 ligand binding site and are constitutively active with respect to ICAM-1 ligand binding.

Figure 4.8: The Adhesion of COS 7 Cells Expressing Wildtype and Modified LFA-1 to ICAM-1

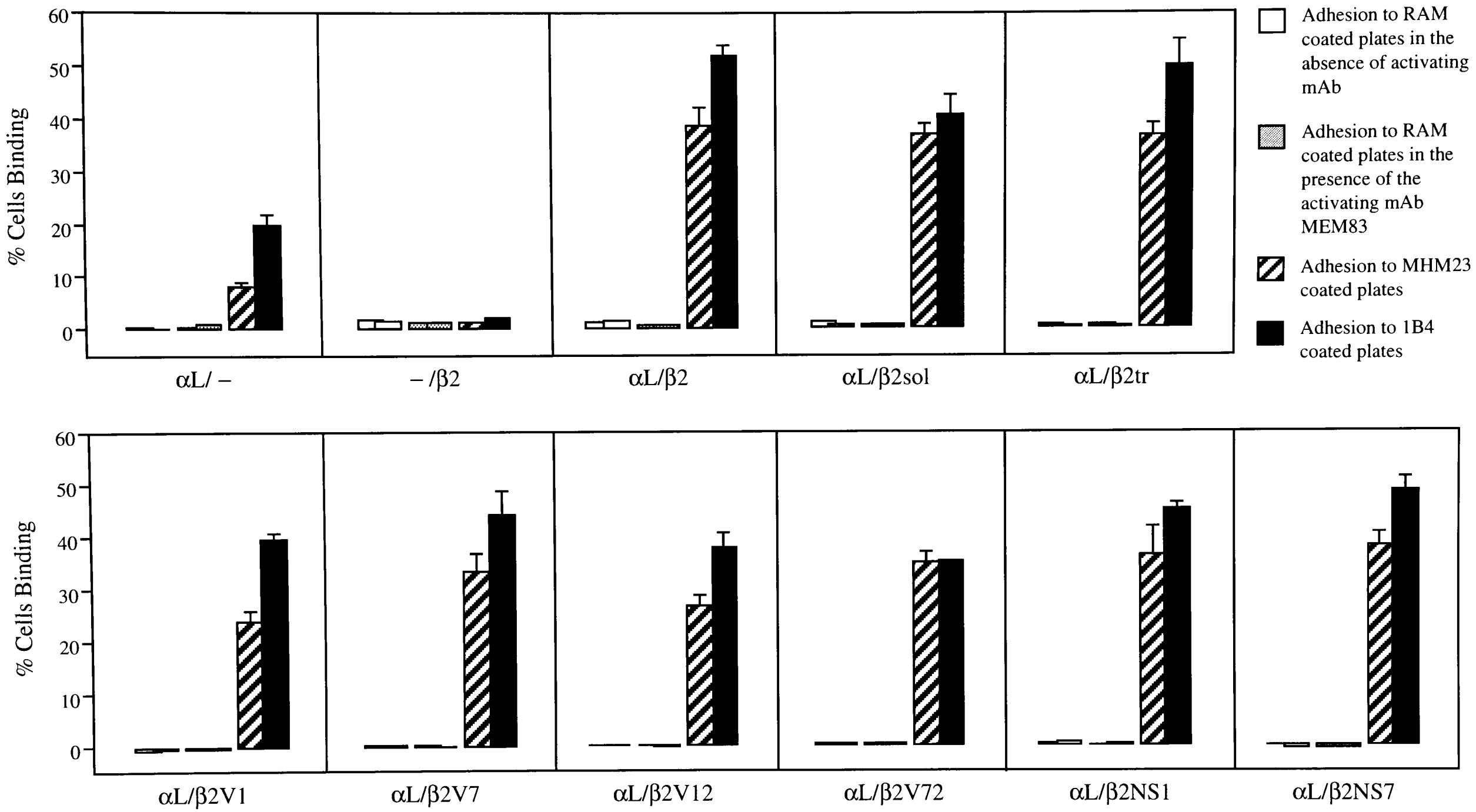
COS 7 cells were transfected with wildtype αL or wildtype β2 alone, or were cotransfected with wildtype αL and wildtype β2, or wildtype αL and β2sol, β2tr, β2V1, β2V7, β2V12, β2V72, β2NS1 or β2NS7, and the resulting transfectants were analysed for their ability to adhere to microtitre plates coated with (a) a goat anti-human Fc polyclonal antibody followed by an ICAM-1/Fc fusion protein (ICAM-1/Fc/GAH plates), and (b) microtitre plates coated with only the goat anti-human Fc polyclonal antibody (GAH-plates). The results for each transfectant are shown in separate panels, with the binding data shown in overlapping pairs of columns, with the right foreground columns showing data obtained in the presence of the blocking mAb MHM23 (anti-β2 heterodimer). The unshaded columns represent the adhesion of transfectants to microtitre plates in the absence of an activating mAb, and the grey shaded columns adhesion to the same plates in the presence of the activating mAb MEM83 (anti-αL). The columns with diagonal lines represent the adhesion of transfectants to microtitre plates coated with the mAb MHM23 (anti-β2 heterodimer), and the black columns adhesion to microtitre plates coated with the mAb 1B4 (also anti-β2 heterodimer). These last two columns provide an estimate of the percentage of cells expressing heterodimeric LFA-1 at levels sufficiently high enough to support adhesion of cells to microtitre plates for the duration of the adhesion assay.

It should be noted that COS transfectants expressing wildtype LFA-1 only adhered to ICAM-1 coated plates in the presence of the activating mAb MEM83, whereas previously (Larson *et al.*, 1990; Hibbs *et al.*, 1991b) it has been reported that wildtype LFA-1 expressed on the surface of COS transfectants is constitutively active with respect to ICAM-1 binding.

(a) Adhesion of Transfectants to Microtitre Plates Coated With ICAM-1/Fc/GAH



(b) Adhesion of Transfectants to Microtitre Plates Coated with GAH Only



4.2.3 EPITOPE MAPPING OF ANTI-β2 MONOCLONAL ANTIBODIES

COS 7 cell transfectants expressing monomeric β2, β2V7, β2V72 and β2NS7 were used to map the epitopes recognised by the anti-human β2 mAbs listed in Table 4.4. The expression of mAb epitopes on the surface of transfectants was assessed by flow cytometry (see Figure 4.9), and the results are summarised in Figure 4.10. All of the transfectants expressed the H52 epitope, confirming expression of the monomeric β2, β2V7, β2V72, and β2NS7 subunits on the cell surface. The KIM182, KIM185, KIM202 and KIM215 epitopes were expressed on the surface of the wildtype β2 transfectants and also on the surface of the chimeric β2V7, β2V72, and β2NS7 transfectants, whereas the KIM89, KIM127, and KIM170 epitopes were only expressed on the surface of the wildtype β2 transfectants. From these results, it is possible to map the epitopes for the H52, KIM182, KIM185, KIM202 and KIM215 mAbs to the N-terminal 436 amino acids of the β2 subunit, whereas the epitopes for the KIM89, KIM127 and KIM170 mAbs can only be mapped to the entire β2 subunit (see Figure 4.10). The epitopes for the KIM series of mAbs have previously been mapped to distinct regions of the human β2 subunit by analysing their expression on a series of mouse/human β2 chimeras (Stephens *et al.*, 1995). By comparing the published epitope mapping results with the results presented in this thesis (See Figure 4.11a and 4.11b), it is possible to localise the KIM182 and KIM185 epitopes to a region of the β2 subunit between amino acids 406-436, the KIM127 and KIM170 epitopes to a region of the β2 subunit between amino acids 406-577, the H52, KIM202, and KIM215 epitopes to the N-terminal 436 amino acids, and the KIM89 epitope to the N-terminal 577 amino acids (See Figure 4.11c). However, it should be noted that the mapping study described in this thesis and the mapping study described by Stephens *et al* (1995) were performed very differently. Whereas in the work presented here, the expression of epitopes on chimeric β subunits was determined for flow cytometric analysis of chimeric β transfectants, in the work published by Stephens *et al* (1995), expression of mAb epitopes on chimeric β subunits was determined by analysing the binding of mAbs to Western blots of whole cell lysates prepared from chimeric β transfectants. Thus, the combined epitope map illustrated in Figure 4.11c must be considered tentative, and will be subject to verification and refinement by future experiments.

Table 4.4: The Monoclonal Antibodies used in the Epitope Mapping Study

The table below lists the mAbs whose epitopes were partially mapped by determining their expression on the chimeric β2V7, β2V72 and β2NS7 subunits.

mAb	Isotype	Epitope Recognised	Reference
H52	IgG1	Human β2	Hildreth and August, 1985
KIM89	IgG2a	Human β2	Stephens *et al.*, 1995
KIM127	IgG1	Human β2	Robinson *et al.*, 1992
KIM170	IgG1	Human β2	Stephens *et al.*, 1995
KIM182	IgG1	Human β2	Stephens *et al.*, 1995
KIM185	IgG1	Human β2	Andrew *et al.*, 1993
KIM202	IgG1	Human β2	Stephens *et al.*, 1995
KIM215	IgG1	Human β2	Stephens *et al.*, 1995

Figure 4.9: Expression of the KIM89, KIM127, KIM170, KIM182, KIM185, KIM202 and KIM215 mAb Epitopes on the Wildtype and Chimeric β2 Subunits

COS 7 cells were transfected with wildtype β2 or chimeric β2V7, chimeric β2V72 or chimeric β2NS7 alone, and the resulting expression of monomeric β subunits on the COS cell surface was analysed by flow cytometry. Transfectants were labelled with an irrelevant mAb (OX34; anti-rat CD2) to indicate the amount of fluorescence due to the non-specific binding of mAbs to COS 7 cells (black profiles), or were labelled with either the mAb H52 (anti-β2; light blue overlays), or one of the KIM mAbs (anti-β2, red overlays). Samples were then stained with a fluorescently labelled rabbit anti-mouse second antibody, and the level of fluorescence on the surface of each cell was measured using a Becton Dickinson FACScan flow cytometer. The flow cytometry profiles obtained are shown opposite. In each profile, fluorescent intensity (in arbitary units) is plotted along the horizontal axis, and cell number is plotted along the vertical axis. The level of expression of wildtype and chimeric β2 monomers on the surface of transfectants is indicated by the level of expression of the H52 epitope. The expression of each KIM mAb epitope on the surface of the β2V7, β2V72 and β2NS7 transfectants was used to partially map the position of these epitopes on the wildtype β2 subunit (see Figure 4.10).

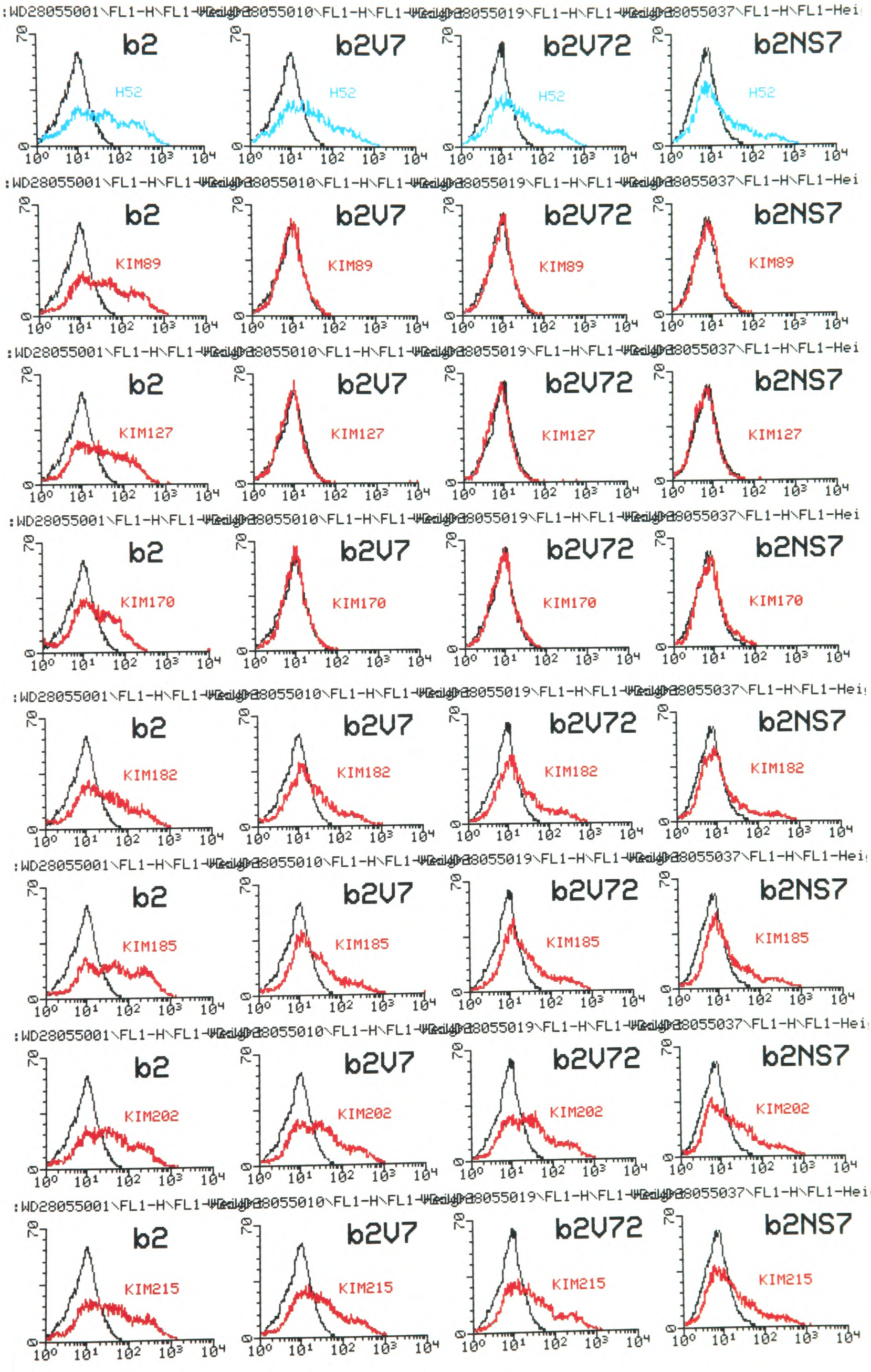

b2
b2V7
b2V72
b2NS7
H52
KIM89
KIM127
KIM170
KIM182
KIM185
KIM202
KIM215

Figure 4.10: Partial Mapping of the KIM mAb Epitopes using the β2/β7 Chimeras

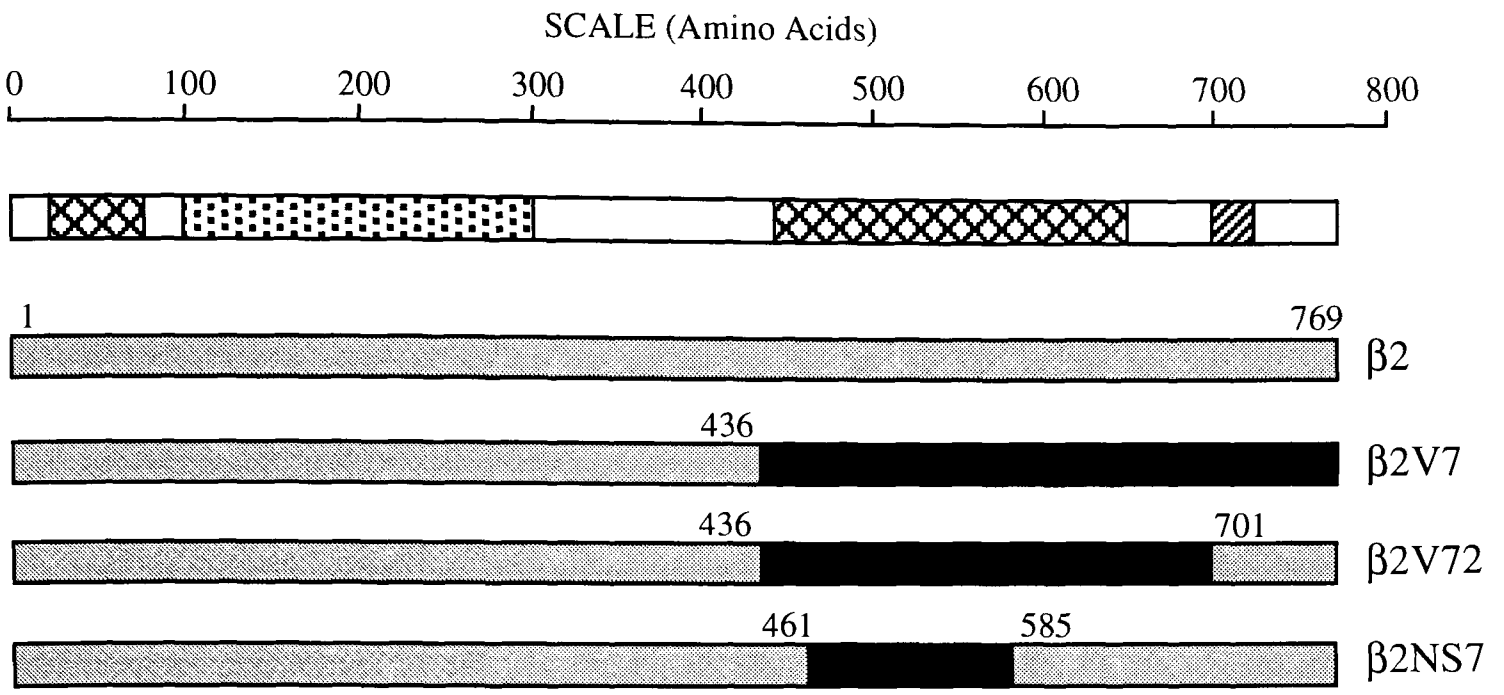
This figure summarises the expression of the KIM mAb epitopes on the chimeric β2/β7 subunits and the mapping of these epitopes to regions within the wildtype β2 subunit using these data:

(a) The chimeric β2V7, β2V72 and β2NS7 subunits are shown, with the β2 regions in each chimera shaded grey and the β7 regions shaded black. The numbers above each subunit refer to the position of β2 amino acid(s) at the chimeric β2/β7 junction(s): amino acids are numbered 1 from the initiation methionine in the β2 leader sequence through to 769 at the C-terminus of the β2 polypeptide. A representative β subunit is shown above the wildtype and chimeric subunits, with the N- and C-terminal cysteine-rich regions indicated by the crosshatched areas, the putative A-domain by the dotted area, and the transmembrane domain by the diagonal lines.

(b) The expression of the H52 and KIM mAb epitopes on the β2V7, β2V72 and β2NS7 chimeras was determined by flow cytometric analysis of COS 7 transfectants (see Figure 4.9). The results are summarised in the table, with the "+" signs indicating expression of an epitope on a chimeric subunit, and the "-" signs indicating loss of an epitope.

(c) As illustrated in the figure, the epitopes for the H52, KIM182, KIM185, KIM202 and KIM215 mAbs were mapped to an N-terminal region of the β2 subunit (amino acids 1-436), but no information on the location of the epitopes for the KIM89, KIM127 and KIM170 mAbs was obtained. For reference, the β subunit is shown in the figure, with the N- and C-terminal cysteine-rich regions indicated by the crosshatched areas, the putative A-domain by the dotted area, and the transmembrane domain by the diagonal lines.

(a) The β2/β7 Chimeras used to Partially Map the KIM mAb Epitopes



(b) Expression of the KIM mAb Epitopes on the β2/β7 Chimeras

Antibody	β2	β2V7	β2V72	β2NS7
H52	+	+	+	+
KIM89	+	−	−	−
KIM127	+	−	−	−
KIM170	+	−	−	−
KIM182	+	+	+	+
KIM185	+	+	+	+
KIM202	+	+	+	+
KIM215	+	+	+	+

(c) Partial Mapping of the KIM mAb Epitopes

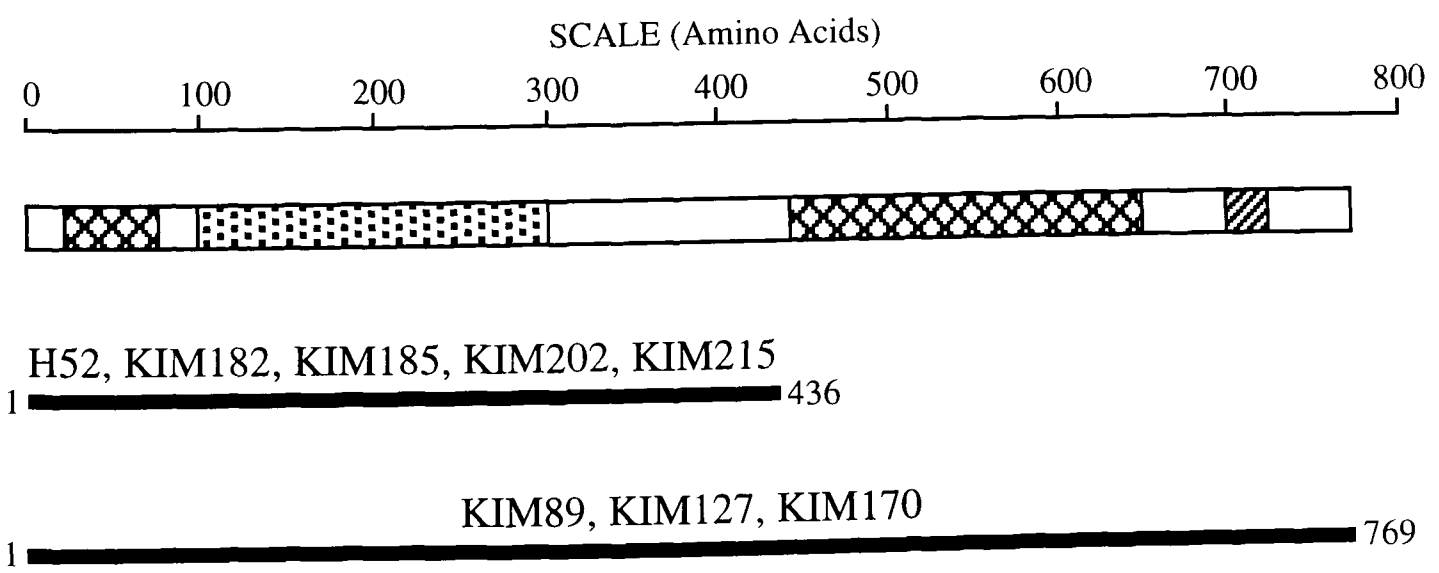


Figure 4.11: Generating an Epitope Map by Combining the Results Presented in this Thesis with the Results Obtained by Stephens *et al* (1995)

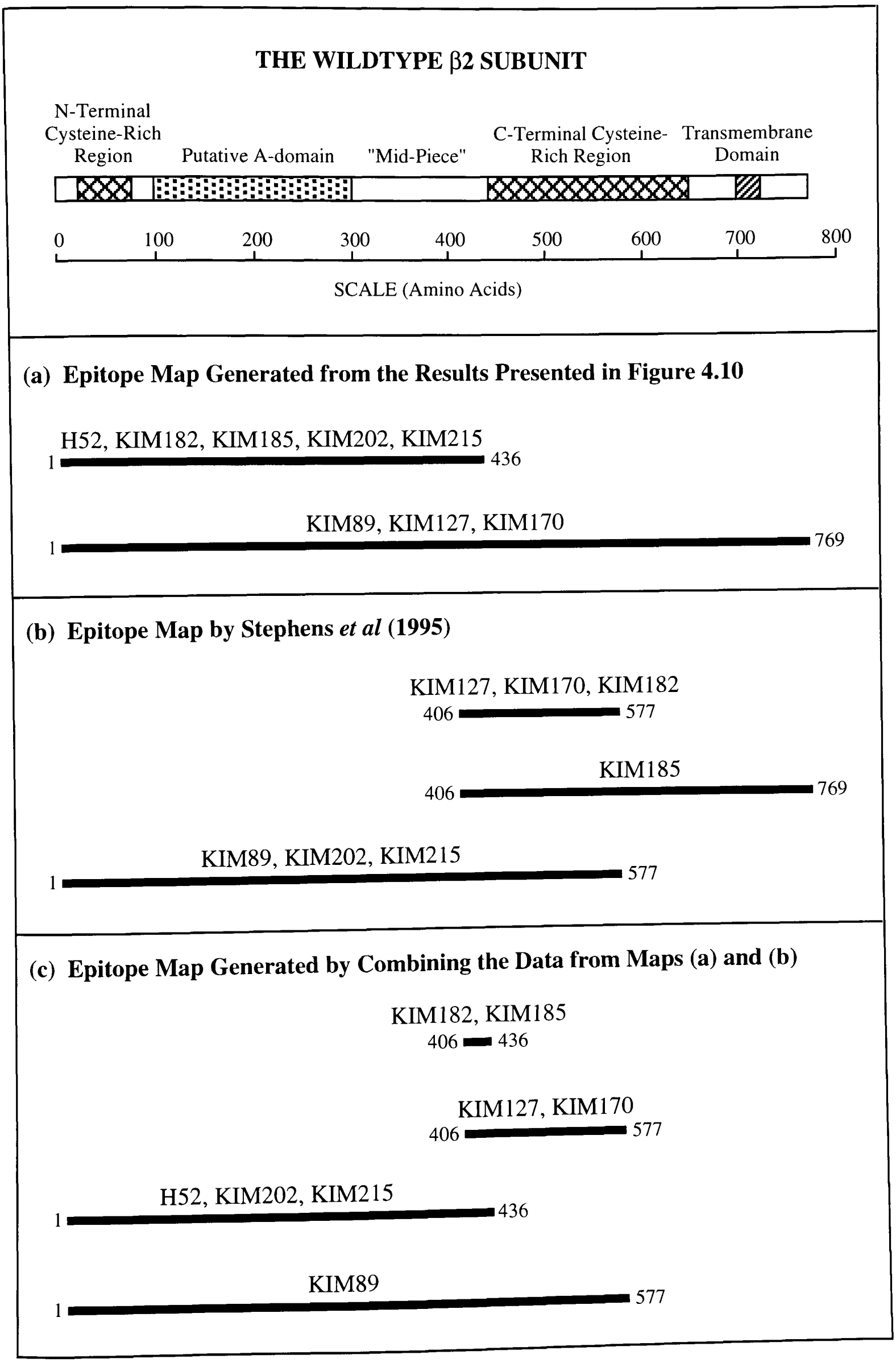


Figure 4.12: Alignment of the Human Integrin β1, β2 and β7 Subunits

The figure below shows the alignment of the human integrin β1, β2 and β7 subunits (without their leader sequences) created using the MULTALIGN programme designed by Dr. G. J. Barton, Laboratory of Molecular Biophysics, Oxford. Amino acid residues which are conserved in all three integrin subunits are shown in blue, whereas residues which are only conserved in two of the subunits are shown in green, and completely unconserved residues are shown in black. For reference purposes, the cysteine residues are shown in red, and are numbered 1 to 56, with C1 representing the first cysteine residue in the extracellular region of the mature β polypeptides, and C56 the last.

```
                                23                                50                                75                               100
HUB1                            ENRCLKANAKSCGECIQAGPNCGWCTNSTFLQEGMPTSARCDDLEALKKKGCPPDDIENPRGSKDIKKNKNVTNRSKGTAEKLKPEDIHQIQPQQLV
HUB2                             QECTKFKVSSCRECIESGPGCTWCQKLNFTGPGDPDSIRCDTRPQLLMRGCAADDIMDPTSLAETQEDHNGGQK                 QLSPQKVT
HUB7  ELDAKIPSTGDATEWRNPHLSMLGSC  QPAPSCQKCILSHPSCAWCKQLNFTASGEAEARRCARREELLARGCPLEELEEPRGQQEVLQDQPLSQGARGEGA       TQLAPQRVR
                                  1       2  3      4  5              6          7

                          125                               150                               175                               200
HUB1    LRLRSGEPQTFTLKFKRAEDYPIDLYYLMDLSYSMKDDLENVKSLGTDLMNEMRRITSDFRIGFGSFVEKTVMPYISTTPAKLRNPCTS EQNCTTPFSYKNVLSLTNKGEVFNEL
HUB2    LYLRPGQAAAFNVTFRRAKGYPIDLYYLMDLSYSMLDDLRNVKKLGGDLLRALNEITESGRIGFGSFVDKTVLPFVNTHPDKLRNPCPNKEKECQPPFAFRHVLKLTNNSNQFQTE
HUB7    VTLRRGEPQQLQVRFLRAEGYPVDLYYLMDLSYSMKDDLERVRQLGHALLVRLQEVTHSVRIGFGSFVDKTVLPFVSTVPSKLRHPCPTRLERCQSPFSFHHVLSLTGDAQAFERE
                                                                                                  8      9

        225                               250                               275                               300                               325
HUB1    VGKQRISGNLDSPEGGFDAIMQVAVCGSLIGWRNVTRLLVFSTDAGFHFAGDGKLGGIVLPNDGQCHLENN MYTMSHYYDYPSIAHLVQKLSENNIQTIFAVTEEFQPVYKEL
HUB2    VGKQLISGNLDAPEGGLDAMMQVAACPEEIGWRNVTRLLVFATDDGFHFAGDGKLGAILTPNDGRCHLEDN LYKRSNEFDYPSVGQLAHKLAENNIQPIFAVTSRMVKTYEKL
HUB7    VGRQSVSGNLDSPEGGFDAILQAALCQEQIGWRNVSRLLVFTSDDTFHTAGDGKLGGIFMPSDGHCHLDSNGLYSRSTEFDYPSVGQVAQALSAANIQPIFAVTSAALPVYQEL
                                  10                                11

                350                               375                               400                               425
HUB1    KNLIPKSAVGTLSANSSNVIQLIIDAYNSLSSEVILENGKLSEGVTISYKSYCK  NGVNGTGENGRKCSNISIGDEVQFEISITSNKCPKKDSDSFKIRPLGFTEEVEVILQYIC
HUB2    TEIIPKSAVGELSEDSSNVVHLIKNAYNKLSSRVFLDHNALPDTLKVTYDSFCS  NGVTHRNQPRGDCDGVQINVPITFQVKVTATECI  QEQSFVIRALGFTDIVTVQVLPQC
HUB7    SKLIPKSAVGELSEDSSNVVQLIMDAYNSLSSTVTLEHSSLPPGVHISYESQCEGPEKREGKAEDRGQCNHVRINQTVTFWVSLQATHCL PEPHLLRLRALGFSEELIVELHTLC
                                                                  12              13                  14                              15

          450                               475                               500                               525                               550
HUB1    ECECQSEGIPESPKCHEGNGTFECGACRCNEGRVGRHCECSTDEVNSEDMDAYCRKENSS EICSNNGECVCGQCVCRKRDNTNEIYSGKFCECDNFNCDRSNGLICGGN  GVC
HUB2    ECRCRDQS RDRSLCH GKGFLECGICRCDTGYIGKNCECQTQGRSSQELEGSCRKDNNS IICSGLGDCVCGQCLCHTSDVPGKLIYGQYCECDTINCERYNGQVCGGPGRGLC
HUB7    DCNCSDTQ PQAPHCSDGQGHLQCGVCSCAPGRLGRLCECSVAELSSPDLEGGCRAPNGTGPLCSGKGHCQCGRCSCSGQSS      GHLCECDDASCERHEGILCGGF  GRC
        1617         18       19 2021       2223            24        25    2627 2829             3031   32      33       34

                          575                               600                               625                               650
HUB1    KCRVCECNPNYTGSACDCSLDTSTCEASNGQICNGRGICECGVCKCTDPKFQGQTCEMCQTCLGVCAEHKECVQCRAFNKGEKKDTCTQECSYFNITKVESRDKLPQPVQPDPVSHC
HUB2    FCGKCRCHPGFEGSACQCERTTEGCLNPRRVECSGRGRCRCNVCEC HSGYQLPLCQECPGCPSPCGKYISCAECLKFEKGPFGKNCSAACPGLQLSNNPVKGR           TC
HUB7    QCGVCHCHANRTGRACECSGDMDSCISPEGGLCSGHGRCKCNRCQCLD GYYGALCDQCPGCKTPCERHRDCAECGAFRTGPLATNCSTACAHTNVTLALAPILDDG         WC
        35 3637       3839     40      41    4243 4445        46 47 48  49    50 51          52  53                            54

                675                               700                               725                               750
HUB1    KEKDVDDCWFYFTYSV NGNNEVMVHVVENPECPTGPDIIPIVAGVVAGIVLIGLALLLIWKLIMIIHDRREFAKFEKEKMNAKWDTGENPIYKSAVTTVVNPKY EGK
HUB2    KERDSEGCWVAYTLEQQDGMDRYLIYVDESRECVAGPNIAAIVGGTVAGIVLIGILLLVIWKALIHLSDLREYRRFEKEKLKSQWNND NPLFKSATTTVMNPKF  AES
HUB7    KERTLDNQLFFF LVEDDARGTVVLRVRPQEK  GADHTQAIVLGCVGGIVAVGLGLVLAYRLSVEIYDRREYSRFEKEQQQLNWKQDSNPLYKSAITTTINPRFQEADSPTL
              55                  56
```

as monomers, and that αβ heterodimer formation is required before the folding process can be completed. Only mature LFA-1 receptors appeared to be expressed on the cell surface, and it was suggested that any monomeric αL and β2 subunits which fail to combine to form LFA-1 heterodimers are retained within the cell and are subsequently degraded. However, the monomeric subunits expressed on the surface of COS cells do appear to be folded correctly. The epitopes of eight different anti-β2 mAbs were expressed on the monomeric β2 subunit (see Figure 4.9), and at least one of these mAbs, KIM127, is known to recognise a conformationally sensitive epitope (Stevens *et al.*, 1995). In addition, under appropriate condtions, the αL transfectants can be stimulated to bind to ICAM-1 and ICAM-2, and the αM transfectants to iC3b and denatured BSA (Dr. S.K.A. Law, unpublished observations). Therefore, it appears that αβ heterodimer formation is not actually required for the correct and complete folding of the leukocyte integrin α and β subunits, suggesting that in leukocytes, a selective mechanism operates to prevent expression of monomeric subunits so that only αβ heterodimeric receptors are expressed on the cell surface. Although COS cells do express other integrins, such as members of the β1 integrin subfamily, they do not normally express β2 integrins, and may therefore lack the correct intracellular machinery required to regulate their expression, explaining the ability of the αL, αM and β2 subunits to be expressed on the COS cell surface in a monomeric, as well as a heterodimeric form. It should be noted that in the experiments discussed here and elsewhere, there is no information on the folding and expression requirements of the αX subunit.

After the initial characterisation of the COS expression system with the wildtype leukocyte integrin subunits, the expression properties of the variant β2 subunits were studied. Like the wildtype β2 subunit, all of the chimeric β2/β1 and β2/β7 subunits could be expressed on the surface of COS cells in a monomeric form, and did not associate with endogenous COS cell counter-subunits. The level of expression of the different chimeric monomers varied, with the two subunits containing the smallest chimeric interchange, β2NS1 and β2NS7, expressing the most efficiently, followed by the β2V7 and β2V72 chimeras, and then the β2V1 and β2V12 chimeras. The expression of the β2/β7 chimeras was generally more efficient than the expression of the β2/β1 chimeras, presumably because the β2 subunit is more closely related to β7 (46.5 % homologous) than it is to β1 (45.7 % homologous). As expected, the β2sol and β2tr subunits were not expressed on the surface of COS cells

transfected with only the β2sol or β2tr constructs, indicating that, like the wildtype and chimeric β2 subunits, the soluble and truncated β2 variants were also unable to combine with endogenous COS cell counter-subunits to form surface expressable hybrid integrin receptors.

The ability of each variant β2 subunit to associate with the wildtype αL, αM and αX subunits to form surface expressable LFA-1, Mac-1 and p150,95 heterodimers was assessed in the COS expression system. All of the chimeric, soluble and truncated β2 variants could efficiently combine with the αL subunit to form modified LFA-1 heterodimers. The six chimeric β2 subunits all appeared to support LFA-1 heterodimer formation with similar efficiency, with the level of expression of each chimeric LFA-1 receptor being limited by the level of expression of the chimeric β2 subunit: the αLβ2NS1 and αLβ2NS7 heterodimers were expressed at high levels, the αLβ2V7 and αLβ2V72 heterodimers at medium levels, and the αLβ2V1 and αLβ2V12 heterodimers at low levels. The modified LFA-1 heterodimers formed with the soluble and the truncated β2 variants, αLβ2sol and αLβ2tr, were expressed at levels similar to the αLβ2V7 and αLβ2V72 heterodimers. Taken together, these results suggest that in LFA-1, the C-terminal cysteine-rich, membrane proximal, transmembrane and cytoplasmic domains of the β2 subunit are not required for interaction with the αL subunit, and that the binding site on β2 for αL must be located within the N-terminal 436 amino acids of the β2 subunit. The ability the variant β2 subunits to form surface expressable Mac-1 or p150,95 receptors was markedly different. All the variant β2 subunits associated far less readily with the αM and αX subunits than they did with the αL subunit, and in each case, the expression of the modified Mac-1 and p150,95 heterodimers was far less efficient than the expression of the modified LFA-1 heterodimers. It therefore appears that the interactions between the β2 subunit and the αM and the αX subunits are far more extensive than the interactions between the β2 and αL subunit, and may involve interaction with regions both N- and C-terminal of residue 436. In addition, each chimeric β subunit, as well as the truncated β subunit, appeared to be able to associate more readily with the αM subunit than with the αX subunit, whereas the soluble β2 subunit appeared to associate more readily with the αX subunit than with the αM subunit. These differences suggest that the regions of the β2 subunit which interact with the αM subunit may be different from the regions of the β2 subunit which interact with the αX subunit. The precise details of the different regions of

the β2 subunit which interact with αL, αM and αX to form LFA-1, Mac-1 and p150,95 heterodimeric complexes could not be determined, but the results presented in this thesis have laid down the foundations for a more detailed experimental analysis of αβ heterodimer formation in Dr. Law's laboratory.

The effect of the various chimeric, soluble and truncated β2 subunit modifications on the ligand binding properties of the intact αβ heterodimers was also investigated. As all the variant β2 subunits supported LFA-1 heterodimer formation far more efficiently and uniformly than they supported the formation of Mac-1 or p150,95, studies were focused on the ligand binding abilites of the modified LFA-1 heterodimers. The ability of these receptors to bind to the LFA-1 ligand ICAM-1 was assessed by examining the adherence of COS cells expressing modified LFA-1 to microtitre plates coated with ICAM-1. All of the modified LFA-1 receptors retained the ability to bind to ICAM-1, indicating that in LFA-1, the C-terminal cysteine-rich and membrane proximal regions of the β2 subunit are not involved in binding ICAM-1, and that the ICAM-1 binding site must therefore be located within the N-terminal 436 amino acids of the β2 subunit. COS cells expressing wildtype LFA-1 adhered to ICAM-1 coated plates poorly unless stimulated with the anti-αL "activating" mAb MEM83. In marked contrast, COS cells expressing the modified LFA-1 receptors adhered readily to ICAM-1 coated plates, even in the absence of the activating mAb, indicating that the modified LFA-1 heterodimers formed from the chimeric, soluble and truncated β2 subunits were all constitutively active with respect to ICAM-1 binding. Therefore, disruption of the conformation of the β2 subunit, either by substituting various regions of β2 with the homologous regions from other β subunits (in the chimeras), or by deleting entire sections of the β2 subunit (in the soluble and truncated variants), resulted in the expression of the activated form of the LFA-1 receptor. A model based on these results, which describes the possible steps involved in the activation of LFA-1, is discussed in detail in Chapter Six.

CHAPTER FIVE

LEUKOCYTE ADHESION DEFICIENCY-I (LAD-I): TRANSIENT EXPRESSION OF MUTANT LFA-1, MAC-1 AND p150,95 IN COS 7 CELLS

5.1 INTRODUCTION

Leukocyte adhesion deficiency-I (LAD-I) is an inherited immunodeficiency disorder caused by defects in the gene encoding the integrin β2 subunit, which results in reduced expression of functional LFA-1, Mac-1 and p150,95 receptors on the surface of leukocytes (reviewed by: Anderson and Springer, 1987; Arnaout, 1990b) (see Chapter 1, Section 1.2.5.3). Adhesion events mediated by the β2 integrins, such as phagocytosis of complement opsonised particles, T cell mediated killing, and trafficking of leukocytes between blood and lymph, are all affected. However, it is the impaired ability of polymorphonuclear leukocytes (PMNs) to migrate across the endothelium to inflammatory sites of infection which results in the classic clinical symptoms of LAD: high white blood cell counts of between 5-15 times that of normal, recurrent bacterial infections of the soft tissues, and impaired pus formation and wound healing. Patients with LAD are generally subdivided into two categories: those with the severe phenotype (where expression of the leukocyte integrins is < 1% of normal) and those with the moderate phenotype (where expression is about 10% of normal). Patients with the severe phenotype usually succumb to infections in early infancy, whereas patients with the moderate phenotype can survive into their 20's or 30's. The defects which result in LAD have been found to be very heterogeneous. Numerous deletions and point mutations have been discovered dispersed throughout the entire β2 gene which affect many stages of β2 subunit synthesis, including initiation of transcription, mRNA stability and splicing, initiation of translation, and the synthesis of mutant β2 subunits which are either aberrantly small or large, or contain amino acid point mutations which affect heterodimer formation or function. Missense point mutations within the coding region of the β2 gene are of particular interest, as they can pinpoint particular residues and regions of the β2 subunit which are critical for αβ heterodimer formation and function. This chapter describes the analysis of three LAD mutations within the coding region of the β2 gene: two missense point mutations and a deletion mutation, and the effect that these mutations have on the expression of the β2 subunit and its ability to associate with the wildtype αL, αM and αX subunits to form functional αβ heterodimeric complexes.

5.2 RESULTS

5.2.1 CHARACTERISATION OF THREE NOVEL LAD MUTATIONS WITHIN THE CODING REGION OF THE β2 GENE

Previous work in Dr. Law's laboratory (Wright *et al.*, 1995; and unpublished observations) had identified three novel, previously uncharacterised mutations within the coding region of the β2 gene (see Table 5.1). Two of these mutations were single base pair substitutions within exon 7 of the β2 gene, which encode single amino acid point mutations within the putative A-domain of the resulting β2 subunits. The other mutation was a two base pair deletion within exon 11 which causes a frameshift and results in a truncated β2 subunit lacking the C-terminal cysteine-rich, transmembrane and cytoplasmic domains. In order to determine whether these defects were LAD mutations, or whether they simply represented alternative but functional forms of the β2 subunit, the effect of each mutation on the expression of the β2 subunit and on its ability to form functional αβ heterodimeric complexes was investigated.

5.2.1.1 Identifying Mutations Within the Coding Region of the β2 Gene

The overall strategy which was employed by Wright *et al* (1995) to identify mutations within the coding region of the β2 gene is summarised in Figure 5.1a. LAD patient EBV transformed B cell lines were used as a source of genetic material. Poly(A) mRNA was isolated from each cell line and was used to synthesise cDNA from each LAD patient. The β2 cDNA was then amplified from LAD patient cDNA by PCR, using taq DNA polymerase. The entire coding region of the β2 cDNA was amplified in five overlapping fragments (see Fig. 5.1a), and these fragments were analysed for the presence of DNA mutations. In order to reduce the amount of nucleotide sequencing required to locate mutations, and also to overcome the problem of confusing PCR errors with real mutations, the chemical cleavage at mismatches (CCM) method (developed by Cotton *et al.*, 1988) was used to screen for mutations in the PCR fragments (see Figure 5.1b). This technique exploits the chemical reactivity of mismatched thymine and cytosine bases in DNA heteroduplexes, and can detect all possible combinations of single-base mismatches, as well as deletions and insertions (Saleeba and Cotton, 1993). The CCM method was used

Table 5.1: The Three Novel Mutations Discovered in the Coding Region of the β2 Gene

Mutation at cDNA Level:			Mutation at Protein Level:		
Position[1]	Nucleotide	Abbreviation[2]	Position[1]	Amino Acid	Abbreviation[2]
809	C to T	C to T^{809}	270	Ala to Val	A270V
850	G to A	G to A^{850}	284	Gly to Ser	G284S
1256	GA deletion	1256ΔGA	418	Frameshift[3]	$T418_{fr*}$

1 The "A" in the initiating "ATG" start codon, and the initiation methionine residue "M" in the resulting polypeptide, were assigned number "1" for the cDNA and protein sequences respectively.

2 The abbreviations used in this chapter for mutations at the cDNA and protein level.

3 The 2 base pair deletion results in a frameshift after the T residue at position 418 and continues with the protein sequence:

VHPGAVVCHPGAGLHGHSDRAGPSPV-Stop

Figure 5.1a: The Overall Strategy Employed to Identify Mutations within the Coding Region of the β2 Gene

EBV transformed B-cell lines from the LAD patients were used as a source of genetic material. For analysis of mutations within the coding region of the β2 gene, total RNA was extracted from each cell line by the guanidine thiocyanate method. Poly(A) mRNA was isolated from the total RNA preps by affinity to oligo dT columns, and was used as a template to prepare cDNA using a cDNA synthesis kit (Amersham Int.). The β2 cDNA, which is shown with its exons and the coding region bounded by the dotted lines in exons 2 and 16, was then amplified from LAD patient cDNA by PCR using Taq DNA polymerase. Two rounds of PCR were required to provide sufficient material for mutation analysis. The first round of PCR synthesised fragments **a** and **b**, which were then used as templates in a second round of PCR to generate fragments **I-V** and fragments **a'** and **b'**. The position of a putative LAD mutation is marked in the figure by a cross (**X**). To reduce the amount of nucleotide sequencing required to identify mutations, and also to overcome the problem of wrongly identifying PCR errors as mutations, the chemical cleavage at mismatches (CCM) method was used to pinpoint the approximate position of mutations in fragments **I-V** (see Figure 5.1b for an explanation of the CCM technique). Fragments **a'** and **b'** were cloned into the vector pBluescript, and the exact position and nature of each mutation was then determined by nucleotide sequencing of regions highlighted by CCM analysis.

LAD Patient

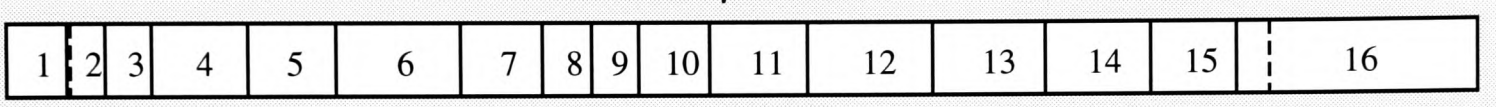
↓

EBV Transformed B-Cell Line

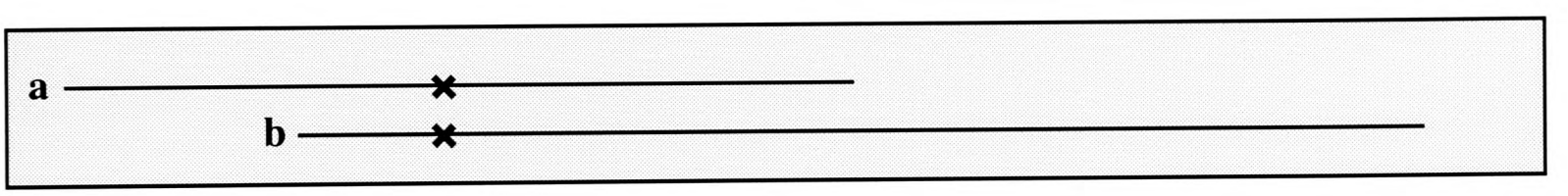
↓

cDNA Library

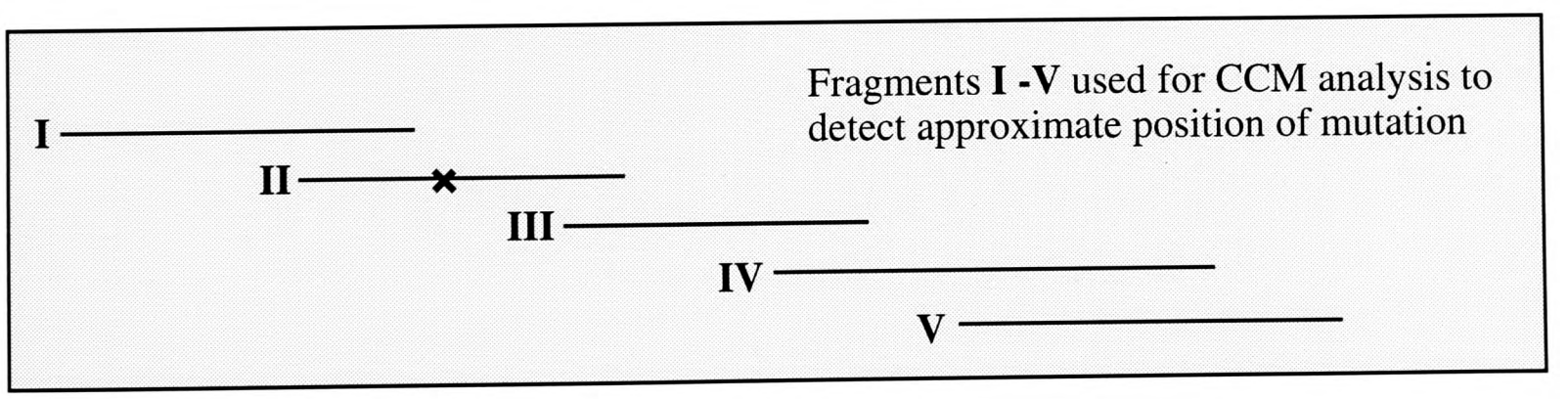
Mutant β2 cDNA



↓ 1st round PCR



↓ 2nd round PCR



+

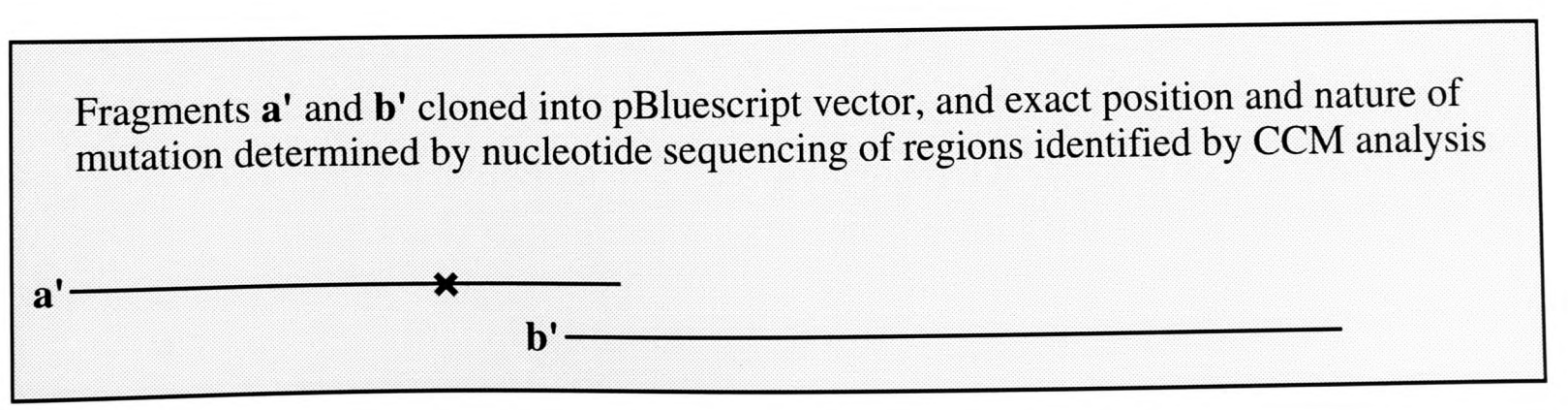
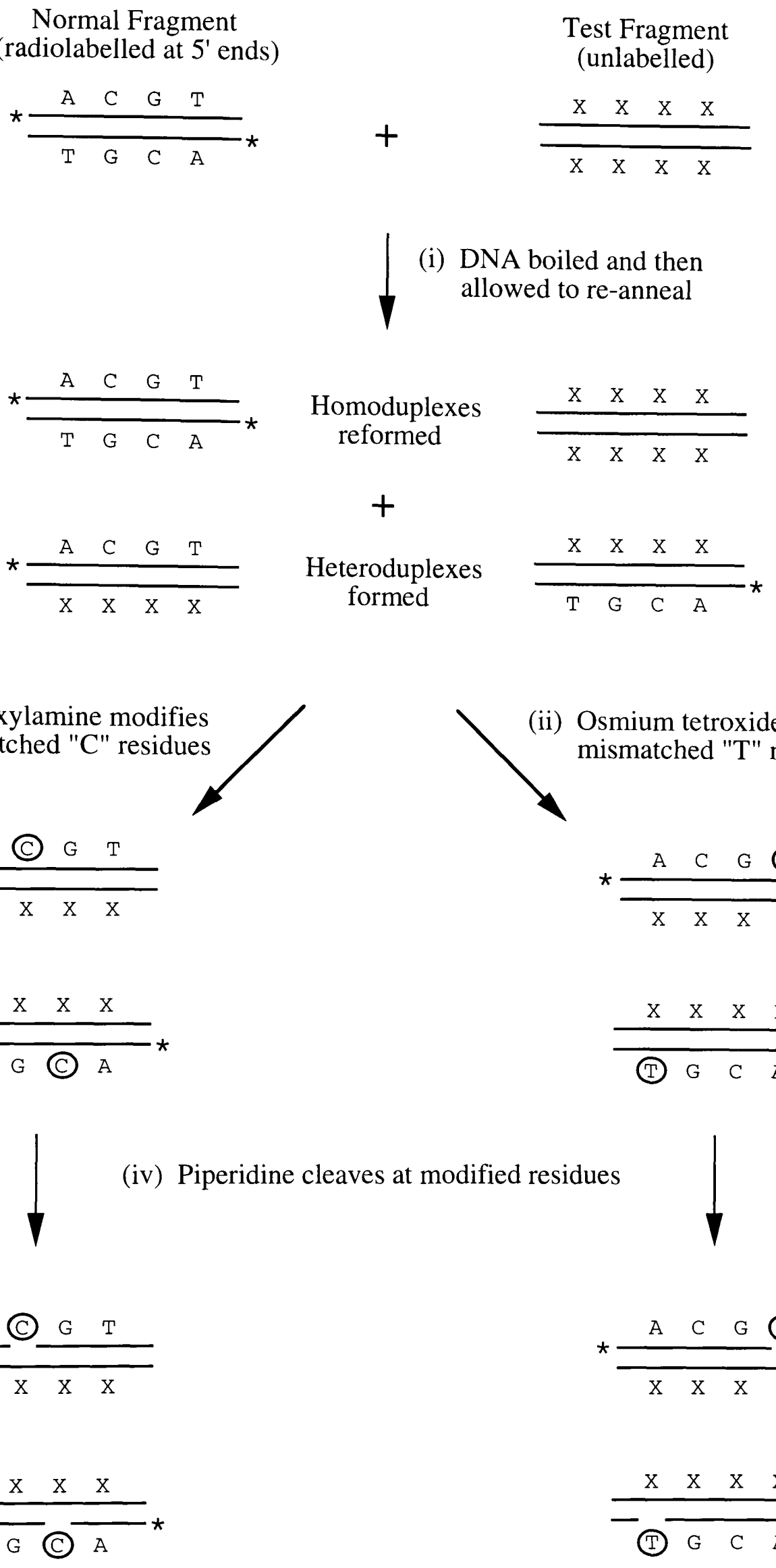


Figure 5.1b: The Chemical Cleavage at Mismatches (CCM) Technique

The chemical cleavage at mismatches (CCM) technique (Cotton *et al.*, 1988; Cotton and Campbell, 1989) was used to pinpoint the approximate position of mutations in the "test" DNA fragments **I-V**, which had been amplified from LAD patient cDNA (see Figure 5.1a). Equivalent "normal" DNA fragments were amplified by PCR from a wildtype β2 cDNA (clone J8; Weitzman *et al.*, 1991), and were radiolabelled at the 5'ends with P^{32}. The radiolabelled normal DNA fragments and the unlabelled test DNA fragments were mixed together, and were then boiled to separate the DNA strands, and were then cooled, allowing the strands to re-anneal. Heteroduplexes containing mismatched or unmatched bases were formed were mutations (indicated in the figure by an X) were present in the test DNA. The mixture was then treated with either hydroxylamine, which modifies mismatched cytosine residues, or osmium tetroxide, which modifies mismatched thymine residues, and the DNA was then cleaved at modified bases by subsequent treatment with piperidine. The cleavage products were then separated on denaturing polyacrylamide gels, and the radiolabelled normal DNA strands were visualised by autoradiography. Cleavage products were detected as smaller bands on gels, and the size of the cleavage products gave an approximate location of the mismatches in the heteroduplex, and hence localised the mutation to one of two possible places within the test fragment. The exact position and nature of the mutation was then determined by nucleotide sequencing these regions in the cloned test fragments **a'** or **b'** (see Figure 5.1a).



(v) Cleavage products are analysed on
denaturing polyacrylamide gels

to locate the approximate position of mutations in the five PCR fragments of each LAD patient, and then the exact location and nature of each mutation was determined by nucleotide sequencing of relevent regions in cloned PCR products. Three novel, previously uncharacterised mutations were discovered by this process (see Table 5.1). In order to determine whether these defects were actually LAD mutations, or whether they simply represented polymorphisms or alternative forms of the β2 subunit present within the normal population, the effect of each mutation on the expression and function of the β2 subunit was investigated.

5.2.1.2 Constructing Full Length Mutant β2 cDNAs

Full length mutant β2 cDNAs containing the A270V, G284S and $T418_{fr*}$ mutations (see Table 5.1), had been previously constructed in Dr. Law's laboratory. A full length wildtype β2 cDNA (J8; Weitzman *et al.*, 1991) in the pBluescript vector had been used as a source of normal cDNA, and the cloned PCR products a' and b', which had been amplified from LAD patient cDNA (see Figure 5.1a), had been used as a source of mutant cDNA. Normal β2 cDNA fragments had been excised from the wildtype β2 clone and had been exchanged for the corresponding mutant fragments using unique restriction enzyme sites. The resulting full length mutant β2 cDNA clones in pBluescript: pBS/β2(A270V), pBS/β2(G284S) and pBS/β2($T418_{fr*}$) (see Figure 5.2) had been nucleotide sequenced to confirm the presence of the mutations, and to confirm the absence of PCR errors in the cDNA sections derived from PCR amplified fragments.

5.2.1.3 Subcloning the Full Length Mutant β2 cDNAs into the pSVL Expression Vector

The entire coding regions of the mutant β2(A270V), β2(G284S) and β2($T418_{fr*}$) cDNAs were then subcloned from pBluescript into the pSVL expression vector (Pharmacia) for transient expression in COS 7 cells.

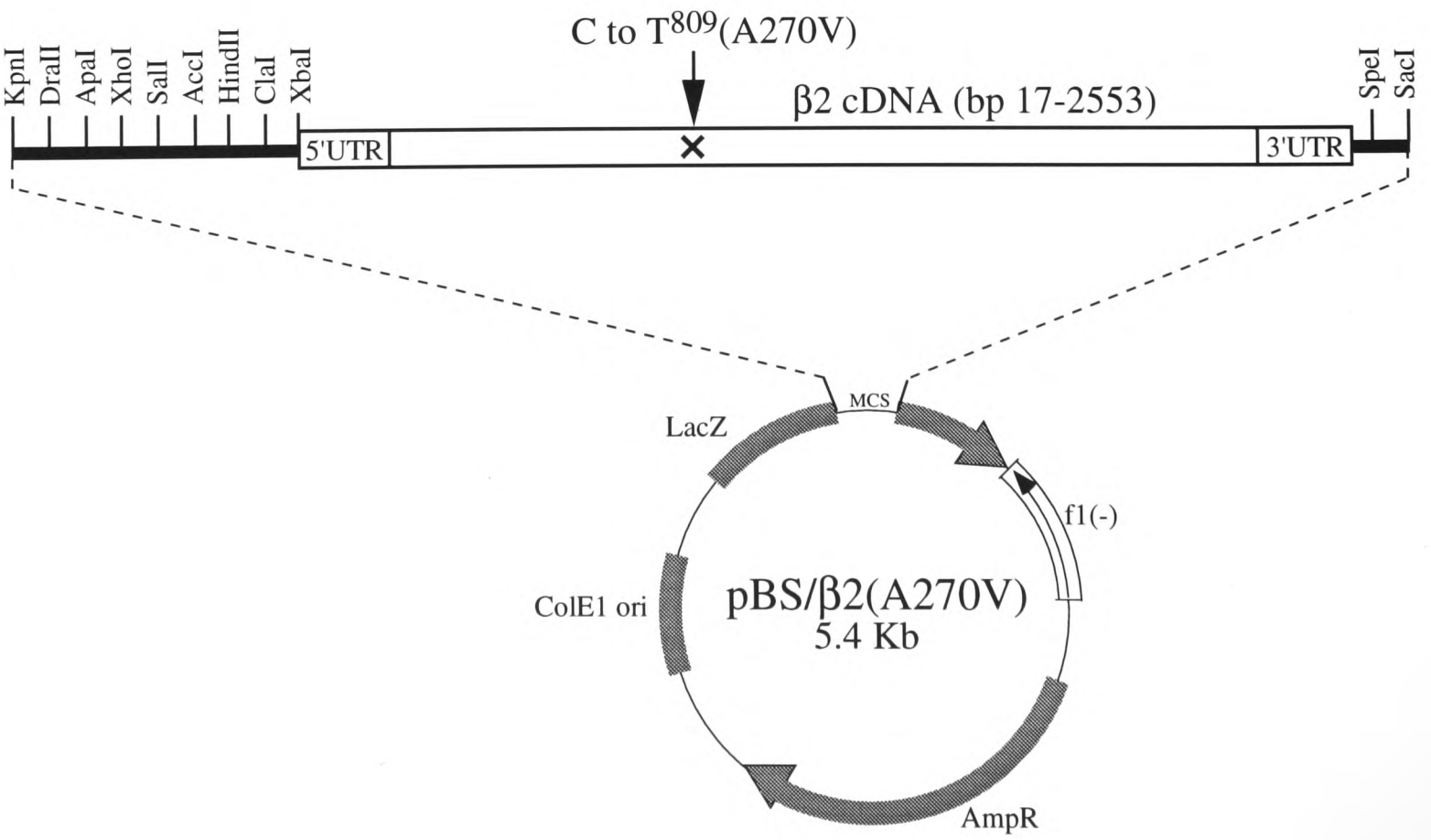
Figure 5.2: The pBS/β2(A270V), pBS/β2(G284S) and pBS/β2($T418_{fr*}$) Clones

(a) pBS/β2(A270V) consists of the entire coding region of the β2 cDNA, carrying the mutation "C to T^{809}(A270V)", cloned into the pBluescript vector.

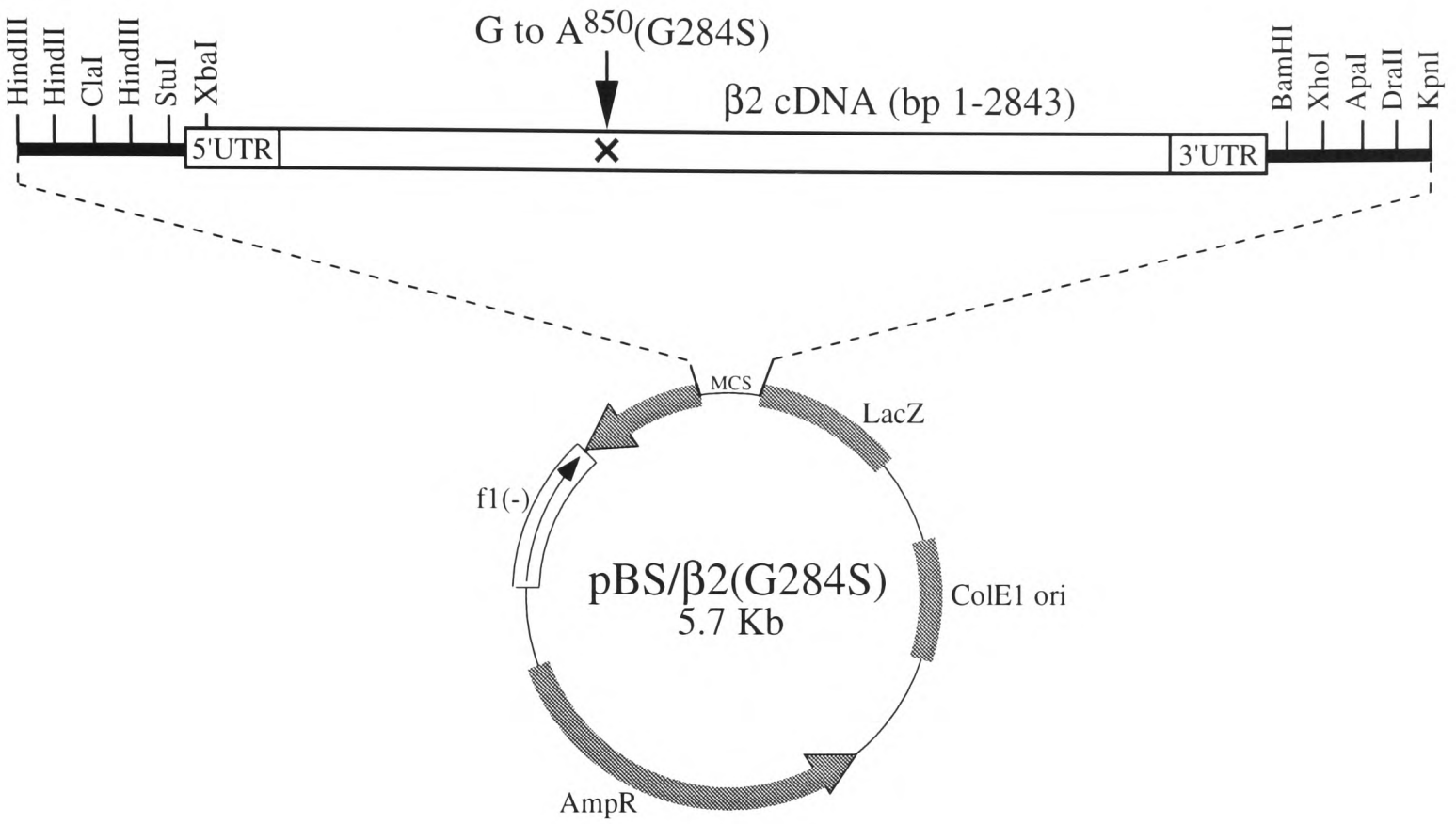
(b) pBS/β2(G284S) consists of the entire coding region of the β2 cDNA, carrying the mutation "G to A^{850}(G284S)", cloned into the pBluescript vector.

(c) pBS/β2($T418_{fr*}$) consists of the entire coding region of the β2 cDNA, carrying the mutation "1256ΔGA($T418_{fr*}$)", cloned into the pBluescript vector.

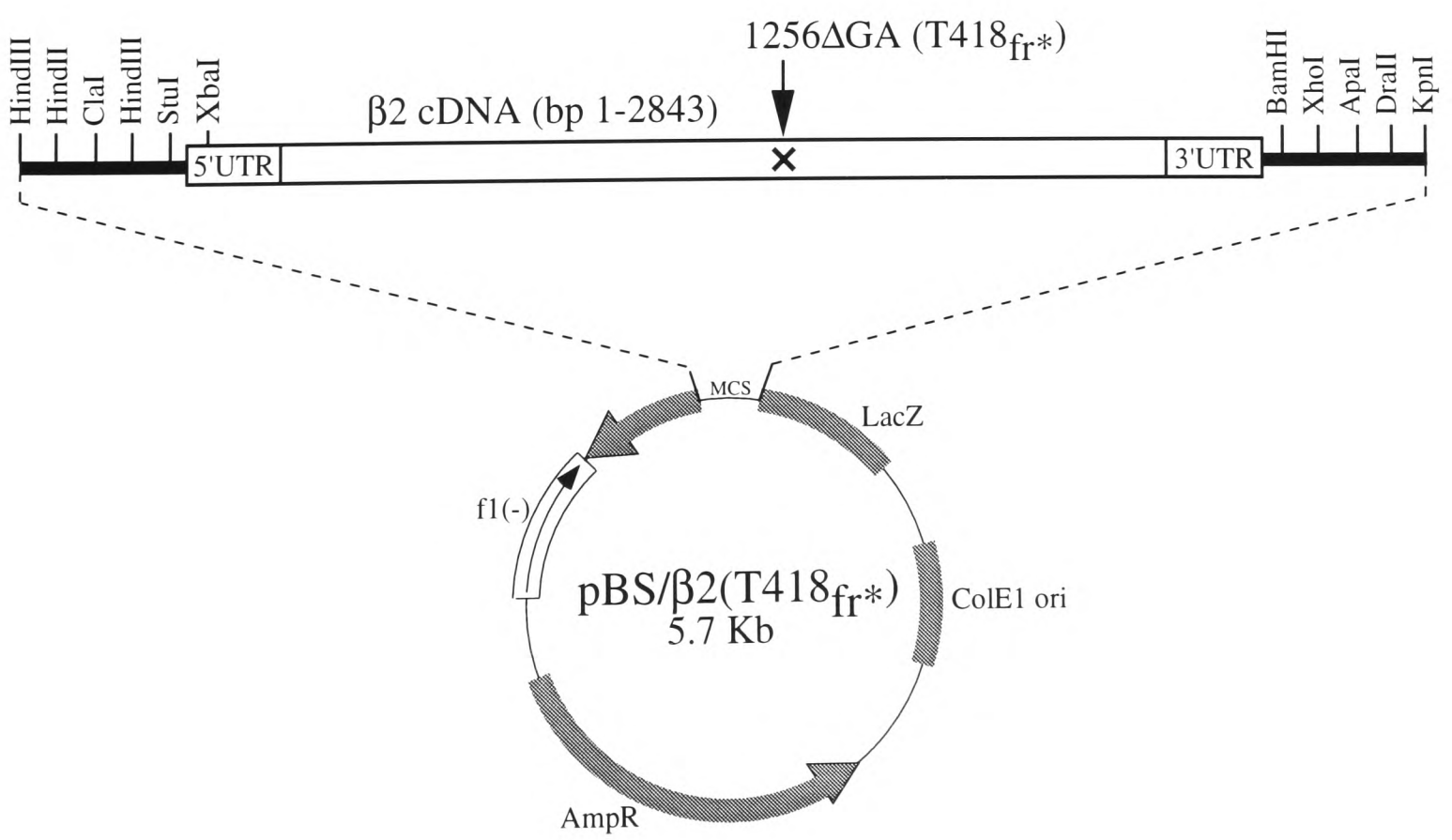
(a) The pBS/β2(A270V) Clone:



(b) The pBS/β2(G284S) Clone:



(c) The pBS/β2(T418$_{fr*}$) Clone:



5.2.1.3.1 Cloning the Mutant β2(A270V) cDNA into pSVL, Creating pSVL/β2(A270V)

The mutant β2(A270V) cDNA was subcloned from pBluescript into the pSVL expression vector as illustrated in Figure 5.3. The entire coding region of the mutant β2(A270V) cDNA was excised from the pBluescript clone pBS/β2(A270V) by restriction digestion with XhoI (pBS/β2(A270V), 5'polylinker) and SacI (pBS/β2(A270V), 3'polylinker), and was then cloned into XhoI/SacI cut pSVL, creating the clone pSVL/β2(A270V).

5.2.1.3.2 Cloning the Mutant β2(G284S) cDNA into pSVL, Creating pSVL/β2(G284S)

The mutant β2(G284S) cDNA was subcloned from pBluescript into the pSVL expression vector as illustrated in Figure 5.4. The pBluescript clone pBS/β2(G284S) was digested with XhoI (pBS/β2(G284S), 3'polylinker) and the resultant 5'overhang was blunted using the end-filling reaction. The entire coding region of the mutant β2(G284S) cDNA was then excised by digestion with XbaI (mutant β2(G284S) cDNA, 5'UTR). The pSVL expression vector was digested with BamHI and the resulting 5'overhang was blunted using the end-filling reaction before subsequent digestion with XbaI. The pSVL/β2(G284S) clone was then constructed by ligating the XbaI-XhoI(blunted) mutant β2(G284S) cDNA insert with the XbaI-BamHI(blunted) pSVL vector.

5.2.1.3.3 Cloning the Mutant β2($T418_{fr*}$) cDNA into pSVL, Creating pSVL/β2($T418_{fr*}$)

The mutant β2($T418_{fr*}$) cDNA was subcloned from pBluescript into the pSVL expression vector in a similar way as the mutant β2(G284S) cDNA, as illustrated in Figure 5.5. The pBluescript clone pBS/β2($T418_{fr*}$) was digested with XhoI (pBS/β2($T418_{fr*}$), 3'polylinker) and the resultant 5'overhang was blunted using the end-filling reaction. The entire coding region of the mutant β2($T418_{fr*}$) cDNA was then excised by digestion with XbaI (mutant β2($T418_{fr*}$) cDNA, 5'UTR). The pSVL expression vector was digested with BamHI and the resulting 5'overhang was blunted using the end-filling reaction before subsequent digestion with XbaI. The pSVL/β2($T418_{fr*}$) clone was then constructed by ligating the XbaI-XhoI(blunted) mutant β2($T418_{fr*}$) cDNA insert with the XbaI-

Figure 5.3: Constructing pSVL/β2(A270V)

The full length β2 cDNA clone containing the mutation "C to T^{809}(A270V)" was subcloned from pBluescript into the pSVL expression vector (Pharmacia) for transient expression in COS 7 cells as described below:

(1) The clone pBS/β2(A270V) was digested with XhoI and SacI, and the 2.5 Kb mutant β2(A270V) cDNA insert band excised was purified by agarose gel electrophoresis.

(2) The pSVL expression vector was also digested with XhoI and SacI, and the resulting 4.8 Kb pSVL vector band purified by agarose gel electrophoresis.

(3) The pSVL vector and the mutant β2(A270V) cDNA insert were then ligated, creating pSVL/β2(A270V).

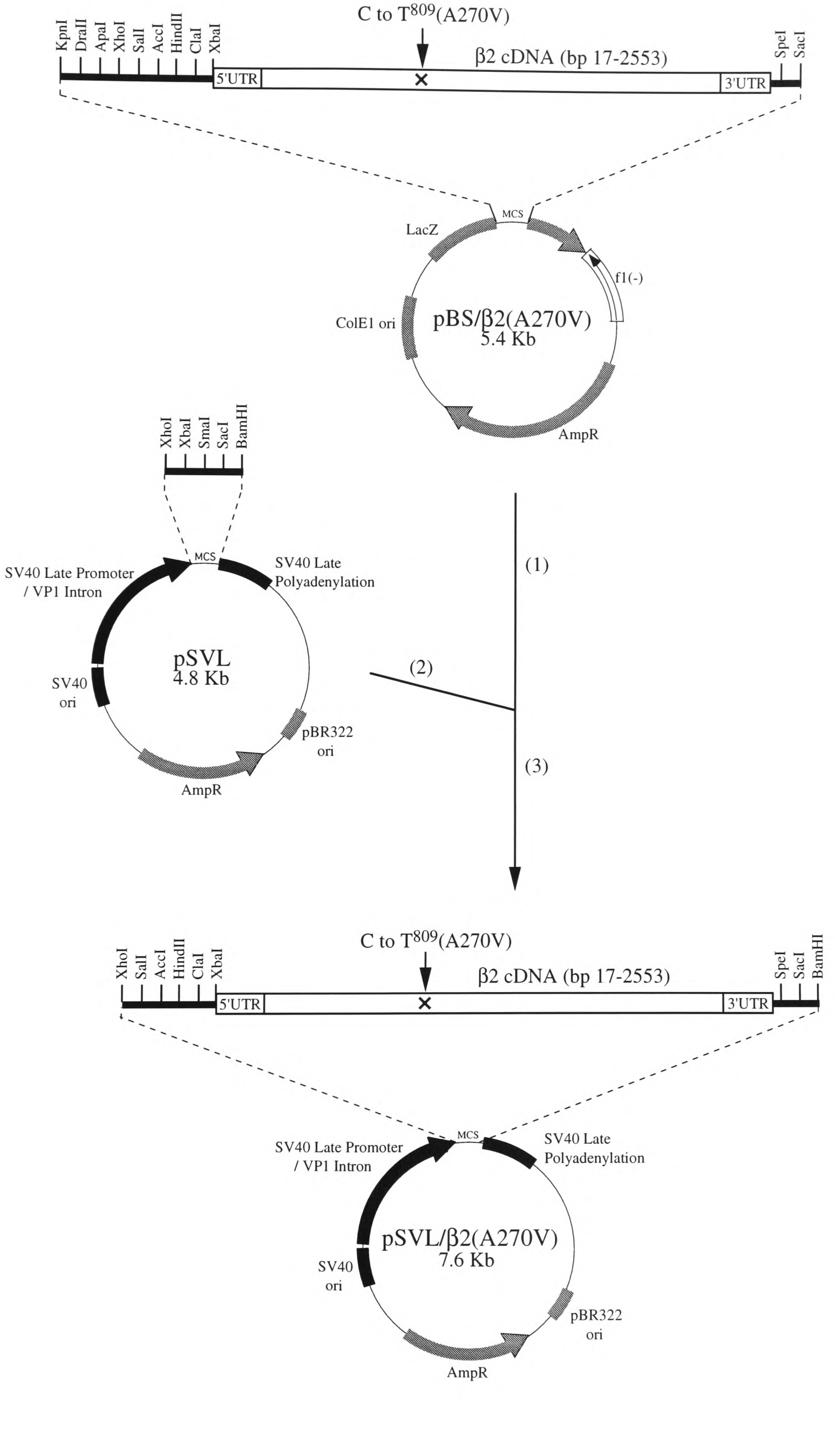

C to T809(A270V)
KpnI
DraII
ApaI
XhoI
SalI
AccI
HindII
ClaI
XbaI
β2 cDNA (bp 17-2553)
SpeI
SacI
5'UTR
3'UTR
MCS
LacZ
f1(-)
ColE1 ori
pBS/β2(A270V)
5.4 Kb
AmpR
XhoI
XbaI
SmaI
SacI
BamHI
MCS
SV40 Late Promoter
/ VP1 Intron
SV40 Late
Polyadenylation
pSVL
4.8 Kb
SV40
ori
pBR322
ori
AmpR
(1)
(2)
(3)
C to T809(A270V)
XhoI
SalI
AccI
HindII
ClaI
XbaI
β2 cDNA (bp 17-2553)
SpeI
SacI
BamHI
5'UTR
3'UTR
MCS
SV40 Late Promoter
/ VP1 Intron
SV40 Late
Polyadenylation
pSVL/β2(A270V)
7.6 Kb
SV40
ori
pBR322
ori
AmpR

Figure 5.4: Constructing pSVL/β2(G284S)

The full length β2 cDNA clone containing the mutation "G to A^{850}(G284S)" was subcloned from pBluescript into the pSVL expression vector (Pharmacia) for transient expression in COS 7 cells as described below:

(1) The clone pBS/β2(G284S) was digested with XhoI and end-filled, and was then digested with XbaI. This excised the 2.8 Kb mutant β2(G284S) cDNA insert band, which was then purified by agarose gel electrophoresis.

(2) The pSVL expression vector was digested with BamHI and end-filled, and was then digested with XbaI. The resulting 4.8 Kb pSVL vector band was also purified by agarose gel electrophoresis.

(3) The pSVL vector and the mutant β2(G284S) cDNA insert were then ligated, creating pSVL/β2(G284S). The XhoI site derived from the insert was reformed in this cloning procedure, whereas the pSVL BamHI site was destroyed.

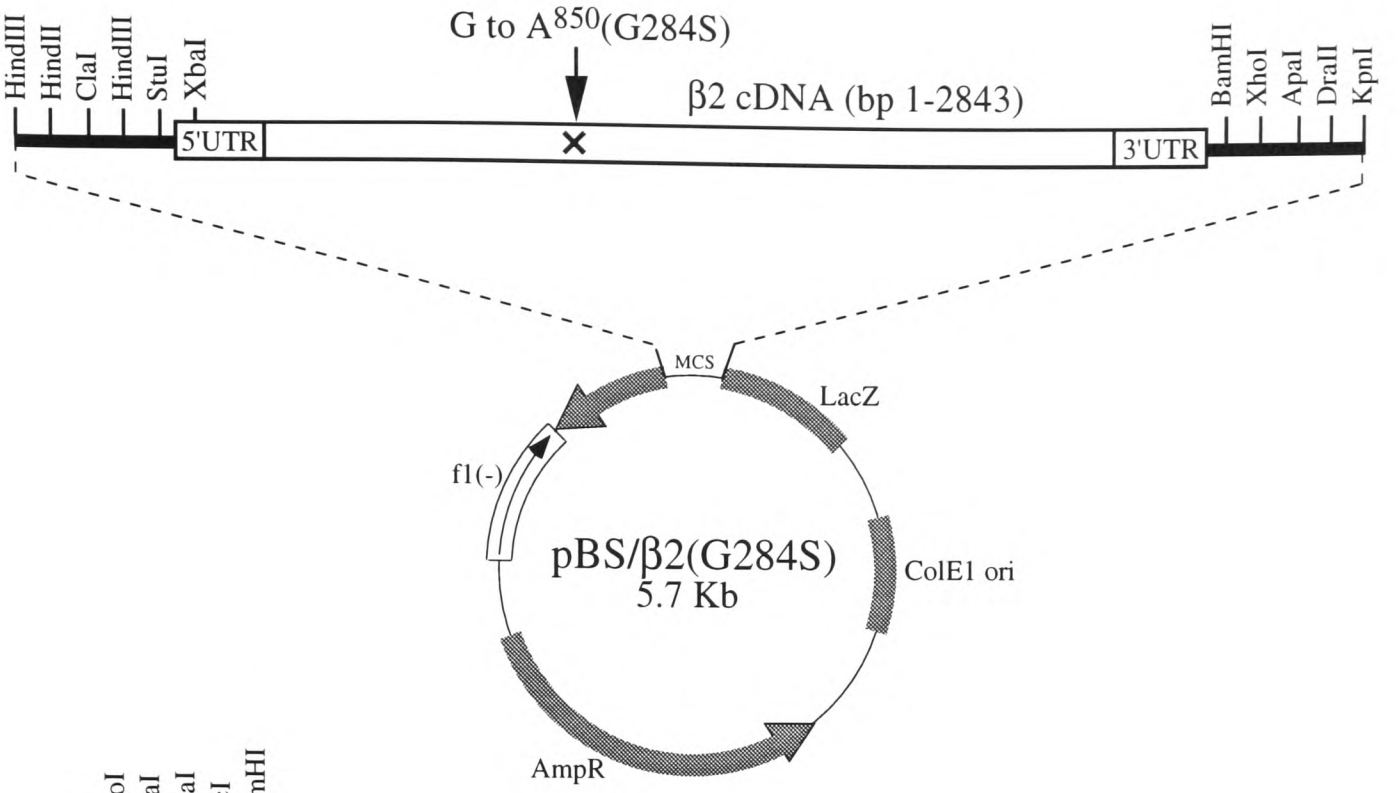

HindIII
HindII
ClaI
HindIII
StuI
XbaI
G to A850(G284S)
β2 cDNA (bp 1-2843)
BamHI
XhoI
ApaI
DraII
KpnI
5'UTR
3'UTR
MCS
LacZ
f1(-)
pBS/β2(G284S)
5.7 Kb
ColE1 ori
AmpR
XhoI
XbaI
SmaI
SacI
BamHI
MCS
SV40 Late Promoter
/ VP1 Intron
SV40 Late
Polyadenylation
pSVL
4.8 Kb
SV40
ori
pBR322
ori
AmpR
(1)
(2)
(3)
G to A850(G284S)
XhoI
XbaI
β2 cDNA (bp 17-2843)
BamHI
XhoI
5'UTR
3'UTR
MCS
SV40 Late Promoter
/ VP1 Intron
SV40 Late
Polyadenylation
pSVL/β2(G284S)
7.6 Kb
SV40
ori
pBR322
ori
AmpR

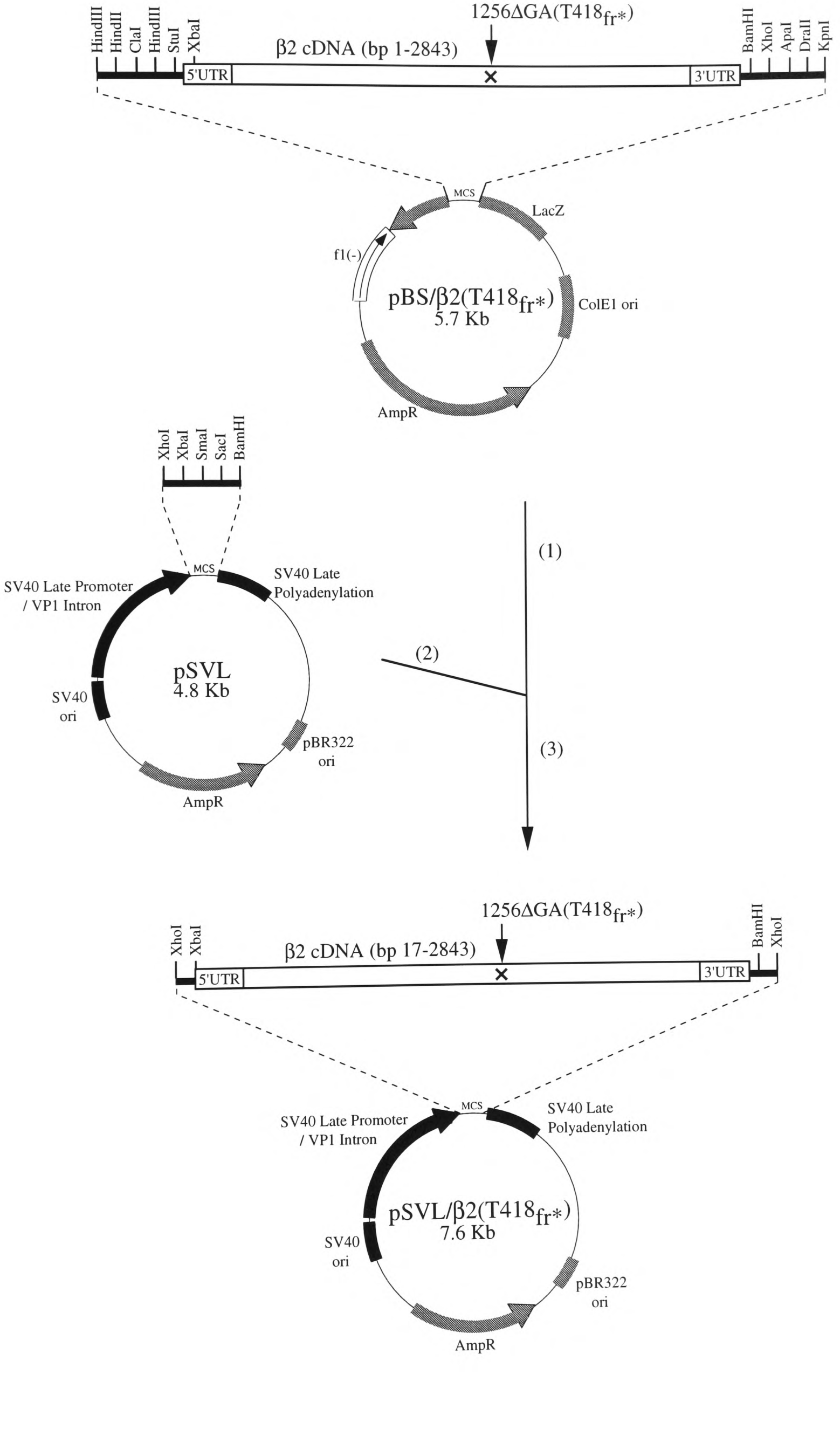
Figure 5.5: Constructing pSVL/β2($T418_{fr*}$)

The full length β2 cDNA clone containing the deletion mutation "1256ΔGA($T418_{fr*}$)" was subcloned from pBluescript into the pSVL expression vector (Pharmacia) for transient expression in COS 7 cells as described below:

(1) The clone pBS/β2($T418_{fr*}$) was digested with XhoI and end-filled, and was then digested with XbaI. This excised the 2.8 Kb mutant β2($T418_{fr*}$) cDNA insert band, which was then purified by agarose gel electrophoresis.

(2) The pSVL expression vector was digested with BamHI and end-filled, and was then digested with XbaI. The resulting 4.8 Kb pSVL vector band was also purified by agarose gel electrophoresis.

(3) The pSVL vector and the mutant β2($T418_{fr*}$) cDNA insert were then ligated, creating pSVL/β2($T418_{fr*}$). The XhoI site derived from the insert was reformed in this cloning procedure, whereas the pSVL BamHI site was destroyed.


HindIII
HindII
ClaI
HindIII
StuI
XbaI
β2 cDNA (bp 1-2843)
1256ΔGA(T418fr*)
BamHI
XhoI
ApaI
DraII
KpnI
5'UTR
3'UTR
MCS
LacZ
f1(-)
pBS/β2(T418fr*)
5.7 Kb
ColE1 ori
AmpR
XhoI
XbaI
SmaI
SacI
BamHI
MCS
SV40 Late Promoter
/ VP1 Intron
SV40 Late
Polyadenylation
pSVL
4.8 Kb
SV40
ori
pBR322
ori
AmpR
(1)
(2)
(3)
1256ΔGA(T418fr*)
XhoI
XbaI
β2 cDNA (bp 17-2843)
BamHI
XhoI
5'UTR
3'UTR
MCS
SV40 Late Promoter
/ VP1 Intron
SV40 Late
Polyadenylation
pSVL/β2(T418fr*)
7.6 Kb
SV40
ori
pBR322
ori
AmpR

BamHI(blunted) pSVL vector.

5.2.1.4 Expressing the Mutant β2 Subunits on COS 7 Cells

The pSVL/β2(A270V), pSVL/β2(G284S) and pSVL/β2($T418_{fr*}$) constructs were then transfected into COS 7 cells as described in Section 2.2.10, either singly or with the full length wildtype αL, αM or αX cDNAs, which had also been cloned into the pSVL vector (see Chapter 3, Section 3.2.4). The expression of mutant β2 subunits on the surface of transfectants was then analysed by flow cytometry, using the mAbs listed in Table 5.2. The level of expression of the H52 mAb epitope on the surface of cells transfected with a mutant β2 construct alone was used to evaluate the ability of the mutant β2 subunits to express on the cell surface without any association with the wildtype αL, αM or αX counter-subunits, whereas the level of expression of the MHM23 and 1B4 mAb epitopes on the surface of cells cotransfected with a wildtype α construct and a mutant β2 construct was used to evaluate the ability of the mutant β2 subunits to associate with the wildtype αL, αM or αX subunits to form LFA-1, Mac-1 or p150,95 heterodimeric complexes. The results obtained by flow cytometry are shown in Figure 5.6.

5.2.1.4.1 Expression of the Mutant β2(A270V) Subunit

When COS 7 cells were transfected with the mutant β2(A270V) construct alone, the H52 epitope was expressed on the cell surface at levels almost as high as on cells which had been transfected with the β2(wildtype) construct alone, indicating that the mutant β2(A270V) subunit can be efficiently expressed on the cell surface without association with the wildtype αL, αM or αX counter-subunits. When the mutant β2(A270V) construct was cotransfected into cells along with the wildtype αL construct, the H52 epitope was again expressed at high levels, but the MHM24, MHM23 and 1B4 epitopes were not expressed at levels any higher than the background levels detected on the αL transfectants, indicating that the β2(A270V) subunit is unable to associate with the wildtype αL subunit to form surface expressable LFA-1 heterodimeric complexes. In contrast, the αMβ2(A270V) cotransfectants expressed the MHM23 and 1B4 epitopes at levels slightly higher than the background levels detected on the αM transfectants, and the αXβ2(A270V) cotransfectants expressed the KB23, MHM23 and 1B4 epitopes at levels much higher than the background detected on the αX transfectants. These results therefore suggest that although the mutant

Table 5.2: The mAbs used for Flow Cytometric Analysis of COS 7 Transfectants

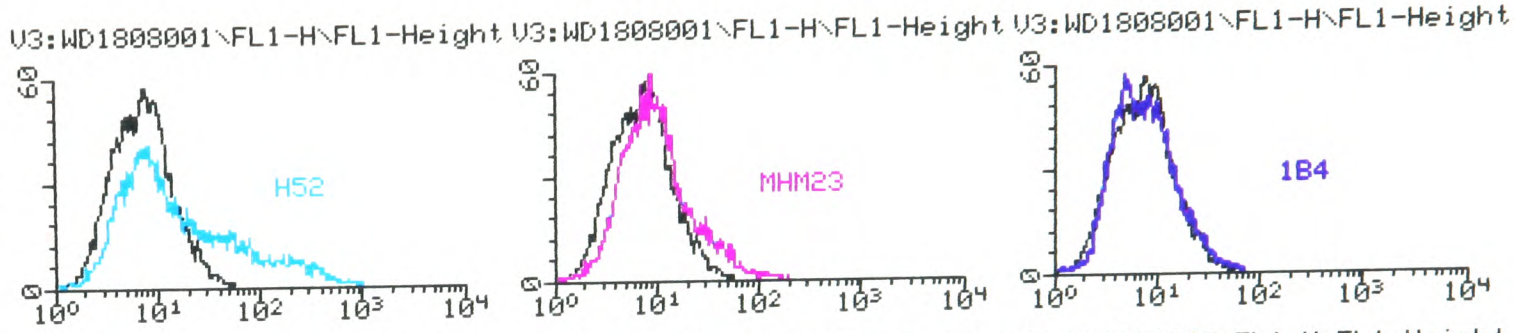
The expression of the MHM24, LPM19C, KB23, H52, MHM23 and 1B4 mAb epitopes on the monomeric and heterodimeric forms of each wildtype subunit was established in Chapter 4 (see Section 4.2.1.1). In the table below, the "+" signs indicate strong expression of an epitope, the "(+)" signs very weak epitope expression, and the "-" signs no epitope expression. The expression of the KB23 epitope on the monomeric form of the αX subunit was not determined, as indicated by the "?" sign. It should be noted that the epitope for the β2-specific mAb H52 is expressed on the monomeric form of the β2 subunit, whereas the epitopes for the β2-specific mAbs MHM23 and 1B4 are only expressed on the LFA-1, Mac-1 and p150,95 heterodimeric forms of the β2 subunit.

mAb	Specificity	Epitope Expressed On:						
		αL	αM	αX	β2	αLβ2	αMβ2	αXβ2
MHM24	αL	+	-	-	-	+	-	-
LPM19C	αM	-	+	-	-	-	+	-
KB23	αX	-	-	?	-	-	-	+
H52	β2	(+)	-	-	+	+	(+)	-
MHM23	β2	(+)	-	-	-	+	+	+
IB4	β2	(+)	-	-	-	+	+	+

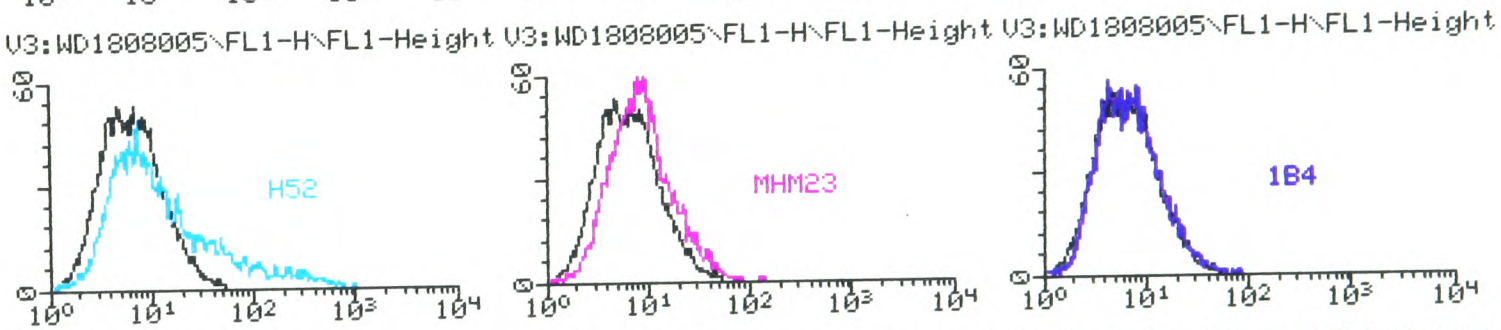
Figure 5.6: The Expression of Mutant β2 Subunits on COS 7 Cells

The flow cytometry profiles obtained from the COS 7 cell transfections described in Section 5.2.1.4 are shown below. Transfectants were labelled with an irrelevant murine mAb (OX34; anti-rat CD2) to indicate the amount of fluorescence due to non-specific binding of mAbs to COS 7 cells (black profiles), or were labelled with the murine anti-human leukocyte integrin mAbs: MHM24 (anti-αL; green overlays), LPM19c (anti-αM; red overlays), KB23 (anti-αX; mauve overlays), H52 (anti-β2; light blue overlays), MHM23 (anti-β2 heterodimer; pink overlays) and 1B4 (anti-β2 heterodimer; dark blue overlays). Samples were then stained with a fluorescently labelled rabbit anti-mouse second antibody, and the level of fluorescence on the surface of each cell (and hence the level of expression of a particular mAb epitope) was measured using a Becton Dickinson FACScan flow cytometer. In the profiles shown below, fluorescent intensity (in arbitary units) is plotted along the horizontal axis, and cell number is plotted along the vertical axis. Cell surface expression of wildtype and mutant β2 subunits is indicated by detection of the H52 mAb epitope, whereas the expression of cell surface wildtype and mutant LFA-1, Mac-1 or p150,95 heterodimers is indicated by the expression of the MHM23 and 1B4 mAb epitopes.

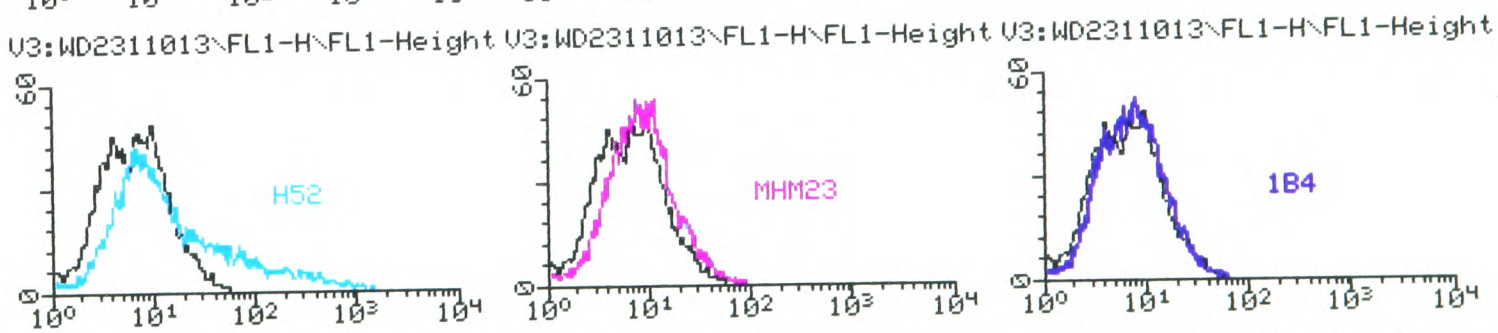
- /β2(wildtype)



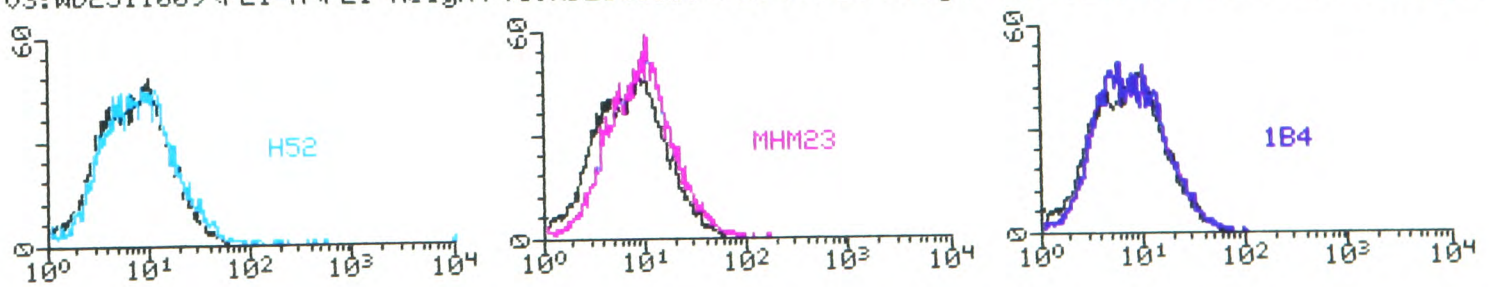
- /β2(A270V)



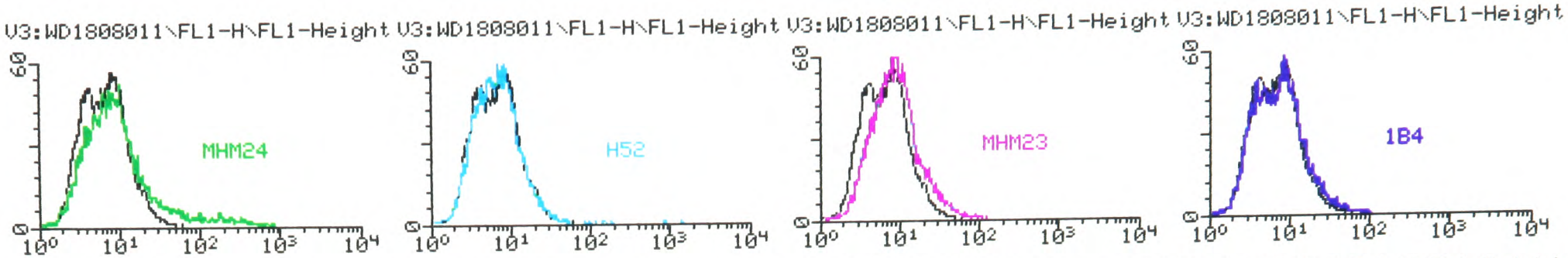
- /β2(G284S)



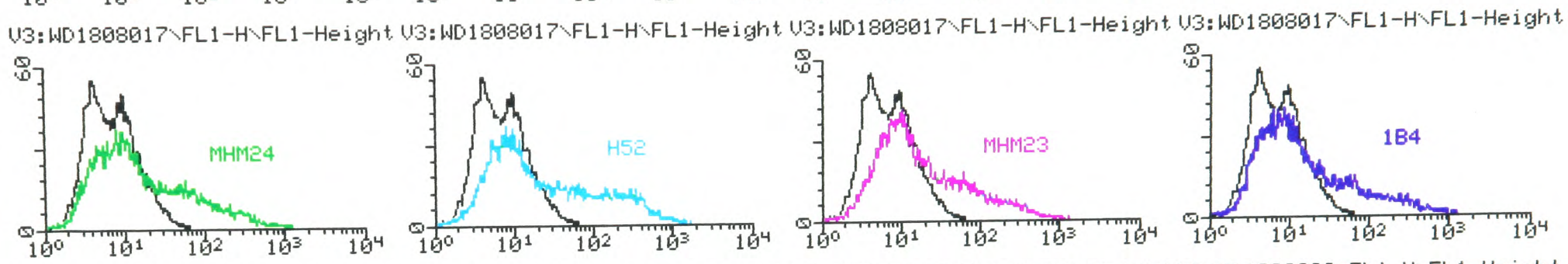
- /β2($T418_{fr*}$)



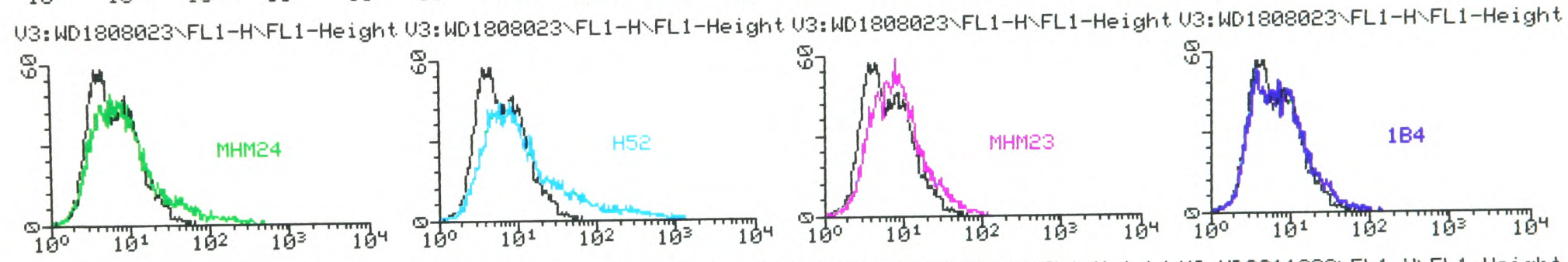
αL/ -



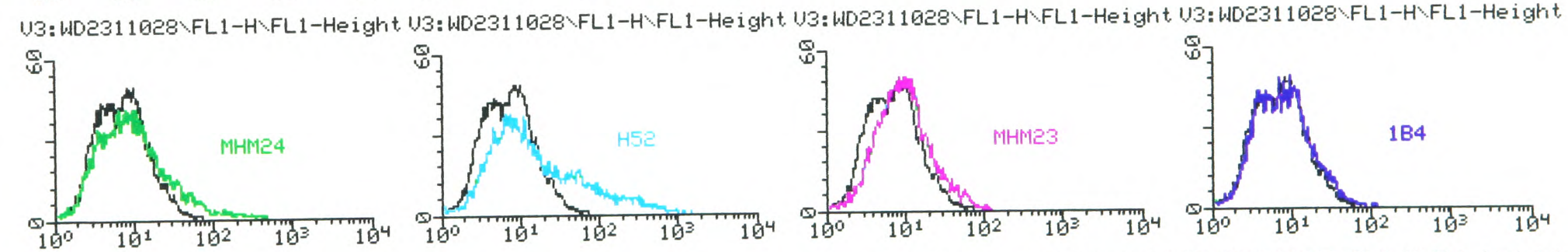
αL/β2(wildtype)



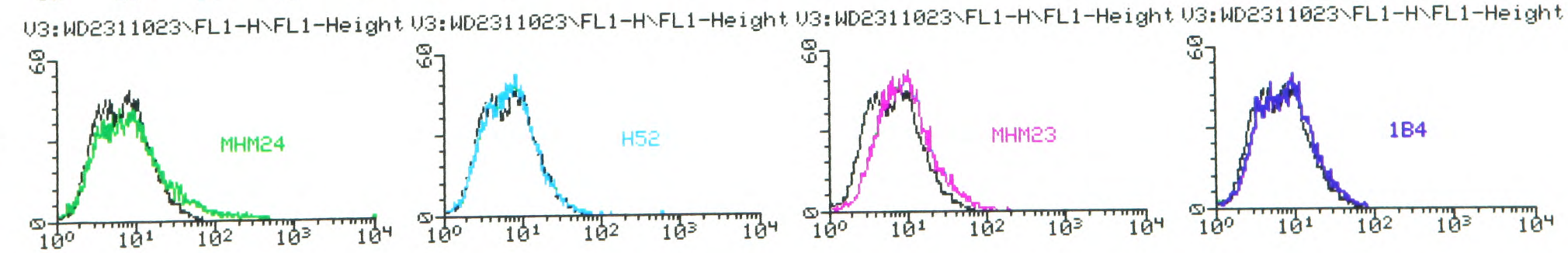
αL/β2(A270V)



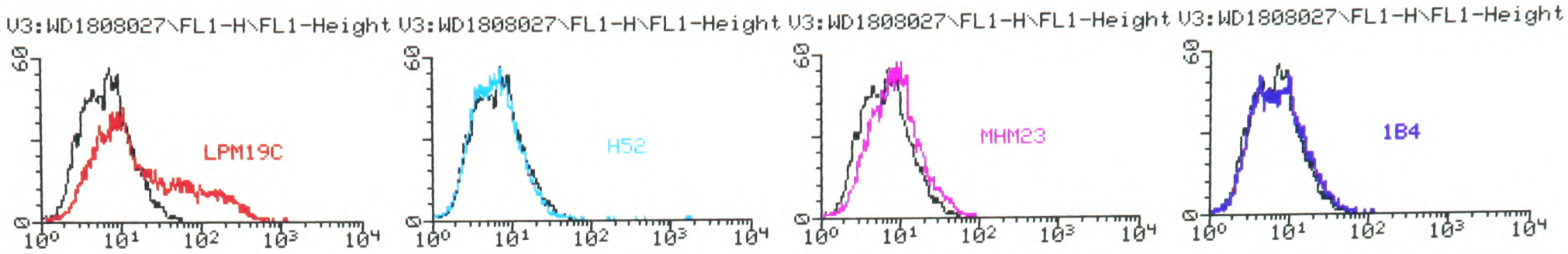
αL/β2(G284S)



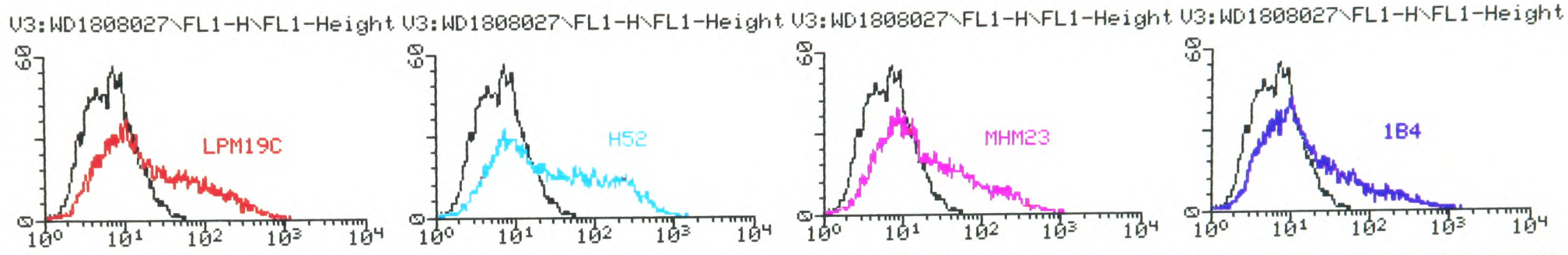
αL/β2(T418$_{fr*}$)



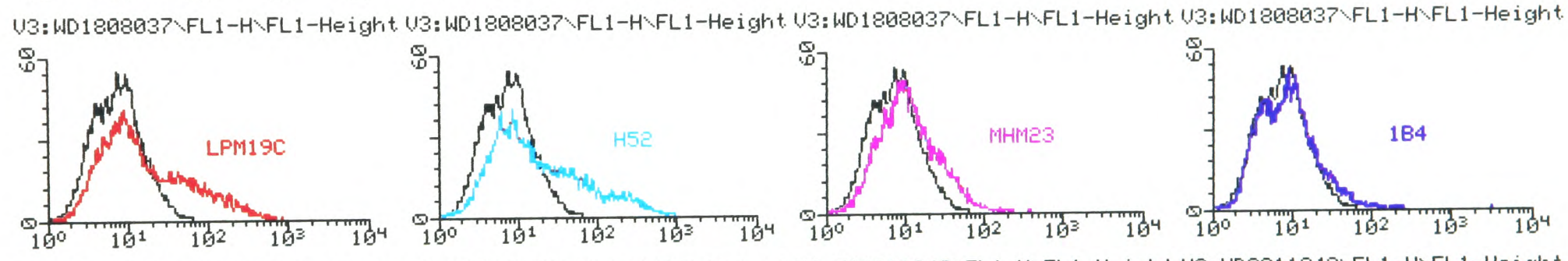
αM/ -



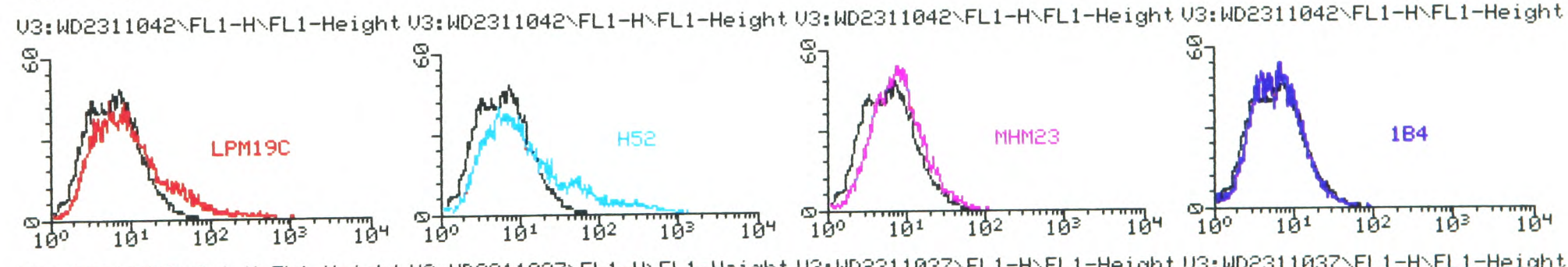
αM/β2(wildtype)



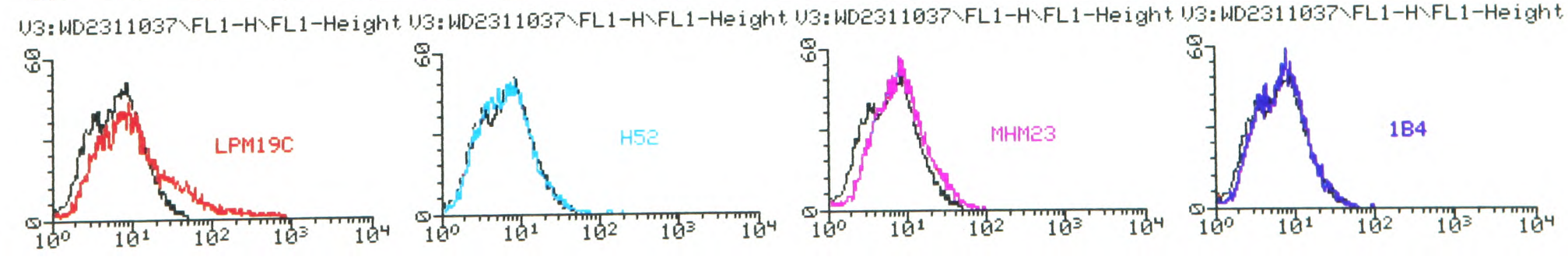
αM/β2(A270V)



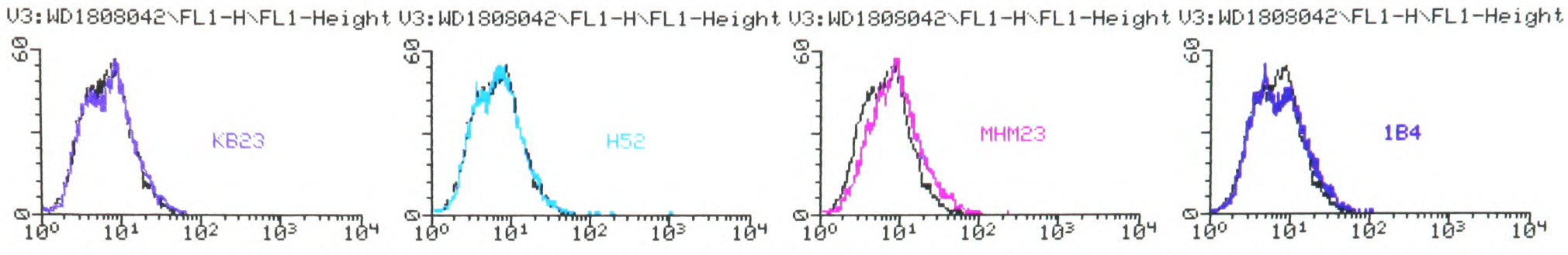
αM/β2(G284S)



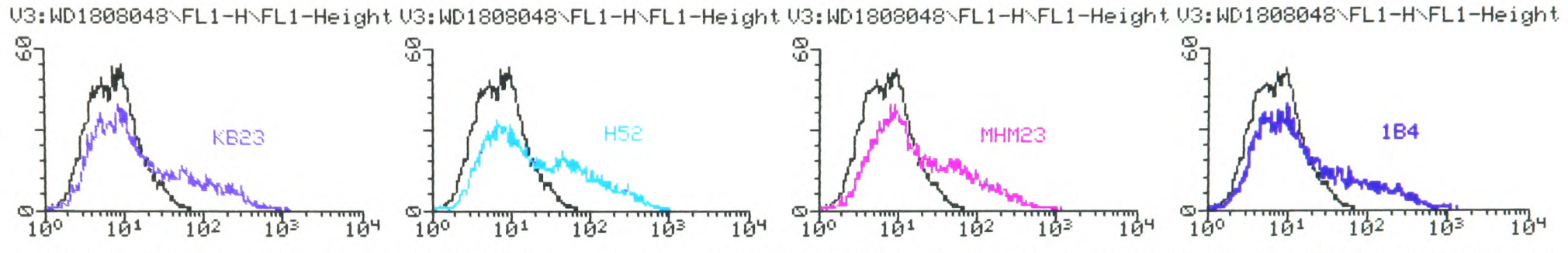
αM/β2(T418$_{fr*}$)



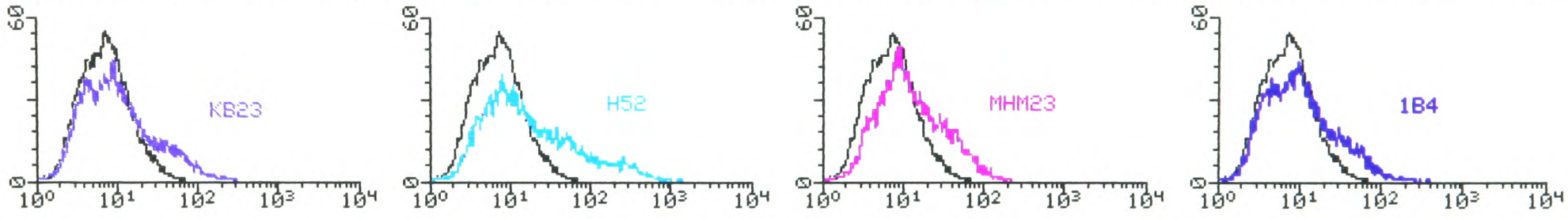
αX/ -



αX/β2(wildtype)



αX/β2(A270V)



β2(A270V) subunit is unable to support LFA-1 heterodimer formation, it can weakly support the formation of Mac-1 heterodimers, and can support the formation of p150,95 heterodimers even more efficiently.

5.2.1.4.2 Expression of the Mutant β2(G284S) Subunit

When cells were transfected with the mutant β2(G284S) construct alone, the H52 epitope was again expressed on the cell surface at levels almost as high as on cells which had been transfected with the β2(wildtype) construct alone, indicating that like the mutant β2(A270V) subunit, the mutant β2(G284S) subunit can also be expressed on the cell surface without interaction with the wildtype αL, αM or αX counter-subunits. When the mutant β2(G284S) construct was cotransfected into cells along with the wildtype αL construct, the H52 epitope was again expressed at high levels, but the MHM24, MHM23 and 1B4 epitopes were not expressed at levels any higher than the background levels detected on the αL transfectants, indicating that again, like the mutant β2(A270V) subunit, the mutant β2(G284S) subunit is unable to associate with the wildtype αL subunit to form surface expressable LFA-1 heterodimers. However, when the mutant β2(G284S) construct was cotransfected into cells along with the wildtype αM construct, the MHM23 and 1B4 epitopes were still not expressed at levels any higher than the background detected on the αM transfectants, suggesting that unlike the mutant β2(A270V) subunit, the mutant β2(G284S) subunit is also unable to associate with the wildtype αM subunit to form surface expressable Mac-1 heterodimers. However, it is possible that αMβ2(G284S) heterodimers can be expressed on the cell surface, but remain undetected simply because the MHM23 and 1B4 epitopes on the β2 subunit are destroyed by the G284S mutation. To address this question, immunoprecipitation analysis of αMβ2(G284S) cotransfectants will be required: the immunoprecipitation of the αM subunit from the surface of αMβ2(G284S) cotransfectants (using an αM specific mAb like LPM19C) without any co-precipitation of the β2(G284S) subunit would confirm that this mutant subunit does not interact with the wildtpye αM subunit to form surface expressable Mac-1 heterodimers. The ability of the mutant β2(G284S) subunit to form p150,95 heterodimeric complexes was not investigated in this experiment.

5.2.1.4.3 Expression of the Mutant β2(T418$_{fr*}$) Subunit

When COS 7 cells were transfected with the mutant β2(T418$_{fr*}$) construct alone, the H52 epitope was not expressed on the cell surface. As this epitope has been localised to a small region of the β2 subunit between amino acids 390-395 (Dr. A. Al-Shamkhani, unpublished observations), it seems likely that it would be preserved on the truncated β2(T418$_{fr*}$) subunit. Therefore, this result suggests that when cells are transfected with the mutant β2(T418$_{fr*}$) construct alone, the resulting truncated β2(T418$_{fr*}$) subunit is either retained and degraded within the cell, or is secreted from the cell into the tissue culture media. When the mutant β2(T418$_{fr*}$) construct was cotransfected into COS 7 cells along with the wildtype αL construct, the H52 epitope was still not expressed on the cell surface, and the MHM24, MHM23 and 1B4 epitopes were also not expressed at levels any higher than the background detected on the αL transfectants. This suggests that like the mutant β2(A270V) and mutant β2(G284S) subunits, the mutant β2(T418$_{fr*}$) subunit is also unable to associate with the wildtype αL subunit to form surface expressable LFA-1 heterodimeric complexes. The H52, MHM23 and 1B4 mAb epitopes were also not expressed on the surface of the αMβ2(T418$_{fr*}$) cotransfectants at levels any higher than the background detected on the αM transfectants, indicating that the mutant β2(T418$_{fr*}$) subunit is also unable to associate with the wildtype αM subunit to form surface expressable Mac-1 heterodimers. The ability of the β2(T418$_{fr*}$) subunit to support p150,95 heterodimer formation was not investigated in this experiment.

5.2.1.4.4 Summary of the Expression of the Mutant β2(A270V), Mutant β2(G284S) and Mutant β2(T418$_{fr*}$) Subunits on COS 7 Cells

The effect of the A270V, G284S and T418fr* mutations on the expression of the β2 subunit and on its ability to form surface expressable LFA-1, Mac-1 and p150,95 heterodimeric complexes is summarised in Table 5.3. The two point mutations, A270V and G284S, did not significantly effect the processing and transport of the β2 subunit to the COS 7 cell surface. However, β2 subunits carrying the G284S mutation were unable to form surface expressable LFA-1 and Mac-1 heterodimers, and β2 subunits carrying the A270V mutation were unable to form LFA-1 heterodimers, and could only weakly support the formation of Mac-1 heterodimers. Thus, both the G284S and A270V mutations are not protein polymorphisms, but can be classified as LAD mutations. The deletion mutation 1256ΔGA,

Table 5.3: Summary of the Expression of the Mutant β2 Subunits on the Surface of COS 7 Cells

The expression of the wildtype and mutant β2 subunits on the surface of COS 7 transfectants was estimated visually from the flow cytometry results shown in Figure 5.6. The expression of β2 subunits as monomers was detected using the anti-β2 mAb H52, whereas the expression of β2 subunits in LFA-1, Mac-1 and p150,95 heterodimeric complexes was detected using the heterodimer-specific anti-β2 mAbs MHM23 and 1B4. Positive expression is indicated by a "+" sign, with the number of "+" signs indicating the level of expression detected. The "-" signs indicate that no cell surface expression was detected, and "ND" indicates that expression was not determined in this particular set of transfections. It should be noted that the expression of the β2(A270V) and β2(G284S) subunits on the cell surface as monomers, as well as the inability of the β2(G284S) subunit to form surface expressable Mac-1 heterodimers, needs to be confirmed by immunoprecipitation analysis of transfectants.

Subunit	Monomer Expression	Heterodimer Expression		
		LFA-1	Mac-1	p150,95
β2(wildtype)	++++	+++++	+++++	+++++
β2(A270V)	+++	-	+	+++
β2(G284S)	+++	-	-	ND
β2($T418_{fr*}$)	-	-	-	ND

which results in a truncated mutant β2 subunit, β2($T418_{fr*}$), completely abolished the expression of cell surface LFA-1 and Mac-1 heterodimers. Therefore, this defect can also be classified as an LAD mutation. It should be noted that although the A270V point mutation completely abolished LFA-1 expression and significantly reduced the expression of Mac-1 heterodimers, it only moderately affected the expression of p150,95 heterodimeric complexes. The ability of the mutant β2(G284S) and mutant β2($T418_{fr*}$) subunits to form surface expressable p150,95 heterodimers was not determined in this experiment.

5.3 SUMMARY

LAD is an autosomal recessive disorder caused by defects in the gene encoding the common β2 subunit of the leukocyte integrins LFA-1, Mac-1 and p150,95. It has been generally described that the defective β2 subunits, if made at all, are unable to combine efficiently with all three leukocyte integrin α subunits to form surface expressable αβ heterodimeric complexes. The resulting combined reduction in LFA-1, Mac-1 and p150,95 expression on the surface of patients' leukocytes is thought to render them adhesion defective, leading to the characteristic immune dysfunctions of LAD. However, this description is probably a rather simplistic characterisation of the disorder. Although LAD patients can be classified as having either the severe phenotype (where expression of the leukocyte integrins is less than 1% of normal), or the moderate phenotype (where expression is about 10% of normal), the clinical symptoms of LAD can vary substantially between patients, and vary particularly between patients with the moderate phenotype. It is difficult to understand how such phenotypic diversity can be attributed solely to a combined reduction in the expression of cell surface LFA-1, Mac-1 and p150,95.

Analysis at the molecular level has shown the disorder to be very heterogeneous. Over 20 different defects in the β2 gene have been described, and the nature of these mutations, and their positions in the β2 gene, are summarised in Figure 5.7. Many of these mutations cause mis-splicing events or frameshifts, and result in the synthesis of mutant β2 subunits with gross abnormalities. These defects tend to completely abolish the cell surface expression of LFA-1, Mac-1 and p150,95, and therefore associate with the severe LAD phenotype. However, at least 13 different point mutations within the coding region of the β2 gene have also been described. These mutations lead to the synthesis of mutant β2 subunits containing single amino acid substitutions, and can associate with either the severe or moderate phenotypes. The study of these mutations is potentially more interesting, as they can provide information on particular residues and regions of the β2 subunit which are critical for αβ heterodimer formation and function.

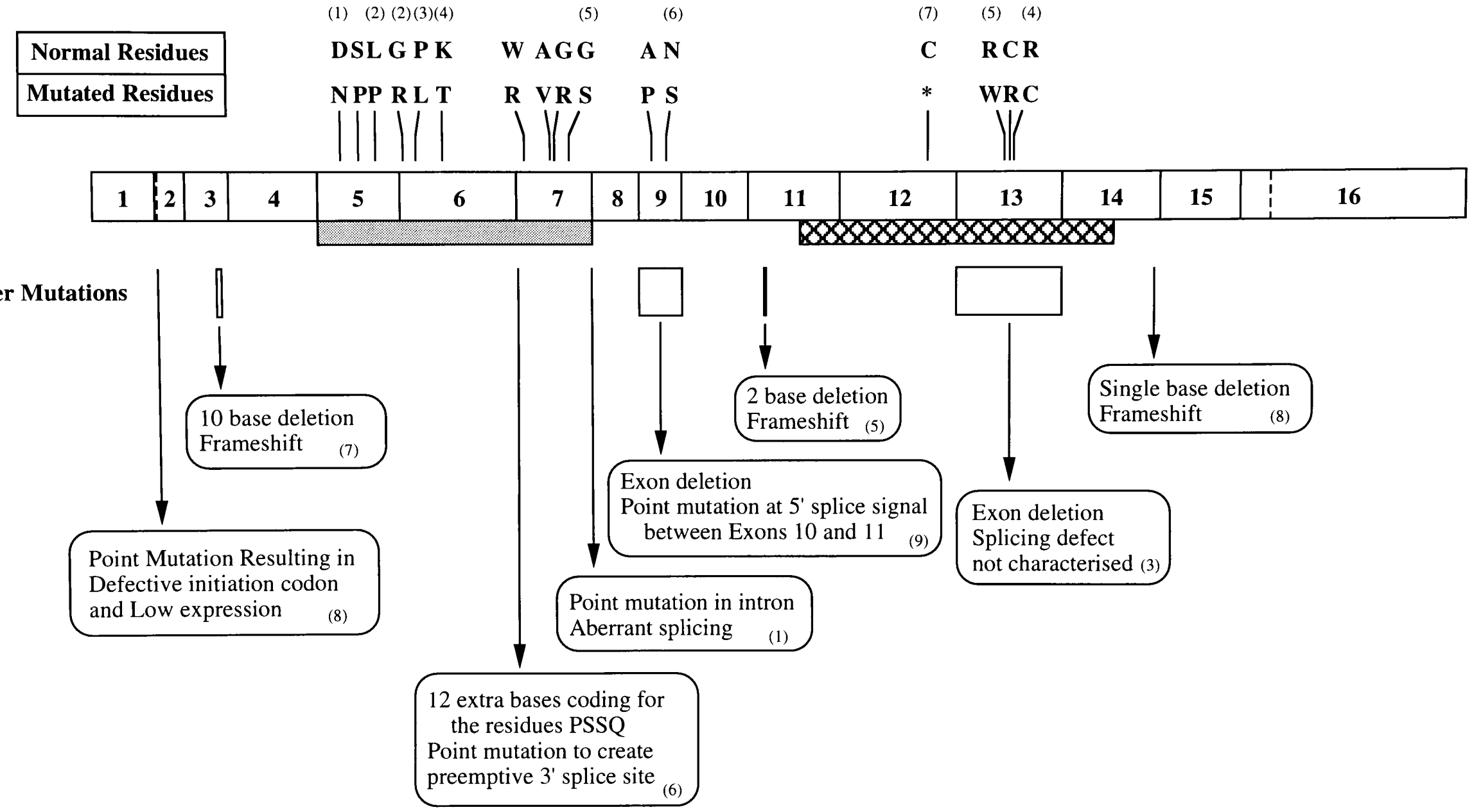
In this chapter, three mutations within the coding region of the β2 gene were studied in detail. These muations had previously been identified in the cDNA of three different LAD patients (Wright *et al.*, 1995; Dr. A. Law and Mrs. J. Shaw, unpublished observations).

Figure 5.7: Summary of LAD Defects

Defects within the β2 gene which are known to contribute to LAD are summarised in the figure below. The entire β2 cDNA, from exon 1 to exon 16 is shown. The coding region is bounded by the dotted lines in exons 2 and 16, and the shaded box below exons 5-7 indicates the region coding for the putative A-domain, whereas the cross-hatched box below exons 11-14 indicates the region coding for the C-terminal cysteine rich region. The position of each LAD defect in the β2 cDNA is marked: mutations which cause aberrant splicing or frameshift events and result in the synthesis of mutant β2 subunits with gross abnormalities are shown below the β2 cDNA, whereas point mutations within the coding region which result in mutant β2 subunits carrying just single amino acid substitutions are shown above the β2 cDNA. Where mutations have been published, the references are as follows:

(1) Matsuura *et al.* (1992)
(2) Wardlaw *et al.* (1990)
(3) Back *et al.* (1992)
(4) Arnaout *et al.* (1990)
(5) Wright *et al.* (1995)
(6) Nelson *et al.* (1992)
(7) Rodriguez *et al.* (1993)
(8) Sligh *et al.* (1992)
(9) Kishimoto *et al.* (1989b)

Point Mutations in coding sequences



To determine whether these defects actually contributed to LAD in these patients, or whether they simply represented polymorphisms or alternative forms of the β2 subunit present within the normal population, mutant β2 subunits carrying the defects were analysed for their ability to form surface expressable LFA-1, Mac-1 and p150,95 heterodimers in COS 7 cells. One of the defects studied was a 2 base pair GA deletion at residue 1256 (1256ΔGA) in exon 11 of the β2 gene, which results in a frameshift mutation and a premature stop codon. The β2(1256ΔGA) cDNA encodes a mutant β2 subunit which has the N-terminal wildtype sequence up to threonine 418 followed by a stretch of 26 aberrant amino acids ($T418_{fr*}$). The mutant $T418_{fr*}$ subunit is truncated in the β2 "mid-piece" region, and therefore lacks the cysteine-rich, transmembrane and cytoplasmic domains. Included in the stretch of 26 aberrant amino acids is an additional cysteine residue and four additional proline residues (see Table 5.1). Not supprisingly, this mutation completely abolished the cell surface expression of LFA-1 and Mac-1 heterodimers, and could therefore be classified as an LAD mutation. The other two defects studied were both single base point mutations within exon 7 of the β2 gene. These mutations, a C to T substitution at residue 809 and a G to A substitution at residue 850, result in mutant β2 subunits containing the single amino acid point mutations A270V and G284S respectively. Both these point mutations are located within the putative A-domain region of the β2 subunit. The G284S mutation completely abolished the cell surface expression of LFA-1 and Mac-1 heterodimers, and the A270V mutation completely abolished the expression of LFA-1 heterodimers and substantially reduced the expression of Mac-1 heterodimers. Therefore, these defects could also be classified as LAD mutations.

During the process of characterising the $T418_{fr*}$, A270V and G284S mutations, a surprising discovery was made: although the A270V mutation completely abolished LFA-1 expression, and substantially reduced Mac-1 expression, it only moderately affected the expression of p150,95 heterodimeric complexes. This result was unexpected, as previously it had been presumed that β2 subunit mutations affecting the expression of one of the leukocyte integrins would similarly affect the expression of all three leukocyte integrins. To date, at least 13 different amino acid point mutations have been discovered in the β2 subunit which contribute to LAD (see Figure 5.7). Most of these amino acids are completely conserved in the β2 subunit cross-species, and are also highly conserved in all

eight human β subunits (see Figure 5.8), indicating their importance in the structure and function of not only the β2 subunit but also the β1, and β3-β8 subunits. These defects have been classified as LAD mutations based on their ability to abolish either LFA-1 or Mac-1 expression. Only rarely has their effect on both LFA-1 and Mac-1 expression been studied, and there are no publications reporting their combined effect on LFA-1, Mac-1 and p150,95 heterodimer formation. In light of the findings with the A270V mutation, the effect of several of the other LAD point mutations on LFA-1, Mac-1 and p150,95 expression has subsequently been studied in Dr. Law's laboratory in detail. Mutant β2 subunits carrying the point mutations were expressed in COS 7 cells along with the wildtype αL, αM or αX subunits, and the expression of αβ heterodimeric complexes on the COS 7 cell surface was assessed by flow cytometry using the heterodimer specific mAbs MHM23 and 1B4. Where expression of mutant LFA-1, Mac-1 or p150,95 was detected on the COS 7 cell surface, transfectants were also tested for their ability to adhere to ligand coated microtitre plates. The results obtained in these experiments are summarised in Table 5.4.

The effect of the different amino acid point mutations on LFA-1, Mac-1 and p150,95 heterodimer formation and expression was surprising. Two of the point mutations studied, P178L and G284S, did completely abolish the cell surface expression of all three leukocyte integrins. However, two other mutations, G273R and A341P, permitted LFA-1 expression but not Mac-1 or p150,95 expression, and two other mutations, C590R and R593C, permitted LFA-1 expression but only weak Mac-1 and p150,95 expression. The contrasting effect of the A270V mutation, to permit p150,95 expression but not LFA-1 or efficient Mac-1 expression, was confirmed in these subsequent experiments.

The effect of the point mutations on the ligand binding abilities of LFA-1, Mac-1 and p150,95 was equally unexpected. COS-7 cells expressing αLβ2(A341P) heterodimeric complexes bound to ICAM-1 coated plates in a similar fashion to cells expressing wildtype LFA-1, as they bound weakly unless stimulated with an activating mAb. However, cells expressing αLβ2(G273R) failed to adhere to ICAM-1 coated plates, even under stimulatory conditions, whereas cells expressing αMβ2(A270V) and αXβ2(A270V) could bind to iC3b coated plates at low levels, but unlike cells expressing wildtype Mac-1 or p150,95, they could not be stimulated to bind at higher levels. Interestingly, cells expressing αLβ2(C590R), and also cells expressing αLβ2(R593C), bound to ICAM-1 plates avidly,

Figure 5.8: Alignment of β Subunits

The entire extracellular and transmembrane regions of all eight human β subunits (HUB1-HUB8), as well as the bovine β2 (BOB2), chicken β2 (CHB2), and murine β2 (MOB2) subunits, were aligned using the MULTALIGN program designed by Dr. G.J. Barton,* Laboratory of Molecular Biophysics, Oxford. Amino acid point mutations which are known to contribute to LAD are shown under the sequence for the human β2 subunit, and are coloured red. The wildtype β2 residues which are affected are coloured blue, and their counter-parts in the other β subunits, if conserved, are also coloured blue. Counter-part residues which are unconserved in the other β subunits are coloured green. The position of a bovine β2 mutation, D128G, which causes bovine LAD (BLAD) in Holstein cattle (Shuster *et al.*, 1992) is also marked. The amino acid numbering refers to the human β2 subunit. It should be noted that the amino acids which are mutated in LAD are completely conserved in the β2 subunit cross-species, and are also highly conserved in the eight different human β subunits. The exceptions are the K196T and R586W mutations: both of these residues are only partially conserved across species, and both residues are completely unconserved in the eight different human β subunits. Arnaout *et al.* (1990) reported that the K196T mutation reduced expression of Mac-1 on the surface of transfected COS 7 cells to 66% normal levels, whereas Nelson *et al.* (1992) reported that the R586W mutation reduced expression of Mac-1 on transfected COS 7 cells to 75% normal levels. Further studies (by Miss M. Gadjeva, Miss S.M Nolan and Dr. S.K.A. Law, unpublished observations) have shown that the K196T mutation has no effect on the expression of LFA-1, Mac-1 or p150,95 on transfected COS 7 cells, and that the binding properties of these receptors is also unaffected (see Table 5.4). Therefore, the classification of K196T, and possibly also of R586W, as LAD mutations is questionable, and they are therefore only tentatively included in the figure below, in brackets.

* Barton, G.J. and Sternberg, M.J.E. (1987) A Strategy for the Rapid Multiple Alignment of Protein Sequences: Confidence Levels from Tertiary Structure Comparisons. *J. Mol. Biol.* **198**, 327.

```
                                                  50
BOB2                          QECTNYKVSTCRDCIESGPGCAWCQKLNFTGQGEPDSIRCDTRAELLSKGCPADDIMEPKSLAETRDSQAGSRK
CHB2                          AECPKIKVGTCKNCIQSGPGCAWCKKLSFTKAGEPDSNRCDTIEQLQQRGCPENEIEFPVNEIKRTQDSAFSNKI
MOB2                          QECTKYKVSSCRDCIQSGPGCSWCQKLNFTGPGEPDSLRCDTRAQLLLKGCPADDIMDPRSIANPEFDQRGQRK
HUB2                          QECTKFKVSSCRECIESGPGCTWCQKLNFTGPGDPDSIRCDTRPQLLMRGCAADDIMDPTSLAETQEDHNGGQK

HUB7  ELDAKIPSTGDATEWRNPHLSMLGSC  QPAPSCQKCILSHPSCAWCKQLNFTASGEAEARRCARREELLARGCPLEELEEPRGQQEVLQDQPLSQGARGEG
HUB1                        ENRCLKANAKSCGECIQAGPNCGWCTNSTFLQEGMPTSARCDDLEALKKKGCPPDDIENPRGSKDIKKNKNVTNRSKGTA
HUB3                       GPNICTTRGVSSCQQCLAVSPMCAWCSDEALP LGSP   RCDLKENLLKDNCAPESIEFPVSEARVLEDRPLSDKGSGDS
HUB5                        LNICTSGSATSCEECLLIHPKCAWCSKEDF GSPRSITSRCDLRANLVKNGC GGEIESPASSFHVLRSLPLSSKGSGSA
HUB6                      RTRWLCLG GAETCEDCLLIGPQCAWCAQENFTHPSGVGE RCDTPANLLAKGCQLNFIENPVSQVEILKNKPLSVGRQKNS
HUB8                       EDNRCASSNAASCARCLALGPECGWCVQEDFISGGSRSE RCDIVSNLISKGCSVDSIEYPSVHVIIPTENEINT
HUB4                         NRCKKAPVKSCTECVRVDKDCAYCTDEMFRDR      RCNTQAELLAAGCQRESIVVMESSFQITEETQIDTTLRRS
HUB1                        ENRCLKANAKSCGECIQAGPNCGWCTNSTFLQEGMPTSARCDDLEALKKKGCPPDDIENPRGSKDIKKNKNVTNRSKGTA
                               1       2  3      4  5              6          7
```

```
                 100                                G                  150
BOB2               QLSPQEVTLYLRPGQAVAFNVTFRRAKGYPIDLYYLMDLSYSMVDDLVNVKKLGGDLLRALNGITESGRIGFGSFVDKTVLPFV NTHPEK
CHB2               QLTPQEVHLKLRIREPAEFDVKFRRATGYPIDIYYLMDLSYSMLDDLENVKKLGGQLLRALESTTPSRRIGFGSFVDKTVLPFV NTHPEK
MOB2               QLSPQKVTLYLRPGQAAAFNVTFRRAKGYPIDLYYLMDLSYSMLDDLNNVKKLGGDLLQALNEITESGRIGFGSFVDKTVLPFV NTHPEK
HUB2               QLSPQKVTLYLRPGQAAAFNVTFRRAKGYPIDLYYLMDLSYSMLDDLRNVKKLGGDLLRALNEITESGRIGFGSFVDKTVLPFV NTHPDK
                                                   N         P          P                    R         L
HUB7    A       TQLAPQRVRVTLRRGEPQQLQVRFLRAEGYPVDLYYLMDLSSSMKDDLERVRQLGHALLVRLQEVTHSVRIGFGSFVDKTVLPFV STVPSK
HUB1    EKLKPEDIHQIQPQQLVLRLRSGEPQTFTLKFKRAEDYPIDLYYLMDLSYSMKDDLENVKSLGTDLMNEMRRITSDFRIGFGSFVEKTVMPYI STTPAK
HUB3    S     QVTQVSPQRIALRLRPDDSKNFSIQVRQVEDYPVDIYYLMDLSYSMKDDLWSIQNLGTKLATQMRKLTSNLRIGFGAFVDKPVSPYMYISPPEA
HUB5    GW    DVIQMTPQEIAVNLRPGDKTTFQLQVRQVEDYPVDLYYLMDLSLSMKDDLDNIRSLGTKLAEEMRKLTSNFRLGFGSFVDKDISPFS YAAPRY
HUB6    S     DIVQIAPQSLILKLRPGGAQTLQVHVRQTEDYPVDLYYLMDLSASMDDDLNTIKELGSGLSKEMSKLTSNFRLGFGSFVEKPVSPFV KTTPEE
HUB8             QVTPGEVSIQLRPGAEANFMLKVHPLKKYPVDLYYLVDVSASMHNNIEKLNSVGNDLSRKMAFFSRDFRLGFGSYVDKTVSPYI SIHPER
HUB4             QMSPQGLRVRLRPGEERHFELEVFEPLESPVDLYILMDFSNSMSDDLDNLKKMGQNLARVLSQLTSDYTIGFGKFVDKVSVPQT DMRPEK
HUB1    EKLKPEDIHQIQPQQLVLRLRSGEPQTFTLKFKRAEDYPIDLYYLMDLSYSMKDDLENVKSLGTDLMNEMRRITSDFRIGFGSFVEKTVMPYI STTPAK
```

```
                      200                                                 250
BOB2    LRNPCPNKE  KECQPPFAFRHVLKLTDNSKQFETEVGKQLISGNLDAPEGGLDAMMQVAACPEEIGWRN VTRLLVFATDDGFHFAGDGK  LGAILTP
CHB2    LKNPCPNKD  SNCQPPFAFKHILSLTDNAEKFESEVGKQFISGNLDAPEG LDAMMQAAVCGDLIGWRN VTRLLVYATDDGFHFAGDGK  LGGILTP
MOB2    LRNPCPNKE  KACQPPFAFRHVLKLTDNSNQFQTEVGKQLISGNLDAPEGGLDAIMQVAACPEEIGWRN VTRLLVFATDDGFHFAGDGK  LGAILTP
HUB2    LRNPCPNKE  KECQPPFAFRHVLKLTNNSNQFQTEVGKQLISGNLDAPEGGLDAMMQVAACPEEIGWRN VTRLLVFATDDGFHFAGDGK  LGAILTP
                 (T)                                                 R                      V  R
HUB7    LRHPCPTRL  ERCQSPFSFHHVLSLTGDAQAFEREVGRQSVSGNLDSPEGGFDAILQAALCQEQIGWRN VSRLLVFTSDDTFHTAGDGK  LGGIFMP
HUB1    LRNPCTS E  QNCTTPFSYKNVLSLTNKGEVFNELVGKQRISGNLDSPEGGFDAIMQVAVCGSLIGWRN VTRLLVFSTDAGFHFAGDGK  LGGIVLP
HUB3    LENPCYDMK  TTCLPMFGYKHVLTLTDQVTRFNEEVKKQSVSRNRDAPEGGFDAIMQATVCDEKIGWRNDASHLLVFTTDAKTHIALDGR  LAGIVQP
HUB5    QTNPCIGYKLFPNCVPSFGFRHLLPLTDRVDSFNEEVRKQRVSRNRDAPEGGFDAVLQAAVCKEKIGWRKDALHLLVFTTDDVPHIALDGK  LGGLVQP
HUB6    IANPCSSIP  YFCLPTFGFKHILPLTNDAERFNEIVKNQKISANIDTPEGGFDAIMQAAVCKEKIGWRNDSLHLLVFVSDADSHFGMDSK  LAGIVIP
HUB8    IHNQCSDYN  LDCMPPHGYIHVLSLTENITEFEKAVHRQKISGNIDTPEGGFDAMLQAAVCESHIGWRKEAKRLLLVMTDQTSHLALDSK  LAGIVVP
HUB4    LKEPWPN      SDPPFSFKNVISLTEDVDEFRNKLQGERISGNLDAPEGGFDAILQTAVCTRDIGWRPDSTHLLVFSTESAFHYEADGANVLAGIMSR
HUB1    LRNPCTS E  QNCTTPFSYKNVLSLTNKGEVFNELVGKQRISGNLDSPEGGFDAIMQVAVCGSLIGWRN VTRLLVFSTDAGFHFAGDGK  LGGIVLP
            8       9                                                  10
```

```
                        300                                                 350
BOB2    NDGRCHLE DNLYKSSNEFDYPSVGQLAHKLAESNIQPIFAVTKKMVKTYEKLTEIIPKSAVGELSEDSRNVVELIKNAYNKLSSRVFLDHSTLPDTLKV
CHB2    NDGQCHLE DNMYKKSNEFDYPSVGQLVQKLAENNIQPIFAVTSKMVDVYKKLSDMIPKSAVGELNEDSSNIIELIQVAYNNLSSRIILDHSTLPDVLDV
MOB2    NDGRCHLE DNMYKRSNEFDYPSVGQLAHKLSESNIQPIFAVTKKMVKTYEKLTEIIPKSAVGELSDDSSNVVQLIKNAYYKLSSRVFLDHSTLPDTLKV
HUB2    NDGRCHLE DNLYKRSNEFDYPSVGQLAHKLAENNIQPIFAVTSRMVKTYEKLTEIIPKSAVGELSEDSSNVVHLIKNAYNKLSSRVFLDHNALPDTLKV
          S                                                                 P          S
HUB7    SDGSCHLDSNGLYSRSTEFDYPSVGQVAQALSAANIQPIFAVTSAALPVYQELSKLIPKSAVGELSEDSSNVVQLIMDAYNSLSSTVTLEHSSLPPGVHI
HUB1    NDGQCHLE NNMYTMSHYYDYPSIAHLVQKLSENNIQTIFAVTEEFQPVYKELKNLIPKSAVGTLSANSSNVIQLIIDAYNSLSSEVILENGKLSEGVTI
HUB3    NDGQCHVGSDNHYSASTTMDYPSLGLMTEKLSQKNINLIFAVTENVVNLYQNYSELIPGTTVGVLSMDSSNVLQLIVDAYGKIRSKVELEVRDLPEELSL
HUB5    HDGQCHLNEANEYTASNQMDYPSLALLGEKLAENNINLIFAVTKNHYMLYKNFTALIPGTTVEILDGDSKNIIQLIINAYNSIRSKVELSVWDQPEDLNL
HUB6    NDGLCHLDSKNEYSMSTVLEYPTIGQLIDKLVQNNVLLIFAVTQEQVHLYENYAKLIPGATVGLLQKDSGNILQLIISAYEELRSEVELEVLGDTEGLNL
HUB8    NDGNCHLK NNVYVKSTTMEHPSLGQLSEKLIDNNINVIFAVQGKQFHWYKDLLPLLPGTIAGEIESKAANLNNLVVEAYQKLISEVKVQVENQVQGIYF
HUB4    NDERCHLDTTGTYTQYRTQDYPSVPTLVRLLAKHNIIPIFAVTNYSYSYYEKLHTYFPVSSLGVLQEDSSNIVELLEEAFNRIRSNLDIRALDSPRGLRT
HUB1    NDGQCHLE NNMYTMSHYYDYPSIAHLVQKLSENNIQTIFAVTEEFQPVYKELKNLIPKSAVGTLSANSSNVIQLIIDAYNSLSSEVILENGKLSEGVTI
           11
```

```
                          400                                                 450
BOB2     TYDSFCS  NGKSQVDQPRGDCDGVQINVPITFQVKVTATECI  Q QQSFTIRALGFTDTVTVRVLPQCE CQCRDAS RDGSICG  GRGSMECGVCRC
CHB2     KYDSICN  NNTGAKNEARGQCDNVKINDEVTFKVKVTANECI  K SQSFTIRPLGFTDTLTVHLDSICD CDCREQ  PDPTACS  GNGKVVCGICSC
MOB2     TYDSFCS  NGASSIGKSRGDCDGVQINNPVTFQVKVMASECI  Q EQSFVIRALGFTDTVTVQVRPQCE CQCRDQS REQSLCG  GKGVMECGICRC
HUB2     TYDSFCS  NGVTHRNQPRGDCDGVQINVPITFQVKVTATECI  Q EQSFVIRALGFTDIVTVQVLPQCE CRCRDQS RDRSLCH  GKGFLECGICRC

HUB7     SYESQCEGPEKREGKAEDRGQCNHVRINQTVTFWVSLQATHCL  PEPHLLRLRALGFSEELIVELHTLCD CNCSDTQ PQAPHCS  DAGHLQCGVCSC
HUB1     SYKSYCK  NGVNGTGENGRKCSNISIGDEVQFEISITSNKCPKKD SDSFKIRPLGFTEEVEVILQYICE CECQSEGIPESPKCH EGNGTFECGACRC
HUB3     SFNATCL  N  NEVIPGLKSCMGLKIGDTVSFSIEAKVRGCPQEK EKSFTIKPVGFKDSLIVQVTFDCD CACQAQAEPNSHRCN NGNGTFECGVCRC
HUB5     FFTATCQ  DGVSYPGQ  RKCEGLKIGDTASFEVSLEARSCPSRHTEHVFALRPVGFRDSLEVGVTYNCT CGCSVGLEPNSARCN  GSGTYVCGLCEC
HUB6     SFTAICN  NG  TLFQHQKKCSHMKVGDTASFSVTVNIPHCE  RRSRHIIIKPVGLGDALELLVSPECN CDCQKEVEVNSSKCH HGNGSFQCGVCAC
HUB8     NITAICP  DG  SRKPGMEGCRNVTSNDEVLFNVTVTMKKCDVTGGKNYAIIKPIGFNETAKIHIHRNCS CQCEDNRGPKG KCVDETFLDSKCFQC
HUB4     EVTSKMF QKTRTGSFHIRRGEVGIYQVQLRALEHVDGTHVCQLPEDQKGNIHLKPSFSDGLKMDAGIICDVCTCELQKEVRSARCS  FNGDFVCGQCVC
HUB1     SYKSYCK  NGVNGTGENGRKCSNISIGDEVQFEISITSNKCPKKD SDSFKIRPLGFTEEVEVILQYICE CECQSEGIPESPKCH EGNGTFECGACRC
             12              13                  14                                15 1617        18        19 2021
```

```
                                500                                                 550
BOB2     DAGYIGKNCECQTQGRSSQELEGSCRKDNSS IICSGLGDCICGQCVCHTSDVPNKKIYGQFCECDNVNCERYDGQVCGGEKRGLCFCGTCRCDEQYEGS
CHB2     NLSYTGKNCECDTKGKTSKELEGSCRKDNSS VICSGLGDCVCGQCVCHTSDVPGKEIYGTFCDCDNMNCEFHNGSLCGGEERGRCDCGECKCTPKYEGS
MOB2     ESGYIGKNCECQTQGRSSQELERNCRKDNSS IVCSGLGDCICGQCVCHTSDVPNKEIFGQYCECDNVNCERYNSQVCGGSDRGSCNCGKCSCKPGYEGS
HUB2     DTGYIGKNCECQTQGRSSQELEGSCRKDNNS IICSGLGDCVCGQCLCHTSDVPGKLIYGQYCECDTINCERYNGQVCGGPGRGLCFCGKCRCHPGFEGS

HUB7     APGALGRLCECSVAELSSPDLESGCRAPNGTGPLCSGKGHCQCGRCSCSGQSS      GHLCECDDASCERHEGMLCGGF  GRCQCGVCHCHANRTGR
HUB1     NEGRVGRHCECSTDEVNSEDMDAYCRKENSS EICSNNGECVCGQCVCRKRDNTNEIYSGKFCECDNFNCDRSNGLICGGN  GVCKCRVCECNPNYTGS
HUB3     GPGWLGSQCECSEEDYRPSQ QDECSPREGQ PVCSQRGECLCGQCVCHSSDFGK  ITGKYCECDDFSCVRYKGEMCSGH  GQCSCGDCLCDSDWTGY
HUB5     SPGYLGTRCECQ DGENQSVYQNLCREAEGK PLCSGRGDCSCNQCSCFESEFGK  IYGPFCECDNFSCARNKGVLCSGH  GECHCGECKCHAGYIGD
HUB6     HPGHMGPRCECGEDMLSTD    SCKEAPDH PSCSGRGDCYCGQCICHLSPYGN  IYGPYCQCDNFSCVRHKGLLCGGN  GDCDCGECVCRSGWTGE
HUB8     DE    NK  CHFDEDQFSSE  SCKSHKDQ PVCSGRGVCVCGKCSCHKIKLGK  VYGKYCEKDDFSCPYHHGNLCAGH  GECEAGRCQCFSGWEGD
HUB4     SEGWSGQTCNCSTGSLSDIQ   PCLREGED KPCSGRGECQCGHCVCYGEGR    YEGQFCEYDNFQCPRTSGFLCNDR  GRCSMGQCVCEPGWTGP
HUB1     NEGRVGRHCECSTDEVNSEDMDAYCRKENSS EICSNNGECVCGQCVCRKRDNTNEIYSGKFCECDNFNCDRSNGLICGGN  GVCKCRVCECNPNYTGS
            2223            24        25    2627 2829            3031   32      33      3435 3637
```

```
                                      600                                                                  650
BOB2     ACQC LKSTQGCLNLDGVECSGRGRCRCNVCQC DPG YQPPLCSE  CPGCPVPC AGFAPCTECLKFDKGPF  AKNCSAACGQTKLLSSPVPGR
CHB2     ACQC KKSTDGCRNSRQNECSLRGSCPCNRCQC RGG YQPPFCEE  CPGCPSPC GRHISCVECKSFNSGPL  AKNCSVACTSIQLADEPRAGSR
MOB2     ACQC QRSTTGCLNARLVECSGRGHCQCNRCIC DEG YQPPMCED  CPSCGSHCRDNHTSCAECLKFDKGPF  EKNCSVQCAGMTLQTIPLKKK
HUB2     ACQC ERTTEGCLNPRRVECSGRGRCRCNVCEC HSG YQLPLCQE  CPGCPSPC GKYISCAECLKFEKGPF  GKNCSAACPGLQLSNNPVKGR
                      (W)  R  C
HUB7     ACEC SGDMDSCISPEGGLCSGHGRCKCNRCQCLD G YYGALCDQ  CPGCKTPC ERHRDCAECGAFRTGPL  ATNCSTACAHTNVTLALAPILDDG
HUB1     ACDC SLDTSTCEASNGQICNGRGICECGVCKCTDPK FQGQTCEM  CQTCLGVC AEHKECVQCRAFNKGEK  KDTCTQECSYFNITKVESRDKLPQ
HUB3     YCNC TTRTDTCMSSNGLLCSGRGKCECGSCVCIQPG SYGDTCEK  CPTCPDAC TFKKECVECKKFDRGALHDENTCNRYCRDEIESVKELKDTGKD
HUB5     NCNC STDISTCRGRDGQICSERGHCLCGQCQCTEPG AFGEMCEK  CPTCPDAC STKRDCVECLLLHSGKP DNQTCHSLCRDEVITWVDTIVKDDQ
HUB6     YCNC TTSTDSCVSEDGVLCSGRGDCVCGKCVCTNPG ASGPTCER  CPTCGDPC NSKRSCIECHLSAAGQA  GEECVDKCKLAGATISEEEDFSKD
HUB8     RCQCPSAAAQHCVNSKGQVCSGRGTCVCGRCECTDPR SIGRFCEH  CPTCYTAC KENWNCMQCLHPHNLSQAILDQCKTSCALM          EQ
HUB4     SCDC PLSNATCIDSNGGICNGRGHCECGRCHCHQQSLYTDTICEINYSAIHPGLC EDLRSCVQCQAWGTGEK KGRTC EECNFKVKMVDELKRAEEV
HUB1     ACDC SLDTSTCEASNGQICNGRGICECGVCKCTDPK FQGQTCEM  CQTCLGVC AEHKECVQCRAFNKGEK  KDTCTQECSYFNITKVESRDKLPQ
         3839      40      41    4243 4445        46   47 48  49     50 51           52  53
```

```
                                                  700
BOB2              KCKERDSEG CWMTYTLVQRDGRD RYDVHVDDMLECVKGPNIAAIVGGTVGGVVLVGILLLVIWK
CHB2              QCKEKDSEN CWISFYMAQDDGEE MYTVTVDPKKECPEPPNIALIVGSTIAGVALIGLLLLLTWR
MOB2              PCKERDSEG CWITYTLQQKDGRN IYNIHVEDSLECVKGPNVAAIVGGTVVGVVLIGVLLLVIWK
HUB2              TCKERDSEG CWVAYTLEQQDGMD RYLIYVDESRECVAGPNIAAIVGGTVAGIVLIGILLLVIWK

HUB7              WCKERTLDN QLFFF LVEDDARA TVVLRVRPQEK  GADHTQAIVLGWVGGIVAVGLGLVLAYR
HUB1     PVQPDPVSHCKEKDVDD CWFYFTYSV NGNN EVMVHVVENPECPTGPDIIPIVAGVVAGIVLIGLALLLIWK
HUB3     AV       NCTYKNEDD CVVRFQYYE DSSG KSILYVVEEPECPKGPDILVVLLSVMGAILLIGLAALLIWK
HUB5     EA     VLCFYKTAKD CVMMFTYVE LPSG KSNLTVLREPECGNTPNAMTILLAVVGSILLVGLALLAIWK
HUB6     GS     VSCSLQGENE CLITF LITTDNEG KTIIHSINEKDCPKPPNIPMIMLGVSLATLLIGVVLLCIWK
HUB8     QHYVDQTSECF                                        SSPSYLRIFFIIFIVTFLIGLLKVLIIR
HUB4     VV       RCSFRDEDDDCTYSYTMEGDGAPGPNSTVLVHKKKDCPPGS FWWLIPLLLLLLPLLALLLLLCWK
HUB1     PVQPDPVSHCKEKDVDD CWFYFTYSV NGNN EVMVHVVENPECPTGPDIIPIVAGVVAGIVLIGLALLLIWK
                  54       55                          56
```

Table 5.4: The Effect of Various LAD Amino Acid Point Mutations on αβ Heterodimer Formation and Ligand Binding

Mutation	LFA-1		Mac-1		p150,95	
	αLβ2 Formation[1]	ICAM-1 Binding[2]	αMβ2 Formation[1]	iC3b Binding[2]	αXβ2 Formation[1]	iC3b Binding[2]
P178L	-		-		-	
K196T[3]	+++++	wt	+++++	wt	+++++	wt
A270V	-		+	low	+++	low
G273R	++++	-	-		-	
G284S	-		-		-	
A341P	+++	wt	-		-	
C590R	+++++	CA	++	CA	ND	
R593C	+++++	CA	++	CA	+/-	

1 The level of expression of cell surface LFA-1, Mac-1 and p150,95 heterodimeric complexes is indicated by the "+" signs, with "+++++" indicating wildtype levels, "++++" slightly lower levels, and "+++", "++" and "+" lower and lower levels of expression. The "-" signs indicate no heterodimer expression, and the "+/-" sign indicates where heterodimer formation was detected at extremely low levels in some experiments, but was not detected at all in others.

2 The ability of COS 7 cells expressing mutant LFA-1, Mac-1 or p150,95 heterodimeric complexes to adhere to microtitre plates coated in ligand is indicated as follows: "wt", wildtype-like binding, ie. binding which is low unless stimulated with an activating mAb; "low", low level of binding even when stimulated with an activating mAb; "-", no binding under any conditions; "CA", constitutively activated, ie. binding at very high levels even in the absence of activating mAbs.

3 The K196T mutation, which is not conserved in the β2 subunit cross-species, or in the human β1–β8 subunits (see Fig. 5.8), has probably been incorrectly characterised as an LAD mutation (Arnaout *et al.*, 1990), as β2 subunits carrying this mutation are able to form cell surface expressable LFA-1, Mac-1 and p150,95 heterodimeric complexes which have normal ligand binding properties.

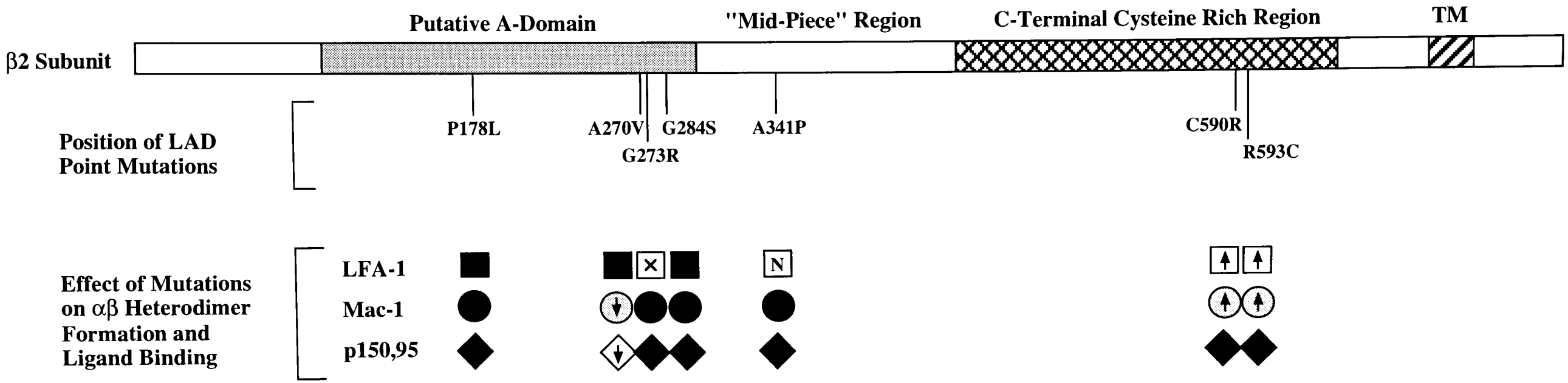
even in non-stimulatory conditions. A similar result was obtained with the adhesion of cells expressing αMβ2(C590R) or αMβ2(R593C) to iC3b coated plates.

The position of these LAD point mutations in the β2 subunit, and their effects on αβ heterodimer formation and ligand binding are summarised in Figure 5.9. Several conclusions can be tentatively drawn from these results. LFA-1 expression was only affected by mutations falling within the putative A-domain region of the β2 subunit, whereas Mac-1 and p150,95 expression was affected by mutations falling within the A-domain as well as by mutations falling within the "mid-piece" and C-terminal cysteine rich regions. This suggests that different regions of the β2 subunit interact with the αL, αM and αX subunits: only the N-terminal putative A-domain region of the β2 subunit appears to interact with the αL subunit to form LFA-1 heterodimeric complexes, whereas more extensive interactions involving the putative A-domain, "mid-piece" and C-terminal cysteine-rich regions appear to be required for Mac-1 and p150,95 heterodimer formation (see Figure 5.9). The results also provided information on functional, as well as structural regions of the β2 subunit. It is generally believed that the ligand binding sites of integrins are composites of regions of the α and β subunits which are brought into close proximity by αβ heterodimer formation. LAD mutations which either abolished or weakened LFA-1, Mac-1 or p150,95 ligand binding were all clustered within the putative A-domain region of the β2 subunit (see Figure 5.9), indicating that this region may contribute to the ligand binding sites in these integrins. However, the adhesive properties of the leukocyte integrins may well be regulated by other, spacially distant regions of the β2 subunit. Mutations within the cysteine-rich region resulted in constitutively activated LFA-1 and Mac-1 receptors, suggesting that the cysteine-rich region may actually play a role in regulating the ligand binding activity of the leukocyte integrins (see Figure 5.9).

It is therefore clear that different amino acid point mutations within the β2 subunit can have completely contrasting effects on the cell surface expression and function of LFA-1, Mac-1 and p150,95. This provides an explanation for the heterogeneity of clinical symptoms seen in LAD patients. Apart from the different phenotypes which can result from each mutation, many LAD patients are compound heterozygotes, carrying two different defective alleles, which can partially compensate for one another in function, and therefore result in even greater phenotypic diversity. It is clear that a thorough re-investigation into the effects of all

Figure 5.9: Summary of the Effect of LAD Amino Acid Point Mutations on LFA-1, Mac-1 and p150,95 Heterodimer Formation and Ligand Binding: Putative Mapping of Functional Regions of the β2 Subunit

In the figure below, the β2 subunit is represented with the position of its putative A-domain, "mid-piece", C-terminal cysteine-rich and transmembrane (TM) regions shown. The positions of the various amino acid point mutations which have been studied in Dr. Law's laboratory are shown below the β2 subunit. The effect of these mutations on αβ heterodimer formation and ligand binding is representated in the figure as follows: LFA-1 heterodimers are represented by squares, Mac-1 heterodimers by circles, and p150,95 heterodimers by diamond shapes. Unshaded shapes represent normal levels of αβ heterodimer expression, grey shaded shapes reduced levels of heterodimer expression, and blackened shapes no heterodimer expression. The ligand binding properties of mutant LFA-1, Mac-1 and p150,95 heterodimers is shown within the shapes: "N" indicates normal binding, ie. a low level of binding which can be stimulated to higher levels with activating mAbs; "X" indicates no binding, even when stimulated with activating mAbs; "↓", indicates a low level of binding which cannot be stimulated to higher levels with activating mAbs; and "↑", very high levels of binding, even without stimulation with activating mAbs. The conclusions which can be tentatively drawn from these results are summarised at the bottom of the figure.


Putative A-Domain
"Mid-Piece" Region
C-Terminal Cysteine Rich Region
TM
β2 Subunit
Position of LAD Point Mutations
P178L
A270V
G273R
G284S
A341P
C590R
R593C
Effect of Mutations on αβ Heterodimer Formation and Ligand Binding
LFA-1
Mac-1
p150,95
N
Regions of the β2 Subunit Interacting With the αL, αM and αX Subunits ?
αL
αM
αX
αM
αX
Functional Regions of the β2 Subunit ?
Ligand Binding Site
Regulatory Region

the LAD point mutations is required, not only to provide valuable information on particular residues and regions of the β2 subunit which are involved in αβ heterodimer formation and function, but also to provide a basis for future research into more effective treatments for individual LAD patients.

CHAPTER SIX

DISCUSSION

6.1 THE EFFECT OF A SERIES OF CHIMERIC, SOLUBLE AND TRUNCATED β2 SUBUNITS ON αβ HETERODIMER FORMATION AND LIGAND BINDING

Exactly how integrin α and β subunits combine to form αβ heterodimeric complexes, exactly how the ligand binding regions within the α and β subunits cooperate to form highly specific ligand binding sites, and exactly how the binding activities of these ligand binding sites are regulated, are inseparable and unanswered questions in the field of integrin-mediated adhesion. In an attempt to address some of these questions, a series of chimeric, soluble and truncated β2 variants were constructed, and were analysed for their ability to combine with the wildtype αL, αM and αX subunits to form modified LFA-1, Mac-1 and p150,95 receptors. The effect of the various β2 subunit modifications on the ligand binding abilities of the resultant LFA-1 heterodimers was also investigated. The composition of these variant β2 subunits is shown in Chapter 3 (see Figure 3.1).

6.1.1 REGIONS OF THE β2 SUBUNIT INVOLVED IN LFA-1, Mac-1 AND p150,95 HETERODIMER FORMATION

All of the variant β2 subunits retained the ability to combine with the wildtype αL subunit to form LFA-1 heterodimers, suggesting that the C-terminal cysteine-rich, membrane proximal, transmembrane and cytoplasmic domains of β2 are not required for its heterodimeric interaction with the αL subunit, and that the αL binding site must therefore reside within the N-terminal 436 amino acid residues of the β2 subunit. This is consistent with the current structural model of integrins, based on electron microscopic studies of α5β1 (Nermut *et al.*, 1988) and αIIbβ3 (Carrell *et al.*, 1985; Weisel *et al.*, 1992), as "two-pronged plugs", in which the N-terminal regions of the α and β subunits interact to form a globular head region, and the remaining C-terminal regions of each subunit are inserted separately into the membrane bilayer (see Figure 1.1).

The "two-pronged plug" model may not be applicable to Mac-1 and p150,95. All of the variant β2 subunits associated far less readily with the αM and αX subunits than they did with the αL subunit, and in some cases, the formation of Mac-1 and p150,95 heterodimeric complexes could not be detected at all. It therefore appears that the heterodimeric

interactions between the α and β subunits in Mac-1 and in p150,95 are far more extensive, and perhaps more complicated, than those in LFA-1, and involve regions from both the N- and C-terminal halves of the β2 subunit. This is consistent with the previous observation that the Mac-1 and p150,95 receptors appear to be more stable than LFA-1 receptors, as under conditions of high pH (pH 11.5) they remain intact, whereas LFA-1 receptors are dissociated (Sanchez-Madrid *et al.*, 1983).

There may also be subtle differences between the regions of the β2 subunit involved in Mac-1 heterodimer formation and those involved in p150,95 heterodimer formation. Although the formation of modified Mac-1 and p150,95 receptors with the variant β2 subunits was very inefficient, all of the variants appeared to support Mac-1 heterodimer formation more efficiently than they supported p150,95 heterodimer formation. The exception was the β2sol subunit, which appeared to support p150,95 heterodimer formation more efficiently than Mac-1 heterodimer formation. This suggests that slightly different regions in the C-terminal half of the β2 subunit may be involved in its heterodimeric interaction with the αM and αX subunits, but further analysis with additional chimeras and β2 mutants will be required to determine the exact details of the regions and residues involved.

6.1.2 REGIONS OF THE β2 SUBUNIT INVOLVED IN LFA-1 BINDING TO ICAM-1

Wildtype LFA-1 heterodimers, and the modified LFA-1 heterodimers formed with the chimeric, soluble and truncated β2 variants, were examined for their ability to bind to the LFA-1 ligand ICAM-1. The wildtype LFA-1 heterodimers, but not the individual αL and β2 monomers, could bind to ICAM-1, indicating that the ICAM-1 binding site is likely to be a composite of regions from both the αL and β2 subunits. All of the modified LFA-1 heterodimers formed with the variant β2 subunits retained the ability to bind to ICAM-1, suggesting that in LFA-1, the C-terminal cysteine-rich and membrane proximal regions of the β2 subunit do not contribute to the ICAM-1 binding site, and that this must therefore be located within the N-terminal 436 amino acid residues of the β2 subunit. These results are consistent with a previous report suggesting that the putative A-domain in the β2 subunit plays an important role in LFA-1 binding to ICAM-1, as two point mutations within this

region, D134A and S136A, completely abolish ICAM-1 binding (Bajt *et al.*, 1995). Two different regions within the αL subunit of LFA-1 have also been implicated in ICAM-1 binding: the A-domain (Landis *et al.*, 1994; Randi and Hogg, 1994; Huang and Springer, 1995) and domains V-VI (Stanley *et al.*, 1994). How the LFA-1 receptor utilises these three regions for ICAM-1 binding, and whether they cooperate somehow in ligand binding, remains to be determined. Interestingly, it has been reported that recombinant αL subunit A-domain can bind ICAM-1 (Randi and Hogg, 1994), and yet as mentioned above, the wildtype αL monomers appear unable to bind to ICAM-1. It therefore appears that the ligand binding activity of the αL A-domain may be regulated by other regions within the αL subunit (see Section 6.1.3).

6.1.3 THE ROLE OF THE β2 SUBUNIT IN THE REGULATION OF LFA-1 BINDING TO ICAM-1

The wildtype LFA-1 heterodimers only bound to ICAM-1 after stimulation with the "activating" mAb MEM83, which recognises an activation epitope located within the A-domain of the αL subunit (Landis *et al.*, 1993). In contrast, all of the modified LFA-1 heterodimers formed with the chimeric, soluble and truncated β2 subunits were constitutively active with respect to ICAM-1 binding: they all bound to ICAM-1 without prior stimulation with MEM83, and the level of binding was actually higher than that observed with MEM83-activated wildtype LFA-1. Therefore, disruption of the C-terminal half of the β2 subunit, either by replacing regions of β2 with the homologous but incompatible regions from the β1 or β7 subunits (in the chimeric variants), or by deleting entire sections of β2 (in the soluble and truncated variants), results in release of the receptor into its high affinity binding state, suggesting that the C-terminal half of the β2 subunit plays a negative regulatory role in LFA-1 function, and under "resting" conditions is required to maintain the receptor in its inactive conformation. As different β2 regions were modified in the various chimeric, soluble and truncated β2 variants, it appears that diverse regions within the C-terminal half of the β2 subunit are involved in maintaining the LFA-1 receptor in its resting state, and that specific intramolecular interactions between these regions appear to be required to constrain the receptor in its inactive conformation, with disruption of any one of these interactions resulting in release of the receptor into its active, high affinity ligand binding conformation.

6.2 THE EFFECT OF A SERIES OF LAD MUTATIONS ON αβ HETERODIMER FORMATION AND LIGAND BINDING

In addition to the chimeric, soluble and truncated β2 variants, three mutant β2 subunits carrying LAD mutations were analysed for their ability to combine with the wildtype αL, αM and αX subunits to form LFA-1, Mac-1 and p150,95 heterodimeric complexes. Two of these mutant subunits, β2(A270V) and β2(G284S), contained single amino acid point mutations within the putative A-domain region of the β2 subunit, whereas the third mutant subunit, β2($T418_{fr*}$), was a truncated frameshift mutant, comprising of the N-terminal 418 amino acid residues of the β2 subunit followed by a stretch of 26 aberrant amino acids, and therefore only contained the N-terminal cysteine-rich, putative A-domain and "mid-piece" regions of the β2 subunit. Not surprisingly, the mutant β2($T418_{fr*}$) subunit was unable to form heterodimers with the αL and αM subunits. However, although the mutant β2(G284S) subunit was also unable to form LFA-1 and Mac-1 heterodimers, the mutant β2(A270V) subunit weakly supported the formation of Mac-1, and efficiently supported the formation of p150,95, even though it did not support the formation of LFA-1 heterodimers. These results, like the results obtained with the chimeric, soluble and truncated β2 variants, suggest that the regions of the β2 subunit involved in its heterodimeric interaction with the αL, αM and αX subunits may differ, and that in the context of these particular mutations, the A270 residue is involved in interactions with the αL subunit and partially involved in interactions with the αM subunit, but is not involved at all in interactions with the αX subunit, whereas the G284 residue is involved in heterodimeric interactions with all three α subunits.

These results prompted a thorough re-investigation into the effects of five other LAD point mutations on LFA-1, Mac-1 and p150,95 heterodimer formation. The results obtained, which are summarised in Chapter 5, Figure 5.9, are consistent with the results obtained with the chimeric, soluble and truncated β2 subunits. Mutations which affected LFA-1 heterodimer formation were localised within the putative A-domain of the β2 subunit, whereas mutations affecting Mac-1 and p150,95 heterodimer formation were localised to regions within the putative A-domain, "mid-piece" and C-terminal cysteine-rich regions, suggesting that the αL subunit only interacts with the A-domain of the β2 subunit, whereas the interactions with the αM and αX subunits are more extensive, involving the A-domain,

"mid-piece" and C-terminal cysteine-rich regions of the β2 subunit. The ligand binding properties of the resultant LFA-1, Mac-1 or p150,95 mutant receptors were also analysed. In all three receptors, mutations which abolished or reduced ligand binding were located within the putative A-domain region of the β2 subunit, whereas mutations which resulted in constitutively active receptors were located within the C-terminal cysteine-rich region. Again, these results are consistent with and supplement those obtained with the chimeric, soluble and truncated β2 variants, as they suggest that in all three leukocyte integrin receptors, ligands bind to a site located within the A-domain of the β2 subunit, and that the C-terminal half of the β2 subunit, and in this case the C-terminal cysteine-rich region, is involved in regulating the activity of this ligand binding site.

6.3 A "CONSTRAINT MODEL" FOR THE REGULATION OF INTEGRIN-LIGAND BINDING EVENTS

The results described in this thesis suggest that an intact, wildtype β2 subunit is required to maintain the LFA-1, Mac-1 and p150,95 receptors in their resting, low affinity ligand binding state, as all of the chimeric, soluble, truncated and LAD mutant β2 subunits which retained the ability to associate with the wildtype αL, αM or αX subunits resulted in the formation of constitutively active LFA-1, Mac-1 or p150,95 receptors. Diverse regions of the β2 subunit were modified in these β2 variants, suggesting that specific intramolecular interactions between different regions in the β2 subunit are required to form a constraint which locks the entire integrin receptor in its inactive state, and that disruption of any one of these intramolecular interactions results in the release of the receptor from this constraint, allowing it to spring into its active, high affinity ligand binding conformation. This concept forms the basis of a novel "constraint model" for the regulation of the LFA-1, Mac-1 and p150,95 receptors, which is illustrated in Figure 6.1. In this model, the integrin receptor is expressed on the cell surface with its β2 subunit locked in an inactive conformation and constraining the entire integrin receptor in its inactive state (Figure 6.1a). In response to appropriate stimuli, the β2 subunit is released from its inactive state, thereby releasing the entire integrin receptor into its active, high affinity ligand binding conformation (Figure 6.1b). The conformational change releasing the constraint imposed by the β2 subunit is envisaged initiating in the cytoplasmic tail of the β2 subunit, and then transmitting through the transmembrane domain and to the extracellular ligand binding site via a long range

Figure 6.1: The "Constraint Model" for the Regulation of Integrin Receptors

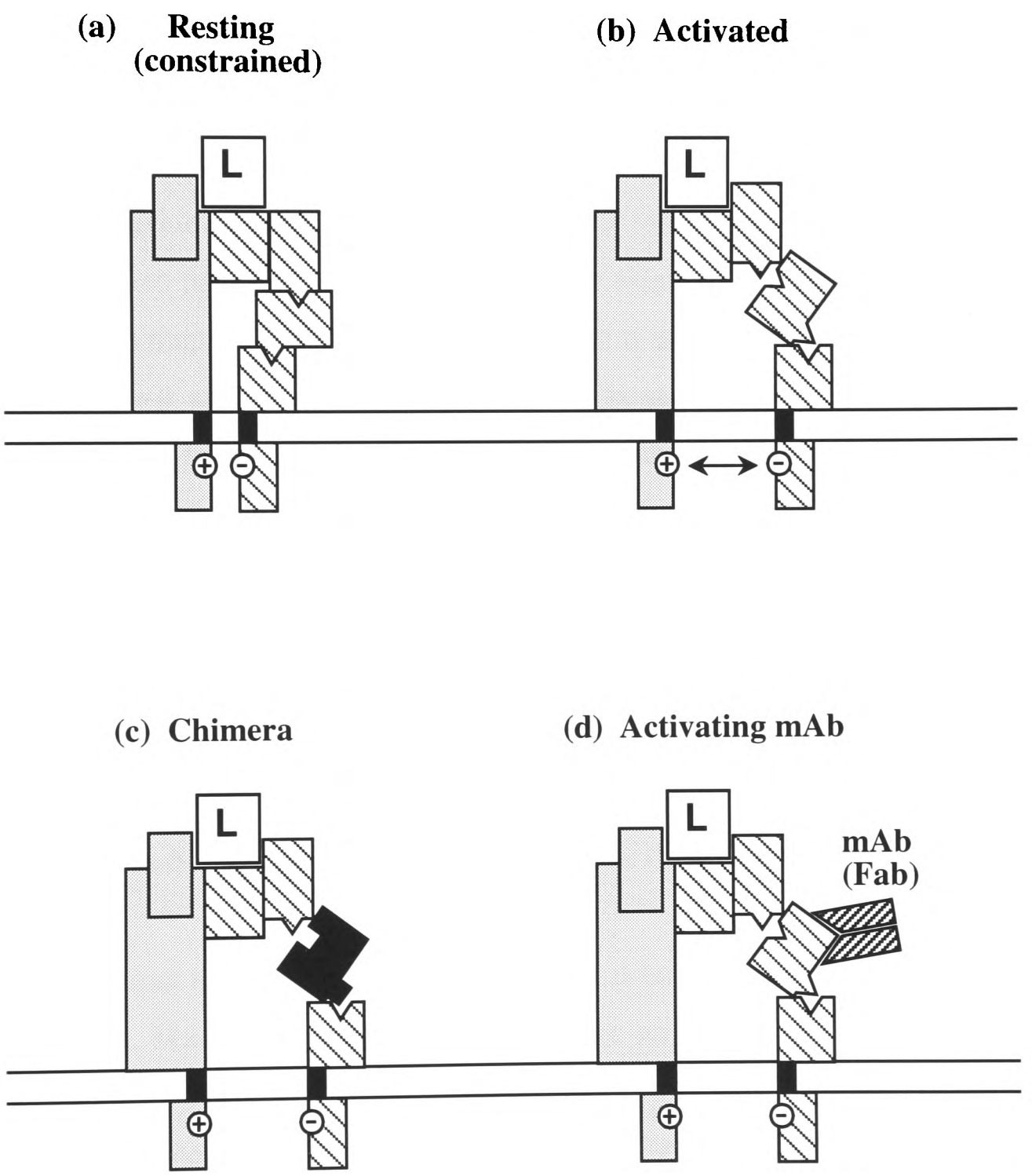
The figure opposite illustrates the "constraint model" proposed for the regulation of integrin receptors. In the figure, the α and β subunits are shaded differently, and the α subunit A-domain, which is only present in some integrins, is shown as a separate box in the α subunit. The different regions in the β subunit represent the N-terminal cysteine-rich, putative A-domain, "mid-piece" and C-terminal cysteine-rich regions. Ligand is shown as a box marked "L". The putative cytoplasmic salt bridge proposed by Hughes *et al* (1996) is also shown.

(a) The β subunit is constrained in its inactive, resting conformation by specific intramolecular interactions between various regions in the β subunit.

(b) Activation of the receptor occurs when these intramolecular interactions are disrupted. During the normal activation of the receptor, a conformational change which disrupts the constraint is envisaged initiating in the cytoplasmic tails of the receptor and this conformational change is then propogated through the transmembrane domains to the extracellular ligand binding site.

(c) In the variant β subunits, the intramolecular interactions constraining the receptor in its inactive, resting state are perturbed, resulting in release of the receptor into its high affinity ligand binding conformation. In the figure, a chimeric β subunit is shown, with its incompatible "mid-piece" shaded black. Similar versions may be drawn for the other β2 variants.

(d) The binding of activating mAbs may also result in integrin activation by disrupting the intramolecular interactions which maintain the receptor in its inactive state. An activating mAb (Fab fragment) is shown in the figure binding to the "mid-piece" region, but similar versions may be drawn for activating mAbs binding to other regions.


(a) Resting
(constrained)
(b) Activated
(c) Chimera
(d) Activating mAb
L
L
L
mAb
(Fab)
⊕
⊖
⊕
⊖
⊕
⊖

conformational change. Hughes *et al* (1996), proposed that a salt bridge between the cytoplasmic domains of integrin α and β subunits may serve to constrain integrin receptors in their inactive conformation, and that disruption of this salt bridge is required to release integrin receptors into their active, ligand binding conformation. This is consistent with the "constraint model" suggested in this thesis, and hence is included in the model illustrated in Figure 6.1: disruption of the cytoplasmic salt bridge can be envisaged initiating the conformational change which releases the β subunit, and possibly also the α subunit, from their inactive states, hence releasing the receptor to participate in high affinity ligand binding events. In the chimeric, soluble and truncated β2 subunits discussed in this thesis, the normal constrained conformation of the β2 subunit is disrupted, and hence all these β2 variants result in activated LFA-1, Mac-1 and p150,95 receptors (Figure 6.1c). The "constraint model" also provides an explanation for the existance of so many activating mAbs whose epitopes map to disparate regions in integrin α and β subunits. For instance, over 12 different anti-β subunit activating mAbs have been described which recognise epitopes located within the N-terminal cysteine-rich region, putative A-domain, "mid-piece", C-terminal cysteine-rich and membrane proximal regions of integrin β subunits (see Figure 6.2). It has been proposed that these mAbs activate integrins by binding to epitopes which are only expressed in the active state, and therefore serve to tip the equilibrium between the inactive and active states in favour of the activated conformation. However, it is also possible that by binding to integrins, these mAbs could disrupt the resting "constrained" conformation of the receptor, and therefore, like the variant β2 subunits, result in its release into the high affinity ligand binding state (Figure 6.1d).

Although the "constraint model" illustrated in Figure 6.1 is based on experiments with the β2 subunit of LFA-1, Mac-1 and p150,95, it may also be applicable to the β subunits of other integrin receptors, as a β3 variant, in which six amino acid residues within the putative β subunit A-domain are changed, has been reported to be constitutively active with respect to fibrinogen binding (Bajt *et al.*, 1992b), and a variant αIIbβ3 receptor comprising of the heavy chain of αIIb and the N-terminal 469 amino acids of β3 has also been reported to adopt the active αIIbβ3 conformation (Wippler *et al.*, 1994). In addition, observations drawn from other publications suggest that the model could be expanded to include intramolecular interactions within the α subunit, and also the interactions between the α and β subunits: chimeric αM subunits, in which regions within the αM A-domain are replaced

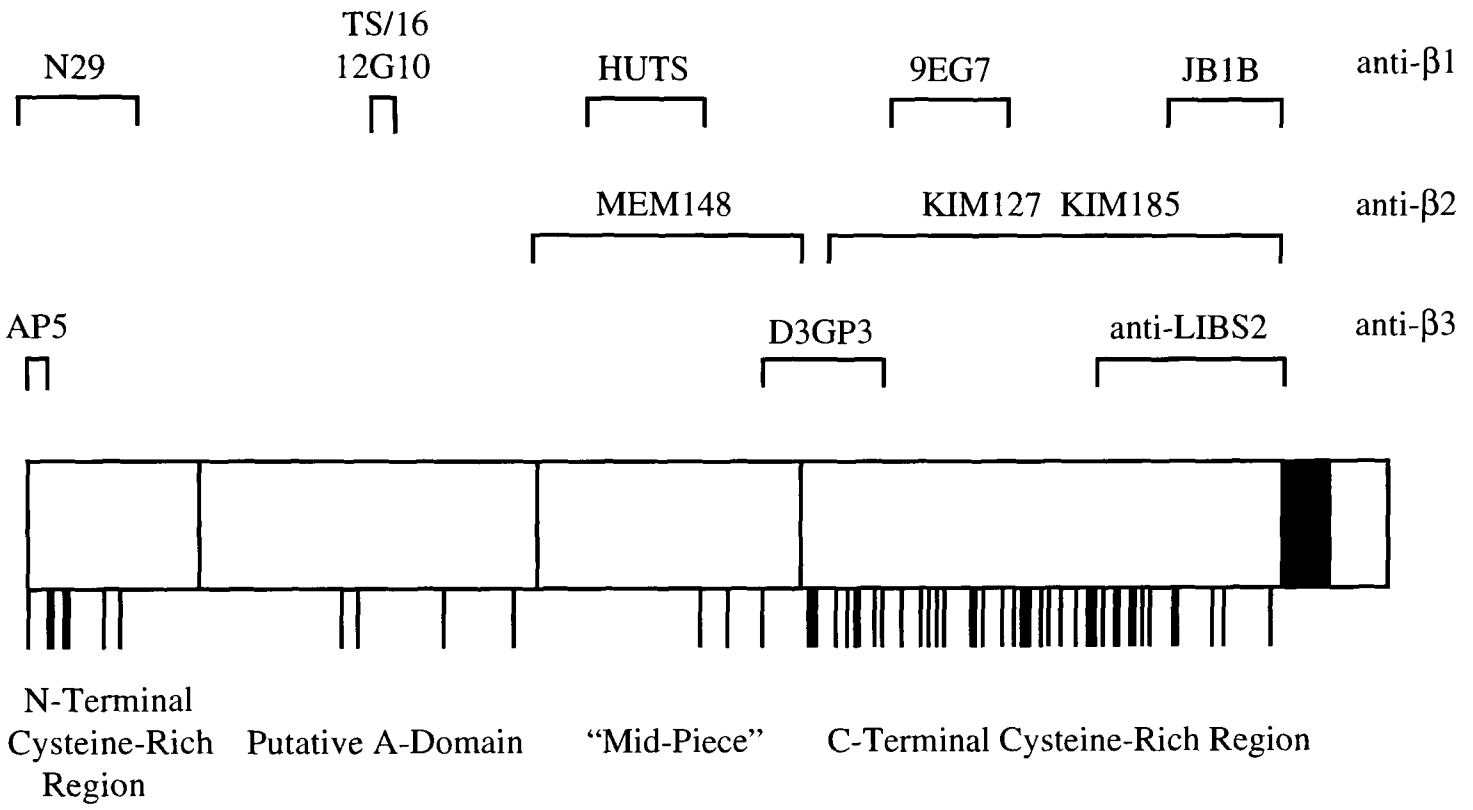


Figure 6.2: Activating Antibodies of the β1, β2 and β3 Integrins

The position of epitopes recognised by mAbs which activate the β1, β2 and β3 integrin subunits are shown. The references for the mapping of these mAb epitopes are as follows: N29 (Wilkins *et al.*, 1996); TS2/16 (Takada and Puzon, 1993); 12G10 (Mould *et al.*, 1995); HUTS (Luque *et al.*, 1996); 9EG7 (Bazzoni *et al.*, 1995); JB1B (Wilkins *et al.*, 1996); MEM148 (unpublished result); KIM127 and KIM185 (Stephens *et al.*, 1995); AP5 (Honda *et al.*, 1995); D3GP3 (Kouns *et al.*, 1991); and anti-LIBS2 (Du *et al.*, 1993).

with the homologous regions from αL, form constitutively active Mac-1 receptors (Zhang and Plow, 1996b), as do interspecies hybrid p150,95 receptors formed from human αX and chicken β2 subunits(Bilsland *et al.*, 1994). Therefore, although the "constraint model" is based on the regulation of the leukocyte integrins LFA-1, Mac-1 and p150,95, it may also be applicable to all integrin receptors.

REFERENCES

Akiyama, S.K., Yamada, S.S., Yamada, K.M. and LaFlamme, S.E. (1994) Transmembrane Signal Transduction by Integrin Cytoplasmic Domain Expressed in Single Subunit Chimeras. J. *Biol. Chem.* **269**, 15961.

Albelda, S.M. and Buck, C.A. (1990) Integrins and Other Cell Adhesion Molecules. *FASEB J.* **4**, 2868.

Altieri, D.C. (1991) Occupancy of CD11b/CD18 (Mac-1) Divalent Ion Binding Site(s) Induces Leukocyte Adhesion. *J. Immunol.* **147**, 1891.

Altieri, D.C., Bader, R., Mannucci, P.M. and Edgington, T.S. (1988) Oligospecificity of the Cellular Adhesion Receptor Mac-1 Encompasses an Inducible Recognition Specificity for Fibrinogen. *J. Cell. Biol.* **107**, 1893.

Altieri, D.C. and Edgington, T.S. (1988) The Saturable High Affinity Association of Factor X to ADP-Stimulated Monocytes Defines a Novel Function of the Mac-1 Receptor. *J. Biol. Chem.* **263**, 7007.

Anderson, D.C., Schmalstieg, F.C., Kohl, S., Arnaout, M.A., Hughes, B.J., Tosi, M.F., Buffone, G.J., Brinkley, B.R., Dickey, W.D., Abrahamson, J.S., Springer, T.A., Boxer, L.A., Hollers, J.M. and Smith, C.W. (1984) Abnormalities of Polymorphonuclear Leukocyte Function Associated With A Heritable Deficiency of High Molecular Weight Surface Glycoproteins (GP138): Common Relationship to Diminished Cell Adherence. *J. Clin. Invest.* **74**, 536.

Anderson, D.C. and Springer, T.A. (1987) Leukocyte Adhesion Deficiency: An Inherited Defect in the LFA-1, Mac-1 and p150,95 Glycoproteins. *Annu. Rev. Med.* **38**, 175.

Andrew, D., Shock, A., Ball, E., Ortlepp, S., Bell, J. and Robinson, M.K. (1993) KIM185, A Monoclonal Antibody to CD18 Which Induces a Change in The Conformation of CD18 and Promotes Both LFA-1 and CR3-Dependent Adhesion. *Eur. J. Immunol.* **23**, 2217.

Aota, S., Nagai, T. and Yamada, K.M. (1991) Characterisation of Regions of Fibronectin Besides the Arginine-Glycine-Aspartic acid Sequence Required for Adhesive Function of the Cell Binding Domain Using Site-Directed Mutagenesis. *J. Biol. Chem.* **266**, 15938.

Aota, S., Nomizu, M. and Yamada, K.M. (1994) The Short Amino Acid Sequence Pro-His-Ser-Arg-Asn in Human Fibronectin Enhances Cell Adhesive Function. *J. Biol. Chem.* **269**, 24756.

Arnaout, M.A. (1990a) Structure and Function of the Leukocyte Adhesion Molecules CD11/CD18. *Blood* **75**, 1037.

Arnaout, M.A. (1990b) Leukocyte Adhesion Molecules Deficiency: It's Structural Basis, Pathophysiology and Implications for Modulating the Inflammatory Response. *Immunol. Rev.* **114**, 145.

Arnaout, M.A., Spits, H., Terhorst, C., Pitt, J. and Todd, R.F. (1984) Deficiency Of A Leukocyte Surface Glycoprotein (LFA-1) in Two Patients With Mo1 Deficiency. *J. Clin. Invest.* **74**, 1291.

Arnaout, M.A., Dana, N., Gupta, S.K., Tenen, D.G. and Fathallah, D.M. (1990) Point Mutations Impairing Cell Surface Expression of the Common β Subunit (CD18) in a Patient with Leukocyte Adhesion Molecule (Leu-CAM) Deficiency. *J. Clin. Invest.* **85**, 977.

Back, A.L., Kwok, W.W. and Hickstein, D.D. (1992) Identification of Two Molecular Defects in a Child with Leukocyte Adherence Deficiency. *J. Biol. Chem.* **267**, 5482.

Bailly, P., Tontti, E., Hermand, P., Cartron, J-P and Gahmberg, C.G. (1995) The Red Cell LW Blood Group Protein is an Intercellular Adhesion Molecule Which Binds to CD11/CD18 Leukocyte Integrins. *Eur. J. Immunol.* **25**, 3316.

Bajt, M.L., Ginsberg, M.H., Frelinger, A.L., Berndt, M.C. and Loftus, J.C. (1992a) A Spontaneous Mutation of Integrin αIIbβ3 (Platlet Glycoprotein IIb-IIIa) Helps Define a Ligand Binding Site. *J. Biol. Chem.* **267**, 3789.

Bajt, M.L., Loftus, J.C., Gawaz, M.P. and Ginsberg, M.H. (1992b) Characterisation of a Gain of Function Mutation of Integrin αIIbβ3 (Platelet Glycoprotein IIb-IIIa). *J. Biol. Chem.* **267**, 22211.

Bajt, M.L. and Loftus, J.C. (1994) Mutation of a Ligand Binding Domain of β3 Integrin: Integral Role of Oxygenated Residues in αIIbβ3 (GPIIb-IIIa) Receptor Function. *J. Biol. Chem.* **269**, 20913.

Bajt, M.L., Goodman, T. and McGuire, S.L. (1995) β2(CD18) Mutations Abolish Ligand Recognition by I Domain Integrins LFA-1 (αLβ2, CD11a/CD18) and Mac-1 (αMβ2, CD11b/CD18) *J. Biol. Chem.* **270**, 94.

Barillari, G., Gendelman, R.,Gallo, R.C. and Ensoli, B. (1993) The Tat Protein of Human Immunodeficiency Virus Type 1, a Growth Factor for AIDS Kaposi Sarcoma and Cytokine-Activated Vascular Cells, Induces Adhesion of the Same Cell Types by Using Integrin Receptors Recognising the RGD Amino Acid Sequence. *Proc. Natl. Acad. Sci. USA.* **90**, 7941.

Bauer, J.S., Varner, J., Schreiner, C., Kornberg, L., Nicholas, R. and Juliano, R.L. (1993) Functional Role of the Cytoplasmic Domain of the Integrin α5 Subunit. *J.Cell. Biol.* **122**, 209.

Bazzoni, G., Shih, D.T., Buck, C.A., and Hemler, M.E. (1995). Monoclonal Antibody 9EG7 Defines a Novel β1 Integrin Epitope Induced by Soluble Ligand and Manganese, but Inhibited by Calcium. *J. Biol. Chem.* **270**, 25570.

Beacham, D.A., Wise, R.J., Turci, S.M. and Handin, R.I. (1992) Selective Inactivation of the Arg-Gly-Asp-Ser (RGDS) Binding Site in von Willibrand Factor by Site Directed Mutagenesis. *J. Biol. Chem.* **267**, 3409.

Beatty, P.G., Ochs, H.D. and Harlan, J.M. (1984) Absence of a Monoclonal Antibody Defined Protein Complex In A Boy With Abnormal Leukocyte Function. *Lancet* **1**, 535.

Beller, D.I., Springer, T.A. and Schreiber, R.D. (1982) Anti-Mac-1 Selectively Inhibits the Mouse and Human Type Three Complement Receptor. *J. Exp. Med.* **156**, 1000.

Bennett, J.S., Vilaire, G. and Cines, D.B. (1982) Identification of the Fibrinogen Receptor on Human Platelets by Photo Affinity labelling. *J. Biol. Chem.* **257**, 8049.

Bennett, J.S., Kolodziej, M.A., Vilaire, G. and Poncz, M. (1993) Determinants of the Intracellular Fate of Truncated Forms of the Platelet Glycoproteins IIb and IIIa. *J. Biol. Chem.* **268**, 3580.

Bergelson, J.M., Chan, B.M., Finberg, R.W. and Hemler, M.E. (1993) The Integrin VLA-2 Binds Echovirus 1 and Extracellular Matrix Ligands by Different Mechanisms. *J. Clin. Invest.* **92**, 232.

Bergelson, J.M. and Hemler, M.E. (1995) Do Integrins Use a "MIDAS" Touch to Grasp an Asp? *Curr. Biol.* **5**, 615.

Berger, M., O'Shea, J., Cross, A.S., Folks, T.M., Chused, T.M., Brown, E.J. and Frank, M.M. (1984) Human Neutrophils Increase Expression of C3bi as well as C3b Receptors Upon Activation. *J. Clin. Invest.* **74**, 1566.

Berman, P.W., Nakamura, G.R., Riddle, L., Chiu, H., Fisher, K., Champe, M., Gray, A.M., Ward, P. and Fong, S. (1993) Biosynthesis and Function of Membrane Bound and Secreted Forms of Recombinant CD11b/CD18 (Mac-1). *J. Cellular Biochem.* **52**, 183.

Bernfield, M.R., Hinkes, M.T. and Gallo, R.L. (1993) Developmental Expression of the Syndecans: Possible Function and Regulation. *Development* **119** (Suppl.), 205.

Bevilacqua, M.P. (1993) Endothelial-Leukocyte Adhesion Molecules. *Annu. Rev. Immunol.* **11**, 767.

Bevilacqua, M.P. and Belson, R.M. (1993) Selectins. *J. Clin. Invest.* **91**, 379.

Bevilacqua, M., Butcher, E., Furie, B., Furie, B., Gallatin, M., Gimbrone, M., Harlan, J., Kishimoto, K., Lasky, L., McEver, R., Paulson, J., Rosen, S., Seed, B., Siegelman, M., Springer, T., Stoolman, L., Tedder, T., Varki, A., Wagner, D., Weissman, I. and Zimmerman, G. (1991) Selectins: A Family of Adhesion Receptors. *Cell* **67**, 233.

Birchmeier, W. and Behrens, J. (1994) Cadherin Expression in Carcinomas: Role in the Formation of Cell Junctions and the Prevention of Invasiveness. *Biochem. Biophys. Acta* **1198**, 11.

Birnboim, H.C. and Doly, J. (1979) A Rapid Alkaline Extraction Procedure for Screening Recombinant Plasmid DNA. *Nucleic Acid Res.* **7**, 1513.

Bilsland, C.A.G., Diamond, M.S. and Springer, T.A. (1994) The Leukocyte Integrin p150,95 (CD11c/CD18) as a Receptor for iC3b. *J. Immunol.* **152**, 4582.

Blackford, J., Reid, H.W., Pappin, D.J.C., Bowers, F.S. and Wilkinson, J.M. (1996) A Monoclonal Antibody, 3/22, To Rabbit CD11c Which Induces Homotypic T Cell Aggregation: Evidence That ICAM-1 Is A Ligand For CD11c/CD18. *Eur. J. Immunol.* **26**, 525.

Blobel, C.P. and White, J.M. (1992) Structure, Function and Evolutionary Relationship of Proteins Containing a Disintegrin Domain. *Curr. Opin. Cell. Biol.* **4**, 760.

Bohnsack, J.F., Akiyama, S.K., Damsky, C.H., Knape, W.A. and Zimmerman, G.A. (1990) Human Neutrophil Adherence to Laminin *in vitro*: Evidence For a Distinct Neutrophil Integrin Receptor For Laminin. *J. Exp. Med.* **171**, 1221.

Boshart, M., Weber, F., Jahn, G., Dorsch-Hasler, K., Fleckenstein, B. and Schaffner, W. (1985) A Very Strong Enhancer Is Located Upstream of an Immediate Early Gene of Human Cytomegalovirus. *Cell* **41**, 521.

Bowditch, R.D., Hariharan, M., Tominna, E.F., Smith, J.W., Yamada, K.M., Getzoff, E.D. and Ginsberg, M.H. (1994) Identification of a Novel Integrin Binding Site in Fibronectin: Differential Utilisation by β3 Integrins. *J. Biol. Chem.* **269**, 10856.

Briesewitz, R., Epstein, M.R. and Marcantonio, E.E. (1993) Expression of Native and Truncated Forms of the Human Integrin α1 Subunit. *J. Biol. Chem.* **268**, 2989.

Briesewitz, R., Kern, A. and Marcantonio, E.E. (1993) Ligand-Dependent and Independent Integrin Focal Contact Localisation: The Role of the α-Chain Cytoplasmic Domain. *Mol. Biol. Cell.* **4**, 593.

Burridge, K., Fath, K., Kelly, T., Nuckolls, G. and Turner, C. (1988) Focal Adhesions: Transmembrane Junctions Between the Extracellular Matrix and the Cytoskeleton. *Ann. Rev. Cell Biol.* **4**, 487.

Buyon, J., Slade, S., Reibman, J., Abramson, S., Philips, M., Weissmann, G. and Winchester, R. (1990) Constitutive And Induced Phosphorylation of the Alpha and Beta Chains of the CD11/CD18 Leukocyte Integrin Family. Relationship to Adhesion Dependent Functions. *J. Immunol.* **144**, 191.

Campanero, M.R., del Pozo, M.A., Arroyo, A.G., Sanchez-Mateos, P., Hernandez-Caselles, T., Craig, A., Pulido, R. and Sanchez-Madrid, F. (1993) ICAM-3 Interacts With LFA-1 and Regulates the LFA-1/ICAM-1 Cell Adhesion Pathway. *J. Cell. Biol.* **123**, 1007.

Calvete, J.J., Henschen, A. and Gonzalez-Rodriguez, J. (1989) Complete Localisation of the Intrachain Disulphide Bonds and the N-Glycosylation Points in the Alpha-Subunit of Human Platelet Glycoprotein IIb. *Biochem. J.* **261**, 561.

Calvete, J.J., Henschen, A. and Gonzalez-Rodriguez, J. (1991) Assignment of Disulphide Bonds in Human Platelet GPIIIa: A Disulphide Pattern for the β-Subunits of the Integrin Family. *Biochem. J.* **274**, 63.

Carrell, N.A., Fitzgerald, L.A., Steiner, B., Erickson, H.P. and Phillips, D.R. (1985) Structure of Human Platelet Membrane Glycoproteins IIb and IIIa as Determined by Electron Microscopy. *J. Biol. Chem.* **260**, 1743.

Charo, I.F., Nannizzi, L., Phillips, D.R., Hsu, M.A. and Scarborough, R.M. (1991) Inhibition of Fibrinogen Binding to GPIIb-IIIa by a GPIIIa Peptide. *J. Biol. Chem.* **266**, 1415.

Chatila, T., Geha, R. and Arnaout, M. (1989) Constitutive and Stimulus-Induced Phosphorylation of CD11/CD18 Leukocyte Adhesion Molecules. *J. Cell. Biol.* **109**, 3435.

Chen, W.J., Goldstein, J.L. and Brown, M.S. (1990) NPXY, A Sequence Often Found in Cytoplasmic Tails, is Required For Coated Pit-Mediated Internalisation of Low Density Lipoprotein Receptor. *J. Biol. Chem.* **265**, 3116.

Chen, Y., O'Toole, T.E., Ylanne, J., Rosa, J. and Ginsberg, M.H. (1994) A Point Mutation in the Integrin β3 Cytoplasmic Domain (S^{752} to P) Impairs Bidirectional Signalling Through αIIbβ3 (Platelet Glycoprotein IIb-IIIa). *Blood* **84**, 1857.

Clements J.M., Newham, P., Shepherd, M., Gilbert, R., Dudgeon, T.J., Needham, L.A., Edwards, R.M., Berry, L., Brass, A. and Humphries, M.J. (1994) Identification of a Key Integrin Binding Sequence in VCAM-1 Homologous to the LDV Active Site in Fibronectin. *J. Cell. Sci.* **107**, 2127.

Coburn, J., Leong, J.M. and Erban, J.K. (1993) Integrin αIIbβ3 Mediates Binding of the Lyme Disease Agent *Borrelia burgdorferi* to Human Platelets. *Proc. Natl. Acad. Sci. USA.* **90**, 7059.

Colombatti, A. and Bonaldo, P. (1991) The Superfamily of Proteins With von Willibrand Factor Type A-Like Domains: One Theme Common to Components of Extracellular Matrix, Hemostasis, Cellular Adhesion and Defense Mechanisms. *Blood* **77**, 2305.

Coppolino, M., Leung-Hagesteijn, C., Dedhar, S. and Wilkins, J. (1995) Inducible Interaction of Integrin α2β1 with Calreticulin. *J. Biol. Chem.* **270**, 23132.

Corbi, A.L., Miller, L.J., O'Connor, K., Larson, R.S. and Springer, T.A. (1987) cDNA Cloning and Complete Primary Structure of the Alpha Subunit of Leukocyte Adhesion Glycoprotein p150,95. *EMBO J.* **6**, 4023.

Corbi, A.L., Larson, R.S., Kishimoto, T.K., Springer, T.A. and Morton, C.C. (1988) Chromosomal Location of the Genes Encoding The Leukocyte Adhesion Receptors LFA-1, Mac-1 and p150,95. Identification of a Gene Cluster Involved in Cell Adhesion. *J. Exp. Med.* **167**, 1597.

Corbi, A.L., Vara, A., Ursa, A., Rodriguez, M.C.G., Fontan, G. and Sanchez-Madrid, F. (1992) Molecular Basis for a Severe Case of Leukocyte Adhesion Deficiency. *Eur. J. Immunol.* **22**, 1877.

Cotton, R.G.H., Rodrigues, N.R. and Campbell, R.D. (1988) Reactivity of Cytosine and Thymine in Single Base Pair Mismatches with Hydroxylamine and Osmium Tetroxide and its Application to the Study of Mutations. *Proc. Natl. Acad. Sci. USA.* **85**, 4397.

Cotton, R.G.H. and Campbell, R.D. (1989) Chemical-Reactivity of matched Cytosine and Thymine Bases Near Mismatched and Unmatched Bases in a Heteroduplex Between DNA Strands With Multiple Differences. *Nucleic Acid Res.* **17**, 4223.

Crowe, D., Chiu, H., Fong, S. and Weissman, I. (1994) Regulation of the Avidity of Integrin $\alpha 4\beta 7$ by the $\beta 7$ Cytoplasmic Domain. *J. Biol. Chem.* **269**, 14411.

Crowley, C.A., Cunnette, J.T., Rosin, R.E., Andre-Schwartz, J., Gallin, J.I., Klempner, M., Snyderman, R., Southwick, F.S., Stossel, T.P. and Babior, B.M. (1980) An Inherited Abnormality of Neutrophil Adhesion: Its Genetic Transmission and Its Asscociation With A Missing Protein. *New Eng. J. Med.* **302**, 1163.

Cunningham, B.A., Hemperly, J.J., Murray, B.A., Prediger, E.A., Brackenbury, R. and Edelman, G.M. (1987) Neural Cell Adhesion Molecule: Structure, Immunoglobulin-Like Domains, Cell Surface Modulation, and Alternative RNA Splicing. *Science* **236**, 799.

Dana, N., Todd, R.F., Pitt, J., Springer, T.A. and Arnaout, M.A. (1983) Deficiency of A Surface Membrane Glycoprotein (Mo1) in Man. *J. Clin. Invest.* **73**, 153.

Dana, N., Fathallah, D.M. and Arnaout, M.A. (1991) Expression of a Soluble and Functional Form of the Human $\beta 2$ Integrin CD11b/CD18. *Proc. Natl. Acad. Sci. USA* **88**, 3106.

Danilenko, D.M, Rossitto, P.V., Van der Vieren, M., Trong, H.L., McDonough, S.P., Affolter, V.K. and Moore, P.F. (1995) A Novel Canine Leukointegrin, $\alpha D\beta 2$, Is Expressed by Specific Macrophage Subpopulations in Tissue and a Minor $CD8^+$ Lymphocyte Subpopulation in Peripheral Blood. *J. Immunol.* **155**, 35.

Davignon, D., Martz, E., Reynolds, T., Kurzinger, K. and Springer, T.A. (1981) Lymphocyte Function Associated Antigen 1 (LFA-1): A Surface Antigen Distinct From Lyt-2,3 That Participates in T Lymphocyte-Mediated Killing. *Proc. Natl. Acad. Sci. USA.* **78**, 4535.

Davis, G.E. (1992) The Mac-1 and p150,95 $\beta 2$ Integrins Bind Denatured Proteins to Mediate Leukocyte Cell-Substrate Adhesion. *Exp. Cell. Res.* **200**, 242.

Dedhar, S. (1994) Novel Functions For Calreticulin: Interaction With Integrins and Modulation of Gene Expression? *Trends Biochem. Sci.* **19**, 269.

de Fougerolles, A.R., Stacker, S.A., Schwarting, R., and Springer, T.A. (1991) Characterisation of ICAM-2 and Evidence For a Third Counter-Receptor For LFA-1. *J.*

Exp. Med. **174**, 253.

de Fougerolles, A.R. and Springer, T.A. (1992) Intercellular Adhesion Molecule-3, A Third Adhesion Counter-Receptor For Lymphoctye Function Associated Molecule-1 On Resting Lymphocytes. *J. Exp. Med.* **175**, 185.

de Fougerolles, A.R., Klickstein, L.B. and Springer, T.A. (1993) Cloning and Expression of Intercellular Adhesion Molecule 3 Reveals Strong Homology to Other Immunoglobulin Family Counter-Receptors For Lymphocyte Function-Associated Antigen 1. *J. Exp. Med.* **177**, 1187.

de Fougerolles, A.R., Qin, X. and Springer, T.A. (1994) Characterisation of the Function of Intercellular Adhesion Molecule (ICAM)-3 and Comparison With ICAM-1 and ICAM-2 in Immune Responses. *J. Exp. Med.* **179**, 619.

Detmers, P.A., Wright, S.D., Olsen, E., Kimball, B. and Cohn, Z.A. (1987) Aggregation of Complement Receptors on Human Neutrophils in the Absence of Ligand. *J. Cell. Biol.* **105**, 1137.

Diamond, M.S., Staunton, D.E., de Fougerolles, A,R., Stacker, S.A., Garcia-Aguilar, J., Hibbs, M.L. and Springer, T.A. (1990) ICAM-1 (CD54): A Counter-Receptor For Mac-1 (CD11b/CD18). *J. Cell. Biol.* **111**, 3129.

Diamond, M.S., Staunton, D.E., Marlin, S.D. and Springer, T.A. (1991) Binding of the Integrin Mac-1 (CD11b/CD18) to the Third Immunoglobulin-Like Domain of ICAM-1 (CD54) and its Regulation by Glycosylation. *Cell* **65**, 961.

Diamond, M.S., Garcia-Aguilar, J., Bickford, J.K., Corbi, A.L. and Springer, T.A. (1993) The I Domain is a Major Recognition Site on the Leukocyte Integrin Mac-1 (CD11b/CD18) for Four Distinct Adhesion Ligands. *J. Cell. Biol.* **120**, 1031.

Diamond, M.S. and Springer, T.A. (1994) The Dynamic Regulation of Integrin Adhesiveness. *Curr. Biol.* **4**, 506.

Dickinson, C.D., Veerapandian, B., Dai, X.P., Hamlin, R.C., Xuong, N., Ruoslhati, E. and Ely, K.R. (1994) Crystal Structure of the Tenth Type III Cell Adhesion Module of Human Fibronectin. *J. Mol. Biol.* **236**, 1079.

Dransfield, I., Cabanas, C., Craig, A. and Hogg, N. (1992) Divalent Cation Regulation of the Function of the Leukocyte Integrin LFA-1. *J. Cell. Biol.* **116**, 219.

D'Souza, S.E., Ginsberg, M.H., Burke, T.A., Lam, S.C.T. and Plow, E.F. (1988) Localisation of an Arg-Gly-Asp Recognition Site Within an Integrin Adhesion Receptor. *Science* **242**, 91.

D'Souza, S.E., Ginsberg, M.H., Burke, T.A. and Plow, E.F. (1990) The Ligand Binding Site of the Platelet Integrin Receptor GPIIb-IIIa is Proximal to the Second Calcium Binding Domain of its α Subunit. *J. Biol. Chem.* **265**, 3440.

D'Souza, S.E., Ginsberg, M.H., Matsueda, G.R. and Plow, E.F. (1991) A Discrete Sequence in a Platelet Integrin is Involved in Ligand recognition. *Nature* **350**, 66.

D'Souza, S.E., Haas, T.A., Piotrowicz, R.S., Byers-Ward, V., McGrath, D.E., Soule, H.R., Cierniewski, C.S., Plow, E.F. and Smith, J.W. (1994) Ligand and Cation Binding are Dual Functions of a Discrete Segment of the Integrin β3 Subunit: Cation Displacement is Involved in Ligand Binding. *Cell* **79**, 659.

Du, X., Gu, M., Weisel, J.W., Nagaswami, C., Bennett, J.S., Bowditch, R. and Ginsberg, M.H. (1993) Long Range Propagation of Conformational Changes in Integrin αIIbβ3. *J. Biol. Chem.* **268**, 23087.

Dustin, M.L. and Springer, T.A. (1989) T Cell Receptor Cross-Linking Transiently Stimulates Adhesiveness Through LFA-1. *Nature* **341**, 619.

Edwards, C.P. and Aruffo, A. (1993) Current Applications of COS Cell Based Transient Expression Systems. *Current Opin. Biotech.* **4**, 558.

Edwards, J.G., Hameed, H. and Campbell, G. (1988) Induction of Fibroblast Spreading by Manganese 2+: A Possible Role for Unusual Binding Sites for Divalent Cations in Receptors for Proteins Containing Arg-Gly-Asp. *J. Cell. Sci.* **89**, 507.

Erle, D.J., Ruegg, C., Shepphard, D. and Pytela, R. (1991) Complete Amino Acid Sequence of an Integrin β Subunit (β_7) Identified in Leukocytes. *J. Biol. Chem.* **266**, 11009.

Etzioni, A. (1994) Adhesion Molecule Deficiences and Their Clinical Significance. *Cell. Adhes. Commun.* **2**(3), 257.

Farrell, D.H. and Thiagarajan, P. (1994) Binding of Recombinant Fibrinogen Mutants to Platelets. *J. Biol. Chem.* **269**, 226.

Faull, R.J., Kovach, N.L., Harlan, J.M. and Ginsberg, M.H. (1994) Stimulation of Integrin-Mediated Adhesion of T Lymphocytes and Monocytes: Two Mechanisms With Divergent Biological Consequences. *J. Exp. Med.* **179**, 1307.

Faull, R.J. and Ginsberg, M.H. (1995) Dynamic Regulation of Integrins. *Stem Cells* **13**, 38.

Fawcett, J., Holness, C.L., Needham, L.A., Turley, H., Gatter, K.C., Mason, D.Y. and Simmons, D.L. (1992) Molecular Cloning of ICAM-3, A Third Ligand For LFA-1, Constitutively Expressed On Resting Leukocytes. *Nature* **360**, 481.

Feinberg, A.P. and Vogelstein, B. (1983) A Technique For Radiolabelling DNA Restriction Endonuclease Fragments to High Specific Activity. *Anal. Biochem.* **132**, 6.

Filardo, E.J. and Cheresh, D.A. (1994) A β Turn in the Cytoplasmic Tail of the Integrin αV Subunit Influences Conformation and Ligand Binding of αVβ3. *J. Biol. Chem.* **269**, 4641.

Fleming, J.C., Pahl, H.L., Gonzalez, D.A., Smith, T.F. and Tenen, D.G. (1993) Structural Analysis of the CD11b Gene and Phylogeneic Analysis of the Alpha Integrin Gene Family Demonstrate Remarkable Conservation of Genomic Organisation and Suggest Early Diversification During Evolution. *J. Immunol.* **150**, 480.

Frelinger, A.L, Du, X.P., Plow, E.F. and Ginsberg, M.H. (1991) Monoclonal Antibodies to Ligand Occupied Conformers of Integrin Alpha IIb-Beta III (Glycoprotein IIb-IIIa) Alter Receptor Affinity, Specificity and Function. *J. Biol. Chem.* **266**, 17106.

Fischer, A., Deschamps-Latscha, B., Gerota, I., Scheinmetzler, C., Virelizier, J.L., Trung, P.H., Lisowskagrospierre, B., Perez, N., Durandy, A., and Griscelli, C. (1983) Bone-Marrow Transplantation For Inborn Error of Phagocytic Cells Associated With Defective Adherence, Chemotaxis, and Oxidative Response During Opsonized Particle Phagocytosis. *Lancet* **ii**, 473.

Gailit, J. and Ruoslhati, E. (1988) Regulation of the Fibronectin Receptor Affinity by Divalent Cations. *J. Biol. Chem.* **263**, 12927.

Garratt, A.N. and Humphries, M.J. (1995) Recent Insights into Ligand Binding, Activation and Signalling by Integrin Adhesion Receptors. *Acta Anat.* **154**, 34.

Gearing, A. J. H. *et al* (1992) Soluble forms of Vascular Adhesion Molecules, E-Selectin, ICAM-1, and VCAM-1: Pathological Significance. *Annals N. Y. Acad. Sci.* **667**, 324.

Gearing, A. J. H. and Newman, W. (1993) Circulating Adhesion Molecules in Disease. *Immunol. Today* **14**, 506.

Ginsberg, M.H., Loftus, J.C., Ryckwaert, J-J., Pierschbacher, M., Pytela, R., Ruoslhati, E. and Plow, E.F. (1987) Immunochemical and Amino Terminal Sequence Comparison of 2 Cytoadhesins Indicates They Contain Similar or Identical Beta-Subunits and Distinct Alpha Subunits. *J. Biol. Chem.* **262**, 5437.

Godin, C., Caprani, A., Dufaux, J. and Flaud, P. (1993) Interactions Between Neutrophils and Endothelial Cells. *J. Cell. Sci.* **106**, 441.

Grunstein, M. and Hogness, D.S. (1975) Colony Hybridization: A Method for the Isolation of Cloned DNAs That Contain a Specific Gene. *Proc. Natl. Acad. Sci. USA.* **72**, 3961.

Gulino, D., Boudignon, C., Zhang, L., Concord, E., Rabiet, M.J. and Marguerie, G. (1992) Ca^{2+} Binding Properties of the Platelet IIb Ligand-Interacting Domain. *J. Biol. Chem.* **267**, 1001.

Gulino, D., Martinez, P., Delechanal, E., Concord, E., Duperray, A., Alemany, M. and Marguerie, G. (1995) Expression and Purification of a Soluble Functional Form of the Platelet αIIbβ3 Integrin. *Eur. J. Biochem.* **227**, 108.

Gumbiner, B.M. (1993) Proteins Associated with the Cytoplasmic Surface of Adhesion Molecules. *Neuron* **11**, 551.

Gumbiner, B.M. (1996) Cell Adhesion: The Molecular Basis of Tissue Architecture and Morphogenesis. *Cell* **84**, 345.

Haas, T.A. and Plow, E.F. (1994) Integrin-Ligand Interactions: A year in Review. *Curr. Opin. Cell. Biol.* **6**, 656.

Hannigann, G.E., Leung-Hagesteijn, C., Fitz-Gibbon, L., Coppolino, M.G., Radeva, G., Filmus, J., Bell, J.C. and Dedhar, S. (1996) Regulation of Cell Adhesion and Anchorage-Dependent Growth by a New β1-Integrin-Linked Protein Kinase. *Nature* **379**, 91.

Haverstick, D.M., Sakai, H. and Gray, L.S. (1992) Lymphocyte Adhesion Can be Regulated by Cytoskeleton-Associated, PMA-Induced Capping of Surface Receptors. *Am. J. Physiol.* **262**, C916.

Heery, D.M., Gannon, F. and Powell, R. (1990) A Simple Method for Subcloning DNA Fragments From Gel Slices. *Trends in Geneticis.* **6**, 173.

Hemler, M.E. (1990) VLA Proteins in the Integrin Family: Structures, Functions, and Their Role on Leukocytes. *Ann. Rev. Immunol.* **8**, 365.

Hibbs, M.L., Wardlaw, A.J., Stacker, S.A., Anderson, D.C., Lee, A., Roberts, T.M. and Springer, T.A. (1990) Transfection of Cells from Patients With Leukocyte Adhesion

Deficiency With An Integrin Beta-Subunit (CD18) Restores Lymphocyte Function Associated Antigen-1 Expression and Function. *J. Clin. Invest.* **85**, 674.

Hibbs, M.L., Jakes, S., Stacker, S.A., Wallace, R.W. and Springer, T.A. (1991a) The Cytoplasmic Domain of the Integrin Lymphocyte Function-Associated Antigen 1 β Subunit: Sites Required for Binding to Intercellular Adhesion Molecule 1 and the Phorbol Ester-Stimulated Phosphorylation Site. *J. Exp. Med.* **174**, 1227.

Hibbs, M.L., Xu, H., Stacker, S.A. and Springer, T.A. (1991b) Regulation of Adhesion to ICAM-1 by the Cytoplasmic Domain of LFA-1 β Subunit. *Science* **251**, 1611.

Hildreth, J.E.K. and August, J.T. (1985) The Human Lymphocyte Function-Associated (HLFA) Antigen and a Related Macrophage Differentiation Antigen (HMac-1): Functional Effects of Subunit Specific Monoclonal Antibodies. *J. Immunol.* **134**, 3272.

Hogervorst, F., Kuikman, I., von der Borne, A.E.G. and Sonnenberg, A. (1990) Cloning and Sequence Analysis of β4 cDNA: An Integrin Subunit that Contains a Unique 118 KDa Cytoplasmic Domain. *EMBO J.* **9**, 765.

Hogervorst, F., Kuikman, I., Noteboom, E. and Sonnenborg, A. (1993) The Role of Phosphorylation in Activation of the α6β1 Laminin Receptor. *J. Biol. Chem.* **268**, 18427.

Hogg, N. (1989) The Leukocyte Integrins. *Immunology Today* **10**, 111.

Hogg, N., Landis, R.C., Bates, P.A., Standley, P. and Randi, A.M. (1994) The Sticking Point: How Integrins Bind to Their Ligands. *Trends Cell Biol.* **4**, 379.

Holness, C.L. and Simmons, D.L. (1994) Structural Motifs for Recognition and Adhesion in Members of the Immunoglobulin Superfamily. *J. Cell. Sci.* **107**, 2065.

Holness, C.L., Bates, P.A., Littler, A.J., Buckley, C.D., McDowall, A., Bossy, D., Hogg, N. and Simmons, D.L. (1995) Analysis of the Binding Site on Intercellular Adhesion molecule-3 for the Leukocyte Integrin Lymphocyte Function Associated Antigen-1. *J. Biol. Chem.* **270**, 877.

Honda, S., Tomiyama, Y., Pelletier, A.J., Annis, D., Honda, Y., Orchekowski, R., Ruggeri, Z., and Kunicki, T.J. (1995). Topography of Ligand-Induced Binding Sites, Including a Novel Cation-Sensitive Epitope (AP5) at the Amino Terminus, of the Human Integrin β3 Subunit. *J. Biol. Chem.* **270**, 11947.

Horwitz, A.F. and Hunter, T. (1996) Cell Adhesion: Integrating Circuitry. *Trends in Cell Biol.* **6**, 460.

Horwitz, A., Duggan, K., Buck, C., Beckerle, M.C. and Burridge, K. (1986) Interaction of the Plasma Membrane Fibronectin Receptor with Talin - A Transmembrane Linkage. *Nature* **320**, 531.

Huang, C. and Springer, T.A. (1995) A Binding Interface on the I-Domain of LFA-1 Required for Specific Interaction with ICAM-1. *J. Biol. Chem.* **270**, 19008.

Huang, C. and Springer, T.A. (1997) Folding of the β-Propellor Domain of the Integrin αL Subunit is Independent of the I Domain and Dependent on the β2 Subunit. *Proc. Natl. Acad. Sci. USA.* **94**, 3162.

Huang, X., Chen, A., Agrez, M. and Sheppard, D. (1994) A Point Mutation in the Integrin β6 Subunit Abolishes Both αVβ6 Binding to Fibronectin and Receptor Localisation to Focal Adhesion Plaques. *Mol. Biol. Cell.* **4**, A283.

Huang, C., Lu, C. and Springer, T.A. (1997) Folding of the Conserved Domain but not of Flanking Regions in the Integrin β2 Subunit Requires Association with the α Subunit. *Proc. Natl. Acad. Sci. USA.* **94**, 3156.

Huber, O., Bierkamp, C. and Kemler, R. (1996) Cadherins and Catenins in Development. *Curr. Opin. Cell. Biol.* **8**, 685.

Hughes, P.E., O'Toole, T.E., Ylanne, J., Shattil, S.J. and Ginsberg, M.H. (1995) The Conserved Membrane-Proximal Region of an Integrin Cytoplasmic Domain Specifies Ligand Binding Affinity. *J. Biol. Chem.* **270**, 12411.

Hughes, P.E., Diaz-Gonzalez, F., Leong, L., Wu, C., McDonald, J.A., Shattil, S.J. and Ginsberg, M.H. (1996) Breaking the Integrin Hinge: A Defined Structural Constraint Regulates Integrin Signalling. *J. Biol. Chem.* **271**, 6571.

Humphries, M.J. (1990) The Molecular Basis and Specificity of Integrin-Ligand Interactions. *J. Cell. Science* **97**, 585.

Hynes, R.O. (1987) Integrins: A Family of Cell Surface Receptors. *Cell* **48**, 549.

Hynes, R.O. (1990) Fibronectins. (New York: Springer-Verlag).

Hynes, R.O. (1992) Integrins: Versatility, Modulation and Signalling in Cell Adhesion. *Cell* **69**, 11.

Hynes, R.O. (1996) Targeted Mutations in Cell Adhesion Genes: What Have We Learned from Them? *Dev. Biol.* **180**, 402.

Hynes, R.O. and Lander, A.D. (1992) Contact and Adhesive Specificities in the Asscociations, Migrations, and Targeting of Cells and Axons. *Cell* **68**, 303.

Irie, A., Kamata, T., Puzon-McLaughlin, W. and Takada, Y. (1995) Critical Amino Acid Residues For Ligand-Binding Are Clustered in a Predicted Beta-Turn of the 3rd N-Terminal Repeat in the Integrin Alpha-4 and Alpha-5 Subunits. *EMBO J.* **14**, 5550.

Ish-Horowicz, D. and Burke, J.F. (1981) Rapid and Efficient Cosmid Cloning. *Nucleic Acid Res.* **9**, 2989.

Jones, E.Y., Harlos, K., Bottomly, M.J., Robinson, R.C., Driscoll, P.C., Edwards, R.M., Clements, J.M., Dudgeon, T.J. and Stuart, D.I. (1995) Crystal Structure of an Integrin-Binding Fragment of Vascular Cell Adhesion Molecule-1 at 1.8 A Resolution. *Nature* **373**, 539.

Juliano, R.L. and Haskill, S. (1993) Signal Transduction From the Extracellular Matrix. *J. Cell. Biol.* **120**, 577.

Kahn, J., Ingraham, R.H., Shirley, F., Migaki, G.I. and Kishimoto, T.K. (1994) Membrane Proximal Cleavage of L-Selectin: Identification of the Cleavage Site and a 6 kd Transmembrane Peptide Fragment of L-Selectin. *J. Cell. Biol.* **125**, 461.

Kamata, T., Puzon, W. and Takada, Y. (1994) Identification of Putative Ligand Binding Sites Within The I-Domain of Integrin Alpha 2 Beta 1 (VLA-2, CD49b/CD29). *J. Biol. Chem.* **269**, 9659.

Kamata, T. and Takada, Y. (1994) Direct Binding of Collagen to the I Domain of Integrin α2β1 (VLA-2, CD49b/CD29) in a Divalent Cation-Independent Manner. *J. Biol. Chem.* **269**, 26006.

Kamata, T., Puzon, W. and Takada, Y. (1995a) Identification of Putative Ligand Binding Sites of the Integrin α4β1 (VLA-4, CD49d/CD29). *Biochem. J.* **305**, 945.

Kamata, T., Wright, R. and Takada, Y. (1995b) Critical Threonine and Aspartic Acid Residues Within The I-Domains of β2 Integrins for Interactions With Intercellular Adhesion Molecule-1 (ICAM-1) and iC3b. *J. Biol. Chem.* **270**, 12531.

Kamata, T., Irie, A., Tokuhira, M. and Takada, Y. (1996) Critical Residues of Integrin Alpha IIb Subunit For Binding of Alpha-IIb-Beta-3 (Glycoprotein IIb-IIIa) To Fibrinogen and Ligand-Mimetic Antibodies (PAC-1, OP-G2, and LJ-CP3). *J. Biol. Chem.* **271**, 18610.

Kansas, G.S., Saunders, K.B., Ley, K., Zakrazewicz, A., Gibson, R.M., Furie, B.C., Furie, B. and Tedder, T.F. (1994) A Role for the Epidermal Growth Factor Like Domain of P-Selectin in Ligand Recognition and Cell Adhesion. *J. Cell. Biol.* **124**, 609.

Kansas, G.S. (1996) Selectins and Their Ligands: Current Concepts and Contreversies. *Blood* **88**, 3259.

Kern, A., Briesewitz, R., Bank, I. and Marcantonio, E.E. (1994) The Role of the I-Domain in Ligand Binding of the Human Integrin α1β1. *J. Biol. Chem.* **269**, 22811.

King, S.L., Cunningham, J.A., Finberg, R.W. and Bergelson, J.M. (1995) Echovirus 1 Interaction with the Isolated VLA-2 I-Domain. *J. Virol.* **69**, 3237.

Kirchhofer, D., Languino, L.R., Ruoslhati, E. and Pierschbacher, M.D. (1990) α2β1 Integrins From Different Cell Types Show Different Binding Specificities. *J. Biol. Chem.* **265**, 615.

Kishimoto, T.K., O'Connor, K., Lee, A., Roberts, T.M. and Springer, T.A. (1987a) Cloning of The Beta Subunit of The Leukocyte Adhesion Proteins: Homology To An Extracellular Matrix Receptor Defines A Novel Gene Superfamily. *Cell* **48**, 681.

Kishimoto, T.K., Hollander, N., Roberts, T.M., Anderson, D.C. and Springer, T.A. (1987) Heterogeneous Mutations of the Beta Subunit Common to the LFA-1, Mac-1 and p150,95 Glycoproteins Cause Leukocyte Adhesion Deficiency. *Cell* **50**, 193.

Kishimoto, T.K., Larson, R.S., Corbi, A.L., Dustin, M.L., Staunton, D.E. and Springer, T.A. (1989) The Leukocyte Integrins: LFA-1, Mac-1 and p150,95. *Adv. Immunol.* **46**, 149.

Kishimoto, T.K., O'Connor, K. and Springer, T.A. (1989b) Leukocyte Adhesion Deficiency: Aberrant Splicing of a Conserved Integrin Sequence Causes a Moderate Deficiency Phenotype. *J. Biol. Chem.* **264**, 3588.

Kloczewiak, M., Timmons, S., Lukas, T.J. and Hawiger, J. (1984) Platelet Receptor Recognition Site on Human Fibrinogen: Synthesis and Structure Function Relationship of Peptides Corresponding to the Carboxyl Terminal Segment of the γ Chain. *Biochemistry* **23**, 1767.

Knott, V., Rees, D.J., Cheng, Z. and Brownlee, G.G. (1988) Randomly Picked Cosmid Clones Overlap the PYRB and ORIC Gap in the Physical Map of the Escherichia-coli Chromosome. *Nucleic Acid Res.* **16**, 2601.

Kolanus, W., Nagel, W., Schiller, B., Zeitlmann, L., Godar, S., Stockinger, H. and Seed, B. (1996) Alpha-L-Beta-2 Integrin/LFA-1 Binding to ICAM-1 Iinduced by Cytohesin-1, a Cytoplasmic Regulatory Molecule. *Cell* **86**, 233.

Komoriya, A., Green, L.J., Mervic, M., Yamada, S.S., Yamada, K.M. and Humphries, M.J. (1991) The Minimal Essential Sequence for a Major Cell Type-Specific Adhesion Site (CS1) Within the Alternatively Spliced Type III Connecting Segment Domain of Fibronectin is Leucine-Aspartic Acid-Valine. *J. Biol. Chem.* **266**, 15075.

Kouns, W.C., Newman, P.J., Puckett, K.J., Miller, A.A., Wall, C.D., Fox, C.F., Seyer, J.M., and Jennings, L.K. (1991) Further Characterization of the Loop Structure of Platelet Glycoprotein IIIa: Partial Mapping of Functionally Significant Glycoprotein-IIIa Epitopes. *Blood* **78**, 3215.

Krauss, J.C., Bond, L.M., Todd, R.F. and Wilson, J.M. (1991) Expression of Retroviral Transduced Human CD18 In Murine Cells: An *in vitro* Model of Gene Therapy For Leukocyte Adhesion Deficiency. *Hum. Gene Ther.* **2**, 221.

Laemmli, U.K. (1970) Cleavage of Structural Proteins During the Assembly of the Head of Bacteriophage T4. *Nature* **227**, 680.

LaFlamme, S.E., Akiyama, S.K. and Yamada, K.M. (1992) Regulation of Fibronectin Receptor Distribution. *J. Cell. Biol.* **117**, 437.

Lafrenie, R.M. and Yamada, K.M. (1996) Integrin-Dependent Signal Transduction. *J. Cellular Biochem.* **61**, 543.

Landis, R.C., Bennett, R.I. and Hogg, N. (1993) A Novel LFA-1 Activation Epitope Maps to the I-Domain. *J. Cell. Biol.* **120**, 1519.

Landis, R.C., McDowall, A., Holness, C.L.L., Littler, A.J., Simmons, D.L. and Hogg, N. (1994) Involvement of the "I" Domain of LFA-1 in Selective Binding to Ligands ICAM-1 and ICAM-3. *J. Cell. Biol.* **126**, 529.

Larson, R.S. and Springer, T.A. (1990) Structure and Function of Leukocyte Integrins. *Immunol. Rev.* **114**, 181.

Larson, R.S., Corbi, A.L., Bermnan, L. and Springer, T.A. (1989) Primary Structure of the Leukocyte Function-Associated Molecule-1 α Subunit: an Integrin with an Embedded Domain Defining a Protein Superfamily. *J. Cell. Biol.* **108**, 703-712.

Larson, R.S., Hibbs, M.L. and Springer, T.A. (1990) The Leukocyte Integrin LFA-1 Reconstituted by cDNA Transfection in a Nonhematopoietic Cell Line is Functionally Active and Not Transiently Regulated. *Cell Regulation* **1**, 359.

Lasky, L.A. (1992) Selectins: Interpreters of Cell-Specific Carbohydrate Information During Inflammation. *Science* **258**, 964.

Lasky, L.A. (1995) Selectin-Carbohydrate Interactions and the Initiation of the Inflammatory Response. *Ann. Rev. Biochem.* **64**, 113.

Law, S.K.L., Gagnon, J., Hildreth, J.E.K., Wells, C.E., Willis, A.C. and Wong, A.J. (1987) The Primary Structure of the Beta Subunit of the Cell Surface Adhesion Glycoproteins LFA-1, CR-3 and p150,95 and its Relationship to the Fibronectin Receptor. *EMBO. J.* **6**, 915.

Laure, L., Ohsugi, M., Hirchenhain, J. and Kemler, R. (1994) E-Cadherin Null Mutant Embryos Fail to Form a Trophectoderm Epithelium. *Proc. Natl. Acad. Sci. USA* **91**, 8263.

Leder, P., Tiemeier, D. and Enquist, L. (1977) EK2 Derivatives of Bacteriophage Lambda Useful in the Cloning of DNA from Higher Organisms: the Lambda gtWES

System. *Science* **196**, 175.

Lee, J-O., Rieu, P., Arnaout, M.A. and Liddington, R. (1995a) Crystal Structure of the A Domain from the α Subunit of Integrin CR3 (CD11b/CD18). *Cell* **80**, 631.

Lee, J-O., Bankston, L.A., Arnaout, M.A. and Liddington, R.C. (1995b) Two Conformations of the Integrin A Domain (I-Domain): A Pathway for Activation? *Structure* **3**, 1333.

Leung-Hagesteijn, C.Y., Milankov, K., Michalak, M., Wilkins, J. and Dedhar, S. (1994) Cell Attachment to Extracellular Matrix Substrates is Inhibited Upon Downregulation of Expression of Calreticulin, An Intracellular Integrin α-Subunit-Binding Protein. *J. Cell. Sci.* **107**, 589.

Li, R., Nortamo, P., Valmu, L., Tolvanen, M., Huuskonen, J., Kantor, C. and Gahmberg, C.G. (1993) A Peptide from ICAM-2 Binds to the Leukocyte Integrin CD11a/CD18 and Inhibits Endothelial Cell Adhesion. *J. Biol. Chem.* **268**, 17513.

Llic, D., Damsky, C.H. and Yamamoto, T. (1997) Focal Adhesion Kinase: At the Crossroads of Signal Transduction. *J. Cell Science* **110**, 401.

Loftus, J.C., O'Toole, T.E., Plow, E.F., Glass, A., Frelinger, A.L., and Ginsberg, M.H. (1990) A β3 Integrin Mutation Abolishes Ligand Binding and Alters Divalent Cation-Dependent Conformation. *Science* **249**, 915.

Loftus, J.C., Smith, J.W. and Ginsberg, M.H. (1994) Integrin-Mediated Cell-Adhesion: The Extracellular Face. *Biol. Chem.* **269**, 25235.

Loftus, J.C., Halloran, C.E., Ginsberg, M.H., Feigen, L.P., Zablocki, J.A., and Smith, J.W. (1996) The Amino-Terminal 1/3 of Alpha IIb Defines the Ligand Recognition Specificity of Integrin Alpha IIb-Beta 3. *J. Biol. Chem.* **271**, 2033.

Logan, D., Abu-Ghazaleh, R., Blakemore, W.,Curry, S., Jackson, T., King, A., Lea, S., Lewis, R., Newman, J., Parry, N., Rowlands, D., Stuart, D. and Fry, E. (1993) Structure of a Major Immunogenic Site on Foot-and-Mouth Disease Virus. *Nature* **362**, 566.

Loike, J.D., Sodeik, B., Cao, L., Leucona, S., Weitz, J.I., Detmers, P.A., Wright, S.D., and Silverstein, S.C. (1991) CD11c/CD18 on Neutrophils Recognises a Domain at the N-Terminus of the Aα Chain of Fibrinogen. *Proc. Natl. Acad. Sci. USA.* **88**, 1044.

Lukashev, M.E., Sheppard, D. and Pytela, R. (1994) Disruption of Integrin Function and Induction of Tyrosine Phosphorylation by the Autonomously Expressed β1 Integrin Cytoplasmic Domain. *J. Biol. Chem.* **269**, 18311.

Luque, A., Gomez, M., Puzon, W., Takada, Y., Sanchez-Madrid, F., and Cabanas, C. (1996). Activated Conformations of Very Late Activation Integrins Detected by a Group of Antibodies (HUTS) Specific for a Novel Regulatory Region (355-425) of the Common β1 Chain. *J. Biol. Chem.* **271**, 11067.

MacKay, B.S., Annis, D.S., Honda, S., Christie, D. and Kunicki, T.J. (1996) Molecular Requirements for Assembly and Function of a Minimised Human Integrin αIIbβ3. *J. Biol. Chem.* **271**, 30544.

Marlin, S.D., Morton, C.C., Anderson, D.C. and Springer, T.A. (1986) LFA-1 Immunodeficiency Disease: Definition of the Genetic Defect and Chromosomal Mapping of Alpha and Beta Subunits of the Lymphocyte Function-Associated Antigen 1 (LFA-1) by Complementation in Hybrid Cells. *J. Exp. Med.* **164**, 855.

Marlin, S.D. and Springer, T.A. (1987) Purified Intercellular Adhesion Molecule-1 (ICAM-1) is a Ligand for Lymphocyte Function-Associated Antigen-1 (LFA-1). *Cell* **51**, 813.

Masumoto, A. and Hemler, M.E. (1993) Mutation of Putative Divalent Cation Sites in the α4 subunit of the Integrin VLA-4: Distinct Effects on Adhesion to CS1/Fibronectin, VCAM-1 and Invasin. *J. Cell. Biol.* **123**, 245.

Masumoto, A. and Hemler, M.E. (1993b) Multiple Activation States of VLA-4: Mechanistic Differences Between Adhesion to CS1/Fibronectin and to Vascular cell Adhesion Molecule. *J. Biol. Chem.* **266**, 228.

Matsuura, S., Kishi, F., Tsukahara, M., Nunoi, H., Matsuda, I., Kobayashi, K. and Kajii, T. (1992) Leukocyte Adhesion Deficiency: Identification of a Novel Mutation in Two Japanese Patients with a Severe Form. *Biochem & Biophys. Res. Comm.* **184**, 1460.

McEver, R.P. (1992) Leukocyte-Endothelial Cell Interactions. *Curr. Opin. Cell Biol.* **4**, 840.

Merrill, J., Slade, S., Weissmann, G., Winchester, R. and Buyon, J. (1990) Two Pathways of CD11b/CD18-Mediated Neutrophil Aggregation With Different Involvement of Protein Kinase C-Dependent Phosphorylation. *J. Immunol.* **145**, 2608.

Michishita, M., Videm, V. and Arnaout, M.A. (1993) A Novel Divalent Cation Binding Site in the A-Domain of the β2 Integrin CR3 (CD11b/CD18) is Essential for Ligand Binding. *Cell* **72**, 857.

Micklem, K.J. and Sim, R.B. (1985) Isolation of Complement-Fragment-iC3b-Binding Proteins by Affinity Chromatography: The Identification of p150,95 as an iC3b-Binding Protein. *Biochem. J.* **231**, 233.

Miller, L.J., Bainton, D.F., Borregaard, N. and Springer, T.A. (1987) Stimulated Mobilisation of Monocyte Mac-1 and p150,95 Adhesion Proteins From An Intracellular Vesicular Compartment to the Cell Surface. *J. Clin. Invest.* **80**, 535.

Mosmann, T. (1983) Rapid Colorimetric Assay For Cellular Growth and Survival: Application to Proliferation and Cytotoxicity Assays. *J. Immunol. Methods* **65**, 55.

Mould, A.P., Garratt, A.N., Askari, J.A., Akiyama, S.K. and Humphries, M.J. (1995) Identification of a Novel Anti-Integrin Monoclonal-Antibody That Recognizes a Ligand-Induced Binding-Site Epitope on the β1 Subunit. *FEBS Lett.* **363**, 118.

Moyle, M., Foster, D.L., McGrath, D.E., Brown, S.M., Laroche, Y., Meutter, J.D., Stannsens, P., Bogowitz, C.A., Fried, V.A., Ely, J.A., Soule, H.R. and Vlasuk, G.P. (1994) A Hookworm Glycoprotein That Inhibits Neutrophil Function is a Ligand of the Integrin CD11b/CD18. *J. Biol. Chem.* **269**, 10008.

Muchowski, P.J., Zhang, L., Chang, E.R., Soule, H.R., Plow, E.F. and Moyle, M. (1994) Functional Interaction Between the Integrin Antagonist Neutrophil Inhibitory Factor and I Domain of CD11b/CD18. *J. Biol. Chem.* **269**, 26419.

Muir, T., Williams, M.,Ginsberg, M. and Kent, S. (1994) Design and Chemical Synthesis of a Neoprotein Structural Model for the Cytoplasmic Domain of a Multisubunit Cell-Surface Receptor: Integrin αIIbβ3 (Platelet GPIIb-IIIa). *Biochemistry* **33**, 7701.

Murray, N.E., Brammar, W.J. and Murray, K. (1977) Lambdoid Phages That Simplify the Recovery of *in vitro* Recombinants. *Mol. Gen. Genet.* **150**, 53.

Myones, B.L., Daizell, J.G., Hogg, N. and Ross, G.D. (1988) Neutrophil and Monocyte Cell Surface p150,95 Has iC3b-Receptor (CR4) Activity Resembling CR3. *J. Clin. Invest.* **82**, 640.

Nagai, T., Yamakawa, N., Aota, S., Yamada, S.S., Akiyama, S.K., Olden, K. and Yamada, K.M. (1991) Monoclonal Antibody Characterisation of Two Distant Sites Required for Function of the Central Cell-Binding Domain of Fibronectin in Cell Adhesion, Cell Migration, and Matrix Assembly. *J. Cell. Biol.* **114**, 1295.

Nelson, C., Rabb, H. and Arnaout, M.A. (1992) Genetic Cause of Leukocyte Adhesion Molecule Deficiency: Abnormal Splicing and a Missense Mutation in a Conserved Region of CD18 Impair Cell Surface Expression of β2 Integrins. *J. Biol. Chem.* **267**, 3351.

Nermut, M.V., Green, N.M., Eason, P., Yamada, S.S. and Yamada, K.M. (1988) Electron Microscopy and Structural Model of Human Fibronectin Receptor. *EMBO J.* **7**, 4093.

Newham, P. and Humphries, M.J. (1996) Integrin Adhesion Receptors: Structure, Function and Implications for Biomedicine. *Mol. Medicine Today* **2**, 304.

Nortamo, P., Salcedo, R., Timonen, T., Patarroyo, M. and Gahmberg, C.G. (1991) A Monoclonal Antibody to the Human Leukocyte Adhesion Molecule Intercellular Adhesion Molecule-2: Cellular Distribution and Molecular Characterisation of the Antigen. *J. Immunol.* **146**, 2530.

Nose, A., Tsuji, K. and Takeichi, M. (1990) Localisation of Specificity Determining Sites in Cadherin Cell Adhesion Molecules. *Cell* **61**, 147.

Nurden, A. and Caen, J. (1974) An Abnormal Platelet Glycoprotein Pattern in Three Cases of Glanzmann's Thrombasthenia. *Br. J. Haematol.* **28**, 253.

Ortlepp, S., Stephens, P.E., Hogg, N., Figdor, C.G. and Robinson, M.K. (1995) Antibodies That Activate β2 Integrins Can Generate Different Ligand Binding States. *Eur. J. Immunol.* **25**, 637.

Osborn, L., Vassallo, C., Browning, B.G., Tizard, R., Haskard, D.O., Benjamin, C.D., Douglas, I. and Kirchhausen, T. (1994) Arrangement of Domains and Amino Acid Residues Required for Binding of Vascular Cell Adhesion Molecule-1 to its Counter-Receptor VLA-4 (α4β1). *J. Cell. Biol.* **124**, 601.

Otey, C.A., Pavalko, F.M. and Burridge, K. (1990) An Interaction Between Alpha-Actinin and the β1 Integrin Subunit *in vitro*. *J. Cell. Biol.* **111**, 721.

Otey, C.A., Schaller, M. and Parsons J. (1994) Characterisation of the Binding Site For Focal Adhesion Kinase on the β1 Integrin Subunit. *Mol. Biol. Cell* **5**, 66a (Suppl.).

O'Toole, T.E., Mandelman, D., Forsyth, J., Shattil, S.J., Plow, E.F. and Ginsberg, M.H. (1991) Modulation of the Affinity of Integrin αIIbβ3 (GPIIb-IIIa) by the Cytoplasmic Domain of αIIb. *Science* **254**, 845.

O'Toole, T.E., Katagiri, Y., Faull, R.J., Peter, K., Tamura, R., Quaranta, V., Loftus, J.C., Shattil, S.J. and Ginsberg, M.H. (1994) Integrin Cytoplasmic Domains Mediate Inside-Out Signal Transduction. *J. Cell. Biol.* **124**, 1047.

O'Toole, T.E., Ylanne, J. and Culley, B.M. (1995) Regulation of Integrin Affinity States Through an NPXY Motif in the β Subunit Cytoplasmic Domain. *J. Biol. Chem.* **270**, 8553.

Overduin, M., Harvey, T.S., Bagby, S., Tong, K.I., Yau, P., Takeichi, M. and Ikura, M. (1995) Solution Structure of the Epithelial Cadherin Domain Responsible for Selective Cell Adhesion. *Science* **267**, 386.

Ozawa, M., Baribault, H. and Kemler, R. (1989) The Cytoplasmic Domain of the Cell Adhesion Molecule Uvomorulin Associates with 3 Independent Proteins Structurally Related in Different Species. *EMBO J.* **8**, 1711.

Pardi, R., Inverardi, L., Rugarli, C. and Bender, J. (1992) Antigen-Receptor Complex Stimulation Triggers Protein Kinase C-Dependent CD11a/CD18-Cytoskeleton Association in T Lymphocytes. *J. Cell. Biol.* **116**, 1211.

Pardi, R., Bossi, G., Inverardi, L., Rovida, E. and Bender, J.R. (1995) Conserved Regions of the Cytoplasmic domains of the Leukocyte Integrin αLβ2 Are Involved in Endoplasmic Reticulum Retention, Dimerisation, and Cytoskeletal Association. *J. Immunol.* **155**, 1252.

Peter, K. and O'Toole, T.E. (1995) Modulation of Cell Adhesion by Changes in αLβ2 (LFA-1, CD11a/CD18) Cytoplasmic Domain/Cytoskeletal Interaction. *J. Exp. Med.* **81**, 315.

Pierschbacher, M.D. and Ruoslahti, E. (1984) Cell Attachment Activity of Fibronectin can be Duplicated by Small Synthetic Fragments of the Molecule. *Nature* **309**, 30.

Pober, J.S., Gimbrone, M.A., Lapierre, L.A., Mendrick, D., Fiers, W., Rothlein, R. and Springer, T.A. (1986) Overlapping Patterns of Activation of Human Endothelial Cells by Interleukin-1, Tumour Necrosis Factor, and Immune Interferon. *J. Immunol.* **137**, 1893.

Postigo, A.A., Corbi, A.L., Sanchez-Madrid, F. and de Landazuri, M.O. (1991) Regulated Expression and Function of CD11c/CD18 Integrin On Human B Lymphocytes. Relation Between Attachment to Fibrinogen and Triggering of Proliferation Through CD11c/CD18. *J. Exp. Med.* **174**, 1313.

Qu, A. and Leahy, D.J. (1995) Crystal Structure of the I-Domain from the CD11a/CD18 (LFA-1, αLβ2) Integrin. *Proc. Natl. Acad. Sci. USA.* **92**, 10277.

Quaranta, V. (1990) Epithelial Integrins. *Cell Differentiation and Development.* **32**, 361.

Quaranta, V. and Jones, J.C.R. (1991) The Internal Affairs of An Integrin. *Trends. Cell. Biol.* **1**, 2.

Rabb, H, Michishita, M., Sharma, C.P., Brown, D. and Arnaout, M.A. (1993) Cytoplasmic Tails of Human Complement Receptor Type 3 (CR3, CD11b/CD18) Regulate Ligand Avidity and the Internalisation of Occupied Receptors. *J. Immunol.* **151**, 990.

Randi, A.M. and Hogg, N. (1994) I Domain of β2 Integrin Lymphocyte Function Associated Antigen-1 Contains a Binding site for Ligand Intercellular Adhesion Molecule-1. *J. Biol. Chem.* **269**, 12395.

Ranscht, B. (1994) Cadherins and Catenins: Interactions and Functions in Embryonic Development. *Curr. Opin. Cell Biol.* **6**, 740.

Richardson, A. and Parsons, J.T. (1995) Signal Transduction through Integrins: A Central Role for Focal Adhesion Kinase? *BioEssays* **17**, 229.

Rieu, P., Ueda, T., Haruta, I., Sharma, C.P. and Arnaout, M.A. (1994) The A-Domain of β Integrin CR3 (CD11b/CD18) is a Receptor for the Hookworm-Derived Neutrophil Adhesion Inhibitor NIF. *J. Cell. Biol.* **127**, 2081.

Riviere, Y., Blank, V., Kourilsky, P. and Israel, A. (1991) Processing of the Precursor of NF-KB By The HIV-1 Protease During Acute Infection. *Nature* **350**, 625.

Robinson, M.K., Andrew, D., Rosen, H., Brown, D., Ortlepp, S., Stephens, P. and Butcher, E.C (1992) Antibody Against The Leu-CAM β-Chain (CD18) Promotes Both LFA-1 and CR3-Dependent Adhesion Events. *J. Immunol.* **148**, 1080.

Rodriguez, C.L., Nueda, A., Grospierre, B., Sanchez-Madrid, F., Fisher, A., Springer, T.A. and Corbi, A.L. (1993) Characterisation of Two New CD18 Alleles Causing Severe Leukocyte Adhesion Deficiency. *Eur. J. Immunol.* **23**, 2792.

Rojiani, M.V., Finlay, R.B., Gray, V. and Dedhar, S. (1991) In vitro Interaction of a Polypeptide Homologous to Human Ro/SS-A Antigen (Calreticulin) with a Highly Conserved Amino Acid Sequence in the Cytoplasmic Domain of Integrin α Subunits. *Biochemistry* **30**, 9859.

Rosen, S.D. and Bertozzi, C.R. (1994) The Selectins and Their Ligands. *Curr. Opin. Cell. Biol.* **6**, 663.

Ross, G.D., Cain, J.A., Myones, B.L., Newman, S.L. and Lachmann, P.J. (1987) Specificity of Membrane Complement Receptor Type Three (CR3) For Beta-Glucans. *Complement* **4**, 61.

Ruoslahti, E. (1991) Integrins. *J. Clin. Invest.* **87**, 1.

Ruoslahti, E. and Pierschbacher, M.D. (1987) New Perspectives in Cell Adhesion: RGD and Integrins. *Science* **238**, 491.

Saiki, R.K., Gelfand, D.H., Stoffel, S., Scharf, S.J., Higuchi, R., Horn, G.T., Mullis, K.B. and Erlich, H.A. (1988) Primer-Directed Enzymatic Amplification of DNA with a Thermostable DNA-Polymerase. *Science* **239**, 487.

Saleeba, J.A. and Cotton, R.G.H. (1993) Chemical Cleavage of Mismatch to Detect Mutations. *Methods Enzymol.* **217**, 286.

Sambrook, J., Fritsch, E.F. and Maniatis, T. (1989) Molceular Cloning: A Laboratory Manual. (Second Edition) Cold Spring Harbor Laboratory Press, N.Y.

Sanchez-Madrid, F., Nagy, J.A., Robbins, E., Simon, P. and Springer, T.A. (1983) A Human Leukocyte Differentiation Antigen Family with Distinct α-Subunits and a Common β-Subunit: The Lymphocyte Function Associated Antigen (LFA-1), the C3bi Complement Receptor (OKM1/Mac-1), and the p150,95 Molecule. *J. Exp. Med.* **158**, 1785.

Sanger, F., Nicklen, S. and Coulson, A.R. (1977) DNA Sequencing with Chain-Terminating Inhibitors. *Proc. Natl. Acad. Sci. USA.* **74**, 5463.

Santoni, M.J., Bartheis, D., Vopper, G., Boned, A., Goridis, C. and Wille, W. (1989) Differential Exon Usage Involving an Unusual Splicing Mechanism Generates at Least Eight Types of NCAM cDNA in Mouse Brain. *EMBO. J.* **8**, 385.

Sastry, S.K. and Horwitz, A.F. (1993) Integrin Cytoplasmic Domains: Mediators of Cytoskeletal Linkages and Extra- and Intracellular Initiated Transmembrane Signalling. *Curr. Opin. Cell Biol.* **5**, 819.

Schaller, M.D. and Parsons, J.T. (1993) Focal Adhesion Kinase: An Integrin-Linked Protein Tyrosine Kinase. *Trends.Cell. Biol.* **3**, 258.

Schaller, M.D., Otey, C.A., Hildebrande, J.D., Parsons, J.T. (1995) Focal Adhesion Kinase and Paxillin Bind to Peptides Mimicking β Integrin Cytoplasmic Domains. *J. Cell. Biol.* **130**, 1181.

Schiffer, S.G., Hemler, M.E., Lobb, R.R., Tizard, R. and Osborn, L. (1995) Molecular Mapping of Functional Antibody-Binding Sites of Alpha-4 Integrin. *J. Biol. Chem.* **270**, 14270.

Schwartz, M.A., Schaller, M.D. and Ginsberg, M.H. (1995) Integrins: Emerging Paradigms of Signal Transduction. *Annu. Rev. Cell Dev. Biol.* **11**, 549.

Seed, B. and Aruffo, A. (1987) Molecular Cloning of the CD2 Antigen, the T-Cell Erythrocyte Receptor, By a Rapid Immunoselection Procedure. *Proc. Natl. Acad. Sci. USA.* **84**, 3365.

Sengelov, H., Kjeldsen, L., Diamond, M.S., Springer, T.A. and Borregaard, N. (1993) Subcellular Localisation and Dynamics of Mac-1 (αMβ2) in Human Neutrophils. *J. Clin. Invest.* **92**, 1467.

Shapiro, L., Fannon, A.M., Kwong, P.D., Thompson, A., Lehmann, M.S., Grubel, G., Legrand, J-F., Als-Neilson, J., Colman, D.R. and Hendrickson, W.A. (1995) Structural Basis of Cell-Cell Adhesion by Cadherins. *Nature* **374**, 327.

Sharma, C.P., Ezzell, R.M. and Arnaout, M.A. (1995) Direct Interaction of Filamin (ABP-280) with the β2-Integrin Subunit CD18. *J. Immunol.* **154**, 3461.

Sharp, P.A., Sugden, B. and Sambrook, J. (1973) Detection of Two Restriction Endonuclease Activities in Haemophilus parainfluenzae Using Analytical Agarose Ethidium Bromide Electrophoresis. *Biochemistry* **12**, 3055.

Shattil, S.J., Hoxie, J.A., Cunningham, M. and Brass, L.F. (1985) Changes in the Platelet Membrane Glycoprotein IIb-IIIa Complex During Platelet Activation. *J. Biol. Chem.* **260**, 11107.

Shattil, S.J., O'Toole, T., Eigenthaler, M., Thon, V., Williams, M., Babior, B.M. and Ginsberg, M.H. (1995) Beta 3-Endonexin, A Novel Polypeptide Which Interacts Specifically with the Cytoplasmic Tail of the Integrin Beta 3 Subunit. *J. Cell. Biol.* **131**, 807.

Shaw, L.M., Messier, J.M. and Mercurio, A.M. (1990) The Activation Dependent Adhesion of Macrophages to Laminin Involves Cytoskeletal Anchoring and Phosphorylation of the α6β1 Integrin. *J. Cell. Biol.* **110**, 2167.

Shaw, L.M. and Mercurio, A.M. (1993) Regulation of α6β1 Integrin Laminin Receptor Function by the Cytoplasmic Domain of the α6 Subunit. *J. Cell. Biol.* **123**, 1017.

Shimizu, Y., Newman, W., Tanaka, Y. and Shaw, S. (1992) Lymphocyte Interactions With Endothelial cells. *Immunol. Today* **13**, 106.

Short, J.M., Fernandez, J.M., Sorge, J.A. and Huse, W.D. (1988) Lambda-ZAP: A Bacteriophage Lambda-Expression Vector With *in vivo* Excision Properties *Nucleic Acid Res.* **16**, 7583.

Shuster, D.E., Kehrli, M.E., Ackermann, M.R., Gilbert, R.O. (1992) Identification and Prevalence of a Genetic Defect That Causes Leukocyte Adhesion Deficiency in Holstein Cattle. *Proc. Natl. Acad. Sci. USA.* **89**, 9225.

Simmons, D.L. (1993) Cloning Cell Surface Molecules by Transient Expression in Mammalian Cells. In "Cellular Interactions in Developement", D. Hartley, ed. (Oxford: Oxford University Press), pp. 93-128.

Singer, S.J. (1992) Intercellular Communication and Cell-Cell Adhesion. *Science* **255**, 1671.

Sligh, J.E., Hurwitz, M.Y., Zhu, C., Anderson, D.C. and Beaudet, A.L. (1992) An Initiation Codon Mutation in CD18 in Association With the Moderate Phenotype of Leukocyte Adhesion Deficiency. *J. Biol. Chem.* **267**, 714.

Smith, J.W. and Cheresh, D.A. (1988) The Arg-Gly-Asp Binding Domain of the Vitronectin Receptor: Photoaffinity Crosslinking Implicates Amino Acid Residues 61-203 of the β Subunit *J. Biol. Chem.* **263**, 18726.

Smith, J.W. and Cheresh, D.A. (1990) Integrin (αVβ3)-Ligand Interaction: Identification of a Heterodimeric RGD Binding Site on the Vitronectin Receptor. *J. Biol. Chem.* **265**, 2168.

Smith, J.W. and Cheresh, D.A. (1991) Labelling of Integrin αVβ3 with ^{58}CO(III): Evidence of Metal Ion Coordination Sphere Involvement in Ligand Binding. *J. Biol. Chem.* **266**, 11429.

Smyth, S.S., Joneckis, C.C. and Parise, L.V. (1993) Regulation of Vascular Integrins. *Blood* **81**, 2827.

Solomon, E., Palmer, R.W., Hing, S. and Law, S.K.A. (1988) Regional Localisation of CD18, the β-Subunit of the Cell Surface Adhesion Molecule LFA-1, On Human Chromosome 21 by *in situ* Hybridisation. *Ann. Hum. Genet.* **52**, 123.

Southern, E.M. (1975) Detection of Specific Sequences Among DNA Fragments Separated by Gel Electrophoresis. *J. Mol. Biol.* **98**, 503.

Sprague, J., Condra, J.H., Arnheiter, H. and Lazzarini, R.A. (1983) Expression of a Recombinant DNA Gene Coding For the Vesicular Stomatitis-Virus Nucleocapsid Protein. *J. Virolology* **45**, 773.

Springer, T.A. (1990) Adhesion Receptors of the Immune System. *Nature* **346**, 425.

Springer, T.A. (1994) Traffic Signals for Lymphocyte Recirculation and Leukocyte Emigration: The Multistep Paradigm. *Cell* **76**, 301.

Springer, T.A. (1995) Traffic Signals on Endothelium For Lymphocyte Recirculation and Leukocyte Emigration. *Annu. Rev. Physiol.* **57**, 827.

Springer, T.A. (1997) Folding of the N-Terminal, Ligand Binding Region of Integrin α-Subunits into a β-Propeller Domain. *Proc. Natl. Acad. Sci.. USA* . **94**, 65.

Springer, T.A., Thompson, W.S., Miller, L.J., Schmalsteig, F.C. and Anderson, D.C. (1984) Inherited Deficiency of the Mac-1, LFA-1, p150,95 Glycoprotein Family and Its Molecular Basis. *J. Exp. Med.* **160**, 1901.

Staatz, W.D., Fok, K.F., Zutter, M.M., Adams, S.P., Rodriguez, B.A. and Santoro, S.A. (1991) Identification of a Tetrapeptide Recognition Sequence for the α2β1 Integrin in Collagen. *J. Biol. Chem.* **266**, 7363.

Stacker, S.A. and Springer, T.A. (1991) Leukocyte Integrin p150,95 (CD11c/CD18) Functions As An Adhesion Molecule Binding To A Counter-Receptor On Stimulated

Endothelium. *J. Immunol.* **146**, 648.

Stanley, P., Bates, P.A., Harvey, J., Bennett, R.I. and Hogg, N. (1994) Integrin LFA-1 α Subunit Contains an ICAM-1 Binding Site in Domains V and VI. *EMBO J.* **13**, 1790.

Staunton, D.E., Dustin, M.L. and Springer, T.A. (1989) Functional Cloning of ICAM-2, A Cell Adhesion Ligand For LFA-1 Homologous to ICAM-1. *Nature* **339**, 61.

Staunton, D.E., Dustin, M.L., Erickson, H.P. and Springer, T.A. (1990) The Arrangement of the Immunoglobulin-Like Domains of ICAM-1 and the Binding Sites for LFA-1 and Rhinovirus. *Cell* **61**, 243.

Stephens, P., Romer, J.T., Spitali, M., Shock, A., Ortlepp, S., Figdor, C.G. and Robinson, M.K. (1995) KIM127, an Antibody that Promotes Adhesion, Maps to a Region of CD18 that Includes Cysteine-Rich Repeats. *Cell Adhesion and Communication* **3**, 375.

Stewart, M and Hogg, N. (1996) Regulation of Leukocyte Integrin Function: Affinity vs. Avidity. *J. Cellular. Biochem.* **61**, 554.

Strynadka, N.C. and James, M.N.G. (1989) Crystal Structures of the Helix-Loop-Helix Calcium-Binding Proteins. *Annu. Rev. Biochem.* **58**, 951.

Stuiver, I. and O'Toole, T.E. (1995) Regulation of Integrin Function and Cellular Adhesion. *Stem Cells* **13**, 250.

Suzuki, S. and Naitoh, Y. (1990) Amino Acid Sequence of a Novel Integrin β4 Subunit and Primary Expression of the mRNA in Epithelial cells. *EMBO J.* **9**, 757.

Suzuki, S., Sano, K. and Tanihara, H. (1991) Diversity of the Cadherin Family: Evidence for Eight New Cadherins in Nervous tissue. *Cell Regulation* **2**, 261.

Suzuki, S. *et al.* (1996) Structural and Functional Diversity of the Cadherin Family. *J. Cell. Biochem.* **61**, 531.

Takada, Y. and Hemler, M.E. (1989) The Primary Structure of the VLA-2/Collagen Receptor α2 Subunit (Platelet GPIa): Homology to Other Integrins and the Presence of a Possible Collagen-Binding Domain. *J. Cell. Biol.* **109**, 397.

Takada, Y. and Puzon, W. (1993) Identification of a Regulatory Region of Integrin β1 Subunit using Activating and Inhibiting Antibodies. *J. Biol. Chem.* **268**, 17597.

Takada, Y., Ylanne, J., Mandelman, D., Puzon, W. and Ginsberg, M.H. (1992) A Point Mutation of Integrin β1 Subunit Blocks Binding of α5β1 to Fibronectin and Invasin But Not Recruitment to Adhesion Plaques. *J. Cell. Biol.* **119**, 913.

Takeichi, M. (1988) The Cadherins: Cell-Cell Adhesion Molecules Controlling Animal Morphogenesis. *Development* **102**, 639.

Takeichi, M. (1990) Cadherins: A Molecular Family Important in Selective Cell-Cell Adhesion. *Ann. Rev. Biochem.* **59**, 237.

Takeichi, M. (1991) Cadherin Cell Adhesion Receptors as a Morphogenetic Regulator. *Science* **251**, 1451.

Takeichi, M. (1993) Cadherins in Cancer: Implications for Invasion and Metastasis. *Curr. Opin. Cell. Biol.* **5**, 806.

Talamas-Rohana, P., Wright, S.D., Lennartz, M.R. and Russell, D.G. (1990) Lipophosphoglycan From *Leischmania mexicana* Promastigotes Binds to Members of the CR3, p150,95 and LFA-1 Family of Leukocyte Integrins. *J. Immunol.* **144**, 4817.

Tamkun, J.W., Desimone, D.W., Fonda, D., Patel, R.S., Buck, C., Horwtiz, A.F. and Hynes, R.O. (1986) Structure of Integrin, a Glycoprotein Involved in the Transmembrane Linkage Between Fibronectin and Actin. *Cell* **46**, 271.

Taniguchi-Sidle, A. and Isenman, D.E. (1992) Mutagenesis of the Arg-Gly-Asp Triplet in Human Complement Component C3 Does Not Abolish Binding of iC3b to the Leukocyte Integrin Complement Receptor Type III (CR3, CD11b/CD18). *J. Biol. Chem.* **267**, 635.

Tedder, T.F. et al. (1995) The Selectins: Vascular Adhesion Molecules. *Faseb. J.* **9**, 866.

Tian, L., Yoshihara, Y., Mizuno, T., Mori, K. and Gahmberg, C.G. (1997) The Neuronal Glycoprotein Telencephalin Is A Cellular Ligand For The CD11a/CD18 Leukocyte Integrin. *J. Immunol.* **158**, 928.

Tozer, E.C., Liddington, R.C., Sutcliffe, M.J., Smeeton, A.H. and Loftus, J.C. (1996) Ligand Binding to Integrin αIIbβ3 is Dependent on a MIDAS-like Domain in the β3 Subunit. *J. Biol. Chem.* **271**, 21978.

Trowald-Wigh, G., Hakansson, L., Johannisson, A., Norrgren, L. and Segerstad, C.H. (1992) Leukocyte Adhesion Protein Deficiency in Irish Setter Dogs. *Vet. Immunol. Immunopathol.* **32**, 261.

Tuckwell, D.S., Brass, A. and Humphries, M.J. (1992) Homology Modelling of Integrin EF-Hands: Evidence for Widespread Use of a Conserved Cation Binding Site. *Biochem. J.* **285**, 325.

Tuckwell, D.S., Calderwood, D.A., Green, L.J. and Humphries, M.J. (1995) Integrin α2 I-Domain is a Binding Site for Collagens. *J. Cell. Sci.* **108**, 1629.

Tuckwell, D.S. and Humphries, M.J. (1997) A Structure Prediction for the Ligand-Binding Region of the Integrin β Subunit: Evidence for the Presence of a Von Willebrand Factor A Domain. *FEBS Letters* **400**, 297.

Tufty, R.M and Kretsinger, R.H. (1975) Troponin and Parvalbumin Calcium Binding Regions Predicted in Myosin Light Chain and T4 Lysozyme. *Science* **187**, 167.

Uciechowski, P. and Schmidt, R. (1989). Cluster Report CD11. In "Leukocyte Typing IV: White Cell Differentiation Antigens", editors: W. Knapp, D. Dorkin, W. Gilks, E. Rieber, R. Schmidt, H. Stein, and A. von dem Borne (Oxford: Oxford University Press). pp 543-551.

Ueda, T., Rieu, P., Brayer, J. and Arnaout, M.A. (1994) Identification of the Complement iC3b Binding Site in the β2 Integrin CR3 (CD11b/CD18). *Proc. Natl. Acad. Sci. USA.* **91**, 10680.

Van der Vieren, M., Trong, H.L., Wood, C.L., Moore, P.F., St. John, T., Staunton, D.E. and Gallatin, W.M. (1995) A Novel Leukointegrin, αDβ2, Binds Preferentially to ICAM-3. *Immunity* **3**, 683.

van Kooyk, Y., van de Wiel-van Kemenade, P., Weder, P., Kuijpers, T.W. and Figdor, C.J. (1989) Enhancement of LFA-1-Mediated Cell Adhesion by Triggering Through CD2 or CD3 on T Lymphocytes. *Nature* **342**, 811.

van Kooyk, Y., Weder, P., Heije, K. and Figdor, C.G. (1994) Extracellular Ca^{2+} Modulates Leukocyte Function-Associated Antigen-1 Cell Surface Distribution on T Lymphocytes and Consequently Affects Cell Adhesion. *J. Cell. Biol.* **124**, 1061.

van Strijp, J.A.G., Russell, D.G., Tuomanen, E., Brown, E.J. and Wright, S.D. (1993) Ligand Specificity of Purified Complement Receptor Type Three (CD11b/CD18, αMβ2, Mac-1). *J. Immunol.* **151**, 3324.

von Andrian, U.H., Berger, E.M., Ramezani, L., Chambers, J.D., Ochs, H.D., Harlan, J.M., Paulson, J.C., Etzioni, A. and Arfors, K.E. (1993) In Vivo Behaviour of Neutrophils from Two Patients with Distinct Inherited LAD Syndromes. *J. Clin. Invest.* **91**, 2893.

Vonderheide, R.H., Tedder, T.F., Springer, T.A. and Staunton, D.E. (1994) Residues Within a Conserved Amino Acid Motif of Domains 1 and 4 of VCAM-1 are Required for Binding to VLA-4. *J. Cell. Biol.* **125**, 215.

Wallace, R.B. and Miyada, C.G. (1987) Oligonucleotide Probes for the Screening of Recombinant DNA Libraries. *Methods Enzymol.* **152**, 432.

Wardlaw, A.J., Hibbs, M.L., Stacker, S.A. and Springer, T.A. (1990) Distinct Mutations in Two Patients With Leukocyte Adhesion Deficiency and Their Functional Correlates. *J. Exp. Med.* **172**, 335.

Weis, W.I. (1995) Cadherin Structure: A Revealing Zipper. *Structure* **3**, 425.

Weisel, J.W., Nagaswami, C., Vilaire, G. and Bennett, J.S. (1992) Examination of Platelet Membrane Glycoprotein IIb-IIIa Complex and its Interaction with Fibrinogen and Other Ligands by Electron Microscopy. *J. Biol. Chem.* **267**, 16637.

Weitzman, J.B. and Law, S.K.A. (1993) CR3 and its Relationship with Other Phagocytic Receptors. In *"Complement in Health and Diseases"* (Ed. K. Whaley). Chapter 10, pp 269-297, Kluwer Academic Press, Lancaster.

Weitzman, J.B., Wells, C.E., Wright, A.H., Clark, P.A. and Law, S.K.A. (1991) The Gene Organisation of the Human β2 Integrin Subunit (CD18). *FEBS Letters.* **294**, 97.

Wencel-Drake, J.D., Flow, E.P., Kunicki, T.J., Woods, V.L., Keller, D.M. and Ginsberg, M.H. (1986) Localisation of Internal Pools of Membrane Glycoproteins Involved in Platelet Adhesive Responses. *Am. J. Pathol.* **124**, 324.

Weskamp, G. and Blobel, C.P. (1994) A Family of Cellular Proteins Related to Snake Venom Disintegrins. *Proc. Natl. Acad. Sci. USA* **91**, 2748.

Wickham, T.J., Mathias, P., Cheresh, D.A. and Nemerow, G.R. (1993) Integrins αVβ3 and αVβ5 Promote Adenovirus Internalisation but Not Virus Attachment. *Cell* **73**, 309.

Wilkins, J.A., Li, A., Ni, H., Stupack, D.G., and Shen, C. (1996). Control of β1 Integrin Function: Localization of Stimulatory Epitopes. *J. Biol. Chem.* **271**, 3046.

Williams, A.F. (1987) A year in the Life of the Immunoglobulin Superfamily. *Immunol. Today* **8**, 298.

Williams, A.F. and Barclay, A.N. (1988) The Immunoglobulin Superfamily-Domains for Cell Surface Recognition. *Ann. Rev. Immunol.* **6**, 381.

Williams, M.J., Hughes, P.E., O'Toole, T.E. and Ginsberg, M.H. (1994) The Inner World of Cell Adhesion: Integrin Cytoplasmic Domains. *Trends Cell Biol.* **4**, 109.

Wippler, J., Kouns, W.C., Schlaeger, E.J., Kuhn, H., Hadvary, P. and Steiner, B. (1994) The Integrin αIIb-β3, Platelet Glycoprotein IIb-IIIa, Can Form a Functionally Active Heterodimer Complex Without the Cysteine-Rich Repeats of the β3 Subunit. *J. Biol. Chem.* **269**, 8754.

Wolfsberg, T.G., Primakoff, P., Myles, D.G. and White, J.M. (1995) ADAM, A Novel Family of Membrane Proteins Containing a Disintegrin and Metalloprotease Domain: Multipotential Functions in Cell-Cell and Cell-Matrix Interactions. *J. Cell. Biol.* **131**, 275.

Wright, S.D., Rao, P.E., Van Voorhis, W.C., Craigmyle, L.S., Iida, K., Talle, M.A., Westberg, E.F., Goldstein, G. and Silverstein, S.C. (1983) Identification of the iC3b Receptor of Human Monocytes and Macrophages by Using Monoclonal Antibodies. *Proc. Natl. Acad. Sci. USA.* **80**, 5699.

Wright, S.D., Weitz, J.I., Huang, A.J., Levin, S.M., Silverstein, S.C. and Loike, J.D. (1988) Complement Receptor Type 3 (CD11b/CD18) of Human Polymorphonuclear Leukocytes Recognises Fibrinogen. *Proc. Natl. Acad. Sci. USA.* **85**, 7734.

Wright, A.H., Douglass, W.A., Taylor, G.M., Lau, Y-L., Higgins, D., Davies, K.A. and Law, S.K. (1995) Molecular Characterization of Leukocyte Adhesion Deficiency in Six Patients. *Eur. J. Immunol.* **25**, 717.

Wright, S.D. and Jong, M.T. (1986) Adhesion-Promoting Receptors on Human Macrophages Recognise *Escherichia coli* By Binding to Lipopolysaccharide. *J. Exp. Med.* **164**, 1876.

Xie, J., Li, R., Kotovuori, P., Vermot-Desroches, C., Wijdenes, J., Arnaout, M.A., Nortamo, P. and Gahmberg, C.G. (1995) Intercellular Adhesion Molecule-2 (CD102) Binds to the Leukocyte Integrin CD11b/CD18 Through the A Domain. *J. Immunol.* **155**, 3619.

Yamada, K.M. and Geiger, B. (1997) Molecular Interactions in Cell Adhesion Complexes. *Curr. Opin. Cell. Biol.* **9**, 76.

Yang, J., Rayburn, H. and Hynes, R. (1993) Embryonic Mesodermal Defects in α5 Integrin-Deficient Mice. *Development* **119**, 1093.

Ylanne, J., Chen, Y., O'Toole, T.E., Loftus, J.C., Takada, Y. and Ginsberg, M.H. (1993) Distinct Functions of Integrin α and β Subunit Cytoplasmic Domains in Cell Spreading and Formation of Focal Adhesions. *J. Cell. Biol.* **122**, 223.

Ylanne, J., Huuskonen, J., O'Toole, T.E., Ginsberg, M.H., Virtanen, I. and Gahmberg, C.G. (1995) Mutation of the Cytoplasmic Domain of the Integrin β3 Subunit. *J. Biol. Chem.* **270**, 9550.

Yoon, P.S., Boxer, L.A., Mayo, A., Angela, Y.Y. and Wicha, M.S. (1987) Human Neutrophil Laminin Receptors: Activation-Dependent Receptor Expression. *J. Immunol.* **138**, 259.

Yorifuji, T., Wilson, R.W., Lorenzo, I., Hughes, B.J., Smith, C.W., Anderson, D.C. and Beaudet, A.L. (1992) Towards Gene Therapy of Leukocyte Adhesion Deficiency. *Pediatr. Res.* **3**, 137A.

Yuan, Q., Jiang, W-M., Krissansen, G.W. and Watson, J.D. (1990) Cloning and Sequence Analysis of a Novel β2-Related Integrin Transcript From T Lymphocytes: Homology of Integrin Cysteine-Rich Repeats to Domain III of Laminin B Chains. *Int. Immunol.* **2**, 1097.

Zhang, L. and Plow, E.F. (1996) Overlapping, But Not Identical Sites, Are Involved in the Recognition of iC3b, Neutrophil Inhibitory Factor, and Adhesive Ligands by the αMβ2 Integrin. *J. Biol. Chem.* **271**, 18211.

Zhang, L. and Plow, E.F. (1996b) A Discrete Site Modulates Activation of I Domains. *J. Biol. Chem.* **271**, 29953.

Zhou, L., Lee, D.H.S., Plescia, J., Lau, C.Y. and Altieri, D.C. (1994) Differential Ligand Binding Specificities of Recombinant CD11b/CD18 Integrin I-Domain. *J. Biol. Chem.* **269**, 17075.

Zimmerman, G.A., Prescott, S.M. and McIntyre, T.M. (1992) Endothelial Cell Interactions With Granulocytes: Tethering and Signalling Molecules. *Immunol. Today* **13**, 93.